Applied Hydrometeorology

BY

PUKH RAJ RAKHECHA

VIJAY P. SINGH

Springer

Applied Hydrometeorology

Applied Hydrometeorology

By

Pukh Raj Rakhecha
Formerly at
Indian Institute of Tropical Meteorology, Pune, India

and

Vijay P. Singh
Department of Biological and Agricultural Engineering and
Department of Civil & Environmental Engineering
Texas A & M University, College Station, USA

Cover photos: Courtesy United States Bureau of Reclamation (USBR)

Printed on acid-free paper

Printed in India.

Dedicated to

Our families

Wife Anusuya, sons Ashok Kumar and Ramesh
—Pukh Raj Rakhecha

*Wife Anita, son Vinay, daughter-in-law Sonali
and daughter Arti*
—Vijay P. Singh

About the Authors

Dr. Pukh Raj Rakhecha, former Dy. Director (Hydrometeorology) with the Indian Institute of Tropical Meteorology in Pune has worked on a variety of hydrometeorological projects including studies of design rainfalls, rainfall statistics, river basin PMP analysis, IFD relations in engineering design, major rainstorms analysis, floods and drought studies, water balance studies and rainfall runoff relations. He has over 250 research papers to his credit and has been consultant on numerous hydrometeorolgical studies. Dr. Rakhecha has travelled widely visiting Australia, Sweden, Switzerland, England, Malaysia, Japan, Iceland and United States for research work and participation in international conferences. He is an internationally recognised hydrometeorologist on PMP studies and member of several scientific societies including International Association of Hydrological Sciences (IAHS).

Dr. Vijay P. Singh holds the Caroline & William N Lehrer Distinguished Chair in Water Engineering, is Professor of Civil and Environmental Engineering, and Professor of Biological and Agricultural Engineering at Texas A & M University. He has published more than 450 journal articles, 70 book chapters, 240 conference proceeding papers, and 70 technical reports and bulletins; authored or co-authored fourteen books and has edited another forty-five texts. Prof. Singh has made pioneering contributions in the application of systems analysis, kinematic wave theory, and entropy theory to a range of problems in hydraulics, water quality engineering, irrigation, hydrology and water resources. Prof. Singh has been the recipient of the ASCE Arid Land Hydraulic Engineering Award (2002) and the Ven Te Chow Award (2005), and most recently the AIH Ray K. Linsley Award for outstanding contributions to surface water hydrology. He has served as Editor-in-Chief of the Water Science and Technology (WST) series for Springer, and also currently serves as Editor-in-Chief of the *ASCE Journal of Hydrologic Engineering* and Editor-Chief of *Water Science and Engineering*. He has directed the organization of 17 international conferences, chaired more than 40 conference sessions, given more than 35 keynote addresses, and examined more than 40 PhD. candidates abroad.

Preface

Water is vital for life. Since the dawn of civilization, much effort has been made to harness sources of fresh water. Recent years have raised global awareness of the need for increasing demand of water worldwide, largely because of growing population, rising standard of living, higher demand for energy, and greater appreciation for environmental quality. As an example, the world population has increased threefold in the past five decades. In order to meet the rising water demand, water resources are being developed by building large dams, reservoirs, barrages and weirs across rivers worldwide. The guiding principle for water resources development has been to ensure adequate supply of water for agriculture, domestic use (including fine drinking water), waste disposal, industries, and energy production, with due attention to maintain the ecosystem functions. This development, however, depends on a holistic, cooperative and scientific approach.

The basic inputs in the assessment of water resources for a given region are from hydrological data and the subject of hydrology forms the core in achieving sustainable development of water resources. Barring a few exceptions, hydrological data for most river basins are sparse and therefore it is difficult to comprehensively assess their water resources. The major source of water is rainfall which occurs as a result of condensation of atmospheric moisture governed by the science of meteorology. Rainfall, therefore, is the principal meteorological element whose recording with other meteorological elements, such as temperature, humidity, wind, and so on, was initiated a long time ago. That is why good networks of raingauge stations have been in existence for several decades in many countries of the world, and long rainfall records are not uncommon these days. Meteorologists, hydrologists and engineers have long recognized the value of hydro-meteorological data and more importantly the rainfall data for hydrologic analyses. Thus, application and analysis of meteorological data for the solution of hydrologic problems has precisely come to be known as the science of

hydrometeorology. In a broad sense, hydrometeorology is a border line science linking meteorology—the science of atmosphere—with hydrology—the science of water of the earth and earth's atmosphere. In engineering hydrology dealing with design and operation of water resource projects, the subject of hydrometeorology occupies a central position. Obviously, the importance of the subject of hydrometeorology has become increasingly recognized and it is now studied not only by hydrologists and engineers but also by students from many different disciplines.

Realizing the importance of the subject, there is a need for a textbook like the present one on applied hydrometeorology oriented towards the Asian environment, particularly to India, which can provide a complete set of tools to practicing engineers and hydrologists engaged in the planning, development and management of water resources. This constitutes the primary objective of this book. The emphasis in the book is on the practical applications of meteorology for water resources development and understanding of the needed meteorological concepts. The subject matter of the book follows this rationale.

The book contains 15 chapters encompassing a wide spectrum of topics of hydrometeorology. Chapter 1 scopes out the area of hydrometeorology, and deals with meteorological variables and their use in hydrology, hydrological cycle, global distribution of land and water, and global water budget. Chapter 2 discusses the earth-atmospheric system. Included in the discussion are composition of the atmosphere, mass of atmosphere and hydrosphere, vertical structure of atmosphere, air density and its variation, hydrostatic equation, hydrostatics of special atmosphere, reduction of pressure to sea level, and atmospheric stability.

The discussion of meteorological processes, constituting the subject matter of Chapter 3, includes compression and expansion of gases, forms of heat, equation of state for a perfect gas, isothermal and adiabatic changes, the first law of thermodynamics, adiabatic process, vertical motion in the atmosphere, mixture of gases, equation of state of moist air, and precipitable water. Chapter 4 deals with radiation and temperature. Beginning with a discussion of the source of heat and light, it goes on to discuss different aspects of radiation, mean annual heat balance, non-radiative heat exchange between the earth and the troposphere, heat balance, and temperature zones. Weather systems for precipitation are discussed in Chapter 5. Included in the discussion are pressure belts; wind systems of the earth; and scales of weather systems including planetary scale, synoptic scale, and meso scale of weather systems. Chapter 6 deals with weather and precipitation in India. The discussion in the chapter includes location and area, land forms, river basins, and seasons of India; climate controls; rainfall and runoff of continents; seasonal variation of pressure and temperature; onset and withdrawal of monsoons; weather systems affecting Indian rainfall; history of rainfall measurement in India; rainfall over India; assessment of rainwater resources; and present status of water utilization in India.

Defining and classifying tropical disturbances and hurricanes, Chapter 7 discusses major hurricanes and super typhoons, wind rotation, conversion of wind speeds, formation of tropical storms, frequency of hurricanes for oceanic regions, absence of hurricanes in South Atlantic Ocean, naming hurricanes, life cycle of hurricanes, structure of hurricanes, hurricane climatology, record hurricane, largest rainfall from tropical storms/hurricanes, longest lasting hurricanes, climatic effects of hurricane activity, global warming and hurricanes, hurricane threats, damages and destruction, seeding of hurricanes, and damage caused by cyclones. Greatest point and areal rainfalls constitute the subject matter of Chapter 8. It includes significant point rainfall occurrences over India, China, Australia, and Japan; world's greatest point rainfalls; importance of greatest areal rainfalls; and greatest areal rainfalls over India, USA, Japan, and China.

Recognizing rainfall as an important source of input for water resources, Chapter 9 covers precipitation and its measurement. It also encompasses mechanisms of precipitation, forms of precipitation, types of precipitation, measurement of precipitation, network design, estimation of missing data, mean depth of rainfall over an area, consistency of rainfall records, extension and interpretation of rainfall data, intensity-duration relationships, and point rainfall and areal rainfall relationships. The physical evaluation of probable maximum precipitation (PMP) based on a hydrometeorological procedure is a topic of considerable importance in designing large dams, reservoirs, and spillways and for the derivation of probable maximum floods (PMF). Techniques for estimating the PMP constitute the subject matter of Chapter 9. They discuss rainstorm analysis, depth-area-duration analysis, design storm, data for design storm studies, methods of estimating design storms, probable maximum precipitation, and methods of estimating PMP.

Chapter 10 deals with design storm estimation. The material contained in this chapter is of particular value to design engineers. The discussion includes rainstorm and its analysis, depth-area-duration analysis of a rainstorm, design storms, data for design storm studies, methods for estimating design storms, probable maximum precipitation, and methods of estimating PMP. Statistical analysis of precipitation is presented in Chapter 11. It deals with data series for frequency analysis, recurrence interval, calculated risk, frequency analysis, measures of central tendency, measures of variability, skewness, and kurtosis (flattening), moments of frequency distribution, standard frequency distributions, tests of significance, homogeneity of data series, and frequency analysis.

Foreshadowing rainfall is covered in Chapter 12. It includes measures of variability, correlation analysis, global scale factors affecting rainfall, types of weather forecasts, techniques for long-range rainfall forecasting in India, Indian summer monsoon and southern oscillation index, statistical techniques used in long range forecasting, multiple regression analysis, and parameters in long-range forecasting of Indian summer monsoon rainfall.

Chapter 13 deals with evaporation. Beginning with a discussion of the physics of evaporation, it goes on to discuss factors affecting evaporation, measurement of evaporation, evaporation measurement in India, and estimation of evaporation by indirect methods.

Extreme hydrometeorological events that arise from unusually high and low precipitation lead to floods and droughts, respectively. These events cause considerable loss of life and property. Droughts constitute the subject matter of Chapter 14. It discusses causes of droughts, evapotranspiration and potential evapotranspiration, types of droughts, droughts in India, El Nino factor relating to droughts, and absence of tropical disturbances and Indian rainfall. The concluding chapter, Chapter 15, is on floods. Defining floods and classifying them, the chapter goes on to discuss the kinds and causes of floods, effects of floods, flood measurements, flood control, estimation of peak floods, flood frequency analysis, floods in Indian rivers, highest floods in India, and comparison of highest floods in India with world's highest floods.

The text material of each chapter contains illustrative examples, which are mostly based on actual, recorded data. It is hoped that the book will be of much use to the professionals engaged in water resources planning, development, and management. Also the book should be useful to university courses concerned with hydrometeorology and its application to water-related issues, as it caters to the requirement of the syllabi of various Indian and foreign universities.

There is vast literature on the topics in this book. A comprehensive list of references has been advertently omitted, and only those studies that are deemed most pertinent have been cited. This is because the intended audience would be more interested in applications rather than advanced literature. This, however, in no way reflects a lack of appreciation for the literature. Indeed this book would not have been completed without reviewing the pertinent literature.

We have tried to make our acknowledgments as specific as possible. We would be most grateful if readers discovering any discrepancies, errors, or misprints would bring them to our attention. Our families provided unwavering support and help, without which this book would not have been completed. As a small token of our appreciation for their love and support, we dedicate this book to them.

January 2009   **Pukh Raj Rakhecha**
                                                      Vijay P. Singh

Contents

1 Introduction

Water, whose importance is rated next to air, is the world's most precious natural resource and is vital for all forms of life. It generally refers to that part of fresh water which is renewable annually and includes surface water, soil water and underground water. Atmospheric precipitation (rainfall, snowfall, and other forms) constitutes the source of all fresh water on the earth. Rainfall, the primary source of water that occurs as a result of condensation of atmospheric moisture, is governed by the science of meteorology and, therefore, is considered to be one of the most important meteorological elements. Similarly, the occurrence and distribution of rainwater on and beneath the earth's surface is governed by the science of hydrology and geology. Both meteorology and hydrology are concerned with the hydrologic cycle (also sometimes referred to as water cycle) dealing with the movement and interchange of water between the oceans, the atmosphere and the earth. The striking elements of the hydrologic cycle, which are generally observed and recorded for purposes of water development, are meteorological elements, such as rainfall and evaporation, as well as hydrologic elements of lake and river levels, river flow, infiltration, and ground water. The river flow data are especially important for determining the total amount of water available in a river that could be stored in reservoirs for irrigation, hydropower generation, and water supply for domestic and other purposes.

Conspicuously, the development of water resources of a region requires hydrological data, such as river flow data, at a number of points along a river. Generally speaking, such data are not available for most of the rivers, especially in developing countries and, moreover, it is rather an expensive and sometimes a difficult task to observe them at a number of sites along a river. On the other hand, meteorological data, such as rainfall, evaporation, temperature, humidity, vapor pressure, radiation, sunshine hours, wind, and so on, are being recorded daily and are available for several years for a close network of stations in many countries of the world. It is now recognized that

in the absence of actual hydrological data, the meteorological data can best be used to assess and develop water resources of a region using the science of hydrometeorology. Thus, hydrometeorology is that branch of meteorological science which deals with the application of meteorology to the solution of hydrologic problems. Broadly speaking, hydrometeorology is concerned with the study of the atmospheric and land phase of the hydrologic cycle with emphasis on the inter-relationships involved. It is a border line science linking meteorology, the science of atmosphere, with surface-water hydrology, the science dealing with the occurrence, distribution, movement and storage of water on the earth's surface.

1.1 SCOPE OF HYDROMETEOROLOGY

The development of hydrometeorology as a science is closely linked with the increasing use of meteorology to the problems of hydrology. Some examples have been chosen to illustrate various aspects of the use of meteorological data in hydrological and agricultural studies. The subject has a very broad scope which will be limited here to a discussion of rainfall and evaporation. Evaporation is commonly used to determine water losses from lakes, ponds, and reservoirs as well as in assessing the water requirements of crops. Estimates of evaporation from river basins are used for conceptual hydrological modeling. Deducting evaporation losses from rainfall, it is possible to estimate surface runoff. The rate at which evaporation takes place greatly depends upon the meteorological elements of temperature, radiation, humidity, vapor pressure, sunshine hours, cloud cover, and wind velocity. These meteorological elements are of great value in estimating evaporation indirectly for hydrologic studies where direct measurement of evaporation is not possible.

Rainfall data are used for the design and construction of water resources projects. Construction of dams and reservoirs across rivers for collection and storage of river runoff water to serve the needs of the people has been in vogue for many centuries. In the planning and design of these dams, long-period rainfall data are used for the estimation of water flowing in a stream. Stream flow data are vital for the assessment of the water yield of river basins and for sizing the storage capacity of dams. In order to protect the dams from large floods caused by heavy rainfall, suitable spillways are designed and built into dams. This requires estimates of the highest floods using discharge records which are often inadequate due to the limited number of surface gauging stations and limited records thereof. In such cases, depending on the type, scope and location of a particular dam, a design flood determined from a design storm is used. The design storm is developed from an analysis of long-period rainfall data from stations in and around the river basin under consideration, and is then converted to a design flood using a rainfall-runoff model. Several techniques of rainfall analysis, such as depth

duration (DD), depth-area-duration (DAD) and transposition of storms have been developed for estimating the design storm. Design storms in common use for deriving design floods are the probable maximum storm (PMS) or the probable maximum precipitation (PMP) and the standard project storm (SPS).

The objective of the PMP is to provide complete safety criterion in situations where extreme loss of life and property would result from failure or overtopping of a dam. Designs of small dams are not based on the PMP storm because there will be little hazard downstream from a dam failure. Instead a frequency approach is used, where extreme rainfalls at a particular point are analyzed statistically to determine the frequency with which a given intensity of rainfall of a specified duration can be expected to occur. Hydrologic methods are then employed to estimate the design flood from the design storm rainfall. The data of recording rain gauges are used for the design of drainage structures for purposes of sizing waterway openings under bridges, culverts for highways and railways, urban storm sewers, airfield drainage, stream control works, and so on. These are designed considering the frequency of rainfall events and the subsequent determination of the required rainfall intensity by statistical methods. Information on rainfall and its forecasts are important inputs concerning the river flow warnings. Efficient operation of a multipurpose dam depends very much on the reliability of rainfall forecasts. Based on rainfall forecasting, the magnitude of inflow is determined and the reservoir is operated to accommodate the incoming flood waters. In the case of storage reservoirs, the water use during dry months would have to be planned carefully. An assessment of the probable wind over reservoirs is needed for calculating water wave heights for the determination of free board requirements.

In light of the above discussion, hydrometeorology has a wide scope in providing rainfall statistics for use in a wide range of design and construction of hydraulic structures. In what follows, the various meteorological variables of importance are described.

1.2 METEOROLOGICAL VARIABLES

Around the earth is a layer of air known as the atmosphere that thins from the ground upward. Weather at a given location is the atmospheric condition at a given time or over a certain period as described by various meteorological variables, such as temperature, pressure, humidity, wind, radiation, rain, sunshine, evaporation, clouds, fog, etc. An understanding of the atmosphere and the associated weather requires continuous measurements of meteorological variables. Measurements are taken using standardized instruments with standardized exposures. The science of meteorology deals with the causes of weather and its variation in space and time. Climate differs from the weather. Climate is the average weather of a place which is determined by averaging several years of meteorological data (usually about

30 years). The reason is that the pattern of variation of meteorological data over time repeats itself in a period of about 30 years.

1.2.1 Temperature

Temperature is a measure of the degree of hotness or coldness of the air and is expressed in degrees on the centigrade scale or the Fahrenheit scale. On the earth, temperature primarily depends on the amount of radiation received by it. Besides radiation, the temperature of any place is dependent on other factors, such as altitude, proximity to the sea, prevailing winds, etc. For meteorological purposes, temperature is recorded by a mercury thermometer in a Stevenson screen and refers to the air temperature in shaded conditions at a height of about 1.5 m. The atmospheric air temperature is an extremely useful parameter for the determination of snow melt and evaporation.

Investigating the nature of a gas, Lord Kelvin put forth the concept of absolute zero beyond which no gas could be cooled any further. This value is about $-273°C$. The absolute scale commences at this scale. The freezing point is $273°A$ and the boiling point $373°A$. It is convenient to use the Kelvin scale when very low or very high temperature values are considered.

1.2.2 Atmospheric Pressure

As pointed out, the earth is surrounded on all sides by a gaseous envelope known as the atmosphere which extends up to a height of many kilometers above the surface of earth. If we consider an imaginary tube of unit area of cross section full of air extending from the earth up to its uppermost limit, the air of this imaginary tube must exercise some force on bodies lying on the earth because of the fact that air has weight. This force exerted on a unit area due to the column of air is called the pressure of the atmosphere and its unit in centimeter-gram-second (CGS) system is dynes/cm^2. If it is assumed that the column at the mean sea level is of height h of air whose average density is ρ, then the atmospheric pressure p is ρgh, where g is the acceleration due to gravity.

The pressure is measured with a mercury barometer (invented by Torricelli in 1643). It is expressed by the height of the mercury column in a barometer balancing the atmospheric pressure. The height of mercury column at the average sea level pressure is about 76 cm. Since the density of mercury at 15°C is 13.59 g/cm^3 and g is 980 cm/s^2, the average sea level pressure $P = 76 \times 13.59 \times 980 = 1,013,200$ dynes/cm^2. The unit dynes/cm^2 is an exceedingly small unit. Bjerknes introduced the millibar, which is 1000 times larger. The millibar (1 millibar = 1000 dynes/cm^2) is the unit of pressure employed in meteorology. The average sea level pressure is about 1013 mb. The unit of pressure in the SI system of units is 1 N/m^2. This unit is known as the Pascal (Pa) and is equal to 10 dynes/cm^2. Hence 1 mb=100 Pa (=1 hecto Pascal or 1 hPa). The atmospheric pressure of 1013 mb is 1013 hPa in the SI unit system.

1.2.3 Atmospheric Humidity

In the atmosphere water vapor is always present in varying proportions. It can be about 4% by mass in hot humid air to more than a hundred times less in very cold air. This atmospheric water vapor is the product of evaporation from water bodies, such as oceans, rivers, lakes, tanks and moist land surfaces. The mean annual global evaporation is estimated to be 1000 mm. The term humidity represents the amount of water vapor present in the atmosphere and can be specified by a number of physical quantities. The important humidity variables are the vapor pressure, relative humidity, specific humidity, mixing ratio, absolute humidity, and dew point.

The water vapor in the air exerts a partial pressure independent of the presence of other gases. This pressure exerted by the water vapor is called the vapor pressure and is the most useful measure of the water content of the atmosphere. It is usually denoted by "e" and is expressed in a manner similar to the atmospheric pressure in millibars or in millimeters of mercury. There is an interesting relationship between the temperature of air and the amount of water vapor that the air can hold. The maximum amount of water vapor that can be present in the atmosphere depends on the air temperature. The higher the temperature the more vapor the air can hold. When the air holds the maximum possible water vapor at a given temperature and pressure then the air is said to be saturated. At this stage, if more vapor is added, or if the air is cooled below the saturation point, the excess vapor condenses into tiny drops of dew. The temperature at which dew begins to form is called dew point and at this temperature the pressure of water vapor in the air becomes saturated. The pressure exerted by the water vapor in a saturated air at a given temperature and pressure is called saturation vapor pressure which for all practical purposes is the largest vapor pressure. It is denoted by "e_s" and is measured in millibars or in millimeters of mercury. The difference "$e_s - e$" is called the saturation deficit. The relative humidity (*RH*) of the air is expressed as:

$$RH = \frac{e}{e_s} \times 100 \tag{1.1}$$

The relative humidity, therefore, is defined as the percentage ratio of the actual vapor pressure (*e*) to the maximum possible vapor pressure (*e_s*) at a given temperature. The air is saturated with the moisture when the relative humidity is 100 percent.

The relationship between the temperature of air and saturation vapor pressure is given as

$$e_s = 6.107 \times 10^{\frac{7.5T}{(237 + T)}} \tag{1.2}$$

where e_s = saturation vapor pressure in millibars, and T = temperature in °C. Equation (1.2) can be used to compute the saturation vapor pressure for

different values of temperatures. Values of saturation vapor pressure for various values of temperature are given in Table 1.1.

The most convenient method for determining the relative humidity of air is by the use of wet and dry bulb thermometers. If the bulb of a thermometer covered by a small piece of muslin is kept moist by a wick dipped in a small water bottle, it will register a lower atmospheric temperature than a similar naked thermometer. Two such thermometers mounted side by side constitute a psychrometer. The lowering of the wet bulb thermometer reading increases as the relative humidity of the air decreases. The low value of temperature from the wet bulb thermometer is due to the fact that when air is unsaturated there is evaporation of water from the wet muslin into the surrounding air. The latent heat of vaporization (evaporation) is taken from the air which is thereby cooled. The cooling of the air and the increase of moisture content by evaporation from the muslin continue until the air surrounding the wet bulb is saturated. Thereafter, the wet bulb thermometer records a steady reading lower than that of the dry bulb thermometer. The difference between the readings of the dry bulb thermometer and the wet bulb thermometer in relation to the air temperature gives a measure of the actual vapor pressure as well as relative humidity. Tables, graphs and equations have been prepared for determining vapor pressure and relative humidity.

Table 1.1: Saturation vapor pressure (mb)

Temp °C	Saturation vapor pressure (mb)*									
	0	1	2	3	4	5	6	7	8	9
00	6.11	6.57	7.06	7.58	8.13	8.72	9.35	10.02	10.73	11.49
10	12.29	13.14	14.03	14.99	16.00	17.07	18.20	19.39	20.66	22.00
20	23.41	24.90	26.45	28.13	29.88	31.73	33.67	35.71	37.87	40.13
30	42.51	45.01	47.65	50.40	53.31	56.35	59.50	62.89	66.40	70.08
40	73.94	77.97	82.20	86.62	91.24	96.08	101.14	106.42	111.94	117.70

* For obtaining the correct saturation vapor pressure value from the table corresponding to a given temperature value, the value of temperature in the first column should be read and then the value in the first row should be added to it. For example, for a temperature of 26°C, go to the fourth row corresponding to the value of 20 and the eighth column corresponding to the value of 6 and the common element of 33.67 mb is obtained, which is the value of the saturation vapor pressure.

The psychrometric equation for deriving the vapor pressure of the air can be expressed as:

$$e = e_s - 0.000660 \, P \, (T - T_w) \, (1 + 0.00115 \, T_w) \qquad (1.3)$$

where e = the pressure of the vapor present in the air in mb, e_s = the saturation vapor present in mb at temperature T_w of the wet bulb thermometer in °C, T = the temperature of the dry bulb thermometer in °C, T_w = the

temperature of the wet bulb thermometer in °C, and P = the pressure of the air in mb. Table 1.2 gives the values of vapor pressure (e) corresponding to specified values of dry bulb and wet bulb temperatures for a pressure of 1000 mb.

In addition to relative humidity, vapor pressure and wet bulb thermometer, humidity can be expressed in other ways which are explained as follows.

The vapor density is the mass of water vapor present in a unit volume of moist air. This is sometimes called the absolute humidity. Its unit is gm/m^3. The specific humidity, denoted as "q", is the mass of water vapor present in one gram of moist air. It hardly ever exceeds 0.04.

The mixing ratio, denoted as "r" is the mass of water vapor present in one gram of dry air. The specific humidity and the mixing ratio are usually expressed as grams per kilogram.

Table 1.2: Values of e in mb

T_w (°C)	$T - T_w$ (°C)									
	0	*1*	*2*	*3*	*4*	*5*	*6*	*7*	*8*	*9*
0	6.11	5.44	4.77	4.11	3.16	2.75	2.09	1.43	0.76	0.09
2	7.06	6.27	5.72	5.04	4.37	3.71	3.03	2.36	1.69	1.03
4	8.13	7.45	6.79	6.12	5.44	4.77	4.09	3.43	2.76	2.08
6	9.35	8.68	8.00	7.33	6.53	5.99	5.31	4.64	3.96	3.29
8	10.73	10.05	9.37	8.70	8.03	7.35	6.68	6.00	5.33	4.65
10	12.29	11.60	10.93	10.25	9.57	8.89	8.23	7.55	6.87	6.19
12	14.03	13.34	12.67	12.00	11.20	10.64	9.96	9.28	8.60	7.92
14	16.00	15.30	14.63	13.95	13.26	12.59	11.91	11.23	10.55	9.88
16	18.20	17.51	16.83	16.15	15.47	14.67	14.51	13.43	12.75	12.05
18	20.66	19.47	19.28	18.60	17.92	17.24	16.56	15.87	15.19	14.51
20	23.41	22.70	22.03	21.35	20.67	19.97	19.29	18.61	17.92	17.24
22	26.45	25.80	25.09	24.40	23.72	23.03	22.35	21.65	20.97	20.29
24	29.88	29.17	28.49	27.80	27.12	26.43	25.75	25.05	24.36	23.68
26	33.67	32.96	32.26	31.59	30.89	30.20	29.52	28.83	28.13	27.45
28	37.87	37.15	36.45	39.77	35.08	34.38	33.69	33.01	32.32	31.63

If P is the total pressure of air and e is the partial pressure of water vapor in it then the partial pressure of the dry air is ($P - e$). The mixing ratio (r) and the specific humidity (q) are expressed as:

$$r = \frac{\varepsilon e}{P - e} = \frac{0.622e}{P - e} \tag{1.4}$$

$$q = \varepsilon \frac{e}{P} = \frac{0.622e}{P} \tag{1.5}$$

where $\varepsilon = 0.622$ is the ratio of the molecular weight of water vapor (18) to the molecular weight of dry air (28.97). The humidity variables can be computed from Tables 1.1 and 1.2 or from equations (1.2) and (1.3).

Example 1.1: The dry bulb and wet bulb thermometer readings, respectively, are: $T = 26°C$ and $T_w = 20°C$. Calculate vapor pressure (e), saturated vapor pressure (e_s), specific humidity (q), mixing ratio (r) and relative humidity (RH). The air pressure (P) is 1000 mb.

Solution:

$$e_s = 6.107 \times 10^{\frac{7.5T}{(237+T)}}$$

$$e_s \text{ (at 26°C)} = 6.107 \times 10^{\frac{7.5 \times 26}{(237+26)}}$$

$$e_s \text{ (at 26°C)} = 33.67 \text{ (see Table 1.1)}$$

$$e_s \text{ (at 20°C)} = 23.41 \text{ (see Table 1.1)}$$

$$e = e_s \text{ (at 20°C)} - 0.000660 \quad P(T - T_w)(1 + 0.00115 \ T_w)$$

$$e = 23.41 - 0.000660 \times 1000 \times 6 \times (1 + 0.00115 \times 20)$$

$$e = 23.41 - 3.96 \times 1.023$$
$$e = 19.36$$

$$RH = \frac{e}{e_s} = \frac{19.36}{33.67} = 0.57 = 57\%$$

$$q = \frac{0.622 \times e}{P}$$

$$q = \frac{0.622 \times 19.36}{1000}$$

$$q = 0.012 \frac{\text{gm}}{\text{gm}} \text{ or 12 gm/kg of moist air}$$

$$r = \frac{0.622 \times 19.36}{1000 - 19.36} \text{ or } r = \frac{12.04}{980.64} \text{ or } r = 0.0123 \text{ gm/kg or 12.3 gm/kg of}$$
dry air

Alternatively, the values can also be calculated from Tables 1.1 and 1.2. The difference between t and t_w is:

$$26 - 20 = 6°C$$

From Table 1.1 the saturation vapor pressure at 26°C = 33.6 mb
The actual vapor pressure under the difference of 6°C from Table 1.2 = 19.29 mb.
Relative humidity = 19.29/33.67 = 57%

Example 1.2: Calculate the amount of water the dry air can hold at 55°C which is one of the highest temperatures ever recorded at a station in the world.

Solution:

$$e_s = 6.107 \times 10^{\frac{7.5T}{(237 + T)}}$$

$$T = 55°C$$

$$e_s = 6.107 \times 10^{\frac{7.5 \times 55}{(237 + 55)}}$$

$$e_s = 157.94 \text{ mb}$$

$$r = \frac{0.622 \times e_s}{1000 - 157.94} \text{ or } r = \frac{0.622 \times 157.94}{1000 - 157.94} \text{ or } r = \frac{98.24}{842.06}$$

$$r = 0.117 \text{ gm/gm}, \ r = 117 \text{ gm/kg}$$

At 55°C, the air can hold 117 gm of water vapor per kg of dry air at 1000 mb.

Example 1.3: On a certain day the dew point was found to be 8° C, while the temperature of the air was 25°C. Find relative humidity on that day.

Solution: The dew point of air which is at 25°C is 8°C. This means that the amount of water vapor actually present in the air at 25°C is not able to saturate the air at that temperature but as the temperature of the air falls to 8°C, the water vapor already actually present in the air is sufficient to saturate the air at 8°C at which dew began to form. Therefore, the relative humidity from saturation vapor pressure (*SVP*) is:

$$\text{Relative humidity} = \frac{SVP \text{ at } 8°C}{SVP \text{ at } 25°C}$$

From Table 1.1

$$SVP \text{ at } 8°C = 10.73 \text{ mb}$$
$$SVP \text{ at } 25°C = 31.73 \text{ mb}$$

$$\text{Relative humidity} = \frac{10.73}{31.73} \times 100 = 33.8\%$$

Example 1.4: The temperatures of dry and wet bulbs are 20°C and 15°C, respectively. Determine the relative humidity and dew point.

Solution: The difference between temperatures of dry and wet bulbs

$$= 20 - 15 = 5°C$$

SVP at 20°C from Table 1.1 = 23.41

Actual vapor pressure under the difference of 5°C from Table 1.2 = 13.63

Relative humidity = $\dfrac{13.63}{23.41} \times 100 = 58\%$

Since the dew point is that temperature at which the saturation vapor pressure is 13.63. From Table 1.1, it is about 11.5°C. Therefore,

Dew point = 11.5°C

1.2.4 Air Density

Air density, denoted as ρ, which is the order of 1/1000 of that of water near the ground, is almost never measured. Instead it is computed from the gas equation ($\rho = P/RT$). It is given in gm/cm^3 or kg/m^3. For a surface pressure of 1000 mb and temperature 290°K the air density is 0.0012 gm/cm^3.

1.2.5 Precipitation

The water cycle in the atmosphere consists of three different parts, namely, evaporation, condensation and precipitation. In this process, the water which falls to the earth surface from the atmosphere in either liquid or solid form is termed precipitation. It includes rain in the liquid form, and snow, sleet and hail in the solid form. Water evaporates from water surfaces, such as seas, rivers, lakes, ponds and also from the land and vegetation in the form of water vapor. This water vapor when rises to considerable heights above the earth's surface gets condensed to form clouds. Essentially, the condensation consists of an accumulation of water vapor molecules into exceedingly small droplets. These small water droplets grow in size and finally fall to the ground as rain or snow. An average rain drop has a radius of about 1000 microns. In order to estimate the total amount of water received from the atmosphere on a given area during a given time, it is necessary to measure precipitation. All forms of precipitation are measured as the vertical depth of water that would accumulate on a level surface if the entire precipitation remained where it fell. The two important parts of precipitation (i.e., rain and snow) are measured separately by measuring devices called raingauges. The standard non-recording raingauge has a receiver five inches in diameter. For hydrologic and water resources development purposes, the most valuable rainfall data are the mean depth of rainfall for different areas for different durations, such as months, seasons or the whole year. The mean annual global precipitation is about 80 cm. However, precipitation is the highest near the equator and between 40° and 50° latitudes. Comparatively heavy

rainfall is received over mountainous areas. For example, Cherrapunji [25.3°N, 91.8°E] in India has an average yearly precipitation of 1087 cm. The various physical processes associated with the formation of precipitation will be discussed in the subsequent chapter.

1.2.6 Horizontal Winds

Wind is the horizontal motion of air over the surface of the earth and is specified in terms of its direction and speed. The wind direction is taken to be the direction from which the wind blows. The wind directions are given in terms of the cardinal directions, such as *N*, *NW*, *NNW*, etc. The north (*N*) wind is one which comes from the north. The wind speed is measured in knot (nautical miles per hour) or kilometer per hour (km/h) or miles per hour (m/h) or meter per second (m/sec). The direction of the wind is measured by the wind vane and the speed by the anemometer. The conversion factor for winds is:

1 knot = 1.853 km/hr = 0.51 m/s = 1.57 miles/hr

1.2.7 Evaporation

It is the process by which a substance changes from the liquid state to the vapor state. Evaporation of surface water from the oceans, lakes, rivers, etc. by the heat of the sun is the cause of water vapor in the atmosphere. The rate of evaporation is measured by the Pan-measurement method or weather pan. In this method, a pan of certain standard dimensions is taken, and the water is filled in this pan to a certain level. The amount of water evaporated from this pan is measured, from which the rate of evaporation per unit time per unit area is calculated.

1.2.8 Visibility

The visibility is defined as the greatest horizontal distance to which an object can be seen. It is measured by selecting a number of objects, such as towers, tall buildings, or hills, known as visibility marks. In the absence of any particles in suspension, the visibility would be unlimited. But in the atmosphere there are always some particles in suspension which reduce the visibility. Particles that restrict visibility are minute particles of smoke, dust or water. Particles of smoke or dust produce haze and that of water produce mist or fog. Dust storms, sand storms, thick drizzle, and heavy rains or snow can reduce the visibility to a few hundred meters.

1.2.9 Vertical Air Motions

Upward vertical motion of air, both small scale and large scale, is responsible for most of the cooling and consequent condensation of air, leading to cloud formation and precipitation. The velocity is not constant vertically and has a distribution which up to certain height follows as logarithmic or power law.

1.2.10 Clouds

Cloud and precipitation play an important role in hydrometeorology. Clouds form when the ascending air becomes super-saturated at high altitudes. The cooling is caused by the expansion of air as it rises gradually to the upper atmosphere. As pointed out earlier the water vapor is created by evaporation of surface water—oceans, lakes, rivers, etc. The water vapor being light rises upwards where it expands adiabatically and is cooled below the saturation point. The excess moisture is condensed on suspended dust particles as minute globules of water which form clouds.

According to their forms as seen from the ground, clouds are classified into three broad categories (Fig. 1.1): (i) Cirrus or feathery streaks of clouds, (ii) stratus or layer clouds, and (iii) cumulus or heap-shaped clouds. On the basis of the height above the ground at which they occur clouds are classified into high, medium and low. According to the international classification, ten principal types are given below and are shown in Table 1.3.

Cirrus clouds have a fibrous structure and can often be seen like a drifting glass wool against the background of a blue sky. Cirrostratus is a thin sheet of high clouds which impart a milky appearance to the sky. Cirrocumulus consists of white globules arranged in a regular pattern.

Altostratus is a dense gray sheet of cloud through which the sun appears dimly. Altocumulus consists of globular masses often arranged in parallel bands with clear gaps between them. Stratus is a sheet of low cloud which looks like fog lifted above the ground. Stratocumulus consists of large lumpy masses with gaps in between. Nimbostratus is a dense dark mass of low cloud from which rain falls.
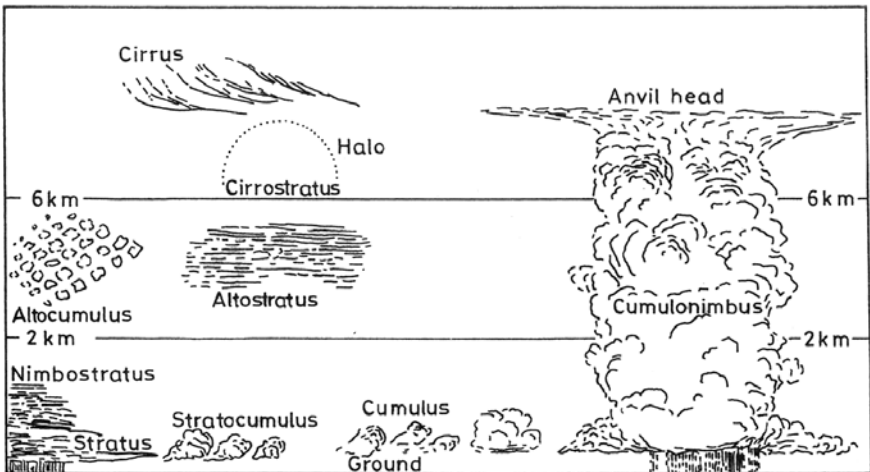
Fig. 1.1. Categories of clouds.

Table 1.3: Classification of clouds

Name of the cloud	Symbol	Height of occurrence
Cirrus	Ci	High (6-15 km)
Cirrostratus	Cs	”
Cirrocumulus	Cc	”
Altostratus	As	Medium (2-6 km)
Altocumulus	Ac	”
Stratocumulus	Sc	Low (< 2 km)
Stratus	St	”
Nimbostratus	Ns	”
Cumulus	Cu	Cloud with great vertical development
Cumulonimbus	Cb	”

Cumulus clouds have a cauliflower appearance with a flat base. On a day of fair weather in summer, one can see these clouds making their appearance around noon, growing in size in the afternoon and dissolving towards evening. Cumulonimbus is the cloud associated with thunderstorms. It is a towering cloud rising like a mountain with a low ragged base and the top extending to very high levels at times above the troposphere. It is accompanied with thunder lightning and heavy rain showers.

1.3 EARTH SYSTEM

Earth is a spheroid slightly flattened at the poles. Its equatorial radius is 6,378 km and the polar radius 6,357 km. The earth may be regarded as a sphere with a mean radius (r_e) of 6,371 km as it has practically the same volume as the earth. The equatorial circumference of the earth is: $2\pi . r_e = 2 \times 3.14 \times 6371 \sim 40,000$ km. The equator is the great circle whose plane is perpendicular to the axis of rotation of the earth. The latitude circles are small circles whose planes are parallel to the equatorial plane. Latitudes are measured in degrees north or south of the equator from 0° at the equator to 90° at the poles. The longitude circles, also known as meridian circles, are great circles passing through the north and south poles. Longitudes are measured in degrees east or west of the meridian of Greenwich from 0° to 180° in either direction. The location of a point on the earth is specified by its latitude (ϕ) and longitude (λ).

1.4 ORBITAL MOTION OF EARTH AND SEASONS

The revolution of earth around the sun, the rotation around its own axis and the inclination of the axis cause the radiation input to differ in time and space. This gives rise to different climatic zones and seasons that exist on the earth. The earth moves around the sun in an elliptical orbit at a speed of 113,000 km/hr taking a year to traverse the 966 million km path. Figure 1.2 shows the orbit of the earth (E) round the sun (S). When the earth is at P

in the course of its motion, it is closest to the sun and is said to be at perihelion. This occurs on or around 1st of January. When the earth is at A, it is farthest away from the sun and is said to be at aphelion. This occurs on or around 2nd of July.
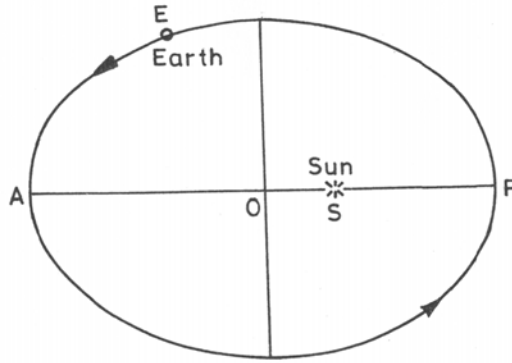
Fig. 1.2. Orbit of the earth around the sun.

The mean distance from the earth to the sun or semi major axis of the earth's orbit is known as the astronomical unit of distance. Its value is 149.6 × 10^6 km. As such, $OA = OP$ = 149.6 × 10^6 km. The present value of the eccentricity (*ec*) of the earth's orbit is 0.01675. Since S is the focus of the ellipse, we have

$$OS = OP \times ec = 149.6 \times 10^6 \times 0.01675 = 2.5 \times 10^6 \, km$$

$$SP = 149.6 \times 10^6 - 2.5 \times 10^6 = 147.1 \times 10^6 \, km$$

$$SA = 149.6 \times 10^6 + 2.5 \times 10^6 = 152.1 \times 10^6 \, km$$

The cause of summer and winter seasons is to be found in the inclination of earth's equator to the plane of its orbit around the sun. The plane of the earth's equator is inclined at an angle of 23.5° to the plane of its orbit which means that as the earth travels around the sun there is an unequal and varying amount of sunlight falling upon the earth (Fig. 1.3).

The earth also rotates around its own tilted axis once in 24 hours. This rotation is from west to east and the axis of the earth maintains its tilt of 23.5° as it rotates and revolves. Viewed from the earth the sun appears to move around the ecliptic and to cross the equator twice in the course of the year. The vernal equinox is the point when the sun crosses from south to north of the equator on or about 21st of March. The other crossing from north to south occurs at the autumnal equinox on or around 22nd of September. On these days the sun appears overhead at noon on the equator with equal duration (12 hours) of day and night all over the earth.
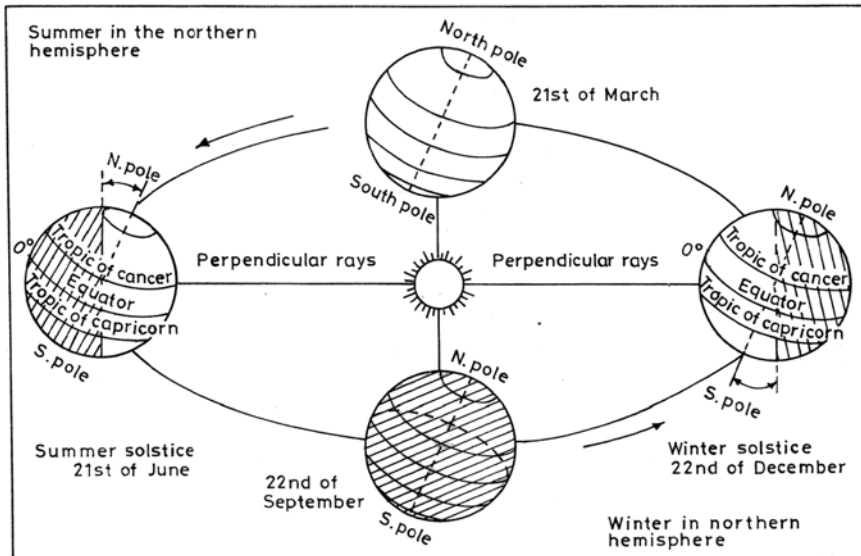
Fig. 1.3. Inclination of earth's equator to its plane around the sun
and summer and winter seasons.

After crossing the vernal equinox (21st of March), the sun appears to move northward reaching the maximum declination of 23½°. This occurs on or around 21st of June. On this day, the sun appears overhead at local noon on the latitude circle of 23.5° N and places in the northern hemisphere have the longest day and shortest night of the year. 21st of June is the summer solstice in the northern hemisphere and the winter solstice in the southern hemisphere. The northern hemisphere receives its maximum amount of solar radiation while the southern hemisphere its least. On 21st of June, the day is of 24 hours at 66½ °N parallel of latitude. The duration of light goes on increasing to the north of 66½ °N parallel of latitude and light lasts for six months at the north pole. During this period it is just opposite in the southern hemisphere. The southern hemisphere is away from the sun. Less than half of the southern hemisphere receives light. At 66½ °S parallel of latitude, night is of 24 hours on 21st of June. The duration of darkness goes on increasing from the south of 66½° parallel of latitude and the south pole remains in darkness for six months.

The apparent southward motion of the sun commences from summer solstice crossing the equator at the autumnal equinox and continuing the southward journey, the sun attains the maximum southern declination of – 23.5° on or around 22nd of December. 22nd of December is the winter solstice in the northern hemisphere and the summer solstice in the southern hemisphere. The southern hemisphere receives its maximum amount of solar radiation while the northern hemisphere its least.

For six months of the sun's apparent motion from the vernal equinox (21st of March) through summer solstice (21st of June) to the autumnal equinox (21st of September), the northern hemisphere of the earth faces the sun more directly than does the southern hemisphere experiencing longer days and receiving more solar radiation. This period of year during which more heat is received from the sun is called the summer season. The southern hemisphere faces the sun more directly than does the northern hemisphere during the other six months of the year and receives more solar radiation.

In the northern hemisphere, it is summer from 21st of March to 22nd of September and from 23rd of September to 20th of March it is winter. The situation in the southern hemisphere is exactly the opposite of that of the northern hemisphere. It is winter in the southern hemisphere from 21st of March to 22nd of September and summer from 22nd of September to 20th of March. These periodical variations in the solar energy received by the two hemispheres give rise to seasons and their associated weather features.

1.5 GLOBAL DISTRIBUTION OF LAND AND WATER

Earth has a nonuniform surface. The earth's surface basically consists of land, ocean, and ice, the last component covering an extremely small portion of the earth's surface (3%). These three components have quite different physical properties. Hence, the distribution of land and ocean over the earth is important for the processes which control weather and climate. For the earth as a whole, 29.2% of the surface area is covered by land and 70.8% by water. For the northern hemisphere the corresponding figures are 39.3% (land) and 60.7% (water); and for the southern hemisphere 19.1% (land) and 80.9% (water). Also, the land portion varies from one latitude belt to another latitude belt and from northern hemisphere to southern hemisphere. Table 1.4 shows the percent distribution of land proportion for different 5° latitudinal belts.

The main points of this distribution are:

(i) In the northern hemisphere, the proportion increases about 20% near the equator to about 70% in the belt of 65°-70°N latitude with a sharp decrease thereafter to zero near the north pole.

(ii) In southern hemisphere, the proportion of land is 20 to 25% up to 30°S thereafter it decreases to zero by 50°S with almost no land in 50°-65°S and a sharp increase to 100% by 80-90°S.

For meteorological purposes, the latitudinal belt from the equator to 30° latitude, from 30° to 60° latitude and from 60° to 90° latitude, are called tropical, the mid latitude and high latitude zones respectively of the two hemispheres.

Table 1.4: Distribution of land areas by latitude [N=north and S=south]

Latitude belt	% of land		Latitude belt	% of land	
	N	*S*		*N*	*S*
0-5°	21	22	45-50°	56	3
5-10°	24	25	50-55°	59	2
10-15°	23	24	55-60°	55	0
15-20°	29	20	60-65°	69	0
20-25°	35	23	65-70°	71	20
25-30°	40	24	70-75°	35	61
30-35°	42	16	75-80°	23	69
35-40°	43	7	80-85°	23	69
40-45°	49	4	85-90°	0	100
			Total land	39	19

1.6 GLOBAL WATER BUDGET

An estimate of global water balance is shown in Table 1.5. The data show that the total volume of global water is estimated as 1.36×10^9 km^3. About 94% of this exists as salt water of the oceans. Most of the remaining water is bound up in the polar ice caps and in glaciers (about 2%); a small part exists as sub-surface water (less than 0.01%). About 4% is found as groundwater. Only a tiny fraction of the global water (~0.01%) exists as fresh water in lakes and rivers for domestic, agricultural and industrial utilization. About 0.001% of the global water exists in the atmosphere in the vapor state as clouds. Atmospheric processes have a fundamental role in the replenishment of the fresh water supply of the world through evaporation from the oceans, transport of the moisture by air currents to distant places and condensation of the vapor to form clouds followed by precipitation as rain or snow.

Table 1.5: Global Water Balance (after L'vovich, 1970)

Location	Volume of Water × 10^6 km^3	Percent of Global Water	Percent of Fresh Water
Oceans	1278.4	94.0	
Polar Ice and Glaciers	27.2	2.0	33.3
Ground water	54.4	4.0	66.6
Soil Water	0.082	0.006	
Lakes and Rivers	0.136	0.01	0.16
Atmosphere	0.0136	0.001	
Total global water	1360	100	
FRESH WATER	81.736	6.0	100

Water Resources of India

It is interesting to know the water balance for a certain part of the globe, such as the Indian region. India, the 7th largest country in the world and the second largest in Asia, has a total geographical area of 3.29 million square kilometers. The country is located within the Asia monsoon region that is characterized by considerable amount of rainfall. The average annual rainfall over the country is about 117 cm (Dhar and Rakhecha, 1979). This is almost one and half times larger than the world average of 80 cm/yr. The total volume of water calculated from the product of the rainfall and the land area of India is approximately 4000 km^3. Of this about 1400 km^3 of water is lost through evaporation and 720 km^3 of water goes into the soil. After deduction for evaporation and infiltration the average surface runoff in the river systems of the country is estimated at 1880 km^3 (Rao, 1975). The groundwater recharge from rainfall in India made by the Central Ground Water Board, New Delhi (1991) is about 432 km^3. The surface water potential is about 1880 km^3 which is dispersed over the different river basins of the country. These river basins are the principal sources of water for more than 1000 million people in India. The water availability per person stands at a volume of 1880 m^3/yr which is about 1/12 of the world average of 21,800 m^3/yr per person. It is estimated that the population of India would be between 1.5 and 1.8 billion in 2050. The per capita availability of water will then be around 1200 m^3/yr, making India as a water stressed country. The water resources of India as a whole and of various Indian river basins are given in Tables 1.6 and 1.7 respectively. Figure 1.4 is a map of India showing river basins. India has 14 major river basins. The Indus River, the Ganga River and the Brahmaputra River are the important Himalayan rivers in the northern part of India. These rivers are both snowfed and rainfed and therefore have continuous flow throughout the year. The Ganga River and its tributaries spread out like a fan on the plain of India forming the largest river basin with an area about one quarter of the total area of India. The main rivers in the central and southern India are the Mahanadi, the Subarnarekha, the Tapi, the Narmada, the Godavari, the Krishna, the Mahi, the Sabarmati, the Cauvery and the Pennar. These rivers are entirely rainfed.

The main characteristics of water resources of these river basins is their uneven regional distribution. The combined runoff of the Indus, the Ganga and the Brahmaputra river basins comprises 65 percent of the total runoff of the country, while the combined runoff of the large rivers to the south of the Ganga, including the Narmada, the Tapi, the Mahanadi, the Godavari and the Krishna is only 17 percent of the total runoff (Table 1.7).
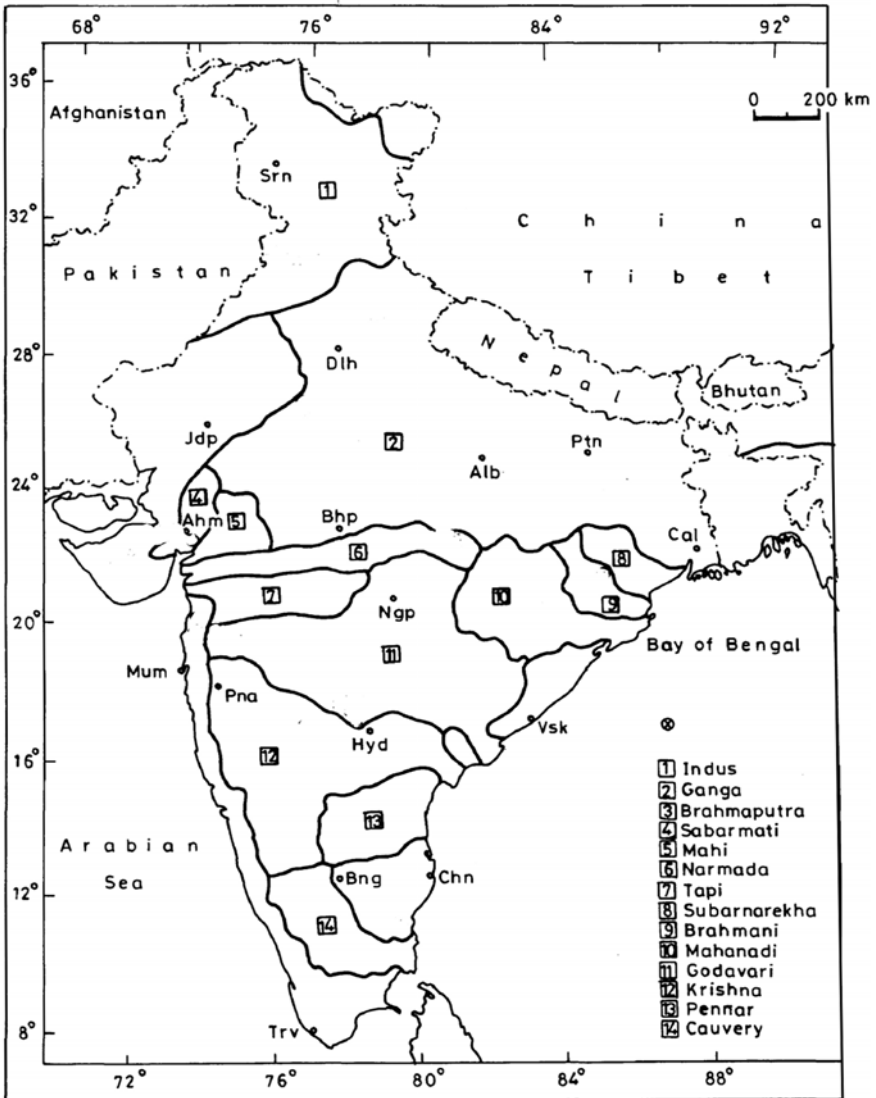
Fig. 1.4. Major river basins of India.

Table 1.6: Water resources of India

Item	*Volume of Water, km^3*
1. Annual Rainfall over India	4000
2. Evaporation loss	1400
3. Runoff from rainfall	1880
4. Seepage into subsoil (1 – 2 – 3)	720
5. Soil Moisture	288
6. Groundwater recharge (4 – 5)	432

Table 1.7: Average annual surface runoff of the main river basins in India

S. No.	River basin	Runoff in km³	% of Total
1.	Indus	80	4.2
2.	Ganga	550	29.3
3.	Brahmaputra	591	31.4
4.	Sabarmati	4	0.2
5.	Mahi	11	0.6
6.	Narmada	40	2.1
7.	Tapi	20	1.1
8.	Subarnarekha	12	0.6
9.	Brahmani	29	1.5
10.	Mahanadi	67	3.6
11.	Godavari	116	6.2
12.	Krishna	58	3.1
13.	Pennar	7	0.4
14.	Cauvery	19	1.0
15.	West flowing rivers of Kutch-Saurashtra including Luni	13	0.7
16.	West flowing rivers south of Tapi	218	11.6
17.	East flowing rivers between Pennar and Cauvery	23	1.2
18.	East flowing rivers between Mahanadi and Godavari	22	1.2
	Total surface runoff	1880	

Although the average annual flow of water in various rivers is 1,880 km³, because of the limitation due to topography, climate and soil conditions only about 720 km³ of water can be used. There are some 3,000 dams in India and the total storage available in these dams is about 132 km³.

1.7 HYDROLOGIC CYCLE

There is a continuous chain of movement and interchange of water between the oceans, the atmosphere and the land surface and below the land surface; this chain, as shown in Fig. 1.5, is known as the hydrologic cycle. The hydrologic cycle has four basic components namely, evaporation and transpiration, precipitation, runoff and ground water. The cycle can be visualized as beginning with the evaporation of water from water surfaces. As shown in Fig 1.5, evaporation occurs from oceans, lakes, streams and land surface and transpiration from vegetation, plant leaves and forests in the form of water vapor due to the heat energy provided by solar radiation. The water vapors move upward and after condensation they form clouds at higher altitudes. While much of the clouds falls back to the oceans as precipitation a part of the clouds is driven to the land area by winds. Through various

processes, clouds cause precipitation on the land surface in different forms, such as rain, snow, hail, sleet, dew, etc. When rain falls from clouds some of it is evaporated from the falling rain drops. Part of the precipitation reaching the ground is quickly evaporated and returned to the atmosphere. The rest seeps into the soil which enriches the moisture content of the soil. Some of the soil water is used up by plants and is returned to the atmosphere by evapotranspiration. The remaining water percolates deep to become ground water. The ground water may come to the surface through springs and other outlets. When rainfall is heavy and the soil is saturated the water flows over the land called runoff. Surface runoff flows into streams and lakes to reach eventually back to the oceans. In this manner, the hydrologic cycle is completed.

Of the four components of the hydrologic cycle, the precipitation component is important to hydrometeorologists, because it represents the quantity of water received over an area for use. The quantity of water going through individual components of the hydrologic cycle can be estimated using the continuity equation known as water budget equation or hydrologic equation. The hydrologic equation is simply a statement of the law of conservation of mass and is given as

$$I = O + \Delta S$$

where I = the inflow volume of water during a given time period, O = the outflow volume of water during the time period and S = change in the storage of the water volume during the given period. In hydrologic calculations, volumes are often expressed as average depths over a given area.

It is important to note that the total water resource of the earth is constant. The mean annual evaporation from the oceans is estimated to be 3,35,000 km^3 and from inland water bodies and the land surface 65,000 km^3 giving a total mean global annual value of 4,00,000 km^3. This must, on average, be equal to the total quantity of water coming back to the earth's surface in the form of precipitation (rainfall and snowfall), because the average amount of water vapor remains constant. Dividing the total volume of evaporation per year by the surface area of the earth ($4\pi r^2 = 4 \times 3.14 \times 6371 \times 6371 = 5.1 \times 10^8$ km^2), we obtain the average annual global rainfall as approximately 80 cm.

The actual distribution of precipitation on the earth is nonuniform. On average, the equatorial zone gets about 200 cm while the subtropical zones get much less than the average of 80 cm. On the whole precipitation exceeds evaporation over the land and evaporation exceeds precipitation over the ocean surface. Most of the excess water goes back to the sea. When rain falls from clouds some of it is evaporated from the falling rain drops. Part of the water reaching the ground is quickly evaporated and returned to the

atmosphere. The rest seeps into the soil. Some of the soil water is used up by plants and is returned to the atmosphere by evapotranspiration. The remaining water percolates to become ground water. The ground water moves slowly and emerges as streamflow or reaches the ocean floor. When the rainfall is heavy and the soil is saturated the surface water flows into streams and lakes to eventually reach the oceans by stream flow.
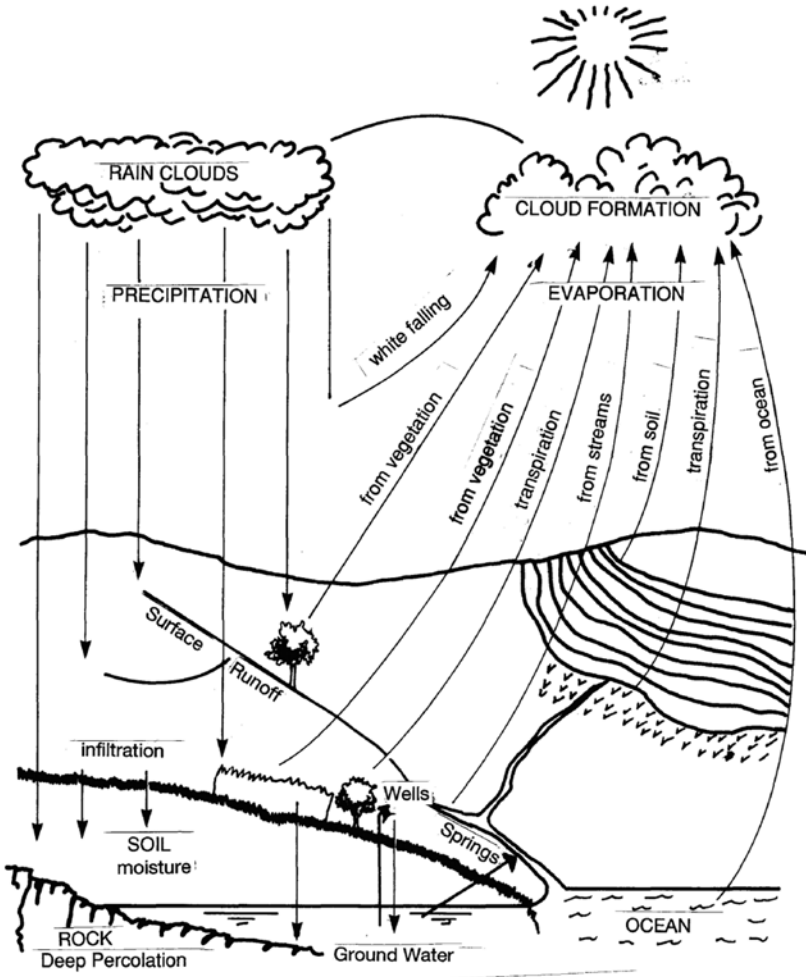
Fig. 1.5. Hydrologic cycle (after Ackermann et al., 1955).

REFERENCES

Ackermann, W.C., Colman, E.A. and Ogrosky, H.O., 1955. From ocean to sky to land to ocean. *In:* U.S. Department of Agriculture Yearbook 1955. U.S. Department of Agriculture, Washington, D.C.

Byers, H.R., 1959. General Meteorology. McGraw-Hill Book Company, New York.

Central Ground Water Board (CGWB), 1991. *Bhujal News*, New Delhi. Special Issue on Ground Water Statistics. Vol 6, No 1, January–March.

Dhar, O.N. and Rakhecha, P.R., 1979. A review of rainfall relationships based upon Indian data. *Water Resources Journal*, ESCAP, Bangkok, Thailand, December.

L'vovich, M.I., 1979. *World Water Resources and Their Future* (English Translation from the Russian), edited by R.L. Nace. American Geophysical Union, Washington, D.C.

Petterssen, S., 1969. Introduction to Meteorology. 2nd ed. McGraw-Hill Book Company, Inc., New York.

Rao, K.L., 1975. India's Water Wealth. Orient Longman, New Delhi.

Smithsonian Institutions, 1939. Smithsonian Meteorology Tables. 5th ed., Published by the Smithsonian Institutions, Washington, D.C.

2 The Atmosphere

The atmosphere is closely related to hydrology in a fundamental manner. It will, therefore, be appropriate to make a brief introduction to the subject of atmosphere. As pointed out in chapter 1, atmosphere is a thin shell of gases, which is held close to the earth by the gravitational attraction and is commonly called the air. These gases seem to have originated slowly over the geological ages from the interior of the solid earth by large scale volcanic activity. The atmosphere of the earth, therefore, consists of gases, water vapor as well as solid and liquid particles. All of the weather phenomena of the earth, such as winds, precipitation, clouds, haze, mist, fog, cyclones and anticyclones, tornados, thunderstorms, fronts and so on, are caused in this layer as a result of solar energy transfers and transformations that take place within the earth-atmosphere system. These weather phenomena associated with solar energy obey the laws of physics. It is necessary, therefore, to understand the relevant physical laws that govern the earth-atmosphere system. This chapter discusses the fundamental properties of the atmosphere.

2.1 EARTH-ATMOSPHERE SYSTEM

The earth rotates from west to east around its axis in 23 hours, 56 minutes and revolves around the sun in about 365¼ days. The earth's rotation produces day and night and its revolution is responsible for the seasons. The earth system includes the atmosphere, oceans, land, ice and all living organisms. Each of these is inexorably linked to others under the influence of energy received from the sun in the form of solar radiation. Also, changes in any single component of the earth's system affect the entire system. People are conscious of weather and the way it affects all living organisms. This weather is caused by the composite effect of several atmospheric or meteorological elements.

The values of the atmospheric elements depend on the conditions within the atmosphere and its interaction with other components, in particular the

land and the ocean surfaces. Apparently, the land-ocean-atmospheric system can be viewed as a vast laboratory where several unbelievable atmospheric phenomena go on all the time under the influence of solar energy. The complexity of the earth's system and many feedbacks among its components make understanding and predicting of atmospheric phenomena exceedingly difficult. However, physical laws, such as the laws of motion, the laws of radiation, the laws of thermodynamics and of evaporation and condensation governing laboratory experiments can well be applied to understand most of the atmospheric characteristics and phenomena. Application of these laws has greatly improved our understanding of the physics and chemistry of the atmosphere. Beginning with a discussion of the composition and the vertical structure of the atmosphere, this chapter discusses various physical laws applicable to the atmospheric domain.

2.2 COMPOSITION OF THE ATMOSPHERE

The composition of atmosphere is an important determinant of the heat balance of the earth-atmosphere system. Atmosphere is largely a mixture of dry air, water vapor and dust particles. Dry air is composed of two main categories of gases—the so called permanent gases that are invariant in their fractional volume and the varying gases. The permanent gases are Nitrogen (N_2), Oxygen (O_2), Argon (A), Krypton (Kr), Xenon (Xe), Neon (Ne), and Helium (He). The varying gases are Methane (CH_4), Ozone (O_3), Nitrous Oxide (N_2O), Carbon monoxide (CO), Carbon dioxide (CO_2), Hydrogen (H_2), Sulphur dioxide (SO_2), Hydrogen sulphide (H_2S), Nitrogen dioxide (NO_2) and Ammonia (NH_3). Of these gases, CO_2 has the greatest concentration, about 0.035 percent, and its concentration seems to be increasing since industrialisation began in 1750. Table 2.1 gives an approximate composition by volume of the constituents of dry air. This measure refers to the volume that each gas would occupy if the component gases were separated and brought to the same temperature and pressure. Of the gases shown in Table 2.1, ninety-nine percent of the atmosphere is made up of N_2 and O_2, with N_2 four times as abundant as oxygen. The average molecular weight of these gases is 29.0. Although these gases play a vital role in complex cycles that support life on earth, they play almost no direct role in radiative processes associated with the heat budget of the earth-atmosphere system. The job of heating and cooling is done by the presence of remaining 1% percent of various trace gases in the earth's atmosphere, notably CO_2, N_2O, CH_4, O_3 and water vapor. These gases act as a glass does in a greenhouse. They permit shortwave radiation to enter earth's atmosphere but impede the longwave terrestrial radiations which causes a positive radiative balance. These gases which absorb terrestrial radiations are called greenhouse gases (GHGs).

Table 2.1: Volume by percentage of gases in the dry air

Permanent Gases			Variable Gases		
Gases	% by volume	Chemical symbols	Gases	% by volume	Chemical symbols
Nitrogen	78.08	N_2	Methane	0.0002	CH_4
Oxygen	20.95	O_2	Ozone	0.000007	O_3
Argon	0.93	Ar	Nitrous oxide	0.00005	N_2O
Neon	0.0018	Ne	Carbon monoxide	0.00002	CO
Helium	0.0005	He	Carbon dioxide	0.0335	CO_2
Xenon	0.000009	Xe	Hydrogen	0.00005	H_2
Krypton	0.00011	Kr	Sulphur dioxide	0.0001	SO_2
			Nitrogen dioxide	0.000002	NO_2
			Ammonia	trace	NH_3

Ozone mainly exists in the upper atmosphere between 10 kms and 50 kms above the earth. It forms primarily due to the photochemical reaction between the ultraviolet (UV) radiation of the sun and the oxygen of the atmosphere. The UV radiation from the sun is absorbed by gaseous oxygen (O_2). Some of these molecules are broken down into atomic oxygen (O) which may recombine with a molecule of oxygen (O_2) to form ozone (O_3). This gas is unstable and easily decomposes to molecular oxygen (O_2) and atomic oxygen (O). Thus, an equilibrium between O, O_2, and O_3 is established and maintained by further absorption of the UV radiation.

The ozone layer in the atmosphere absorbs most of the harmful UV radiation from the sun, thus providing a protective layer over the earth. The substances that damage the ozone layer are chlorofluorocarbons (CFCs), chlorine, and bromine containing gases, and some others which are used for refrigeration, air-conditioning, foam blowing and fire extinguishing purposes. It has been demonstrated that emissions of the above gases have led to the depletion of ozone in both the southern and northern hemispheres that will last for decades and cause adverse impacts on human health and ecological systems (IPCC, 2001). Upsetting of the O_3 balance in the atmosphere can cause significant changes not only in the weather and climate of the earth but also for the very existence of life on the earth's surface.

CO_2 is a potent green house gas along with the other gases. The sources of atmospheric CO_2 are agricultural decay, volcanic eruption, burning of coal, oil and natural gas. CO_2 is a vital ingredient in photosynthesis, the process by which green plants synthesize food for themselves. It is, therefore, consumed by plants and produced by animal and burning processes. It has been found that the atmospheric concentration of CO_2 is currently rising from fossil fuel burning and land use change (IPCC, 2001). CO_2 significantly absorbs long wave terrestrial radiation and any increase in the total amount of CO_2 in the atmosphere will promote global warming and will have severe

environmental repercussions. The current rate of increase of CO_2 is about 0.5% per annum. At this rate the concentration of atmospheric CO_2 will double by the end of the 21st century. A doubling of atmospheric CO_2 will force a 1.4°C to 5.8°C increase in global mean temperature (Houghton et al., 2001). This rise in the mean global temperature will cause changes in temperature regimes and a shift in precipitation patterns as well on the earth.

Agricultural fertilizers, volcanic eruptions, nuclear blasts, burning of aviation fuels, and CFCs are important sources of atmospheric nitrous oxide (N_2O). N_2O in the atmosphere absorbs terrestrial radiation and thus contributes to the warming of the atmosphere (IPCC, 2001). On a per molecule basis, N_2O is about 200 times more potent than CO_2 in this respect and it has been concluded that an increase of 0.2 to 0.3 percent in atmospheric concentrations would contribute about 5% to the supposed green house warming. N_2O is also a destroyer of ozone. It has been estimated that doubling the concentration of N_2O in the atmosphere would result in a 10% decrease in the ozone layer and this would increase the UV radiation reaching the earth by 20%.

Water vapor is an important constituent of the atmosphere whose proportion is highly variable in space and time. The concentration can be as high as about 4% by volume in hot humid air to more than a hundred times less in very cold air. The concentration decreases with altitude. Water vapor enters the atmosphere by evaporation from water surfaces and also by transpiration from plants. In condensation it forms clouds which consist of water droplets or ice crystals depending on the altitude. Thus, water has the unique feature that it exists in the atmosphere in all three forms:gaseous, liquid and solid. The water vapor is a major absorber of terrestrial radiation in certain wave-length bands. Important among these are the intense absorption bands around 6.3 μm.

Besides the gases mentioned above, the atmosphere also contains in suspension fine particulate matter called aerosols. These are solid particles or liquid droplets whose sizes cover a wide range. They have an important role in condensation processes in the atmosphere leading to cloud formation. Over the past century regional meteorological measurements have shown that global climate is changing (Easterling et al., 1997). Some of this change has been the result of rising atmospheric concentration of CO_2 and other gases. Global climate models predict significant changes in the mean global temperature which will cause alteration in the amount and distribution of precipitation.

2.3 MASS OF THE ATMOSPHERE AND THE HYDROSPHERE

It is seen that the average pressure of air at sea level is about 76 cm of mercury column of a unit cross section. Since the density of mercury is about 13.6 gm/cm^3, the mass of the column would be $76 \times 13.6 = 1034$ gm/cm^2 or 10^{10} kg/km^2. Using this value, the mass (M) of whole atmosphere on the surface of the earth with a mean radius (r) of 6371 km works out to be

$$M = 4\pi r^2 \times 10^{10} \text{ kg}$$
$$= 4 \times 3.14 \times 6371 \times 6371 \times 10^{10} \text{ kg} \cong 5 \times 10^{18} \text{ kg}$$

Thus, the mass of whole atmosphere is 5×10^{18} kg.

As pointed out in Chapter 1, the total volume of water in the hydrosphere is 1.36×10^9 km^3. Dividing by the surface area of the earth gives the depth of water distributed uniformly over the earth.

$$\text{Depth of water} = \frac{1.36 \times 10^9}{4 \times 3.14 \times 6371 \times 6371} \cong 2.7 \text{ km}$$

and the mass of the whole water as:

Mass of water = $1.36 \times 10^9 \times 10^{12}$ kg = 1.36×10^{21} kg (1 km^3 of water weight 10^{12} kg).

$$\frac{\text{Mass of water}}{\text{Mass of atmosphere}} = \frac{1.36 \times 10^{21}}{5 \times 10^{18}} \cong 270$$

The mass of the hydrosphere is about 270 times the mass of the atmosphere.

2.4 AVERAGE VERTICAL STRUCTURE OF ATMOSPHERE

Atmosphere is held close to the earth by gravitational attraction and in a large measure rotates with it. It has no real upper boundary but presently the limit of the atmosphere is fixed quite arbitrary at about 1000 km above the earth and at this distance it is extremely tenuous. Roughly one-half of the total mass of the atmosphere is found below a height of 5 km and over 99% is under 100 km. While pressure decreases steadily with height, temperature shows much more complicated distribution. Figure 2.1 gives the percentage of the total mass of the atmosphere with elevation.

Vertical temperature observations by balloon ascents, aircraft and rockets and more recently by remote sensing techniques from orbiting satellites have shown that the atmosphere contains three relatively warm regions with cold layers in between. Figure 2.2 gives the average vertical temperature distribution that is used to divide the atmosphere into four layers or spheres: the troposphere, the stratosphere, the mesosphere and the thermosphere. The warm regions are located near the ground, at a height of about 50 km and far above 100 km.

(a) *Troposphere*: It is the lowest layer of the atmosphere and contains about 80% of the atmosphere. The top of the troposphere is called the tropopause. The height of the tropopause varies with latitude and season from about 8 to 10 km in polar latitudes, 10 to 12 km in the middle latitudes and about 16 km in the tropics. The main characteristics of this layer are: (1) more or less uniform decrease in temperature with height
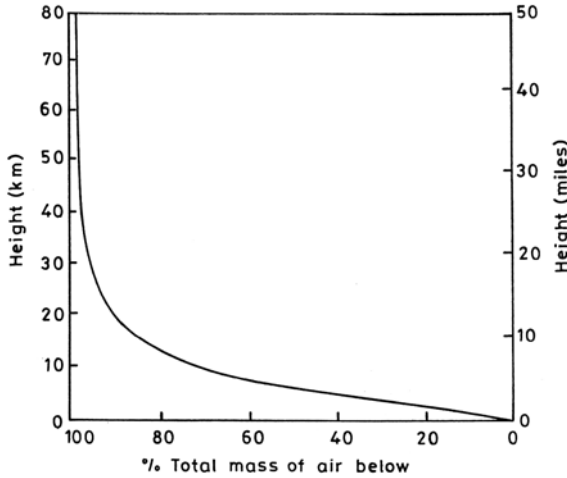
Fig. 2.1. The percentage of total mass of atmosphere lying below 80 km elevation.
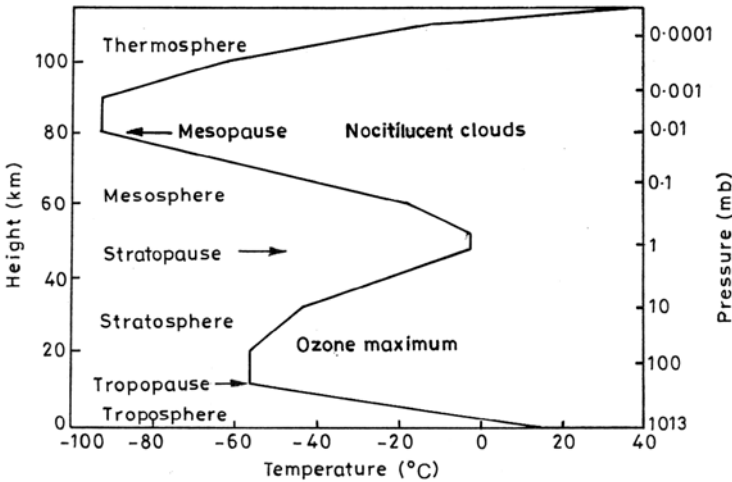
Fig. 2.2. Vertical distribution of temperature and pressure.

at the mean rate (also called environmental lapse rate γ) of 6.5°C per km, (2) increasing of wind speed with height, (3) principal medium for the movement of mass (water as liquid, solid or gas, dust, and pollutants), (4) energy (heat energy from the sun) and momentum (winds) over the earth's surface, and (5) practically all weather phenomena, such as clouds and precipitation, take place.

(b) *Stratosphere*: The layers above the troposphere up to a height of about 50 km is called the stratosphere. The lower stratosphere has a remarkably stable and approximately isothermal temperature distribution. Cirrus

clouds occasionally form in the lower stratosphere but the visible weather phenomena usually are absent above the tropopause. The isothermal character of the lower stratosphere terminates at a height of about 20 km and beyond this the temperature increases sharply up to stratopause at a height of about 50 km. This region is known as upper stratosphere. The convective currents and moisture usually do not cross tropopause. Hence, the stratosphere is hydrostatically stable and poorly mixed. The stratosphere contains about 97% of the ozone in the atmosphere.

(c) *Mesosphere*: Above the stratosphere is the mesosphere where temperature again decreases with increasing height, reaching a minimum at about 80 km (mesopause). This is a region of strong winds, steady from the east in the summer and variable from the west in the winter. Mesopause is the coldest layer of the atmosphere with a temperature of –80°C to –90°C.

(d) *Thermosphere*: The thermosphere is a very high temperature region and extends from the mesopause (80 km) to the outer edge of the atmosphere several hundred kilometers aloft. High temperature is caused by the absorption of extremely short wave UV radiation from the sun.

The layer from the surface to the tropopause is known as the lower atmosphere and the layer extending from the tropopause to about 100 km is referred to as middle atmosphere where photochemical processes are important.

2.5 HYDROSTATIC EQUATION

The hydrostatic equation relates changes in pressure to changes in height in the atmosphere. It is known that the force of gravity amounting to 981 dynes per gram is acting vertically downward on air. In spite of this we do not observe that atmosphere is accelerating downward under the influence of gravity. This shows that another force or forces must be acting upward on the air to balance gravity.

Figure 2.3 shows an atmospheric column of unit cross sectional area on the surface of the earth. The atmospheric pressure is the weight of air in a vertical column of unit cross section above the surface of the earth. It is known that the amount of air decreases upwards so the pressure also decreases. Thus, if one considers a small segment of thickness dz in this column, there must be a decrease of pressure, say dP, from the bottom to the top of the segment (Fig. 2.3). That is if P be the pressure at z then $P - dP$ the pressure at $z + dz$. Because of this pressure difference a pressure gradient force is operating upward on the segment. The value of this pressure gradient force per unit volume is dP/dz. If ρ be the density of the air then,

$$\text{Force per unit mass} = \frac{1}{\rho}\frac{dP}{dz} \qquad (2.1)$$
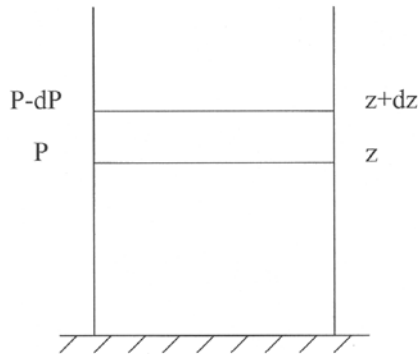
Fig. 2.3. Vertical column of unit cross section.

Thus, $\dfrac{1}{\rho}\dfrac{dP}{dz}$ is the value of the upward force owing to the normal decrease of pressure with elevation. Hence, for the equilibrium of dz the upward pressure gradient force balances the downward gravity force, and hence

$$\frac{1}{\rho}\frac{dP}{dz} = -g \qquad (2.2)$$

or
$$\frac{dP}{dz} = -\rho g \qquad (2.3)$$

Evidently, the rate of change of pressure with height (dP/dz) is dependant on the acceleration due to gravity (g) multiplied by the air density (ρ).

The negative sign indicates that as height increases the atmospheric pressure decreases. The reason being that as we go higher up the air column above us becomes smaller. At the same time, the density of air also goes on decreasing. Equation (2.3) can be used to obtain the value of pressure at any point in the atmosphere, provided it can be assumed that the density ρ is either constant or it is a function of pressure. Equation (2.3), known as the hydrostatic equation, is a fundamental equation in meteorology. It may be applied to compute heights since the air density can be computed from observations of pressure and temperature.

The relation between the pressure (P), the density (ρ) and the absolute temperature (T) of the dry air is given by the gas law as

$$P = \rho RT \qquad (2.4)$$

where R is the gas constant for dry air whose value in CGS unit is 287×10^4 cm^2 sec^{-2} k^{-1} and in MKS units is 287 m^2 sec^{-2} k^{-1}.

Example 2.1: Determine the change in pressure from the bottom to the top of a 30 meter high building. The density of air $= 1.205 \times 10^{-3}$ gm/cm^3.

Solution: From equation (2.3), $dP = -\rho g dz$, $g = 981$ cm sec^{-2}, $\rho = 1.205 \times 10^{-3}$ gm cm^{-3}, $dz = 3,000$ cm,

$$
\begin{aligned}
dP &= -1.205 \times 10^{-3} \text{ gm cm}^{-3} \times 981 \text{ cm sec}^{-2} \times 3000 \text{ cm} \\
&= -3.55 \times 10^3 \text{ gm cm sec}^{-2} \text{ cm}^{-2} \text{ (gm cm sec}^{-2} = \text{dyne)} \\
&= -3.55 \times 10^3 \text{ dynes cm}^{-2} = -3.55 \text{ mb } (10^3 \text{ dynes cm}^{-2} = 1 \text{ mb})
\end{aligned}
$$

Example 2.2: Calculate the density of air (a) under standard temperature and pressure (STP) and (b) under standard pressure and at a temperature of 20°C.

Solution: The density (ρ) of air is given as $\rho = \dfrac{P}{RT}$.

(a) The standard temperature and pressure (STP) values for the air are:

$$P = 1013 \text{ mb} = 1013 \times 10^3 \text{ gm cm}^{-1} \text{ sec}^{-2}$$
$$T = 273 \text{ °K}, R = 287 \times 10^4 \text{ cm}^2 \text{ sec}^{-2} \text{ K}^{-1}$$
$$\rho = \frac{1013 \times 10^3}{287 \times 10^4 \times 273} = 0.00129 \text{ gm cm}^{-3} = 1.29 \text{ kg m}^{-3}$$

(b) $P = 1013$ gm cm^{-1}sec^{-2}, $T = 273 + 20 = 293$°K

$R = 287 \times 10^4$ cm^2 sec^{-2} K^{-1}

$$\rho = \frac{1013 \times 10^3}{287 \times 10^4 \times 293} = 0.001205 \text{ gm cm}^{-3} = 1.205 \text{ kgm}^{-3}$$

Example 2.3: Calculate the density of air at the tropopause level where pressure is 100 mb and a temperature of 200 °K.

Solution: We know that

$$\rho = \frac{P}{RT}$$
$$P = 100 \times 10^3 \text{ gm cm}^{-1} \text{ sec}^{-2}$$
$$T = 200 \text{ °K}$$
$$R = 287 \times 10^4 \text{ cm}^2 \text{ sec}^{-2} \text{ K}^{-1}$$
$$\rho = \frac{100 \times 10^3 \text{ gm cm}^{-1} \text{ sec}^{-2}}{287 \times 10^4 \text{ cm}^2 \text{ sec}^{-2} \text{ K}^{-1} \times 200 \text{K}} = 0.000174 \text{ gm cm}^{-3}$$
$$= 0.174 \text{ kgm}^{-3}$$

Example 2.4: Find the mass of the air at 27°C in a room 4 m × 3 m × 3 m size.

Solution: We have

$$\rho = \frac{P}{RT}$$

$$P = 1013 \times 10^3 \text{ gm cm}^{-1} \text{ sec}^{-2}$$
$$T = 300 \text{ °K}$$
$$R = 287 \times 10^4 \text{ cm}^2 \text{ sec}^{-2} \text{ k}^{-1}$$

Density of air $(\rho) = \dfrac{1013 \times 10^3}{287 \times 10^4 \times 300}$

$$= 0.001176 \text{ gm cm}^{-3} = 1.176 \text{ kg m}^{-3}$$

Mass of air $= 4 \times 3 \times 3 \times 1.176 \text{ kg} = 42.3 \text{ kg}$

2.6 HYDROSTATICS OF SPECIAL ATMOSPHERE

2.6.1 Isothermal Atmosphere

If the temperature of the atmosphere does not change with height, such an atmosphere is called an isothermal atmosphere. Using the following equations of state and hydrostatic relation one obtains

$$P = \rho RT \tag{2.5}$$

$$\frac{dP}{dz} = -\rho g \tag{2.6}$$

Eliminating the density (ρ) from equations (2.5) and (2.6) one obtains

$$\frac{dp}{P} = -\frac{g}{RT} dz \tag{2.7}$$

In an isothermal atmosphere $g/(RT)$ is a constant and equation (2.7) can be integrated from the mean sea level $(z = 0, P = P_0)$ to some level $z(z = z, P = P_z)$ where pressure is P_z to yield the following equation for the vertical variation of pressure with height:

$$\int_{P_0}^{P_z} \frac{dP}{P} = -\frac{g}{RT} \int_0^z dz \tag{2.8a}$$

$$\log_e \frac{P_z}{P_0} = -\frac{gz}{RT}$$

$$P_z = P_0 \ \exp[-\frac{g}{RT} z] \qquad (2.8b)$$

Thus, in an isothermal atmosphere, pressure decreases exponentially with height. This equation is of great importance because it expresses an explicit relationship between pressure, temperature and height.

For air $R = 287$ J kg^{-1}K^{-1}, $g = 9.8$ m/s^2, $T = 273$ °K, $P_0 = 1000$ mb, the variation in pressure with height is obtained as follows:

Altitude above sea level (km)	0	5	10	20	30	50	80	100
Pressure (mb)	1000	535	287	82	24	1.9	0.05	0.004

Example 2.5: For an isothermal atmosphere, the sea level pressure and temperature are 1000 mb and 273 °K respectively. Determine the pressure on the top of the hill 10 km high.

Solution: From equation (2.8b), $P_z = P_0 e^{\frac{-g}{RT} z}$

$P_0 = 1000$ mb, $g = 9.81$ m/s^2, $T = 273$ °K

$R = 287$ m^2 sec^{-2}K^{-1}, $z = 10{,}000$ m

For an isothermal atmosphere, $\dfrac{g}{RT} = $ constant

$$\frac{g}{RT} = \frac{9.81 \ \text{m/s}^2}{287 \ \text{m/s}^2/\text{K}^{-1} \times 273 \ °\text{K}} = 1.25 \times 10^{-4}$$

$$P_z = 1000 \times e^{-1.25 \times 10^{-4}} = 287 \ \text{mb}$$

Example 2.6: Determine the height of the atmosphere containing half of the total mass of air.

Solution:

$$P_z = P_0 e^{\frac{-g}{RT} z}, \ z = \frac{RT}{g}\left[\ln P_0 - \ln P_z\right]$$

At the point where half of the mass of the atmosphere is above and half below $P_z = P_0/2$. On substituting the values of R, T and g and assuming a temperature of 270°K, we have:

$$z = \frac{287 \times 270}{9.81}\ln 2 = \frac{287 \times 270 \times 0.6931}{9.81} \quad \left[\ln 2 = \log_e 2 = 0.6931\right]$$

$$z = 5475 \ \text{m}$$

2.6.2 Atmosphere with Constant Lapse Rate

In the troposphere, temperature varies in both time and space, and decreases with height at a given time and place. The rate of decrease is not constant but is about 6.5°C per kilometer on the average. The rate of decrease of temperature with height is known as environmental lapse rate (γ) and bears no relation to air parcels rising or falling. In an atmosphere with surface pressure P_0, surface temperature T_0 and constant lapse rate γ, the variation of pressure with height can be shown as:

We have

$$\frac{dP}{P} = -\frac{g}{RT}dz \tag{2.9}$$

The temperature T of the air at height z will be

$$T = T_0 - \gamma z$$

Now putting the value of T in equation (2.9) we obtain

$$\int_{P_0}^{P_z}\frac{dP}{P} = \int_0^z -\frac{g}{R(T_0 - \gamma z)}dz \tag{2.10}$$

$$P_z = P_0\left(\frac{T_0 - \gamma z}{T_0}\right)^{g/(R\gamma)}$$

or

$$P_z = P_0\left(\frac{T}{T_0}\right)^{g/(R\gamma)} \tag{2.11}$$

An estimate of atmospheric pressure (P_z) at any level z can be estimated using information on the sea level pressure (P_0) and temperature (T) and by assuming the temperature decreasing at the rate of 6.5 °C/km.

For P_0 = 1000 mb, T_0 = 300°K, and γ = 6.5 °C/km the changes of pressure (P) with altitude (z) are as follows:

Altitude above sea level (km) :	0	1	3	6	9	12
Pressure (mb) :		1000	891	703	483	323	210

Example 2.7: Given the atmospheric pressure at the mean sea level as 1000 mb, temperature 27°C, estimate the pressure on the top of the hill corresponding to an altitude of 3 km.

Solution: We have $P_z = P_0\left(\frac{T_0 - \gamma z}{T_0}\right)^{\frac{g}{R\gamma}}$,

$P_0 = 1000$ mb, $T_0 = 273 + 27 = 300°K$, $z = 3000$ m, $g = 9.81$ msec^{-2},

$R = 2.87$m^{2}sec^{2}K^{-1}, $\gamma = 6.5 °C/1000$m

$$\frac{g}{R\gamma} = \frac{9.81 \times 1000}{287 \times 6.5} = 5.2533$$

$$\frac{T_0 - \gamma z}{T_0} = \frac{300 - 6.5 \times 3}{300} = 0.935$$

$$P_z = 1000(0.935)^{5.2533} = 703 \text{ mb}$$

2.7 REDUCTION OF PRESSURE TO SEA LEVEL

The height above the mean sea level varies from station to station because the surface of earth is irregular. To study the horizontal variation of pressure over an area it is necessary that the surface pressure data observed at different stations are reduced to a common base level. This is taken as the mean sea level. For this purpose the weight of the air column of unit cross section between the station level and the sea level has to be added to the station level pressure. This is known as reduction of pressure to sea level for which the following formula is used:

$$\log_e \frac{P_z}{P_o} = -\frac{g}{RT} z \qquad (2.12)$$

where P_0 and P_z are the pressure levels at the sea level and some height z respectively g is the acceleration due to gravity and T is the temperature of the air at the station level.

Example 2.8: A station is located at a height of 1610 m above the sea level. The pressure recorded at this station is 833 mb. What will be the pressure reduced to the mean sea level if the station level temperature is 20 °C?

Solution: We have, $\log_e \dfrac{P_z}{P_0} = -\dfrac{gz}{RT}$ or $\log_e P_0 - \log_e P_z = \dfrac{gz}{RT}$

P_0 = pressure at sea level, P_z = station level pressure = 833 mb,

$g = 9.8$ m sec^{-2}

$R = 287$ m^2 sec^{-2} K^{-1}, $T = 273 + 20 = 293°K$, $z = 1610$ m

Substituting the values in the equation, we get:

$$\log_e P_0 - \log_e 833 = \frac{9.8 \times 1610}{287 \times 293} \text{ or } \log_e P_0 = \log_e 833 + 0.18763$$

$$\log_e P_0 = 6.72503 + 0.18763 = 6.91266 \text{ or } P_0 = 1004.9 \text{ mb}$$

which is the pressure reduced to sea level.

2.8 ATMOSPHERIC STABILITY AND INSTABILITY

When a parcel of air is disturbed from its position upward or downward and if the parcel returns to its original position, the atmosphere is said to be in a state of stable condition. On the other hand, if the environmental conditions are such that the parcel tends to move away from its initial position, the atmosphere is said to be in a state of unstable condition.

We consider that the atmospheric air is dry. Suppose that the air parcel at a level AA, where the pressure is P and the temperature is T, is displaced by a small distance dz upward to the level BB where the pressure is $P - dP$ (Fig. 2.4). Since the air is compressible, the parcel will expand and cool at the dry adiabatic lapse rate γ_d (10°C/km). The temperature (T_B) of the displaced air parcel at the level BB will be $T_B = T - \gamma_d\, dz$. Assuming that the environmental lapse rate is γ, then the environmental temperature T'_B at the level BB will be $T'_B = T - \gamma dz$.
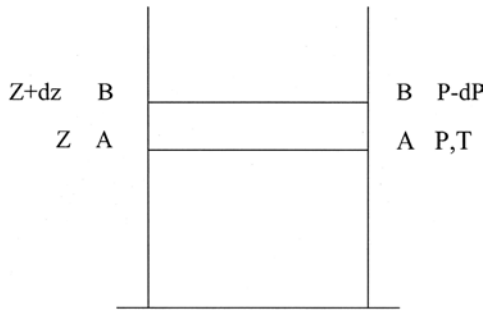
Fig. 2.4. Vertical atmospheric column.

If $T_B > T'_B$, i.e., $\gamma > \gamma_d$, the air parcel is warmer and less dense than the environmental air. Hence, the air parcel will rise further. This shows that when the atmospheric lapse rate (γ) is greater than the dry adiabatic lapse rate (γ_d), the atmosphere is said to be in a state of unstable equilibrium.

If $T_B < T'_B$, i.e., $\gamma < \gamma_d$, the disturbed air parcel will be cooler and denser than the environmental air. Hence the air parcel will sink back to the original level. This shows that when the atmospheric lapse rate (γ) is less than the dry adiabatic lapse rate (γ_d), the atmosphere is said to be in a state of stable conditions.

If $T_B = T'_B$, i.e., $\gamma = \gamma_d$, the disturbed air parcel will have the same temperature as the environmental air temperature and would have no tendency to move upwards or downwards. In this case the atmosphere is in a state of neutral condition. Obviously, the environmental lapse rate determines whether the atmosphere is stable, unstable or neutral for vertical air movement. The principal criteria for finding the stability or instability for a dry atmosphere are as follows:

$$\gamma < \gamma_d \quad \text{stable atmosphere}$$
$$\gamma > \gamma_d \quad \text{unstable atmosphere}$$
$$\gamma = \gamma_d \quad \text{neutral}$$

In the saturated atmosphere, a parcel of air disturbed upward will cool at the saturated adiabatic lapse rate γ_s. The stability and instability criteria for a saturated atmosphere are similar to those for a dry atmosphere, i.e.,

$$\gamma < \gamma_s \quad \text{stable atmosphere}$$
$$\gamma > \gamma_s \quad \text{unstable atmosphere}$$
$$\gamma = \gamma_s \quad \text{neutral}$$

The actual atmosphere is normally neither dry nor fully saturated. When an unsaturated air parcel is displaced upwards from its starting position it initially cools at the dry adiabatic lapse rate until saturation is reached and thereafter further upward movement is accompanied by cooling at the saturation adiabatic lapse rate.

REFERENCES

Easterling, D.R., Horton, B., Jones, P.D., Peterson, T.C., Karl, T.R., Parker, D.E., Salinger, M.J., Razuvayeu, V., Plummer, N., Jamason, P. and Folland, C.K., 1997. Maximum and Minimum temperature trends for the globe. *Science*, Vol. 227, pp. 364-367.

Houghton, J.T., Ding, Y. and Griggs, D.J., 2001. Climate Change: The scientific basis. IPCC Third Assessment report., Cambridge University Press, London, New York

Intergovernmental Panel on Climate Change (IPCC), 2001. Climate change: The scientific basis. Cambridge University Press, London, New York.

3 <u>Atmospheric Processes</u>

Atmosphere is the most dynamic part of the terrestrial environment. It is driven by the energy received from the sun. Almost all weather phenomena mentioned in Chapter 2 result from the differences in the amount of solar energy received and utilization thereof. It is, therefore, necessary to understand as to how the energy from the sun is converted into heat and shared by the earth and the atmosphere. Thermodynamics provides quantitative relationships between heat and other forms of energy and can thus be utilized to analyze the ways in which changes in the heat content of a substance affects the dynamics of the substance. A typical thermodynamic process involves the addition of heat to a fluid causing pressure and volume to change. The laws of thermodynamics relate these changes in heat content, pressure and volume. Thermodynamics has, therefore, wide applications in hydrometeorology. This chapter briefly discusses physical laws which are important for understanding variations in heat, temperature, pressure and density of air which are needed for understanding the various atmospheric processes.

3.1 HEAT AND TEMPERATURE

Heat is defined as the energy which produces in us the sensation of hotness while temperature is a measure of the degree of hotness or coolness of a body. The change in the heat content of a body is generally the cause of the change in its temperature. Heat always flows from a body at a higher temperature to a body at a lower temperature when the two are placed in contact, no matter what the amount of heat present in either body is. It is similar to the nature of liquids which always flow from a higher level (potential) to a lower level (potential). The direction of flow of the liquid does not depend on the quantity of liquid present at either level. Even if there is a lesser amount of liquid present at the higher level than at the lower level, the flow will be from the higher level to the lower level. In this respect, temperature may be called the level of heat and heat energy flows

in response to a temperature difference. There are instruments designed to measure the temperature of a given body in degrees on the Centigrade scale or the Fahrenheit scale. The Centigrade scale was first introduced by Celsius in 1742. In this scale the freezing point of water is marked 0°C and the boiling point 100°C and the interval is divided into 100 equal parts. The unit of heat is the gram calorie. It is the amount of heat required to raise the temperature of one gram of water by 1°C.

3.2 COMPRESSION AND EXPANSION OF A GAS

Gases like solids and liquids expand on heating. But there is an important difference in the behavior of gases as compared to solids and liquids, when the effect of pressure on their volumes is considered. While solids and liquids are practically incompressible, the effect of pressure on the volume of gases is very marked. For example, when compressed at a constant temperature, the volume of a gas is halved on doubling the pressure and becomes one third when the pressure is made three fold. Hence, in the case of gases three variables namely, volume (V), pressure (P) and temperature (T) have to be considered:

  (i) The effect of a change of pressure (P) on the volume (V) of a gas when temperature (T) remains constant, i.e., $P_1V_1 = P_2V_2$ (Boyles' Law)
 (ii) The effect of a change of temperature (T) on the volume of a gas (V) when pressure (P) remains constant, i.e., $V_1T_2 = V_2T_1$ (Charles' Law)
(iii) The effect of a change of temperature (T) on the pressure of a gas (P) when its volume (V) remains constant, i.e., $P_1T_2 = P_2T_1$

When a gas is compressed, the external work done on the gas is transformed into heat resulting in an increase of temperature. Similarly, when a compressed gas expands against an external pressure, the gas does work and heat energy is transformed into mechanical work. Heat and mechanical work are different forms of energy. The equivalent amount of mechanical energy, known as the mechanical equivalent of heat is 4.186 Joules (1 Joule = 10^7 ergs); 1 calorie = 4.2 Joules = 4.2×10^7 ergs).

3.3 FORMS OF HEAT

The amount of heat stored in a body is expressed in calorie. If an equal amount of heat is applied to equal masses of different substances, it is found that their temperature changes are different. The term "specific heat" is defined in the following manner. If dQ is the heat given to one gram of any substance, there will be a certain temperature rise, say dT. The two quantities dQ and dT are connected by a factor C which is called specific heat:

$$\frac{dQ}{dT} = C, \; dQ = CdT$$

Thus the specific heat is the quantity of heat required to raise the temperature of a unit mass of a substance (one gram) by 1°C.

Unlike solids and liquids, gases are highly compressible. Hence, the specific heat of a gas depends on the conditions under which heat is supplied to it. If the volume of gas is kept constant during application of heat, the gas does not do any external work and the heat is utilized entirely for increasing its internal energy. The pressure of the gas would increase in this case but this does not affect the internal energy which depends only on the temperature of the gas. The heat required to raise the temperature of a unit mass of gas through 1°C when its volume is kept constant is known as the specific heat at a constant volume denoted as C_v. The value of C_v for air is 0.171 cal/gm/K (0.718 J/gm/K).

If, on the other hand, the pressure of the gas is kept constant during the application of heat, the gas would expand doing external work. The quantity of heat required to raise the temperature of unit mass of gas by 1°C when its pressure is kept constant is known as the specific heat at a constant pressure denoted as C_p. The value of C_p for air is 0.240 cal/gm/K (1.005 J/gm/K). The ratio of C_p/C_v of the specific heats is an important parameter. Its value for air is 1.40.

3.4 EQUATION OF STATE FOR A GAS: PERFECT GAS

For meteorological purposes, the atmosphere can be regarded as a perfect gas with a molecular weight of 28.96 gm which is the weighted mean value of the molecular weights of N_2, O_2, Argon and CO_2, according to their relative proportions. A perfect gas or ideal gas is one in which there is no inter-molecular attraction and the molecular dimensions are negligibly small. Air under atmospheric conditions nearly satisfies these requirements. The density ρ of a particular gas is related to its pressure P and absolute temperature T by the equation of state which, for a perfect gas, takes the form:

$$P = \rho RT \text{ or } P\alpha = RT \tag{3.1}$$

in which R is the gas constant and α is the specific volume (volume occupied by the unit mass of the gas) $\alpha \times \rho = 1$. The gas constant is defined by equation (3.1) as $P/(\rho T)$ and, therefore, in SI units, constant R is expressed as Newton-meter per kilogram per Kelvin (Nm/kg/K). For air the value of R is 287 Nm/kg/K or 287 J/kg/K (1 Joule = 1 Newton-meter).

Example 3.1: Calculate the gas constant (R) for one gram of air of density 0.001293 gm/cm^3 at N.T.P.

Solution: From the gas equation,

$$R = \frac{P}{\rho T}$$

$$P = 76 \times 13.6 \times 980 \text{ gm cm}^{-1} \text{ sec}^{-2}$$
$$\rho = 0.001293 \text{ gm cm}^{-3}$$
$$T = 273°\text{K}$$

$$R = \frac{76 \times 13.6 \times 980}{0.001293 \times 273}$$
$$R = 287 \times 10^4 \text{ cm}^2 \text{ sec}^{-2} \text{ K}^{-1} \text{ gm}^{-1}$$
$$\quad = 287 \times 10^4 \text{ ergs K}^{-1} \text{ gm}^{-1}$$

3.5 ISOTHERMAL AND ADIABATIC CHANGES

Isothermal changes are those in which the temperature of the system undergoing change remains constant. When a gas is compressed isothermally, the heat equivalent of the work done on the gas has to be removed from it to keep the temperature constant. Similarly in an isothermal expansion, the heat has to be supplied to maintain its constant temperature. Thus, isothermal processes involve an exchange of heat between the gas and its environment.

Adiabatic changes are those in which the system undergoing a change is kept thermally isolated from the environment, i.e., no heat is added or taken away from the system. If heat exchanges are involved the process is said to be non-adiabatic. Near the earth's surface non-adiabatic processes are common since air readily exchanges heat with earth's surface. At higher levels, air is far from hot and cold sources and considered to be nearly adiabatic.

3.6 FIRST LAW OF THERMODYNAMICS

This law is a statement of the physical changes that take place when heat is supplied to or withdrawn from a gas. It is a very important law, for, together with equations of state and the hydrostatic equation, it accounts for many of the processes which occur in the atmosphere. The law states that when a quantity of heat (dQ) is supplied to a gas, part of it is used for increasing its internal energy and the remainder is used for doing work by the gas against an external force. Thus, when a small quantity of heat dQ is supplied to a unit mass of a gas, and if its internal energy is increased by du and the gas performs work dw, the first law takes the form:

$$dQ = du + dw \tag{3.2}$$

The internal energy of a perfect gas depends only on its absolute temperature (T). Hence, for a small increase of temperature dT by the application of heat, the increase in internal energy $du = C_v \, dT$. If the pressure of the gas is P and its specific volume increases from α to $\alpha + d\alpha$ by the application of heat, the work done by the gas is $Pd\alpha$. Hence, equation (3.2) can be written as

$$dQ = C_v \, dT + Pd\alpha \tag{3.3}$$

Using the equation of state, we have:

$$P\alpha = RT$$

Therefore, its differentiation yields

$$Pd\alpha + \alpha dP = RdT \tag{3.4}$$

Eliminating $d\alpha$ between equations (3.3) and (3.4), one has

$$dQ = (C_v + R)\, dT - \alpha dP \tag{3.5}$$

If pressure is kept constant then $dP = 0$, and equation (3.5) becomes dQ
$= (C_V + R)dT$. Therefore, $\left(\dfrac{dQ}{dT}\right)_P = C_V + R$, where $\left(\dfrac{dQ}{dT}\right)_P$ is the specific
heat at a constant pressure denoted as C_p. Thus,

$$C_P = C_V + R \quad \text{or} \quad C_P - C_V = R \tag{3.6}$$

$$dQ = C_p dT - \alpha dP \tag{3.7}$$

Equations (3.3) and (3.7) are two different forms of the first law of thermodynamics.

Example 3.2: A gas occupying $0.5\ \text{m}^3$ at a pressure of 1000 mb is compressed isothermally to a volume of $0.004\ \text{m}^3$. Find its final pressure.

Solution: During isothermal change, $PV = $ constant,

$$P_1V_1 = P_2V_2, \quad P_1 = 1000\ \text{mb}, \quad V_1 = 0.5\ \text{m}^3, \quad V_2 = 0.004\ \text{m}^3$$

$$P_2 = \frac{P_1V_1}{V_2} = \frac{1000 \times 0.5}{0.004} = 125000\ \text{mb} = 125000 \times 10^3\ \text{dynes}/\text{cm}^2$$

$$= 1.25 \times 10^7\ \text{N}/\text{m}^2 \ \left[1\,\text{N}/\text{m}^2 = 10\ \text{dynes}/\text{cm}^2\right]$$

Example 3.3: A gas expands from a volume of 5000 cc to 30,000 cc at a pressure of 1520 mb. Determine the work done and also the change in internal energy, if 2000 calories of heat are supplied to the system.

Solution: Heat added = change in internal energy + work done

$$Q = du + PdV$$

Work done $= P(V_2 - V_1)$

$P = 1520\ \text{mb} = 1520 \times 10^3\ \text{dynes}/\text{cm}^2$, $V_1 = 5000\ \text{cc}$, $V_2 = 30{,}000\ \text{cc}$

Work done $= 1520 \times 10^3(30000 - 5000) = 1520 \times 10^3 \times 25000$

$= 3800 \times 10^7\ \text{ergs}$

One calorie $= 4.2 \times 10^7$ ergs

Work done $= 3800 \times 10^7/4.2 \times 10^7 = 905$ calories

Change in internal energy $=$ heat added $-$ work done

$$= 2000 - 905 = 1095 \text{ calories}$$

3.7 VERTICAL MOTION IN THE ATMOSPHERE

In hydrometeorology, it is required to know how the temperature changes with height when air rises or sinks adiabatically. To develop the concepts associated with vertical motions, we consider a small element of air which is often referred to as a parcel of air. We make the assumption that the vertical motion of this parcel is so fast that it does not exchange heat with its surroundings. That is the process which is adiabatic. In such a case, as the parcel rises through the atmosphere its pressure decreases along with that of the surrounding environment and as such the parcel expands and cools.

3.7.1 Dry Adiabatic Rate of Cooling

If the air is dry and no heat is supplied the process is said to be dry adiabatic and the temperature changes are entirely due to expansion or contraction. Suppose a parcel of dry air at level z, where the atmospheric pressure is P, moves adiabatically to a higher level $z + dz$ where the pressure is $P - dP$ (Fig. 3.1). On account of the decrease of pressure, the air parcel would expand and cool. Applying the first law of thermodynamics in the form given by equation (3.7) to the moved air parcel, one has

$$dQ = C_p \, dT - \alpha \, dP \tag{3.8}$$

Since the process is adiabatic $dQ = 0$,

$$C_p \, dT = \alpha \, dP \tag{3.9}$$

From the hydrostatic equation,

$$dP = -\rho g dz \tag{3.10}$$

Substituting the value of dP in equation (3.9) one has

$$C_p \, dT = -\alpha \rho g dz \text{ or } C_p dT = -g dz \, [\alpha \times \rho = 1] \text{ or } -\frac{dT}{dz} = \frac{g}{C_p} \tag{3.11}$$

The minus sign shows that the air cools when it ascends and warms when it descends. The quantity $-dT/dz$ is the rate at which the air cools and since the process is dry adiabatic, it is called the dry adiabatic rate of cooling and is denoted by γ_d. Thus,

$$\frac{-dT}{dz} = \frac{g}{C_p} = \gamma_d \tag{3.12}$$

It is interesting to note that the rate of dry adiabatic cooling is constant. For air $C_p = 1.005 \times 10^7$ ergs/gm/K, $g = 980$ cm/s². Then the variation in temperature per meter can be obtained from equation (3.12) as:

$$\frac{dT}{dz} = \frac{980}{1.005 \times 10^7} \times 100 = 0.0098 \ °C/m \approx 9.8 \ °C/km$$

Thus,

$$\gamma_d \approx 10 \ °C/km$$

Under adiabatic conditions, the atmosphere produces cooling by about 10°C for each one kilometer increase in elevation and warming by about 10°C for each one kilometer decrease in elevation. Such vertical motions producing warming and cooling are always present in the atmosphere and are linked with weather producing systems, such as thunderstorms, storms, cyclones, and depressions, etc.
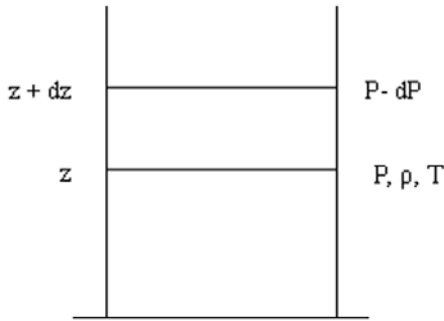
Fig. 3.1. Vertical atmospheric column.

3.7.2 Wet Adiabatic Rate of Cooling

If a parcel of saturated air ascends adiabatically, air will cool by expansion but this cooling will be reduced by the liberation of latent heat. As a result, the wet adiabatic rate of cooling is less than the dry adiabatic lapse rate. Suppose the parcel of air consists of one gram of dry air and r gm of water vapor (r = mixing ratio). Through condensation a small amount of water vapor is changed to liquid water so that the mixing ratio decreases by a small amount dr. If L is the latent heat of vaporization, the liberated heat is $-Ldr$. From the first law of thermodynamics, one has

$$- Ldr = C_p dT - \alpha dP \tag{3.13}$$

$$dT = \frac{\alpha\, dp - Ldr}{C_p} \tag{3.14}$$

From the hydrostatic equation,

$$dP = -\rho g dz$$

Substituting the value of dP in equation (3.14) one has

$$-\frac{dT}{dz} = \frac{g}{C_p} + \frac{L}{C_p} \cdot \frac{dr}{dz} \tag{3.15}$$

or

$$-\frac{dT}{dz} = \gamma_d + \frac{L}{C_p} \cdot \frac{dr}{dz} \tag{3.16}$$

Let the wet adiabatic rate be denoted by γ_s. Then,

$$\gamma_s = -\frac{dT}{dz} = \gamma_d + \frac{L}{C_p} \frac{dr}{dz} \tag{3.17}$$

Since dr is negative, we see that the effect of condensation is to cause the rising air to cool more slowly than in a dry adiabatic process. Unlike the dry adiabatic rate, the wet adiabatic rate is not a constant.

3.7.3 Relation between *P*, *V*, and *T* in Adiabatic Processes

Air that rises or falls from one level to another in the atmosphere instantly assumes the pressure of its environment, but not the temperature. Air that descends is compressed by the higher pressure and warms while air that rises expands and is cooled. When it does so, its temperature change, according to the gas law and the first law of thermodynamics which can be combined as

$$P\alpha = RT$$
$$dQ = C_p dT - \alpha dp$$

For adiabatic process. $dQ = 0$. Eliminating α, one obtains

$$C_p dT = \frac{RT}{P} dP \quad \text{or} \quad \frac{dT}{T} = \frac{R}{C_P} \frac{dP}{P}$$

Integrating,

$$\log_e T = \frac{R}{C_P} \log_e P + \text{const or } TP^{-R/C_P} = \text{const} \tag{3.18}$$

The value of R/C_p for the dry air is 0.286. Obviously, when no heat is added to or taken from the gas, the temperature change is the result entirely of the pressure change. That is

$$\frac{T_2}{T_1} = \left(\frac{P_2}{P_1}\right)^{0.286} \tag{3.19}$$

where T_1 and P_1 are the temperature and pressure, respectively, at an initial level, P_2 is the pressure at another level to which air moves, and T_2 is the resulting temperature at the new level. This is known as Poisson's law. It relates adiabatic temperature changes experienced by a parcel of air undergoing vertical displacement in the atmosphere.

Suppose a gas whose pressure is P and temperature T is adiabatically compressed or expanded till its pressure becomes 1000 mb. The temperature attained by the gas is known as potential temperature (θ) of the gas. From equation (3.19) one has

$$\theta = T \left(\frac{1000}{P} \right)^{0.286}$$

The potential temperature of the dry air remains constant in an adiabatic process.

Example 3.4: A parcel of air with a temperature of 300 °K rises from a height where the pressure is 1000 mb to a height where the pressure is 600 mb. Find the resulting temperature of air at 600 mb.

Solution: From $\dfrac{T}{T_0} = \left(\dfrac{P}{P_0} \right)^{0.286}$, $T_0 = 300°K$, $P_0 = 1000$ mb and $P = 600$ mb

$$T = 300 \left(\frac{600}{1000} \right)^{0.286} = 300 \times 0.864 = 259 °K$$

3.8 MIXTURE OF GASES

Air is a mixture of gases. To understand the behavior of mixtures so long as condensation does not take place, Dalton's law is considered. This law states that the total pressure (P) exerted by a mixture of gases is equal to the sum of the partial pressures (P_1, P_2,..., P_n) exerted by each constituent. Thus,

$$P = P_1 + P_2 + P_3 + ... + P_n = \sum_{i=1}^{n} P_i \qquad (3.20)$$

Let the volume of the mixture be V, the mass of the nth constituent be M_n and its molecular weight be m_n. If each gas obeys the ideal gas law, then

$$P_n = \frac{R^x M_n}{m_n V} T$$

$$P = \sum_{i}^{n} P_i = \frac{R^x T}{V} \sum_{i}^{n} \frac{M_n}{m_n}$$

$$P\alpha = R^x T \frac{\sum_{i}^{n} \frac{M_n}{m_n}}{\sum_{i}^{n} M_n}$$

where α is the specific volume of the mixture. This can be written as

$$P\alpha = \frac{R^x}{\overline{m}} T \ , \ \text{where} \ \frac{1}{\overline{m}} = \frac{\sum_{i}^{n} \frac{M_n}{m_n}}{\sum_{i}^{n} M_n} \tag{3.21}$$

$\overline{m}$ = mean molecular weight. Equation (3.21) shows that a mixture of ideal gases obeys a gas law which is of the same form as the ideal gas law for a single constituent.

3.9 EQUATION OF STATE OF MOIST AIR

The dry air and water vapor separately satisfy the equation of an ideal gas with sufficient accuracy for meteorological purposes. The mean molecular weight of the moist air is obtained by taking the weighted harmonic mean of molecular weights of dry air and water vapor. The mean molecular weight ($\overline{m}$) of the moist air is given as

$$\frac{1}{\overline{m}} = \frac{1}{M_d + M_V} \left[\frac{M_d}{m_d} + \frac{M_V}{m_v} \right] \tag{3.22}$$

where M_d = the mass of dry air, M_v = the mass of water vapor, m_d = the molecular weight of dry air, and m_v = the molecular weight of water vapor. Therefore, equation (3.22) is expressed as

$$\frac{1}{\overline{m}} = \frac{1}{m_d} \frac{M_d}{M_d + M_V} \left[1 + \frac{M_V / M_d}{m_V / m_d} \right] \tag{3.23}$$

The ratio M_v/M_d is the mass of vapor per unit mass of dry air and is the mixing ratio (r). The mixing ratio can be given as:

$$r = \frac{M_V}{M_d} = \frac{\rho_V}{\rho_d}$$

If P is the total pressure of the air and e is the partial pressure of the water vapor in it, the partial pressure of the dry air will be $P - e$.

For water vapor,

$$e = \rho_e \frac{R^x}{m_V} T$$

For dry air,

$$P - e = \rho_d \frac{R^x}{m_d} T$$

$$\rho_V = \frac{e\,m_V}{R^x T} \quad \text{and} \quad \rho_d = \frac{(P-e)m_d}{R^x T}$$

$$r = \frac{\rho_V}{\rho_d} = \frac{m_V}{m_d}\frac{e}{(P-e)}$$

But m_v/m_d is the ratio of the molecular weight of water vapor (18) to the mean molecular weight of dry air (29); therefore the value of $m_v/m_d = 18/29 = 0.622$. Substituting the values of $M_v/M_d = r$ and $m_v/m_d = 0.622$ in equation (3.23) we have

$$\frac{1}{\overline{m}} = \frac{1}{m_d}\left[\frac{1 + 1.61r}{1 + r}\right]$$

Thus, the mean molecular weight of the moist air is expressed in terms of the molecular weight of the dry air and the variable mixing ratio.

The equation of the moist air is

$$P\alpha = \frac{R^x}{m_d}\left(\frac{1+1.61\,r}{1+r}\right)T \tag{3.24}$$

This equation is the same as the equation of state for dry air, except for the factor in the bracket which is a correction to be applied to the specific gas constant for the dry air to obtain the gas constant value for the moist air containing an amount of vapor given by r. This means a variable gas constant which is awkward. To avoid this, a correction to the temperature is applied and a new temperature is defined as

$$T^v = \frac{1+1.61r}{1+r}T$$

This new temperature T^v is called virtual temperature and is a function of the real temperature T and γ. It is a fictitious temperature that satisfies the equation of state for dry air. The r is the mixing ratio in gm of water vapor per gram of dry air. Thus,

$$P\alpha = \frac{R^x}{m_d}T^v$$

The virtual temperature is obviously the temperature that dry air would have if its pressure and specific volume were equal to those of a given sample of moist air. Since water vapor is less dense than air, its presence always increases the specific volume. Hence the virtual temperature is always higher than the observed temperature.

Example 3.5: The temperature of air is 20 °C and the mixing ratio to be 10 gm/kg. What is the virtual temperature?

Solution: We have

$$T^v = \left(\frac{1+1.61r}{1+r}\right)T, \; T = 273 + 20 = 293, \; r = \frac{10}{1000} = 0.010$$

$$T^v = \left(\frac{1+1.61 \times 0.010}{1+0.010}\right)293 = \frac{1.0161}{1.010} \times 293 = 294.8$$

The difference between the virtual temperature and the real temperature is about 294.8 – 293 = 1.8 °C.

3.10 PRECIPITABLE WATER

Precipitable water is another useful measure of the water vapor content of the atmosphere. It is defined as the amount of water that would form in an atmospheric column of unit cross section if all water vapor in it (extending from the top of the atmosphere to the surface) were condensed. It is expressed as the height in mm or inches. Estimation of precipitable water in the atmosphere is extremely useful from meteorological and hydrological standpoints.

An equation for computing water in the atmosphere can be derived as follows. Consider a column of air having a base of 1 cm^2, as shown in Fig. 3.1. If dz is an element of air of height z, the amount of precipitable water (w) in a column of air of height z is calculated as

$$w = \int_0^Z \rho_w \, dz \qquad (3.25)$$

where ρ_w is the density of water vapor. From the hydrostatic equation

$$dP = -\rho_a \, g \, dz \qquad (3.26)$$

where ρ_a is the density of air, and g is the acceleration of gravity. From equations (3.25) and (3.26) we have

$$w = -\frac{1}{g}\int_{P_0}^{P_z} \frac{\rho_w}{\rho_a} \, dP = -\frac{1}{g}\int_{P_0}^{P_z} q \; dP \qquad (3.27)$$

where $q = \rho_w/\rho_a$ is the specific humidity and P_z is the atmospheric pressure at altitude z. Using P in mb and q in gm/kg, it is found that the value of the depth of precipitable water (w) in cm:

$$w \text{ (in cm)} = 0.001 \int_{P_z}^{P_0} q \, dP \qquad (3.28)$$

The above equation can be used to determine the precipitable water between two levels in an air mass knowing the variation of humidity and pressure with height.

Nomograms for computing the precipitable water (w) have been given by Peterson (1961) and Solot (1939). Precipitable water values can also be obtained from publications by the U. S. Weather Bureau (USWB) [now National Weather Service (NWS)] (1951) and WMO (1986). USWB (1960) and Reitan (1963) showed that the precipitable water in an air mass, from which large precipitation occurs, can be estimated from the surface dew points decreasing with height at the saturated pseudo-adiabatic lapse rate. Tables are available to determine the precipitable water content in the atmosphere as a function of dew point at 1000 mb (WMO,1986). For estimation of the probable maximum precipitation (PMP) the use of the 12-hour or 24-hour persisting 1000 mb dew points is made to estimate the highest value of the atmospheric precipitable water. Table 3.1 gives precipitable water between the surface and the levels indicated for air masses of certain surface dew points with assumed saturated pseudo-adiabatic lapse rates. This table shows that the higher the dew point temperature, the more precipitable water the air can carry. Details of PMP estimation will be discussed in a separate chapter.

The mean precipitable water over the northern hemisphere is estimated at 23.85 mm and that over the southern hemisphere at 25.49 mm. This gives a mean global value of 24.67 mm or 2.467 gm/cm^2. During the summer monsoon over India the precipitable water may be as large as 50 to 60 mm and it may be as small as 1 or 2 mm at higher latitudes.

The average water content of 24.67 mm in the atmosphere is sufficient only for some ten days' supply of rainfall over the earth as a whole. Obviously, a frequent and intensive turnover of moisture through evaporation, condensation and precipitation must occur. While atmospheric moisture is essential for precipitable water, the relationship between precipitable water and moisture is determined by the efficiency of rain producing systems in any particular climatic region. For example, observations show that on average only 5% of the water vapor crossing Illinois is precipitated there and in the case of the Mississippi River basin only about 20% does.

Table 3.1: Precipitable water (mm) between 1000 mb surface and indicated height (m) in a saturated pseudo-adiabatic atmosphere as a function of the 1000 mb dew point (°C).

Height (m)	Dew point (°C) at 1000 mb				
	10°C	*15°C*	*20°C*	*25°C*	*30°C*
200	2	2	3	4	6
400	4	5	6	9	12
600	5	7	10	13	17
800	7	9	13	17	22
1000	8	11	15	21	28
2000	13	19	27	37	50
3000	17	25	35	50	68
4000	19	28	42	60	83
5000	20	31	46	67	94
6000	21	32	49	72	102
7000	21	33	51	76	110
8000	21	33	52	78	116

As the first onslaught of monsoon currents strike the Indian region at Trivandrum in India late in May or the first week of June, the precipitable water content over this station is given in Table 3.2.

Table 3.2: Monthly values of precipitable water content in mm over Trivandrum

Month	J	F	M	A	M	J	J	A	S	O	N	D	Annual
W(mm)	36.6	37.1	40.6	45.7	47.5	45.0	43.4	42.9	42.9	43.9	41.4	37.8	42.1

It is seen that there is a gradual increase in precipitable water over the months, with a maximum in the month of May and a minimum in January.

Example 3.6: The variations of vapor pressure (e) with height (h) and pressure (P) are given in Table 3.3. Compute the depth of precipitable water in cm for a column of atmosphere 18,000 feet in height.

Table 3.3: Variation of vapor pressure with height and pressure

Height (1000 ft)	0	2	4	6	8	10	12	14	16	18
P (mb)	1013	942	875	812	753	697	644	595	550	500
e (mb)	7.0	5.0	3.8	3.2	2.0	1.6	1.1	0.8	0.6	0.4

Solution: We can compute the precipitable water in cm from the following equation:

$$w \text{ (in cm)} = 0.001 \int_{P_1}^{P_2} q \ dP$$

where q is specific humidity in g/kg, and P is pressure in mb. Since the values of q are not given we can find q from $q = \dfrac{622e}{P}$ gm/kg , where e is the vapor pressure. To solve the integral the air column is divided into 2000 ft zones and the mean values of q for each zone is used. The equation can be written as

$$w = 0.001 \sum \bar{q} \ dP$$

where $\bar{q}$ is the mean value of q for each zone. The computations are shown in Table 3.4.

Table 3.4: Calculation of precipitable water (w)

Level (1000 ft)	P (mb)	(e) mb	q=622e/P (gm/kg)	($\bar{q}$) = ($q_n + q_{n+1}$)/2	dP= $P_n - P_{n+1}$ (mb)	($\bar{q}$)dP
0	1013	7.0	4.30	-	-	-
2	942	5.0	3.30	3.8	71	270
4	875	3.8	2.70	3.0	67	201
6	812	3.2	2.45	2.57	63	162
8	753	2.0	1.65	2.05	59	121
10	697	1.6	1.43	1.54	56	86
12	644	1.1	1.06	1.25	53	66
14	595	0.8	0.84	0.95	49	47
16	550	0.6	0.68	0.76	45	34
18	500	0.4	0.50	0.56	50	28

$$\sum \bar{q} \ dP = 1015$$

$$w \text{ (in cm)} = 0.001 \sum \bar{q} \ dP = 0.001 \times 1015 = 1.015 \text{ cm} = 0.41 \text{ inch}$$

REFERENCES

Peterson, K.R., 1961. A precipitable water nomogram. *Bull. Am. Meteorol. Soc.* 1942, 119-121.

Pettersen, S., 1969. Introduction to meteorology. McGraw Hill Book Company Inc., New York.

Reitan, C.H., 1963. Surface dew point and water vapor aloft. *J. Appl. Met.*, 2, pp. 776-779.

Solot, S., 1939. Computation of depth of precipitable water in a column of air. *Monthly Weather* Rev., 67, pp. 100-103.

USWB, 1951. Tables of precipitable water and other factors in a saturated pseudo adiabatic atmosphere. U.S. Dept of Commerce, Tech paper No 14, 27 pp.

USWB, 1960. Technical Paper No. 38.

World Meteorological Organization, 1986. Manual for estimation of probable maximum precipitation. Operational Hydrology Report No. 1, WMO No 332, 269 pp.

4 Radiation and Temperature

Hydrologic characteristics of an area depend primarily on its climate and geology. Climate is particularly important, because it determines the distribution of rain water for agriculture, hydropower generation, and other human activities with significant economic consequences. Hence, it is essential to have a basic knowledge of the factors that make our climate what it is.

Climate is defined as the long-term average (usually 30 years or longer) of the variations in daily weather in the atmosphere over an area. Weather in the atmosphere at a place is caused by the composite effect of several atmospheric or meteorological variables. The values of these meteorological variables depend upon the composition of the earth's surface and the exchange of heat and moisture between the earth and the atmosphere resulting from the interaction of many physical processes (see Fig. 4.1).

The various interactive physical processes determining weather and climate are: (a) the motion of earth (orbiting around the sun and the rotation around its own axis); (b) variability in solar radiation; (c) radiation budget; (d) atmospheric circulation; (e) oceanic circulation; (f) the atmospheric content of gases, aerosols, and dust; (g) changes in the land surface, (h) hydrologic cycle; (i) air-sea interaction; and (j) energy exchange. Most fundamental of these processes are radiation and temperature and they constitute the subject matter of this chapter.

The orbital motion of the earth around the sun affects the seasonal amount of radiation received by each hemisphere. Solar radiation varies over time and affects the energy received at the top of the atmosphere. The radiation balance accounts for the heat energy coming from the sun and that radiated by the earth system. Atmospheric circulation determines the flow patterns of air as well as the exchange of heat and moisture over the land and ocean surface. Oceanic circulation strongly affects the temperature of the sea surface and the rate of energy exchange between the atmosphere and oceans. Atmospheric concentration of gases, aerosols and dust affect the amount and type of radiation emitted or absorbed by the atmosphere. Changes
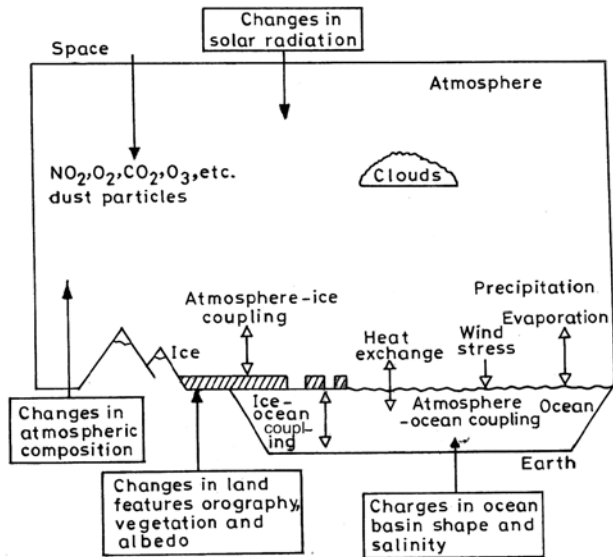
Fig. 4.1. Earth's climate system and interactions among its components.

on the land surface affect the distribution and exchange of energy and moisture, and the albedo (reflectivity). The hydrologic cycle determines the interchange of moisture between earth, oceans and atmosphere. The energy exchange process explains the heat transfer through evaporation, condensation and turbulence. The air-sea interaction involves upwelling and the El Nino and La Nina phenomena.

The above processes and other factors affect atmospheric and oceanic circulation. Hence climate processes are replete with combinations of interactions, feedbacks, and changes. Apparently, changes in these processes and factors affect the distribution of heat and moisture of the earth system and lead to weather and climate variability. During the last two decades, the complexity of atmosphere, land and ocean interactions and the potential for climate change caused by increasing human activities have prompted the development of numerical models to assess the impact of changes in climate in many areas, including agriculture, water resources and land use.

4.1 SUN: THE SOURCE OF HEAT AND LIGHT

Life on earth depends on the immense nuclear furnace we call sun. Larger than a million earths, the sun is practically the main source of heat to drive the climate system. It is a gaseous sphere, and the gases are mostly hydrogen and helium. The sun derives its energy by the gradual conversion of hydrogen into helium by thermonuclear fusion in its deep interior under the extreme conditions of pressure and temperature prevailing there. The radius of the sun is 6.96×10^5 km (6.96×10^{10} cm) which is about 109 times the radius

of earth. The visible surface of the sun from which most of the radiation is emitted is called the photosphere. Measurements on the radiation emitted by the sun combined with the laws of radiation show that the temperature of the photosphere is approximately 6000° K. Instrumental observations of the sun reveals a wealth of features of which most important are the sunspots which are dark areas on the solar disc. They are about 1500° C cooler than the surrounding photosphere and, having a radius of about 4000 km, are centers of strong magnetic fields. The number of spots on the sun increase and decrease with a periodicity of about 11 years known as the sunspot cycle (Fig. 4.2). Solar radiation varies by about 0.1 percent over the 11-year sunspot cycle and it may vary by larger amounts (0.6%) over longer periods. Table 4.1 gives the astronomical particulars of the sun.
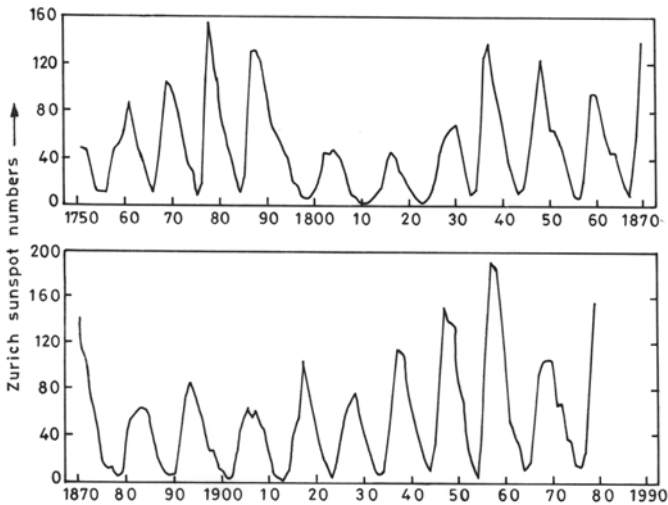
Fig. 4.2. The sunspot cycle: 1751-1980.

Table 4.1: Astronomical particulars of the sun

Parameters	Values
Radius	6.960×10^8 m or 4.326×10^5 miles
Surface area	6.087×10^{18} m^2
Volume	1.412×10^{27} m^3
Mass	1.99×10^{30} kg
Mean density	1.409 gm cm^{-3} or 1409 kg m^{-3}
Rate of energy production	56×10^{26} calories/minute
Gravity at surface	2.74×10^4 cm s^{-2}
Moment of inertia	6.0×10^{53} gm cm^2
Escape velocity at surface	618 km s^{-1}
Sidereal period of rotation	25.38 days
Period of rotation with respect to the earth	27.28 days

4.1.1 Solar Constant

Sun provides 99.97% of the heat energy required for the physical processes taking place in the earth-atmosphere system. Each minute sun radiates about 56×10^{26} calories of energy. This amount of energy from the sun is usually expressed in terms of solar constant which is defined as an amount of energy received in unit time on a unit surface area perpendicular to the sun's rays at the outer boundary of the atmosphere at the mean distance between the earth and the sun. This distance is about 1.5×10^8 km (1.5×10^{13} cm). As such, the energy per unit area incident on a spherical cell with a radius of 1.5×10^{13} cm and concentric with the sun is calculated as

$$S = \frac{E}{4\pi r^2} = \frac{56 \times 10^{26}}{4 \times 3.14 \times (1.5 \times 10^{13})^2} \approx 2 \text{ cal/cm}^2/\text{min}$$

where S = the solar constant (cal/cm^2/min), E = the rate of energy production (cal/min), and r = radius (cm).

The solar constant is not a true constant but fluctuates by as much as ± 1.5% about its mean value. Meteorologists measure the rate of input of heat energy in terms of the watt per square meter of earth's surface (W/m^2) and its value is:

$$S = 2 \text{ cal/cm}^2/\text{min} = \frac{2 \times 4.2 J \times 100 \times 100}{60} \text{ Joules/sec/m}^2$$

$$= 1390 \text{ Joules/sec/m}^2 = 1390 \text{ W/m}^2 \quad (1 \text{ Joule/sec} = 1 \text{ watt})$$

The current best estimate is 1370 Wm^{-2}.

Earth intercepts only a tiny fraction of the energy radiated by sun. We know that at any instant one half of the surface of the earth is exposed to the sun. The projected area normal to the solar rays which intercepts the radiation is πr^2, where r is the radius of the earth (6.37×10^8 cm or 6.37×10^5 km).

Energy intercepted = $\pi r^2 S = 3.14 \times (6.37)^2 \times 10^{16} \times 2 = 2.55 \times 10^{18}$ cal/min.

The energy intercepted during a complete rotation is distributed uniformly over the entire surface area of the earth ($4\pi r^2$). Hence, the average solar energy that arrives at the top of the atmosphere is

$$\overline{Q_s} = \frac{\pi r^2 S}{4\pi r^2} = \frac{S}{4} = 0.50 \text{ cal/cm}^2/\text{min} = 263 \text{ k cal/cm}^2/\text{year} = 348 \text{ W/m}^2$$

This energy flows down through the atmosphere, interacting with it, so that some energy is reflected back to space, some is absorbed and converted into heat and some reaches the surface of the earth. The energy that arrives at the surface and is absorbed can heat the surface, evaporate water, melt snow, and heat the underlying soil by radiation processes. Variations in the energy received from the sun and variations in the interaction with the earth

and the atmosphere create temporal and spatial variations in energy exchanges which lead to our climate. Radiation processes, therefore, play an important role in the formulation of the climate. It is therefore important to study some simple laws of radiation.

4.2 RADIATION

Radiation is the physical process by which energy is emitted by all objects having a temperature above absolute zero in the form of electromagnetic waves. The waves travel in straight lines with the speed of light until they hit objects from which they are partly reflected and partly absorbed. The absorption gives rise to a change in the heat content of the object. The various kinds of electromagnetic waves which are characterized by its wavelength (λ) measured in micrometer (μm) (1 μm $= 10^{-6}$ m $= 10^{-10}$ Angstrom) are as follows:

Type of radiation	Range of wavelength
Cosmic rays, gamma rays, x rays, etc.	$\leq 10^{-3}$ μm
Ultraviolet	$10^{-3} - 0.4$ μm
Visible	$0.4 - 0.8$ μm
Near infrared	$0.8 - 4.0$ μm
Infrared	$4.0 - 100$ μm
Microwave	$100 - 10^{7}$ μm
Radio	$>10^{7}$ μm

All bodies (solid, liquid, and gas) absorb and emit radiation depending on the nature of the body and its temperature. In the study of radiation, much importance is given to the radiation emitted by a black body. In the theory of radiation, a black body is a body that completely absorbs the radiation in all wavelengths falling on it. The radiation emitted by such a body is known as black body radiation. The term black has nothing to do with the color of the body. Black is really an absence of all the colors of the visible spectrum. For example, snow behaves like a black body for radiation of wavelengths greater than 1-5 μm. The sun, the earth and the clouds radiate very nearly as a black body over a wide range of wavelengths. The laws of radiation enable us to determine the temperature of the radiating body and the radiation emitted by it. This principle is utilized in remote sensing of the temperature of cloud tops, sea surface, etc. by meteorological satellites.

4.3 LAWS OF RADIATION

The fundamental laws of radiation are presented below.

Kirchoff's law: Kirchoff's law states that a body which is a good absorber of radiation in certain wavelengths is also a good emitter in the same wavelengths.

Stefan-Boltzmann's law: The Steffan-Boltzmann law states that the amount of energy radiated per unit time and wavelength from a unit surface area of an ideal black body is proportional to the fourth power of the absolute temperature of the body. It is expressed as

$$I = \sigma T^4 \qquad (4.1)$$

where I is the amount of radiation in cal/cm^2/min, T is the absolute temperature of the black body in absolute degrees, and σ is the Boltzmann constant. The value of σ depends on the units used. Its value in CGS units is 5.67×10^{-5} erg cm^{-2} s^{-1} K^{-4} or 5.67×10^{-8} J m^{-2} s^{-1} K^{-4}.

Wein's law: The Wein law states that the wavelength of maximum intensity (λ_m) in black body radiation is inversely proportional to the absolute temperature (T), i.e.,

$$\lambda_m = \frac{2897}{T} \qquad (4.2)$$

It shows that higher the temperature of the black body the shorter is the wavelength of the radiation.

Planck's law: Planck's law gives the relationship between radiation energy, temperature and wavelength of the electromagnetic radiation, and is given by

$$I_\lambda = \frac{C^1}{\lambda^5} \frac{1}{e^{c/(\lambda T)} - 1} \qquad (4.3)$$

Equation (4.3) gives the amount of radiational energy emitted per unit time and within a unit of wavelength by the unit area of a black body. Figure 4.3 gives the distribution of radiation with wavelength from Planck's law for temperatures corresponding to the sun surface, the earth and the atmosphere. It is seen from Fig. 4.3 that the intensity falls off to small values for very short and very long wavelengths and attains a maximum for an intermediate wavelength, the value of which depends on the temperature of the emitting body. It can be seen that the wavelength λ emitted by a body corresponding to the sun surface temperature of approximately 6000 °K ranges from about 0.3 μm to about 3 μm. The wavelength of the maximum radiation is about 0.5 μm. The wavelength of the radiation emitted by the earth's surface (300 °K) and by the atmosphere (200 °K) ranges from about 3 μm to 100 μm. The maximum of the emitted radiation has a wavelength of near 10 μm. Most of the radiation at the temperature of the sun is contained in the short wavelength range as compared with the radiation at the temperature of the earth's surface. Hence the radiation which is emitted by the sun is often called as short wave radiation and the radiation from the earth's surface and the atmosphere as long wave radiation. The radiation from the earth's system is commonly called terrestrial radiation.
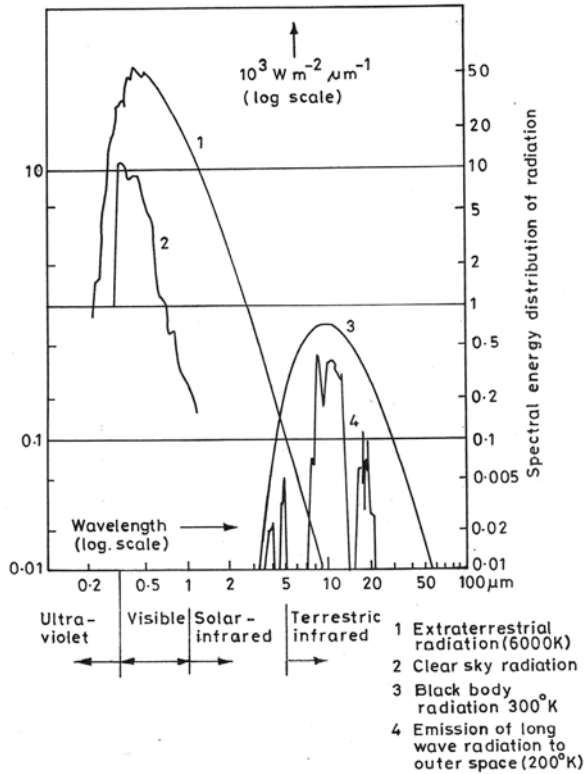
Fig. 4.3. Distribution of radiation with wave length.

Example 4.1: Calculate the energy radiated in one minute by a perfectly black body sphere of 5 cm radius maintained at 127 °C.

Solution: Energy radiated per sec per unit area (I) = σT^4

Total energy radiated per sec = area × σT^4

Total energy radiated per minute = 60 × area × σT^4

Area of sphere = $4\pi r^2$

$r = 0.05$ m, $T = 273 + 127 = 400$ °K,

$\sigma = 5.67 \times 10^{-8}$ J m^{-2} s^{-1} K^{-4}

Energy = $60 \times 4\pi r^2 \times 5.67 \times 10^{-8} \times (400)^4$

$= 60 \times 4 \times 3.14 \times (0.05)^2 \times 5.67 \times 10^{-8} \times 400^4 = 2751$ Joules

4.4 INCOMING SOLAR RADIATION WITHOUT ATMOSPHERE AT THE EARTH'S SURFACE

The seasonal variation in solar radiation reaching the earth's surface is caused by the inclination of the earth's axis to the plane of its orbit and the revolution of the earth around the sun. The amount of daily solar radiation received

over a unit area of the earth's surface at different latitudes have been calculated from astronomical considerations. In this calculation, one has to take into account the fact that the inclination of the solar rays to the surface at any latitude varies in the course of the day and also depends on the time of the year. If the solar rays make an angle θ with the normal to the surface, the effective solar radiation received per unit area is $S \cos \theta$, where S is solar constant. Figure 4.4 gives the distribution of daily values of incoming solar radiation received by the earth's surface at five latitudes 0°, 20°, 40°, 60°, and 90° in the course of a year. The main features of this distribution are:
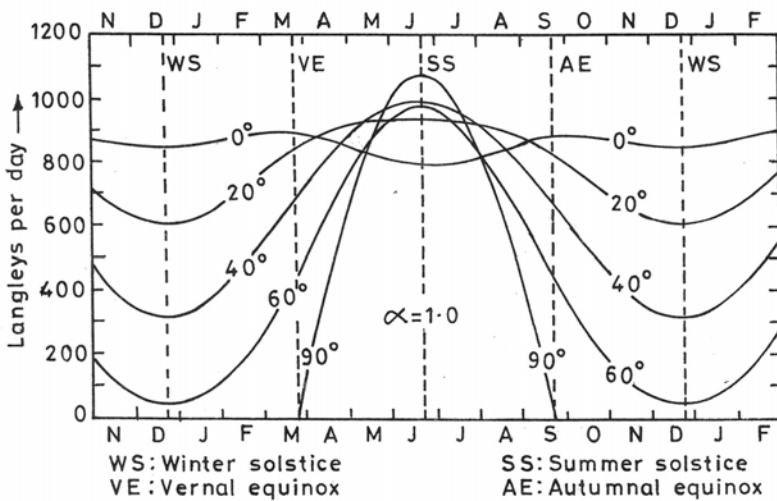
Fig. 4.4. Daily totals of solar radiation in langleys per day at five different latitudes over the northern hemisphere for a transparent atmosphere.

(*a*) The seasonal variation of solar radiation is least at the equator and increases with increasing latitude. At the equator the daily radiation varies between 800 and 900 langleys (cal/cm^2) during the year. High radiation over the equator is due to the fact that the zenith angle of mid day sun never exceeds 23°. The equatorial region is one of annual maximum radiation.

(*b*) The largest variation occurs at the poles. At the north pole, the daily radiation is zero from 23rd of September to 21st of March to a maximum of 1000 cal/cm^2/day on 22nd of June (summer solstice). At the south pole, it is zero from 21st of March to 23rd of September with a maximum of 1150 cal/cm^2/day on 22nd of December. It can be seen from these values that the north pole receives the maximum solar radiation per day and the equator the minimum at summer solstice.

(*c*) A secondary maximum occurs near latitude 40° at the summer solstice.

(*d*) The solar radiation at any latitude depends on the day of the year.

(*e*) The latitudinal variation is small close to the summer solstice and very large close to the winter solstice.

The atmosphere is not fully transparent and this modifies the distribution of solar radiation over the surface of the earth. Before it reaches the ground it is attenuated by reflection from and absorption by the constituents of the atmosphere. The net effect is that only a fraction of the solar radiation reaches the ground; the rest is extinguished and redistributed.

4.5 PASSAGE OF SOLAR RADIATION THROUGH AVERAGE ATMOSPHERIC CONDITION

When solar radiation passes through the atmosphere it is attenuated by scattering and reflection due to air molecules, water droplets, ice crystals, aerosols, dust, and clouds and depending on the wavelength, it is absorbed by varying degrees by O_3, CO_2 and H_2O. The net effect is that the radiation reaching the ground is less than what is received without atmosphere and seasonal variations are subsequently different from that discussed in the previous section. A schematic representation of solar energy in the earth-atmosphere system is shown in Fig. 4.5. Radiation is indicated by arrows and the percentage of the numerical values appearing on the arrows. The figure represents the average conditions for the whole atmosphere.
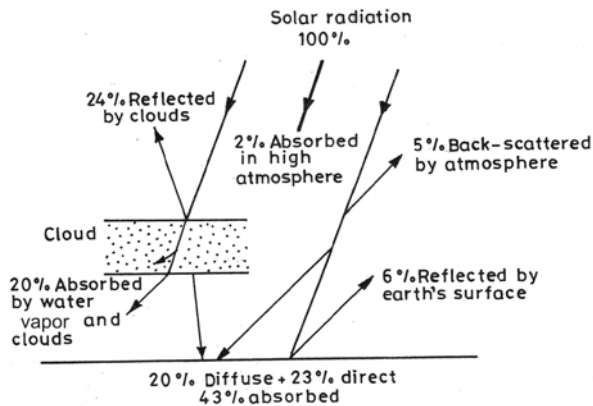
Fig. 4.5. Approximate budget of solar radiation for the earth-atmosphere system.

The solar energy in the earth-atmosphere system involves absorption, scattering, and diffuse reflection.

(i) **Absorption:** The solar radiation of the wavelength less than 0.29 μm is absorbed by O_3 and partly by O_2 in the stratosphere. About 2% of the incoming radiation is absorbed in this manner in the stratosphere. About 20% is absorbed by H_2O and clouds in the troposphere.

(ii) **Scattering**: When the incoming solar radiation encounters small particles (air molecules, dust, aerosols, and water droplets) of the atmosphere, the radiation energy is diffusely scattered in all directions from the particles. Scattering of radiation by air molecules is more effective for the shortest wavelengths. About 25% of the energy is scattered by the atmosphere of which 20% reaches the earth's surface and 5% returns to space. In absorption, part of the energy is removed by absorbing gases, whereas in scattering the energy is redistributed in different directions.

(iii) **Diffuse reflection**: Clouds reflect much incoming solar radiation to space. Depending upon the height, clouds consist of tiny water droplets or ice crystals. A large percentage of the incident solar radiation is diffusely reflected backwards and part of the energy is absorbed within the clouds. The amount of reflection depends on the nature of the clouds and the total amount of clouds. It is estimated that about 24% of the total radiation is reflected from clouds and a further 6% is reflected from the earth's surface.

The resulting values indicate that about 35% of the incoming solar radiation is returned back to space during its journey from the top of the atmosphere to the surface of the earth by scattering in the atmosphere and by diffused reflection from clouds and also at the earth's surface. The rest of the energy is absorbed partly by the atmosphere and mostly by the earth. About 43% of the incident radiation is absorbed by the earth. It is this part of solar energy that is available for physical processes associated with weather and climate.

The fraction of the total incoming radiation which is reflected back to space is called albedoe. We have seen that 24% of the total radiation is reflected from the clouds and a further 6% from the earth's surface. When 5% of the scattered radiation is added then a planetary albedo of 35% is obtained. Under average conditions, the albedo (reflectivity) of the earth as a whole is about 35%. Of the remaining 65%, a small part (22%) is absorbed in the atmosphere but the bulk (43%) is absorbed by the earth's surface.

(i)	Absorption above troposphere by ozone and oxygen	2%
(ii)	Absorption in the troposphere by clouds and water vapor	20%
(iii)	Absorption by the surface of the earth	43%
(iv)	Reflection back as short wave radiation to space	35%

In the absence of a compensating mechanism, continuous absorption of the solar energy by the earth and atmosphere as indicated above would lead to a progressive increase in the temperature of the system. Experience shows that this is not happening.

4.6 TERRESTRIAL RADIATION

The amount of solar energy absorbed by the earth-atmosphere system is $(1-A)S/4$ cal/cm^2/min, where S is the solar constant and A is the planetary

albedo, i.e., the percentage of the incoming radiation which is reflected back to space and amounts to approximately 35%. Because of the law of conservation of energy for earth in the thermodynamic equilibrium, the incoming radiation must be balanced by an amount equal to $(1–A)S/4$ cal/cm^2/min. This loss must be sought in the long wave radiation that goes from the earth-atmosphere system back to space. If we assume the mean surface temperature of the earth as T_E, then, from the Stefan-Boltzmann law, the average long wave radiation, R_E, per unit area of the earth's surface is

$$R_E = \sigma T_E^4$$

where σ is the Boltzmann constant. The incoming solar radiation is balanced by the long wave terrestrial radiation:

$$\sigma T_E^4 = (1 - A)\frac{S}{4}$$

where $\sigma = 5.67 \times 10^{-8}$ Wm^{-2} K^{-4}, $S = 1359$ Wm^{-2}, and $A = 0.35$. Introducing numerical values of quantities σ, S and A, we obtain

$$T_E^4 = (1–0.35) \times \frac{1359}{4} \times \frac{10^8}{5.67}$$

$$T_E^4 = 250 \text{ K } (–23 \text{ °C})$$

However, temperature measurements averaged over all latitudes and all seasons give a mean temperature of the earth as 15° C. The difference of 38 degrees is due to the fact that much of radiation emitted by the earth's surface does not go straight into space because certain gases in the atmosphere absorb and redirect it back to the earth, adding to the warmth of the earth. This process of warming is called the greenhouse effect and makes the earth and the adjoining atmosphere warmer than what it would have been if the atmosphere did not have greenhouse gases.

The greenhouse gases include water vapor, carbon dioxide, nitrous oxide, methane and ozone. As a matter of fact, if our atmosphere did not absorb or trap the sun's heat in this manner, the earth would be as lifeless as the moon. The atmospheric concentration of each greenhouse gas is a result of the interaction of the biological systems on the earth with hydrologic and other biogeochemical cycles that involve various sinks and sources of greenhouse gases. Changes in amounts of greenhouse gases throughout the earth's history, whether natural or recently human induced, have coincided with changes in the earth's climate. The most popular paradigm for the correlation between greenhouse gas concentrations and climate variations is that as concentrations of greenhouse gases increase, the atmosphere becomes an increasingly efficient trap for the redirected energy, and global atmospheric warming could occur (IPCC, 2001).

4.7 MEAN ANNUAL HEAT BALANCE OF THE EARTH-ATMOSPHERE SYSTEM

The earth-atmosphere system receives energy from the sun in the form of short wave radiation and returns the same amount of energy to space in the form of long wave radiation. A complex mechanism of physical and dynamical processes within the system are involved in maintaining this energy balance. As most of the weather phenomena occur within the troposphere, we deal here with the heat balance of the earth and troposphere being regarded as a coupled system.

4.7.1 Shortwave Radiation

It is known that the solar radiation which is received by the entire earth's surface of area $4\pi r^2$ (r is radius of earth) is, on average, equal to one fourth the solar constant or about 0.4855. If this amount is arbitrarily set at 100 units then for this amount two units of energy is absorbed by O_3 and O_2 above the tropopause level. The remaining 98 units enter the troposphere. Of this 35 units are returned to space. Of the remaining 63 units, 43 units are absorbed by the earth's surface and 20 units in the troposphere.

4.7.2 Long Wave Radiation

 (i) **Emission from the surface of the earth:** The mean surface temperature of the earth is 288° K (15° C). The radiation emitted (I) per unit area of the surface per unit time is given by the Stefan-Boltzmann formula as

$$I = \sigma T_E^{\,4}$$
$$\sigma = 8.12\times10^{-11} \text{ cal/cm}^2/\text{min/K}^4$$
$$I = 8.12\times10^{-11} \times (288)^4$$
$$= 0.5600 \text{ cal/cm}^2/\text{min}$$

Expressed on the same scale as for the incident solar radiation, this is equal to 116 units (0.56/0.4855 ~ 116). This is roughly 2.5 times the 43 units of solar radiation absorbed by the earth's surface. Of this emitted radiation 106 units are absorbed by the water vapor and CO_2 in the troposphere, while 10 units escape to space.

 (ii) **Emission by the troposphere (including clouds):** It is estimated from the radiative transfer that 158 units of long wave radiation are emitted by the troposphere. Of this 102 units are directed downwards and absorbed by the earth. The balance of 56 units escapes to space at the tropopause.

(iii) **Downward radiation from the stratosphere and energy balance:** The total long wave radiation emitted to space by the earth and the troposphere together is 66 units (10+56). This is more than the 63 (43+20) units of short wave radiation absorbed by the earth and the

troposphere. The balance of three units is made up by long wave radiation directed downward from the stratosphere through the tropopause and absorbed by the troposphere. Thus, the earth-troposphere system absorbs 66 units of energy, 63 units as short wave radiation from the sun and three units as long wave radiation emitted by the stratosphere. The same amount of energy escapes to space at the tropopause level in the form of long wave radiation. Thus, the overall energy balance of the earth-troposphere system is maintained.

4.8 NON-RADIATIVE HEAT EXCHANGE BETWEEN THE EARTH AND THE TROPOSPHERE

We have seen that the earth emits 116 units of energy. It absorbs 43 units of short wave radiation from the sun and 102 units of long wave radiation emitted by the troposphere. These add up to 145 units; thus, by the radiative exchange process the earth gains 29 units. Also the troposphere absorbs 20 units of short wave radiation from the sun, 106 units of long wave radiation from the earth and three units of long wave radiation from the stratosphere. These add up to 129 units. The troposphere emits 158 units of radiation which is in excess of what it absorbs by 29 units. Apparently, by the radiative process alone, the earth gains 29 units of energy while the troposphere loses 29 units of energy. This imbalance is compensated for by the transfer of heat from the earth to the troposphere by the following non-radiative heat exchange processes.

(i) The solar energy received at the earth's surface is utilized for evaporating water from the water bodies, such as seas, oceans, lakes, rivers, etc. In doing so, the latent heat of evaporation at the rate of about 600 calories per gram of water is utilized. The water vapor enters the troposphere and is transported both horizontally and vertically by air currents. Finally, the vapor condenses to form clouds. During condensation the latent heat is released and goes to heat the troposphere. In this way, water vapor acts as a medium for the transport of heat from the surface of the earth to the troposphere. It is estimated that about 23 units of heat are transferred in this manner.

(ii) The solar radiation absorbed by the surface raises its temperature and the air in contact with the surface also gets heated. The heating sets up turbulent air motion in the lower layers of the atmosphere which transports sensible heat from the surface to higher layers. It is estimated that about six units of heat is transferred in this manner. By these two non-radiative processes the excess heat from the surface is transferred to the troposphere and the heat balance of the earth-troposphere is maintained.

4.9 HEAT BALANCE

Of particular interest to meteorology is the so-called net heat balance, which is the difference between the total incoming radiation and the total outgoing radiation. Houghton (1954) has computed the heat balance for each 10° latitude strips from the equator to poles for the whole year for northern hemisphere. This is shown in Fig. 4.6.
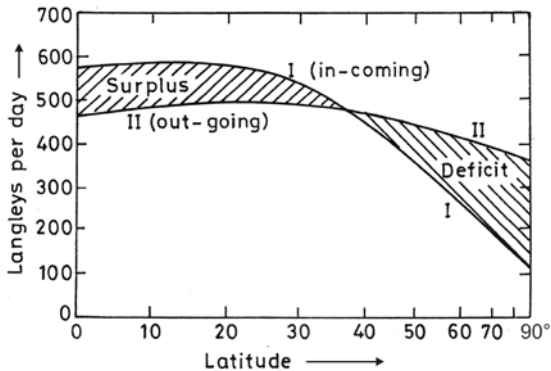
Fig. 4.6. Latitudinal variation of the earth's heat budget (after Houghton, 1954).

Curve I represents the mean annual absorption of solar radiation by the earth-troposphere system as a function of latitude and curve II shows the corresponding outgoing long-wave radiation. Figure 4.6 shows that the solar energy absorbed by the system is largest in the tropics and decreases to small values towards the pole. The outgoing long-wave radiation shows much less variation with latitude. The two curves intersect at nearly 35° where the absorbed short-wave radiation and outgoing long wave radiation balance. Equatorwards of this latitude the absorbed energy is in excess of the outgoing radiation (energy surplus), while poleward, the outgoing radiation exceeds the absorbed solar energy (energy deficit). This feature is of much meteorological significance. In a fluid medium, one portion cannot get heated continuously and other cannot get depleted of heat continuously. If this situation is allowed to persist, the tropics would grow hotter and hotter and higher latitudes would grow colder and colder. In a fluid medium like atmosphere the situation cannot persist and hence circulation of the atmosphere starts and carries the excess heat from the tropics to the poles to maintain the observed temperature distribution from the equator to the pole in each hemisphere. The atmosphere can be considered as a heat engine absorbing net heat in a high temperature reservoir in the tropical belt and giving up heat in the low temperature reservoir in the polar region.

4.10 TEMPERATURE ZONES

The duration or the length of the day changes throughout the year, causing the seasons—summer and winter of varying temperatures. If we go from the

equator to the north or to the south, we find that the length of the day goes on changing and the sun's rays go on more and more oblique. The sun's rays are never very oblique near the equator and hence occupy less space. That is why this region gets more heat. Towards the poles, the sun's rays slant and occupy more space and hence this region gets less heat. As we go from the equator to the poles, we come across regions with varying temperatures. These are called the temperature zones of the earth (Fig. 4.7).

 (i) **Torrid zone:** The region lying between the Tropic of Cancer (23½° N) and the Tropic of Capricorn (23½° S) is known as the Torrid zone. In this zone, the sun is directly overhead twice a year and its rays are never very oblique. The region gets more heat and the weather in general is always hot.

 (ii) **Temperate zone:** The region in the northern hemisphere between the Tropic of Cancer (23½° N) and 66½° N and in the southern hemisphere between the Tropic of Capricorn (23½° S) and 66½° S is called temperate zone. The sun is never overhead in these regions but its rays vary considerably in direction. There are well marked warm and cool seasons or summer and winter.

(iii) **Frigid zone:** The region in the northern hemisphere between 66½° N and the north pole, in the southern hemisphere between 66½° S and the south pole is known as Frigid zone. In this region the sun's rays are always very oblique so the weather, in general, is never warm. In summer it is cool and in winter it is extremely cold. Moreover, the sun's rays do not reach this region at all in winter.

Temperature zones have an effect on climate and as well as on human and plant life.
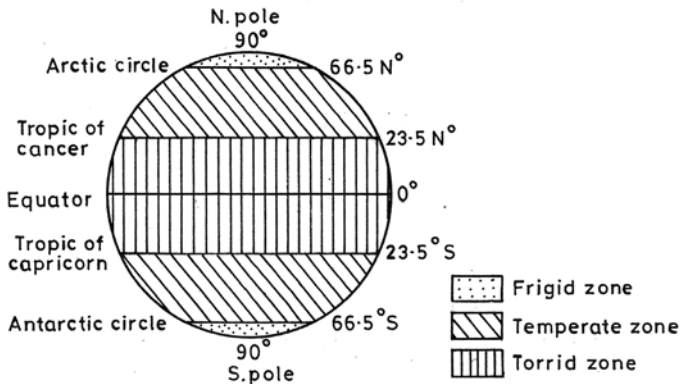
Fig. 4.7. Temperature zones of the earth.

REFERENCES

Houghton, H.G., 1954. On the annual heat balance of the northern hemisphere. *Journ. of Met.,* 11, pp. 1-9.

Intergovernmental Panel on Climate Change (IPCC), 2001. Climate change: The scientific basis. Cambridge University Press, London, New York.

Petterssen, S., 1969. Introduction to Meteorology. 2nd ed. Mc Graw-Hill Book Company, Inc. New York.

Plate, E.J. (editor), 1982. Engineering Meteorology. Elsevier, Scientific Publishing Co., New York.

Sellers, A.H. and Robinson, P.J., 1986. Contemporary Climatology. Longman Group, U.K. Ltd.

5 Weather Systems for Precipitation

The theme of this chapter is to provide a general discussion of weather systems, such as Inter Tropical Convergence Zone (ITCZ), jet streams, cyclones and anticyclones, tropical depressions, extra tropical cyclones, fronts, trade winds, monsoon winds and easterly waves. Radiation, temperature, wind and pressure are the fundamental factors that govern these weather systems. All these factors are inter-related. Consequently, in the study of weather systems the knowledge of radiation and temperature as well as pressure belts and wind systems of the world is obviously of prime importance. Radiation and temperature were discussed in Chapter 4. Before discussing weather systems, a short discussion of the major pressure belts and wind systems of the earth is given first.

5.1 PRESSURE BELTS AND WIND SYSTEMS OF THE EARTH

5.1.1 Major Pressure Belts

Figure 5.1 shows how belts of high and low pressure would appear on the earth with an alternating rhythm of low pressure, high pressure, low pressure and high pressure at $0°$, $30°$, $60°$ and $90°$, respectively. It is known that temperature and atmospheric pressure are inversely related to each other. The atmospheric pressure decreases with a rise in air temperature and increases when the air temperature falls. Air expands with a rise in its temperature. In other words, air becomes less dense and exerts less pressure. At low temperatures, however, the air becomes denser and exerts greater pressure.

The air pressure is not uniform at the earth's surface. It changes from place to place because of the modification of thermal circulation due to the rotation of earth. The rays of the sun fall perpendicular on the equator throughout the year. That is why the temperature at the equator is always high. Owing to high temperatures near the equator, the air near the surface of the earth gets heated and expands. The expanded air is lighter and therefore,

it rises rapidly, producing a low pressure belt all along the equator. This low pressure belt lies between 5° north and 5° south parallels of latitudes.

The rising air at the equator cools down as it goes higher and higher and starts moving towards the polar regions. In the middle latitudes, this air becomes cool and heavy and comes down near 30° north or south latitudes and piles up there. This process of piling up results in the formation of subtropical high pressure belts around 30° latitude in both the hemispheres.

Temperature is extremely low in Polar Regions. The air being cold and heavy throughout the year, a high pressure belt is formed in both the North Pole and South Pole regions. At about 60° north and south latitude, the air moving from the polar cold meets the air coming from the subtropical high pressure belts. This causes air to rise and low pressure belts around 60° are developed in both hemispheres. The major pressure belts with approximate latitudes within which they lie are (see Fig. 5.1):

 (i) belt of low pressure along the equator;
 (i) belts of high pressure at about 30° north and south;
 (ii) belts of low pressure at about 60° north and south; and
(iii) belts of high pressure at each pole:

These pressure belts are commonly known as the equatorial low pressure trough; the subtropical high pressure belts or the subtropical anticyclones; the subpolar low pressure troughs or the arctic belts; and the polar anticyclones.
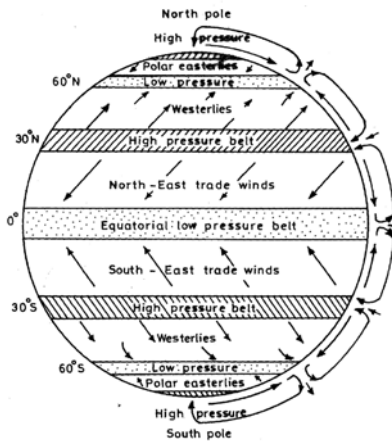
Fig. 5.1. Average wind and pressure belts.

5.1.2 Wind Systems of the Earth

The atmospheric pressure patterns described above give rise to the horizontal motion of air. The air starts blowing from a high pressure area to a low pressure area. As pointed out in Chapter 1, the horizontal motion of air relative to the earth is called wind. Winds are one of the major factors that affect the weather at a place. The average wind systems over a smooth

uniform earth are as shown in Fig. 5.1. In low latitudes, the winds blowing from the subtropical high pressure belts towards the equatorial region of low pressure are called the easterlies or trade winds. These winds are very strong in winter. If the earth were at rest, this would have produced a north wind in the northern hemisphere and a south wind in the southern hemisphere. But on account of earth's rotation, the direction of these winds is from the northeast to the southwest in the northern hemisphere and from the southeast to the northwest in the southern hemisphere. In many areas, they blow with extreme regularity throughout the year, especially over the oceans. Sailing vessels traveling westward once made good use of these winds. That is why they are known as trade winds. The trade winds converge towards the equator, where we find a belt of calm or light and variable winds. This belt is commonly known as Inter Tropical Convergence Zone (ITCZ). Although weather in the trade wind regions is normally fine and quiet, tropical depressions, cyclones and hurricanes are often formed there. These weather systems travel east to west and produce widespread and prolonged heavy rainfall over land areas which often cause severe floods in river catchments.

The winds blowing from the subtropical high pressure belts towards the low pressure areas near 60º parallel of latitudes are called westerlies. These winds blow from west to east. On account of the earth's rotation, these winds blow from the southwest to the northeast in the northern hemisphere and from the northwest to the southeast in the southern hemisphere. The weather of this region is dominated by a fairly regular progression from west to east of low and high pressure systems which are known as extratropical cyclones and anticyclones. These cyclones bring strong winds and cloudy skies accompanied by rainfall or snowfall. The anticyclones are generally associated with fair weather.

In extreme latitudes, the winds blowing from the polar high pressure belts towards the low pressure belt near 60º parallel of latitude are called the polar easterlies. These winds lack force and speed. As they generally blow from east they are called polar easterlies. These winds are extremely cold and dry.

The trade winds, and westerly and easterly winds blow throughout the year and are called planetary winds. The general patterns of pressure and winds are, however, distorted with the seasonal changes. For example, in northern winter intense cooling of the atmosphere over Canada and Siberia interrupts the temperate low pressure belt. The Siberian high pressure intensifies the northeast winds over south Asia. In summer intense heating over subtropical latitudes causes formation of heat lows over the southern part of Asia and southwestern U.S.A., interrupting the subtropical high pressure belt and reversing the normal northeast trade winds to southwest.

5.2 SCALE OF WEATHER SYSTEMS

There are different scales of weather systems ranging from planetary scale to micro scale. All these weather systems of different scales interact with

each other and exchange energy and moisture. For better understanding of their physical and dynamical aspects, the weather systems have been classified into four broad categories as given in Table 5.1.

Table 5.1: Classification of weather systems

Weather Systems	Phenomena	Horizontal Scale (km)	Vertical Scale (km)	Time
1. Planetary scale	Trade winds, ITCZ	5000-10,000	10	> 7 days
2. Synoptic scale	Cyclones	500-2000	10	2-7 days
3. Meso scale	Land and sea breeze	1-100	1-10	1-10 hrs
4. Micro scale	Dust whirl, thunderstorm	< 1	< 1	< 1 hr

The planetary, synoptic, meso, and micro scale systems have wavelengths of order of 5000–10,000 km, 500–2000 km, 1–100 km and less than 1 km, respectively, with time scales of about a week or more, 2–7 days, 1–10 hours and less than one hour, respectively. Some of the important planetary scale systems are the inter-tropical convergence zone (ITCZ), the sub-tropical westerly jet stream in the upper troposphere during the period October to May over northern India, and the tropical easterly jet stream in the upper troposphere during the monsoon season of June through September. The important synoptic scale systems are cyclones, anticyclones, monsoon depressions, extra tropical cyclones, easterly waves in the trade winds, and the Rossby waves in the mid-tropospheric levels in middle latitudes. Over the Indian region these synoptic scale systems form over preferred regions.

Weather systems of tropics are quite different from those of middle or temperate latitudes. The temperate latitude regions do not have a specific rainy season as against tropical areas particularly those affected by tropical depressions and storms. The weather of the temperate latitudes is dominated by a fairly regular progression from west to east of low and high pressure systems which are known as extra-tropical cyclones and anticyclones. In what follows many facts on the weather systems would be gleaned.

5.3 PLANETARY SCALE WEATHER SYSTEMS

5.3.1 Inter Tropical Convergence Zone (ITCZ)

The subtropical high pressure belts lie at about $30°$ North and South parallels of latitudes in both the hemispheres. The area of the globe between these two subtropical high pressure belts is called tropical region. From these high pressure regions, the northeast and southeast trade winds blow towards the equator where they converge in a zone of low pressure known as the inter tropical convergence zone (ITCZ). The ITCZ surrounds the whole earth. Because of the convergence of the moisture laden trade winds from the north

and the south ITCZ is a zone of ascending motion and high convective activity. It is a zone of cloudiness which is the breeding place for tropical migratory systems, such as lows, depressions, storms and cyclones as can be seen most clearly in satellite pictures. At the earth's surface, ITCZ generally coincides with warmest temperatures and lowest pressures. For this reason it is also called Thermal equator.

The apparent annual migration of the sun latitudinally between the tropics of Cancer and Capricon, the ITCZ moves northward and southward into the subtropics during the year. It occupies northern-most position during July and southern-most position during January. The surface position of ITCZ during January and July is shown in Fig. 5.2. The time of its extreme northern-most position lags behind the northern summer solstice by about 3-4 weeks as also the time of its extreme southern-most position lags behind the southern summer solstice with a period of about 3-4 weeks. The shift position of the ITCZ is known as the monsoon trough. With the northward movement of the ITCZ, southwesterlies begin to intrude into southeast Asia. As such, ITCZ is closely associated with monsoons in Southeast Asia.
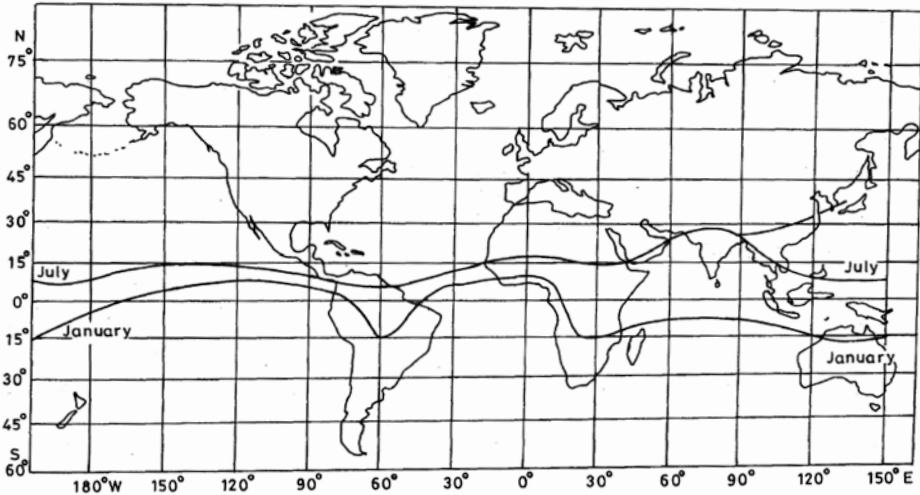
Fig. 5.2. Surface position of ITCZ during January and July
(after Asnani, 1993).

5.3.2 Jet Stream

In the prevailing westerlies of middle latitudes in the northern hemisphere, high speed winds blow from west to east near the tropopause. Its existence in westerlies was discovered in the 1940s. These westerly winds which often record speeds as high as 200 to 300 km/h are known to meteorologists as the westerly jet streams of middle latitudes. Normally, a jet stream is thousands of kilometers in length, hundreds of kilometers in width and a few kilometers in depth. A jet stream follows a sinuous path and achieves its maximum

force and extent in winter when there may be two or even three different currents. In summer it has a mean position at higher latitudes and its speed and extent are reduced.

Observations in the southern hemisphere indicate the existence of a similar jet stream system in comparable latitudes crossing South America, Australia and New Zealand. Over the low latitude margins of the westerlies the subtropical westerly jet stream persists through most of the year. There is a generic relationship between the jet stream and cyclone development. The jet stream seems to exert a definite steering control over cyclonic paths and in the forecasting of cyclonic motion.

Another jet stream system blowing from east to west is the easterly jet stream of low latitudes. It exists mainly over southern India and the Gulf of Aden during the monsoon months. Two types of jet streams, namely the subtropical westerly jet stream (STWJ) and the tropical easterly jet stream, that occur over the Indian monsoon region are shown in Fig. 5.3.
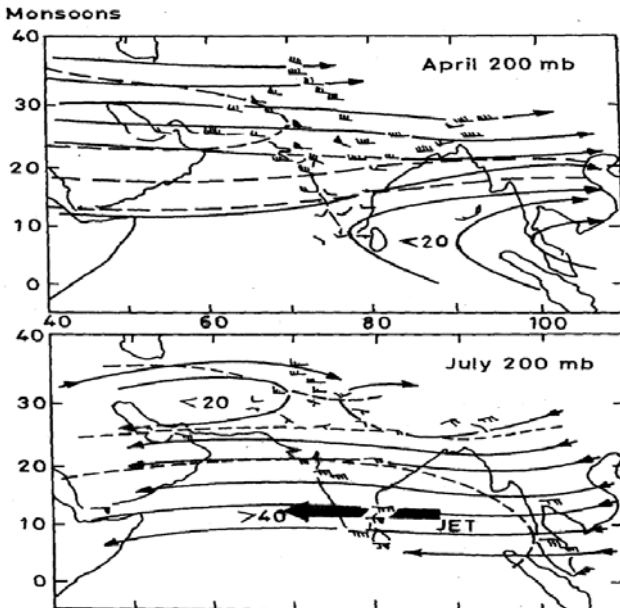
Fig. 5.3. Position of the tropical easterly jet (TEJ) in July and the subtropical westerly jet (STWJ) in April.

5.4 SYNOPTIC SCALE WEATHER SYSTEMS

5.4.1 Cyclones

The word cyclone is used in meteorology to indicate a system of winds blowing around a low pressure center. Winds around such a center circulate anticlockwise in the northern hemisphere and clockwise in the southern

hemisphere. Figure 5.4(a) shows schematically the pressure pattern and wind circulation associated with cyclonic system. The diameter of cyclones is of the order of 1000 km and cause cloudy skies, heavy rainfall and strong winds. Cyclones are of two types. First, cyclones developing in middle latitudes are usually called extratropical cyclones. They develop in middle latitudes and move from west to east and being steered by the westerlies of the mid latitudes. Second, a much more violent phenomena, characteristic of the tropics which are usually called tropical cyclones.

Cyclones in the tropics form over different oceans within a low latitude belt which is a little beyond 5° from the equator. They are known as *hurricanes* over north Atlantic and the portion of the Pacific Ocean close to west coast of U.S.A. and of Mexico, *typhoons* in the west Pacific, Willey Willey over Australian coast and *cyclones* in the Indian Ocean. Upon formation these tropical cyclones move from east to west. On average approximately 80 tropical cyclones with maximum sustained winds of 40-50 knots occur each year over the earth. Of these, about 70% form over northern hemisphere. Most cyclonic storms form over northern west Pacific Ocean (26%). The frequency of occurrence of cyclonic storms over north India is about 6%. Cyclonic storms do not form within five degrees of the equator. Cyclogenesis is specially favored near the seasonal location of the ITCZ. Southeast Pacific and south Atlantic oceans are free of cyclonic storms because in these areas Sea Surface Temperature (SST) is low and equatorial trough does not form. A detailed discussion on tropical cyclones is given in Chapter 7.
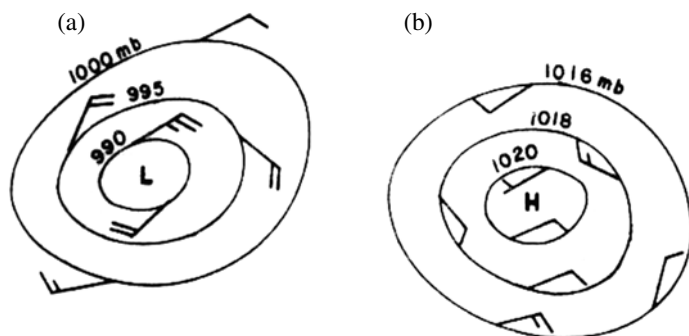
Fig. 5.4. Pressure patterns and wind circulation in (a) cyclonic and (b) anticyclonic.

5.4.2 Anticyclones

The word anticyclone is used to indicate a system of winds blowing around a center of high pressure. In other words a high pressure system is usually called an anticyclone. Winds around such a center circulate clockwise in the northern hemisphere and anticlockwise in the southern hemisphere [see Fig. 5.4(b). These are regions of descending air motion, clear skies and dry weather. Anticyclones are a permanent feature over the continental areas in

the northern winter months. They form because of the large radiative cooling of the land surfaces compared with the oceanic areas. A large quasi stationary anticyclone lies over Siberia throughout the northern winter season. A system of elongated and persistent anticyclones extend round the globe over the sub-tropical belts at 30 degrees latitude of both the northern and southern hemispheres throughout the year. They are known as subtropical anticyclones.

5.4.3 Asian Monsoon Winds

In some regions of the world a system of alternating winds blow in the year due to the seasonal heating and cooling of oceans and continents. They are called monsoon winds. The name monsoon which is derived from the Arabic word 'mausim' meaning season was originally given about six hundred years ago by Arab navigators of sailing ships to those seasonal winds of the Arabian sea which blow consistently for about six months from the northeast during the northern winter and six months from the southwest during the northern summer. The physical cause of these winds has been found to be in the differential heating of land and sea by the Sun's radiations. The effect of differential land-sea heating will be illustrated by the land and sea breeze phenomena later in this chapter. Meteorologically the Asian monsoon is the best known example of an alternating circulation wind system which develops in response to the differential heating of land and sea. Characteristics of the Asian monsoons have been described by several workers (Ramage, 1971; Krishnamurti, 1979; Das, 1995; Fen and Stephen, 1987; Warren, 1987).

In the northern hemisphere, a low pressure area is created in central Asia on account of the excessive heat in summer. This being the winter season in the southern hemisphere, a high pressure area is created there. As a result of this pressure gradient, the winds start blowing from the high pressure area in the southern hemisphere towards the low pressure area in the northern hemisphere. When these winds reach the northern hemisphere after crossing the equator they are deflected due to the action of Coriolis force and become southwesterly (Fig. 5.5a). These winds blow during the period from June to September. After a long journey over the ocean they get highly charged with moisture and on reaching the Indian subcontinent they cause rainfall. Normally, the monsoon strikes the southern tip of the west coast of India in early June, advances northward, and is established over most of the country by the end of June. Most of the annual rainfall over India occurs during the southwest monsoon winds from June to September. In this season cyclonic storms from the Bay of Bengal and the Arabian Sea produce very heavy and widespread rainfall. Monsoon winds are observed in India and its neighboring countries as well as in North Australia, East Africa and Central America.

As the winter season approaches, in the northern hemisphere a high pressure area is created in central Asia. Since there is summer at this time in the southern hemisphere, a low pressure area is formed there. Hence, under its influence the winds reverse the direction and start blowing from

cold central Asia to southern hemisphere in the northeast direction. They are called the northeast monsoon winds (Fig. 5.5b). They are not as strong as the southwest monsoon winds. These northeast winds being of continental origin are dry but during their passage over the south China sea and the Bay of Bengal they pick up moisture and cause much rains over southeast Asian countries (Malaysia, Indonesia, Singapore, etc.) and east coast of India, respectively, during October to December.
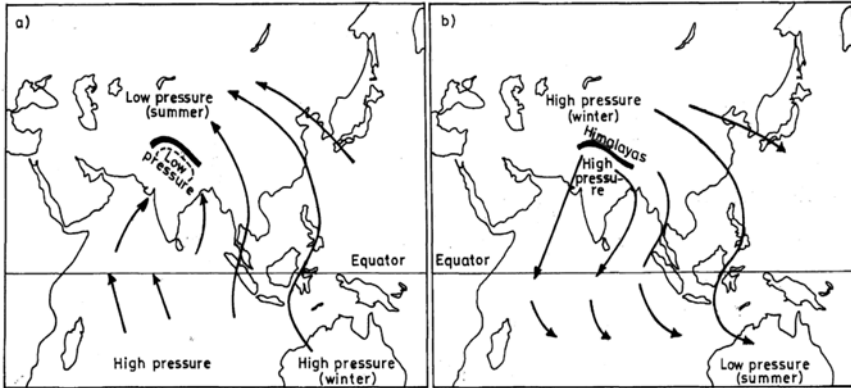
Fig. 5.5. (a) Southwest monsoon winds, and
(b) northeast monsoon winds.

Although the word monsoon is used as a name for the periodic winds in south and southeast Asia, similar systems exist everywhere where large temperature differences develop between oceans and continents. In high and mid latitudes these seasonal winds tend to be overshadowed by global winds.

5.4.4 Causes of Monsoon

The most important cause of monsoons is the differing nature of the land and sea to seasonal changes in solar energy. The conduction of heat into the earth is a slow process as compared to ocean. In summer, only a few centimeters of soil depth is heated by the solar energy, whereas solar energy is able to penetrate to a depth of at least 200 meters in the ocean. Most of the energy received by the earth is used up in heating the air rather than earth's surface. Consequently, a smaller part of solar heat is available for heating the air. Thus, the rise in temperature in summer is more over continents than over the oceans. The mean summer temperature over land often exceeds those over oceans along the same latitudes by as much as 5 to 10°C. In winter, the situation is reversed, and the large heat storage of oceans leads to higher temperature there than over land. It has been previously pointed out that temperatures are related to pressure by virtue of the fact that warm air is less dense than the cold air and hence exerts less pressure. Thus, warmer areas are associated with low pressure and cold areas with high pressure. This

gives a pressure gradient from south to north in summer for winds to blow from ocean to land. In principle, the causes are essentially the same as those of land and sea breezes but they exist on much larger time and distance scales and interact with the winds of the upper troposphere.

If it was only a difference in the response of the land and oceans to incoming solar energy, then why are monsoons not observed wherever large areas of land are surrounded by oceans? The answer is the energy required to set up a reversal of winds on a scale comparable to the monsoons. So the temperature contrast between land and sea must be very pronounced and persistent to be able to generate a monsoon (Das, 1995). If the thermal contrast was on a smaller scale and lasted for a short time we will observe a phenomenon that is similar to the monsoon. That is a sea breeze.

The importance of differential heating was recognized by Halley in 1686. He suggested this to be the main cause of monsoon winds. While the wind changed the direction every six months over the northern Indian Ocean, this reversal was not observed either over the southern Indian Ocean or over the Atlantic Ocean and the Pacific Ocean. Halley explained this by emphasizing the proximity of the northern Indian Ocean to the land which received an excess of solar radiation. Hadley in 1735 noted that the winds of his model would blow directly towards the coast (either northerly or southerly depending on the season) and not obliquely as the southwesterly or northeasterly observed by the sea traders. Hadley argued that the rotation of the earth would cause the moving air to turn to the right in the northern hemisphere and to the left in the southern hemisphere. These two workers were able to identify that planetary scale monsoon circulation was due to (a) the differential heating of land and ocean, and (b) the deflection of wind due to the rotation of the earth. Both summer and winter monsoons are characterized by seasonal changes in wind and weather as a result of the differential heating of land.

In the case of the summer monsoon there is strengthening of low level winds, pressure gradient and building up of moisture prior to the onset (see Fig. 5.5a). However, in the case of winter monsoon (see Fig. 5.5b), the band of the low level westerlies is less extensive and the activity is mainly confined to southeast Asia and the adjoining areas of the southern hemisphere up to Australia (streams that cross the equator have a greater tendency to become westerly).

5.4.5 Monsoonal Extent

Figures 5.5a and 5.5b show surface winds and the approximate boundaries of separation between the winds of the northern and southern hemispheres in January (winter) and July (summer). In July (summer) over a large part of the Pacific and Atlantic oceans, the ITCZ (see Fig. 5.2) lies a little to the north of the equator, whereas the SE trade winds from the southern hemisphere penetrate deep into the northern hemisphere into India, southeast Asia and

to a smaller extent into Africa. It is interesting to see how the winds are deflected to the right as they cross the equator. On the other hand, in January (winter) the NE trade winds from the northern hemisphere penetrate farthest southward into South America, east Africa, and northeast Australia. Also, another branch of the NE trade winds blowing across Siberian high penetrates into Indonesia, Malaysia and southern half of Indian peninsula. These areas of extensive penetration of air from the colder into the warmer hemisphere are the main monsoon areas. About half of tropics has the monsoon regime. A tendency for NW winds to blow from Atlantic into Europe in summer months sometimes is referred to as European monsoon.

Attempts have been made to separate monsoon regions from non-monsoon regions (for example, Khoromov, 1957; Ramage, 1971). All these attempts are based on changes in surface wind direction between summer and winter seasons. Ramage (1971) discreetly improved on all previous work and has defined the monsoon area by the following criteria:

  i) the prevailing wind direction shifts by at least 120° between January and July;
 ii) the average frequency of the respective prevailing wind directions in January and July exceeding 40%;
iii) the mean resultant wind in at least one of the months exceeding 3 m/sec; and
iv) fewer than one cyclone-anticyclone alternation occurring every two years in either months in a 5° latitude-longitude region.

Figure 5.6 shows the monsoon regions of the earth as defined above. An area 35°N to 25°S and 30°W to 170°E lies in the monsoon climate zone. The monsoon climate regions are: (a) the entire African continent; (b) Indian subcontinent; (c) Southeast Asia (Myanmar, Thailand, Laos, Vietnam,
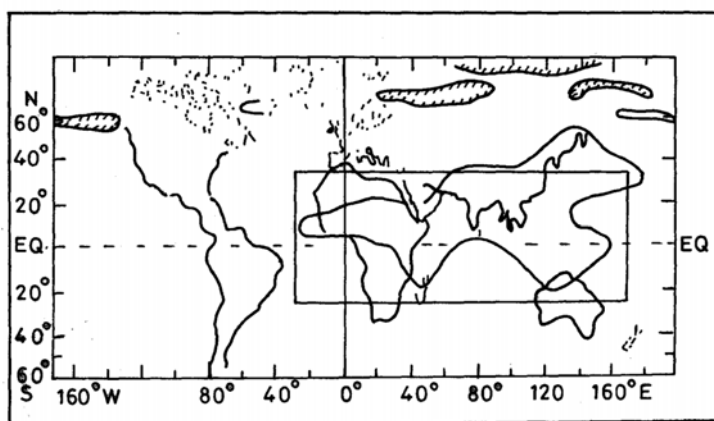
Fig. 5.6. The monsoon regime (after Ramage, 1971). Hatched area is monsoonal and the rectangle broadly indicates the extent of the monsoon regime.

Table 5.2: Mean monthly precipitation (mm) at selected stations in the monsoon climate regions

Location	Jan	Feb	Mar	April	May	June	July	Aug	Sept	Oct	Nov	Dec	Total
Peshawar	39	41	65	42	15	7	34	41	14	10	10	15	333
New Delhi	25	22	17	7	8	65	211	173	150	31	1	5	715
Bombay	2	1	Tr.	3	16	520	709	439	297	88	21	2	2098
Pune	2	Tr.	3	18	35	103	187	106	127	92	37	5	715
Trivandrum	20	20	43	122	249	331	215	164	123	271	207	73	1838
Colombo	88	96	118	260	353	212	140	124	153	354	324	175	2397
Kathmandu	18	17	38	48	90	248	385	286	179	78	6	1	1395
Patna	11	21	35	55	181	293	267	289	235	169	19	1	1576
Madras	24	7	15	25	52	53	83	124	118	267	209	139	1216
Calcutta	14	24	27	43	121	259	301	306	290	160	35	3	1583
Dacca	18	31	58	103	194	322	437	305	236	169	28	2	1903
Rangoon	2	5	8	51	307	483	582	528	394	180	69	19	2619
Bangkok	9	29	34	89	166	171	178	191	306	255	47	7	1492
Chiang Mai	7	11	15	51	139	154	188	220	292	124	38	10	1246
Phnom Penh	7	10	40	77	134	155	171	160	224	257	127	45	1407
Ho Chi Minh City	16	3	13	42	320	331	314	269	336	269	115	56	1984
Kuala Lumpur	171	169	237	279	216	126	102	157	188	275	259	230	2409
Singapore	252	175	200	196	174	171	167	191	179	208	251	266	2430
Manila	13	7	6	24	110	236	253	480	271	201	129	56	1791
Jakarta	335	241	201	141	116	97	61	50	78	91	151	193	1755
Surigao	589	405	398	258	184	112	195	149	197	308	415	653	3863
Sian	5	11	23	41	68	49	89	97	116	57	24	8	578
Nan Chang	55	100	191	250	289	295	257	111	109	57	70	70	1862
Canton	27	65	101	135	256	291	264	249	149	49	51	34	1720
Yülin	11	7	21	29	150	197	149	189	293	190	54	43	1332
Darwin	341	338	274	121	9	1	2	5	17	66	156	233	1562
Cocos Island	216	136	229	236	294	202	262	204	81	109	56	86	2108
Wyndham*	202	163	122	34	10	10	5	Tr	2	9	42	104	703
Marble Bar*	82	70	58	21	23	19	11	5	2	5	8	31	340

[* Western Australia]

Indonesia, Malaysia, Philippines, Kampuchea, Singapore); and (d) North Australia. Table 5.2 gives monthly rainfall at a few selected stations in the monsoon climate regions.

It may be pointed out that the best known of the monsoon winds of the world are those that flow over the Indian subcontinent in the 100-day period between the beginning of June to mid-September each year. The southwest monsoon from June to September provides 75 to 80% of the total annual rainfall over most stations. Cherrapunji in northeast India holds the world's record of maximum rainfall for one month i.e. 930 cm in July 1861 and also for one year – 2646 cm.

5.4.6 Tropical Disturbances and Monsoon Depressions

Tropical disturbances belong to the family of low pressure systems in the tropical areas. A depression or a low is an atmospheric whirlpool with a central region of low pressure. It has been previously pointed out that in the northern hemisphere the winds around such a low pressure center circulate in the anticlockwise direction. The intensity of the whirlpool is measured by the strength of winds. Thus, when the winds round the low pressure center are strong, the depression is classified as a cyclonic storm and so on. The criteria for classifying the atmospheric low pressure systems are given in Table 5.3.

Table 5.3: Classification of atmospheric low pressure systems

System	*Range of wind speed*
Low	< 17 knots (8.5 m/s)
Depression	17-33 knots (8.5-16.5 m/s)
Cyclonic storms	34-47 knots (17-23.5 m/s)
Severe cyclonic storms	48-63 knots (24-31.5 m/s)
Hurricanes/Typhoons	> 63 knots (31.5 m/s)

Monsoon depressions are low pressure areas with two or three closed isobars (at 2 mb intervals) and the surface wind in cyclonic circulation is between 17 and 33 knots. They form over Bay of Bengal (18°N), Arabian Sea and even over land. On average, seven depressions are generated in the SW monsoon season. Their formation in the Bay of Bengal is highest. The most favorable conditions are the areas with the sea surface temperature higher than 29°C and presence of lower tropospheric monsoon trough over North Bay of Bengal. They have a life period of 2 to 7 days. They move westward from the Bay of Bengal across the Indian region and cause heavy to very heavy rainfall along and near their tracks. Heavy rains (often exceeding 10 cm in 24 hr) fall over a 400 km wide strip to the left of monsoon depression tracks. The strip extends from about 500 km ahead to about 500 km behind the center. An interesting sea level pressure map of monsoon

depression at 0830 hrs IST 8 August 1979 is shown in Fig. 5.7. The depression developed in the Bay of Bengal then moved westward over the Indian land with a NW/SE orientation. It is noted that pressure at the center is about 950 mb.

Saha et al. (1981) found that a fair number of monsoon depressions in the Bay of Bengal are activated by westward moving remnants of disturbances that have had their origin far to the east of the Bay of Bengal. There is also a direct relationship between monsoon depressions and tropical cyclones in the South China Sea.
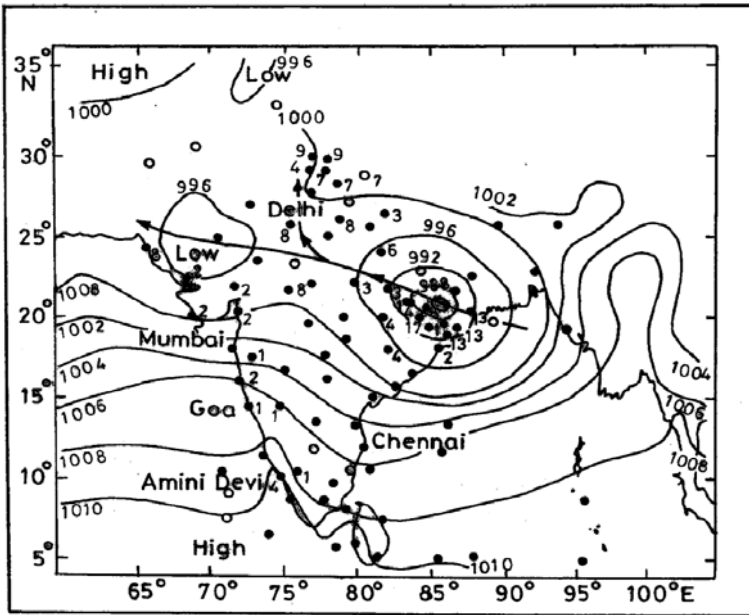
Fig. 5.7. Sea level pressure map of a monsoon depression at 0830 hrs IST 8 August 1979.

5.4.7 Importance of Monsoons

The Asian monsoon circulation brings water to the land areas which are of crucial importance for human life. Population expansion, rapid industrialisation, commercialization of agriculture and quantum jumps in economic activities demand more and more water. Catastrophes occur when there is too much or too little water at both spatial and temporal scales. Because of its profound importance on economy, the monsoon is by far the most important event in meteorology. Numerous studies have been carried out to understand the space-time variation of rainfall during monsoons. Also, beginning from the 1960s, several regional and global scientific initiatives for monsoon research have been sponsored by international organizations/agencies, including the World Meteorological Organization (WMO). Among

those which were relevant to the Asian region were the efforts of the International Indian Ocean Expedition (IIOE) during 1962-65, GARP Atlantic Tropical Experiment (GATE) in 1974, Monsoon Experiments (MONEX) during 1978-79, Tropical Ocean and Global Atmosphere (TOGA) during 1985-95, and the South China Sea Monsoon Experiment (SCSMEX) in 1999. The large volumes of observation data collected during these experiments have been impressive in understanding of the physical causes leading to floods and droughts in the monsoonal regions. The Asian monsoon has a strong seasonal effect on the rainfall regime of India. The spatial and temporal characteristics of rainfall in relation to the weather of India will be discussed in the next chapter.

5.4.8 Easterly Waves

Easterly waves exist in the tropical region of both hemispheres all year round. They are more marked in the northern tropical region during June-September. Starting from the west Pacific, easterly waves begin as weak low pressure systems, near the equatorial ITCZ growing into tropical depressions and occasionally into typhoons which affect the Philippines, South China Sea, Vietnam, south-east China, and Japan. The easterly waves cross Vietnam, Thailand, Myanmar and reach the Bay of Bengal. Under favorable conditions, they may lead to the formation of monsoon depressions over the head of the Bay of Bengal. The easterly waves move across India into the east Arabian Sea and weaken over the west Arabian Sea. They can again be traced over north Africa, west of 30°E. They gain intensity as they move westwards, attaining maximum strength near longitude 5°W. Crossing the west Africa coast, they move into the east Atlantic and then into Atlantic. Here some of the easterly waves trigger the development of west Atlantic hurricanes which affect the West Indies, Gulf of Mexico and the southeast (SE) coast of the United States.

5.4.9 Extra-Tropical Cyclones

Extra-tropical cyclones arise in the belt of westerly winds. They originate at the boundary separating the cold dry air from Polar Regions with the warm moist air from tropical regions, when the two air masses come near each other. The surface separating such different air masses is known as a front. A wave perturbation develops at the frontal surface, gets amplified and begins to move. Under the combined influence of the low level perturbation and the outflow of air at upper levels, a progressive fall of pressure takes place and the system intensifies affecting the weather over large areas as it moves from west to east, being steered by the westerly flow of the mid latitudes.

5.5 MESO SCALE WEATHER SYSTEMS

Land and Sea Breeze

In this section we examine the land and sea breeze phenomenon which is caused by heat capacity differences between land and water. The heat capacity (*H*) of a given substance is the quantity of heat needed to raise its temperature through 1°C. Thus if ρ be the density of the given substance and *s*, its specific heat, the heat capacity of the substance is

$$H = \rho \times s \quad \text{cal/cm}^3/^\circ\text{C} \tag{5.1}$$

The heat capacity of water and soil are 1.0 and 0.6 cal/cm³/°C. Water has, therefore, a relatively large heat capacity as compared to soil. This shows that water requires much more heat to warm up than that for an equivalent volume of soil. Both the land and the sea are warmed during the day by the solar radiation. The land surface, because of low heat capacity, heats up more rapidly than the sea during the day. The land in turn heats up the lower layer of air above it. The warm air rises over the land, producing a lower pressure over the land. On the other hand, because the water has a higher heat capacity and also solar radiation is capable of penetrating to a greater depth the time needed to warm the sea is greater. As a result, the lower layer of air above the sea surface is cooler, producing greater pressure over the sea. As a result of this pressure difference between the land and sea, the cooler air from the sea starts to blow towards the land. This wind is known as sea breeze, as shown in Fig. 5.8a.

The situation is reversed at night because solar radiation is now cut off. The land cools much faster than the sea. As a result, the sea remains warmer than the land. The air pressure on the sea is therefore lower than what it is on the land. The relatively cold air from the land starts to blow towards the sea. This wind blowing from the land to the sea is known as land breeze, as shown in Fig. 5.8b.
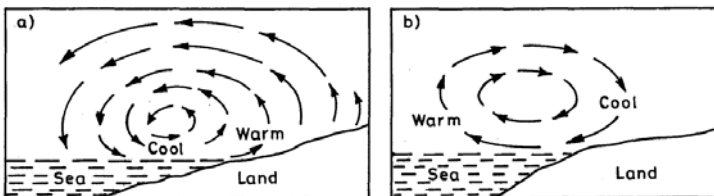
Fig. 5.8. (a) Sea breeze—day time, and (b) land breeze—night time.

The land and sea breeze is important for understanding the periodic winds like monsoons. In summer, which corresponds to the daytime cycle of the sea breeze, monsoon winds blow from the sea towards the land. On the other hand, in the northern winter, which is similar to the land breeze,

there are winds that blow from the land to the sea. The monsoons represent winds on a much larger scale. This scale of motion extends over thousands of kilometers.

5.6 OCEANIC CIRCULATION

Similar to atmospheric circulation, oceans also exhibit oceanic circulation. The movement of a big mass of water in definite direction along the surface of the ocean is called the ocean current. The ocean circulation is slow and most of it is confined to shallow layers on the top. Oceanic circulation occurs because of the action of winds on the water surface and the temperature and salinity differences in different regions of the ocean.

Temperature generally goes on decreasing from the equator to the poles. The water in the equatorial regions of the earth receives much of heat than the water near the poles and expands due to this heat. Its volume increases but its density is reduced and becomes lighter. On the other hand, temperature is low in the polar regions and the water is very cold and dense. Thus, there is a great difference in the density of oceanic waters in the equatorial and polar regions. Hence, surface currents of warm and light waters flow from the equatorial region towards the polar region. Similarly, cold water currents flow from the cold polar region towards the equatorial region. The planetary winds blowing over the surface of the ocean lend speed and direction to these ocean currents. Thus, planetary winds are an important factor driving ocean currents. All the important ocean currents flow in the direction of planetary winds. The factors, such as the rotation of the earth, the difference in the salinity of oceanic waters and the configuration of the continental coastlines, affect the direction of oceanic currents. We find a specific pattern of ocean currents which is a consequence of the location of the continents on the earth, their size and their north-south extent. The main features of the ocean current circulation are shown in Fig. 5.9.
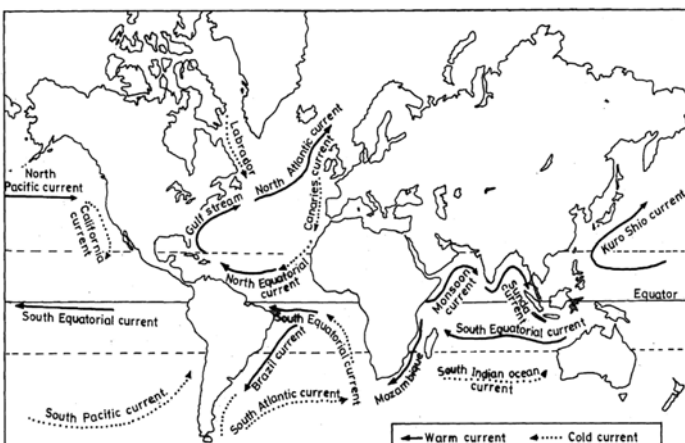
Fig. 5.9. Important ocean currents.

The ocean currents are of two types: warm water currents and cold water currents. Ocean currents flowing from relatively warm waters towards cold water are called warm currents. Currents flowing from cold water towards warm water are called cold currents. Ocean currents are generally named after the regions along which they flow. The warm ocean current flowing along the Brazilian coast is called the Brazil current and the cold current flowing along the Labrador coast is known as the Labrador current. Waters of the North Atlantic Ocean flow west from the west coast of Africa. This current flows parallel to the equator and is divided by the corner of Brazil into two branches. One of the branches flows towards the northwest and enters the Gulf of Mexico and extends toward the Norwegian Sea and the Barents Sea. Hence, it is called the Gulf Stream. This is a warm current and vast masses of warm water are transported from low to high latitude and this reduces the meridional temperature contrast that otherwise would exist.

The counterpart to the warm Atlantic current is the Labrador current, which transports cold water of low salt content out of the Arctic Ocean extending southward to the Grand Bank and the New England coast. The cold Labrador current meets the Gulf Stream near the eastern coast of North America. Foggy weather prevails where these two currents meet. Figure 5.9 shows that the Gulf Current, while flowing northward, enters the zone of westerlies and flows along the coast of the British Isles. Here this warm current is called the North Atlantic current. One branch of this current enters the North Sea in the north. The other branch flows along the west coast of Portugal and Morocco towards the equator. It is called the Canaries current. Particularly during the warmer part of the year, when the prevailing winds are from north, the upwelling of cold water from the depths along these coasts creates a strong temperature contact between the coastal waters and the adjacent land areas.

On the North Pacific Ocean the current system is essentially the same as on the North Atlantic. In particular, here the Kuroshio current brings much warm water toward the Gulf of Alaska, the cold polar current, the Oyashio along the east coast of Asia.

The ocean currents have a great effect on human life. The climate of the coastal areas is influenced by these currents. The climate of Western Europe is warmer because of the warm North Atlantic current. That is also why water near the ports there does not freeze even in winter. Similarly, it moderates the climate of the British Isles to some extent. On account of the difference in temperature, foggy weather prevails near the meeting point of warm and cold ocean currents. At the same time, it creates conditions favorable for fishing. That is why places where the warm and cold currents unite develop into well-known fishing grounds.

REFERENCES

Asnani, G.C., 1993. Tropical Meteorology. Published by G.C. Asnani, Pune, India, 1202 pp.

Das, P.K., 1995. The Monsoons. National Book Trust, India, 252 p.

Fein, J.S. and Stephens, P. L. (eds.), 1987. Monsoons. New York, John Wiley and Sons.

Khromov, S.P., 1957. Die Geographische Verbreitung der Monsune Petermanns Geogr. Mitt., 101, pp. 234–237.

Krishnamurti, T.N., 1979. Tropical Meteorology: Compendium of Meteorology, Vol. II. WMO No. 364, WMO, Geneva.

Lau, K.H. and Li, M.T., 1984. The monsoon of east Asia and its global associations– A survey. *Amer. Meteor. Soc.*, 65, pp. 114–125.

Ramage, C.S., 1971. Monsoon Meteorology. London, Academic Press.

Saha, K.R., Shukla, J. and Sanders, F., 1981. Westward propagating predecessors of monsoon depressions. *Mon. Weather Rev.*, USA, 139 (2), pp. 330-343.

Warren, B.A., 1987. Ancient and medieval records of the monsoon winds and currents of the Indian Ocean. *In*: Monsoons. J.S. Fein & P.L. Stephens (eds.), pp.137– 158, New York, John Wiley & Sons.

6 Weather and Precipitation in India

Currently, water is used in five major sectors: domestic (including drinking water), agriculture, industry, power generation and environmental conservation. As a result, sustainable access to safe water and improved sanitation has become an urgent issue in many countries of the world. We know that precipitation brings water to the earth's surface and the occurrence of precipitation can be considered to be a process of weather systems. More detailed discussion on various weather systems that produce precipitation have been presented in the previous chapter. The theme of this chapter, therefore, is to provide an overview of weather systems and precipitation in the context of an ideal region to get a realistic picture of the status of water availability.

The region of India was selected as the study area because the country with one sixth of the world's population and diversity of topography, soils, climate, etc., has always been facing challenges in the area of water resources. For example, the water availability per capita in India was over 5000 m^3 per annum in 1950. It now stands at hardly more than 2000 m^3 per capita. With every increase in population, there is a corresponding decline in per capita availability of water. Obviously, judicious use of water resources requires a detailed account of various characteristics of weather systems and the distribution of rainfall provided by them over different parts of the country so that renewable water resources can be harnessed effectively to serve man's needs.

6.1 LOCATION AND AREA OF INDIA

India is one of the major countries of the Asian subcontinent. It is separated from the rest of Asia by high mountains of Suleman, the Karakoram and the Himalayas, as shown in Fig. 6.1. To the northwest of India is Pakistan, while China, Nepal, and Bhutan are in the north and Myanmar and Bangladesh in the east. The Bay of Bengal is in the east, the Arabian Sea in the west and the Indian Ocean is to the south of the country.

The Indian mainland extends north-south from about 8°N to 37°N and east-west from 68°E to 97°E. The total area of the country is 32,87,263 km² and by size it is the 7th largest country in the world. The tropic of cancer passes through the middle of the country. The population, according to 2001 census, is over one billion. It is important to identify how big the size of India is in comparison with other countries of the world. The area of India in comparison with areas of some European and Asian countries is shown in Table 6.1. The area of India is almost one third of China and 14 times that of the United Kingdom.

Table 6.1: Land area of India in comparison with other countries of the world

Country (European)	Population (million)	Area (km²)	Country (Asian)	Population (million)	Area (km²)
France	61	543965	India	1080	3287263
Spain	41	504750	China	1806	9561000
Sweden	9	449793	Pakistan	162	796095
Norway	5	323895	Indonesia	242	1904569
Italy	38	301278	Thailand	66	513115
United Kingdom	61	244108	Malaysia	24	330434
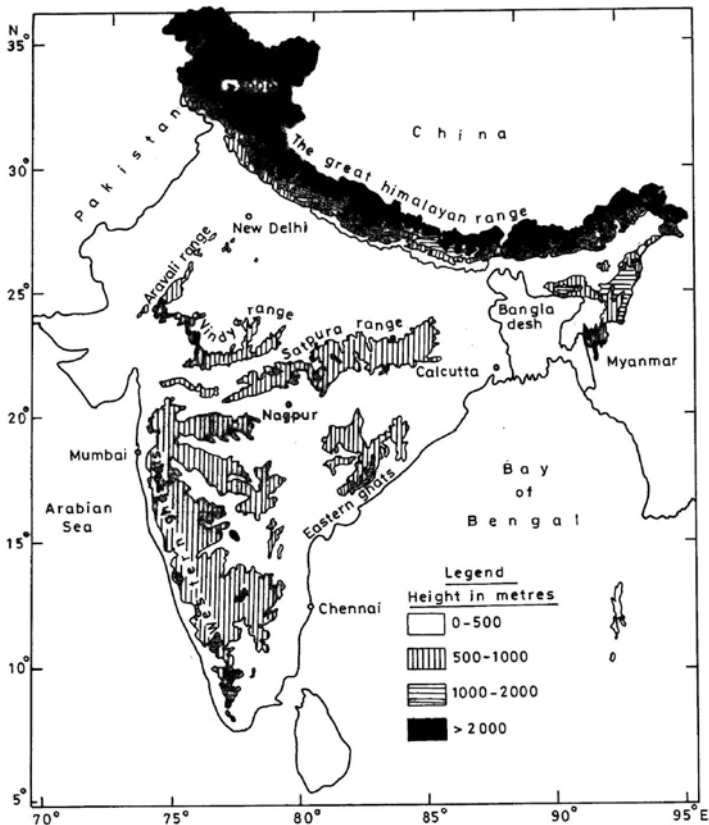
Fig. 6.1. Physical map of India showing mountains.

6.2 LAND FORMS OF INDIA

The most salient fact with regard to both the physical geography and geology of the Indian region is that it is composed of three distinct units or land forms which are as unlike in their physical as in their geological character (Wadia, 1978). These three land forms are:

- The triangular plateau of the peninsula south of the Tropic of Cancer (23.5°N).
- The mountainous region of the Himalayas which borders India to the north, west and east.
- The great Indo-Gangetic Plain separating the above two areas and extending from the valley of the Indus to the Brahmaputra in Assam.

The peninsular India consists mainly of a plateau of altitude 500-1000 meters. The main ranges of peninsula are Western and Eastern Ghats, and Vindhya-Satpura. The Western Ghat is 1400 km long, with peaks usually 1200-1800 m high.

To the north of the peninsula is the low land area formed by the valleys of the Indus River, the Ganga River and the Brahmaputra River. The area extends from west to east for about 2400 km and from north to south for about 240 km to 320 km. To the north of this extensive plain is the high barrier of the Himalayan Mountains rising to an average height of 6.5 km and further north is the Tibetan plateau with an average elevation of 3 km. The Himalayas extending for more than 2400 km from the Indus to the Brahmaputra comprise three parallel ranges interspersed with large plateaus and valleys:

 (i) Greater Himalayas (average height 6000 m) with high glacier concentrations near peaks, such as Nanga Parbat (8125 m), Mount Everest (8848 m) in Nepal, Kanchanjunga (8597 m), and Nanda Devi (7816 m).
 (ii) Middle Himalayas with an average height of 3700 to 4000 m and alternate ridges and valleys of 60-80 km wide.
(iii) Siwalik with an average height of 900-1200 m.

For administrative purposes the country is divided into 28 states and seven Union Territories, as shown in Fig. 6.2 and Table 6.2.

6.3 CLIMATIC CONTROL

The main factors which control the weather and climate of a region are geographical and atmospheric conditions. These include (a) latitude, (b) mountain ranges, (c) land and water distribution, (d) altitude, (e) wind, (f) air mass, (g) ocean currents, and (h) depressions and storms. India has a wide range of weather and climatic regimes from arid to humid arising due

Table 6.2: States and union territories of the Indian Union

S.No	States of India	Area (km^2)
1	Andhra Pradesh	275069
2	Arunachal Pradesh	83743
3	Assam	78438
4	Bihar	94163
5	Chattisgarh	136034
6	Goa	3702
7	Gujarat	196024
8	Haryana	44212
9	Himachal Pradesh	55673
10	Jammu & Kashmir	222236
11	Jharkhand	79714
12	Karnataka	191791
13	Kerala	38863
14	Madhya Pradesh	308144
15	Maharashtra	307713
16	Manipur	22327
17	Meghalaya	22429
18	Mizoram	21081
19	Nagaland	16579
20	Orrisa	155707
21	Punjab	50362
22	Rajasthan	342239
23	Sikkim	7096
24	Tamil Nadu	130058
25	Tripura	10491
26	Uttaranchal	53483
27	Uttar Pradesh	238566
28	West Bengal	88752
-	India	3290000

Union Territories		
1	Andaman & Nicobar Islands	8249
2	Chandigarh	114
3	Dadra & Nagar Haveli	491
4	Daman & Diu	112
5	Delhi	1483
6	Lakshadweep	32
7	Pondicherry	480

to the influence of these factors. The tropic of cancer passes through the middle of the country. A large part of the peninsula comprising nearly 1/3 of the country lies to the south of this parallel. This region experiences high temperatures over a large part of the year.

Fig. 6.2. Map of India showing different states.

The Himalayas run along the northern border of India in an east west direction. It exercises a dominant influence, vitally affecting both climate and hydrology of India. Central Asia that lies to the north of these ranges has abnormally low temperatures in winter. The cold winds that blow towards south, i.e., towards India, are blocked by the Himalayas. Excluding the northern high lands, the entire northern plains experience mild winter. Its high snowing ranges have a moderating influence on the temperature and humidity of northern India. Due to its high altitude and its situation directly in the path of the monsoons, it is most favorably conditioned for precipitation of much of their contained moisture either as rain or snow. Glaciers of enormous magnitudes are nourished on the higher ranges by this precipitation which together with the abundant rainfall in lower ranges feeds a number of rivers flowing down to the fertile plains.

6.4 RIVER BASINS OF INDIA

River basins are highly integrated hydrological systems with the same water flowing and recycling through the domestic, agricultural, industrial and environmental sectors. The major river basins of India which are 14 in number have been shown in Chapter 1 (see Fig. 1.4). These rivers can be grouped into five different zones: (1) the west flowing rivers, such as the Narmada and the Tapi; (2) the east flowing rivers, such as the Mahanadi, the Godavari, the Cauvery, and the Pennar; (3) the Ganges and its tributaries, (4) the Indus and its tributaries, and (5) the Brahmaputra River. The total catchment area of all the rivers in India is approximately 3.05 million km^2. The rivers in the northern part of India are both snow-fed and rain-fed and continuously flow throughout the year. The rivers in southern India are entirely rain-fed, with the result that many of them have low or negligible flow during hot summer season. The surface water potential of these river systems is given in Table 6.3.

Table 6.3: Surface water resources for different rivers in India

River basins	Surface runoff (km^3)	% of the total
1. West flowing rivers like Narmada and Tapi	306	16
2. East flowing rivers like Mahanadi, Godavari, Krishna, Cauvery and Pennar	356	19
3. The Ganges and its tributaries	550	29
4. Indus and its tributaries	79	4
5. Brahmaputra River	590	32
Total surface runoff	1880	100

The total annual surface runoff in the rivers of India, including the groundwater recharge from rainfall, has been found to be 1880 km^3. On the basis of rainfall data, the mean annual rainfall of India (given later in this chapter) is estimated to be about 117 cm. This mean annual rainfall over the country is equivalent to a volume of water of about 3840×10^9 m^3. This shows that for India as a whole about 49% of the annual rainfall is converted into surface runoff and ground water and the remaining 51% of the total rainfall is lost to the atmosphere by evaporation and evapotranspiration. Because of the limitations imposed by topography, climate and soil conditions, only about 720 km^3 can be used, which represents about 39% of the average total in the various river systems of the country.

6.5 RAINFALL AND RUNOFF OF CONTINENTS

The extent of India's surface water resources is given in Table 6.4 where rainfall and runoff are compared for the six continents.

Table 6.4: Rainfall and runoff of the continents
[E=evaporation, and ET= evapotranspiration]

Region	Area (1000 km²)	Annual rainfall (cm)	E & ET as a % of rainfall	Runoff as a % of rainfall
Africa	30210	66	76	24
North America	24260	66	60	40
South America	17790	135	64	36
Asia	44030	61	64	36
Europe	9710	58	60	40
Australia	7690	42	87	13
India	3290	117	51	49

6.6 THE SEASONS OF INDIA

From the stand point of weather and climate the year in India can be divided into the following four seasons:

  (i) Winter (January and February)
 (ii) Hot weather (March to May)
(iii) Rainy southwest monsoon (June to September)
(iv) Northeast monsoon (October to December)

6.6.1 Winter Season

The winter season remains from January through February and January is the coldest month. The season is characterized by low temperatures, generally clear skies and fine weather for the country as a whole. The extreme northern parts of India experience the influence of extra-tropical weather systems which cause periodic spells of cloudiness and rainfall or snowfall. These are known as western disturbances. In the rear of some of these disturbances, the northern and central parts of the country experience pronounced spells of cold weather, known as cold waves, due to the invasion of cold air from higher latitudes. Depressions and storms in the Indian seas are rare in these months.

6.6.2 Hot Weather Season

The month of March marks the beginning of hot weather and the temperature starts rising progressively from April through June. On the 21st of March the sun rays fall vertically on the equator. Thereafter the apparent movement of the sun is towards north. During this period the sun rays are more or

less vertical in India. The days are long and nights are short. As a result, temperature rises, thereby creating hot weather conditions in India. In the month of May, the highest temperature is recorded in northwest India. In this season, the afternoon temperature rises to about 40°C and very hot winds blow in north India. They are called *Loos*. Over Rajasthan and adjoining areas, convective activity is often manifested as dust storms. During this season, there is an increasing thunderstorm activity over the southern parts of the peninsula and over northwest India. The thunderstorms over northwest India, known as Norwesters, are of great severity. Cyclonic storms form in the Bay of Bengal in April and their frequency increases in May.

6.6.3 Southwest Monsoon Season

The southwest (SW) monsoon is the major rainy season for India. Most parts of the country receive 75-80% of the annual rainfall during the four months of the SW monsoon season. The monsoon circulation gets established and rainfall sets in over south Kerala and over northeastern India in early June. The rains advance from south to north across the peninsula and from east to west across north India. By the second week of July the monsoon rains spread over the entire country. The rains begin receding from northwest India by the beginning of September. Although the SW monsoon season is taken to be four months but its actual period varies from less than 75 days in the western parts to above 150 days over certain parts of peninsular India.

From time to time monsoon weather systems (cyclonic storms) which develop in the Bay of Bengal move through the central parts of the country beyond Rajasthan where they dissipate. In their journey across the country they cause heavy rains along and around their tracks. Many of these disturbances do not intensify beyond the depression stage (see Table 5.3). Widespread and heavy rains can produce deadly and destructive floods. The India Meteorological Department maintains a constant vigilance on cyclonic storms throughout the season. Figures 6.3 and 6.4 show tracks of depressions/storms for the months of July and August.

6.6.4 Northeast Monsoon

The month of October is the transition period between the southwest monsoon and winter conditions. The northeast (NE) monsoon period is comparatively drier throughout the country except for the states of Andhra Pradesh and Tamil Nadu. The NE monsoon winds blow from the land towards the sea. While blowing over the waters of the Bay of Bengal they acquire moisture and give rains to Tamil Nadu as well as the east coast of Andhra Pradesh. Cyclonic storms of severe intensity form in the Bay of Bengal and the Arabian Sea during the months of October and November and with less frequency in December. Tracks of cyclonic storms for October are shown in
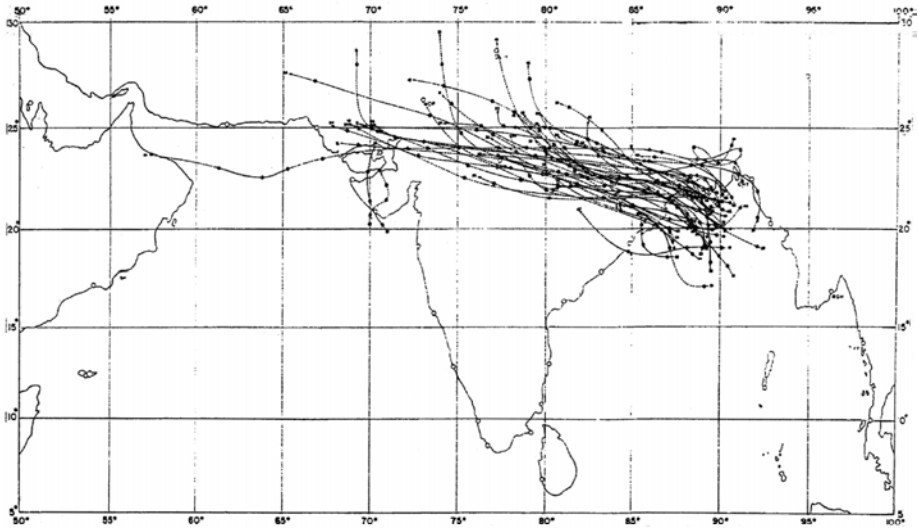
Fig. 6.3. Tracks of cyclonic storms in July.
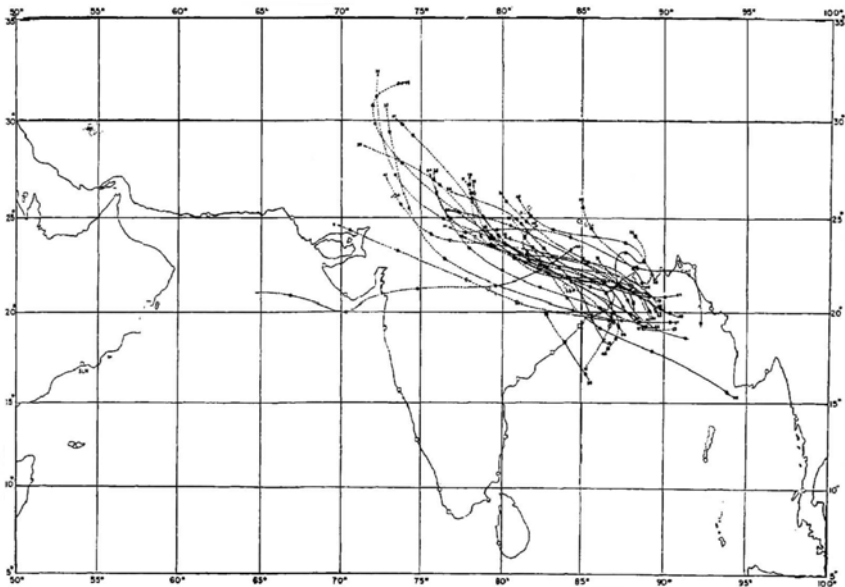
Fig. 6.4. Tracks of cyclonic storms in August.

Fig. 6.5. These cyclones strike coastal areas and cause intense rainfall and heavy damage to life and property.
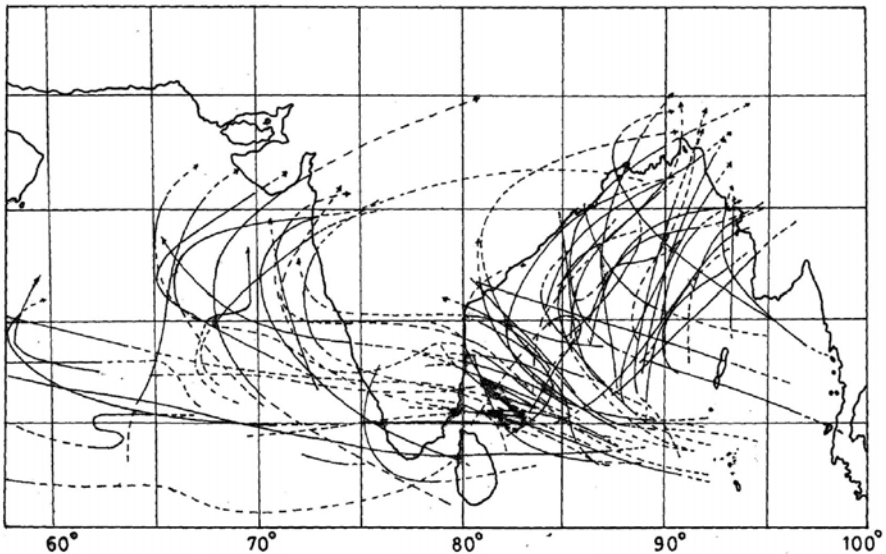
Fig. 6.5. Tracks of cyclonic storms in October.

6.7 SEASONAL VARIATION OF PRESSURE

The pressure distribution for January is shown in Fig. 6.6. This figure shows a weak ridge of high pressure over north India and trough of low pressure from Kerala to Gujarat. In general surface pressure increases from south to north.

The month of March marks the beginning of summer and temperature starts arising progressively. The increase in temperature in April causes a fall in the atmospheric pressure. The pressure distribution for April is shown in Fig. 6.7. The pressure gradient across the country is weak and the surface pressure decreases from south to north.

The pressure distribution for July is shown in Fig. 6.8. The lowest pressure is over central Pakistan with average pressure around 994 mb. A trough of low pressure lies over north India with its axis from northeast of Rajasthan to the northern part of the Bay of Bengal which is referred to as the monsoon trough. A strong south to north pressure gradient from south Arabian Sea/south Bay of Bengal up to the monsoon trough exists which is about 12 mb.

Figure 6.9 shows pressure distributions for October. The pressure field is flat over India and its neighborhood. However, by the middle of October surface pressure gradients reverse across the country with higher pressure building up over north India. Winds now blow from the high pressure area on land to the low pressure area on the Indian Ocean.
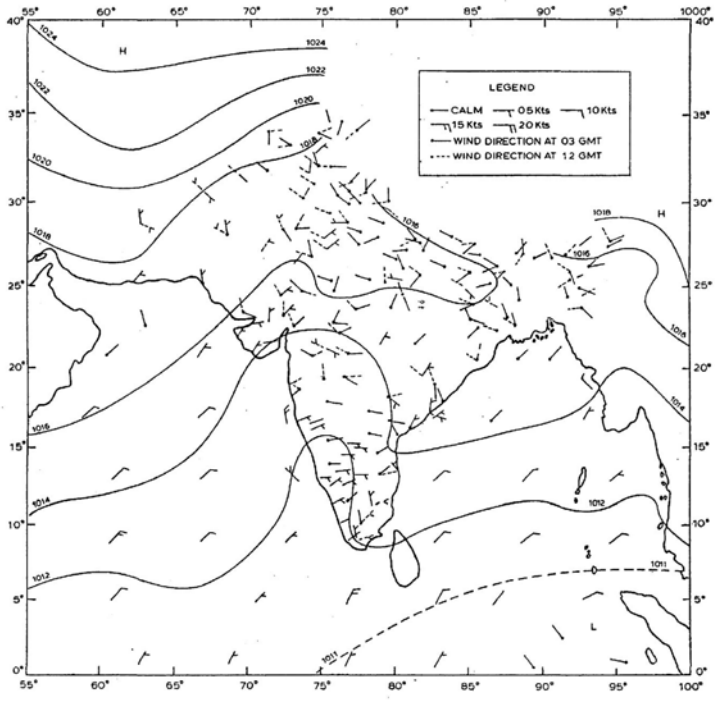
Fig. 6.6. Mean pressure (mb) and surface wind distribution during January.
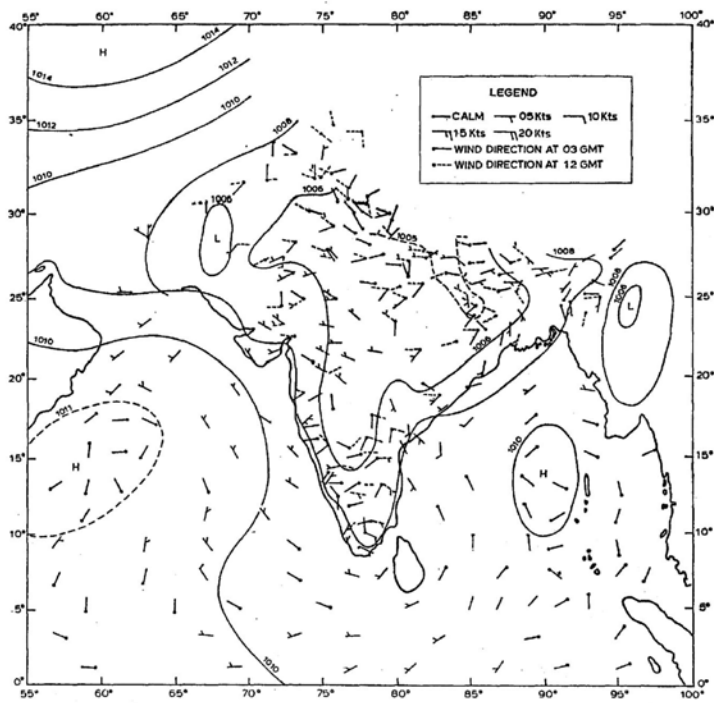
Fig. 6.7. Mean pressure (mb) and surface wind distribution during April.
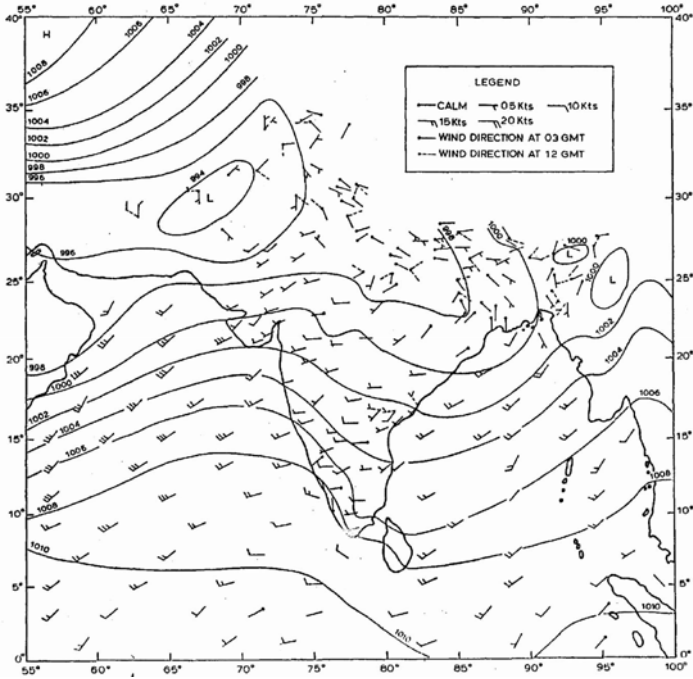
Fig. 6.8. Mean pressure (mb) and surface wind distribution during July.
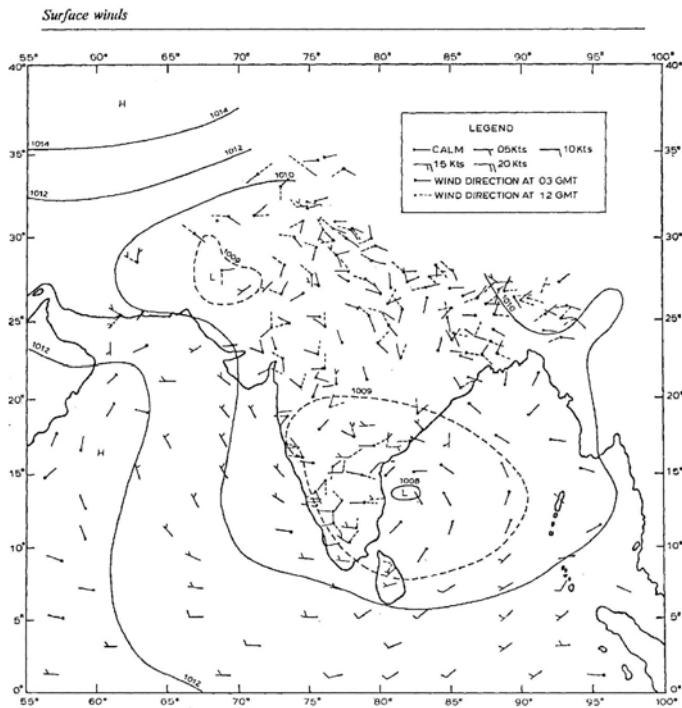
Fig. 6.9. Mean pressure (mb) and surface wind distribution during October.

6.8 MEAN SEASONAL VARIATION OF AIR TEMPERATURE

6.8.1 Average Temperature

Figure 6.10 shows the distribution of the average daily air temperature (reduced to the sea level) for the four representative months of January, April, July and October. The average daily air temperature as shown in the figures is the average of daily maximum and the minimum temperatures. The temperatures range from about 15° to 25°C in January, from 25° to 35°C in April, from 28° to 35°C in July, and from 27° to 29°C in October.

   In January, a more regular latitudinal distribution of the average temperature is evident. Average temperatures range from 15°C in the north to 25°C in the south. This is the month with the lowest temperature in all parts of the country. The months with the highest average temperature are April or May in the south and June in the north. The slightly lower temperature of July is due to the increase in cloudiness during the monsoon season.
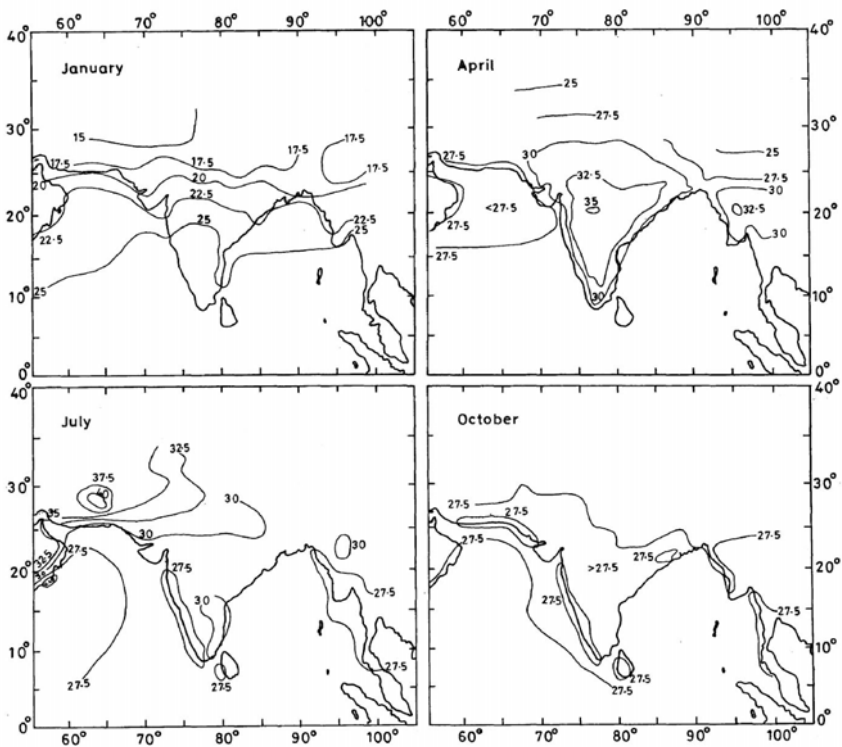
Fig. 6.10. Average daily air temperature (°C).

6.8.2 Average Daily Maximum Temperature

Maps of average maximum and minimum temperatures (January, April, July and October) are shown in Figs 6.11 and 6.12, respectively. In April average
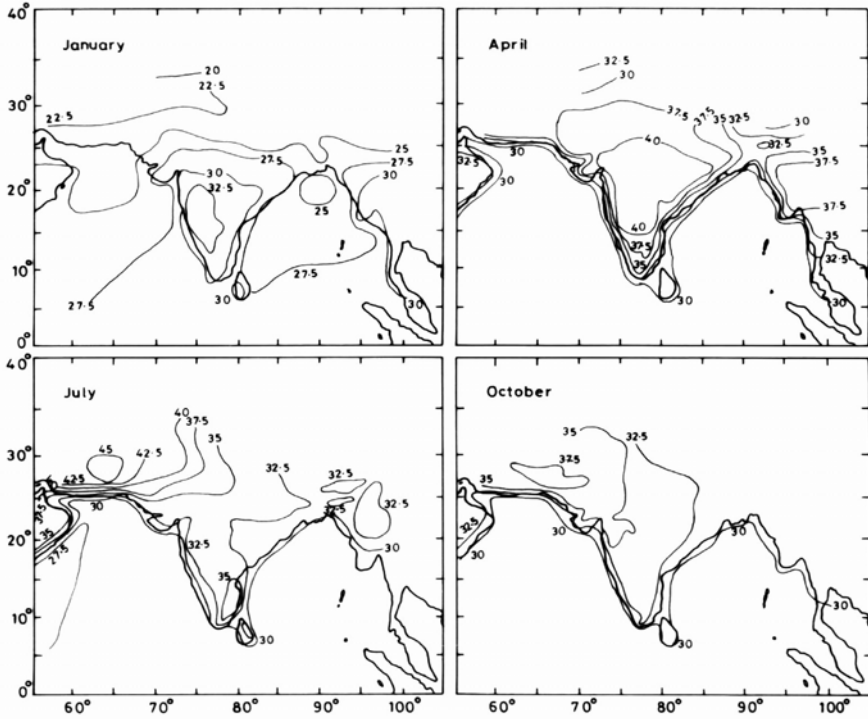
Fig. 6.11. Mean daily maximum temperature (°C).

maximum temperatures exceed 40°C over a vast area of the peninsula and exceed 42°C over appreciable areas of northwest in June-July. The consistently hottest part of India is around west Rajasthan where the average temperature is 40°C and daily maximum during summer may exceed 40°C consistently for several days at a time. The marked gradients of isotherms of maximum temperature in summer in coastal areas, particularly along the west and east coasts, are due to the inland penetration of fresh sea breezes resulting from the sharp temperature differences between the land and sea surfaces. Maximum temperatures for different months for 10 selected stations are given in Table 6.5.

6.8.3 Average Daily Minimum Temperature

The minimum temperature is likely to be affected by micro-meteorological conditions. Figure 6.12 gives the average daily minimum temperature in January, April, July and October. The spatial range is 10°-25°C in January, 20°-28°C in April, 25°-30°C in July and 20°-25°C in October. Table 6.5 contains minimum temperature values for different months at selected stations. The winter season remains from January through February with a marked decline in the minimum temperature in January which may fall to minus 2.3°C at some stations, such as Srinagar.
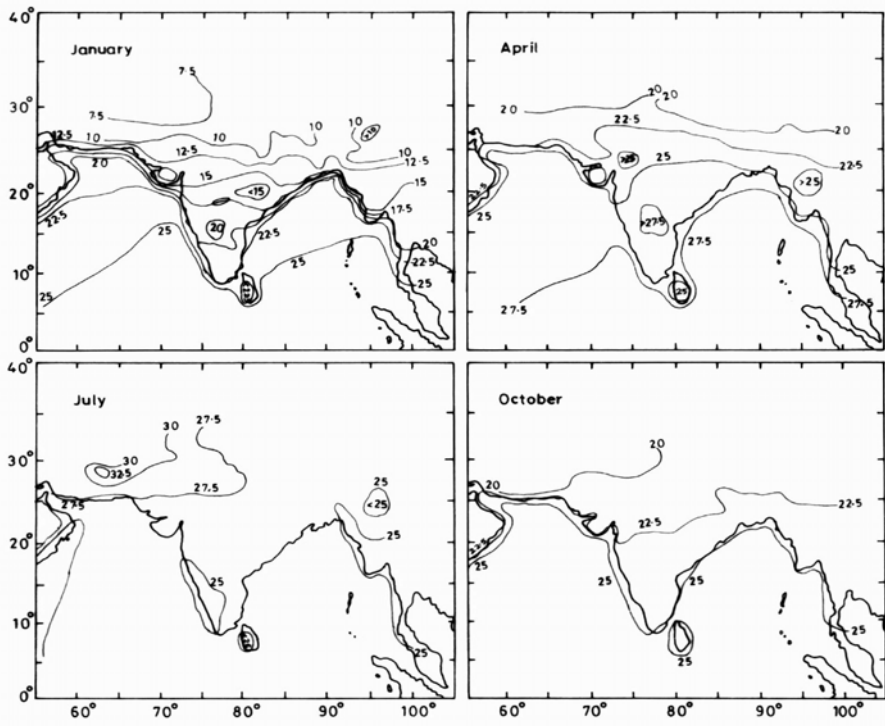
Fig. 6.12. Average daily minimum temperature (°C).

6.9 ONSET AND WITHDRAWAL OF MONSOONS

The hydro-climate of India is characterized by the southwest and northeast monsoons which bring water to the country. Agriculture is India's largest enterprise and its prosperity to a large extent depends on timely arrival and subsequent distribution of monsoon rains.

The monsoonal rains in India are much influenced by two air masses in the lower level of the atmosphere, namely, dry air from the north which originates from the Siberian high pressure and moist air from the Indian Ocean. The boundary between these two air masses is the ITCZ (see Fig. 5.3) as defined in Chapter 5. The ITCZ with migratory tendency controls the monsoons of India.

In the month of May, the ITCZ moves northward and lies at about 15° N. As a result, southeasterly winds from the Indian Ocean begin to intrude into Southeast Asia. Once the winds cross the equator they turn in the southwesterly direction and shed their water load first over the south Kerala beginning rains and is called the onset of the southwest monsoon. In July, the ITCZ is located at about 30° N and the depth of moist winds is about 6000 m below the ITCZ. The greater part of the country receives copious rainfall with peak period in July/August.

Table 6.5: Average daily maximum and minimum temperatures (°C) (Period 1931-1960)

Station		Jan	Feb	Mar	Apr	May	Jun	Jul	Aug	Sept	Oct	Nov	Dec
Agra	Max	22.2	25.7	31.9	37.7	41.8	40.5	34.8	32.8	33.2	33.3	29.2	24.1
	Min	7.4	10.3	13.7	21.4	27.2	29.5	27.0	25.8	24.6	19.1	12.0	8.2
Ahmedabad	Max	28.7	31.0	35.7	39.7	40.7	38.0	39.2	31.8	33.1	35.6	33.0	29.6
	Min	11.9	14.5	18.6	23.0	26.3	27.4	25.7	24.6	24.2	21.2	16.1	12.6
Bhopal	Max	25.7	28.5	33.6	37.8	40.7	36.9	29.9	28.6	30.1	31.3	28.5	26.1
	Min	10.4	12.5	17.1	21.2	26.4	25.4	23.2	23.5	21.9	18.0	13.3	10.6
Jodhpur	Max	24.6	27.9	33.3	38.3	41.6	40.1	35.7	33.2	34.7	35.7	31.4	26.7
	Min	9.5	12.0	17.1	22.4	27.3	28.5	26.8	25.2	24.1	19.6	13.9	10.7
Kolkata	Max	26.4	29.0	33.8	36.0	35.7	33.8	31.8	31.8	32.0	31.4	29.4	26.5
	Min	12.3	15.1	20.4	24.3	26.0	26.2	26.0	26.0	25.9	23.6	17.6	13.0
Mumbai	Max	29.1	29.5	31.0	32.3	33.3	31.9	29.8	29.5	30.1	31.9	32.3	30.9
	Min	19.4	20.3	22.7	23.1	26.9	26.3	25.1	24.8	24.7	24.8	22.8	20.8
New Delhi	Max	21.3	23.5	30.2	36.2	40.5	39.9	35.3	33.7	34.1	33.1	28.7	23.4
	Min	7.3	10.1	15.1	21.0	26.6	28.7	27.2	26.1	24.6	18.7	11.8	8.0
Pune	Max	30.7	32.9	36.1	37.0	37.2	31.9	27.8	27.7	29.2	31.8	30.8	30.1
	Min	12.0	13.3	16.8	20.6	22.6	23.0	22.0	21.5	20.8	19.3	15.0	12.0
Srinagar	Max	4.4	7.9	13.4	19.3	24.6	29.0	30.8	29.9	28.3	22.6	15.5	0.8
	Min	-2.3	-0.8	3.5	7.4	11.3	14.4	19.4	17.9	12.7	5.7	-0.1	-1.8
Trivandrum	Max	31.3	31.7	32.5	32.4	31.6	29.4	29.1	29.4	29.9	29.9	30.1	30.9
	Min	22.3	22.9	24.2	25.1	25.0	23.6	23.2	23.3	233	23.4	23.1	22.5

In January, the ITCZ reaches its farthest position between latitudes 10-15° south. The areas north of ITCZ are characterized by dry subsiding winds of north easterlies. As a consequence, the northeast monsoon period is drier throughout the country except for Tamil Nadu.

From the above discussion one finds that the important perceptible changes in the circulation associated with the onset of the southwest monsoon over India are:

- ITCZ with usual features arrives over the region;
- Blowing of winds from about southwest— extending to at 6 km above mean sea level;
- Decrease of temperature from the heat of April-May;
- Heavy rains accompanied by heavy thunderstorms;
- The trough of low pressure well marked on synoptic charts;
- Appearance of easterly jet over the southern half of the Indian peninsula; and
- Weakening of westerly jet and its shift to the far north of the Himalayas.

The dates of the onset can be determined by the changes in any of these features for any year. Although these features are associated with the onset of the monsoon, they do not simultaneously occur. Southwesterlies set in the Arabian Sea in May itself but the rains occur only in the next month. On account of the preponderant importance of rains, the India Meteorological Department (IMD), on the basis of statistical analysis, has fixed the normal dates for the onset and withdrawal of the monsoon in relation to the sharp increase and decrease, respectively, in the five-day means of rainfall and the changes in the circulations.

6.9.1 Statistical Method for Determining the Onset Date

There is a statistical method for fixing the normal dates for the onset of the monsoon. In this method, a month is divided into five-day periods (pentads) and the normal rainfall for each pentad from rainfall records of a station is determined. Around the time of arrival of the monsoon, the normal rainfall over a particular pentad would show a well-marked rise over its two or three preceding pentads. The increase is not transient but is maintained. The middle day of such a pentad is taken as the date of onset. On this basis the normal dates for the onset of the monsoon have been determined for several stations in India. Figure 6.13 shows the five-day rainfall figures at some coastal stations to illustrate an increase of rainfall at the onset.

6.9.2 Normal Dates of Onset of Monsoon

The normal dates of onset of the southwest monsoon have been worked out by the India Meteorological Department from the successive 5-day normals of rainfall for a large number of stations in the country. The middle day of
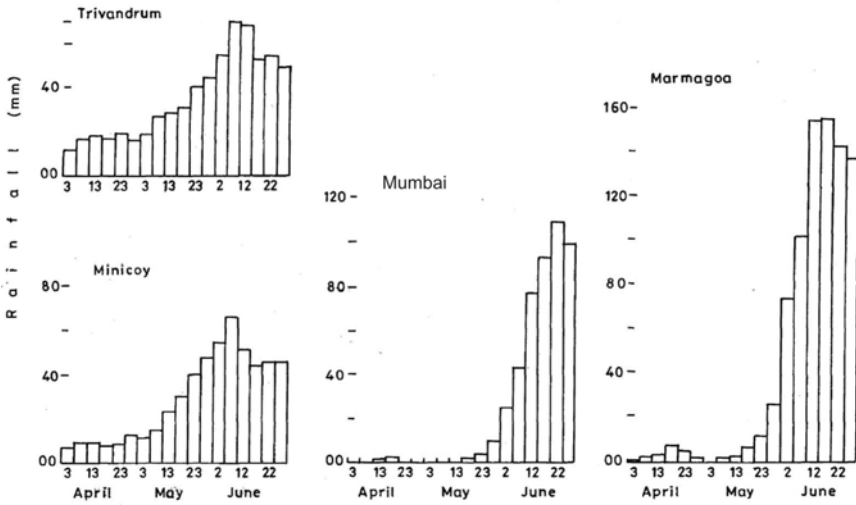
Fig. 6.13. Normal pentad rainfall.

the 5-day period showing the characteristic monsoon rainfall rise in the five-day normal rainfall curve of a station is taken to denote the normal onset date of monsoon for that station. The spatial variation of these normal dates over India is shown in Fig. 6.14. This map shows that the earliest date of
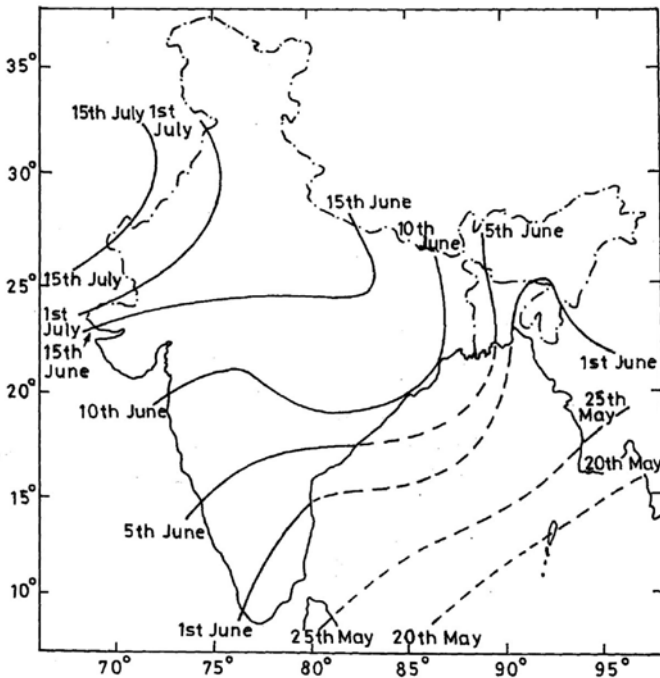
Fig. 6.14. Normal dates of onset of the southwest monsoon.

the onset of the SW monsoon is May 20 over the Islands of Bay of Bengal and May 25 is in Srilanka. Thereafter, it reaches the extreme southern tip of the Indian peninsula on June 1. The subsequent progress of the monsoon may be seen in the form of two branches, namely, the Arabian Sea branch and the Bay of Bengal branch. The Arabian Sea branch gradually advances northward to Bombay (now called Mumbai) by June 10. The Bay of Bengal branch moves northward in the central Bay of Bengal and reaches over Assam (NE part) by the first week of June. On reaching the southern periphery of the Himalayan barrier it is deflected westwards and advances towards the Gangetic plains of India. The arrival of the monsoon over Calcutta (now called Kolkata) (7 June) is slightly earlier than over Bombay (10 June). By the middle of June the Arabian branch spreads over Saurashtra and Kutch and the central parts of the country. Thereafter, the deflected current from the Bay of Bengal and the Arabian Sea branch of the monsoon tend to merge into a single current.

The remaining parts, including western Uttar Pradesh, Haryana, and eastern Rajasthan, experience their first monsoon showers by the first of July. The arrival of monsoon at a place like Delhi (28°N, 77°E) often raises an interesting question. Sometimes the first monsoon showers in Delhi arrive from the east as an extension of the Bay of Bengal branch but on a number of other occasions the monsoon is received from the south that is from the Arabian Sea. The meteorologist is often confronted with the problem of trying to decide whether the monsoon would strike Delhi from the east or from the south. By mid July the monsoon extends into Kashmir. By the first week of July the onset of monsoon gets established over most of the country. This is the normal behavior of the onset of monsoon.

From the normal dates given in Fig. 6.14 it should not be concluded that the advance takes place progressively, once the monsoon has set in the southern tip of the Indian peninsula. The activity often weakens after an advance of about 500 km and a fresh surge is needed to spread the monsoon air mass further. Figure 6.15 shows the onset dates for the Asian countries.

6.9.3 Normal Dates of Withdrawal of Monsoon

The displacement of the monsoon air mass by the continental dry air mass and the development of an anticyclonic flow determine the dates of withdrawal of monsoon over north and central India. The easterly jet which was a feature of the onset of monsoon disappears after the recession of the monsoon by early October. Many features that were associated with the onset phase of the monsoon disappear, as the winter Asian monsoon begins to set in over India.

Figure 6.16 gives normal dates for the withdrawal of the monsoon. It shows that the monsoon begins to withdraw from northwest India by the middle of September. The withdrawal of monsoon is a more gradual process than its onset. The monsoon withdraws from the upper half of the peninsula by October 15 and from the remaining parts of the country by early December.
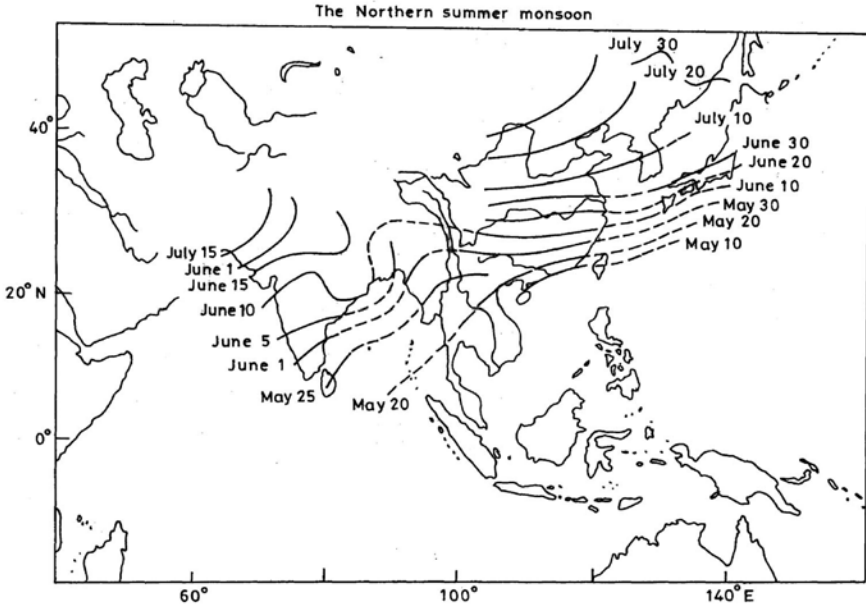
Fig. 6.15. Normal dates of onset of the southwest monsoon over Asian countries.
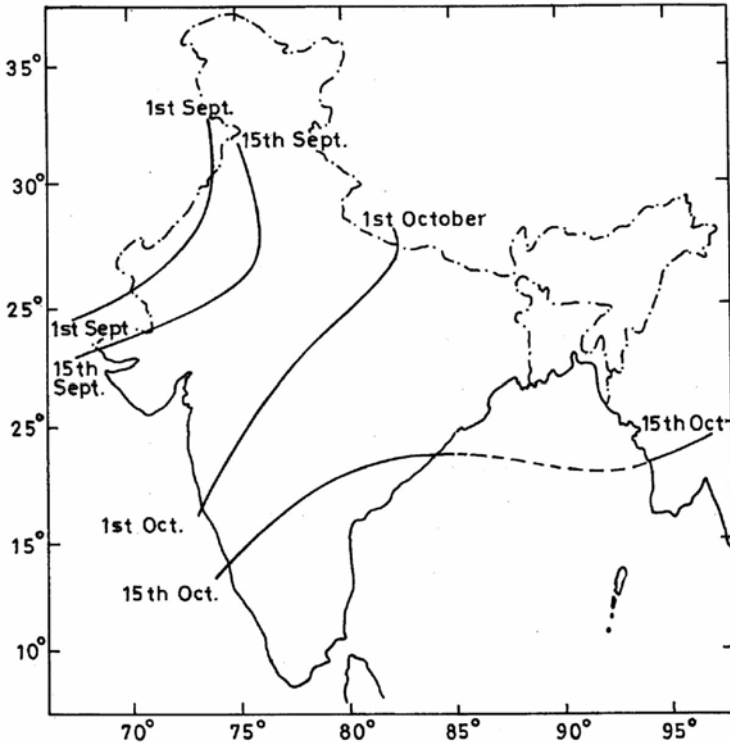
Fig. 6.16. Normal dates of withdrawal of the southwest monsoon.

6.9.4 Variability of Dates of Onset of Monsoon

Marked year-to-year variations in the dates of onset and withdrawal of the monsoon occur. There were several occasions in the past when the monsoon arrived over certain parts of the country about 2 to 3 weeks earlier or later than the normal dates of onset. To illustrate the variability in the onset of monsoon, a histogram giving the dates of the onset over Bombay (Mumbai) during 1879-1975 is given in Fig. 6.17. The extreme dates of onset of the monsoon for some parts of the country are given below:

Area	Normal dates	Earliest	Latest
1. Kerala	1 June	11 days	17 days
2. Coastal Karnataka	4 June	16 days	12 days
3. Konkan	8 June	11 days	17 days

It may be surmised that such variations may influence the amount of rainfall received during the monsoon season and cause great concern to agriculturists and hydrologists dealing with water management.
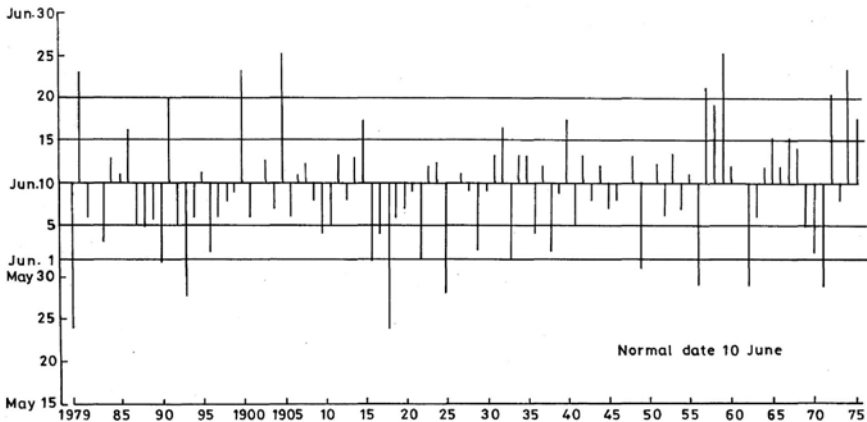
Fig. 6.17. Onset dates of southwest monsoon over Bombay (Mumbai) during 1879-1975.

6.9.5 Influence of Early or Late Onset of Monsoon on the Amount of Rainfall

Investigations were carried out by Dhar et al. (1980) to see whether or not an early or late onset of monsoon exercises any significant influence on the amount of rainfall that would fall during the monsoon season. This was done by examining the rainfall distribution over Kerala, coastal Karnataka and Konkan—the west coast subdivisions of India. These subdivisions were chosen because they experienced the first onslaught of monsoon during its advance over the country. The variability of the onset of the monsoon over these three
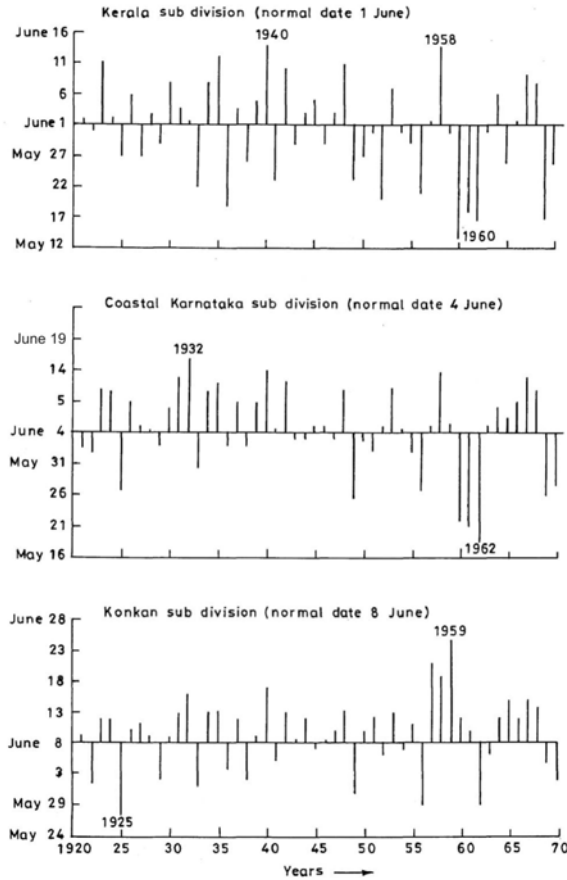
Fig. 6.18. Onset dates of southwest monsoon over three subdivisions (1921-1970).

subdivisions is shown in Fig. 6.18. The results revealed that the total rainfall received in these subdivisions during the early monsoon month of June and the monsoon season as a whole is independent of onset date. They correctly surmised that monsoon is an oscillating current which can gather momentum even after a late start.

6.10 MAIN WEATHER SYSTEMS AFFECTING INDIAN RAINFALL

The important weather systems that affect the Indian rainfall are:

- Formation and movement of tropical disturbances across the country
- Monsoon trough
- Breaks in the monsoon
- Mid tropospheric low pressure systems over the Gujarat area
- Low level easterly jet
- Thunderstorms

6.10.1 Tropical Disturbances

We have already discussed the characteristics of the tropical disturbances that form in the Bay of Bengal and the Arabian in Chapter 5 and their tracks are shown in this chapter. These weather systems bring rainfall over India. Normally, during the summer monsoon season, tropical disturbances (mainly depressions) from the Bay of Bengal and the Arabian Sea move across the country and bring heavy rainfall. The rainfall area may be as large as 400,000 km^2 and point rainfall may range from 40 to 90 cm in a day (Pisharoty and Asnani, 1957; Bao, 1987; Rakhecha and Pisharoty, 1996). Disturbances from the Arabian Sea move in a northerly or northeasterly direction and produce heavy rainfall over the Mahi River and the Sabarmati River basins (see Fig. 1.4). When a depression from the Head of the Bay of Bengal moves, a belt of heavy rainfall spreads to the eastern part of the Ganga River basin and the lower Brahmaputra River basin. With the further movement of the depression, the area receiving rain extends to the Mahanadi River and adjoining basins. By the time the depression moves over central India, it is weakened due to the depletion of moisture supply. Sometimes the depression after reaching central India intensifies due to the fresh feed of moisture from the Arabian Sea. This causes another spell of heavy rains over central and peninsular river basins. Towards the end of the monsoon, i.e., in September some depressions after reaching central India turn northwards, causing heavy rains and serious flooding both in the Indus River and upper reaches of the Ganga River basin. The magnitudes and frequencies of the heavy rainfalls, however, differ significantly because of wide variations of physiography and climatic types across the country.

During the northeast monsoon months (October-December) more severe cyclonic disturbances form in the south Bay of Bengal in the latitude belt of 10°-15° N. These systems move inland and produce heavy to very heavy rainfall over the Cauvery River and Pennar River basins.

6.10.2 Monsoon Trough

At the end of the hot weather a zone of low pressure develops over northwest India as a result of excessive solar heating. With the advance of the monsoon, this heat low gradually extends eastwards until it forms an elongated low pressure zone running parallel to the Himalayan Mountains in a west to east direction. This trough line is called the *monsoon trough*. The axis of this trough at the sea level normally extends from NW India to the Head Bay of Bengal. This trough is a semi-permanent feature of the summer monsoon. When the trough is located in its normal position, rainfall over most parts of India is generally well distributed but relatively much less rain in sub-Himalayan and adjoining areas. If the trough shifts south of its normal position, the rainfall belt shifts south and the rainfall will occur mostly south of the axis of the monsoon trough. However, when the monsoon trough
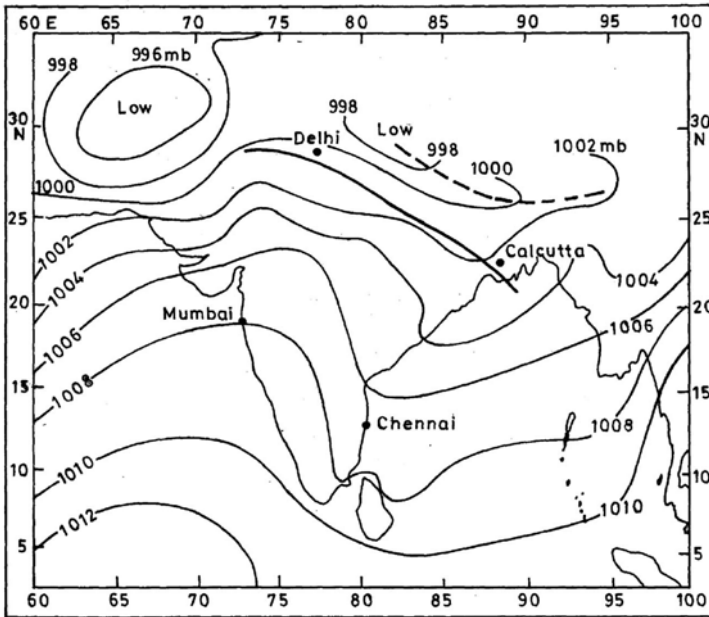
Fig. 6.19. Normal position of the axis of monsoon trough is shown by a thick continuous line. Dotted line indicates its position during a 'break'.

shifts north and lies over the foot of the Himalayas, there is a well marked change in the rainfall distribution over the country. Most parts of India generally receive much less rainfall but the sub-Himalayan area gets heavy rainfall resulting in floods in the Himalayan rivers. The monsoon trough can be seen up to a height of about 6 km. The normal position of the monsoon trough is shown in Fig. 6.19.

6.10.3 Mid-Tropospheric Low Pressure System over Gujarat

The monsoon depressions that form over the North Bay of Bengal and move westwards across the country are the main rain producing weather systems of the monsoon. It has also been observed that very heavy rainfall over western India, especially over northern parts of Maharashtra and Gujarat, is associated with cyclonic vortices (upper air lows) that develop in the middle troposphere. These disturbances occur mainly as circular vortices over northeast Arabian Sea and the Gujarat region during active monsoon epochs and have their largest intensity near 600 mb (4 km). The dimensions of these vortices are roughly of the order of 300 km in the horizontal direction and about 3 km in the vertical direction. A peculiar feature of these vortices is that they are only confined to the middle troposphere and are not visible at the surface. Fig. 6.20 shows the mid-tropospheric low pressure system over the Gujarat coast.
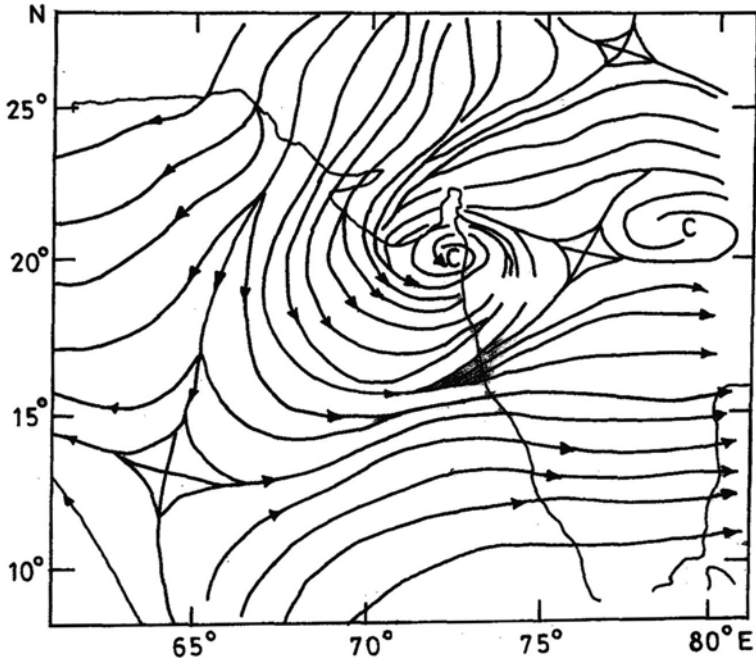
Fig. 6.20. Mid-tropospheric low pressure system.

6.10.4 Breaks in Monsoon

Rainfall during the monsoon period is not continuous but it alternates with active and break monsoon conditions. When the monsoon trough shifts north and lies over the foot of the Himalayas, there is a well marked change in rainfall distribution over the country. Most parts of India generally get little rainfall but the sub-mountain area gets heavy rainfall resulting in floods in the rivers originating in the Himalayas. During the break monsoon situations, sometimes Tamil Nadu gets heavy rainfall. Such a situation in which the monsoon trough lies close to or over the foot of the Himalayas and in which there is a marked decrease in rainfall over most parts of India is called a 'break' in the monsoon. The average number of breaks each year during July and August per year is 1.5 and the average duration of the 'break' is about six days. The situation for a typical monsoon break is shown in Fig. 6.19.

Figure 6.21 shows the time series of the daily average rainfall over central India during the monsoon seasons of 1965 and 1967. The average rainfall for the monsoon period was computed by a simple arithmetic average method taking all the available rainfall stations into consideration. In 1965, the period of August 4-15 was a long period of below normal rainfall. This was a typical long break. Prolonged breaks during a monsoon season result in drought conditions. During 1967, on the other hand, there was only a short break in the second week of July and 1967 was thus a good monsoon year.
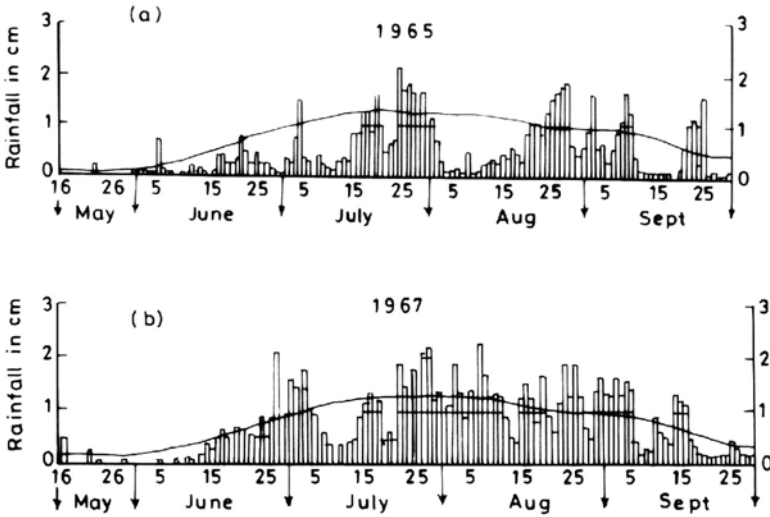
Fig. 6.21. Daily average rainfall over central India for the monsoon seasons of (a) 1965 and (b) 1967.

6.10.5 Jet Stream

A jet stream is a strong narrow current, concentrated along a quasi horizontal axis in the upper troposphere (200 mb). Two types of jet streams namely the subtropical westerly jet stream (STWJ) and the tropical easterly jet stream (TEJ) that occur over the Indian region are shown in Fig. 5.7. The subtropical westerly jet stream (STWJ) is located at about 12 km high during the period of October to May over north India to the south of Himalayas (20°-30°N). It is circumpolar in nature. It shifts to the north of Himalayas, often abruptly as the monsoon gets established over India.

The tropical easterly jet (TEJ) is located at about 14 km high during the monsoon season (June-September) around 10°N (Fig. 5.7). The TEJ originates somewhere in the low latitude western Pacific region and gets accelerated downstream up to south India. The TEJ over Asia is an integral part of the Asian monsoon circulation and exerts a dynamical control on the maintenance of the large-scale monsoon circulation as well as the development of monsoon depressions.

6.10.6 Thunderstorms

A thunderstorm is defined by the World Metrological Organization (WMO) as one or more sudden electrical discharges manifested by a flash of light (lightning) and a sharp rumbling sound (thunder). It usually develops in an unstable and moist atmosphere. Thunderstorms frequently occur in eastern India in the month of April and May. They are capable of releasing considerable amounts of rainfall, although their areal extent is smaller. In some years an excessive thunderstorm activity in the eastern region can lead

to flooding in the Brahmaputra River even in late May or early June. Every thunderstorm produces lightning which has the potential to kill people.

6.11 HISTORY OF RAINFALL MEASUREMENT IN INDIA

A study of water resources rightly commences with rainfall measurement. Rainfall measurement in India began towards the 18th century, when the first rainfall station was set up in 1784 at Calcutta (Kolkata) by the East India Company. From 1785 to 1840 rainfall stations were established at Madras (Chennai) in 1792, at Bombay (Mumbai) in 1823 and at Shimla in 1840. Thereafter, more rainfall gauges were installed at about 50 stations in different provinces of the country. With the establishment of the India Meteorological Department (IMD) in 1875 by the then government of India, the rainfall station network grew rapidly. At the time of independence in 1947 there were around 2750 rainfall stations (Ahuja, 1960). The need for increasing the rainfall station network in support of agriculture and water resources development work was felt after 1947 and as a result more rainfall stations were set up throughout the country. Presently, there are some 5000 rainfall stations whose data are processed and archived by IMD. In addition to these there are about 4050 rainfall stations that are being maintained by the railways, forest, agriculture and irrigation departments. There are also about 600 self-recording rainfall stations which provide records of rainfall intensity variations. The rainfall data are available with the National Data Centre, IMD, Pune. Apparently the rainfall records in India are excellent by world standards.

6.12 RAINFALL OVER INDIA

Rainfall (also called precipitation sometimes) is the quantity of water available naturally. Therefore, a proper assessment of rainfall for various regions and river basins give their rain water potential. The India Meteorological Department, the Indian Institute of Tropical Meteorology, and the Central Water Commission have undertaken comprehensive assessment studies of Indian rainfall. Maps on seasonal distribution of rainfall are valuable in the development of water resources. The seasonal and annual rainfall distributions for India are discussed in the following sections.

6.12.1 Winter Season (January and February)

The distribution of rainfall during winter season is shown in Fig. 6.22. In winter moderate to heavy snow and rainfall occur mostly over Himalayas and Jammu and Kashmir and is caused by western disturbances which generally move eastward across northwest India. Some light rainfall also occurs in northern plains. The highest rainfall of 10-30 cm occurs in Jammu and Kashmir. Punjab, Haryana, east Madhya Pradesh, Bihar Plateau, Assam,
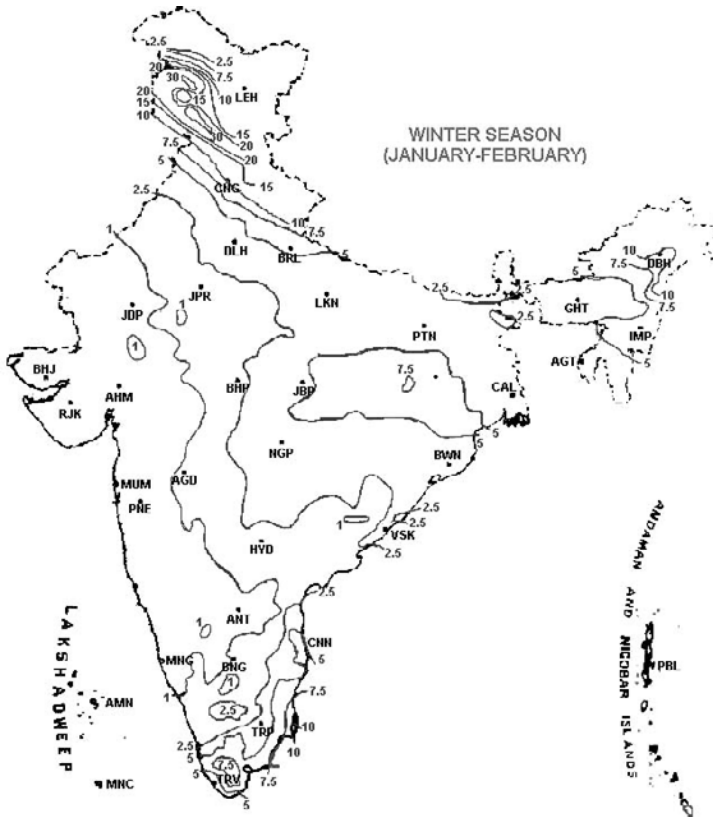
Fig. 6.22. Seasonal rainfall (cm) for January and February.

Orissa and Vidarbha receive 2.5 to 10 cm. This rainfall is useful for winter crops. Low pressure areas in the Bay of Bengal formed in these months cause 20 to 25 cm of rainfall over the southern part of the Indian peninsula.

6.12.2 Hot Weather Season (March to May)

Western disturbances continue affecting north India in the first half of the season causing rain, thunder, and hail. Convective cells cause thunderstorms mainly in Kerala, West Bengal and Assam. Figure 6.23 shows the rainfall distribution during hot weather season. In this season, the highest rainfall of 50-100 cm occurs in south Assam, 30-50 cm of rainfall occurs in north Assam, Jammu and Kashmir and Kerala. 10-20 cm of rainfall occurs in Bengal, Orissa and coastal Andhra Pradesh. Only 1-5 cm of rainfall occurs in U.P., Punjab, Haryana, Rajasthan, Madhya Pradesh and Maharashtra.

6.12.3 Southwest Monsoon Season (June to September)

The southwest monsoon (June to September) is the major rainy season of India. It has been said that the southwest monsoon produces about 75 to 80%
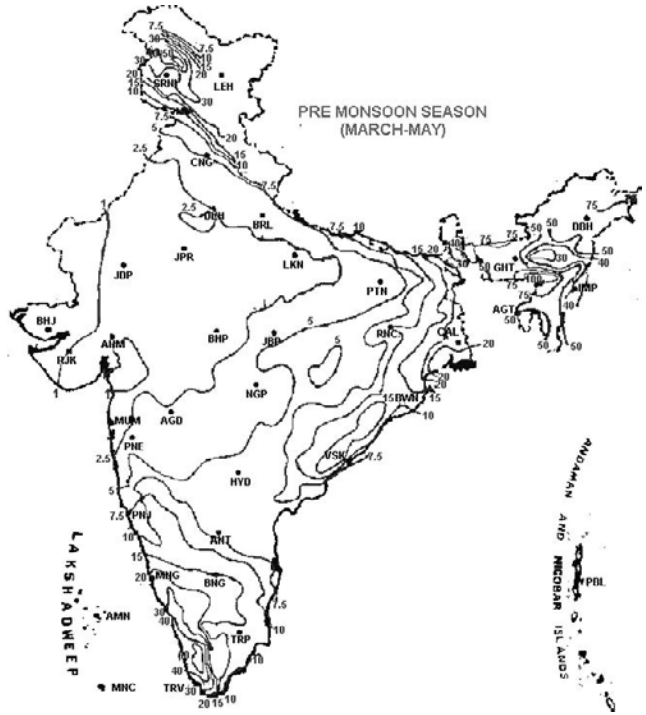
Fig. 6.23. Seasonal rainfall (cm) for March to May.
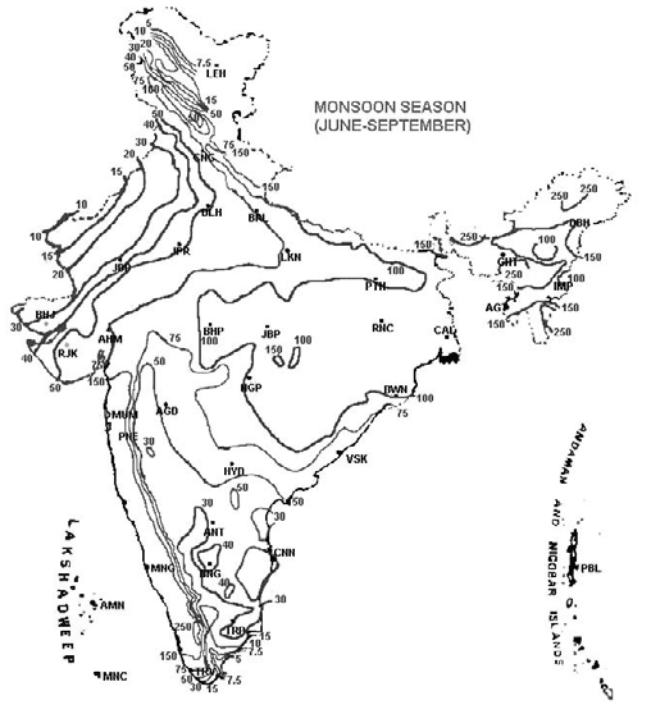
Fig. 6.24. Seasonal rainfall (cm) for June to September.

of the annual rainfall. The spatial distribution of the mean monsoon rainfall is shown in Fig. 6.24. As seen from this figure, the southwest monsoon produces a heavy rainfall of 200 to 300 cm over the areas of Assam, West Bengal, Kerala and west coasts of Maharashtra-Karnataka. However, rainfall is from 100 to 150 cm in the areas of Bihar, Himachal Pradesh and Madhya Pradesh and from 50 to 100 cm in the areas of Uttar Pradesh, eastern Rajasthan, Andhra Pradesh, Maharashtra and Gujarat. However, it produces less rain of the order of 50 cm in the western Rajasthan, Saurashtra and Kutch, Haryana, Punjab, Jammu and Kashmir and Tamil Nadu. The wettest area is Mawsynram (25° 18′ ; 9° 35′ E) in northeast India with a rainfall of 1140 cm and the driest area is the desert of western Rajasthan with a rainfall of less than 10 cm.

6.12.4 Northeast Monsoon Season (October to December)

The highest seasonal rainfall of 60-80 cm occurs in the north Tamil Nadu coast; 40-60 cm rainfall in coastal Andhra Pradesh, south Tamil Nadu and Kerala; and 20-40 cm in south interior Karnataka and coastal Karnataka (Fig. 6.25). During this season cyclones from the south Bay of Bengal strike coastal areas and cause heavy to very heavy rainfall in Tamilnadu, Andhra Pradesh and Kerala.
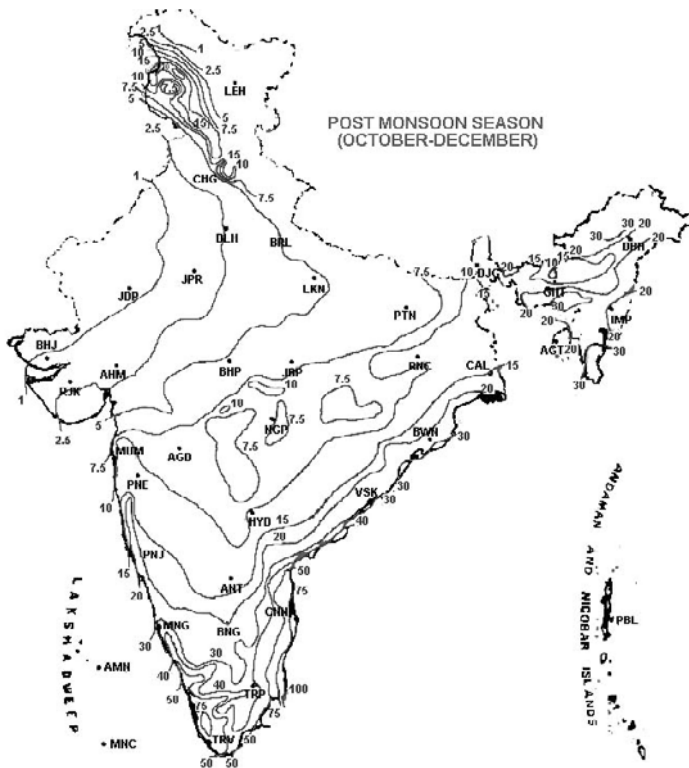
Fig. 6.25. Seasonal rainfall (cm) for October to December.

6.12.5 Annual Rainfall

The mean annual rainfall distribution over the country is shown in Fig. 6.26. Considerable variation in rainfall exists with an annual rainfall of 250 cm or more over the Western Ghats, the sub-Himalayan West Bengal, and Assam. There is a steep decrease of rainfall to the east of the Western Ghats, with a further gradual increase towards the east coast. From the Orissa coast to west Rajasthan, rainfall progressively decreases from 150 cm to 15 cm. The average annual rainfall for the country as a whole is 117 cm.
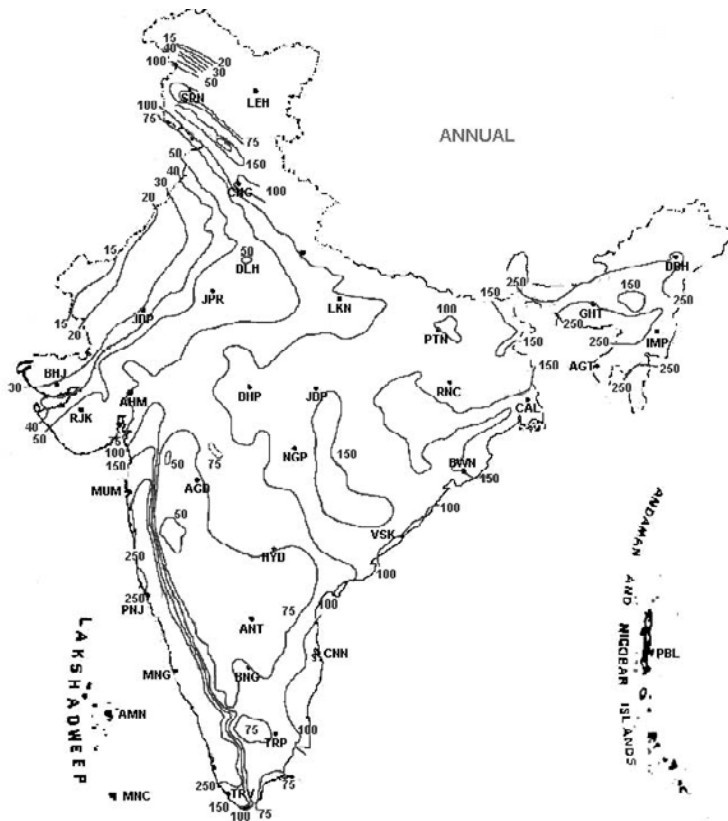
Fig. 6.26. Mean annual rainfall (cm).

Figure 6.27 shows the mean monthly rainfall totals for India as a whole for 1871-1990. Monthly rainfall totals increase progressively from January, peak in July/August due to the southwest monsoon and decline in November and December. The southwest monsoon month of June has a mean monthly rainfall of 16.3 cm which increases to 27.5 cm in July and 24.4 cm in August. The mean value then falls sharply to 7.7 cm in October. The rainfall drops to 1.2 cm in December.
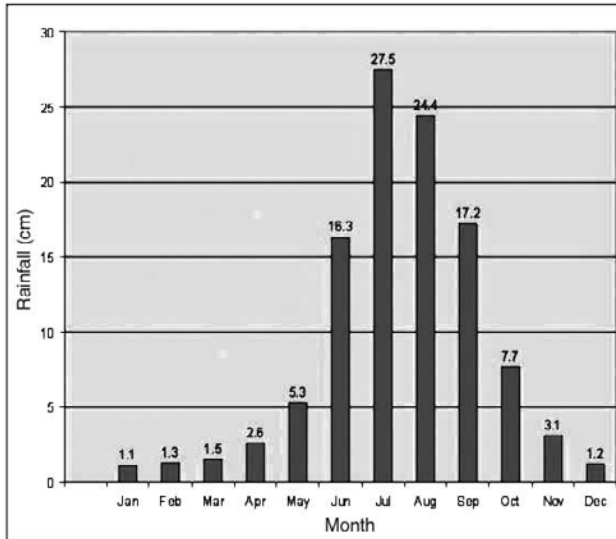
Fig. 6.27. Mean monthly rainfall of India, 1871-1990.

6.13 ASSESSMENT OF RAINWATER RESOURCES OF INDIA

India is divided into 28 states and seven union territories (Fig. 6.2). The distribution of rainfall over these regions is dependent on the southwest (June-September) and northeast (October-December) monsoons, cyclonic disturbances, and thunderstorms. Mean seasonal and annual rainfall values, together with the coefficient of variability of annual rainfall for these 28 states as well as for the country as a whole, are given in Table 6.6 (IMD, 1962). The rainfall in India varies widely from one state to another. Among the 28 states of the country, the highest average annual rainfall is 300 cm in Kerala and the lowest annual rainfall is 55 cm in Haryana. According to Table 6.6, seven states have the mean annual rainfall values between 50 and 100 cm, nine between 100 and 150 cm, two between 150 and 200 cm and 10 have over 200 cm. About 10% of India has an annual rainfall greater than 200 cm while about 40% has less than 100 cm. These proportions play an important part in the relative water availability status of the 28 states. Table 6.6 shows that about 75-85% of the total annual rain over most parts of India falls during the southwest monsoon period between June and September.

In the winter season (October-December) a high atmospheric pressure zone hovers over Mangolia and Siberia. Under its influence the general flow of winds is from the northeast. These winds being of continental origin are therefore dry. During their passage over the Bay of Bengal these winds pick up moisture and cause rains over Tamil Nadu, Andhra Pradesh, Karnataka and Kerala.

Reliability of Indian Rainfall

The coefficient of variability (CV) of the annual rainwater for each of the 28 states is given in Table 6.6. It is a statistical measure of the reliability of rainfall. The CV is a ratio of the standard deviation of yearly rainfall to average annual rainfall. A CV value of 25% tells that in about 68 years out of every 100, the rainfall in the region will range from an excess of 25% over the mean annual rainfall to a deficiency of 25% (or plus or minus 25% of the region's mean annual rainfall). The deviation will be over 25% in the rest of the 32 years – a deficit of over 25% in about 16 years and an excess of over 25% in another 16 years. For instance, in Uttar Pradesh where annual average rainfall is around 99 cm and CV is 20% it will be observed that in about 68 years out of 100 years, the annual rainfall will be between 79 cm and 119 cm. In the 16 years, the annual rainfall may be reduced to less than 79 cm, while in another 16 years it may exceed 119 cm.

6.14 PRESENT STATUS OF WATER UTILIZATION IN INDIA

The total annual surface water runoff of India is of the order of 1880 km^3. Because most of the annual rainfall over different parts of India occurs during the southwest monsoon season from June to September, dams are built to store water for use throughout the year. Prior to India's independence there were only 250 storage dams in India. After independence, the water resources development and utilization in India have proceeded rapidly. A great number of dams for storage of water have been built in response to meeting water needs. Table 6.7 gives the number of dams built every 10 years.

At present there are about 3634 large dams in India. Out of these about 2154 dams are big, each having a storage of more than 60 million m^3. These dams are used for water supply, irrigation, power generation and flood protection. The storage build-up in the completed projects up to the year 1989 was about 252×10^9 m^3, indicating that about 36% of the usable flow is being stored. Thus, there is great potential for increasing reservoir storage capacity for monsoon water by constructing new dams.

Table 6.6: Average annual rainfall over different states of India

S. No.	States of India	Area (km²)	Average annual rainfall (cm)	CV (%)	Rainfall during SW monsoon (cm)	Monsoon rainfall as % of annual
1	Andhra Pradesh	275069	88	20	55	63
2	Arunachal Pradesh	83743	228	11	150	67
3	Assam	78438	252	11	165	65
4	Bihar	94163	134	13	113	82
5	Chattisgarh	136034	135	16	119	88
6	Goa	3702	254	20	239	94
7	Gujarat	196024	83	30	79	95
8	Haryana	44212	55	28	46	84
9	Himachal Pradesh	55673	175	21	135	77
10	Jammu & Kashmir	222236	100	22	47	47
11	Jharkhand	79714	119	16	102	86
12	Karnataka	191791	136	18	99	73
13	Kerala	38863	300	14	200	68
14	Madhya Pradesh	308144	122	20	108	89
15	Maharashtra	307713	132	21	116	88
16	Manipur	22327	252	11	165	65
17	Meghalaya	22429	283	11	181	64
18	Mizoram	21081	283	11	181	64
19	Nagaland	16579	283	11	181	64
20	Orissa	155707	149	14	113	76
21	Punjab	50362	63	34	50	80
22	Rajasthan	342239	59	31	54	92
23	Sikkim	7096	274	12	192	70
24	Tamil Nadu	130058	101	14	33	33
25	Tripura	10491	252	11	165	65
26	Uttaranchal	53483	103	19	88	86
27	Uttar Pradesh	238566	99	20	86	87
28	West Bengal	88752	165	15	125	76
-	India	3290000	117	10	89	76

Table 6.7: Number of dams built every 10 years in different states of India (CWC, 1990)

S.No.	Name of state	Up to 1950	1951-1960	1961-1970	1971-1980	1981-1990	Under construction	Year of construction unknown	Total
1	Andhra Pradesh	21	13	17	16	9	17	9	102
2	Assam	-	-	-	-	2	1	-	3
3	Arunachal Pradesh	-	-	-	-	-	-	-	-
4	Bihar	-	12	6	15	23	33	3	92
5	Gujarat	37	64	82	57	57	68	-	365
6	Goa	-	-	-	-	-	2	3	5
7	Haryana	-	-	-	-	-	-	-	-
8	Himachal Pradesh	-	-	1	2	1	1	-	5
9	Jammu & Kashmir	-	-	-	2	1	2	4	9
10	Karnataka	16	7	32	41	38	24	55	213
11	Kerala	1	4	16	7	5	16	5	54
12	Madhya Pradesh	73	38	83	165	207	144	42	752
13	Maharashtra	53	25	143	586	290	320	91	1508
14	Manipur	-	-	-	1	-	3	1	5
15	Meghalaya	-	1	3	2	-	1	-	7
16	Nagaland	-	-	-	-	-	-	-	-
17	Orissa	2	3	5	48	72	18	1	149
18	Punjab	-	1	-	-	-	1	-	2
19	Rajasthan	12	30	19	18	18	4	27	128
20	Sikkim	-	-	-	-	-	-	-	-
21	Tamil Nadu	11	10	24	27	9	13	3	97
22	Tripura	-	-	-	1	-	-	-	1
23	Uttar Pradesh	24	17	22	9	7	12	18	109
24	West Bengal	-	1	1	5	1	15	4	27
	Total	256	226	454	1002	740	696	266	3634

REFERENCES

Ahuja, P.R., 1960. Planning of precipitation network for water resources developmert in India. WMO flood control series No 15, 106–112.

Bao, C.L., 1987. Synoptic Meteorology in China. Springer Verlag, Berlin, 269 p.

Central Water Commission (CWC), 1990. National Register of large dams. CWC: Dam Safety Organisation, New Delhi, 102 pp.

Dhar, O.N., Rakhecha, P.R. and Mandal, B.N., 1980. Does the early or late onset of monsoon provide any clue to subsequent rainfall during the monsoon season? *Monthly Weather Review*, 108, 7, pp 1069–1072.

India Meteorological Department (IMD), 1962. Monthly and annual normals of rainfall and of rainy days. Memoirs of IMD, 31, Part 3, 208 pp.

India Meteorological Department (IMD), 1989. Climatological Tables of Observatories in India (1931–1960).

India Meteorological Department (IMD), 2004. www.imd.ernet.in/section/climate/annual-rainfall.htm

Pisharoty, P.R. and Asnani, G.C., 1957. Rainfall around monsoon depression over India. *J. Met. Geophys.*, 8, pp 1-6.

Rakhecha, P.R. and Pisharoty, P.R., 1996. Heavy rainfall during monsoon: Point and spatial distribution. *Current Sci.*, 71, pp 177–186.

Wadia, D.N., 1976. Geology of India. Tata McGraw Hill Publishing Co., New Delhi, 508 p.

7 Tropical Storms and Hurricanes

The tropical disturbances having wind speeds below 63 knots are known as depressions, cyclonic storms and severe cyclonic storms. More intense cyclonic storms with winds over 63 knots around a low pressure center spirally form over the tropical oceans at latitudes between 7° and 15°. Such systems are known as cyclones in India, hurricanes in North America and the Caribbean area, and typhoons in Japan. After their formation they start moving at a speed of around 15 km per hour generally to the west over the open waters of the oceans. The tropical cyclones produce heavy clouds, rough seas and very heavy rainfall. A well-developed hurricane is a hazard to ships in its proximity as well as to the coastal area where it strikes. The storm piles up a huge sheet of sea water in its forward sector which can inundate low lying coastal areas causing large scale death and destruction. This is known as storm surge, which can be 80 km wide and four meters deep and is the most devastating feature associated with a hurricane. Nine out of ten hurricane fatalities are caused by storm surges. For example, the infamous tropical cyclone, which struck Bangladesh in November 1970, was responsible for killing nearly 300,000 people as a result of storm surge, while hurricane Mitch that struck central America in October, 1998, caused fatalities in excess of 11000 and the total damage was worth millions of U.S. dollars. When tropical cyclones move over land areas they produce widespread and heavy rainfall for several days. The importance of tropical cyclones in hydrology, therefore, lies in the circumstance that they bring water to the land, which is essential for life, and the damage to coastal areas. Hurricanes are responsible for most of the rains in the central parts of America.

Tropical cyclones, therefore, have received much attention because of the destructive power and consequent damage and socio-economic upheaval they cause: a direct result of strong winds and an indirect result of large rainfall amounts. This makes it appropriate to discuss in this chapter these events particularly in the context of the hurricanes in the USA.

7.1 DEFINITION

Air in motion is called wind. Any weather system having strong winds is called a storm. Hurricanes meaning big winds are part of a family of cyclonic storms. In meteorology a cyclonic storm is a center of low pressure around which winds are generally less than 17 knots. From the center of the storm the pressure increases markedly with distance outwards. The amount of the pressure drop in the center and the pressure gradient prevailing near the center contribute to the intensity of the cyclonic storm and the intensity of winds. The central pressure in a severe storm may be more than 50 mb lower than the pressure at the outskirts and maximum winds sometimes exceeding 63 knots occur usually within about 30 km of the storm center. Thus, the intensity of a cyclonic storm or tropical storm is expressed in terms of wind speed as indicated in Table 5.3.

Table 5.3 shows the tropical storms that occur over the sea areas, covering a wide range of intensities from a low pressure area with winds less than 17 knots to a hurricane or tropical cyclone with winds over 63 knots. The word "cyclone" is derived from a Greek word 'Cyclos' meaning the coil of a snake, and was first used in India by Henry Piddington, a British Officer at the Calcutta (now Kolkata) Port about the middle of the nineteenth century for tropical revolving storms in the Bay of Bengal and the Arabian Sea. To Henry Piddington, the tropical storms looked like the coiled serpents in the sea and he named them as cyclones. What are known as cyclones in India are called hurricanes in North America and the Caribbean area, typhoons in Japan, willy willies in Australia, and Baguios in the Philippines. These weather systems have diameters of around 500-1000 km but some typhoons have been larger. The pressure at the center of a tropical cyclone would be a couple of millibars less than pressure in the surrounding area. Because of very strong pressure gradients prevailing near the center of a cyclone, wind speeds usually exceed 63 knots and on rare occasions wind speeds can be as high as 115 knots. The winds around such a low-pressure center rotate anti-clockwise in the northern hemisphere and clockwise in the southern hemisphere.

Figure 7.1 shows a fully developed hurricane over the southern tip of Florida. From the inset barogram, it is seen that the pressure at Miami dropped by about 75 mb. It was a storm of unusual intensity. Since the atmospheric pressure is very nearly equal to the weight of the air column, it is found that the total pressure drop as calculated below was equivalent to a removal of 765,680 tons of air/km^2. It is evident that tremendous forces were involved.

1013 mb pressure = 76 cm of mercury height (1 mb = 1.033 gm/cm^2)
75 mb pressure = 5.63 cm of mercury height
Mass of air = 5.63 × 13.6 gm/cm^2 ≅ 77.568 gm/cm^2 = 765,680 tons/km^2
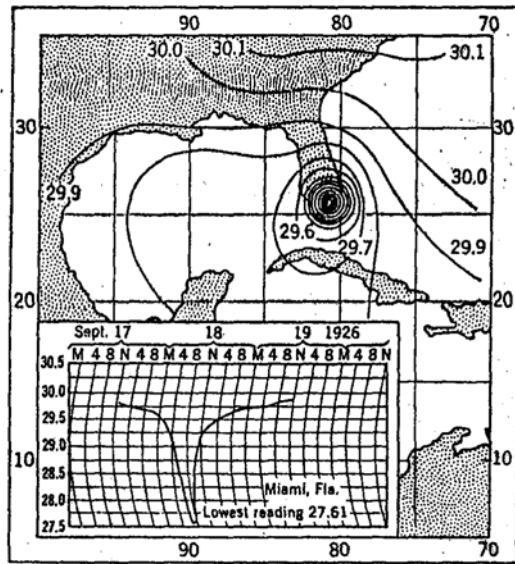
Fig. 7.1. Hurricane of September, 1926 over the southern tip of Florida (after Petterssen, 1969).

Saffir-Simpson Hurricane Scale

The hurricane damage is caused not only by high winds but also by heavy rains, floods and storm surge. Hence, a classification scheme that ranks tropical storms and hurricanes on the basis of the wind speed alone is not sufficient to describe hurricanes in their entirety, particularly in terms of the ensuing consequences.

In 1970, Robert Simpson, a meteorologist and Director of the National Hurricane Center, and Herbert Saffir, a consulting engineer in Dade County Florida, developed a scale to measure and classify the destructive potential of hurricanes. In addition to wind speed and central pressure, the Saffir-Simpson classification includes storm surge height and coastal destruction potential. Depending on wind speed, air pressure and storm surge height, the intensity of a hurricane is ranked on a scale of 1-5 called the Saffir-Simpson Scale. Table 7.1 shows the Saffir Simpson scale and the corresponding criteria for damage classification.

The United States utilizes the Saffir-Simpson hurricane intensity scale to give an estimate of potential property damage and flooding expected along the coast from the hurricane landfall.

During an average year about 8 to 9 tropical storms develop in the Atlantic, including the Gulf of Mexico and the Caribbean Sea from June to

Table 7.1: Saffir-Simpson hurricane scale

Saffir-Simpson Category	Winds			Central Pressure		Storm Surge Height		Damage	North American Examples
	mph	*m/s*	*Knots*	*inches*	*mb*	*ft*	*m*		
1	74-95	33-42	64-82	>28.94	>980	3-5	1.0-1.7	Minimal	Agnes 1972
2	96-110	43-49	83-95	28.91-28.50	979-965	6-8	1.8-2.6	Moderate	Cleo 1964
3	111-130	50-58	96-113	28.47-27.19	964-945	9-12	2.7-3.8	Extensive	Fran 1996
4	131-155	59-69	114-135	27.88-27.17	944-920	13-18	3.9-5.6	Extreme	Andrew 1992
5	>156	>70	>136	<27.12	<920	>18	>5.7	Catas-trophic	Camille 1969

November. Of these, 4-5 are likely to develop into hurricanes but only 2 to 3 are likely to reach the Saffir-Simpson category 3 or more intensity. Category 5 hurricanes are very rare, occurring about once every one hundred years.

7.2 MAJOR HURRICANES AND SUPER TYPHOONS

Sometimes, the speed of winds is much larger than what is observed in a hurricane. Also the amount of damage caused by hurricanes does not increase linearly with wind speed. Instead the damage produced increases exponentially with winds. The classification of hurricanes into major hurricanes is on the basis of the maximum sustained winds associated with them. Accordingly, 'major hurricane' is a term used by the National Hurricane Center for hurricanes that reach maximum sustained 1-minute surface winds of at least 96 knots. This is equivalent of Category 3, 4, or 5 on the Saffir-Simpson Scale. The World Meteorological Organization guidelines suggest utilizing a 10-minute average to get a sustained measurement. However, the National Hurricane Center and the Joint Typhoon Warning Center (JTWC) of the U.S.A. use a 1-minute averaging period to get sustained winds. "Super Typhoon" is a term used by the U.S. JTWC for typhoons that reach maximum sustained 1-minute surface winds of at least 130 knots. This is equivalent of a strong Saffir-Simpson Category 4 or 5 hurricane in the Atlantic Ocean.

7.3 WIND ROTATION

Winds around a low-pressure center circulate counter-clockwise in the northern hemisphere and clockwise in the southern hemisphere because of the rotary motion of the earth about its axis from west to east. The earth's rotation introduces an apparent force called the Coriolis force or deviating

force. When an object approaches the equator the Coriolis force pushes it to the west, and in general the rotation of the earth turns the straight-line travel into a curved path. In the northern hemisphere there is then a tendency for moving objects to deflect to the right of their line of movement, whereas in the southern hemisphere to the left. Thus, the Coriolis force pulls the winds to the right in the northern hemisphere and to the left in the southern hemisphere. When a low pressure starts to form north of the equator, the air will move from a high to a low pressure area in order to create equilibrium. Because of the rotation of the earth, the wind does not move in a straight line from high to low. With low pressure areas, the winds aiming towards the center of the low deflect to the right in the northern hemisphere and this means an anticlockwise circulation around the low pressure area rather than a direct impingement onto it from all directions.

The wind speed is commonly measured by a revolving cup anemometer and expressed in terms of knots (nautical miles per hour), kilometers per hour (km/hr), miles per hour (mph), and meters per second (m/s). The conversion factors are:

knot = nautical miles per hour

$$1 \text{ knot} = 1.853 \text{ km/hr} = 0.5148 \text{ m/s} = 1.1574 \text{ mph}$$
$$1 \text{ mph} = 0.864 \text{ knot} = 1.609 \text{ km/hr} = 0.447 \text{ m/s}$$
$$1 \text{ km/hr} = 0.538 \text{ knot} = 0.621 \text{ mph} = 0.278 \text{ m/s}$$
$$1 \text{ m/s} = 3.6 \text{ km/hr} = 1.94 \text{ knot} = 2.2 \text{ mph}$$

7.4 FORMATION OF TROPICAL STORMS

The subtropical high-pressure belts lie roughly at 30° on both sides of the equator (see Fig. 5.1). The region of the globe between these two high-pressure belts is called the tropical region. From these high pressure regions, the northeast (NE) and southeast (SE) trade winds blow towards the equator where they converge in a zone of low pressure, known as the ITCZ (see Fig. 5.2 in Chapter 5). Because of the convergence of trade winds, the ITCZ is a region of ascending motion and maximum cloudiness. This ITCZ, however, has a large seasonal movement from winter to summer due to the apparent north-south movement of the sun between the tropics of Cancer and the tropics of Capricorn in the course of a year. As such, the center of the weather systems of the two hemispheres is to the north of the equator during northern summer and to the south of the equator during the southern summer. Furthermore, within the tropical areas the sun is directly overhead twice a year and its rays are never very oblique. Thus, the air over tropical oceans generally is warm and possesses ample moisture. Warm air with high moisture content over tropical oceans is much lighter than warm air with low moisture content elsewhere. Warm moist air, therefore, produces low-pressure areas with a high convective activity. A small drop in the atmospheric pressure in an area of the ocean starts the neighboring air to move in a circular or nearly

circular manner around the center of low pressure and eventually in a spinning manner. The wind around such a low-pressure center circulates counterclockwise in the northern Hemisphere and clockwise in the southern Hemisphere because of the rotary motion of the earth about its own axis from west to east. The system of pressure and winds surrounding such a low-pressure center is called a tropical storm. On the surface weather map, tropical storms are characterized by almost circular isobars around the center of low pressure.

The formation of low-pressure tropical storms is quite frequent near the ITCZ over these tropical oceans, where a relative twist or vorticity is always present. Sometimes, the fall of pressure is large and very strong winds exceeding 63 knots prevail with much greater cyclonic spin. Such a system is then said to be a tropical cyclone. It is a huge mass of revolving moist air and has a diameter of 500-1000 km. Also, just as the spinning top tends to move, so the spinning motion of air in a cyclone moves as a whole gaining intensity as it moves over warm waters. This movement is caused in part due to the general air movement in the area, where a cyclone is formed and trade winds tend to push it. Another feature that needs to be emphasized is that air parcels do not move around in circular paths. They move more or less in a spiral path towards the center. Figure 7.2 shows the spiral motion of air parcels, and the steady movement of the system in a course of two days.
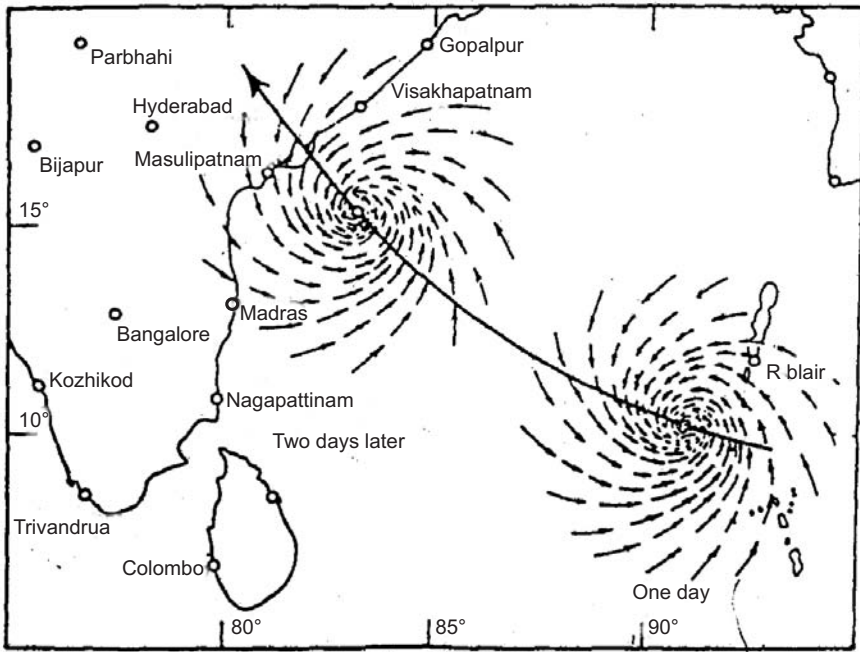
Fig. 7.2. Tropical cyclone in the Bay of Bengal.

The circulation of air around the center of low pressure can well be compared with the water draining from a kitchen sink that has a drain in its center. First, there is a slight circular motion of water around the center, but in a short time a definite funnel like depression (vortex) forms with the water circulating more rapidly around the sink until all the water is drained. The development of a tropical cyclone or hurricane is based somewhat on the same sort of conditions.

7.5 ORIGIN OF HURRICANES

Hurricanes over the Atlantic Ocean often originate near Africa particularly during the northern summer. They are driven westward by easterly trade winds and eventually these storms turn northward as they meet the prevailing winds coming eastward across North America. It has been recognized since the 1930s that lower tropospheric (from ocean surface to about 5 km) westward traveling disturbances often serve as the seedling circulations for a large proportion of hurricanes over the North Atlantic Ocean. These westward traveling disturbances are called easterly waves and have their origins over North Africa as described in Chapter 5. These easterly waves are generated by instability of the African jet. These easterly waves move westward in the lower troposphere trade wind belt across the Atlantic Ocean and produce cloudy weather and rain for a day or so over the areas coming under their influence. These waves occur usually in April or May and continue until October or November throughout the trade wind belt.

Waves have a period of about 3 or 4 days and a wavelength of 2,000 to 2,500 km (1,200 to 1,500 miles). The distinguishing feature is that there is a weak low-pressure center often present at the equatorial end of the trough of an easterly wave. On occasions, such a center associated with the easterly wave may develop to a tropical depression, to a storm, and then into a hurricane. On average, about 60 waves are generated over North Africa each year, but it appears that the number that is formed has no relationship to how much hurricane activity there is over the Atlantic each year.

Hurricanes over the Eastern Pacific beginning in the warm waters off the Central American and Mexican coasts can also be traced back to Africa. Hurricanes cannot be generated spontaneously. For development, they require a weak organized system with sizable spin and low-level inflow. A substantial amount of such a large-scale spin is available from easterly waves.

7.6 FREQUENCY OF HURRICANES FOR OCEANIC REGIONS

The main oceanic regions where tropical cyclones/hurricanes occur and the average tracks they follow are shown in Fig. 7.3. The interesting point worthy of careful note is that tropical cyclones do not form close to the

equator but they form quite far from the equator. This is mainly due to the fact that there is no Coriolis force (the deviating force due to the earth's rotation) at the equator to cause the winds to cyclonic spin around the low-pressure center. Most cyclones form in the belts between 7° and 15° from the equator. Secondly, we find that they form over the ocean areas, where the sea temperatures are high of the order of 27° or more (Fig. 7.4). Such high temperatures are necessary to produce a steep rate of change of temperature with height in the atmosphere that is necessary to maintain the vertical circulation in a cyclone.
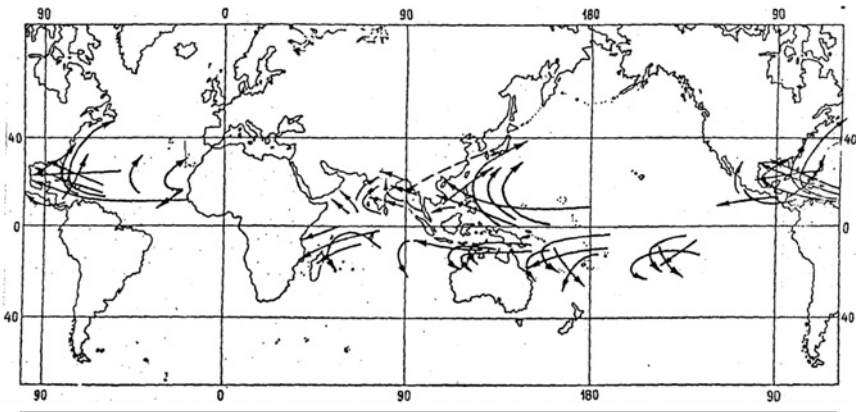
Fig. 7.3. Main tracks of tropical cyclones/hurricanes/typhoons (after Khromov, 1964).

Figure 7.3 shows that all cyclones begin at sea and move westward. After some time they re-curve to northwest, then to north and finally to northeast. Some of them move over land areas and there is a strong tendency for them to dissipate over land mainly due to the depletion of moisture. The frequency of occurrence of tropical cyclones which include tropical storms (winds > 33 knots) and hurricanes (winds > 63 knots) for the various ocean regions are given in Table 7.2. Looking at the table it is seen that an average of 128.5 tropical cyclones (include tropical storms and hurricanes) have been generated each year in the various ocean areas of the world. Of these, 90.1 form over the northern hemisphere and 38.4 over the southern hemisphere. Apparently the number of tropical cyclones in the northern hemisphere is much greater than over the southern hemisphere. An average of 12%, 20%, 32%, 6%, 12%, 8% and 10% tropical cyclones (including tropical storms and hurricanes) are generated each year in the Atlantic, the Northeastern Pacific, the Northwestern Pacific, the North Indian Ocean, the Southwest Indian Ocean, Southeast Indian Ocean and the Southwest Pacific Ocean, respectively.
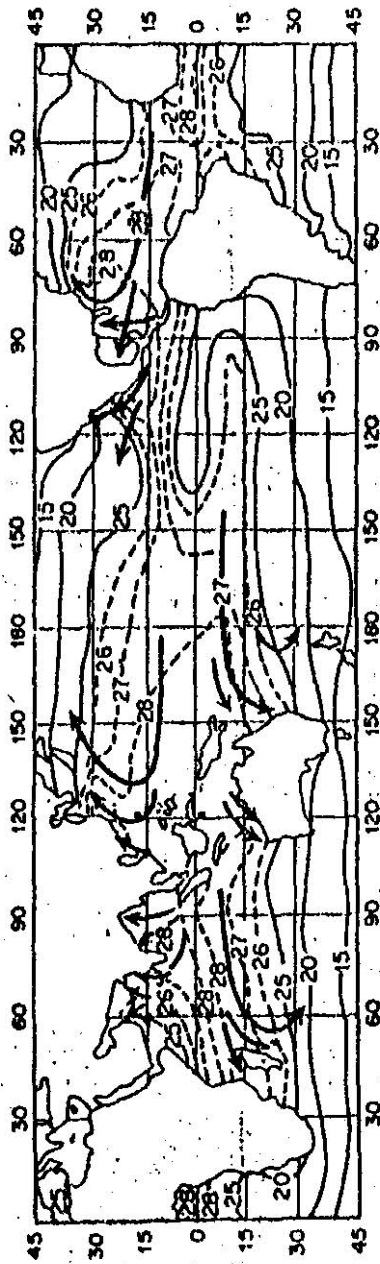
Fig 7.4. Tropical tracks and sea surface temperatures during the warmest season.

Table 7.2: Frequency of tropical cyclones for various ocean regions (1968-1989)

Ocean Region	Tropical Storms winds > 17 ms^{-1}			Hurricane/Typhoon/Tropical cyclone > 33 ms^{-1}		
	Max	*Min*	*Mean*	*Max*	*Min*	*Mean*
Atlantic	18	4	9.7	12	2	5.4
Northeastern Pacific	23	8	16.5	14	4	8.9
Northwestern Pacific	35	19	25.7	24	11	16.0
North Indian Ocean	10	1	5.4	6	0	2.5
Southwest Indian Ocean	15	6	10.4	10	0	4.4
Southeast Indian Ocean	11	1	6.9	7	0	3.4
Southwest Pacific	16	2	9.0	11	1	4.3
Global	103	75	83.6	65	34	44.9

Source: Neumann, 1993

An average of 16.5 tropical cyclones is generated each year in the Northeast Pacific Ocean. The main area of cyclone generation is off the West Coast of Mexico between latitudes 10° and 15°N and between longitudes 95° and 100°W. However, a summary of maximum and minimum number of hurricanes that have occurred in the Atlantic Ocean and hit the U.S.A. (1901-2000) is given in Table 7.3.

Table 7.3: Frequency of maximum and minimum tropical storm/hurricanes for Atlantic Ocean and striking the U.S.A.

Category	Maximum	Minimum
Tropical storms/hurricanes	21 (1933)	1 (1914)
Hurricanes	12 (1969)	0 (1907,1914)
Major Hurricanes	7 (1950)	0 (many times)
USA land falling storms/hurricanes	8 (1916)	1 (many times)
USA land falling hurricanes	6 (1916, 1985)	0 (many times)
USA land falling major hurricanes	3 (1909, 33, 54)	0 (many times)

The average number of cyclones each year forming over the North Indian Ocean (the Bay of Bengal and the Arabian Sea) is about 5.4. During the monsoon months of June-September, the tropical storms in the Bay of Bengal are usually of small intensity. They form in the north of Bay of Bengal and follow a northwesterly course. They cause widespread and intense rainfall and floods in India because of northwest penetration of tropical storms. The tropical storms that form in the Bay of Bengal and the Arabian Sea during pre-monsoon months of April and May and the post-monsoon months of October to December are generally of great intensity and often have the inner core of hurricane winds. They usually form between 8°N and 14°N.

7.7 ABSENCE OF HURRICANES IN SOUTH ATLANTIC OCEAN

The formation of hurricanes is totally absent over the South Atlantic Ocean. This is mainly because of the following factors:

(a) The ocean surface temperature is rather low due to cold ocean currents that flow equatorward along the coasts of South America and Africa.

(b) The troposphere vertical wind shear is strong.

(c) The absence of ITCZ, because it remains to the north of the equator throughout the year (Fig. 5.2 in Chapter 5).

The low sea surface temperature, the absence of ITCZ as well as having strong wind shear make it difficult to have a genesis of tropical cyclones.

7.8 NAMING OF HURRICANES

There are seven tropical cyclone oceanic areas where storms occur on a regular basis (see Table 7.2). The National Hurricane Center (NHC) in Miami, Florida, USA, has a responsibility for monitoring and forecasting hurricanes in the Atlantic and Northeast Pacific Ocean. All tropical cyclones or hurricanes are given names by their respective forecasting offices to provide to general public information and warning about the storm's movement over the ocean. In the past without naming hurricanes confusion arose when more than one tropical storm was in progress in the same ocean at the same time. The public got confused as to which storm was being described. Therefore, naming hurricanes reduces the confusion about the type of storm being described and warned for. Also it becomes useful, especially when exchanging detailed storm information between hundreds of widely scattered stations, airports, coastal bases, and ships at sea.

For hundreds of years hurricanes in the Caribbean Sea were named after the Saints on whose day the hurricane occurred. However, this practice was never followed in the USA. The first use of naming a tropical cyclone was introduced by an Australian meteorologist before the end of the 19th Century. According to Dunn and Miller (1964), he named tropical cyclones after political figures that he did not like. By properly naming a hurricane, the meteorologist can publicly describe a politician as causing great distress or wandering aimlessly about the Pacific.

It appears that during World War II, tropical cyclones were informally given women's names by the US Weather Service of the Air Force and the Navy who were monitoring and forecasting tropical cyclones over the Northwest Pacific Ocean. In 1953, the U.S. National Weather Service, which is the federal agency that tracks hurricanes and issues warnings in the Atlantic Ocean made an official weather service policy to use female names for hurricanes. The notion was that the hurricanes like women are totally unpredictable. In 1979 the U.S. National Weather Service (NWS) started using both women's and men's names. One name for each letter of the

alphabet is selected except for Q, U, and Z. For Atlantic Ocean hurricanes, the names may be French, Spanish or English, since these are the major languages bordering the Atlantic Ocean where tropical storms occur. Table 7.4 gives six lists in rotation that are being used. The same lists are reused every six years.

Table 7.4: Names of Atlantic, Gulf of Mexico, and Caribbean hurricanes

2002	2003	2004	2005	2006	2007
Arthur	Ana	Alex	Arlene	Alberto	Andrea
Bertha	Bill	Bonnie	Bret	Beryl	Barry
Cristobal	Claudette	Charley	Cindy	Chris	Chantal
Dolly	Danny	Dannielle	Dennis	Debby	Dean
Edouard	Erika	Earl	Emily	Ernesto	Erin
Fay	Fabian	Frances	Franklin	Florence	Felix
Gustav	Grace	Gaston	Gert	Gordon	Gabrielle
Hanna	Henri	Hermine	Harvey	Helene	Humberto
Isidore	Isabel	Ivan	Irene	Issac	Ingrid
Josephine	Juan	Jeanne	Jose	Joyce	Jerry
Kyle	Kate	Karl	Katrina	Kirk	Karen
Lili	Larry	Lisa	Lee	Leslie	Lorenzo
Marco	Mindy	Matthew	Maria	Michael	Melissa
Nana	Nicholas	Nicole	Nate	Nadine	Noel
Omar	Odette	Otto	Ophelia	Oscar	Olga
Paloma	Peter	Paula	Philippe	Patty	Pablo
Rene	Rose	Richard	Rita	Rafael	Rebekah
Sally	Sam	Shary	Stan	Sandy	Sebastien
Teddy	Teresa	Thomas	Tammy	Tony	Tanya
Vicky	Victor	Virginie	Vince	Valerie	Van
Wilfred	Wanda	Walter	Wilma	William	Wendy

The names in the first column of the list have already been used in 2002. The 2008 names will be identical to the list for 2002. The northeast Pacific Ocean tropical cyclones were named using women's names starting in 1959 for storms occurring near Hawaii. From 1978 both men's and women's names have been used.

As discussed above, for over a half century (since 1945) the weather service of the US Air Force and the Navy have named tropical cyclones forming in the Northwest Pacific Ocean using women's names, but from 1979 men's names were also included. From January 1, 2000, tropical cyclones in the northwest Pacific are being named from a new and very different list of names. The new names are Asian names and were contributed by all the nations that are members of the WMO Typhoon Committee. The new names will be allotted to developing tropical storms by the Tokyo Typhoon Center of the Japanese Meteorological Agency (JMA). These newly selected names have two main differences from the rest of the world's tropical cyclone name

roster. First, the names are not personal names. There are a few men's and women's names but most of them are names of flowers, animals, birds, trees or even food items. Secondly, the names will not be allotted in alphabetical order, but are arranged by contributing nation with the countries being alphabetized.

The North Indian Ocean region tropical cyclones are not named. The Southwest Indian Ocean tropical cyclones were first named during the 1960-61 season. The southwest Pacific and Australian region started giving women's names to the storms in 1964 and both men's and women's names since 1974.

In the Atlantic Ocean, tropical cyclone names are retired that is those names are not used again if a hurricane has been found to be big and destructive. So when a hurricane name is retired or removed from the list it will not be used again for a new storm. This is done to prevent confusion with a historically well known hurricane with a current one in the Atlantic Ocean. Some of the retired names are listed below:

Agnes 1972	Betsy 1965
Alicia 1983	Bob 1991
Allen 1980	Camille 1969
Andrew 1992	Carla 1961
Anita 1977	Carmen 1974
Audrey 1957	Carol 1955

7.9 LIFE CYCLE OF HURRICANES

The life cycle of a hurricane can be divided into four stages:

  (a) The formative stage
  (b) The developing stage
  (c) The mature stage, and
  (d) The dissipating stage

The average life span of a tropical cyclone in the Indian seas is about six days from the formative stage to the dissipating stage. The average life span of Atlantic hurricanes is around nine days, although in the month of August, it may be around 12 days. The hurricanes developing over Africa and the Cape Verde Island are of longer duration. They cross the Atlantic Ocean twice and move farther to the north. Their duration is in the range of 3 to 4 weeks. The famous hurricane of San Ciriaco (1899) lasted for five weeks.

7.9.1 Formative Stage

In the formative stage, a shallow and fairly large area of low pressure is formed in the oceanic region. This is characterized on the surface weather map by almost circular isobars around the center of low pressure. The winds

around the low-pressure center are moderate and cumulus clouds and showers of rain occur. Such low-pressure areas may be present for several days before further development commences.

7.9.2 Development Stage

In the developing stage, the pressure drop continues, the wind speed increases, and cloudiness and rainfall increase. All these lead to inflow of moist air into the area and consequent upward motion and further increase of rainfall. The pressure over the central parts of the low-pressure area falls by 5-10 millibars during the course of a day or two. The meteorological services usually describe this stage as a depression. The maximum winds in the circulation are less than 33 knots. From this stage onwards the area of the low pressure, the depression, and the associated wind system together with the weather of clouds and rains begin to acquire a progressive movement over the ocean surface. The entire system moves at a rate of 15 km/hr (350 km/day) to the west. Many of these depressions die out before intensifying into tropical storms (central pressure fall of 15 mb) or cyclones (central pressure fall of 30 mb).

7.9.3 Mature Stage

This stage is called Tropical Cyclone. The pressure deficiency at the center would be more than 30 mb. The central pressure stops falling and the maximum winds no longer increase. Instead, the storm area expands horizontally and vast masses of air are drawn into the whirl.

A mature tropical cyclone has a central region of light winds with little or no clouds known as eye of the cyclone. Another feature that needs to be emphasized is that the air parcels do not move around on circular paths. They move more or less on a spiral path towards the center. The spiral nature of cyclones and the eye of the cyclone can be seen distinctly in the satellite cloud pictures of a tropical cyclone as shown in Fig. 7.5. The eye that may have a diameter of 20-30 km is surrounded with steep walls of massive clouds (known as wall clouds) that may extend vertically to 15 km or more. This area of the cyclone experiences the severest winds and torrential rains. Figure 7.1 shows the fully developed hurricane of September 1926 approaching the Florida coast, U.S.A.

7.9.4 Dissipating Stage

In the developing and mature stages, most tropical storms move westward. The majority of them dissipate on coming over land. Friction effects over the land decrease the wind speed, and the central pressure begins to rise. The decreased supply of water vapor reduces the energy supply to the system.
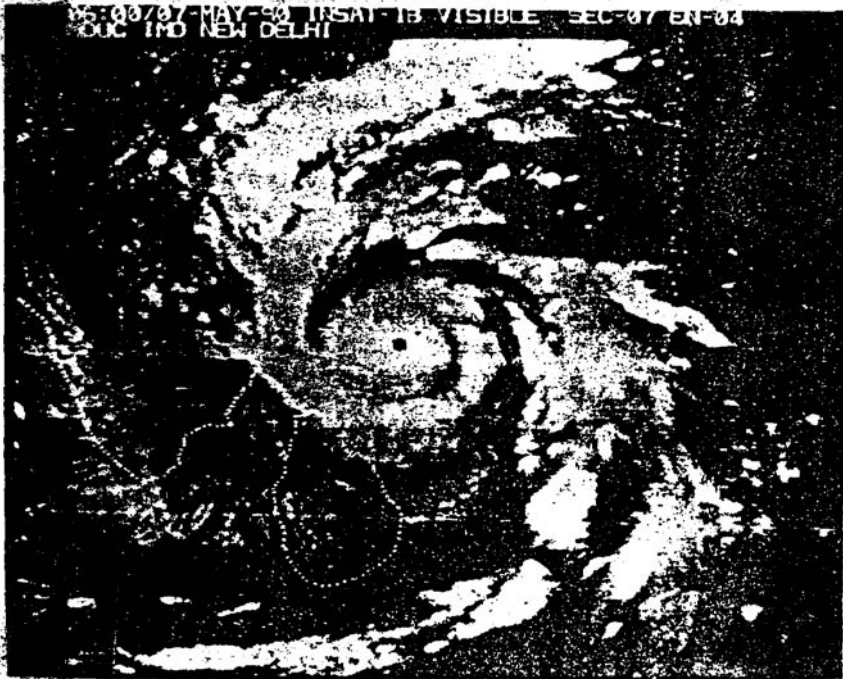
Fig. 7.5. Spiral bands and the eye at the center
(satellite cloud picture of tropical cyclone).

Nevertheless, rainfall from the already contained moisture continues for a day or two over coastal areas till the entire system weakens into a depression. In this stage, the system continues to move over the land for a few more days causing widespread and intense rainfall. While a tropical cyclone causes large-scale destruction to coastal areas, in its later stage it is very beneficial to the land. It brings water to the land and is essential for life. Rainfall from dissipating tropical storms can range from several centimeters to more than 80 cm in 2 to 3 days.

It is interesting to note that a tropical cyclone represents a tremendous generation of energy. The total production and dissipation of kinetic energy is estimated to be 7.0×10^{21} ergs per second from a cyclone with a diameter around 1300 km. This is equivalent to 1.5×10^{13} kwh per day. The energy of a large (megaton) nuclear explosion is about 10^9 kwh.

It was suggested that if the walls of clouds of a mature cyclone were seeded with AgI (silver iodide), it would release considerable amounts of latent heat. This could imbalance the forces within the storm, and the end result would be a decrease in the maximum wind speeds and consequently a reduction in the power of the cyclone.

7.10 STRUCTURE OF HURRICANES

A tropical cyclone is a huge rotating mass of moist air like rotating column 500-1000 km in diameter and 10-15 km in height. The most interesting feature of this large rotating mass of moist air is that it has a funnel in shape at the center called the 'eye' of the cyclone. The eye is about 20-30 km in diameter. Here the atmospheric pressure is the lowest. A listing of record measurements of lowest pressures in tropical cyclones/hurricanes/typhoons is given in Table 7.5.

For hurricanes in the U.S.A., the lowest pressure on record is 892 mb (27.35 inches) measured at Matecumbe Key, Florida, on September 2, 1935, while in Indian cyclones the lowest pressure at the center is about 919 mb that occurred at False Point on September 22, 1885. The eye is best seen in a satellite cloud picture. The eye appears as a dark spot in the center of a large patch of bright clouds (Fig. 7.5). The eye (funnel) is open at the top almost without cloud and wind is either absent or very weak. On the other hand, the walls of the funnel are a zone of very strong rotation of wind. The structure of a hurricane is given in Fig. 7.6 (Tannehill, 1956).
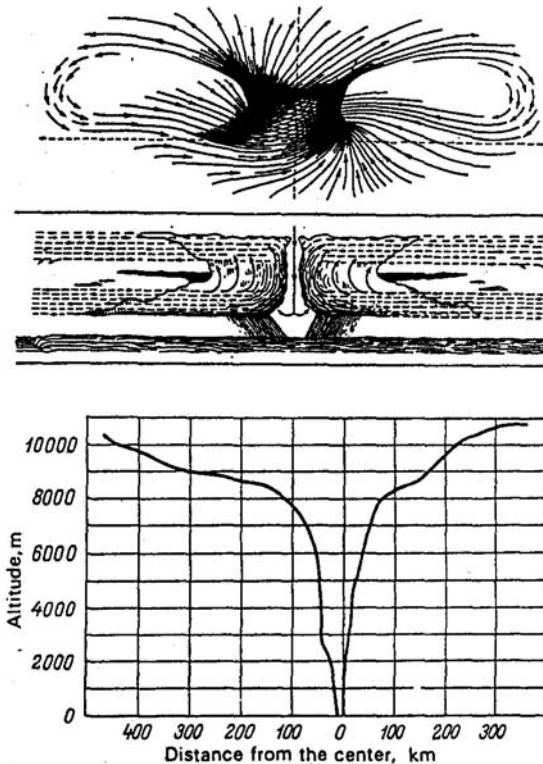
Fig. 7.6. Structure of a hurricane (after Tannerhill, 1956).

Table 7.5: Record low pressure readings in tropical cyclones/hurricanes

| Sr. No. | Place | Location | Date | Pressure | |
				Inches	mb
1	SS Saporoea	600 km east of Luzon	August 18, 1927	27.18	887
2	Matecumbe Key	Florida	September 2, 1935	27.35	892
3	Basilan	Frank Helm Bay P. I	September 25, 1905	27.85	909
4	Cossak	Australia	January 7, 1881	27.00	914
5	Chetumal	Mexico	September 27-28, 1955	27.00	914
6	SS Phemius	Western Caribbean	November 5,1932	27.01	915
7	SS Laisang	27.7° N 123° E	August 2, 1901	27.03	915
8	Havana	Cuba	October10-11, 1846	27.06	916
9	False Pt	India	September 22,1885	27.14	919
10	Hurricane Esther	Atlantic	September 17,1961	27.26	923
11	Hurricane Inez	East Caribbean	September 28, 1966	27.37	927
12	West Palm Beach	Florida	September 16,1928	27.43	929

At the top is a sketch of the direction of the rotating air; the middle sketch shows that the hurricane has a well-shaped central funnel in which the movement of air is directed downward, while at sides air moves upward. The bottom figure shows a section of funnel of the hurricane of 1882 over Manila, Philippines. It can be seen that up to a height of 8 km the side of the funnel is quite steep, becoming gentler higher up.

7.11 HURRICANE CLIMATOLOGY

7.11.1 Hurricane Season

All tropical storms, which include hurricanes/tropical cyclones, form in much the same way and in the same seasons of the year all over the world. The main oceanic regions where they form are shown in Fig. 7.3. The average frequency of tropical storms forming in different months of the year over different oceanic regions is given in Table 7.6.

According to Table 7.6, the hurricane season in the North Atlantic Ocean, which affects the USA, is from June through November. They are very rare outside these months. However, Hurricane Alice, which occurred in the vicinity of the Lesser Antilles during January 1955 is the only one definitely known to have developed in that month. An average of 8 to 9 tropical storms, including hurricanes, are generated each year in the Atlantic Ocean, of which approximately 50% attain hurricane intensity. The months of August, September and October have the largest number of storms: 1.8, 2.7 and 1.9, respectively. However, their frequencies, intensities and movement vary considerably from year to year. The highest frequency was 21 in 1933 and the lowest was one in 1914 (See Table 7.3).

The hurricane season off the west coast of Mexico (Eastern Pacific) is about the same as in the Atlantic. The main area of hurricane generation is between latitudes 10° and 15°N and between longitudes 95° and 100°W. Most of the hurricanes originate about 300 km south of Cabo San Lucas, the southernmost point in Baja California. After leaving their area of origin storms move usually northward off the coast and may intensify into hurricanes. Farther north and west, strong wind shear and colder waters dissipate the storms. Occasionally some storms meander and move into the U.S.A. or Mexico causing heavy precipitation and flooding. About six tropical storms each year develop off the West Coast of Central America or Mexico but less than 50% reach hurricane intensity. Several eastern Pacific hurricanes have crossed Central America and regenerated in the Caribbean Sea or in the Gulf of Mexico.

The Northwestern Pacific Ocean is the most active region where tropical storms (typhoons) occur all year round with an annual average of more than 21. Most of these form to the east of the Philippine Islands, and may move westward across the Philippines into the China Sea or northwestward towards

Table 7.6: Average monthly frequency of tropical storms

Ocean Region	J	F	M	A	M	J	J	A	S	O	N	D	A
Atlantic													
a) All tropical storms	*	0	*	0	0.1	0.5	0.5	1.8	2.7	1.9	0.4	0.1	8
b) Hurricane intensity	*	0	*	0	*	0.2	0.2	0.9	1.6	0.8	0.1	*	3.8
North Pacific-West of Mexico													
a) All tropical storms	*	*	*	*	0.1	0.8	0.7	1	1.9	1	0.1	0	5.7
b) Hurricane intensity	*	*	*	*	0.1	0.2	0.2	0.5	0.7	0.5	0	0	2.2
Northwestern Pacific Ocean	0.4	0.2	0.3	0.4	0.7	1	3.2	4.2	4.6	3.2	1.7	1.2	21.1
North Indian Ocean (Bay of Bengal & Arabian Sea)	0.2	0	0.2	0.3	0.7	0.9	0.9	0.6	0.8	1.1	1.3	0.5	7.5
Southwest Indian Ocean (Vicinity of Madagascar)	1.3	1.7	1.2	0.6	0.2	0	0	0	0	0	0	0.1	5.1
Southeast Indian Ocean/ NW Australia	0.3	0.2	0.2	0.1	0	0	0	0	0	0	0	0.1	0.9
Southwest Pacific/Australia													
South Atlantic Ocean	0	0	0	0	0	0	0	0	0	0	0	0	0

* less than 0.1

China coast then veer towards Japan or the open Pacific. The main hurricane (typhoon) season is from July to November with a maximum number occurring in the months of August and September.

Tropical cyclones in the north Indian Ocean are quite frequent in May and November with the commencement of the summer season. During the height of the southwest monsoon season, their frequency is relatively low, but it increases again during the winter monsoon. The severe cyclones (>63 knots) occur almost exclusively from April to June and October to December.

In the southern hemisphere, hurricanes occur in three main areas:

i. in the Southwest Indian Ocean in the vicinity of and to the east of Madagascar;
ii. in the Southeast Indian Ocean off the northwest of Australia; and
iii. in the South Pacific Ocean off the east coast of Australia.

These regions have similar annual cycles with tropical storms occurring in November through April, corresponding to the summer and fall months of the northern hemisphere. In the southern hemisphere the wind blows clockwise around the center of the cyclonic storm.

7.11.2 Reasons for Seasonal Occurrence

We have seen that tropical storms/hurricanes primarily develop during the summer months from June to November for the northern hemisphere and from December to March for the southern hemisphere. The first comprehensive attempt to specify the necessary climatological conditions for tropical storm formation was by Palmer in 1948. The conditions postulated by him were:

(a) Sea surface temperature must be warmer than about 26°C. Warm waters are necessary to fuel the heat engine of the tropical storm.
(b) Some type of weather disturbance must be present that can easily initiate convection (i.e., thunderstorm). It is the thunderstorm activity which allows the heat stored in the ocean waters to be liberated for the tropical storm.
(c) There must be a proper latitudinal location (at least 5-10 degrees of latitude from the equator).
(d) Tropical storms cannot generate spontaneously. To develop, they need a weak organized system with sizable spin and low-level inflow. Low vertical shear in the troposphere and a substantial amount of large-scale spin is available either from the monsoon trough or easterly waves.

The necessary conditions, as described above, are mostly encountered in summer season. As a result one would expect tropical storms to form in the summer season.

7.11.3 Yearly Frequency of Tropical Storms and Hurricanes in America

Mitchell (1932), Tannerhill (1956), Dunn and Miller (1964) and the annual hurricane summaries prepared by the US Weather Service (1956) all gave information on the frequency of tropical storms and those of hurricanes for all areas in the Atlantic Ocean. Since 1956, the U.S. Weather Bureau began a systematic and comprehensive compilation of the tracks of all tropical storms and hurricanes for the Gulf of Mexico, the Caribbean Sea and the North Atlantic Ocean. From these one can readily find: how many storms have passed any given area, at what month of the year, moving in what direction and with what speed? Based on these, the frequency of tropical storms and those that reached hurricane and major hurricane intensity during each year of the period 1901-1999 for all areas in the Atlantic is given in Table 7.7 and Fig. 7.7. This table shows that the frequency of tropical storms varies considerably from year to year. The highest frequency was 21 in the year 1933 and the lowest was one in 1914. It has been seen that during the 99-year period (1901-1999) about 863 tropical storms, including hurricanes, developed in the adjacent waters of the United States giving an average of 8.7 each year. Of these, about 496 became hurricanes.

During recent years there has been a speculation on the possibility that the annual number of hurricanes is on the increase. According to Dunn and Miller (1964) this increase is due in part to better detection but there also appears to have been a significant increase in the number of hurricanes beginning around 1930. A gradual warming of the atmosphere apparently began about that time, and the greater number of tropical storms is probably due to that warming trend. One hypothesis is that the oceans would warm, thereby creating the potential for more intense hurricanes (Emanuel, 1987). However, Gray (1990) suggests that the variability in hurricane incidence and intensity is a function of natural climate variability.

7.11.4 Frequency of Hurricanes on Atlantic and Gulf Coasts

On average, two hurricanes strike the U.S. coast each year, with two intense hurricanes striking the U.S. coast every three years. These hurricanes that make landfall cause considerable damage and loss of life. They are therefore of great concern. It is of great importance to determine the frequency of tropical storms and hurricanes that have penetrated various sections of the U.S. coast. The number of all tropical storms for three intensity groups that penetrated different sections of the Atlantic Coast and Gulf Coast during the period 1901-1955 is shown in USWB (1955). The three intensity groups are:

(a) All tropical storms and hurricanes regardless of intensity.
(b) All hurricanes having a minimum central pressure of less than 29.0 inches (982 mb). The group includes storms with maximum winds exceeding 135 km/hr (80 mph) and maximum storm surges exceeding 2 m in height.

Table 7.7: Frequency of tropical storms and hurricanes in the United States

Year	Tropical Storms and Hurricanes	Hurricanes Intensity	Major Hurricanes	Hurricane days
1901	10	2		
1902	5	3		
1903	9	8		
1904	6	2		
1905	5	1		
1906	11	6		
1907	4	0		
1908	8	4		
1909	11	4		
1910	4	3		
1911	4	3		
1911	8	5		
1913	4	3		
1914	1	0		
1915	5	4		
1916	14	11		
1917	3	2		
1918	5	3		
1919	3	1		
1920	4	4		
1921	5	4		
1922	4	3		
1923	5	4		
1924	8	5		
1925	2	1		
1926	10	8		
1927	7	4		
1928	6	4		
1929	3	3		
1930	2	2		
1931	10	2		
1932	11	6		
1933	21	9		
1934	11	6		
1935	6	5		
1936	17	8		
1937	9	2		
1938	7	3		
1939	5	2		
1940	8	4		
1941	6	4		
1942	10	4		
1943	10	5		

(Contd.)

Table 7.7: (*Contd.*)

Year	Tropical Storms and Hurricanes	Hurricanes Intensity	Major Hurricanes	Hurricane days
1944	11	7	3	27
1945	11	5	2	14
1946	6	3	1	6
1947	9	5	2	28
1948	9	6	4	29
1949	13	7	3	22
1950	13	11	7	60
1951	10	8	2	36
1952	7	6	3	23
1953	14	6	3	18
1954	11	8	2	32
1955	12	9	5	47
1956	8	4	2	13
1957	8	3	2	21
1958	10	7	4	30
1959	11	7	2	22
1960	7	4	2	18
1961	11	8	6	48
1962	5	3	0	11
1963	9	7	2	37
1964	12	6	5	43
1965	6	4	1	27
1966	11	7	3	42
1967	8	6	1	36
1968	8	4	0	10
1969	16	12	3	40
1970	10	5	2	7
1971	13	6	1	29
1972	7	3	0	6
1973	8	4	1	10
1974	11	4	2	14
1975	69	6	3	21
1976	10	6	2	26
1977	56	5	1	7
1978	12	5	2	14
1979	9	5	2	22
1980	11	9	2	38
1981	12	7	3	23
1982	6	2	1	6
1983	4	3	1	4
1984	13	5	1	18
1985	11	7	3	21
1986	6	4	0	11
1987	7	3	1	5

1988	12	5	3	21
1989	11	7	2	32
1990	14	8	1	27
1991	8	4	2	1
1992	7	4	1	16
1993	8	4	1	10
1994	7	3	0	7
1995	19	11	5	60
1996	13	9	6	45
1997	8	3	1	16
1998	14	10	3	49
1999	12	8	5	41
2000				
Total	**863**	**496**	**126**	
Mean	**87**	**5.0**	**2.3**	

(c) All hurricanes having a minimum central pressure of less than 28.25 inches (957 mb). This group includes the very intense hurricanes with maximum winds ranging from 190-300 km/hr (120-200 mph) and maximum storm surges exceeding 3 to 5 m in height. These are the storms that cause damage to all except carefully designed buildings to withstand high winds.

It has been shown that the coastal region most vulnerable to tropical storms is the southern quarter of the state of Florida where 16 hurricanes were experienced in 65 years. This shows that the risk of heavy rainfall, damaging winds and flooding from the surge is high in Florida. Other more vulnerable areas are the Texas coast, the mid Gulf coast and the North Carolina coast.

7.11.5 Absence of Hurricanes along West Coast

Hurricanes form in the Atlantic Ocean, including the Gulf of Mexico and Caribbean Sea, to the east of the U.S. mainland and in the Northeast Pacific Ocean to the west of the U.S.A. However, the hurricanes that form in the northeast Pacific almost do not strike the U.S., whereas those forming in the Atlantic Ocean strike the U.S. coast. There are two reasons for this. First, hurricanes in the northeast Pacific Ocean form between latitudes 10° and 15°N and longitudes 95° and 100°W. After formation they move usually west-northwest off the U.S. coast. As a result they move farther away from the U.S. west coast. On the other hand, in the Atlantic Ocean their movement often brings the hurricanes into the vicinity of the U.S. east coast. Second, along the east coast the Gulf Stream brings a source of warm water of about over 27°C (about 80°F), which is ultimately the source of energy for hurricanes. However, along the U.S. west coast, the ocean temperatures are relatively cool even in the middle of summer, which weaken the hurricanes rapidly when they travel over cool ocean waters.
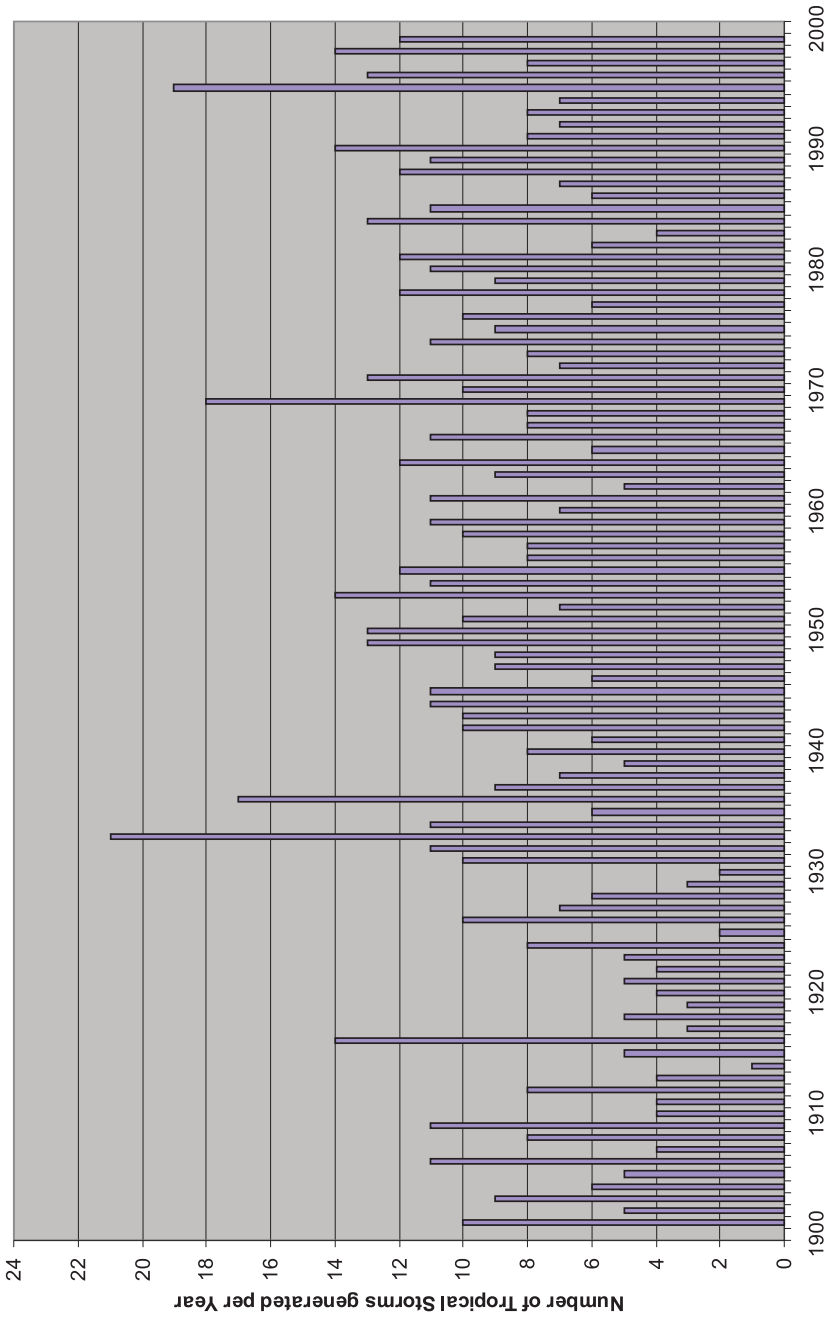
Fig. 7.7: Variation in the number of tropical storms in the Atlantic Ocean.

7.12 MOST INTENSE HURRICANES ON RECORD

Intense hurricane is a term used by the National Hurricane Center (NHC) for hurricanes that attain winds of at least 96 knots. This is equivalent to Category 3, 4, and 5 on the Saffir-Simpson Scale. Intense hurricanes that form in the Atlantic Ocean, Caribbean Sea, Gulf of Mexico and in the eastern Pacific Ocean become hazardous to the United States, when they come on to the land or parallel to the coast. They bring storm surge, high winds, torrential rains and flooding, all of which result in tremendous property damage and loss of life in coastal areas. The meteorological services at the NHC by means of weather satellites, radar and specially equipped airplanes keep a continuous watch on the intensity and movement of hurricanes and provide frequent warnings to alert the public and the various government authorities held with the responsibility of organizing rescue and safety measures to minimize the loss of life and property. It may also be mentioned that the modern forecasting and communication techniques make it possible to quickly warn people sufficiently in advance in areas likely to be affected so that they can take steps needed to reduce property damage and move to higher grounds.

Most lethal of all damages is a storm surge (a huge dome of water of 80-100 km wide and a few meters deep) which causes inundation of low-lying coastal areas where a hurricane makes landfall, producing large scale death and destruction. Also, strong winds in a hurricane do a great deal of destruction to man-made structures. Huge trees can be blown over and loose objects and roofing are carried far away. Also, heavy and widespread rainfall for several days from the hurricane produce destructive floods, landslides, levee breaches, overtopping of dams, and so on.

Table 7.8: Most intense hurricanes of the U.S.A.

No.	Hurricane	Year	Category at the time of landfall	Pressure (mb)	Deaths	Damage, million dollars*
1	Galveston, Texas	1900	4	931	12000	30856
2	Hazel	1954	4	938	95	8160
3	Audrey	1957	4	945	390	-
4	Donna	1960	4	930	107	13967
5	Carla	1961	4	931	46	8194
6	Betsy	1965	3	948	75	14413
7	Camille	1969	5	909	256	12711
8	Celia	1970	3	945	-	3869
9	Gilbert	1988	5	888	318	-
10	Hugo	1989	4	934	-	10872
11	Andrew	1992	4	922	27	38362

* Normalized to 1998, dollars by inflation, wealth increases and coastal country population changes

In the past intense hurricanes of extreme intensity have hit coastal areas of south Atlantic states (North Carolina, South Carolina, and Georgia), the middle Gulf Coast (Louisiana, Mississippi, and Alabama), Florida, the middle Atlantic states (from Virginia to New York), and Texas and have caused enormous loss of life and property. The intensity of a hurricane is an indicator of damage. The damage from winds is proportional to the energy of the wind (Energy = ½ mv^2). Thus a wind of 100 km/hr is four times as effective in causing damage as a wind of 50 km/hr. It is therefore pertinent to briefly discuss some of the most intense hurricanes of the Atlantic Ocean, which produced large-scale damage and destruction in the United States. Table 7.8 gives the list of most intense hurricanes hitting the United States. The listed hurricanes are all of Category 3 and above.

7.13 LARGEST RAINFALL FROM TROPICAL STORMS/HURRICANES

Tropical storms and hurricanes are known to generate heavy to very heavy rainfall for several days. The converging moisture-laden air of the storm on rising is cooled by the adiabatic expansion and after becoming saturated it releases its copious moisture as rain. The water vapor of the air in condensing to moisture releases great amounts of heat and this heat is added to drive the tropical storm system. After leaving their area of formation, some storms strike the land areas. It has been found that rainfall over the land commences when the center of the storm is about 500 km away from the seacoast. Heavy rainfall continues along and near the track of the storm even after it crosses the coast and moves over the land. Depending upon the tracks of tropical storms, heavy rains associated with them on a particular day are spread over an area that could be of the order of 400,000 km^2 (Bao, 1987). Daily maximum rainfalls from tropical storms can be surprisingly high and may range from 50 to 80 cm in a day. This magnitude of rainfall, however, varies from storm to storm and from place to place. It is of great value to know the largest rainfalls from tropical storms. Such magnitudes of the largest rainfalls over different parts of the world are important not only in the design of a wide range of water resources projects but also useful to assess the physical upper limit to the rainfall which is possible over an area. Table 7.9 gives the largest point and areal rainfalls for one-day duration from tropical storms over different parts of the world.

Table 7.9 shows that the largest known one-day rainfall over various sizes of area in different parts of the world generated from tropical storms, hurricanes and typhoons, are comparable. Also the largest known Atlantic hurricane one-day point rainfall value is 98 cm observed at Yankeetown, Florida, on September 6, 1950. For a Pacific Ocean typhoon, the largest value is 97 cm observed at Linzhuang, China on August 7, 1975 and for the Bay of Bengal, the largest value is 99.0 cm at Dharampur, India on July 2, 1941. Table 7.10 gives the world's largest recorded rainfall values for different durations associated with tropical storms.

Table 7.9: Largest areal rainfalls (cm) for one-day duration associated
with tropical storms and hurricanes

Country	Area (km²)							Tropical Storm
	10	*100*	*500*	*1000*	*2000*	*5000*	*10000*	
USA	98	97	87	85	80	65	46	Sept. 6, 1950
India	99	97	90	85	77	65	54	July 2, 1941
China	97	90	80	74	66	53	41	August 7, 1975
Australia	91	85	77	73	66	56	46	1898

Table 7.10: Largest rainfall values associated with tropical storms

Duration	Amount (cm)	Location	Storm Date
12 hours	115 cm	Foc-Foc, La Reunion Island	7-8 Jan., 1966
24 hours	183 cm	Foc-Foc, La Reunion Island	7-8 Jan., 1966
48 hours	247 cm	Aurere, La Reunion Island	8-16 April, 1958
72 hours	324 cm	Grand - Ilet, La Reunion Island	24 -27 Jan., 1980
10 days	508 cm	Commerson, La Reunion Island	18-27 Jan., 1980
5 days	80 cm	Abbeville, Louisiana	6-10 Aug., 1940
5 days	86 cm	Crowley, Louisiana	6-10 Aug., 1940

7.14 LONGEST LASTING HURRICANES

The average life of a hurricane in the Atlantic Ocean is about nine days. We
have seen that during the months of June and July, hurricanes form entirely
on the western side of the Atlantic in the lower latitudes, most frequently in
the western Caribbean Sea and the Gulf of Mexico. These hurricanes are
relatively short lived, simply because the region of formation is so near to
land areas that they do not have to travel far before landfall takes place.
During the months of August and September, they form frequently on the
eastern side of the Atlantic Ocean fairly close to the Cape Verde Islands.
These storms have the longest life span with an average of 12 days; obviously
hurricanes developing in the Cape Verde region have to travel long distances.
Therefore, the factors which determine the life time of a hurricane are the
time and place of origin and the general circulation features existing in the
atmosphere at the time of formation. A number of hurricanes have lasted for
3 to 4 weeks. Table 7.11 gives the long lasting Atlantic hurricanes.

Table 7.11: Longest lasting Atlantic hurricanes

S.No.	Hurricane Name and Year	Life Span (days)
1	Ginger 1971	27.3
2	Inga 1969	24.8
3	Kyle	22
4	Carrie	20.8
5	Inez 1966	20.3
6	Alberto	19.8

Table 7.11 shows that hurricane Ginger of 1971 lasted for 27.3 days in the North Atlantic Ocean. It is worth mentioning that Hurricane/Typhoon John lasted for 31 days as it traveled both the northeast and northwest Pacific Oceans during August and September 1994. This hurricane, formed in the northeast Pacific Ocean, reached the hurricane force there, then moved across the date line and was renamed Typhoon John, and then finally curved back across the dateline and was renamed Hurricane John again.

7.15 CLIMATIC EFFECTS OF HURRICANE ACTIVITY

Giving frequencies of tropical storms and those that reached the hurricane intensity for the period of 1901-1999 in the Atlantic Ocean, Table 7.7 shows a large variation from year to year. During the 99-year period, the highest number of tropical storms including hurricanes in any one year was 21 in 1933 and the lowest was one in 1914. The cause of these variations appears to be non-seasonal in the ocean-atmosphere system. Of these, El Nino-Southern Oscillation (ENSO) is a major ocean-atmosphere phenomenon which influences weather not only in the neighborhood of its occurrence but even at far away locations through a complicated interactive process. It seems ENSO might be playing also an important role in influencing the variability of tropical storm generation for some of the oceanic regions. In this context, it is of interest to know whether the ENSO conditions influence the tropical storm frequency in the Atlantic and east Pacific regions of the United States. It can be done by examining the frequencies of occurrence of tropical storms and hurricanes in the Atlantic Ocean during the ENSO and non-ENSO years. Before investigating the relationship between the ENSO events and tropical cyclone frequencies, it is important to understand what exactly ENSO is all about. Chapter 12 provides details on the occurrence and characteristics of ENSO.

Major El Nino events occur generally at intervals of 3 to 5 years and once commenced, an El Nino episode continues for 12 to 18 months. Of course, there are examples of El Nino aborting only in a few months. ENSO affects various meteorological and oceanographic conditions worldwide and it seems to have some effect on the frequency of occurrence of tropical storms and hurricanes. The relationship between ENSO events and the frequency of tropical storms that form in the Atlantic Ocean has been examined for the period 1901-1999.

Several indices have been developed that indicate the ENSO conditions. The difference in the sea-level pressure between Darwin [12.4°S, 130.9°E], Australia and Tahiti [17.5°S, 149.5°W] is commonly used to create an index of the Southern Oscillation. Precipitation in the Line Islands of the equatorial Pacific Ocean [latitude 0° to 10°N, longitude 160°W] also has been used as an index of the ENSO condition. Distinct precipitation surges occur in these normally dry islands under ENSO conditions. The sea level pressure difference

between Easter Island [27.1°S, 109.5°W] and Darwin [12.4°S, 130.9°E] was shown by Quinn and Burt (1972) to be statistically related to the El Nino phenomena and was shown to be a good index for prediction of the ENSO phenomenon. Quinn et al. (1978) developed a chronology of El Nino events since 1726 and have classified them as strong (S), moderate (M), weak, and very weak. The strong and moderate El Nino events as given by Quinn et al. (1978) for the period 1901-1999 along with the frequency of tropical storms are shown in Table 7.12.

Table 7.12: El Nino years and frequency of tropical storms in the Atlantic Ocean

Number	Year	Storms and Hurricanes	Hurricanes
1	1902	5	3
2	1905	5	1
3	1911	4	3
4	1914	1	0
5	1918	5	3
6	1925	2	1
7	1929	3	3
8	1939	5	2
9	1941	6	4
10	1953	14	6
11	1957	8	3
12	1965	6	4
13	1972	7	3
14	1976	10	6
15	1982	6	2
16	1986	6	4
17	1992	7	4
18	1994	7	3
19	1997	8	3
	Total	115	58
	Average	6.0	3.0

Table 7.12 shows a total of 19 ENSO (strong and moderate) events that occurred during the 99-year period giving an average of one event every 5.2 years. Table 7.13 gives detailed statistics about the frequency of tropical storms and hurricanes during the ENSO and non-ENSO conditions. The table shows that an average of 6.0 and 3.0 tropical storms and hurricanes, respectively, per year were generated under ENSO conditions and 9.4 and 5.5 tropical storms and hurricanes, respectively, per year under non-ENSO conditions. Apparently, the frequency of tropical storms and hurricanes is reduced during ENSO conditions in the Atlantic Ocean. The primary reason for the decline is due to the increased tropospheric vertical wind shear in the environment. The increased wind shear helps prevent tropical disturbances from developing into tropical storms and hurricanes in the Atlantic Ocean.

The wind shear is defined as the amount of change in the direction or speed of wind with increasing altitude. When the wind shear is weak, the storms that are part of the cyclone grow vertically and the latent heat from condensation is released into the air directly above the storm aiding in the development. When there is a strong wind shear, this means that storms become more slanted and the latent heat release is dispersed over a much larger area.

Table 7.13: Frequency of tropical storms/hurricanes during ENSO and no ENSO conditions

	ENSO Years		No ENSO Years		Total
	Total	*Average*	*Total*	*Average*	
All tropical storms	115 (19 years)	6.0	748 (80 years)	9.4	863
Hurricanes	58 (19 years)	3.0	438 (80 years)	5.5	496

7.16 GLOBAL WARMING AND HURRICANES

According to the International Panel on Climate Change (IPCC), carbon dioxide, methane and other greenhouse gases are likely to warm the atmosphere by 3.6 degrees Fahrenheit (2 degrees Celsius) by 2100. This may result in the increased tropical sea surface temperature. Since tropical storms derive their heat input from warm tropical oceans, it is quite possible that an increase in the surface ocean temperature would lead to more frequent and intense hurricanes, tropical cyclones and typhoons. However, the variability in tropical cyclone frequency and intensity depends on the natural climate variability (Gray, 1990).

A number of investigators have argued that the recent impacts of hurricane Andrew in 1992 and Hugo in 1989 are evidence of global warming. In this context several investigators became interested to know whether the global warming or warmer globe would influence the frequency of occurrence of tropical cyclones. Several researchers investigated the relationship between the occurrence of tropical cyclones and global warming using a Global Climate Model (GCM). A GCM is a locomotive strength software that simulates how radiation, wind, temperature and oceans interact to produce climate. They are run to predict the effects of rising levels of greenhouse gases. Using a coupled ocean-atmosphere GCM, Royer et al. (1998) showed that global warming would result in about a 10% increase in numbers of tropical cyclones in the northern hemisphere and about a 5% increase in numbers in the southern hemisphere. Similarly, Druyan et al. (1999) found that the global warming would produce more tropical cyclones over the North Pacific Ocean, east of the Philippines and the North Atlantic Ocean. Although modeling studies to date have shown possible increases in tropical

cyclone frequency with a warmer globe, most studies have assumed that the relationship between tropical cyclone generation and environmental parameters would remain stationary. For example, recently Henderson-Sellers et al. (1998) assessed the impact of global warming on tropical cyclones and found no possibility of major changes in the area or global location of tropical cyclone genesis in greenhouse conditions. Further they concluded that the peak intensity of tropical cyclones may increase by 5 to 10% in wind speeds for a doubled carbon dioxide climate but the other factors, such as ocean spray and lapse rate (surface to 300 mb) changes, would act to reduce changes in wind speeds.

Although no definitive answers have been provided as to how the tropical cyclones may alter due to global warming, the fact remains that intense hurricanes have been decreasing in the Atlantic over the past 50 years, despite a rapid increase in tropical cyclone-caused losses. This indicates that societal factors, as opposed to physical factors, are important and that impacts of tropical cyclone would continue to rise unless measures are taken to reduce vulnerability. This need is largely independent of the number of future tropical cyclone frequency. The main coastal impacts resulting from tropical cyclone are flooding from storm surge, wind related structural damage, and risk to life from flying debris; rainfall which is often heavy and widespread after a tropical cyclone makes landfall, and large scale flooding from excessive rainfall are the main threats to life and property.

7.17 HURRICANE THREATS, DAMAGE AND DESTRUCTION

7.17.1 Energy and Lightning due to Hurricanes

A hurricane is essentially a heat engine. It derives its heat input from the warm humid air over the tropical ocean. The hurricane releases this heat energy through the condensation of water vapor into water droplets. The huge amount of heat released in the condensation process is used to cause rising motions in the storm and also maintain the strong spiraling winds of the hurricane. Many scientists have drawn our attention to the fact that a hurricane represents a tremendous generation of heat energy. If we could divert even a small part of the energy of a hurricane from its path of destruction, then benefits will be substantial. The total energy released through the condensation process of rain formation is as follows. Let us assume that an average hurricane extending over a radius of 665 km produces rainfall (p) of about 1.5 cm per day. Therefore, the total amount of rainwater received would be:

$$
\begin{aligned}
\text{Amount of rainwater} &= \pi r^2 \times p \\
&= 3.14 \times 665 \times 665 \times 1.5{\times}10^{10} \text{ cm}^3/\text{day} \\
&= 2.1{\times}10^{16} \text{ cm}^3/\text{day} \\
&= 2.1{\times}10^{16} \text{ gm/day [1 cm}^3 \text{ of water} = 1 \text{ gm]}
\end{aligned}
$$

Using the latent heat of condensation of water to be 597 cal/gm, this amount of rain produced would generate heat of :

$$\text{Heat generated } = 597 \times 2.1 \times 10^{16} \text{ calories/day}$$
$$= 1.3 \times 10^{19} \text{ calories/day}$$
$$= 5.4 \times 10^{19} \text{ Joules/day [1 calorie = 4.2 Joules]}$$
$$= 6.0 \times 10^{14} \text{ Joules/sec}$$
$$= 6.0 \times 10^{14} \text{ Watts}$$

Computations show that about 5.4×10^{19} Joules/day (6.0×10^{14} Watts) of heat is generated by a hurricane. This enormous amount of heat released in a hurricane is equivalent to 200 times the worldwide electrical generating capacity.

7.17.2 Highest Damages and Death Tolls on Record

The data existing in the last several years indicated that among several kinds of natural disasters occurring in the world the destructive power of hurricanes/cyclones is the largest. As killers, they were far ahead of earthquakes. The annual worldwide damage for around 80-100 tropical cyclones each year has been estimated at about 1.5 billion U.S. dollars with a human death toll of 15,000-20,000 [Pearce et al., 1996].

There are three elements associated with a hurricane, which cause destruction and damage. (i) Hurricanes are associated with high-pressure gradients and consequent strong winds. These in turn generate storm surges. A storm surge is an abnormal rise of sea level that occurs as a storm approaches a coastline. The sea water associated with storm surge inundates low lying areas of coastal regions drowning human beings and live stock, eroding beaches and embankments, destroying crops and reducing soil fertility. In 1900, up to 12,000 deaths occurred in Galveston, Texas, primarily as a result of the storm surge that was associated with a Gulf of Mexico hurricane. In 1957, a storm surge, which was associated with hurricane Audrey and which was over four meters and extended as far as 40 kilometers in this particularly low-lying region, was the major cause of death of 500 people in Louisiana. In September 1928, the waters of Lake Okeechobee, driven by hurricane winds, overflowed the banks of the lake and were the main cause of more than 1800 deaths. A tropical cyclone in Bangladesh in November 1970 caused the death of nearly 300,000 people due to storm surge. (ii) Very strong winds of a hurricane produce considerable damage to structures and communication systems and cause risk to life from flying debris. (iii) Heavy and prolonged rains due to cyclones/hurricanes cause river floods and submergence of low lying areas. Table 7.14 gives the death toll caused by cyclones in various parts of the world during the period 1864-1999.

Table 7.14: Deaths from cyclones and hurricanes

Number	Cyclone/Hurricane	Deaths	Location
1	October 1864	50,000	Bengal (now Bangladesh)
2	1 Nov. 1876	100,000	Bengal (now Bangladesh)
3	8 Sept. 1900	12,000	Galveston Texas, USA
4	12-17 Sept. 1928	4,000	West Indies, FL
5	3 Sept. 1980	2,000	San Domingo
6	15-16 Oct. 1942	11,000	Bengal, India
7	Oct. 1949	700	Masulipatnam, Andhra Pradesh, India
8	25-27 Sept. 1953	1,300	Vietnam
9	27 Sept. 1954	1,218	Japan
10	June 1957	500	Louisiana, USA
11	17-19 Sept. 1959	2,000	Far East
12	26-27 Sept. 1959	4,466	Honshu, Japan
13	4-6 Oct. 1963	6,000	Cuba, Haiti
14	13 Nov. 1970	300,000	Bangladesh
15	19-20 Sept. 1974	2,000	Honduras
16	19 Nov. 1977	10,000	Andhra Pradesh, India
17	4 June 1982	243	Orissa Coast, India
18	9 May 1990	1,000	Andhra Pradesh, India
19	Nov. 1999	10,000	Orissa Coast, India

A list of 25 damaging hurricanes that caused large-scale deaths and destruction is given in Tables 7.15 and 7.16.

Table 7.15: 25 deadliest hurricanes in USA during 1900-1998
(from Hebert et al., 1997)

Rank	Hurricane	Year	Category	Deaths
1	Galveston, TX	1900	4	12,000
2	Okeechobee, FLOOD	1928	4	1,836
3	FL (Keys), TX	1919	4	600
4	New England	1938	3	600
5	FL (Keys)	1935	5	408
6	Audrey (SW LA/N TX)	1957	4	390
7	NE US	1944	3	390
8	Grand Isle, LA	1909	4	350
9	New Orleans, LA	1915	4	275
10	Galveston, TX	1915	4	275
11	Camille (MS/LA)	1969	5	256
12	FL (Miami)/MS/AL	1926	4	243
13	Diane (NE US)	1955	1	184
14	SE FLOOD	1906	2	164

(*Contd.*)

Table 7.15: (*Contd.*)

Rank	Hurricane	Year	Category	Deaths
15	MS/AL/FL	1906	3	134
16	Agnes (NE US)	1972	1	122
17	Hazel (NC/SC)	1954	4	95
18	Betsy (SE FL/SE LA)	1965	3	75
19	Carol (NE US)	1954	3	60
20	Floyd - Eastern US	1999	2	57
21	SE FL/LA/MS	1947	4	51
22	Donna (FL/Eastern US)	1960	4	50
23	GA/NC/SC	1940	2	50
24	Carla - TX	1961	4	46
25	TX (Velasco)	1909	3	41

One can take some comfort in the fact that even with the massive damage amounts that hurricanes can cause, none of these hurricanes in recent years have caused huge numbers of deaths in the United States. This is because of the increasingly skillful forecasts of hurricane tracks, and the ability to communicate warnings to the public.

Table 7.16: 25 costliest hurricanes (normalized to 1998 dollars by inflation, wealth increases and coastal county population changes)

Rank	Hurricane	Year	Category	Damage (100s US Dollars)
1	E Florida/Alabama	1926	4	83,814
2	Andrew (SE FL/LA)	1992	4	38,362
3	Galveston, TX	1900	4	30,856
4	Galveston, TX	1915	4	26,144
5	SW Florida	1944	3	19,549
6	New England	1938	3	19,275
7	Okeechobee, FLOOD	1928	4	15,991
8	Betsy (SE FL/LA)	1965	3	14,413
9	Donna (FL/Eastern US)	1960	4	13,967
10	Camille (MS/LA)	1969	5	12,711
11	Agnes (NE US)	1972	1	12,408
12	Diane (NE US)	1955	1	11,861
13	Hugo (SC)	1989	4	10,872
14	Carol (NE US)	1954	3	10,509
15	SE FL/LA/MS	1947	4	9,630
16	Carla (TX)	1961	4	8,194
17	Hazel (NC/SC)	1954	4	8,160
18	NE US	1944	3	7,490
19	SE Florida	1945	3	7,318
20	Frederic (AL/MS)	1979	3	7,295

21	SE Florida	1949	3	6,707
22	FL (Keys), TX	1919	4	6,200
23	Alicia (N TX)	1983	3	4,702
24	Floyd (Eastern US)	1999	2	4,500
25	Celia (S TX)	1970	3	3,869

The previous table shows that Andrew is no longer the most destructive hurricane on record. 23 of the top 25 destructive hurricanes were major hurricanes of Saffir-Simpson Scale 3 or higher.

The most devastating cyclone of the Indian Sea have occurred in the Bay of Bengal and have caused considerable damage to life and property in coastal areas of Tamilnadu, Andhra Pradesh, Orissa, and West Bengal. The cyclone hit the Orissa Coast on June 4, 1982, which caused loss of life and destruction on a massive scale as shown in Table 7.17.

Table 7.17: Damage caused by cyclones

Population affected	7,323,000
Villages affected	15,536
Area affected	25,000 km^2
Deaths	243
Injuries	493
Cattle lost	11,468
Crop area damaged	15,890 km^2
Area saline-inundated	890 km^2
Houses collapsed/damaged	819,000
Power lines lost	2,566 km
Canal breaches	1,840
Embankment breaches	302
Embankments/channels damaged	796 km
Irrigation projects damaged	2,384
Roads damaged	13,478 km
Public buildings damaged	5,591
Schools damaged	6,876
Tube wells damaged	2,500
Drinking water wells damaged	1,600

The cyclone was associated with hurricane wind speeds of 220 km/hr and a storm surge of 2 to 4 meters in height of seawater.

REFERENCES

Bao, C., 1987. Synoptic Meteorology in China. Springer, Berlin.

Druyan, L.M., Lonegran, P. and Eichler, T., 1999. A GCM investigation of global warming impacts relevant to tropical cyclone genesis. *Int. J. of Climatology*, 19, pp. 607-618.

Dunn, G.E. and Miller, B.I., 1964. Atlantic Hurricanes. Louisiana State University Press, Baton Rouge, LA., 377 p.

Emanuel, K.A., 1987. The dependence of hurricane intensity on climate. *Nature*, 326, pp. 483-485.

Gray, W.M., 1990. Strong association between west African rainfall and US landfall of intense hurricanes. *Science*, 249, pp. 1251-1256.

Hebert, P.J., Jarrell, J.D. and Mayfield, M., 1997. The deadliest, costliest and most intense United States hurricanes of this century. NOAA. Tech. Memorandum NWS, TPC-1, National Hurricane Centre, Florida.

Henderson-Sellers, Zhang, A., Berz, H., Emmanual, G., Gray, K.A., Landsea, W., Holland, C., Lighthill, G., Shieh, J., Webster, S.L. and McGuffee, P., 1998. Tropical cyclones and global climate change: A post IPCC assessment. *Bulletin AMS*, 79, pp. 19-38.

Khromov, S.P., 1964. Meteorologiya i Klimatologiya dlya geograficheskikh fakul tetoy (Meteorology and Climatology for Geography Faculties). Leningrad, 499p.

Lourensz, R.S., 1981. Tropical cyclones in the Australian region—July 1909 to June 1980. Bureau of Meteorology Australia., 94 p.

McGregor, G.R., 1995. The tropical cyclone hazard over the South China Sea, 1970-1989: Annual spatial and temporal characteristics. *Applied Geology*, 15, pp. 35-52.

Mitchell, C.L., 1932. West Indian hurricanes and other tropical cyclones of the North Atlantic Ocean. *Monthly Weather Review*, 60, No. 12, p. 250.

Neumann, C.J., 1993. Global overview in global guide to tropical cyclone forecasting. WMO TC-No. 560, Report No. TCP-31, World Meteorological Organization, Geneva.

Petterssen, S., 1969. Introduction to Meteorology. McGraw Hill Book Company, Inc., New York.

Quinn, W.H. and Burt, W.V., 1972. Use of Southern Oscillation in weather prediction. *J. Appl. Meteorol.*, 11, pp. 616-628.

Quinn, W.H., Zopf, D.O., Short, K.S. and Kuo Yang, R.T.W., 1978. Historical trends and statistics of the Southern Oscillation, El Nino and Indonesian droughts. *Fish. Bull.*, 76, pp. 663-678.

Riehl, H., 1954. Tropical Meteorology. McGraw-Hill Book Company, New York.

Royer, J.F., Chauvin, B., Timbal, P. and Grimal, D., 1998. A GCM study of the impact of greenhouse gas increase on the frequency of occurrence of tropical cyclones. *Climate Change*, 38, pp. 307-343.

Tannerhill, I.R., 1956. Hurricanes. Princeton University Press, New Jersey.

U.S. Weather Bureau, 1956. The hurricanes. Revised edition, Washington, D.C.

U.S. Weather Bureau, 1956. Rainfall associated with hurricanes. National Hurricane Research Project, Report No. 3, U.S. Department of Commerce, 305 pp., Washington, D.C.

8 Greatest Point and Areal Rainfalls

Weather systems of the tropics and extra tropics generate heavy to very heavy rainfall for periods of days in various parts of the world, as discussed in Chapter 5. The heavy rainfall events may last 3 to 4 days and are responsible for causing floods, landslides, levee breaches, dams overtopping, sedimentation, erosion and other such occurrences. Flooding from some of the abnormally heavy rainfall events have destroyed dams, causing enormous loss of life and property damage. This happened in India in 1979 when a heavy rainfall event over the Machhu River catchments totally destroyed the Machhu-2 dam on 11 August. The disaster killed as many as 2000 people and totally devastated urban and rural property downstream of the dam (Purohit et al., 1993). Another instance is the catastrophic flood generated from a heavy rainfall event caused by typhoon Nina of August 1975 in the Hongru River basin in China which destroyed the Banqiao and Shimantan dams (Tan and Lu, 1994). There are many dam failures (see Table 8.11) caused by flooding due to heavy rains in various parts of the world (Lemperiere, 1993). In fact, the first recorded dam failure in the USA occurred on 16 May, 1874 in Williamsburg, Massachusetts. It is evident from the above examples that tropical and extra tropical storms and associated heavy rainfalls cause floods which are undoubtedly one of the mightiest and most devastating forces of nature. However, there are ways to prevent or minimize the impacts of flood disasters from heavy rainfall on people and property by adopting the following measures:

- Constructing flood walls and levees to constrict the overflow of rivers
- Increasing capacity of existing channels by river improvement and cutoff
- Constructing flood control dams on rivers to store runoff and reduce flooding downstream
- Constructing diversion channels for flood waters
- Monitoring spillway gates in times of heavy rainfall
- Creating and enforcing effective building codes to prevent property from tropical storms.

For designing the above flood control works ranging from urban drainage systems to dams and spillways and also making better management decisions about floodplain land use, knowledge of the greatest point and areal rainfalls for various durations is essential for determining flood peaks and volumes for maximum protection against structural failure. The information on these extreme events is also of value to people curious about the size of unusual or rare natural phenomena. The information on heavy rainfall may also serve as a background material in evaluating the value of probable maximum storm (PMP) for spillways of large water supply dams as will be discussed in Chapter 10. Moreover, in the regions of sparse or no data, it enables the hydrologist to transfer information from a region of its occurrence to a similar rainfall climate region. The primary purpose of this chapter is to provide available information on greatest point and areal rainfall values for a number of countries from various sources.

8.1 DEFINITIONS

Before proceeding further with the subject of this chapter, it is important to define some terms concerning the use of rainfall information.

 (a) Point rainfall: It is the rainfall at any station at any instant. Suppose the amount of rainfall from 0830 hours on 15 July to 0830 hours on 16 July is 20.5 cm then 20.5 cm is called the point 1 day rainfall of 16 July.
 (b) Average annual rainfall: It is the average value obtained by adding of the annual or seasonal rainfall of any station for a number of years, say 30 years or more, and dividing the sum by the number of years.
 (c) Annual maximum rainfall: It is the highest of the 365 daily observed rainfall values in a year.
 (d) Intensity of rainfall: The rate of rainfall in cm/hr is called the intensity of rainfall. An intensity of less than 0.5 cm/hr is called low and more than 2.5 cm/hr is called high intensity. Intensity can be obtained from records of automatic rainguages and is useful in the estimation of maximum flood discharge.

8.2 SIGNIFICANT RAINFALL OCCURRENCES OVER INDIA

8.2.1 Greatest Mean Annual Rainfalls in the Indian Monsoon

The greatest rainfall accumulation for periods of several days is associated with the Asian monsoons. Most of China, India and Southeast Asia are the prime areas of monsoon rain during the Asian summer season. During the height of the summer monsoon season, rather high moisture is present in the air throughout the monsoonal areas. Thus, mechanisms for releasing the ever present moisture become important in determining the rainfall magnitude. These mechanisms may vary from small-area showers or thundershowers set off by the sun's heating of the earth to tropical storms which may provide heavy rainfall amounts over areas as large as 400,000 km^2.

As regards India, the southwest monsoon is the heavy rain season lasting from June through September. Rainfall is measured on a daily basis at about 5000 stations and measurements at many stations are available for over 100 years. The available mean annual rainfall records (IMD, 1962) for several stations in India indicate that there are only 14 stations which receive mean annual rainfall in excess of 500 cm (Table 8.1). Of these, 10 stations are located in the Western Ghats and the other four in northeast India. The maximum mean annual rainfall recorded in India is 1141 cm at Mawsynaram in Khasi Jaintia hills which has an altitude of 1401 m. Cherrapunji and Mawsynram in Khasi Jaintia hills are world's highest rainfall areas. Cherrapunji holds the world's record rainfall for durations from 15 days to 2 years (see Table 8.10). Agumbe in the Western Ghats of south India has an annual maximum rainfall of 828 cm.

8.2.2 Greatest Point Rainfalls in the Indian Monsoon

During the monsoon season (June to September) much of the heavy to very heavy rainfall for periods of days in India comes mainly from the monsoonal depressions. The rainfall events may last 3 to 4 days and point rainfall may range from 40 to 80 cm a day. Recently, Rakhecha et al. (1990) and Rakhecha and Pisharoty (1996) have made comprehensive studies on heavy rainfall events having durations of 1 to 3 days in India during the 100 years and this has provided much information for the first time on the spatial and temporal characteristics of the greatest point rainfalls. Table 8.2 gives the stations that have recorded rainfalls exceeding 50 cm in one day. This table shows that the one-day greatest rainfalls can be surprisingly high in India. According to Table 8.2, 26 stations have recorded greatest daily rainfall values between 50 and 60 cm, nine between 60 and 70 cm, nine between 70 and 80 cm, four between 80 and 90 cm and five have recorded more than 90 cm. Dharampur (plain area station) in the Surat district of Gujarat in Western India recorded the highest rainfall of 99 cm due to a monsoon depression from the Bay of Bengal on 2 July 1941 (see Fig. 8.9). Cherrapunji, a mountainous station, has recorded the highest rainfall of 104 cm. This demonstrates that one-day rainfall potential caused by topography is more or less equal to that for flat areas caused by the monsoon depression. All the highest rainfalls for the storm periods of 1 to 3 days listed in Table 8.2 were caused by tropical storms except those by orographic influence. In order to identify certain prefered areas, the spatial patterns for one-day greatest rainfalls is shown in Fig. 8.1 This figure is based on the greatest recorded 1-day rainfall (ending 0830 IST) from 1875 to 1982 inclusive for about 300 first order rainfall measuring stations uniformly distributed over the country.

Figure 8.1 shows the pattern of the greatest 1-day rainfall across the Indian region. The isohyets of the greatest 1-day rainfall range from less than 20 cm over large part of the interior peninsula, the arid region of western Rajasthan and northeast of Jammu and Kashmir to over 40 cm on

Table 8.1: Stations recording mean annual rainfall in excess of 500 cm in India

S. No.	Station	State (Fig. 1.2)	Latitude	Longitude	Elevation (m)	Mean annual rainfall (cm)
1.	Amboli	Maharashtra	13^0 31'	75^0 06		748
2.	Agumbe	Karnataka	12^0 23'	75^0 44'	659	828
3.	Bhagamandala	Karnataka	26^0 46'	89^0 35'	876	603
4.	Buxa	West Bengal	25^0 17'	91^0 43'	-	532
5.	Cherrapunji	Meghalaya	27^0 52'	94^0 30'	1313	1087
6.	Denning	Tripura	16^0 33'	73^0 50'	-	532
7.	Gaganbavada	Maharashtra	17^0 56'	73^0 40'		621
8.	Mahabaleshwar	Maharashtra	18^0 59'	73^0 17'	1382	623
9.	Matheran	Maharashtra	25^0 18'	91^0 35'		517
10.	Mawsynram	Meghalaya	12^0 05'	25^0 44'	1401	1141
11.	Makut	Karnataka	10^0 03'	76^0 47'		506
12.	Neriamangalam	Kerala	19^0 34'	76^0 09'		588
13.	Peermade	Kerala	12^0 20'	75^0 34'		517
14.	Pulingoth	Karnataka				594

and near coastal strips, including the Gujarat and Saurashtra coasts, the mountainous regions of the Western Ghats, the hills of Assam and the foothills of the Himalayas. Heavy rainfalls exceeding 30 cm in one day have also occurred over the central parts of India lying between 19° N and 25° N and 70° E to 85° E. Heavy rains exceeding 30 cm in one-day have also occurred even in the arid and semi arid tracts of Rajasthan and Kutch, where annual rainfall is 30 cm or less. There is a general tendency for daily maximum rainfalls to be highest along the coasts and in the mountainous areas. For example, Mumbai (Bombay), Harnai, Cuddalone, Wandiwash, Kakinada, Gopalpur on or near the coasts and some places such as Agumbe, Mt. Abu, Khandala, Mawsynram and Cherrapunji, in the hills have recorded 60 to 100 cm rainfall in one day. It is interesting to mention that the magnitude of the largest measured rainfall at Mumbai increased from 57 cm in July 1974 to 94 cm in 26 July 2005.

The greatest rainfalls for 2 and 3 days are presented in Table 8.3 and their spatial patterns are shown in Fig. 8.2 and Fig. 8.3, respectively. The 2-day rainfall varies from 53 cm to 165 cm and for 3-day from 57 cm to 224 cm. It is mentioned that the rainfall values presented in different tables and figures are at a point, but areal rainfalls are often of greater interest in hydrology and this will be discussed later in this chapter.

Table 8.2: Stations recorded rainfalls exceeding 50 cm in one day duration in India

S. No.	Station	Lat.		Long.		Ht (m)	1-day (cm)	Date
1.	Aliwal	31°	45'	75°	05'	-	50	5.10.1955
2.	Agumbe	13°	31'	75°	06'	659	62	27.7.1963
3.	Bansada	20°	46'	73°	22'	-	51	2.7.1941
4.	Bassi	26°	50'	76°	04'	351	56	19.7.1981
5.	Bamanwas	26	30	76	35	252	51	19.7.1981
6.	Bano	22°	40'	84°	56'	452	81	13.9.1959
7.	Bhagamandala	12°	23'	75°	31'	876	84	25.7.1924
8.	Balehonur	13°	22'	75°	27'	907	73	6.7.1968
9.	Champua	22°	05'	85°	40'	-	57	30.7.1927
10.	Cherrapunji	25°	15'	91°	44'	1313	104	14.6.1876
11.	Contai	21°	47'	87°	45'	11	71	3.8.1977
12.	Chandbali	20°	47'	86°	44'	6	52	16.9.1879
13.	Cuddalore	11°	46'	79°	46'	12	57	18.5.1943
14.	Dakor	22°	45'	78°	09'		54	28.7.1927
15.	Dausa	26°	54'	76°	20'	3	55	19.7.1981
16.	Dharampur	20°	33'	73°	11'	38	99	2.7.1941
17.	Dhampur	29°	18'	78°	31'	238	77	18.7.1880
18.	Goalpara	26°	11'	90°	38'	-	71	8.6.1970
19.	Gopalpur	19°	16'	84°	53'	17	51	24.10.1954
20.	Hardwar	29°	57'	78°	10'		50	18.9.1880
21.	Harnai	17°	49'	73°	06'	20	80	5.8.1968

(Contd..)

Table 8.2 (*Contd.*)

S. No.	Station	Lat.		Long.		Ht (m)	1-day (cm)	Date
22.	Jowai	25°	26'	92°	12'	1390	102	11.9.1877
23.	Kilba	31°	30'	78°	08'	-	61	27.12.1958
24.	Kurseong	26°	53'	88°	17'	1476	64	5.10.1968
25.	Khandala	18°	46'	73°	22'	539	52	19.7.1958
26.	Karjat	18°	55'	73°	20'	107	61	18.7.1958
27.	Kakinada	16°	57'	82°	14'	8	50	2.6.1941
28.	Mount Abu	24°	36'	72°	43'	1195	56	1.9.1973
29.	Mawsynram	25°	18'	91°	35'	1401	99	10.7.1952
30.	Mongpoo	26°	55'	88°	30'	-	55	12.6.1950
31.	Mumbai	18°	54'	72°	49'	11	57	5.7.1974
32.	Mavelikara	09°	15'	76°	32'	-	65	24.7.1967
33.	Navasari	20°	57'	72°	56'	25	78	2.7.1941
34.	New Kandla	23°	00'	70°	13'	14	51	12.8.1979
35.	Nagina	29°	27'	78°	26'	250	82	18.9.1880
36.	Najibabad	29°	37'	78°	21'	240	72	18.9.1880
37.	New Delhi	28°	35'	77°	12'	216	50	9.9.1875
38.	N. Lakhimpur	27°	14'	94°	07'	102	51	22.9.1956
39.	Porbander	21°	37'	69°	38'	12	51	4.9.1977
40.	Pindwara	24°	47'	73°	03'	370	64	1.9.1973
41.	Purnea	25°	46'	87°	28'	38	90	13.9.1879
42.	Paradip port	20°	19'	86°	44'	4	70	10.11.1969
43.	Palhera	22°	03'	80°	46'	-	57	30.6.1961
44.	Ponnampet	12°	09'	75°	56'	857	52	16.7.1965
45.	Rewa	24°	32'	81°	18'	286	77	16.6.1882
46.	Sambalpur	21°	28'	83°	58'	148	58	9.8.1982
47.	Tezu	27°	55'	96°	10'	197	64	30.9.1972
48.	Taldangra	23°	02'	87°	06'	-	60	10.8.1950
49.	Tellicherry	11°	45'	75°	30'	-	64	25.5.1969
50.	Satna	24°	34'	80°	50'	549	54	16.6.1882
51.	Vengurla	15°	52'	73°	38'	9	53	15.6.1958
52.	Wandiwash	12°	30'	79°	37'	-	71	5.8.1965
53.	Quilandi	11°	27'	75°	42'	8	91	28.5.1961

Table 8.3: Stations recorded rainfalls exceeding 60 cm
in 2- and 3-day durations in India

S. No.	Station	Height (m)	2-day	3-day	Date
1.	Agumbe*	659	93	95	July 1963
2.	Bamnwas	252	76	103	July 1981
3.	Bansada		91	107	July 1941
4.	Bassi	351	84	85	July 1981
5.	Bhagmandala*	876	136	136	July 1924
6.	Mumbai	11	80	88	July 1974
7.	Champua		71	74	July 1927

8.	Cherrapunji*	1313	165	224	June 1876
9.	Cuddalore	12	82	95	May 1943
10.	Dausa		64	69	July 1981
11.	Dakor		100	114	July 1927
12.	Dhampur	258	99	99	Sept. 1880
13.	Dharampur	38	126	145	July 1941
14.	Gopalpur	17	65	70	October 1954
15.	Hardwar		81	81	Sept. 1880
16.	Khandala*	539	67	73	July 1958
17.	Kakinada	8	53	57	June 1941
18.	Karjat*	107	67	73	July 1958
19.	Mawsynram*	1401	143	201	July 1952
20.	Nagina	250	104	104	Sept. 1880
21.	Najibabad	240	98	98	Sept. 1880
22.	Navasari		124	126	July 1941
23.	Ponnampet	857	61	67	July 1965
24.	Porbandar	12	62	66	Sept. 1977
25.	Quilandi	8	109	113	May 1961
26.	Rewa	286	77	82	June 1882
27.	Satna	549	58	61	June 1882
28.	Vengurla	9	82	88	June 1958

*Orographic rainfall
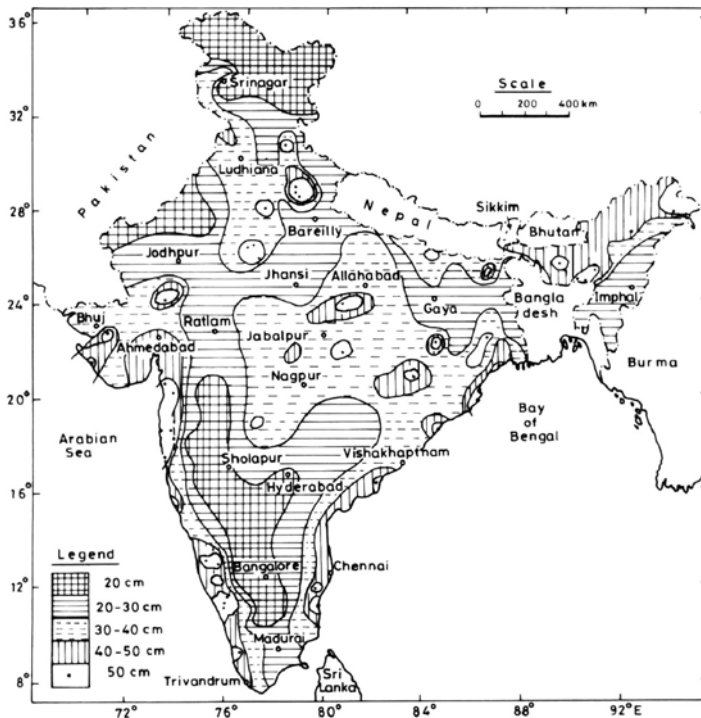
Fig. 8.1. Greatest rainfalls for 1-day duration (1875-1982)
(after Rakhecha and Pisharoty, 1996).
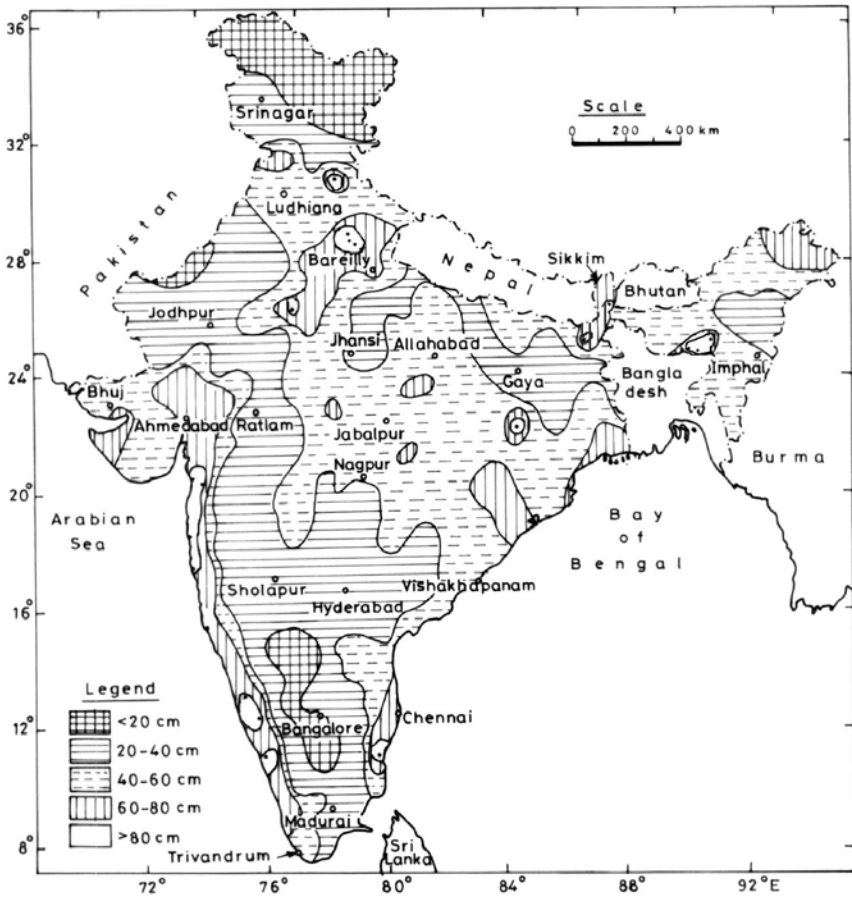
Fig. 8.2. Greatest rainfalls for 2-day duration (1875-1982)
(after Rakhecha and Pisharoty, 1996).
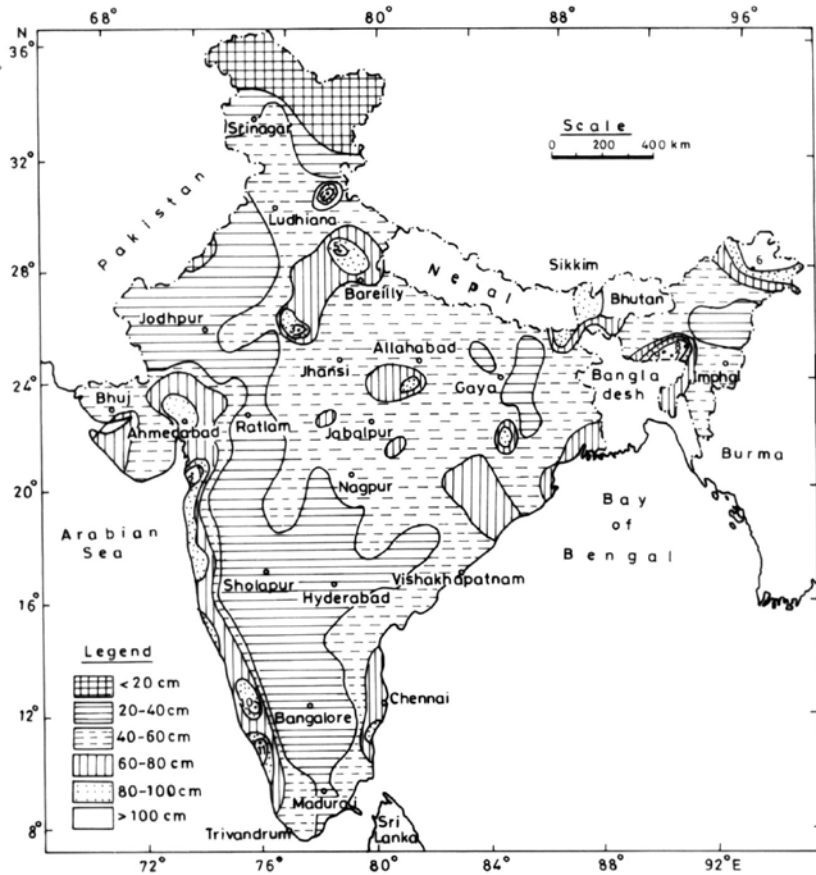
Fig. 8.3. Greatest rainfalls for 3-day duration (1875-1982)
(after Rakhecha and Pisharoty, 1996).

8.2.3 Greatest Hourly Rainfalls in India

Table 8.4 gives the highest 1-hour rainfall values for some stations in India.
There is a general tendency for hourly rainfalls to be highest along the
coastal and mountainous areas. The highest 1-hour rainfall of 12.9 cm occurred
in Mumbai. These values represent intensities only over small areas around
the recording points for turbulence and exposure characteristics of the
measuring gauge can vary even a small distance of a few meters.

Table 8.4: Greatest 1-hour rainfall amounts (cm) in India

S. No.	Station	Lat		Long		Ht (m)	Rainfall (cm)
1.	Allahabad	25°	27'	81°	44'	98	7.5
2.	Asansol	23°	41'	86°	59'	126	8.6
3.	Amritsar	31°	38'	74°	52'	234	6.5
4.	Aurangabad	19°	53'	75°	20'	581	6.1
5.	Agartala	23°	53'	91°	15'	-	6.6
6.	Ahmedabad	19°	05'	74°	55'	55	8.0
7.	Vadodara	22°	18'	73	15'	38	6.7
8.	Mumbai	19°	07'	72°	51'	15	12.9
9.	Bangalore	12°	57'	77°	38'	921	6.1
10.	Bhopal	23°	17'	77°	21'	523	7.2
11.	Cherrapunji	25°	15'	91°	44'	1313	12.7
12.	Calcutta	22°	39'	88°	27'	6	6.8
13.	Dibrugarh	27°	28'	94°	55'	106	6.0
14.	Gaya	24°	45'	84°	57'	116	7.0
15.	Hyderabad	17°	27'	78°	28'	545	10.2
16.	Hazaribagh	23°	59'	85°	22'	611	6.7
17.	Jamshedpur	22°	49'	86°	11'	129	8.6
18.	Jodhpur	26°	18'	73°	01'	224	5.1
19.	Jaipur	26°	49'	75°	48'	390	5.7
20.	Jabalpur	23°	11'	79°	57'	393	7.4
21.	Jagadalpur	19°	05'	82°	02'	553	7.3
22.	Kodaikanal	10°	14'	77°	28'	2343	6.9
23.	Lucknow	26°	45'	80°	53'	111	7.0
24.	Chennai	13°	00'	80°	11'	16	6.2
25.	Mangalore	12°	52'	74°	51'	22	6.4
26.	Mahabaleshwar	17°	56'	73°	40'	1382	4.9
27.	New Delhi	28°	35'	77°	12'	216	7.9
28.	Nagpur	21°	06'	79°	03'	310	7.8
29.	Pune	18°	32'	73°	51'	559	4.7
30.	Trivandrum	8°	29'	76°	57'	64	7.1
31.	Tiruchirapalli	10°	46'	78°	43'	88	7.8
32.	Veraval	20°	54'	70°	22'	8	12.2
33.	Vengurla	15°	52'	73°	38'	9	6.6
34.	Viskhapatnam	17°	43'	83°	14'	3	6.3

8.3 SIGNIFICANT RAINFALL OCCURRENCES OVER CHINA

Most of China is situated in the tropical East Asia monsoon region. Southern and eastern parts of China are frequently hit by typhoons which stem from the southwest Pacific ocean. These typhoons bring exceptionally heavy rainfalls in coastal areas. Sometimes a strong typhoon can move inland causing a heavy rainfall if the area is influenced by cold air at the same time.

Pan and Teng (1988) in their work on determination of design flood in China gave a list of extraordinary rainfalls for six hours to seven days for stations in China as shown in Table 8.5.

Table 8.5: Stations recorded greatest rainfalls (cm) in China

S. No.	Location	Date	Rainfall in cm			
			6 hr	24 hr	3 days	7 days
1.	Guangdong, Tangkou	22 April 1965	61.0	76.9	90.0	104.2
2.	Guangdong, Litong	20 May 1959	28.1	85.8	103.0	123.4
3.	Guangdong Guoziyuan	27 May 1973	51.5	76.0	85.9	117.8
4.	Guangdong, Baishiman	30 May 1977	46.0	88.4	122.2	151.3
5.	Guangxi, Qishi	31 May 1971	36.7	61.7	69.0	70.6
6.	Fujian, Gaoshan	21 June 1974	31.8	73.8	76.5	85.2
7.	Hubei, Yufeng	3 July 1935	-	42.3	107.7	131.8
8.	Guangdong, Zhenhai	12 July 1955	38.6	85.1	94.9	98.2
9.	Guangxi, Laohutan	11 July 1960	44.1	65.8	103.6	114.1
10.	Nei Mongol, Uxinqi	1 August 1977	-	140.0	-	-
11.	Jiangsu, Chaoqiao	4August 1960	-	82.2	93.4	93.4
12.	Hebei, Zhangmo	4 August 1963	42.6	95.0	145.8	205.1
13.	Henan, Lingzhuang	7 August 1975	83.0	106.0	160.5	163.1
14.	Anhui, Yangyin	17 August 1975	30.7	65.3	82.9	88.0
15.	Jiangxi, Lu Shan	17 August 1953	-	90.0	107.3	-
16.	Jiangxi, Dafeng	21 August 1965	29.2	67.3	91.7	93.3
17.	Zhejiang, Hualong	12 September 1963	27.3	51.9	73.3	77.0
18.	Taiwan, Baishi	10 September 1963	-	124.8	179.4	-
19.	Hainan Dao, Jianfengling	8 September 1963	33.9	77.7	91.2	91.4
20.	Guangdong, Wuyang	21 September 1976	45.0	79.4	102.9	102.9
21.	Hainan Dao, Tunchang	11 October 1954	-	69.7	85.2	92.9
22.	Taiwan, Xinliao	17 October 1967	-	167.2	274.9	-
23.	Guangdong, Kangdong	29 September 1965	51.0	67.4	143.9	-

Source: Pan and Teng (1998)

According to Pan and Teng (1988), the intensities of several observed point rainfalls exceeded the highest that occurred at the same latitude in the world. In August 1975, Typhoon Nina caused heavy to very heavy rainfall in the Hongru River Basin. The rainfall lasted for five days during August 4-8. A rainfall of 106 cm in 24-hr occurred in Lingzhuang, Henan province, which is about 600 km away from the coast. Also, the storm with the highest intensity 83 cm in six hours in Lingzhuang set a new world record. The heavy rainfall caused huge inflow of water into the reservoirs of Banqiao and Shimantan dams. The magnitude of the generated flood was so large that it ultimately destroyed the Banqiao and Shimantan dams as mentioned earlier. Figure 8.4 shows the distribution of highest 24-hour rainfalls in China. According to Table 8.5 and Pan and Teng (1988), 13 stations in China

recorded daily values between 40 and 80 cm, six between 80 and 100 cm, three between 100 and 140 cm, and one (Xinliao) recorded 167.2 cm.

In the inland plateau of China (the arid and semi arid regions) heavy rainfalls are much less frequent than in coastal areas. It was found that heavy rainfalls of short duration over small areas have very high intensity. Some high intensity rainfalls have been observed in the arid region such as rainfall of 50-60 cm during a 3-6 hour period.
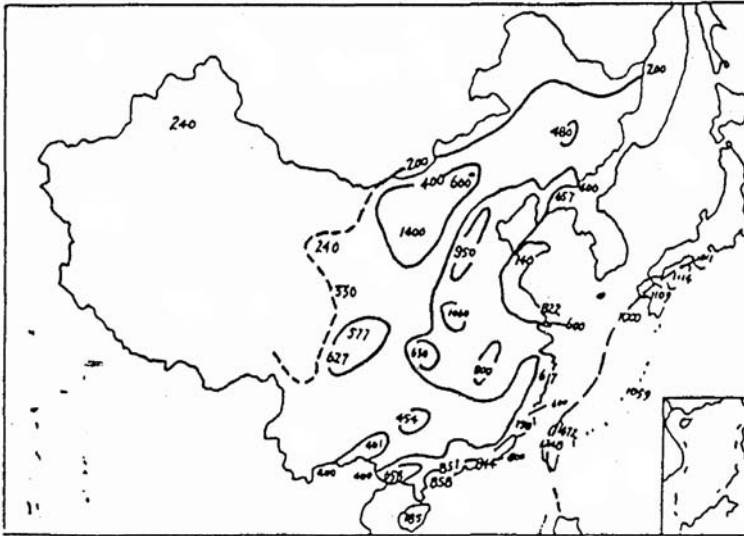
Fig. 8.4. Highest rainfall (mm) for 24-hour in China.

8.4 SIGNIFICANT RAINFALL OCCURRENCES OVER AUSTRALIA

The heaviest rainfalls in Australia are caused by tropical cyclones. The average season for tropical cyclones in the Australian region is in November/December and continues to March/April. The month of greatest activity is January. The Australian Bureau of Meteorology (1976, 1996) in their Climate of Australia and the hydrology report series-3 gave the listing of stations which recorded extreme rainfalls in different durations (see Table 8.6) as also the stations that recorded the highest 24-hour rainfalls (see Table 8.7). Most of the very high 24-hour falls (above 70 cm) have occurred in the coastal strip of Queensland where a tropical cyclone moving close to mountainous terrain provides ideal conditions for spectacular falls. Brunt (1958) describes an event that produced 90.7 cm of rainfall in 24 hours on 3 February at Crohamhurst, Queensland. The Australian record for 24 hours is 96.0 cm at Bellenden Ker Top, Queensland on 4 January 1979. Cyclone Tracy produced 82 cm of rain over Darwin in northern Australia in 1974. Comparison of notable Australian point rainfalls with the world's greatest observed point rainfalls is shown in Fig. 8.6.

Table 8.6: Stations recorded greatest rainfalls (cm) for different
durations in Australia

S. No.	Station	Period	Duration-hours				
			1	3	6	12	24
1.	Adelaide	1897-1967	6.9	13.3	14.1	14.1	14.1
2.	Alice Springs	1951-1970	5.4	5.5	6.4	8.7	10.6
3.	Brisbane	1911-1968	8.8	14.4	18.2	24.4	30.8
4.	Broome	1948-1970	7.2	11.9	13.0	17.2	22.8
5.	Canberra	1932-1970	5.1	6.8	7.1	8.9	13.8
6.	Carnarvon	1956-1971	3.2	6.3	8.2	9.5	10.8
7.	Charleville	1953-1971	4.2	6.6	7.5	11.1	14.2
8.	Cloncurry	1953-1972	4.6	11.8	16.4	17.3	20.4
9.	Darwin	1953-1970	8.8	10.1	10.9	15.2	19.1
10.	Esperance	1963-1972	2.3	45	6.2	6.8	7.9
11.	Hobart	1911-1970	2.8	5.6	8.7	11.7	16.8
12.	Meekathara	1953-1971	2.6	6.7	8.0	9.8	11.2
13.	Melbourne	1878-1969	4.9	5.7	8.6	10.2	12.9
14.	Mildura	1953-1971	4.9	6.0	6.5	6.5	9.1
15.	Perth	1946-1971	3.2	3.8	4.7	6.4	9.3
16.	Sydney	1913-1967	6.9	13.4	16.2	18.0	28.1
17.	Townsville	1953-1970	8.7	11.1	12.2	16.1	27.5

Source: Climate of Australia, Bureau of Meteorology Australia, 1975.

Table 8.7: Stations recording the greatest daily rainfalls in Australia

S. No.	State	Station	Amount (cm)	Date
1.	Queensland	Bellenden Ker Top	96.0	4 January 1979
		Crohamhurst	90.7	3 February 1893
		Finch Hatton	87.8	18 February 1958
		Mount Dangar	86.9	20 January 1970
		Port Douglas	80.1	1 April 1911
2.	Western Australia	Whim Creek	74.7	3 April 1898
		Fortescue	59.3	3 May 1890
3.	New South Wales	Dorrigo	63.6	24 June 1950
		Cordeaux River	57.4	14 February 1898
4.	Northern Territory	Darwin	82.0	1974
		Roper Valley	54.5	15 April 1963
		Groote Eylandt	51.3	28 March 1953
5.	Tasmania	Mathinna	33.6	5 April 1929
		Cullenswood	28.2	5 April 1929
6.	Victoria	Balook	27.5	18 February 1951
		Hazel Park	26.7	1 December 1934
7.	South Australia	Ardrossan	20.6	18 February 1946
		Carpa	19.9	18 February 1946

Source: Climate of Australia, Bureau of Meteorology Australia, 1975.
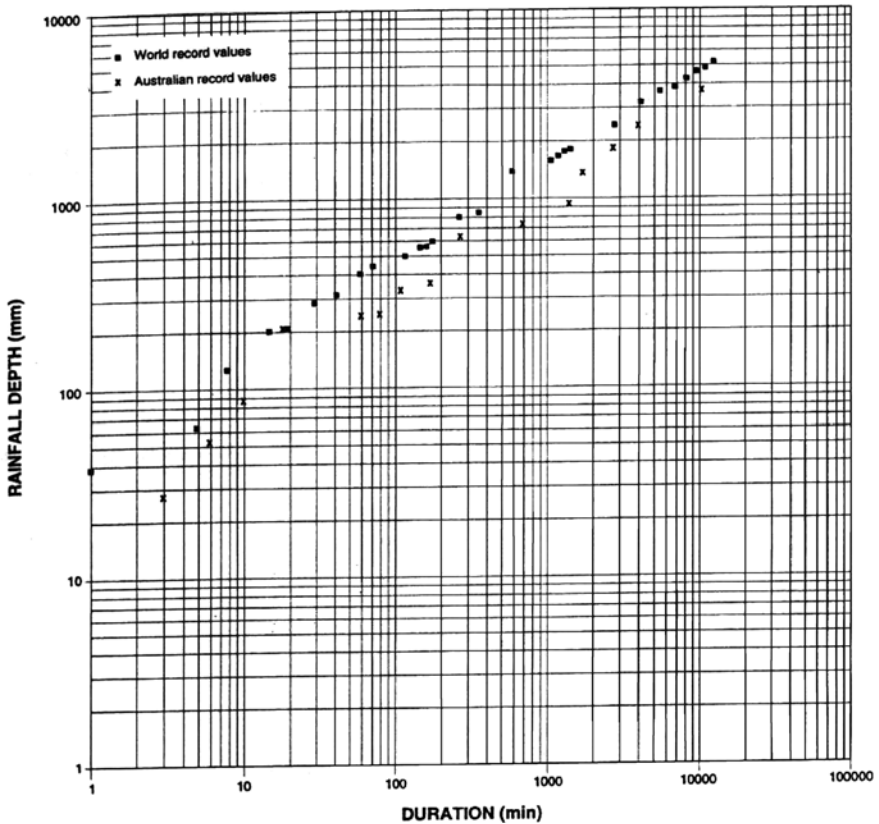
Fig. 8.5. Comparison of Australian greatest point rainfalls
with the world's greatest point rainfalls.

8.5 SIGNIFICANT RAINFALL OCCURRENCES OVER JAPAN

Most of the annual rainfall in Japan occurs in the rainy season in June and
during the typhoon season from September to October. Almost every year an
average 30 typhoons affect Japan and about three move into the country.
Typhoons in Japan have produced some of the greatest rainfalls. The greatest
observed point rainfalls for different durations ranging from 10 minutes to
72 hours in Japan are given in Table 8.8. The largest typhoon rainfall in
Japan for 24 hr, 48 hr and 72 hr are 113.8 cm, 169.2 cm and 223.7 cm,
respectively.

Table 8.8: Stations recording greatest rainfalls (cm) in Japan

Duration	Depth (cm)	Location	Date
10 min	5.6	Shionomisaki Wakayama	19.4.1944
20 min	8.5	Koubtsu Nagasaki	25.7.1982
30 min	11.0	Do	25.7.1982
60 min	18.7	Do	25.7.1982
2 hr	29.6	Ashizuri Kochi	18.10.1944
3 hr	37.7	Saigou Nagasaki	25-26.7.1957
4 hr	46.7	Do	25-26.7.1957
5 hr	57.5	Do	25-26.7.1957
6 hr	64.7	Do	25-26.7.1957
8 hr	74.2	Do	25-26.7.1957
10 hr	84.5	Do	25-26.7.1957
16 hr	105.3	Do	25-26.7.1957
24 hr	113.8	Hisou Tokyshima	10-11.9.1976
36 hr	140.7	Do	10-11.9.1976
48 hr	169.2	Do	9-11.9.1976
72 hr	223.7	Do	10-13.9.1976

8.6 WORLD'S GREATEST POINT RAINFALLS

The greatest 24-hr point rainfall values gathered for different countries of the world are given in Table 8.9 whereas Table 8.10 gives some of the world's greatest recorded rainfall values for various durations (WMO, 1994). The enveloping curve to the world's greatest rainfall values is shown in Fig. 8.6. It can be seen that the enveloping line shown is a very good fit on the log-log scale to most points and enables an easy calculation of world's higest rainfall for any period to be assessed. The equation can be approximated by

$$R = 42.2 \ D^{0.475}$$

in which R = rainfall depth in cm, and D = the duration of rainfall in hours.

Table 8.9: World greatest recorded 24-hr point rainfall (cm) values

S. No.	Station	Rainfall (cm)	Date
1.	Yankeetown, Florida, USA	98.3	6 September 1950
2.	Kadena AF Base, Okinawa	107.2	8 September 1956
3.	Cilaos, La Reunion	187.0	16 September 1952
4.	Belouve, La Reunion	168.9	28 February 1964
5.	Aurere, La Reunion	158.3	8 April 1958
6.	Dharampur, India	99.0	2 July 1941
7.	Nagina, India	82.3	18 September 1880
8.	Linzhuang, China	97.0	5 August 1975
9.	Hisou, Tokushima, Japan	113.8	11 September 1976
10.	Bellenden Ker Top, Queensland, Australia	96.0	4 January 1979
11.	Roebourne, Western Australia	74.7	3 April 1898

Table 8.10: World's record point rainfall values for various durations

| Duration	Depth (cm)	Location	Date
1 min	3.8	Barot, Guadeloupe	26.11.1970
5 min	6.2	Port Bells, Panama	29.11.1911
8 min	12.6	Fussen, Bavaria	25.5.1920
15 min	19.8	Plumb Point, Jamaica	12.5.1916
20 min	20.6	Curtea-de-Arges, Rumanla	8.7.1947
40 min	23.5	Guinea, Virginia USA	24.8.1906
42 min	30.5	Holt, Missouri USA	22.6.1947
2 hr 10 min	48.3	Rockport, West Virginia USA	18.7.1889
2 hr 45 min	55.9	D'Hanis, Texas USA	31.5.1935
4 hr	58.4	Bessetere, St. Kitts, West Indies	12.1.1880
4 hr 30 min	78.2	Smethport, Pennsylvania USA	18.7.1942
6 hr	83.0	Lingzhuang, China	August 1975
9 hr	108.7	Belouve, La Reunion	28.2.1964
12 hr	134.0	Belouve, La Reunion	28-29.2.1964
18 hr 30 min	168.9	Belouve, La Reunion	28-29.2.1964
24 hr	187.0	Cilaos, La Reunion	15-16.3.1952
48 hr	250.0	Cilaos, La Reunion	15-17.3.1952
72 hr	324.0	Cilaos, La Reunion	15-18 March 1952
96 hr	372.1	Cherrapunji, India	12-15 September 1974
120 hr	385.4	Cilaos, La Reunion	13-18 March 1952
144 hr	405.5	-do-	13-19 March 1952
7 days	411.0	-do-	12-19 March 1952
8 days	413.0	-do-	11-19 March 1952
15 days	479.8	Cherrapunji, India	24 June-8 July 1931
31 days	930.0	-do-	July 1861
61 days	1276.7	-do-	June-July 1861
92 days	1636.9	-do-	May-July 1861
122 days	1873.8	-do-	April-July 1861
153 days	2041.2	-do-	April-August 1861
183 days	2245.4	-do-	April-September 1861
334 days	2299.0	-do-	January-November 1861
365 days	2646.1	-do-	August 1860-July 1861
731 days	4076.8	-do-	1860-1861
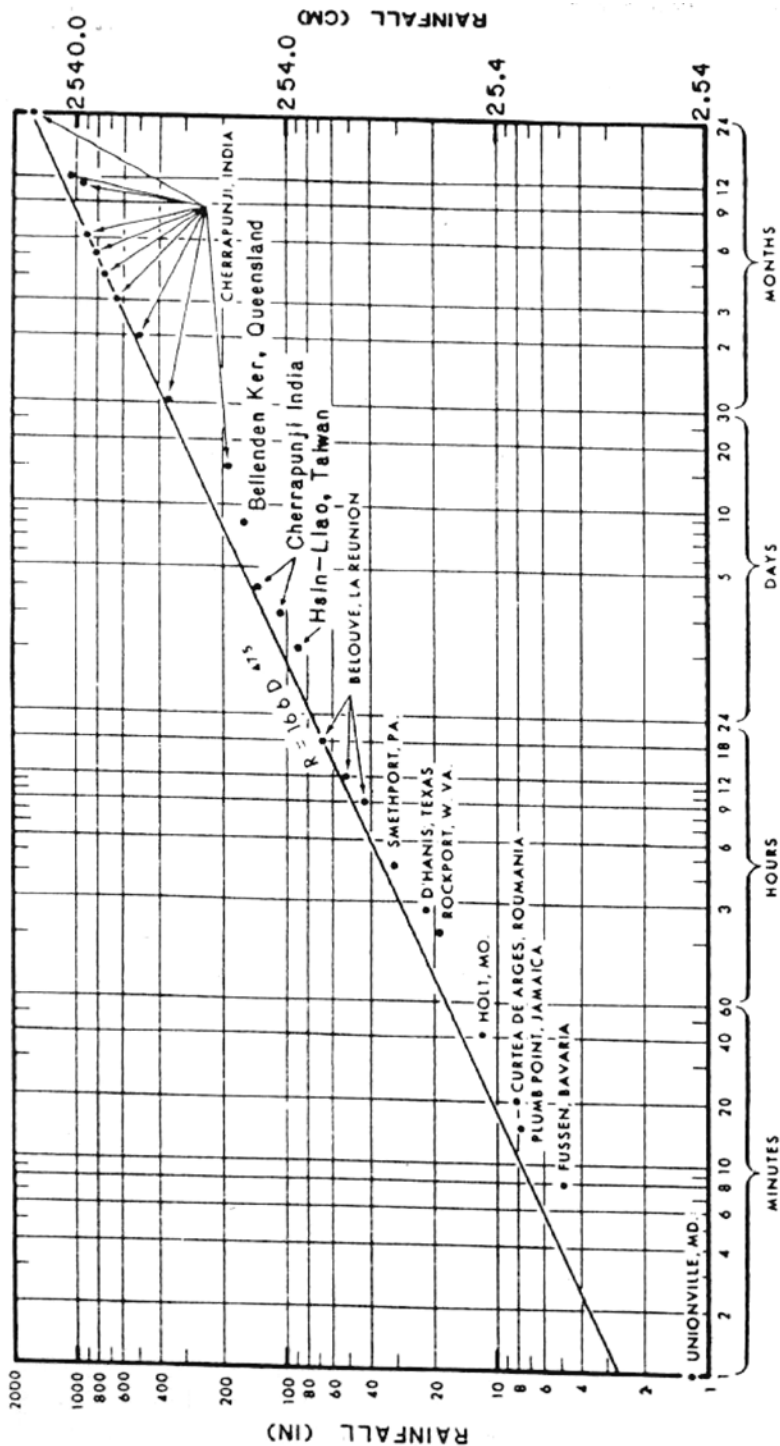
Fig. 8.6. World's greatest observed point rainfalls.

Table 8.9 shows that the greatest recorded point rainfalls for 24 hour duration were 98.3 cm at Yankeetown, Florida, from an Atlantic hurricane; 107.2 cm on 8 September 1956 at Kadena Air Force Base at Okinawa from the Pacific Ocean typhoon and 99.0 cm on 2 July 1941 at Dharampur from the Bay of Bengal depression.

It may be said that not all the rainfall values in Table 8.9 were associated with tropical disturbances but they are indicative of the tremendous amounts of rain that have been generated all over the world. The interesting point worthy of careful note is that how very large amounts of rain are generated within short intervals of time. The table shows, for example, rainfall amounts of the order of 187 cm on the island of Reunion in 24 hours.

8.7 IMPORTANCE OF THE GREATEST AREAL RAINFALLS

The greatest areal rainfall values are used for determining design storms and the probable maximum storm (PMP) for spillways on large dams. Large amounts of money are being spent by every country of the world in the construction of dams and reservoirs for various purposes, such as irrigation, hydropower generation, flood control, water supply for domestic and industrial use, navigation, fisheries, etc. For design of these structures, it is most important that every care is taken in the estimation of spillway design flood so that the dam should stand without overtopping or damage. The design flood for a dam is the flood of suitable probability and magnitude adopted to ensure the safety of dams. The past has seen some significant failures of dams in the world, releasing storages suddenly and causing calamities in the downstream areas. There have been about 200 notable dam failures in the world in the 20th century. Some dam failures in various parts of the world resulting from inadequate design floods are given in Table 8.11.

A recent survey indicated that about 30% of 66,000 existing dams in the USA have been found unsafe and 75% of these are because of inadequate spillway capacities. Many old dams in India and other parts of the world could be similarly unsafe based on hydrological considerations.

The design flood for a dam is estimated from the river discharge data. However, for most cases where major dams are envisaged, discharge records over a long period are not generally available. In such a situation, the magnitude of the design flood can be determined from the greatest areal rainfalls obtained from severe rainstorms experienced by the concerned basin because they are the main cause of floods. The hydrologist, therefore, looks at the information on extreme areal rainfalls from severe rainstorms to obtain estimates of design storm/flood. Information on the greatest areal rainfalls, therefore, assumes importance in the context of dam design works. The method for computing areal rainfalls from a rainstorm is detailed in Chapter 10.

Table 8.11: Major dam failures

S. No.	Dam	Height (m)	Country	Year of Failure	Lives Lost
1.	Southfork	22	USA	1889	2209
2.	Briseis	24	Australia	1929	14
3.	Sellazerbino	47	Italy	1935	-
4.	Kadam	23	India	1958	-
5.	Malpasset	-	France	1959	421
6.	Panshet	53	India	1961	-
7.	Khadakwasla	20	India	1961	-
8.	Valnot	265	Italy	1963	2600
9.	Gibson	61	USA	1964	-
10.	Chikkhole	37	India	1972	-
11.	Shimantan	-	China	1975	-
12.	Banqiao	-	China	1975	-
13.	Teton	-	USA	1976	11
14.	Euclides Da Cunha	40	Brazil	1977	-
15.	Machhu-2	25	India	1979	2000
16.	Noppikoski	19	Sweden	1985	19
17.	Tailings	-	Italy	1985	200
18.	Kantle	-	Srilanka	1986	100
19.	Spitskop	13	South Africa	1988	13

8.8 GREATEST AREAL RAINFALLS OVER INDIA

The historical rainfall data of India, especially after 1891, show that there have been about 1000 major rainstorms which have occurred in different parts of the country. Rakhecha and Pisharoty (1996) and IITM (1994) in their comprehensive storm studies have found that during the 105-year period (1891-1995), 12 rainstorms have given the greatest areal rainfalls for different sized areas and durations. The areal rainfalls observed in India from 12 most predominant rainstorms for storm periods of 1 to 3 days and areas of 10 to 30,000 km^2 are given in Table 8.12 and their locations are shown in Fig. 8.7. Table 8.12 shows that for 10, 100, 1000, 5000, 10,000, 20,000, and 30,000 km^2 the maximum areal rainfalls from these 12 storms varied from 24-99 cm, 23-97 cm, 23-85 cm, 22-65 cm, 21-54 cm, 19-43 cm, and 15-36 cm, respectively, for 1-day duration; from 44-127 cm, 43-126 cm, 32-118 cm, 27-70 cm, 25-83 cm, 20-66 cm and 19-56 cm, respectively, for 2-day duration; and from 58-145 cm, 57-143 cm, 45-134 cm, 30-117 cm, 27-105 cm, 23-86 cm, and 21-76 cm, respectively, for 3-day duration. Therefore, Table 8.12 may serve as a guide in evaluating practical design storm rainfalls for designing hydrologic projects.
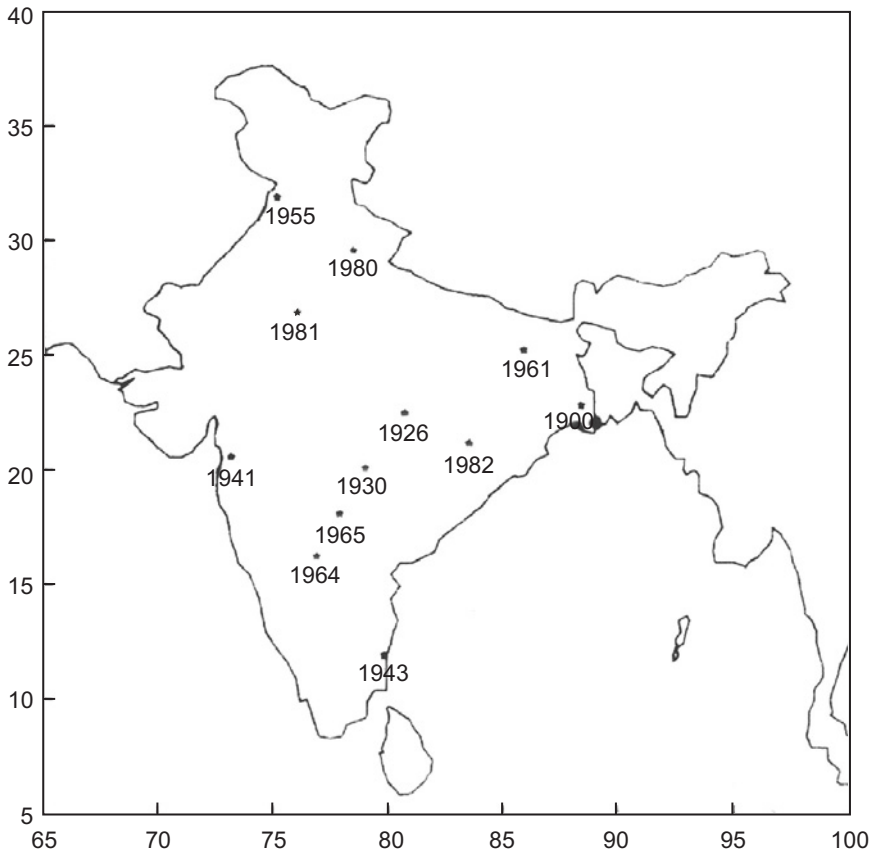
Fig. 8.7. Locations of rainstorms centers.

Table 8.12 indicates that two rainstorms stand out above all others for 1, 2, and 3-day durations that produced the largest areal rainfalls for various sized areas during the 105-year period of available records in India. These were the storms of September 17-18, 1880 over north-west Uttar Pradesh and of July 1-3, 1941, over Gujarat.

The September 17-18, 1880 rainstorm over northwest (NW) Uttar Pradesh was caused by a depression in the Bay of Bengal (see Fig. 8.8). The rainfall lasted two days from 17 to 18 September. The 60-cm isohyet for those days encompasses 20,000 km². The station Nagina recorded 104 cm in two days. The rainstorm caused huge inflows of water in the rivers of these areas. A particularly hard hit area was Nainital, where according to the Imperial Gazetteer (1908), the landslip at Nainital took a heavy toll of human lives, killing about 150 persons including 43 Europeans.

The July 1941 rainstorm was caused by the depression from the Bay of Bengal (see Fig. 8.8). After reaching central India it intensified from the Arabian sea branch of the monsoon and produced a severe rainstorm in the

Table 8.12: Greatest areal rainfalls (cm) in India (Rakhecha and Pisharoty, 1996)

S. No.	Rainstorm date	Storm center	Area affected	Duration	Area in 100 sq. km²						
					0.1	1	10	50	100	200	300
1.	17-18 September 1880	Nagina	Uttar Pradesh	1	28	82	78	63	52	40	34
				2	104	103	99	87	77	62	54
2.	20-22 September 1900	Serampore	West Bengal	1	44	43	41	36	33	28	24
				2	73	72	67	58	52	44	38
				3	83	82	78	69	62	52	45
3.	19-21 September 1926	Bichhia	Madhya Pradesh	1	36	36	35	33	30	26	23
				2	65	65	63	57	53	47	42
				3	83	82	81	76	71	62	55
4.	1-3 July 1930	Wani	Maharashtra	1	36	36	31	24	22	19	16
				2	71	70	58	40	33	28	26
				3	77	76	66	47	39	35	32
5.	1-3 July 1941	Dharampur	Gujarat	1	99	97	85	65	54	43	36
				2	127	126	118	97	83	66	56
				3	145	143	134	117	105	86	76
6.	17-19 May 1943	Vanur	Tamil Nadu	1	42	41	37	29	25	21	19
				2	72	72	69	55	46	37	33
				3	95	95	91	73	61	49	42
7.	3-5 October 1955	Batala	Punjab	1	50	47	45	40	35	29	24
				2	72	70	64	56	51	44	39
				3	72	71	67	59	53	47	43

(Contd.)

Table 8.12 (*Contd.*)

| S. No.	Rainstorm date	Storm center	Area affected	Duration	Area in 100 sq. km²						
					0.1	1	10	50	100	200	300
8.	1-3 October 1961	Sheikhpura	Bihar	1	37	37	36	32	28	23	19
				2	55	54	53	49	44	35	30
				3	58	57	57	54	50	42	37
9.	28-30 September 1964	Atmakur	Karnataka	1	24	23	23	22	21	19	17
				2	44	43	32	27	25	22	21
				3	62	61	51	38	34	30	27
10.	13-15 July 1965	Nizamsagar	Andhra Pradesh	1	51	49	39	25	20	16	15
				2	54	52	41	27	23	20	19
				3	60	57	45	30	27	23	21
11.	18-20 July 1981	Bassi	Rajasthan	1	56	56	54	45	37	27	20
				2	84	83	76	62	52	40	33
				3	97	95	85	71	61	48	40
12.	28-30 July 1982	Bijapur	Orissa	1	52	52	51	45	38	30	24
				2	70	70	69	65	59	50	43
				3	88	88	84	74	66	55	46
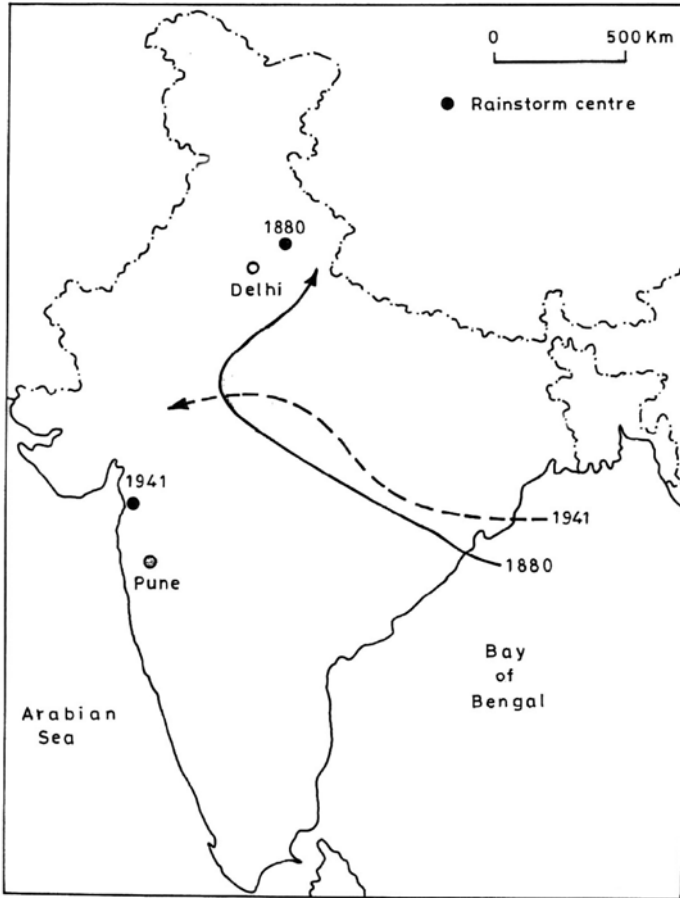
Fig. 8.8. Tracks of two depressions.

Gujarat state. Several stations recorded rainfalls exceeding 40 cm in one day. The Dharampur station recorded 99 cm of rainfall in one day on July 2. This is a record rainfall for a plain area station in India for one-day duration. However, the record value established in the July 1941 storm is far below the world's one-day highest value of Table 8.9. The July 1941 rainstorm has been recognized as the highest recorded storm so far not only in the Gujarat state but also in the entire region of India. Torrential rainfalls from this rainstorm caused severe flooding in the Tapi River. During the same event, a heavy landslide from the Western Ghats had buried an electric locomotive near Karjat railway station. As a result, rail traffic was paralyzed between Pune and Mumbai for 10 days. The largest values of areal rainfalls in India are comparable and even exceed the largest areal rainfalls from Australia, China and the USA. Also the spatial pattern of rainfall for one-day duration for July 1941 storm which is considered to be the world record storm is shown in Fig. 8.9.
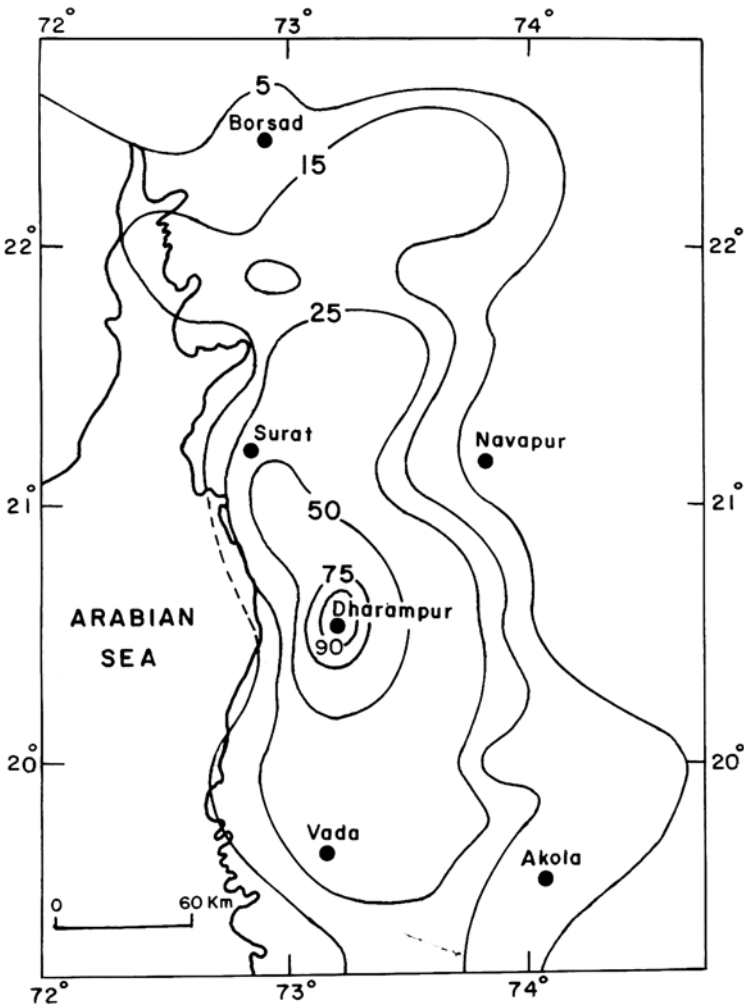
Fig. 8.9. Isohyets (cm) of one-day (2 July 1941) rainstorm.

8.9 GREATEST AREAL RAINFALLS OVER THE USA

Tropical storms and hurricanes form over the Gulf of Mexico, Caribbean sea and the southern north Atlantic Ocean during June to November, as stated in Chapter 7. After formation over the seas, some of them move into the US and cause heavy to very heavy rainfall over thousands of square kilometers. Heavy rainfalls occur in the front sector to the right of the path of the hurricane and point rainfall caused by such hurricanes range from 40 cm to 80 cm in 24 hours. Shipe and Riedel (1976) show that in the rainfall records of the US, the following three rainstorms contributed the greatest areal rainfalls for one-day to three-day duration. These rainstorms are:

- 27 June-1 July 1899 with center at Hearme, Texas.
- 13-15 March 1929 with center at Elba, Alabama.
- 3-5 September 1950 with center at Yankeetown, Florida.

The storm of 3-5 September 1950 brought very heavy rainfall and destructive floods in areas around Yankeetown in the state of Florida. This rainstorm produced the greatest rain depths in one day for areas from 10 to 10,000 km^2 and in two and three days for areas of 10 to 5,000 km^2. On the other hand the June 1899 rainstorm produced the greatest rain depths in one day for areas from 20,000 to 50,000 km^2 and in two and three days for areas of 10,000 to 50,000 km^2. The greatest areal rainfalls produced from these two storms for 1, 2 and 3 days durations in the USA are shown in Table 8.13.

Table 8.13: The greatest areal rainfalls (cm) in the USA

Area (km^2)	One day	Two days	Three days
10	98	110	115
100	97	107	110
500	87	96	102
1000	85	93	97
2000	80	89	92
5000	65	74	77
10,000	46	57	66
20,000	33	48	57
30,000	27	43	53
50,000	21	36	46

8.10 GREATEST AREAL RAINFALLS OVER CHINA

Most of the rainfall in China is received in the summer season. As indicated in Section 8.3, during this season, typhoons form in the northwest Pacific Ocean and travel westwards towards China. Some recurve northward off the coast, whereas others move in over the land. These typhoons cause most of the intense rainstorms in China (Tan and Lu, 1994). The total area covered by the typhoon rainfall reaches about one million km^2. According to the records from 1950 (Pan and Teng, 1988), typhoon Nina produced the highest areal rain depth in August 1975 for most durations and areas in the Hongru River basin. The rainfall lasted five days from 4-8 August with most rain falling between 5-7 August. The station at Lingzhuang recorded rainfall up to 83 cm in a six-hour period, setting a new world record (Pan and Teng, 1988). Table 8.14 gives the greatest areal rain depths from 5-7 August, 1975 rain storm (Svensson and Rakhecha, 1998).

The greatest areal rainfall values for different catchment sizes should be more useful for the flood and design storm studies in China.

Table 8.14: Areal rainfall values (cm) from the August 1975 rainstorm

Area (km²)	One day	Two days	Three days
10	97.0	117.1	152.7
100	90.3	109.3	141.8
500	80.0	98.6	127.3
1000	74.0	92.1	118.4
2000	66.0	84.2	107.8
5000	52.7	71.6	91.0
10,000	41.0	60.4	76.4
15,000	34.2	53.5	67.2
20,000	29.4	48.4	60.7
25,000	25.8	44.5	55.0

8.11 GREATEST AREAL RAINFALLS OVER AUSTRALIA

The area of Australia is almost as large as that of the USA, excluding Alaska. In the Australian region the most extreme known rainfalls are caused from tropical cyclones (Willy Willies). Tropical cyclones form over the seas to the northeast and the northwest of Australia between November and April. On an average, about three Coral Sea cyclones directly affect the Queensland coast and about two the north western coast. Tropical cyclones approaching the coast usually produce very heavy rains in coastal areas. Some cyclones move inland and produce widespread heavy rainfall. Kennedy (1982) gives the list of the following six rainstorms in Australia:

- Crohamhurst, 1893 over Queensland
- Whim CK, 1898 over Western Australia
- Clermante, 1916 over Queensland
- February, 1955 over New South Whales
- Mackay, 1958 over Queensland
- TC Joan, 1975 over Western Australia

Table 8.15 gives the largest areal rainfalls for 1, 2 and 3 days durations produced by the most severe rainstorms in Australia.

Table 8.15: Greatest areal rainfalls (cm) in Australia

Area (km²)	One day	Two days	Three days
10	91	-	-
100	85	135	170
500	77	115	149
1000	73	110	140
2000	66	93	120
5000	56	75	97
10,000	46	60	74
20,000	35	45	55
30,000	25	33	44
50,000	12	17	23

REFERENCES

Brunt, A.T., 1958. Analysis of two Queensland storms. Proceedings of Conference on Extreme Precipitation, Melbourne. Bureau of Meteorology, Australia.

Bureau of Meteorology, Australia, 1976. Climate of Australia. Extract for official year book of Australia. No 61, 1975 and 1976, 76 p.

Bureau of Meteorology, Australia, 1996. Catalogue of significant rainfall occurrences over Southeast Australia. Hydrology report series 3, 85 p.

Fu, A., 1991. A brief introduction of river system in Hongruhe River basin. Unpublished report, Henan Province Prospecting and Designing Institute of Water Conservancy, Zhengzhou, China.

India Meteorological Department (IMD), 1962. Monthly and annual normals of rainfall and of rainy days. *Memoirs of IMD*, 31, Part 3, 208 p.

Indian Institute of Tropical Meteorology (IITM). 1994. Severe rainstorms of India atlas. IITM, Pune.

Kennedy, M.R., 1982. The Estimation of Probable Maximum Precipitation in Australia: Past and Current Practice. Proc. Workshop on Spillways designs. AWRC Conf. Ser. No. 6. AGPS. Canberra. 26-52.

Lemperiere, F., 1993. Dams that have failed by flooding: An analysis of 70 failures. *Int. Water Power and Dams Constr.*, 45, 9, pp. 19-24.

Pan, J. and Teng, W., 1988. Determination of design flood in China. Seizieme Congres des Grands Barrages, San Francisco, California. Commission International des Grands Barrages, pp. 1515-1527.

Pisharoty, P.R. and Asnani, G.C., 1957. Rainfall around monsoon depressions over India. *Journal of Meteorology and Geophysics*, 8, pp. 1-8.

Purohit, M.U., Modhwadia, K.E., Nathani, K.U. and Dave, A.A., 1993. Unusual storms in Gujarat: Characteristics of the storm of August 1979 over Machhu basin of Saurashtra region. CBIP Publ. No 234, Conference on unusual storm events and their relevance to dam safety and snow hydrology, New Delhi. 243-246.

Rakhecha, P.R., 2003. Counting on perfect storms. *International Water Power and Dam Construction*, October Issue, 14-16.

Rakhecha, P.R., Kulkarni, A.K., Mandal, B.N. and Deshpande, N.R., 1990. Homogenous zones of heavy rainfall of 1-day duration over India. *Theor. Appl. Climatol.*, 41, pp. 213-219.

Rakhecha, P.R. and Pisharoty, P.R., 1996. Heavy rainfall during monsoon season: Point and spatial distribution. *Current Science*, 71, pp. 177-186.

Shipe, A.P. and Riedel, J.T., 1976. Greatest Areal Storm Rainfall Depths for the Contigous United States. NOAA, Tech Memorandum NWS Hydro33.

Svensson, C. and Rakhecha, P.R., 1998. Estimation of Probable Maximum Precipitation for dams in the Hongru River Catchment, China. *Thero. Appl. Climatol*, 59, pp. 79-91.

Tan, F. and Lu, Y., 1994. Reconstruction of the Banqiao and Shimantan dams. *Int. J. on Hydropower and Dams*, 1, 4, pp. 49-53.

World Meteorological Organisation, 1994. Guide to hydrological Practices. 5th edition. WMO No. 168.

9 Precipitation and Its Measurement

The term precipitation denotes all forms of water that reach the earth from the atmospheric weather systems. In other words, precipitation is the quantity of naturally available water. Precipitation, however, exhibits marked variability in time and space owing to meteorological causes. As a result, the annual total precipitation may range from half of the normal in one year to twice the normal the next year. Also, we have noted a large spatial variation in the distribution of seasonal and annual rainfall of India, as shown in Figs 6.22 to 6.26 (Chapter 6). This variability in precipitation is responsible for many hydrological problems, such as floods, droughts, land slides, erosion, etc. The study of precipitation therefore forms a major portion of the subject of applied hydrometeorology. This chapter deals with various forms and types of precipitation and in particular with the measurement and analysis of precipitation data for their use in hydrological problems.

9.1 MECHANISMS OF PRECIPITATION

Of the several meteorological processes taking place in the atmosphere, the phenomena of precipitation and evaporation in which atmosphere interacts with water surface are the most important from a hydrometeorological point of view. In hydrometeorology, precipitation is defined as the deposition of water in either liquid or solid form which falls from the atmosphere on to the earth. For precipitation to occur, the presence of moisture in the atmosphere is essential. As a result of evaporation from water sources at the earth's surface, such as oceans, lakes, rivers, wetlands and of transpiration from plants, the moisture in the form of water vapor is always present in the atmosphere. The vast expanse of oceans is the main source of the moisture evaporating into the atmosphere. As evaporation continues, the amount of water vapor in the atmosphere goes on increasing and as there is a maximum limit to the quantity of water vapor that air can absorb, a stage is reached when the air becomes saturated with the amount of water vapor contained

in it. This limit, however, varies with the changing temperature of the air. It may be stated that warm air can hold more water vapor than cold air. The temperature of the air at which the air becomes saturated is known as the dew point temperature. At this temperature, however, if more water vapor is added or the air is cooled below the dew point temperature, the excess water vapor condenses into tiny water droplets of a cloud. Observations indicate that the condensation of the water vapor into water droplets occurs on hygroscopic particles, such as salt crystals, combustion products containing sulfur and nitrogen compounds present in countless numbers in the atmosphere. The diameter of such particles is usually less than one micron (one micron (μ)=10^{-3} mm). When condensed water droplets grow in size and become heavy enough, they come down to the earth's surface as drizzle, rain, snow, sleet, hail, dew, etc., and are collectively known as precipitation. The rate and amount of precipitation depend largely on the rate and amount of cooling, similar to the moisture supply in the air.

9.2 FORMS OF PRECIPITATION

Different combinations of states of water, temperature and wind conditions give rise to the various forms of precipitation. The discussion here is limited to the more common forms which are important for hydrometeorological purposes.

 (i) *Drizzle*: Drizzle is a fine sprinkle of very small and rather uniform water droplets, with a diameter of less than 0.5 mm. It occurs from low clouds (stratus type) and its intensity is generally less than 1 mm per hour.

 (ii) *Rain*: Rain is precipitation in the form of liquid water drops. The size of rain drops is larger than 0.5 mm in diameter. Rain drops in the tropics, especially during thunderstorms, and rain showers are much larger and can be of the order of 5 mm in diameter. Depending on the intensity, the rain is termed as light (< 10 mm per day), moderate (10-40 mm per day), and heavy (> 40 mm per day).

(iii) *Snow*: Snow is precipitation comprising ice crystals which are either translucent or white. Snow crystals are of several types but the most prominent shape is hexagonal with complex branches. About a fall of 250 mm of snow is regarded as equivalent to the 25 mm of rain. For meteorological records, snow is melted and its amount is expressed in terms of the equivalent depth of rain.

(iv) *Sleet*: Sleet is precipitation of melting snow or a mixture of snow and rain. Much of the precipitation in high and mid latitudes begins as snow in the upper layers, turns into sleet at and below the melting level and comes down to the earth as rain.

 (v) *Glaze*: The ice coating formed when rain or drizzle freezes as it comes in contact with cold objects at the ground is called glaze. It can occur only when the air temperature is near 0° C.

(vi) *Hail*: Hail is precipitation of irregular balls or lumps of ice which fall from cumulonimbus clouds and are often associated with thunderstorms. The average diameter of hails ranges from 5 to 50 mm. Sometimes hail stones fall in very large sizes weighing more than 500 gm each. Hails are caused by the rapid ascent of moist air. The water drops freeze and the size of drops increases as more water vapor freezes on their surface. When lumps are heavy enough to overcome the resistance of the ascending air currents, they fall and may still grow in their downward journey by assuming fresh layers of ice from the super-cooled water drops in the moist air. A severe hailstorm is capable of causing much damage to growing crops.

(vii) *Dew*: Dew is formed at late nights or in early mornings. It appears as beautiful globules of clear water on grass blades, flower petals and other objects on the ground. It is generally formed in open when the temperature has fallen sufficiently during the night under clear sky conditions. The critical value to which the temperature of the surrounding air should fall for dew to form is known as dew point or dew point temperature of air. At this temperature air gets saturated with the amount of water vapor contained in it. In rainy climates, dew is of little importance for vegetation, but in dry climates the night dew may contribute substantially to plant growth. While drizzle, rain, snow and hail form in the air and fall to the ground, dew forms directly on the ground or on the cool surfaces of objects on the ground.

It may, however, be mentioned that out of the various forms of precipitation, a major part of precipitation occurs in the form of rain and a minor part occurs in the form of snow. The contribution of the other forms of precipitation is relatively small and is generally ignored in hydrologic studies.

9.3 TYPES OF PRECIPITATION

Although moisture is always present in the atmosphere but whenever and wherever it precipitates, the fundamental cause is the cooling of large masses of air containing water vapor to below their dew point. The usual mechanism by which the air is cooled is necessarily the upward lifting of the air mass. When air rises, it expands on being surrounded by air at a lower pressure than itself. This expansion causes air to cool. The ascending air is, therefore, accompanied by cloud and precipitation. Three different types of mechanisms are generally recognized in which air is forced to rise. They are the cyclonic circulation, mountain barrier, and thermal convection. The precipitation associated with these mechanisms is called cyclonic precipitation, orographic precipitation, and convective precipitation, respectively.

9.3.1 Cyclonic Precipitation

A cyclonic circulation results from the movement of air mass from a region of high pressure to a region where the atmospheric pressure is low and in so doing displaces low pressure air upward. The lifted air expands, cools, and finally condenses to cause precipitation. The pressure differences are created by the unequal heating of the earth's surface. The wind in response to the low pressure gradient picks up a whirling mass of cyclonic circulation which is counterclockwise in the Northern Hemisphere and clockwise in the Southern Hemisphere because of the rotary motion of the earth about its own axis. The intensity of the cyclonic circulation is expressed in terms of the velocity of wind as mentioned in Chapter 5.

Cyclonic precipitation may further be classified as frontal or nonfrontal. Any barometric low can produce nonfrontal precipitation as air is lifted through horizontal convergence of the inflow air. If one airmass lifts over another airmass, the precipitation is called frontal cyclonic precipitation. When two airmasses, having different characteristics, meet each other, condensation and precipitation occur at the surface of contact. This surface is called a front. If a cold airmass displaces a warm airmass, the front is said to be cold front and if a warm airmass replaces the retreating cold airmass, the front is known as warm front. On the other hand, if the two airmasses are drawn simultaneously towards a low pressure area, the front developed is called a stationary front.

9.3.2 Convectional Precipitation

The transmission of heat from one part of a liquid or gas to another by the movement of particles themselves is called convection. Rain that is caused by the process of convection in the atmosphere is known as convective rain. When the air layer of the atmosphere close to the warm earth gets heated, the air expands and its density is reduced and it rises as a convection current. The rising air cools adiabatically and finally condenses to cause precipitation. This type of precipitation generally occurs in tropics where on a hot day the ground surface gets heated unequally. Convective precipitation is of shower type and its intensity may vary from light showers to cloudbursts, depending on the temperature and moisture conditions. The average life of a convective cell is about half an hour.

Some areas are subjected to severe convective precipitation in the form of whirling thunderstorms. They are typical of the humid tropical regions, such as Indonesia, Malaysia, and Central and West Africa. A thunderstorm usually develops in an unstable moist atmosphere. A cumulus cloud is formed when warm moist air from the surface rises to a higher altitude and condenses. It grows laterally and vertically into a larger dense cloud called cumulonimbus with strong turbulence within the cloud and strong outflow below the base of the cloud. A mature thunderstorm often has a cellular structure with a

diameter ranging from 3 to 6 km and its top exceeding 10 km. Thunderstorms are capable to produce hail, heavy rain, frequent lightning, and strong gusty winds. Some characteristics of thunderstorms have already been discussed in Chapter 6.

9.3.3 Orographic Precipitation

Orographic precipitation is caused from the mechanical lifting of moist air currents over mountainous barriers. When a wind stream encounters a mountainous barrier, it cannot move forward and hence tends to rise over the mountains. The lifting of air leads to adiabatic cooling which in turn produces clouds and precipitation. The most prominent effect, of course, is heavy precipitation on the windward side of mountains and the less precipitation on the leeward side. The Western Ghats in India is an excellent example of an area where heavy rainfall occurs due to orographic effects.

Orographic precipitation generally increases with elevation to the crest of a barrier. For very high barriers, however, the maximum precipitation on the windward slope quite often occurs below the crest. Hill (1881) made a detailed study of the distribution of rainfall in the northwest Himalayas and found that rainfall increases with elevation up to a height of about 1.2 km and thereafter it diminishes as the elevation increases. In the Sierra Nevada Mountains in the U.S.A., rainfall increases up to a height of 1.5 km (Linsley et al., 1949). Rumley (1965) investigated the distribution of rainfall with elevation in the Andes Mountains in Ecuador and found two zones of maximum rainfall along western and eastern slopes at an elevation of 1.0 and 1.4 km, respectively. Dhar and Rakhecha (1980) investigated the variation of rainfall with elevation in central Himalayas and found two zones of maximum rainfall, one near the foothills and other at an elevation of 2.0 to 2.4 km.

9.4 MEASUREMENT OF PRECIPITATION

Precipitation is the major contributor to water resources. Information on the amount of rain water, and its variability in space and time in respect of various river catchments is valuable to the development of water resources. Also, for almost all hydrological designs, it is necessary to have precipitation records of long periods. It is, therefore, necessary to measure the amount of precipitation at a particular point and also determine its distribution at various points in the river catchment. Nearly all the measurable precipitation occurs as rain or snow, depending on the latitude and season. It is measured as the vertical depth of water or water equivalent which would accumulate on a level surface, if all the precipitation remained where it fell. Apparently, it can therefore be measured in any open container with vertical sides calibrated to determine the amount of precipitation that fell between measurement intervals.

    Since the size, shape, and exposure of a measuring container affect the amount caught by the container, it is desirable to use a standard container so that observations taken at different places are comparable. This standard instrument which is used for measuring rainfall is called a "raingauge." Two types of raingauges are commonly used. The first is the non-recording raingauge and the second is the recording raingauge. These two types are described in what follows.

9.4.1 Non-recording Raingauges

Non-recording raingauges are most widely used throughout the world. The non-recording raingauges are commonly used where measurements are needed only once or at the most a few times daily. As the name indicates, these raingauges do not record rainfall but only collect the rain water. The collected rain water is then measured by means of a graduated cylinder which gives the total amount of rainfall in mm of water depth at the raingauge station. Many different instruments have been designed for such gauges. Out of them Symon's type raingauge is most widely used. As shown in Fig. 9.1, Symon's raingauge consists of a cylindrical metal case of internal diameter 127 mm with its base enlarged to 203.2 mm diameter. Over the cylinder a funnel is fixed with a circular brass rim of 127 mm in diameter. The funnel shank is inserted in a metal or glass bottle placed inside the case. The case of the raingauge is fixed in masonry or concrete foundation such that the funnel rim is exactly 305 mm above the ground level. The rain water enters the bottle through the funnel and gets collected in the bottle. The rain water is measured with the help of a graduated measuring glass which indicates the millimeters of rain that have fallen at the raingauge station.
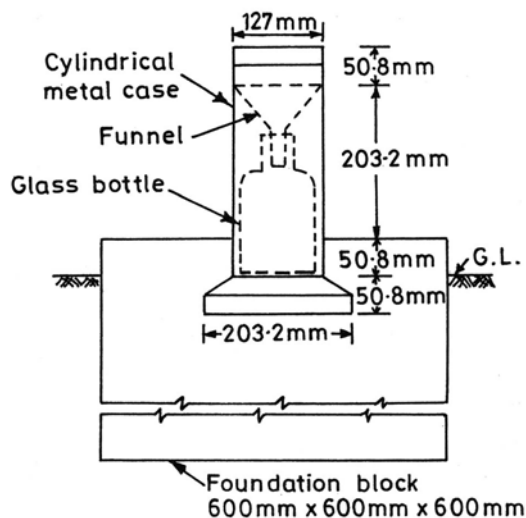

Fig. 9.1. Symon's raingauge.

At each gauge station, rainfall observations are taken daily two times at 08:30 and 17:30 (IST) in India. However, if rainfall is likely to exceed the capacity of the bottle then a few intermediate observations are also taken. The sum of the observations taken will represent the total rainfall of the past 24 hours of the day on which the observation at 08:30 hrs was taken.

9.4.2 Recording Raingauges

When a continuous record of precipitation is required so that indications of the time distribution can be obtained, recording raingauges are used. These raingauges automatically record the amount of rainfall and the time of its occurrence and cessation in the form of a pen trace on a clock driven chart. There are three types of recording gauges: (i) tipping bucket raingauge, (ii) weighing type raingauge, and (iii) float type raingauge.

The gauges provide a record of cumulative rain with time in the shape of a mass curve of rainfall. From this mass curve, the depth of rainfall in a given time, the rate or intensity of rainfall at any instant during a storm, the time of onset and cessation of rainfall can be determined. These data are of great value for the design of flood control structures, urban drainage, and soil erosion problems.

(i) *Tipping bucket raingauge*: A tipping bucket raingauge consists of a cylindrical receiver of a 300 mm diameter with a funnel inside. Just below the funnel as shown in Fig. 9.2, a pair of tipping buckets is pivoted. The buckets are so designed that when 0.25 mm of rainfall is caught in one bucket it gets overbalanced and it tips and empties into the storage tank below and at the same time the other bucket comes under the funnel and the process is repeated. The tipping of the bucket activates an electric circuit which causes a pen to mark a record on a

Fig. 9.2. Tipping bucket raingauge.

chart wrapped on a clock-driven revolving drum. Since each mark on the record sheet corresponds to 0.25 mm of rainfall, by counting the same the intensity of rainfall can be determined.
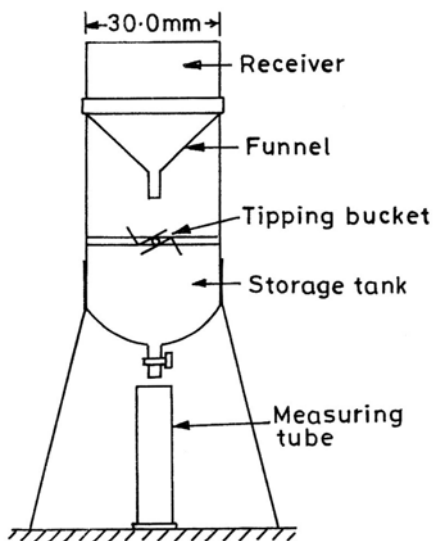
(ii) *Weighing type raingauge*: In the weighing type of raingauge the rain water enters through a funnel into a bucket which is supported on the
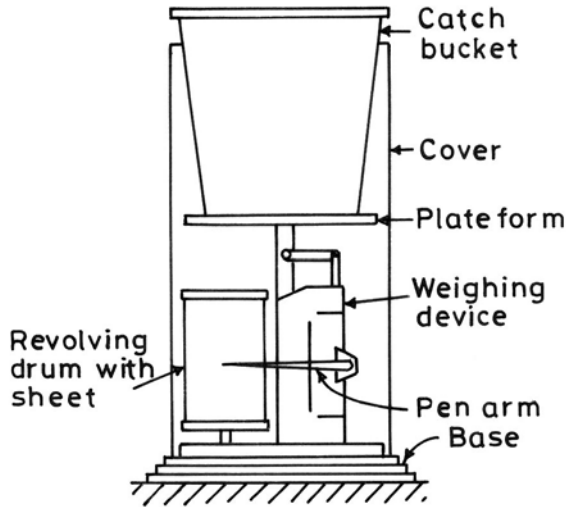
Fig. 9.3. Weighing type raingauge.

weighing platform of a spring or lever balance as shown in Fig. 9.3. The increase in the weight of the bucket due to the addition of the rain water causes the platform to move. The movement of the platform is linked through a system of levers to a pen which makes trace of accumulated amounts of rainfall on a suitable graduated chart wrapped round a clock-driven revolving drum. The rainfall record produced by this gauge is in the form of a mass curve of rainfall in which the total rainfall is plotted with respect to time.

(iii) *Float type raingauge*: In this raingauge the rain water enters a chamber which contains a float (as shown in Fig. 9.4). As the level of the rain water collected in the float chamber rises, the float moves up, which activates a pen connected to it through a connecting rod. The pen makes a trace of the accumulated amount of rainfall on a suitable graduated chart wrapped round a clock-driven revolving drum. Thus, in the case of this gauge the rainfall record is also in the form of a mass curve of rainfall. When the float chamber gets filled, the water siphons out automatically through a siphon tube as shown in Fig. 9.4.

9.5 NETWORK DESIGN

Precipitation data are very useful for the assessment and management of water resources of a catchment. The amount of rainfall varies from place to place in the catchment. It is therefore necessary to install raingauges at various key points in the area if one is concerned with the tapping of the overall reliable amount of water availability in the catchment.

Perhaps, the best known earliest studies concerned with network design were those of Horton (1923) and Drozdov (1936). Later investigations on
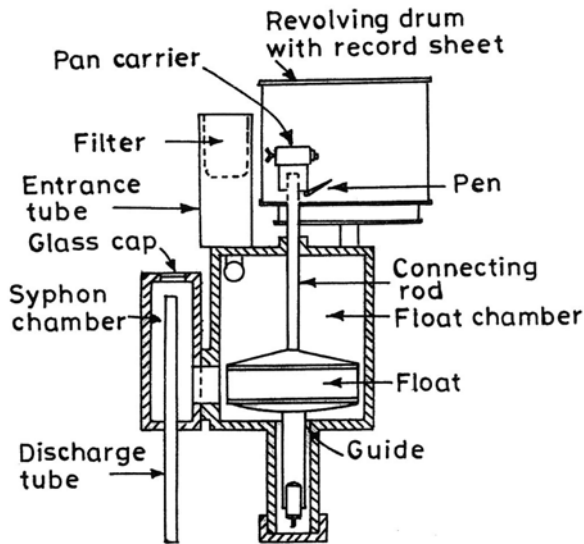
Fig. 9.4. Float type raingauge.

the network design of raingauges for hydrologic purposes have been carried out by several investigators and these have guided the design of networks in river catchments. The WMO/IAHS Symposium on Design of Hydrological Networks held in Quebec in June 1965 discussed many methods of network design and planning of precipitation gauges related to different types of catchments. Rodda (1969) summarized much of the work on network design.

9.5.1 Number of Rainfall Stations Required

Many hydrologic studies require an estimation of the average depth of rainfall for various durations over some area which is either fixed (for example, a river catchment) or variable in space. Depending on the problem, a network of non-recording raingauges is required to ensure that areal variability is sampled adequately. For a catchment where raingauges have not been installed there is no simple method of finding as to how many raingauges are needed. In these circumstances, WMO (1974) has recommended the following as minimum network densities for general hydrometeorological purposes:

1. For flat area of temperate, Mediterranean and tropical regions, one station per 600-900 km^2
2. For mountainous area of temperate, Mediterranean, and tropical regions, one station per 100-250 km^2
3. For mountainous islands with very irregular precipitation, one station per 25 km^2
4. For arid and polar regions, one station per 1500-10,000 km^2

In the following section methods of determining the optimum number of raingauges are discussed.

9.5.2 Optimum Number of Raingauges

Rycroft (1949) used the variance in space to determine the optimum number of raingauges in the Jonkershook catchment. The equation developed by Rycroft for obtaining the optimum number of raingauges, N, is:

$$N = \left[\frac{2v}{x}\right]^2 \qquad (9.1)$$

where N = the optimum number of raingauges, v = the variance in space of the rainfall based on existing stations, and x = the allowable variance in the estimate of mean rainfall.

Ganguli et al. (1951) used the coefficient of variation in space of the monthly rainfall to determine the optimum number of raingauges. Their formula is:

$$N = \left[\frac{CV_m}{x}\right]^2 n \qquad (9.2)$$

where N = the optimum number of raingauges, CV_m = the coefficient of variation of space mean monthly rainfall based on existing raingauge stations, x = the tolerance value of CV_m, and n = the number of existing raingauge stations.

Ahuja (1960) developed a method for obtaining the optimum number of raingauges, N, based on the coefficient of variation in space of rainfall to estimate the mean areal rainfall within a desired accuracy. The basis behind the method is that a certain number of raingauge stations is necessary to give an average rainfall with a certain percentage of error:

$$N = \left[\frac{CV}{x}\right]^2 \qquad (9.3)$$

where N = the optimum number of raingauge stations to be established in the catchment, CV = the coefficient of variation of rainfall based on existing raingauge stations, and x = the desired percentage error in the estimate of the average rainfall depth over the catchment. CV can be computed as follows:

 (i) Calculate the mean rainfall, $\overline{R}$, based on existing raingauges:

$$\overline{R} = \frac{\sum\limits_{i=1}^{n} R_i}{n} \qquad (9.4)$$

   where n is the number of existing raingauges, and ΣR is the total rainfall of all stations (i = 1, 2, …, n).

(ii) Calculate the standard devision (σ):

$$\sigma = \sqrt{\frac{1}{n-1} \sum\limits_{i=1}^{n} (R_i - \overline{R})} \qquad (9.5)$$

(iii) Calculate the coefficient of variation:

$$CV = 100 \times \frac{\sigma}{R} \qquad (9.6)$$

The additional raingauges $(N - n)$ are then distributed in different rainfall areas demarcated by isohyets in proportion to their areas.

Example 9.1: There are five raingauge stations in a catchment. The average annual rainfall values of these stations are 85, 100, 126, 78, and 56 cm, respectively. Determine the optimum number of raingauges. It is desired to limit the error in the average value of rainfall in the catchment to 10%. Indicate how many additional raingauges are distributed.

Solution: The locations of five raingauges in a typical catchment are shown in Fig. 9.5. The various steps involved are tabulated as follows:

Station	Rainfall (x, cm)	$(x - \bar{x})$	$(x - \bar{x})^2$	Statistical parameters
1	85	–4	16	$\bar{x} = \dfrac{\Sigma x}{n} = \dfrac{445}{5} = 89$ cm
2	100	11	121	$\sigma = \sqrt{\dfrac{\Sigma (x - \bar{x})^2}{n - 1}} = \sqrt{\dfrac{2716}{4}} = 26.1$
3	126	37	1369	$CV = \dfrac{26.1}{89} = 29.3\%$
4	78	–11	121	
5	56	–33	1089	
$n = 5$	$\Sigma x = 445$		$\Sigma (x - \bar{x})^2 = 2716$	

Mean rainfall = 89 cm
Standard deviation = 26.1 cm
CV = 29.3%

Now the optimum number of raingauges (N) that would be necessary to estimate the average rainfall depth with a percentage error of less than or equal to 10% is:

$$N = [\frac{CV}{x}]^2 \qquad (9.7)$$

$$N = [\frac{29.3}{10}]^2 \approx 9 \qquad (9.8)$$

The optimum number of raingauges in the catchment should be nine. Therefore, the additional number of raingauges to be installed is four $(= 9 - 5)$.
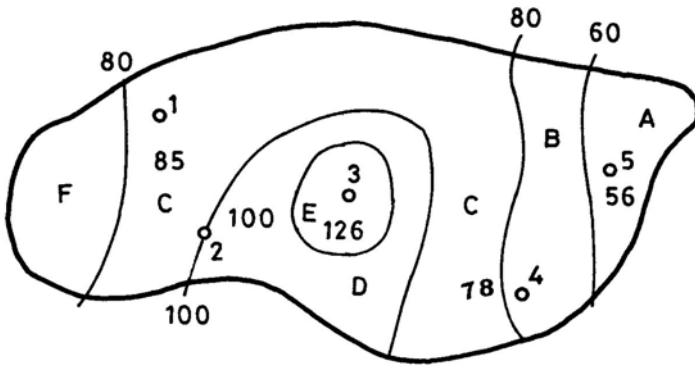
Fig. 9.5. Isohyets.

Once the number of raingauges is determined for a catchment, the selection of sites is the next step. For allocating the additional raingauges in the catchment, isohyets, as shown in Fig. 9.5, are first drawn. Then the areas bounded by different consecutive isohyets within the catchment are measured by a planimeter. The proportionate areas of different isohyetal zones A, B, C, D, E, and F, as shown in Fig. 9.5, are found to be 0.09, 0.11, 0.37, 0.24, 0.07, and 0.12, respectively. The four raingauges are then allocated to the different zones in proportion to their areas. Details are given in Table 9.1.

Table 9.1: Calculations for allocation of raingauges

Zone	A	B	C	D	E	F	Total Area
Area (km^2)	700	800	2760	1840	500	900	7500
% of total area	0.09	0.11	0.37	0.24	0.07	0.12	
$N \times$ % of total area	0.81	0.99	3.3	2.1	0.6	1.1	
Rounded as	1	1	3	2	1	1	
Existing raingauges	1	1	1	1	1	0	
Additional gauges	0	0	2	1	0	1	

The optimum number of raingauges in different isohyetal zones of A, B, C, D, E, and F are found to be 1, 1, 3, 2, 1, and 1, respectively. The number of raingauges to be installed depends upon the spatial distribution of the existing raingauges. The percentage error (p) in the estimation of the average depth of rainfall in the existing network is:

$$p = \frac{29.3}{\sqrt{5}} = 13\%$$

9.6 ESTIMATION OF MISSING RAINFALL

Sometimes the rainfall amount at a certain station for a certain day may be missing due to the absence of the observer or an instrumental failure. In such a case, it is necessary to supplement the missing rainfall amount from the data of nearby raingauge stations. The following methods are used.

Suppose, for a certain day, that there is no record of the rainfall at station A. We select three rainfall stations as close and evenly spaced around station A as possible. Assume that there are three stations: x_1, x_2, and x_3. The rainfall values for these three stations on the day for which the data at A is missing are collected. The normal annual rainfall values for all the four stations should be known. Now if the normal annual rainfall at each of these three neighbouring stations differ within 10% of the normal annual rainfall of the station A, with missing data, then the simple way of estimating the missing rainfall at A is to take the simple arithmetic mean of the amounts known for the three stations. Suppose N_1, N_2, N_3, and N_A are the normal annual rainfall amounts at stations x_1, x_2, x_3, and A, respectively; and P_1, P_2, P_3, and P_A are their rainfall values for the day on which the rainfall at station A was missing, then the rainfall at the missing station is

$$P_x = \frac{P_1 + P_2 + P_3}{3}$$

Here the values of N_1, N_2, and N_3 differ from N_A by 10% or less only.

However, when the normal annual rainfall at any of the three stations chosen differs from that of the missing station's normal rainfall by more than 10%, the normal ratio method is used as follows:

The value of missing rainfall at A with reference to

(1) The value of missing rainfall at A with reference to $x_1 = P_1 \dfrac{N_A}{N_1}$

(2) The value of missing rainfall at A with reference to $x_2 = P_2 \dfrac{N_A}{N_2}$

(3) The value of missing rainfall at A with reference to $x_3 = P_3 \dfrac{N_A}{N_3}$

The amount of missing rainfall at the station A is the mean of the above three values:

$$P_A = \frac{1}{3}[P_1 \frac{N_A}{N_1} + P_2 \frac{N_A}{N_2} + P_3 \frac{N_A}{N_3}]$$

Example 9.2: A 3-hr storm occurred at a place *A* and rainfall values at the neighboring stations x_1, x_2 and x_3 were measured as 107, 89, and 122 mm,

respectively. The rainfall at station A could not be measured since the raingauge bottle was broken. Estimate the missing rainfall value for station A. The normal annual rainfall values of A, x_1, x_2 and x_3 are 978, 1120, 935, and 1200 mm, respectively.

Solution: N_A = 978 mm for the station A. 10% of 978 = 97.8 mm. The maximum permissible normal annual rainfall at either of three stations for taking simple arithmetic average is: 97.8 + 978 = 1075.8 mm. Apparently the normal annual rainfall at the three stations differ by more than 10% of N_A. Hence, the normal ratio method should be used to estimate the missing amount of rainfall at A.

$$\begin{aligned} P_A &= \frac{1}{3}\left[P_1 \frac{N_A}{N_1} + P_2 \frac{N_A}{N_2} + P_3 \frac{N_A}{N_3}\right] \\ &= \frac{1}{3}\left[107 \times \frac{978}{1120} + 89 \times \frac{978}{935} + 122 \times \frac{978}{1200}\right] \\ &= \frac{1}{3}[93.5 + 93.1 + 99.4] = 95.3 \text{ mm} \end{aligned}$$

Hence, the missing value of rainfall is 95.3 mm at station A.

9.7 MEAN DEPTH OF RAINFALL OVER AN AREA

For many hydrometeorological problems, the mean or average depth of rainfall over a particular area is needed. There are several methods for computing the mean or average depth of rainfall, depending upon the physiographic features and the network of raingauges in the area. However, the following three methods are generally used for calculating the average rainfall over an area.

9.7.1 Arithmetic Mean Method

The simplest method for determining the average depth of rainfall is the arithmetic mean method. It consists of averaging the rainfall values recorded at a number of stations in the catchment as shown in Fig. 9.6. For example, if R_1, R_2, R_3...., R_n are rainfall values recorded at n raingauge stations distributed over an area, then the average depth of rainfall $\bar{R}$ is given as:

$$\bar{R} = \frac{R_1 + R_2 + R_3 + \dots R_n}{n} = \frac{\sum_{i=1}^{i=n} R_i}{n} \tag{9.9}$$

The results obtained by this method are satisfactory if raingauges are uniformly distributed over the area and the individual gauge measurements do not vary greatly about the mean.
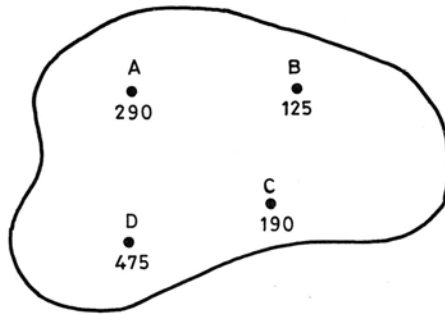
Fig. 9.6. Raingauge locations and rainfall measured by them.

Example 9.3: Rainfall during the month of July measured at four raingauge stations A, B, C, and D in a catchment was 290, 125, 190, and 475 mm, respectively. Compute the mean rainfall using the arithmetic method.

Solution: For the arithmatic mean method (see Fig. 9.6),

Station	Rainfall (mm)
A	290
B	125
C	190
D	475
	1080

    Average rainfall = 1080 mm/4 = 270 mm

9.7.2 Thiessen Method

Another method for computing the average depth of rainfall over an area with a relatively few rainfall stations unevenly distributed is the Thiessen polygon method. The method assumes that at any point in the area rainfall is the same as that at the nearest rainfall station so the depth recorded at a given station is applied to a distance half way to the next station in any direction. In this method, the adjacent raingauge stations are joined by straight lines, thus dividing the entire area into a number of triangles as shown in Fig. 9.7. Perpendicular bisectors are drawn on each of these lines, thus forming polygons around raingauge stations. It is assumed that the entire area within any polygon is nearer to the rainfall station that is included in the polygon than to any other rainfall station. The area enclosed by the polygon surrounding each station is then planimetered. If R_1, R_2, R_3..., R_n is the rainfall recorded at stations 1, 2, 3,...., n surrounded by polygons having areas as A_1, A_2, A_3..., A_n, then the average depth of rainfall $\bar{R}$ for the area A is given as:

$$\bar{R} = \frac{A_1 R_1 + A_2 R_2 + \ldots A_n R_n}{A_1 + A_2 + \ldots A_n} = \frac{\sum\limits_{i=1}^{n} R_i A_i}{A} \tag{9.9}$$

where A is the total area of the catchment. In the Thiessen polygon method, each raingauge station is given a weight according to its position with respect to the boundary of the area under consideration and hence this method is better than the arithmetic method.
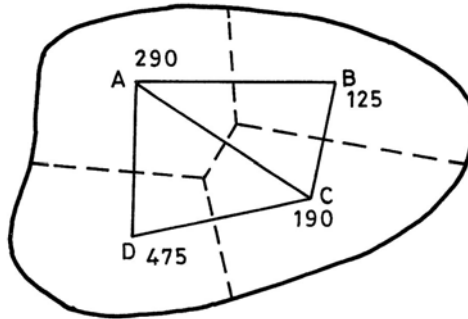

Fig. 9.7. Thiessen polygons.

Example 9.4: Consider four stations A, B, C, and D within a catchment as shown in Fig. 9.7. The rainfall measured by these stations is that given in Example 9.3. Compute the mean areal rainfall by the Thiessen method.

Solution: First, a Thiessen diagram is constructed. To that end, join the consecutive stations A, B, C, and D. Then, divide the area into triangles. To divide the area into triangles, most frequently the shorter of the two diagonals is to be joined. Perpendicular bisectors are then drawn so as to divide the area into polygons. Calculation of the average rainfall by the Thiessen method is as follows:

Station	Observed rainfall (mm)	Area of the corresponding polygon (km²)	Weight rainfall (mm)
A	290	37	10730
B	125	24	3000
C	190	30	5700
D	475	34	16150
		125	35580

Average rainfall = 35580 mm/125 = 284.6 mm

The greatest limitation of the method is that any change in the number or location of stations in the catchment makes it necessary to reconstruct the

Thiessen polygons. The method is not suitable for hilly areas because the method does not directly account for the orographic influence on rainfall.

9.7.3 Isohyetal Method

The least mechanical and conceptually more accurate method for computing the average rainfall from observations taken at a number of rainfall stations is the isohyetal method. Isohyets are the contours of equal rainfall. They are drawn after rainfall at each station is plotted. Then, assuming a linear variation of rainfall between two stations, the positions of rainfall values at some interval are interpolated between the stations. The points with equal values of rainfall are joined by smooth lines called isohyets. Taken together, they form the isohyetal pattern for the area as shown in Fig. 9.8. Isohyetal maps can also be drawn using computer programs. Once the isohyetal map is prepared, the area between two adjacent isohyets is measured by a planimeter and for this area rainfall is assigned to be equal to the mean of the two isohyet values. If A_1, A_2, A_3..., A_n are the areas between two isohyets and R_1, R_2, R_3..., R_n the average rainfall between two isohyets, then the average depth of rainfall $\bar{R}$ over the area A is given as:

$$\bar{R} = \frac{R_1 A_1 + R_2 A_2 + \dots R_n A_n}{A_1 + A_2 + \dots A_n} \tag{9.10}$$
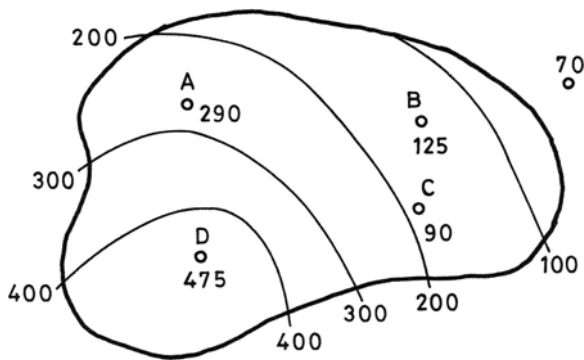

Fig. 9.8. Isohyets of catchment of Fig. 9.6.

The isohyetal method is possibly the best of the three methods and has the advantage that isohyets may be drawn to take into account the physiographic features of the region. Also, the results obtained by this method remain practically unaffected whether any new station is added to or is missing from the network over the area under study. One limitation of this method, however, is that the accuracy of the results depends upon the skill of the analyst.

Example 9.5: Rainfall values at different raingauge stations in a catchment are shown in Fig. 9.8. Compute the mean areal rainfall using the isohyetal method.

Solution: First, isohyets are constructed using rainfall values recorded at different stations. Then the isohyetal method is applied to calculate the average rainfall depth in the catchment as shown in Fig. 9.8. Calculations are shown below.

Isohyets (mm)	Area between isohyets (km²)	Average rainfall (mm)	Rainfall volume (km² × mm)
475-400	24	437	10488
400-300	25	350	8750
300-200	34	250	8500
200-100	36	150	5400
100-70	6	85	510
	125		33648

Average rainfall = 33648 mm/125 = 269.2 mm

9.8 CONSISTENCY OF RAINFALL RECORDS

Inconsistency or nonhomogeneity in rainfall records may arise from changes in the raingauge location, changes in the immediate surroundings due to the construction of buildings or growth of trees and changes in the rainfall observation methods. Such changes may cause an apparent change in the precipitation catch, which may not be due to meteorological causes. Often these changes do not show in published rainfall records. It is, therefore, desirable to test the consistency or homogeneity of records and adjust them if necessary. The consistency of records at a station is determined by the use of the double mass curve technique. In this technique, the cumulative rainfall of a station in question is plotted against the average cumulative rainfall of a number of other nearby stations which are influenced by the same meteorological conditions. About 10 stations should be selected. From the plot, the year in which a change in rainfall record has occurred is indicated by the change in slope of the double mass curve. The rainfall records of the station are then adjusted by multiplying the record values of rainfall by the ratio of slopes of the straight lines before and after the change. The double mass curve technique is best explained by an example.

Example 9.6: Table 9.2 gives annual rainfall values at a typical station A and the average annual rainfall of 10 stations in the vicinity of station A for a period of 30 years. It is suspected that there has been a change in the location of raingauge at A during the period of record. Check the consistency

Table 9.2: Computation of double mass curve for a typical station A

Year	Rainfall at A		Avg. rainfall of 10 stations	
	Rainfall (cm)	Cum Rainfall (cm)	Rainfall (cm)	Cum Rainfall (cm)
1921	50	1178	72	1322
1922	90	1128	57	1250
1923	6	1038	27	1193
1924	22	1032	25	1166
1925	50	1010	61	1141
1926	62	960	22	1080
1927	70	898	55	1058
1928	36	828	57	1043
1929	42	792	37	946
1930	42	750	19	909
1931	36	708	27	890
1932	42	672	60	863
1933	18	630	55	803
1934	30	612	39	748
1935	54	582	38	709
1936	48	528	48	671
1937	12	480	50	623
1938	36	468	24	573
1939	41	432	44	549
1940	36	391	60	505
1941	45	355	47	445
1942	10	310	30	398
1943	45	300	41	367
1944	31	255	56	326
1945	44	224	40	270
1946	40	180	37	230
1947	24	140	55	193
1948	44	116	42	138
1949	36	72	46	96
1950	36	36	50	50

of record at station A and determine the year when the change has occurred and adjust the records prior to the change.

Solution: In order to test the consistency in the rainfall records of station A, the cumulative rainfall of station A and the average cumulative rainfall of 10 stations are plotted in Fig. 9.9. It can be seen from the figure that there is a distinct change in the slope in the year 1931, indicating that a change in rainfall had occurred in the year 1931 when the slope of 1.10 changes to 0.80. The change in slope is accounted for by the fact that the station was moved to another place in 1931. On the basis of the difference in slope of the two
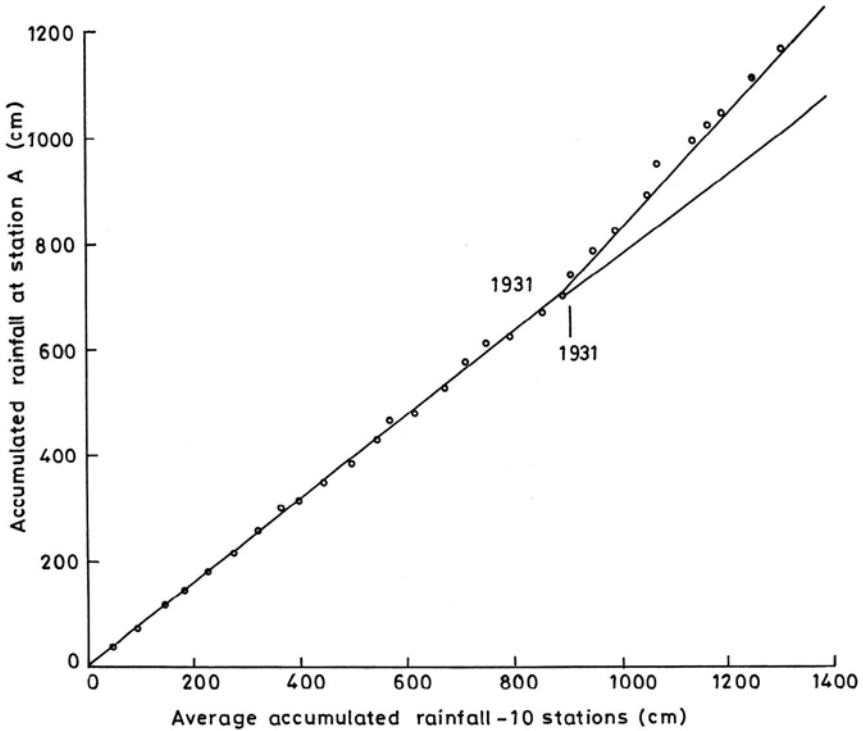
Fig. 9.9. Double mass analysis.

sections of the curve, the records for station A should be adjusted by a factor 0.80/1.1 to make the records prior to 1931 comparable with those for the recent period. The adjusted values prior to 1931 are given in Table 9.3.

$$\text{Correction factor} = \frac{0.80}{1.1} = 0.727$$

Table 9.3: Adjusted values of rainfall

Year	Original value (cm)	Adjusted value (cm)
1930	42	42 × .727 = 31
1929	42	42 × .727 = 31
1928	36	36 × .727 = 26
1927	70	70 × .727 = 51
1926	62	62 × .727 = 45
1925	50	50 × .727 = 36
1924	22	22 × .727 = 16
1923	6	6 × .727 = 4
1922	90	90 × .727 = 65
1921	50	50 × .727 = 36

9.9 EXTENSION AND INTERPRETATION OF RAINFALL DATA

Rainfall at any place can be adequately described if the intensity, duration and frequency of the various storms occurring at that place are known. Whenever rainfall occurs, its magnitude and duration are known from meteorological readings. Thus, at a given station the magnitudes of the rains of various durations, such as 5 minutes, 10 minutes, 15 minutes, etc., are generally known. These data can be used to determine the intensity-duration-frequency relations (IFD). The IFD data are used in the rational method for urban storm drainage design. In applying the rational method rainfall intensity is used which represents the average intensity of a storm of given frequency for a selected duration.

  (i) Intensity: This is a measure of the quantity of rain falling in a given time or in other words, the intensity of rain is the rate at which rain is falling. It is expressed in inches/hr, mm/hr or cm/hr.
 (ii) Duration: The duration is the period of time during which rain falls.
(iii) Frequency: This refers to how often a rainfall of a particular magnitude occurs in a given duration.

   The intensity of rainfall at which the rain falls changes continuously throughout the storm. If 5 cm of rain falls in one hour then it gives an average rainfall intensity of 5 cm/hr. However, during this particular time period, sometimes, the rainfall intensity will greatly exceed 5 cm/hr and sometimes it may be much less than 5 cm/hr. The variation of rainfall depth or intensity with time (duration) can be shown graphically by (a) a hyetograph and (b) a mass curve. A rainfall hyetograph is a plot of rainfall depth or intensity against time shown in the form of a histogram as in Fig. 9.10. It is useful in determining the maximum intensity of rainfall during a particular storm.

   A mass curve of rainfall is a plot of cumulative rainfall against time as shown in Fig. 9.11. From the mass curve the total depth of rainfall and the intensity of rainfall for any duration can be computed. A mass curve of
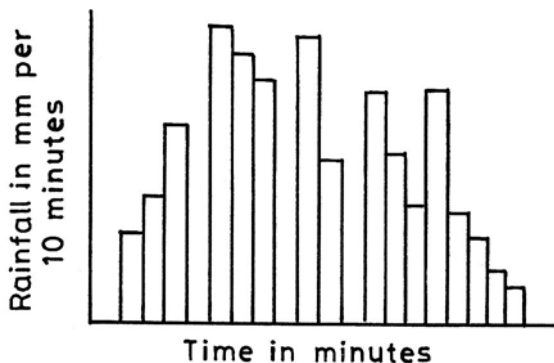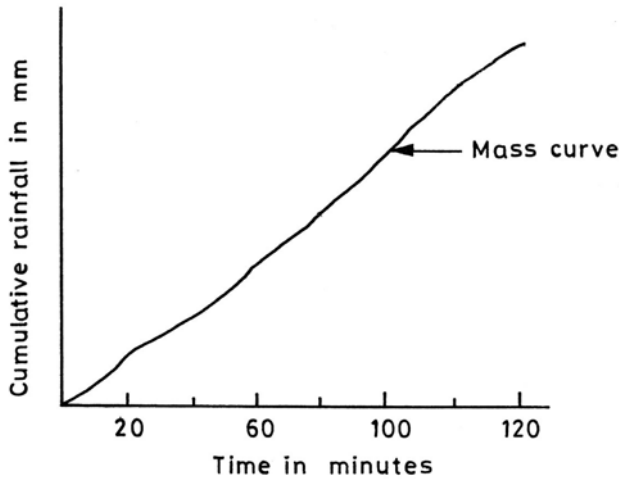

Fig. 9.10. Rainfall hyetograph.

Fig. 9.11. Diagrammatic representation of mass curve.

rainfall is always a rising curve and may have some horizontal sections which indicate periods of no rainfall. The mass curve for a design storm is generally obtained from the maximum rainfall depths recorded in different time intervals in a storm.

The maximum rainfall depth or intensity recorded in a given time interval in a storm is found by computing a series of running totals of rainfall depth for that time interval starting at various points in the storm, then selecting the maximum value of this series. For example, for a 15-minute time interval, Table 9.4 shows running totals beginning with 0.8 cm recorded in the first

Table 9.4: Computation of rainfall depth and intensity at a location

Time (*min*)	*Rainfall* (*cm*)	*Cumulative* *rainfall (cm)*	*Rainfall totals*		
			15 m	*30 m*	*40 m*
0					
5	0.1	0.1			
10	0.1	0.2			
15	0.6	0.8	0.8		
20	0.7	1.5	1.4		
25	0.3	1.8	1.6		
30	0.2	2.0	1.2	2.0	
35	0.5	2.5	1.0	2.4	
40	0.2	2.7	0.9	2.5	2.7
45	0.2	2.9	0.9	2.1	2.8
50	0.2	3.1	0.6	1.6	2.9
Max depth	0.7		1.6	2.5	2.9
Max intensity (cm/hr)	8.4		6.4	5.0	4.3

15 minutes, 1.4 cm from 5 minutes to 20 minutes, 1.6 cm from 10 minutes to 25 minutes, and so on. The maximum 15-minute recorded depth is 1.6 cm recorded between 10 minutes and 25 minutes, corresponding to an average intensity of 6.4 cm/hr. Table 9.4 shows similarly computed maximum depths and intensities for 30-minute and 40-minute intervals. It can be seen that as the time period increases, the average intensity of the storm decreases. Computations of the maximum rainfall depth and intensity carried out in this way give an idea of how severe a particular storm is compared to other storms recorded at the same location. They also provide useful data for design flow studies for important water projects.

9.10 INTENSITY-DURATION RELATIONSHIPS

Point rainfall data are used to derive intensity-duration curves. The greater the intensity of rainfall, in general, the shorter length of time it continues for. Many formulas have been derived to express the relationship between intensity and duration of point rainfall for durations of 5 to 120 minutes. A formula expressing the relationship between intensity and duration for durations of 5 to 120 minutes is of the type:

$$i = \frac{a}{t + b} \qquad (9.11)$$

in which i is the average intensity for duration t, and a and b are locality-dependent constants.

For durations of over 120 minutes, the relationship between the average rainfall intensity and duration is expressed by a formula of the type:
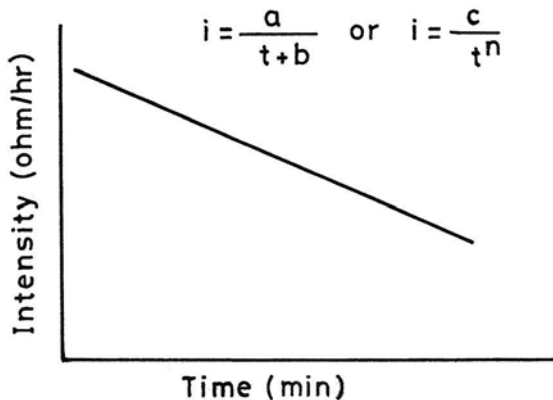
$$i = \frac{C}{t^n} \qquad (9.12)$$

Fig. 9.12. Rainfall intensity versus time.

in which C and n are locality-dependent constants. From equation (9.11) we have:

$$\log i = \log a - \log (t + b) \qquad (9.13)$$

The relation between the rainfall intensity and duration can be obtained as a straight line by plotting the intensity against duration in time on a double log paper as shown in Fig. 9.12.

Example 9.7: The table below gives values of rainfall of various durations during a storm. Construct (a) hyetograph, (b) mass curve of rainfall, (c) maximum depth duration values, and (d) maximum intensity-duration curve.

Time (min)	5	10	15	20	25	30	35	40	45	50
Rainfall (cm)	0.1	0.1	0.6	0.7	0.3	0.2	0.5	0.2	0.2	0.2

Solution: Computation of rainfall depth and intensity is shown in Table 9.5.

Table 9.5: Computation of rainfall depth and intensity

Time (min)	Rainfall (cm)	Cumulative rainfall (cm)	Running totals									
			5m	10m	15m	20m	25m	30m	35m	40m	45m	50m
5	0.1	0.1	0.1									
10	0.1	0.2	0.1	0.2								
15	0.6	0.8	0.6	0.7	0.8							
20	0.7	1.5	0.7	1.3	1.4	1.5						
25	0.3	1.8	0.3	1	1.6	1.7	1.8					
30	0.2	2	0.2	0.5	1.2	1.8	1.9	2				
35	0.5	2.5	0.5	0.7	1	1.7	2.3	2.4	2.5			
40	0.2	2.7	0.2	0.7	0.9	1.2	1.9	2.5	2.6	2.7		
45	0.2	2.9	0.2	0.4	0.9	1.1	1.4	2.1	2.7	2.8	2.9	
50	0.2	3.1	0.2	0.4	0.6	1.1	1.1	1.6	2.3	2.9	3	3.1
Max depth	0.7		0.7	1.3	1.6	1.8	2.3	2.5	2.7	2.9	3	3.1
Max intensity	8.4		8.4	7.8	6.4	5.4	5.5	5	4.6	4.4	4	3.7

(a) Hyetograph: The rainfall at successive 5-minute intervals is given in column 2 of Table 9.5. The rainfall hyetograph plot of rainfall depth (cm) against time (minutes) is shown in Fig. 9.13a.

(b) Mass curve of rainfall: The plot of cumulative rainfall (cm) against time (minutes) gives the mass curve of rainfall. The cumulative rainfall obtained by summing the rainfall increments (column 2) through time is given in column 3 of the table. The rainfall mass produced by plotting the cumulative rainfall against time (minutes) is shown in Fig. 9.13b.
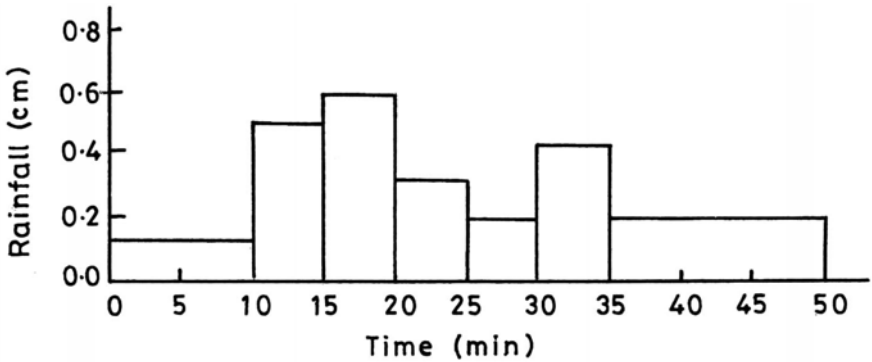
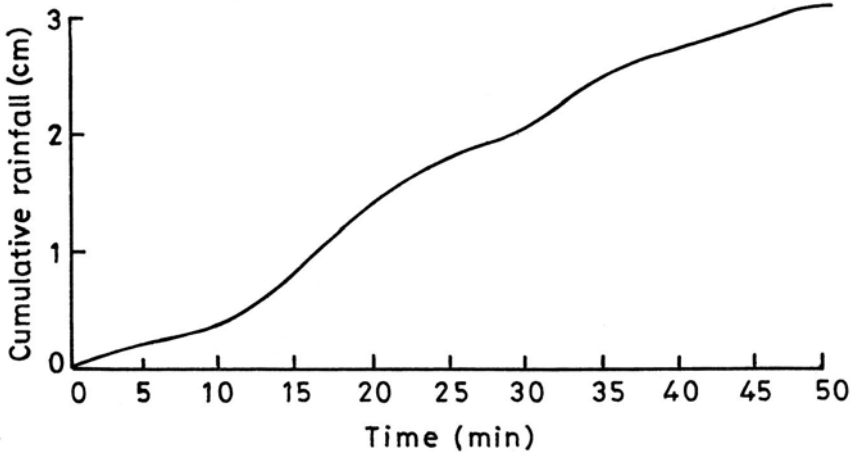**Fig. 9.13a.** Rainfall hyetograph.

Fig. 9.13b. Mass curve of rainfall.

(c) Maximum depth-duration values: The maximum rainfall depth recorded in a given time interval in a storm is determined by computing a series of running totals of rainfall depth for that time interval starting at various points in the storm, then selecting the maximum value of this series. The running totals for 5, 10, 15, 20, 25, 30, 35, 40, 45, and 50 minute durations are listed in columns 4 to 13 of Table 9.5. The maximum rainfall values recorded during the 5, 10, 15, 20, 25, 30, 35, 40, 45, and 50 minute durations are 0.7, 1.3, 1.6, 1.8, 2.3, 2.5, 2.7, 2.9, 3.0, and 3.1 cm, respectively.

(d) Maximum intensity duration curve: Corresponding to the maximum rainfall depths for different durations obtained in (c) above, the corresponding maximum intensities for 5, 10, 15, 20, 25, 30, 35, 40, 45, and 50 minute durations are as follows:

$$5 \text{ min} = \frac{0.7 \times 60}{5} = 8.4 \text{ cm/hr}$$

$$10 \text{ min} = \frac{1.3 \times 60}{10} = 7.8 \text{ cm/hr}$$

$$15 \text{ min} = \frac{1.6 \times 60}{15} = 6.4 \text{ cm/hr}$$

$$20 \text{ min} = \frac{1.8 \times 60}{20} = 5.4 \text{ cm/hr}$$

$$25 \text{ min} = \frac{2.3 \times 60}{25} = 5.5 \text{ cm/hr}$$

$$30 \text{ min} = \frac{2.5 \times 60}{30} = 5.0 \text{ cm/hr}$$

$$35 \text{ min} = \frac{2.7 \times 60}{35} = 4.6 \text{ cm/hr}$$

$$40 \text{ min} = \frac{2.9 \times 60}{40} = 4.4 \text{ cm/hr}$$

$$45 \text{ min} = \frac{3.0 \times 60}{45} = 4.0 \text{ cm/hr}$$

$$50 \text{ min} = \frac{3.1 \times 60}{50} = 3.7 \text{ cm/hr}$$

It can be seen that as the time period increases, the average intensity of the storm decreases.

The equation for the maximum intensity (i) and duration (t) is of the form:

$$i = \frac{C}{t^n} \tag{9.14}$$

or $$\log i = \log C - n \log t$$

We have for $t = 15$ minutes, $i = 6.4$ cm/hr; and for $t = 40$ minutes, $i = 4.4$ cm/hr. Substituting the values in the equation gives

$$0.806 = \log C - 1.176n \tag{9.15}$$

$$0.643 = \log C - 1.602n \tag{9.16}$$

Solving the above equations we have: $n = 0.382$, and $C = 18.0$. Hence, the formula becomes:

$$i = \frac{18}{t^{0.382}} \tag{9.17}$$

9.11 POINT RAINFALL TO AREAL RAINFALL RELATIONSHIP

A spatial distribution of rainfall giving the average rainfall depth exceeding a specified threshold value over a region in association with some meteorological phenomena, such as depression, cyclonic storm, etc., is called a rainstorm. The isohyetal patterns of rainstorms show that variations in intensity and the total depth of rainfall occur from the centers to the peripheries of rainstorms. The maximum intensity of rainfall in a rainstorm occurs at a point at the center of storm and away from this the rainfall intensity gradually decreases. The form of variation is shown in Fig. 9.14, which shows for a particular rainstorm how the average depth of rainfall progressively decreases over a progressively increasing area from the center of the rainstorm to its periphery. This shows that the maximum rainfall at the center of the rainstorm appears to have a definite relationship to the average amount of rainfall over an area. Horton (1924) found that the depth-area curve, as shown in Fig. 9.14, can be represented in a non-linear form as:

$$\bar{P} = P_m e^{-kA^n} \tag{9.18}$$

in which $\bar{P}$ is the average depth of rainfall for a given duration over an area A, P_m is the highest rainfall at the center of the storm and k and n are constants whose values vary with the durations of a given storm. The equation relates storm central rainfall to storm areal rainfall.
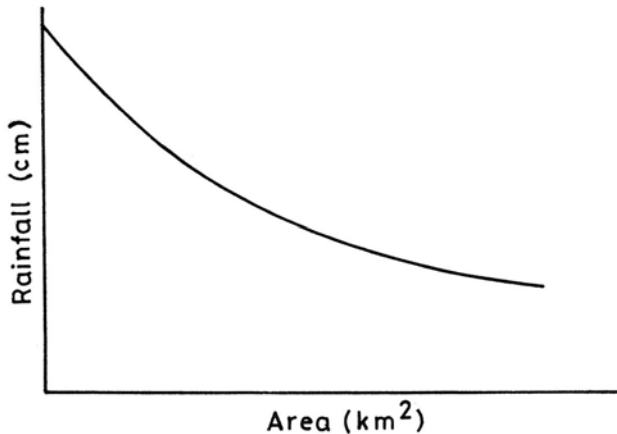

Fig. 9.14. Depth area curve of rainfall.

Using storm data of Gangetic West Bengal, Rakhecha et al. (1993) found that the envelope curves of 1-, 2- and 3-day duration amounts for storms could be represented as:

$$\bar{P_1} = P_1 e^{-0.00120 A^{0.600}} \qquad (9.19)$$

$$\bar{P_2} = P_2 e^{-0.00118 A^{0.627}} \qquad (9.20)$$

$$\bar{P_3} = P_3 e^{-0.0005 A^{0.693}} \qquad (9.21)$$

where $\bar{P_1}, \bar{P_2},$ and $\bar{P_3}$ are the average rainfall depths over an area A (km^2), and P_1, P_2 and P_3 are the maximum central rain depths (cm) for 1-, 2-, and 3-day durations. If the depth-area curve associated with a rainstorm is available, it can be used to convert the storm center rainfall to areal average rainfall for hydrologic purposes.

Example 9.8: The table gives depth-area values from a rainstorm. Compute the relationship of point to a real rainfall.

Area km^2	10	100	500	1,000	5,000	10,000	20,000
Rainfall (cm)	54	53	51	48	39	33	29

Solution: By using equation $p = P_m e^{-KA^n}$ we have:

$$\log_e \frac{p}{P_m} = - KA^n$$

$$\log_e \frac{P_m}{p} = KA^n$$

$$\log_e \log_e \frac{P_m}{p} = \log_e K + n \log_e A$$

The equation reduces to a straight line which can be fitted by the least square method or by a simple method. Here $P_m = 54$ cm. For $p = 51$ cm, $A = 500$ km^2,

$$\log_e \log_e \frac{P_m}{p} = - 2.86, \ \log_e 500 = 6.21$$

for $p = 39$ cm, $A = 5000$ km^2,

$$\log_e \log_e \frac{P_m}{p} = - 1.12 \ \log_e 5000 = 8.52$$

Putting the values in the above equation we have:

$$-2.86 = \log K + 6.21 \ n \qquad (1)$$
$$-1.12 = \log K + 8.52 \ n \qquad (2)$$

Solving above equations (1) and (2) we have:

$$1.74 = 2.31 \ n$$

$$n = 0.753$$
$$\log_e K = -2.86 - 6.21 \times 0.753$$
$$\log_e K = -2.86 - 4.68$$
$$\log_e K = -7.54$$
$$K = 0.00053$$
$$p = Pm\ e^{-0.00053\ A^{0.753}}$$

is the relationship required.

REFERENCES

Ahuja, P.R., 1960. Planning of precipitation network for water resources development in India. WMO flood control series No 15, 106–112.

Dhar, O.N. and Rakhecha, P.R., 1981. The effect of elevation on monsoon rainfall distribution in the central Himalayas. Proc. Int. Symp. Monsoon Dynamics. Cambridge Univ. Press. London, 253–260.

Drozdov, O.A., 1936. A method for setting up a network of meteorological stations for a level region. Trudy, No. 12, 2.

Ganguli, M.K., Rangarajan, R. and Panchang, G.M., 1951. Accuracy of mean rainfall estimates – Data of Damodar catchment. *Irrigation and Power, J.*, 8.

Hill, S.A., 1881. Meteorology of northwest Himalayas. Memoirs of the India Meteorological Department, 1, 377–426.

Horton, R.E., 1923. The accuracy of areal rainfall estimates. *Mon. Weather Rev.*, 51.

Horton, R.E., 1924. Discussion of the distribution of intense rainfall and some other factors in the design of storm water drains. *Proc. Amer. Meteor. Civil Engineers*, 50, pp. 660–667.

Linsley, R.K., Kohler, M.A. and Paulhus, J.R.H., 1949. Applied Hydrology. McGraw Hill, New York.

Rakhecha, P.R., Mandal, B.N., Kulkarni, A.K. and Sangam, R.B., 1993. A hydrometeorological analysis of the severe rainstorm of 20–23 Sept. 1900 over the Gangetic West Bengal. *Advances in Atmos. Sciences, China*, 10, 1, pp. 113–120.

Rodda, J.C., 1969. Hydrological network design – Needs, problem and approaches. WMO/IHD Report No. 12, Geneva.

Rumley, G.B., 1965. An investigation of the distribution of rainfall with elevation for selected stations in Ecuador. M.S. Thesis, Texas A & M University, USA.

Rycroft, H.B., 1949. Random Sampling of rainfall. *J. South African Forestry Assoc*. 18.

World Meteorological Organization, 1974. Guide to hydrological practice. Third Edition WMO, No. 168. Geneva.

10 <u>**Design Storm Estimation**</u>

Construction of dams and reservoirs across rivers for collecting and storing the runoff water to serve the needs of the people has been in vogue for many centuries. It was known that these dams often breached due to overtopping or seepage instability. Later, the discovery of concrete in the late 19th century gave a tremendous push to the dam construction work throughout the world. In all these dams, a spillway is built that not only allows water to pass over the dam structure in normal day to day operation but is also a safety device to pass the largest flood discharge arising from heavy rainfall after the reservoir is filled so that the dam would not be damaged. The magnitude of the largest flood, called the spillway design flood, was earlier based on professional judgement and historical flood marks. As a consequence, the largest flood that would be expected at the dam site was estimated from flood marks and the spillway capacity was provided accordingly. In the later part of the 19th century, the magnitude of the spillway design flood was determined by empirical formulae relating discharge to drainage area in the form $Q = K A^n$, where Q is the peak flood discharge, A is the drainage area, K is an empirical coefficient depending upon the rainfall-runoff characteristics of the drainage area, and n is a constant whose value usually lies between 0.5 and 1.0. The empirical formulae were based on the catchment area, with the assumption of constant coefficients. The degree of conservatism implied by these formulae was obviously unknown. The dams based on these formulae were often breached due to inadequate spillway capacities as pointed out in Chapter 8.

In 1930, Sherman introduced the concept of the unit hydrograph by which it became possible to estimate flood runoff from a storm rainfall. The word storm rainfall, which is also called a rainstorm, is usually used to denote heavy rainfall for a certain period of time. It then became possible to use the principles of hydrometeorology to derive a spillway design flood from the storm rainfall using a runoff model or the unit hydrograph method. Before discussing design storms it is important to have knowledge of rainstorms and the methods used to analyze them.

10.1 RAINSTORM AND ITS ANALYSIS

The previous chapters show that when a weather system like depression/storm etc. moves from the ocean over to a land area, it brings moisture and as a consequence produces heavy and wide spread rainfall for a number of days. Several stations in the affected area simultaneously record heavy rainfalls and the values may range from 40 to 80 cm per day. Such a large scale spatial distribution of heavy rainfall yielding the average depth of rainfall exceeding a threshold value over a region is called a rainstorm. The period for which the storm rainfall depth equals or exceeds the threshold value is known as the storm period.

The rainfall measured by a gauge is a point measurement, that is, it represents rainfall at the point where the gauge is located. Floods, however, result from substantial volumes of rain spread out over a river basin or a substantial portion thereof. Thus, any appraisal of storm rainfall for purposes of estimating flood magnitudes from rainfalls spread out over an area, it is necessary to estimate the average rainfall amounts for various size areas during the storm period. Thus, the form of information required is the largest average depth of rainfall (in millimeters or inches) yielded by it over specified sizes of area (in square kilometers or square miles) during the storm period. That is, rainstorm data should be expressed in terms of Depth-Area-Duration (DAD) values. These values are required for purposes of evaluating design storms. The following section describes the manner in which DAD values are derived from the point rainfall measurements. The standard method for computing the depth-area relationship of a rainstorm is detailed in a manual for Depth-Area-Duration analysis of Storm Precipitation (WMO, 1969).

10.2 DEPTH-AREA-DURATION ANALYSIS OF A RAINSTORM

The Depth-Area-Duration (DAD) analysis of a rainstorm is carried out to quantify rainfall depths over specified sizes of area falling in specified durations of time, say, 1-day, 2-day, 3-day, and so on. The steps involved in the DAD analysis are as follows:

 (i) The first step is the selection of a severe rainstorm.
 (ii) The selected storm is assigned a duration. This is the period for which the daily storm rainfall depths are equal to or greater than the threshold value.
(iii) For each day of the storm duration, obtain rainfall amounts at all of the available stations in the storm area. These rainfall data are mostly available in published form and are typically daily and hourly amounts at rainfall measuring stations.
(iv) For each day of the storm duration, daily rainfall values at all the available stations in the storm region are extracted.

(v) The 1-day, 2-day, or *n*-day (*n* = any number) rainfall amounts for the entire storm period are plotted on rainfall base maps separately in respect of all rain gauge stations within the storm area. These maps should preferably be on a scale 1 inch = 16 miles with contour heights, catchment boundaries and location of rain gauge stations.

(vi) After plotting rainfall amounts, isohyets are constructed by interpolation between stations. Topographic features should be taken into account. If the storm is of a type that is common in a region where topographic effects play an important part in the geographic distribution of rainfall, the mean annual rainfall map may give some guidance on the distribution of the storm rainfall. For a typical storm the 1-day storm isohyetal map is shown in Fig. 10.1.
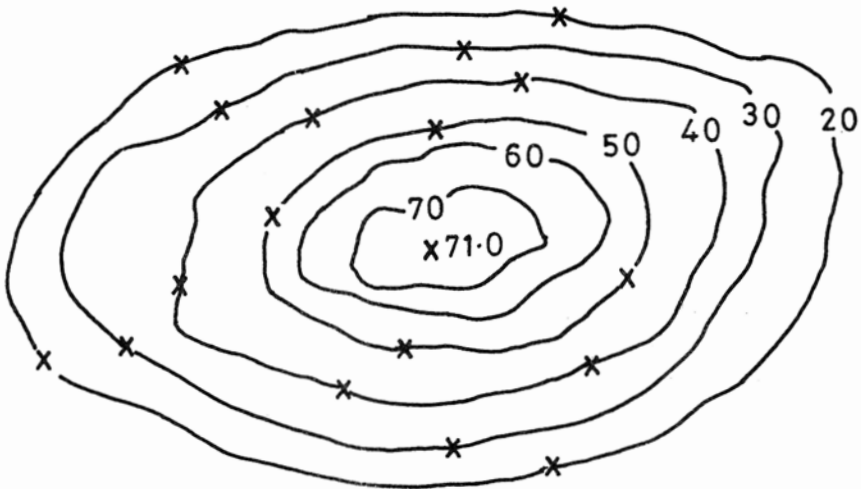

Fig. 10.1. Isohyetal pattern for a typical 1-day storm.

(vii) To determine the average depth of rainfall that fell over the area between two isohyets, the area enclosed between them are measured with the help of a planimeter. The manner in which the computations are entered is given in the computational sheet as in Table 10.1.

(viii) For constructing the Depth-Area-Duration curve, the average rain depths in column 7 of the computation sheet are plotted against the accumulated area (km^2) given in column 3. The starting point is taken to be the central rainfall value (71.0 cm) of the storm and plotted against point area (~ 10 km^2). After plotting all the points, a smooth DAD curve is drawn which passes through all the points. Figure 10.2 shows the Depth-Area relation curve from an isohyetal map (Fig. 10.1) for 1-day duration. The rainfall value for any size area can be obtained from this curve.

Table 10.1: Computational sheet for DAD analysis

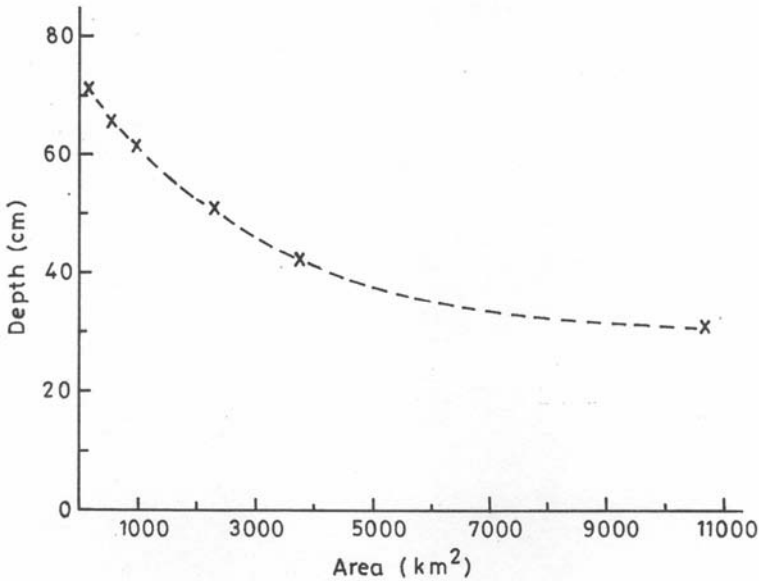| Isohyetal range (cm)	Mean rainfall (cm)	Accumulated area (km²)	Area between isohyets (km²)	Volume of water (cm × km²)	Accumulated volume (cm × km²)	Average depth (cm)
1	2	3	4	5	6	7
71-70	70.5	97	97	6839	6839	71
70-60	65.0	432	335	21775	28614	66
60-50	55.0	780	348	19140	47754	61
50-40	45.0	1722	942	42390	90144	52
40-30	35.0	3599	1877	65695	155839	43
30-20	25.0	10454	6855	171375	327214	31

Fig. 10.2. DAD curve for one day.

10.3 DESIGN STORM

In the design of any hydrologic project connected with irrigation, hydropower or flood control, it is necessary to determine the areal and time distribution of the greatest rainfall associated with a rainstorm and to evaluate the average depth of rainfall over a specified area during the storm. The specified area for such a hydrologic project is the natural drainage basin which is called a river catchment. By definition, a design storm of a catchment is an estimate of the highest rainfall of a specified recurrence interval over the catchment which is accepted for use in determining the spillway design flood.

Categories of Design Storms

Three types of design storms are commonly used for deriving spillway design floods: (i) Standard Project Storm (SPS), (ii) Probable Maximum Storm (PMS) or Probable Maximum Precipitation (PMP), and (iii) Frequency-based storms.

Standard project storm (SPS): The Standard Project Storm (SPS) is the most severe rainstorm that has actually occurred over the catchment during the period of available records. It is used in the design of all water projects where not much risk is involved and economic considerations are taken into account. SPS is used by U.S. Army Corps of Engineers for design work.

Probable maximum precipitation (PMP): The probable maximum storm, also called the probable maximum precipitation (PMP), over a river basin refers to that amount of rainfall depth that is close to the physical upper limit for a given duration over a particular drainage area. WMO (1986) defines PMP as the greatest depth of precipitation for a given duration that is physically possible over a particular area and geographical location at a certain time of the year. Estimates of PMP are required for calculating the resulting probable maximum flood (PMF) hydrograph which is the design flood for spillways of large dams, where no risk of failure can be accepted. An estimate of PMP is made either by a statistical method in which a very large return period value of rainfall depth is calculated or by the physical method in which major historical rainstorms are moisture maximized. It is generally determined from the greatest storm rainfall depths associated with severe rainstorms and from increasing this rainfall in accordance with meteorologically possible increases in the atmospheric factors that contribute to storm rainfall.

Frequency-based storm: A design flood can be estimated using a frequency-based method or rainfall runoff method. The former involves a frequency analysis of long-term streamflow data at a site of interest. When such data are not available, then a frequency analysis of rainfall data is performed and coupled with a rainfall-runoff model to get the design flood. The rainfall-runoff model can be empirical, conceptual, or physically based. On the other hand, regional frequency analysis can also be employed to obtain the design flood. The index method is one of the most popular regional frequency analysis methods.

10.4 DATA FOR DESIGN STORM STUDIES

The basic data required in design storm studies are: (i) long-term daily rainfall records from all the stations in and around the catchment area of the dam site, (ii) rainfall data from automatic recording rainfall stations, and (iii) data of storm dew point and maximum dew point temperatures. As regards

India, rainfall is measured on a daily basis at about 5000 stations and measurements at some stations are available for over 100 years. Also there are about 525 automatic recording rainfall stations which provide rainfall records not only of the total daily rainfall but also the intensity variation throughout the day. Hourly, daily, and monthly rainfall data of these stations are available with the National Data Centre of India Meteorological Department (IMD) at Pune. Also a systematic preparation of daily weather charts for the whole of India has been done by the IMD since August 1871. Daily weather reports and daily weather maps for India in printed form are available since 1878. The Indian Weather Review gives a summary of the main features of the weather of India month by month and it also gives an annual summary. The monthly Weather Review contains accounts of depressions, and cyclonic storms while the annual summary gives a consolidated list of these cyclonic disturbances, including the greatest observed pressure, intensity of disturbances, heavy rainfall, and so on. The publication "Tracks of tropical storms and depressions in the Bay of Bengal and the Arabian Sea," contains valuable information about severe rainstorms, as shown in Chapter 6.

10.5 METHODS FOR ESTIMATING DESIGN STORMS

The first and foremost requirements for estimating the SPS or PMP storm is the selection of major rainstorms that have occurred in and around the catchment under study. These storms are determined by reviewing all daily rainfall records of stations located in and around the catchment. If daily rainfall data are available electronically then computer methods can be employed for quickly listing major rainstorms. Before selecting the storms, it is pertinent to consider an appropriate threshold value based on rainfall regime and catchment size for the purpose of storm selection. The following criteria may be used for storm selection: (a) If the catchment lies in a low rainfall region a slightly lower threshold value is chosen for storm selection, whereas for a high rainfall region a higher threshold value is chosen. Normally, about 10% of the seasonal normal rainfall is taken for the most frequent storm duration over the region. For example, if the seasonal rainfall is 100 cm and the most frequent storm duration is two days, then a threshold value

of $\left[100 \times \dfrac{1}{10} \times \dfrac{1}{2} = 5.0 \text{ cm} \right]$ i.e. 5 cm per day can be chosen.

As regards catchment size, for smaller catchments, a higher threshold value and for larger catchments a lower threshold should be chosen. An average rainfall depth of 5 cm per day over a catchment of 10,000-15,000 km^2 would be appropriate. After obtaining a suitable severe rainstorm data base, the following four methods are generally used for estimation of the SPS or PMP design storm rainfall:

 (i) Depth-Duration analysis
 (ii) Depth-Area-Duration analysis
(iii) Storm transposition
(iv) Statistical method

The main objective of these methods is to estimate the highest rainfall that might occur over the catchment. In estimating the PMP, the highest observed rainfall is maximized for a moisture maximization factor (MMF). The design storm rainfall values are then used in determining the design flood hydrograph by the unit hydrograph method or some other transformation function.

10.5.1 Depth-Duration Method

The depth-duration method is normally employed when daily rainfall data for a good number of stations within a catchment under study are available for a sufficiently long period of time (years). The daily rainfall data of stations within the catchment are examined and for each year the heaviest rainstorm that gave maximum rainfall for 3 to 4 days over the entire catchment is selected. The areal average rainfall for each day of the storm period is then computed by the arithmetic average method, isohyetal method or Thiessen polygon method as described in Chapter 9. With a view to obtaining the highest areal rain depths for different durations over the catchment, the areal average rain depths are plotted against their duration. Such a curve is called the depth-duration (DD) curve. The curve enveloping all such curves is then drawn. The enveloping curve gives design storm ranfalls for different durations over the catchment.

Rakhecha et al. (1995) estimated the design storm rainfall for the Upper Krishna River catchment upstream of the Almatti dam in the Karnataka state of India by the DD method. The maximum rainfalls of 10 heavy rainstorms for 1 to 3-day durations determined by the DD method are listed in Table 10.2.

Table 10.2: Ten highest areal rainfall (cm) recorded over the Krishna River catchment above the Almatti dam

Year	1-day rainfall (cm)	2-day rainfall (cm)	3-day rainfall (cm)
1912	9.9	15.0	21.8
1914	14.0	21.5	24.6
1943	9.5	16.2	20.0
1946	8.2	13.9	16.8
1956	6.8	12.0	15.8
1966	9.5	13.2	16.0
1967	6.1	11.7	15.8
1975	9.5	13.4	16.1
1976	9.0	12.5	16.7
1983	8.2	14.7	19.7

In order to obtain the highest rainfall depths recorded over the catchment, the rain depths for 1, 2, and 3-day durations for the 10 highest storms are plotted as depth-duration (DD) curves (Fig. 10.3). The design storm values for the catchment are 14.0 cm, 21.5 cm, and 24.6 cm for 1, 2, and 3 days, respectively.
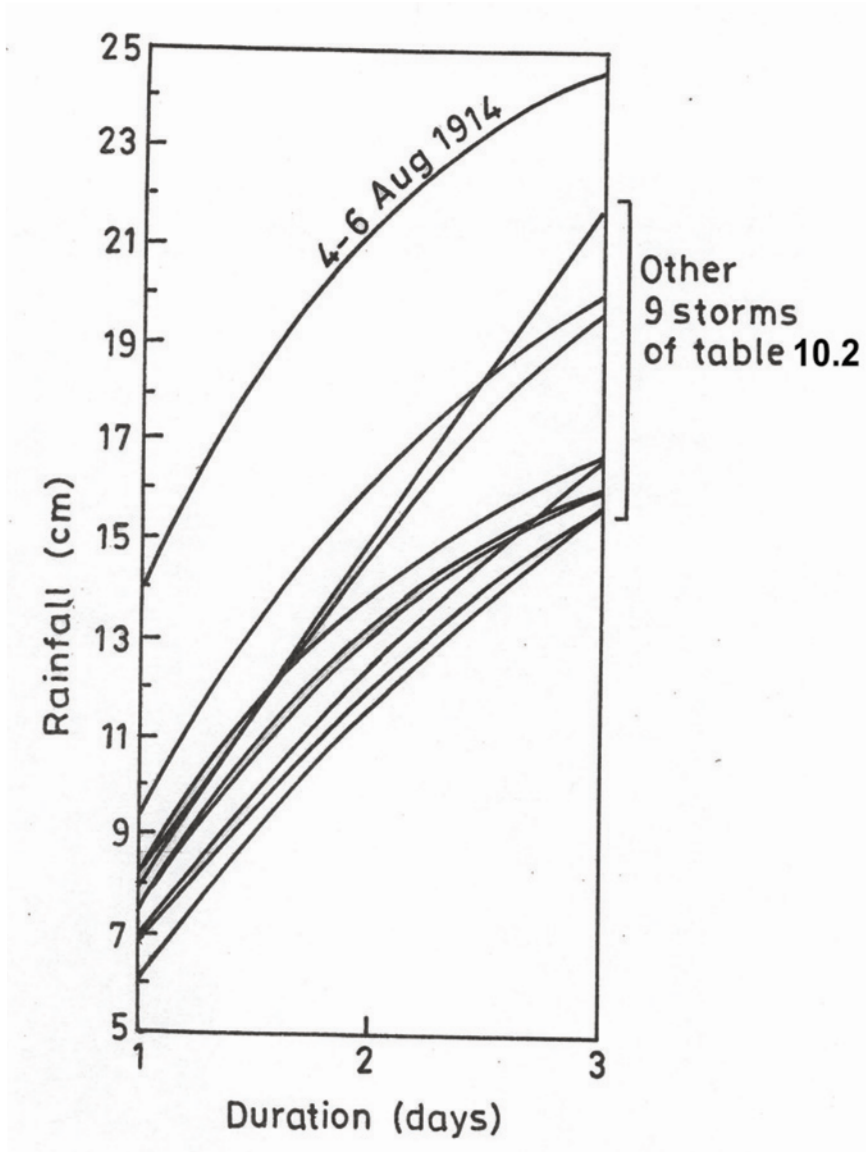

Fig. 10.3. Depth duration curves for the 10 highest storms.

10.5.2 Depth-Area-Duration Method

The depth-duration (DD) method considers major rain storms which have occurred within the catchment. Although these rainstorms are probably the critical ones for estimating design storm rainfalls, it is quite possible that some more spectacular storms with higher rainfall depths that have occurred remote from the river catchment could occur over the catchment. For these reasons there should be a careful examination of all the rainstorms which have occurred away from the catchment for their possible use. If rainstorms are to be used to derive design storm rainfalls then these should be analyzed in such a manner as to determine the largest depth of rainfall that fell over areas of various sizes and durations. The steps involved in the depth-area-duration (DAD) analysis have been explained in a preceding section. The DAD values of 12 major rainstorms for 1 to 3-day durations in India are given in Table 8.12 (Chapter 8). The rainfall values for small area sizes are useful for the estimation of design storms for design of bridges, drainage works, and rainfall values for large areas are useful for the estimation of design storms for major and medium dams.

10.5.3 Storm Transposition

Storm transposition implies the transfer or application of an outstanding or a major rainstorm from where it occurred to other neighboring areas where it could occur. If a catchment has not experienced the number of storms necessary for design storm estimation then the record of storms is increased by transposing storms over the catchment from another catchment lying in the same meteorologically homogeneous region. Two regions are said to be meteorologically homogeneous if they have: (i) similar features of climate (mean annual temperature, mean annual rainfall, direction of prevailing winds, etc.), (ii) identical topographic features, (iii) the same moisture source, and (iv) experience the same type of storms.

For purposes of transposition, a rainstorm refers to the isohyetal pattern which is to be brought over to the catchment. The isohyetal pattern is drawn at the place of storm occurrence. Its outer-most isohyet is fixed to suit the size of the project catchment. The isohyetal pattern is then shifted over to the project catchment and adjusted in a way so as to yield maximum rainfall depth over the catchment. In doing so the axis of isohyetal pattern can undergo an angular rotation up to a maximum of 20 degrees. After transposing the storm pattern over the catchment, the average depth of the transposed storm over the catchment is computed by the DD method. As an example, Fig. 10.4 shows the transposed isohyetal pattern of September 19-21, 1926 rainstorm over the Betwa catchment in India.
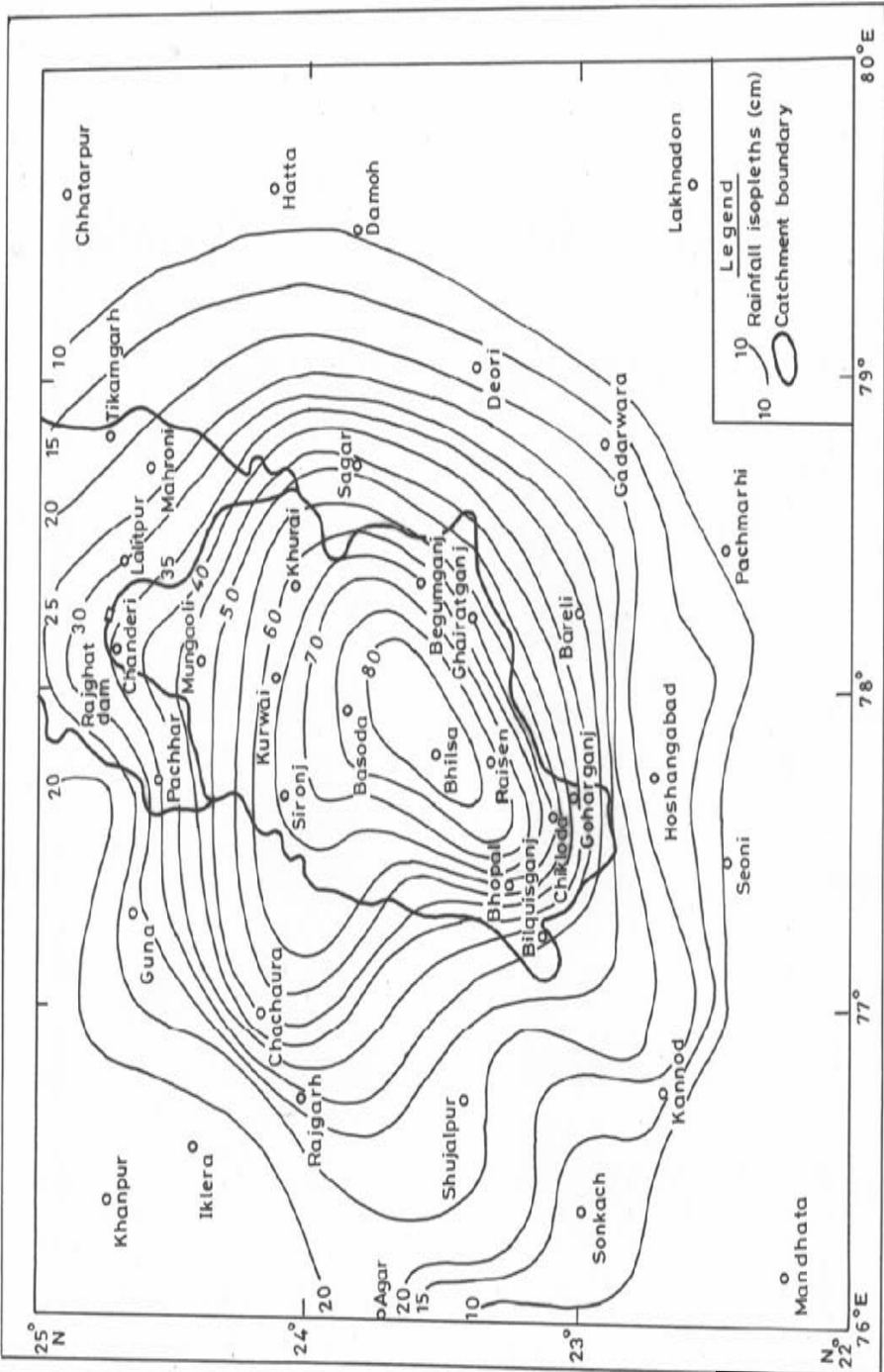
Fig. 10.4. Isohyetal pattern of the September 19-21, 1926, rainstorm transposed over Betwa basin up to Rajghat dam.

The following guidelines for transposition of storms should be considered:

(i) Coastal storms should not be transposed to inland areas. Such storms should be considered for transposition along coastal catchments.

(ii) Storms occurring over mountains should not be transposed to other plains or mountainous areas.

(iii) Transposition should be avoided if it requires crossing a barrier having an elevation of more than 800 m. If hill ranges are of lower elevation, transposition may be undertaken with the application of a suitable barrier adjustment factor.

(iv) In middle latitudes, it is suggested that the homogeneous regions for transposition should be characterized by the same type of air mass. Too much latitudinal transposition may involve a change in the air mass characteristics of the storm. In general, latitudinal transposition over 10° latitude should be avoided.

10.5.4 Statistical Method

Annual maximum areal rainfall values for a catchment or for a station for various durations are subjected to frequency analysis and the estimates of design rainfalls for different return periods are determined. To that end, the annual maximum rainfall series and the daily rainfall data of stations within the catchment are processed for the period of record and for each year the heaviest rainstorm that was sustained for 3 to 4 days is selected. The arithmetic average or the isohyetal method then calculates the areal average rainfall for each day of the storm period. Thus, for N years of data the annual maximum series will consist of N rainfall values. The annual maximum rainfall series for different durations of the catchment are then subjected to an extreme value analysis and the estimates of design storm rainfall for a specific return period is determined. In India, according to the Central Water Commission (1969) guidelines, the minimum return period of the inflow design flood for the safety of the dam should be as follows:

(a) For large dams with a storage capacity of more than 60×10^6 m^3 and a hydraulic head greater than 30 m, a recurrence interval of 1000 years is used.

(b) For minor dams with storage of less than 60×10^6 m^3, a recurrence interval of less than 1000 years is used.

10.6 PROBABLE MAXIMUM PRECIPITATION

There are varying design storm rainfall values, depending on the designer's viewpoint. It has been recognized that there is a physical upper limit to the amount of precipitation that can fall over a specified area in a given time. This precipitation associated with the physical upper limit is known as the probable maximum precipitation (PMP). The dams for which a high degree

of safety is required are needed to be designed to pass the flood resulting from the physical upper limit to precipitation. The PMP as defined by the American Meteorological Society (1954) as "the greatest depth of precipitation for a given duration that is physically possible over a particular drainage area at a certain time of the year". In a WMO publication (1986), however, the definition has been modified by substituting the words "over a given size storm area in a particular geographical location" for the words "over a particular drainage". The modification recognizes the fact that there is a difference in the storm depths over a storm area and those over a specific basin of the same size because storm patterns do not coincide exactly with the shape of the basin.

10.7 METHODS OF ESTIMATING PMP

WMO (1986) gives the following methods that can be used to estimate the PMP:

  (i) Storm model approach based on realistic meteorological processes.
 (ii) Maximization and transposition of actual storms.
(iii) Use of generalized depth-area-duration data.
(iv) Statistical analyses of extreme rainfalls.

10.7.1 Storm Model Approach

Determination of the PMP from a storm model requires maximization of all the variables that cause precipitation. The main assumption is that the PMP will result from a storm in which there is the optimum or most effective combination of maximum water content in the atmosphere and the efficiency of the storm generation mechanism. Factors which determine the storm efficiency are:

  (i) horizontal mass convergence,
 (ii) vertical velocities,
(iii) condensation of water vapor into cloud particles, and
(iv) frontal or topographically induced lifting.

The maximum water content in the atmosphere can be estimated with an acceptable accuracy by an appropriate interpretation of climatological data. However, at present there is neither an empirical nor a satisfactory theoretical method for assigning maximum values individually or collectively to various factors that constitute storm efficiency. In view of the uncertainties and limitations of the knowledge of the precipitation processes, the use of storm models is not well accepted for determining the PMP. The solution to this problem has been to use observed storm rainfall as an indirect measure of storm efficiency. In practice, the PMP is determined by moisture maximization and transposition of the actual observed storm.

10.7.2 Maximization and Transposition of Actual Storms

The PMP for different durations over an area is derived by maximizing the highest rainfalls obtained for major historical rainstorms that have occurred over the area under study. This maximization consists of simply multiplying the highest rainfall values by the moisture maximization factor (MMF). The MMF is a ratio of the highest amount of moisture recorded in the study area during the period when the storm occurred to the amount of moisture recorded during the storm. The objective of maximization is to determine the physical upper limit of rainfall which would result if the moisture available to the storm is maximum. Obviously, the most important factor in the moisture maximization is the estimation of moisture or precipitable water available in the atmosphere. U.S. Weather Bureau (USWB) (1960), now National Weather Service (NWS), and Reitan (1963) showed that the precipitable water or moisture in the air mass from which large precipitation occurs can be estimated from the surface dew point temperatures when saturation and pseudo-adiabatic conditions are assumed. The MMF therefore is determined on the basis of 12-hour or 24-hour maximum persisting storm and the maximum ever recorded persisting dew point for the area under study. The meaning and the method of determining the 12-hour or 24-hour persisting dew point temperature will be discussed later. Both storm and maximum dew points are reduced pseudo-adiabatically to the 1000 mb level by means of Fig. 10.5 so that dew points obtained at different elevations are comparable. Figure 10.6 gives values of precipitable water (mm) between 1000 mb surface and various pressure levels up to 200 mb in a saturated pseudo-adiabatic atmosphere as a function of the 1000 mb dew point. In practice the dew points are converted to precipitable water by the use of Fig. 10.6 or from tables such as those given in WMO (1986).
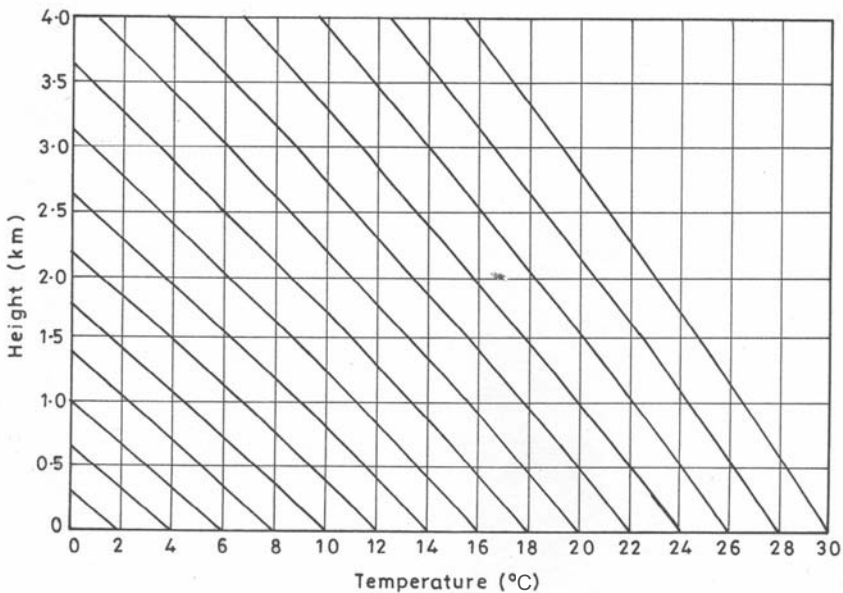

Fig. 10.5. Pseudo-adiabatic diagram for dew point reduction to 1000 mb.
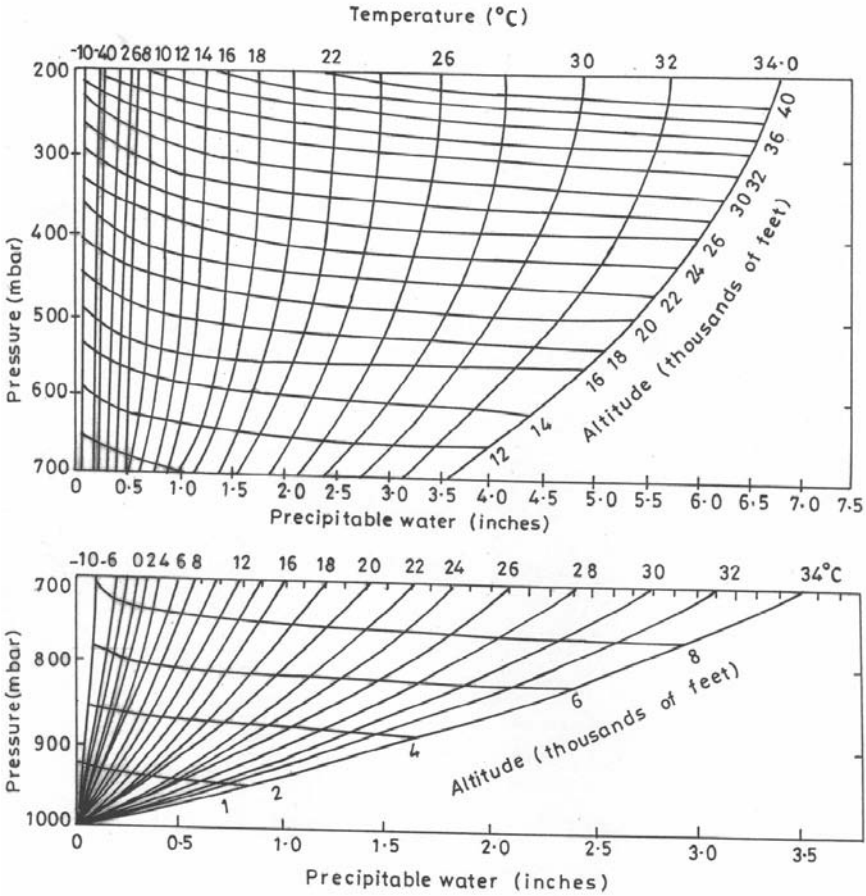
Fig. 10.6. Precipitable water above 1000 mb assuming saturation with pseudo adiabatic lapse rate for the indicated surface temperature.

The highest rainfall values from the storm where it occurred, i.e., without change in location, are maximized so as to obtain the PMP rainfall as

$$R_m = R_0 \frac{W_m}{W_s} \tag{10.1}$$

where R_m is the maximized rainfall, R_0 is the highest observed storm rainfall for a particular duration and size of area, W_m – the precipitable water corresponding to the maximum surface dew point at the location of storm occurrence, and W_s is the precipitable water corresponding to the storm dew point.

Example 10.1: A rainstorm over an area of 892 km^2 produced the highest rainfalls of 38 cm, 69 cm, and 98 cm in 1, 2, and 3 days, respectively. The

24-hour persisting 1000 mb dew point temperature for the storm was 22.8°C and the highest 24-hour persisting dew point for the concerned area was 25.5°C. Calculate the MMF as well as PMP rainfall depths.

***Solution*:** Persisting storm dew point temperature = 22.8°C
        Storm precipitable water (1000 mb – 200 mb) = 66.7 mm
        Highest dew point for the concerned area = 25.5°C
        Precipitable water (1000 mb – 200 mb) = 84.3 mm
        MMF = 84.3 mm/66.7 mm = 1.26

The highest rainfall values are then maximized by a factor of 1.26 to obtain the PMP values which are as follows:

$$1\text{-day PMP} = 38 \times 1.26 = 48 \text{ cm}$$
$$2\text{-day PMP} = 69 \times 1.26 = 87 \text{ cm}$$
$$3\text{-day PMP} = 93 \times 1.26 = 117 \text{ cm}$$

10.7.2.1 Adjustment for storm elevation

If the storm elevation is not at mean sea level but it occurred at some elevated place, then a correction is to be applied for the elevation of the storm. In case the elevation of the storm is less than 300 m, the adjustment for storm elevation is not made (Schreiner and Riedel, 1978). If the storm has occurred on a sloping plain at an elevation of 400 m with no intervening topographic barrier between the rain area and the moisture source, then the moisture maximization factor for the data given in Example 10.1 is as follows:

        Storm dew point = 22.8°C
        Precipitable water above 400 m = 58.7 mm
        Highest dew point = 25.5°C
        Precipitable water above 400 m = 75.8 mm
        MMF = 75.8/58.7 = 1.29
        1-day PMP = 38 × 1.29 = 49 cm
        2-day PMP = 69 × 1.29 = 89 cm
        3-day PMP = 93 × 1.29 = 120 cm

Tables in WMO (1986) provide precipitable water values above specified heights (meters).

10.7.2.2 Adjustment for transposition

When no severe rainstorm has occurred in the study area then in that case the nearest available storm from a meteorologically homogeneous region has to be physically moved to the area under study. This movement is called transposition of storm which involves a number of guidelines as discussed previously. The transposed rain depths are then maximized by an MMF. The transposed location may either be in the proximity of the moisture source or be away from the source. In the storm transposition, the moisture content

entering the storm cell will change and an adjustment is to be made for this change. The storm is first adjusted at its original location. If d_1 is the maximum dew point at the original location and d_2 is the storm dew point and w_1 and w_2 are the corresponding precipitable waters then MMF for the original location of the storm (K_m) is:

$$K_m = \frac{w_1}{w_2} \qquad (10.2)$$

Now the storm needs to be adjusted for its new location. If d_3 is the maximum dew point over the new transposed location where the storm is transposed and w_3 is the corresponding precipitable water then the transposition adjustment (K_t) is

$$K_t = \frac{w_3}{w_1} \qquad (10.3)$$

The combined storm maximization factor is given as:

MMF = adjustment for original location times the adjustment for transposed location

$$\text{MMF} = \frac{w_1}{w_2} \times \frac{w_3}{w_1} = \frac{w_3}{w_2}$$

$$= \frac{\text{Precipitable water corresponding to dew point at the transposed location}}{\text{Precipitable water corresponding to the storm dew point}}$$

Example 10.2: The 1000 mb dew point temperature of a storm at its original location is 25°C. The 1000 mb maximum dew point at the storm occurrence is 28°C and at its transposed location the maximum dew point is 27°C. Find the MMF.

***Solution*:** Storm dew point (d_2) = 25°C
Precipitsable water at 25°C (w_2) = 81 mm
Dew point at original place (d_1) = 28°C
Precipitable water at 28°C (w_1) = 105 mm
Dew point at transposed location (d_3) = 27°C
Precipitable water at 27°C (w_3) = 96 mm

$$\text{MMF} = \frac{w_1}{w_2} \times \frac{w_3}{w_1} = \frac{105}{81} \times \frac{96}{105} = \frac{96}{81} = 1.19$$

10.7.2.3 Adjustment for barrier

A barrier adjustment is applied to compensate for the difference in elevations of the original and transposed sites. This is a common situation because catchments upstream from suitable dam sites are often surrounded by mountains. The barrier adjustment is the ratio of precipitable water in a column of air above the top of the barrier to the transposed site for the maximum dew point to the precipitable water above the barrier at the original site for the same maximum dew point. This adjustment is better understood with the help of an example given below.

Example 10.3: A rainstorm occurred over an area whose average elevation is 300 m and the 1000 mb dew point of the storm was 20°C. This storm is transposed to a catchment with an average elevation of 500 m. The maximum persisting dew points at the transposed and original sites were 24° and 25°C, respectively. Calculate the moisture adjustment factor.

Solution: The moisture adjustment factor considering the difference in elevation between original and transposed sites is worked out as follows:

> Storm dew point = 20°C
> Precipitable water $(w_{20})_{300}$ above 300 m at 20°C = 47.4 mm
> Max persisting dew point at original site = 25°C
> Precipitable water $(w_{25})_{300}$ above 300 m at 25°C = 74.4 mm
> Maximum persisting dew point at transposed site = 24°C
> Precipitable water $(w_{24})_{500}$ above 500 m at 24°C = 63.7 mm
> Precipitable water $(w_{24})_{300}$ above 300 m at 24°C = 67.7 mm
> MMF = $(w_{25})_{300}\ /(w_{20})_{300} \times (w_{24})_{300}/(w_{25})_{300} \times (w_{24})_{500}/(w_{24})_{300}$
> $\quad = 74.4/47.4 \times 67.7/74.4 \times 63.7/67.7$
> $\quad = 63.7/47.4 = 1.34$

10.7.2.4 Persisting dew points

The moisture maximization procedure used for the estimation of the probable maximum precipitation for specific areas consists of moisture adjustment of observed areal rainfall values associated with severe rainstorms occurring within the specific areas as well as those transposed over the areas. For moisture adjustment the observed areal rainfall values are multiplied by the ratio of the highest amount of moisture recorded in the specific area to that recorded during the storm period.

The amount of moisture in the air can be obtained from the single observation of dew point temperature, but these have certain synoptic limitations and are also susceptible to observational error. The moisture itself must be such that which persists for a period of several hours rather than minutes. Thus the dew point values used to estimate moisture during the storm as well as over the specific area is based on three or more consecutive dew point values by a reasonable time interval. The value of the dew point

so obtained is called the persisting dew point. The daily dew point data for meteorological stations are published by various meteorological departments worldwide. The daily dew point data during a storm period can be collected from such publications. The general practice is to use the 12-hour or 24-hour persisting dew point. The maximum persisting 24-hour dew point can be obtained from the series of 12-hour intervals on days as in Table 10.3:

Table 10.3: 12-hour interval dew point

	Day 1		*Day 2*		*Day 3*		*Day 4*	
Time (GMT)	03	12	03	12	03	12	03	12
Dew point (°C)	22	22	23	24	26	24	20	21
Persisting dew point (°C)		22	22	23	24	20	20	

In determining the persisting dew point, the consecutive dew points during a 24-hour period are examined for their reliability and the lowest of these values is selected. The highest persisting 24-hour dew point for the above series is 24°C which is obtained from a period 12 hours of the second day to 12 hours of the third day.

10.7.2.5 Storm dew point

In order to obtain the storm moisture, dew points in respect of stations located in the warm air flowing into the storm are identified from the surface weather map. While selecting the stations, care should be taken such that the storm centre should invariably fall close to the stations. Also, dew points between the rain area and moisture source have to be given prime consideration. Dew points in the rain area may be too high because of precipitation, but they need not be discarded if they appear to agree with dew points outside the rain area. Figure 10.7 gives a weather map from which the storm dew point is determined based on the available dew points of four stations enclosed by rectangles. Of course, one station is inside the heavy rainfall area and the other three in the path of moisture inflow. The storm dew point is then determined by averaging of these four stations. Before averaging, the dew point values are reduced pseudo-adiabatically to the 1000 mb level, so that dew points for stations at different elevations are comparable.

10.7.2.6 Highest persisting 24-hour 1000 mb dew points

For obtaining the maximum persisting dew point for any specific area, the long period (say, 20 to 30 years) dew points at several stations within the study area are scanned for a period of 15 days during which the storm has occurred. For example, if the storm has occurred during the period August 10-12, the data for the period of August 3-17 is scanned and the highest persisting dew point for each year for each station is determined. From these values, the maximum dew point is selected.
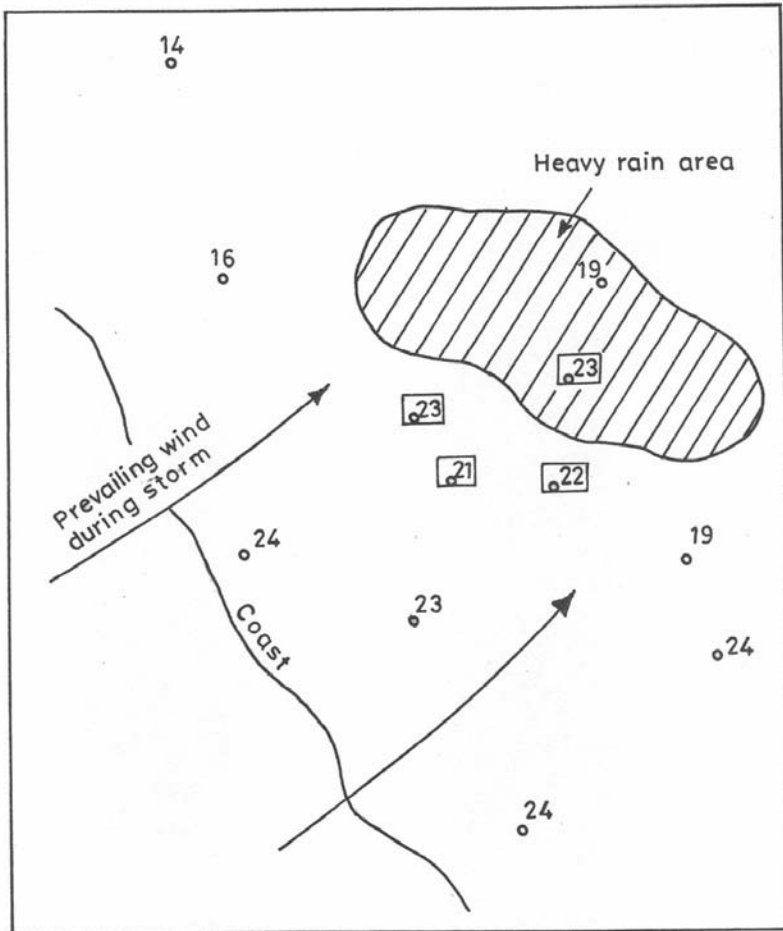
Fig. 10.7. Determination of maximum dew point in a storm.

In some regions where numerous estimates of PMP are made, the maximum dew points for each month of the year are inadequate to estimate the maximum moisture. For these reasons, generalized maps of the highest 24-hour persisting dew points for individual months of the year as well as for the year as a whole are available. Such maps for the Indian region developed by Rakhecha and Kennedy (1985) and Rakhecha et al. (1990) are shown in Figs 10.8 and 10.9. These dew point maps can be used to calculate the maximum moisture content of the atmosphere for any location. Also, these maps will not only provide a ready convenient source of maximum persisting dew point for any area, but will also aid in maintaining consistency between estimates for various parts of the country. Details of the development of these maps and procedures used in obtaining the persisting dew points are given by Rakhecha et al. (1990).
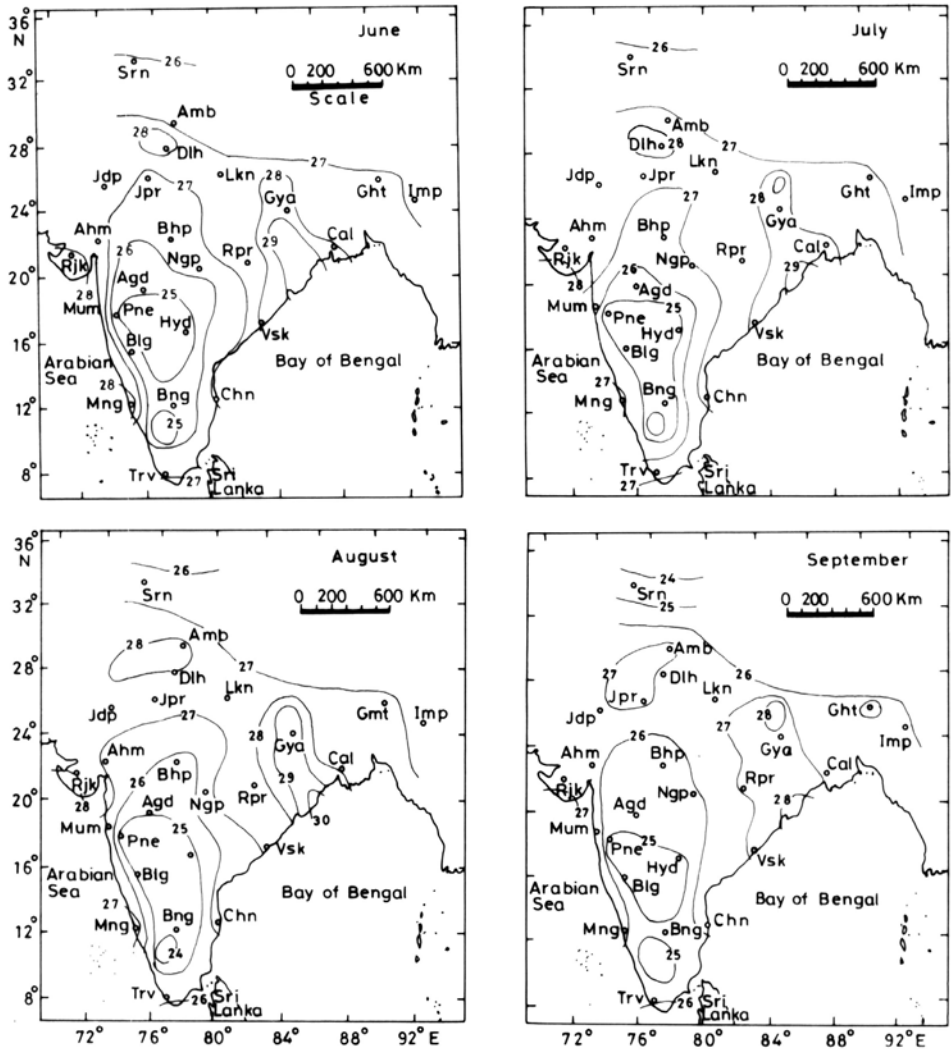
Fig. 10.8. Monthly maximum persisting 24-hour 1000 mb dew point temperature (°C) for June-September months.
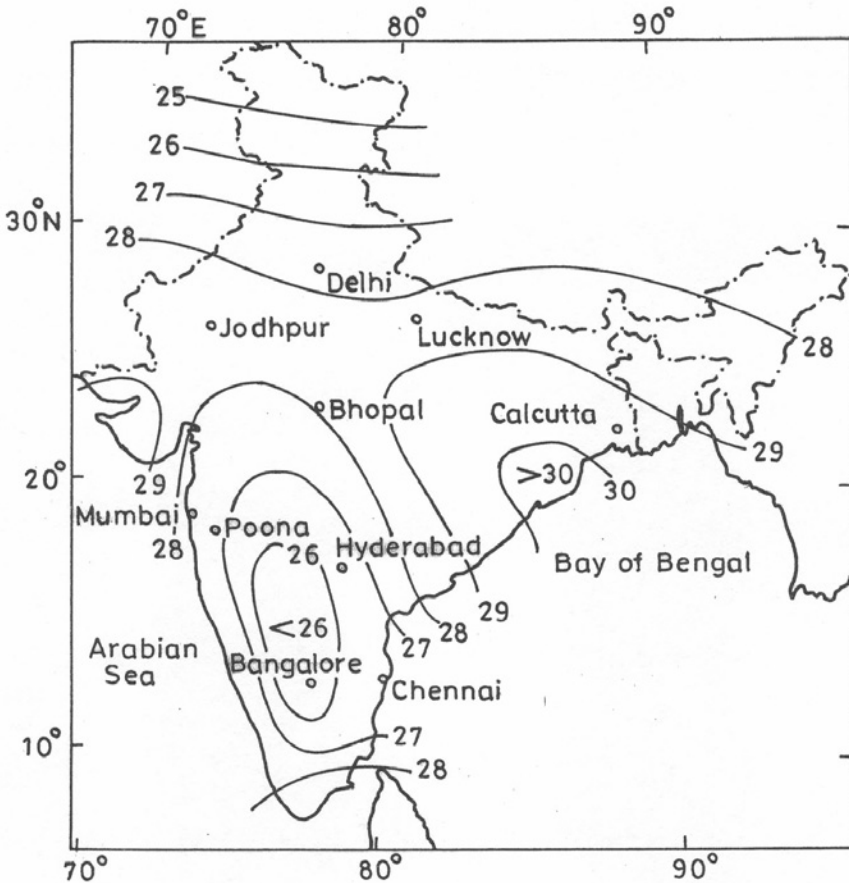
Fig. 10.9. Annual maximum persisting 24-hour
1000 mb dew point temperature (°C).

10.7.3 Statistical Analysis of Extreme Rainfall

A different type of statistical method for estimating PMP for small areas has been developed by Hershfield (1961, 1965), based on a general frequency equation given by Chow (1951). The use of the Hershfield statistical method in the U.S.A. (Myers, 1967), Canada (Bruce and Clark, 1966), and India (Dhar et al., 1981; Rakhecha et al., 1992, 1994) has shown that the PMP estimates obtained by this method are closely comparable to those obtained by the elaborate physical method consisting of moisture maximization and transposition of actual observed storm. However, WMO (1969, 1970, 1986) has suggested this method for estimating PMP for those stations whose daily rainfall data are available for a long period of time but where data for storm maximization are lacking. The statistical formula for estimating the PMP for small areas suggested by Hershfield (1965) is:

$$X_{PMP} = \bar{X}_n + K_m \sigma_n \qquad (10.4)$$

where

$$K_m = \frac{X_1 - \bar{X}_{n-1}}{\sigma_{n-1}} \qquad (10.5)$$

where X_{PMP} is the PMP rainfall for a given station for a specified duration, K_m is the frequency factor, and X_1, $\bar{X}_n$ and σ_n are, respectively, the highest, mean, and standard deviation for a series of n annual maximum rainfall values of a given duration and $\bar{X}_{n-1}$, σ_{n-1} are respectively the mean and standard deviation for this series excluding the highest value from the series. Hershfield (1965) showed that the empirically derived coefficient K_m varies directly with rainfall duration and inversely with the mean of the series.

Estimates of PMP for 1-day duration have been made for several stations in India using the Hershfield statistical method. Rakhecha and Soman (1994) calculated estimates of PMP for a 2-day duration for stations in India using the Hershfield method. Maximum annual 2-day duration data of 80 years from 1901 for about 400 stations were used. Based on these PMP estimates a generalized map showing the spatial distribution of 2-day PMP was prepared (Fig. 10.10). The 2-day PMP over the Indian region varies from 40 to 130 cm.

10.7.4 PMP by Generalized Method

The approach used to estimate PMP has been the physical method, based essentially on limited transposition and maximization. The method is applied on a project by project basis. Such a method can be unreliable if highly efficient rainstorms have not been recorded over the region under study. For this reason, generalized methods have been developed in which the maximum recorded rain depths from a large area are used and adjustment factors are applied for the moisture, distance from the moisture source, topographic effects and intervening mountain barriers when applying the maximum recorded rain depths to the particular area. In the absence of severe storm data in a study of PMP for the Mekong River basin, Southeast Asia, USWB (1970) applied a generalized technique using the U.S. hurricane rainfall data. The current trend in hydrometeorological practice is to develop generalized studies and subsequently use these studies to prepare estimates for individual catchments. No doubt the generalized PMP studies require a considerable investment of time but there are several advantages which are:

(a) Maximum use can be made of all data over a region.
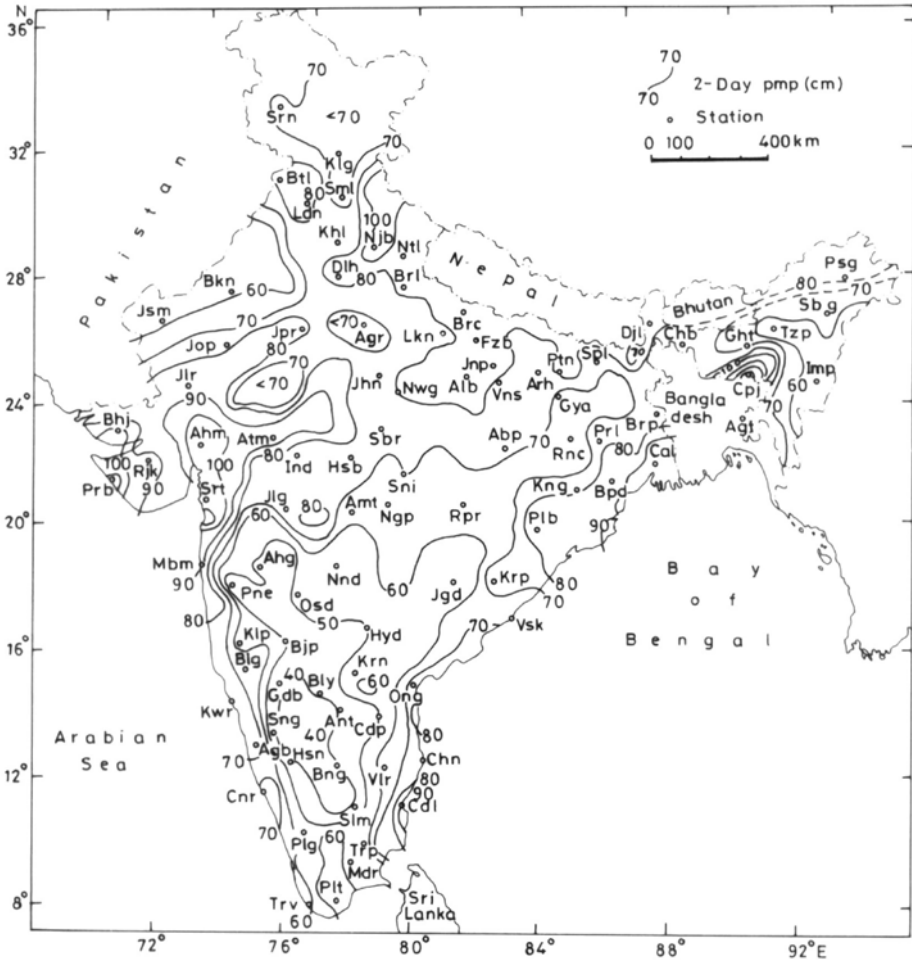(b) Regional durational and areal smoothing is done in a consistent manner for the region.

Fig. 10.10. Generalized map of 2-day PMP (cm) over India.

(c) Amount of subjectivity is reduced.

(d) Uniform practice and consistent rules are maintained.

(e) Once completed, the reliable estimates for individual catchments can be made accurately and easily.

Rakhecha and Kennedy (1985) developed a generalized method to estimate the PMP for the Indian region. This method was further modified by Rakhecha et al. (1995) and applied to the region east of 80° E. The main steps for developing the generalized method consist of:

(i) Determination of the maximum average depths of rainfall for varying area sizes and durations from major rainstorms that have occurred over a large area.

(ii) Moisture maximization of areal rainfall values to an extreme moisture content which is determined from dew point temperature.

(iii) Normalizing the maximized rainfall values for the land close to the sea coast. This is done by applying in reverse the adjustments for the distance of the storm from the coast, topographic effects, and any intervening mountain barrier between rainfall and the moisture source.

(iv) Plotting of the normalized values to obtain a smooth envelop representing the initial PMP values for flat land close to the sea.

These normalized values can be applied to any individual catchment with application of appropriate adjustment factors for deriving reliable PMP estimates.

REFERENCES

Bruce, J.P. and Clark, R.H., 1966. Introduction to Hydrometeorology. Pergamon, New York, 319 pp.

Central Water and Power Commission (CWPC), 1969. Estimation of design flood. Recommended procedures. Govt. of India Publ. New Delhi, 130 pp.

Chow, V.T., 1951. A general formula for hydrologic frequency analysis. *Trans. Am. Geophys Union*, 32, pp. 231–237.

Hershfield, D.M., 1961. Estimating the probable maximum precipitation. *J. Hyd. Div. Am. Soc. of Civil Eng.*, 87, Hy 5, pp. 99–116.

Hershfield, D.M., 1965. Method for estimating probable maximum precipitation. *J. Am. Water Works Assoc.*, 57, pp. 965–972.

Myers, V.A., 1967. Meteorological estimation of extreme precipitation for spillway design floods. U.S. Weather Bureau, WBTM, *Hydro.*, 5, pp. 1-39.

Rakhecha, P.R. and Kennedy, M.R., 1985. A generalized technique for the estimation of probable maximum precipitation in India. *J. Hydrology*, 78, pp. 345-359.

Rakhecha, P.R., Deshpande, N.R. and Nandargi, S.S., 1990. Maximum persisting dew points during the southwest monsoon season over India. *Mausam*, 41, 1, pp. 140–142.

Rakhecha, P.R. and Soman, M.K., 1994. Estimation of Probable maximum precipitation for a 2–day duration: Part 2 – North Indian Region. *Theor. Appl. Climatol.* 49, pp. 77–84.

Rakhecha, P.R., Deshpande, N.R., Kulkarni, A.K., Mandal, B.N. and Sangam, R.B., 1995. Design storm studies for the upper Krishna River catchment upstream of the Almatti Dam site. *Theor. Appl. Climatol.* 52, pp. 219–229.

Reitan, C.H., 1963. Surface dew point and water vapor aloft. *J. Appl. Meteor.* 9, pp. 776–779.

Schreiner, L.C. and Riedel, J.T., 1978. Probable maximum precipitation estimates. United States east of the 105th meridian. Hydrometeorological Report No. 51. National Weather Service. National Oceanic and Atmospheric Administration, US Department of Commerce, Washington, DC. 67 pp.

United States Weather Bureau (USWB), 1960. Generalized estimates of probable maximum precipitation for the United States west of the 105th meridian. USWB Tech. Pap. No. 38, Washington, D.C.

United States Weather Bureau (USWB), 1970. Probable maximum precipitation, Mekong River basin. USWB., Hydrometeorol. Rep. No. 46, Silver Spring Md.

World Meteorological Organization (WMO), 1969. Estimation of maximum floods. Tech. Note. No. 98, WMO, No. 233, TP. 126.

World Meteorological Organization (WMO), 1969. Manual for depth–area duration analysis of storm precipitation. WMO. 237, TP. 129.

World Meteorological Organization (WMO), 1970. Guide to hydrometeorological practices, WMO, No. 168, TP. 82.

World Meteorological Organization (WMO), 1986. Manual for estimation of probable maximum precipitation. WMO operational hydrology report No. 1 WMO No 232. (Second edition).

11 Statistical Analysis of Precipitation

It has been noted in Chapter 10 that an important problem in hydrometeorology is to estimate the frequency of maximum rainfall or design storm rainfall of a specified duration that is likely to occur at a selected station or in a selected river catchment for designing hydraulic structures subject to flooding, such as bridges, culverts and dams. In the same chapter it was also mentioned that the statistical method is one of the four methods for estimating design storms. In this method an estimate of the frequency with which a given magnitude of rainfall may be exceeded in the future is based upon the study of the frequency with which it has been exceeded in the past in a probabilistic sense.

In design problems, extreme values are usually used. This is based on the philosophy that if the designed structure can withstand the highest value in a year, it can withstand all other values. Two types of data are generally selected: (1) the annual extreme value series and (2) the partial duration series. This chapter presents some of the applications of statistical methods by which extreme rainfall data series may be quantified and presented in a standard frequency frame work. Before proceeding with the application of statistical analysis we define some useful terms.

A hydrometeorological variable (X) is one which measures the magnitude of some element of hydrological cycle, say rainfall. The value of X changes with the individual observation. A variable which can theoretically assume any value between two given values is called a continuous variable, otherwise it is called a discrete variable. A 30-year continuous record of rainfall at a place is a sample of the rainfall history at that place. The set of all records of the same station under a fixed set of conditions is called a population. Statistical theory is based on the concept that the sample is assumed to be representative of the population. In order to draw inferences about a population, the data in the sample must be random, independent and homogenous. When every value in the population has an independent chance of being chosen, the sample is called a random sample. A degree of

independence varies with the nature of the data being considered. Successive daily rainfalls or stream flows are not independent because a stream that is high one day will probably be high the next day. Monthly or extreme daily rainfall data are much more independent of each other. Homogenous data belong to the same population. Homogeneity and randomness of data may be tested through the use of statistical tests described later in this chapter.

11.1 DATA SERIES FOR FREQUENCY ANALYSIS

11.1.1 Annual Extreme Value Series

The highest observed value (daily rainfall) at any rainfall station during a year is called the annual extreme value. The annual extreme value series, therefore, consists of only one highest value for each year of record. Thus, for *N* years of data an annual extreme value series will consist of *N* values one for each year.

11.1.2 Partial Duration Series

This is also called partial series. The annual extreme series ignores the second and third highest values of a year which may be higher than many of the extreme annual values of other years in the series. This type of situation is overcome by selecting all the values above an arbitrary threshold value. The series obtained in this manner is known as a partial duration series. Therefore, a partial duration series contains the largest values greater than a base value. The lowest value is generally chosen as a base value in the annual extreme data series. In a complete partial duration series if the lowest values are truncated so that the number of values in the series is equal to the number of years of record then this truncated series is called the annual exceedance series.

Both these types of series or selected data are used in frequency analysis. It is important to mention that if the time interval between the two values is less than a year, the seasonal variation may introduce inhomogeneities in the data series. However, if the data are selected only from a particular season or month, the homogeneity may largely be maintained. Since the partial series is not a true series, the values selected may not be independent of each other and as a result such a series cannot be considered to be completely homogeneous and independent. Nevertheless, the use of both types of the selected data for frequency analysis gives almost similar estimates for frequency of more than 10 years. The difference is significant in the lower frequency estimates. Langbein (1949) studied these two types of selected data series and suggested an empirical relationship between their frequencies based on annual and partial duration floodseries:

$$T_{AM} = \frac{1}{1 - \exp\left(-\dfrac{1}{T_{PD}}\right)}$$

where T_{AM} and T_{PD} are the average recurrence intervals corresponding to a given flood magnitude calculated from an annual series and a partial duration series, respectively. The relationship between the two series is shown in Table 11.1.

Table 11.1: Frequency relationship based on partial duration and extreme annual series

Partial-duration series	Annual series
Frequency (years)	Frequency (years)
0.5	1.16
1.0	1.58
1.45	2.00
1.75	2.33
2.0	2.54
5.0	5.52
10.0	10.5
20.0	20.5
50.0	50.5
100.0	100.5

Table 11.1 shows that for all practical purposes the partial duration series and the annual series do not differ much except in the values of low magnitudes. Estimate of the maximum rainfall of a particular magnitude is provided in terms of what is called as a return period or recurrence interval.

11.2 RECURRENCE INTERVAL

The main objective of frequency analysis of hydrometeorological data is to estimate the recurrence interval or return period (T) of a given magnitude x of a hydrometeorological variable (X), that is, how often does the given magnitude x of the variable occur? The average interval of time within which the value x of variable X will be equaled or exceeded once is called the recurrence interval or return period. The return period is a measure of the probable time interval between the occurrence of a given event and that of an equal or greater event. If the basic data are truly representative, then, for example, a rainfall having a return period of 100 years will be equaled or exceeded, on an average, once in 100 years over a great length of time. Thus, if we have 10,000 years of record, there will be 100 such values.

If a hydrometeorological variable (X) equal to or greater than x occurs on the average once in T years, then the probability of occurrence $P(X \geq x)$ of such a variable is

$$P(X \geq x) = \frac{1}{T} \qquad (11.1)$$

or

$$T = \frac{1}{P(X \geq x)} \qquad (11.2)$$

The probability that x will not occur is

$$P(X \leq x) = 1 - P(X \geq x) \tag{11.3}$$

or $\qquad P(X \leq x) = 1 - \dfrac{1}{T} \tag{11.4a}$

$$T = \frac{1}{1 - P(X \leq x)} \tag{11.4b}$$

The concept of a return period does not imply that an event of a determined value occurs at regular intervals of T years or that having occurred once, it will not occur again for the next T years. It means that when calculated over a long period of record the probable mean interval between two events of the determined magnitude is equal to the return period T. For example, a rainfall value of the 30-year return period over a long period of record of, say 600 years, will occur 20 times or in any one year there is a 3.3 percent chance that a rainfall of this value will occur $P = 1/T = 1/30 = 3.3\%$. Furthermore, it says nothing as to by what amount and how many times can this rainfall value be exceeded during a period of 30 years?

11.3 CALCULATED RISK

If there is a sequence of extreme rainfall values then it is assumed that this sample represents the parent population of extremes of rainfall and can therefore be used to deduce inferences about that population. Suppose a station has a long period of rainfall records which would give a good estimate of the true average return periods of all rainfall values up to the 100-year value. Now we would like to know that in any 30-year sample of rainfall records what the probabilities are that the sample contains one, two, etc., true 30-year return period values. Also, what is the probability of a 30-year sample to have a 100-year return period value? The following equations will give the probability of various combinations of events.

The probability that a value of a variable equal to or greater than x will occur in any year is:

$$P = \frac{1}{T} \tag{11.5}$$

The probability that such an event will not occur in any year is:

$$q = 1 - P = 1 - \frac{1}{T} \tag{11.6}$$

Now the probability that x will not occur for n successive years is:

$$q \times q \times q \times q \ldots q_n = q^n = \left(1 - \frac{1}{T}\right)^n \tag{11.7}$$

The probability R, called risk, that x will occur at least once in n successive years is

$$R = 1 - \left(1 - \frac{1}{T}\right)^n \tag{11.8}$$

Equation (11.8) can be used to calculate the probability that a value of the variable equal to or greater than x will occur within its return period as:

$$P_T = 1 - \left(1 - \frac{1}{T}\right)^T \tag{11.9}$$

The term $\left(1 - \frac{1}{T}\right)^T$ equals e^{-1} in the limit when T becomes larger. Thus, for large values of the return period, $P_T = 0.632$. Table 11.2 gives some values of P_T as a function of T.

It is seen that if a hydraulic structure is designed for a design storm of 30-year return period, then there is a 64% chance that a design storm equaling or exceeding the 30-year return period occurs before the end of the first 30-years. Also, by substituting $T = 100$ and $n = 30$ in equation (11.8) it is found that there would be a 26% probability that a 30-year sample may contain a design storm of 100 years.

Table 11.2: Probability P_T that an event with a return period T will occur within the next T years

T	P_T	T	P_T
2	0.7500	50	0.6358
5	0.6723	100	0.6340
10	0.6513	200	0.6330
20	0.6415	500	0.6325
30	0.6380	1000	0.6323
40	0.6369	Infinite	0.6321

For design purposes, it seems more practical to specify at the beginning the admissible probability $R\%$, in other words, the allowable risk for the undesirable event (here the occurrence of a design storm equal to or greater than a certain limit QL) to occur during the minimum life period n assigned to the structure, and to compute, consequently, the corresponding return period T. The probability R (called risk) of the design storm rainfall having a given return period occurring at least once in n successive year is

$$R = 1 - \left(1 - \frac{1}{T}\right)^n \tag{11.10}$$

Table 11.3 gives the value of the calculated return period for various values of risk R from 1 to 75% and of the nominated life between 2 and 100

years. It is seen that if a dam is to be built for a nominal life span of 25 years, and the designer takes a risk of 10% of the structure being overtopped by a flood during this 25-year period, its spillway should be designed for a design storm of 238-year return period.

Table 11.3: Return periods associated with various degrees of risk and expected design life

Risk (%)	Expected Design Life (years)							
	2	5	10	15	20	25	50	100
75	2.0	4.02	6.69	11.0	14.9	18.0	35.6	72.7
50	3.43	7.74	14.9	22.1	29.4	36.6	72.6	144.8
40	4.44	10.3	20.1	29.9	39.7	49.5	98.4	196.3
30	6.12	14.5	28.5	42.6	56.5	70.6	140.7	281
25	7.46	17.9	35.3	52.6	70.0	87.4	174.3	348
20	9.47	22.9	45.3	67.7	90.1	112.5	224.6	449
15	12.8	31.3	62.0	90.8	123.6	154.3	308	616
10	19.5	48.1	95.4	142.9	190.3	238	475	950
5	39.5	98.0	195.5	292.9	390	488	976	1949
2	99.5	248	496	743	990	1238	2475	4950
1	198.4	498	996	1492	1992	2488	4975	9953

Example 11.1: What return period must a design engineer use in his design of a highway bridge if he is willing to accept only a 10% risk that flooding will not damage it in the next five years?

Solution: $R = 1 - \left(1 - \dfrac{1}{T}\right)^n$. We have $R = 10\%$, and $n = 5$ years. Then

$$10 = 1 - \left(1 - \frac{1}{T}\right)^5 = 48.1 \text{ years (see Table 11.3)}$$

Example 11.2: If an event has a probability of 1/5 or a return period of five years then what is the probability that it will occur at least once in the next three years.

Solution: The probability P that an event will occur at least once in n years is

$$P = 1 - \left(1 - \frac{1}{T}\right)^n$$

Here $T = 5$, $n = 3$

$$P = 1 - \left(1 - \frac{1}{5}\right)^3 = 0.488 = 48.8\%$$

The chances are about one out of two that the 5-year return period value will be exceeded once in the next three years.

Example 11.3: If an event has a return period of 10 years then what is the probability that it will occur in the next 10 years?

Solution: The probability P that an event will occur at least once in n years is

$$P = 1 - \left(1 - \frac{1}{T}\right)^n$$

Here $T = 10$, $n = 10$

$$P = 1 - \left(1 - \frac{1}{10}\right)^{10}$$

$$= 0.6513 \text{ (see Table 11.2)}$$

11.4 FREQUENCY ANALYSIS

The collection of data observed in time relating to any hydrometeorological variable is called a data series. For example, all the rainfall (variable) measurements recorded at a station over many years form a data series. When such a data series of any variable is collected or available, there usually arises a need to reduce the large amount of data to a manageable size so that an overview can be obtained of the variable under study. In order to sum up the information contained in the data series, mathematical statistics is employed in hydrometeorology. Before treating the data series for statistical analysis, it is useful to understand concepts of population, sample and statistical variable.

In statistics, a finite or an infinite collection of observations on some variable is called a population. The event constitutes a statistical variable and is generally denoted by a capital letter X and a specified observation value of the population by a small letter x. A subpopulation drawn from a larger population constitutes a sample. The number of observations in a sample is the sample size of the variable. The procedure of extracting a sample from a population is called the sampling technique. The concept of a sample is important in statistics, because it is rather uneconomical to consider the entire population to get any information about it. For example, it would be impossible to check every drop of water in a city water supply for purity. A variable can be either a discrete variable or a continuous variable.

A discrete variable is that whose individual values are real numbers whereas a continuous variable is that which takes on every value between certain limits, say a and b. For example, let $x_1, x_2, x_3..., x_{100}$ be a finite set of 100-year values of a statistical variable X. The set of all the 100-year values is often considered in practice a population of 100 values and the set

of values for the first ten years is a sample of this population having a size of 10 years. If we characterize the variable as annual extreme rainfall then the values x_1, x_2, x_3,…, x_{100} make up a statistical series of annual extreme rainfall. Important features of the data series can be better viewed in the form of frequency distribution as well as by preparing frequency diagrams.

11.4.1 Frequency Distribution

It is one of the ways to reduce the large amount of data by grouping the values in a number of equal class intervals (intervals of similar values). There is no set rule governing the width of the class interval but the number of classes should not be more than five times the logarithm of the number of observations. We can then list each class interval in a row and find the number of observations whose values lie within that class interval. This number is the frequency with which observations in that class occur. The table bringing together all the classes and their respective frequencies gives the frequency distribution of the statistical variable. The frequency distribution of the annual average rainfall for the Krishna River catchment up to the Almatti dam site in India for an 85-year period is given in Table 11.4

Table 11.4: Frequency distribution of annual rainfall for the Krishna River catchment up to Almatti dam site

Class intervals (cm)	Frequency	Relative frequency (%)	Cumulative frequency	Cumulative relative frequency
61–70	1	1	1	1
71–80	4	5	5	6
81–90	4	5	9	11
91–100	15	18	24	28
101–110	18	21	42	49
111–120	18	21	60	71
121–130	16	19	76	89
131–140	2	2	78	92
141–150	4	5	82	96
151–160	2	2	84	99
161–170	1	1	85	100
Total	85	100		

By giving each class a width of 10 years, the length of yearly rainfall data has been condensed from a series of 85 to a frequency distribution of 11 rows.

Sometimes, instead of the actual number of values for each class interval, it is better to give the percentage of the total number of values in each interval. When the total number of observations is large, percentages are more meaningful than actual numbers. These percentages are called relative frequencies. Also, it may be quite useful to present the data as a cumulative

frequency distribution. The cumulative frequency for a given class is the sum of the frequencies of all classes up to and including the frequency in the given class. Table 11.4 gives the absolute frequency, the relative frequency (percentage of observations) and the corresponding cumulative frequency of the average annual rainfall for the Krishna River catchment.

11.4.2 Frequency Diagrams

There are several types of frequency diagrams that are used for graphical representation of statistical data. The most common in use are: (1) histogram, (2) frequency polygon, (3) frequency curve, and (4) cumulative frequency or Ogive. These diagrams show frequencies with which different values occur. These frequency diagrams are prepared as follows:

 (a) A horizontal axis is labeled with the name of the variable and the possible values of the variable with suitable scale are marked along this axis.
 (b) The number of observations (frequency) is labeled on a vertical axis and the frequency values are marked along this axis.

11.4.3 Histogram

Histograms are the most commonly used diagrams to depict the group frequency distribution of both continuous and discontinuous variables. A histogram consists of a series of continuous vertical rectangles (i.e., a set of vertical bars drawn side by side). The width of each rectangle represents the width of a class interval and the height of each rectangle bar represents the frequency with which observations occur in that interval. The area of a rectangle is proportional to the frequency of the corresponding class and the total area under the histogram is proportional to the total frequency of all the classes. It may be mentioned that when all the classes are not of equal width, the height of the rectangles are taken equal to the corresponding class frequencies. But when all the classes are not of equal width, the height of a rectangle is taken equal to the frequency density of the corresponding class interval, where

$$\text{Frequency density} = \frac{\text{class frequency}}{\text{width of class interval}}$$

Figure 11.1 shows the histogram for the annual rainfall values given in Table 11.4.

11.4.4 Frequency Polygon

In the case of ungrouped frequency distribution of a discrete variable the values of the variable versus their frequency are plotted on the horizontal
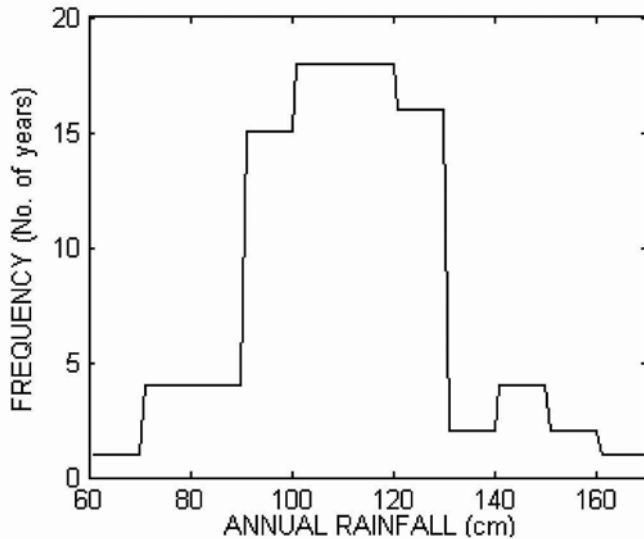
Fig. 11.1. Histogram of annual rainfall.

and vertical axes, respectively, on a graph paper by using suitable scales. The points so plotted are then joined by straight lines. The frequency polygon is completed by joining the extremities of the figure so obtained to the two points on the horizontal axis corresponding to the values before the first and after the last tabulated values each of them having zero frequency. The polygon so constructed is called a frequency polygon.

In the case of a grouped frequency distribution, a frequency polygon is a line chart of class frequencies plotted against mid values of the corresponding class intervals. When all the classes have a common width, it is usually constructed from the histogram of the grouped frequency distribution by joining the mid points of the tops of the consecutive rectangles. The two end points of the polygon are joined to the next lower and higher class mid points each having zero frequency.

11.4.5 Frequency Curve

If the class intervals of a frequency distribution are made smaller so that the number of classes becomes larger then in the limiting case, when the class intervals are indefinitely small and the number of classes indefinitely large, the histogram and frequency polygon take on the shape of a smooth curve called frequency curve. This curve indicates the shape of the frequency distribution which may be symmetrical or asymmetrical or J shaped or U shaped. Figure 11.2 shows the frequency curve of annual rainfall for the Krishna River catchment.
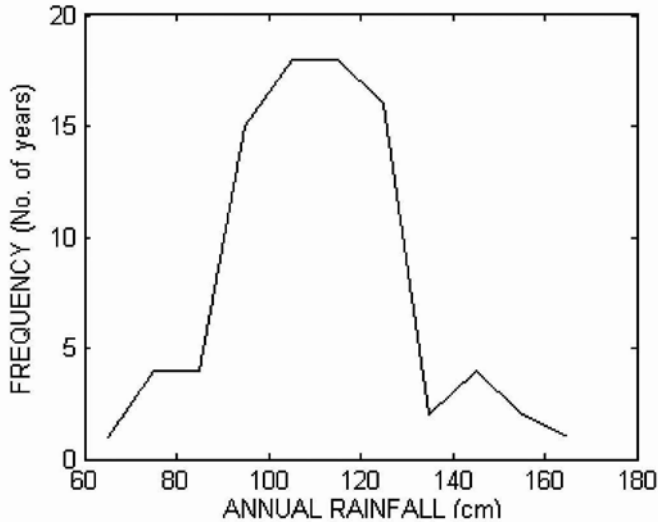
Fig. 11.2. Frequency curve of annual rainfall.

11.4.6 Cumulative Frequency or Ogive

Another convenient form of the frequency diagram is the cumulative curve or "ogive." In this diagram, cumulative frequencies are plotted corresponding to their class boundary values. These points are then joined by straight lines giving the cumulative frequency distribution diagram. There are two types of cumulative frequency diagrams: (a) The curve showing the cumulated frequency of more than any value, and (b) the curve showing the cumulative frequency of less than any value.

Example 11.4: The following table gives the frequency distribution of annual rainfall (cm) of a station for 100 years.

Rainfall	Number of years
20-29	8
30-39	10
40-49	25
50-59	31
60-69	11
70-79	12
80-89	2
90-99	1

Draw the cumulative frequency curves both for less than and more than types from the given data.

Solution: A cumulative frequency distribution of both less than and more than from the given data is first constructed.

Class boundary rainfall	Less than	More than
20	0	100
29	8	92
39	18	82
49	43	57
59	74	26
69	85	15
79	97	3
89	99	1
99	100	0

A graph of this table can be plotted. For this purpose, rainfall is placed along the horizontal axis and number of years from 0 to 100 along its vertical axis. The cumulative frequencies both less than and more than are plotted corresponding to the class boundaries of rainfall. These points are then joined by straight lines, giving the cumulative frequency diagram shown in Fig. 11.3.
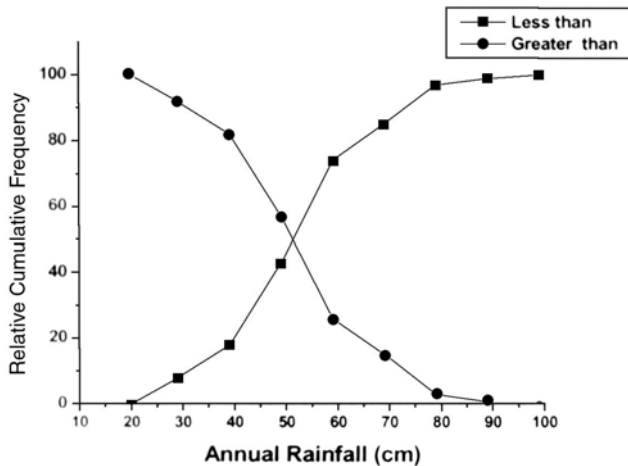

Fig. 11.3. Cumulative frequency curve of annual rainfall.

11.5 MEASURES OF CENTRAL TENDENCY

The main purpose of statistical analysis is to sum up the information contained in a series of observations. The statistical parameters for this purpose are the central or dominant value of the series, the dispersion (fluctuation) of various values of the series about the central value, and the shape of the statistical frequency curves. The purpose of the central value is to characterize the series as a whole by a single number which can represent, as a rough

approximation, the order of magnitude of the values as a whole and also provide a comparison between two different series. The central value or a dominant value of a statistical distribution is expressed by the arithmetic mean, the median, and the mode or modal value.

11.5.1 Arithmetic Mean ($\bar{x}$)

Let x cm be the rainfall of a station in a particular year. Then, in general X (rainfall) will be a variable whose values change with year. It may be possible that N values of x will not all be different. Suppose there are only n different values $x_1, x_2, x_3..., x_n$ which occur, respectively, $f_1, f_2,..., f_n$ times. These f_1, $f_2,..., f_n$ are called the frequencies of the values x_i of the variable X so that

$$N = f_1 + f_2 + f_3 +...f_n$$

The number N is the total frequency. The mean of the distribution is the arithmetic mean $\bar{x}$ of the N values of the variable and is therefore given by

$$\bar{x} = \frac{1}{N}\sum [f_1 x_1 + f_2 x_2 +.................. + f_n x_n] = \frac{1}{N}\sum_{i=l}^{n} f_i x_i \qquad (11.11)$$

11.5.2 Median

The middle value of the variable X, which divides the frequencies in the distribution into two equal parts, is called median. To find median the N values of the variable in the distribution have to be arranged in ascending or descending order of magnitude. Then the median is the middle value, if N is odd; while if N is even, it is the arithmetic mean of the middle pair.

11.5.3 Mode

The value of the variable whose frequency is a maximum in a distribution is called a mode or modal value of the distribution. When, as usually happens, there is only one mode, the distribution is said to be unimodal.

The arithmetic mean is the value most frequently used as the central value. However, for the annual maximum series, where the values are very asymmetrically distributed, median is more representative as it shows that one half of the values of the series are above and the other half are below the median.

11.6 MEASURES OF VARIABILITY

The statistical parameters that measure the variability or dispersion of individual observations are the mean deviation, the standard deviation, the variance, the range and the coefficient of variation.

11.6.1 MEAN DEVIATION FROM THE MEAN

The arithmetic mean value of the absolute deviations from the mean of the distribution is called the mean deviation from the mean. Thus,

$$\text{Mean deviation} = \frac{1}{N} \sum | x_i - \bar{x} | \qquad (11.12)$$

11.6.2 Variance and Standard Deviation

The average of the squared deviations of each of the terms of the series from the mean ($\bar{x}$) is called the variance of X and is denoted by μ_2 or σ^2. Thus,

$$\mu_2 = \sigma^2 = \frac{1}{N} \sum_{i=1}^{n} f_i (x_i - \bar{x})^2 \qquad (11.13)$$

The positive square root of the variance is called standard deviation (*SD*) of X and is denoted by σ. The variance or *SD* may be taken as an indication of the extent to which the values of X are scattered. This scattering is called dispersion. When the values of X cluster closely round the mean, the dispersion is small. When those values, whose deviations from the mean are large, also have relatively large frequencies, the dispersion is large. The variance and *SD* play a prominent part in the study of hydrometeorological variables, particularly rainfall.

11.6.3 Range

The difference between the largest and the smallest values of the distribution is called the range. Thus,

$$\text{Range} = x_{max} - x_{min} \qquad (11.14)$$

11.6.4 Coefficient of Variation

The ratio of the standard deviation to the mean value of the variable is called the coefficient of variation. It is an absolute measure of dispersion in the sense that it is independent of the unit employed. By means of this coefficient we are able to compare the variabilities of distributions of different characteristics, such as rainfall and discharge. Thus,

$$\text{Coefficient of variation} = \frac{\sigma}{\bar{x}} \qquad (11.15)$$

Example 11.5: The daily rainfall (cm) values produced by a cyclonic storm at a station during a period 1 to 7 days were 14, 24, 20, 36, 15, 21, and 10 cm, respectively. Determine (a) the mean rainfall, (b) the range, (c) the standard deviation, and (d) coefficient of variability of rainfall.

Solution:

Daily rainfall (x)	14	24	20	36	15	21	10	$\sum x = 140$
Deviation $(x - \bar{x})$		−6	4	0	16	−5	1	−10	$\sum (x - \bar{x}) = 0$
Squared deviation $(x - \bar{x})^2$		36	16	0	256	25	1	100	$\sum (x - \bar{x})^2 = 434, n = 7$

(i) $\bar{x} = \dfrac{\sum x}{n} = \dfrac{140}{7} = 20$ cm = mean rainfall

(ii) Range: $36 - 10 = 26$ cm

(iii) $\sigma = $ standard deviation $= \sqrt{\dfrac{\sum (x - x)^2}{n}} = \sqrt{\dfrac{434}{7}} = \sqrt{62} = 7.87$

(iv) Coefficient of variability $= \dfrac{\sigma}{\bar{x}} = \dfrac{7.87}{20} \times 100 = 39.0\%$

The rainfall of seven days varied by an average of 7.8 cm from the mean of 20.0 cm.

Example 11.6: For the distribution expressed by

$x =$	5	6	7	8	9	10	11	12	13	14	15
$f =$	18	25	34	47	68	90	80	62	38	27	11

the total frequency is 500. Show that the mean value of x is 10.1, the variance 5.58, SD 2.36, and the median 10.

Solution:

Calculations for Mean, Variance and Standard deviation

x	f	fx	$(x - \bar{x})$	$f(x - \bar{x})^2$	Cumulative frequency
5	18	90	−5.1	468.2	18
6	25	150	−4.1	420.3	43
7	34	238	−3.1	326.7	77
8	47	376	−2.1	207.3	124
9	68	612	−1.1	92.3	192
10	90	900	−0.1	0.9	282
11	80	880	0.9	64.8	362
12	62	744	1.9	223.8	424
13	38	494	2.9	319.6	462
14	27	378	3.9	411.7	489
15	11	165	4.9	264.1	500
	500	5027		2788.7	

$$\text{Mean} = \frac{1}{N}\sum f_i x_i$$

$$N = 500$$

$$\sum f_i x_i = 5027$$

$$\text{Mean} = \frac{5027}{500} = 10.1$$

$$\text{Variance } (\sigma^2) = \frac{1}{N}\sum_i f_i (x_i - \bar{x})^2$$

$$= \frac{1}{500} \times 2788.7$$

$$\sigma^2 = 5.58$$
$$\sigma = 2.36$$

The value of x corresponding to the cumulative frequency $\frac{N+1}{2}$ is the median.

Here $\frac{N+1}{2} = \frac{500+1}{2} = 250.5$

Median is the arithmetic mean of the 250th and 251st values. From the last column we see that 250th and 251st values are equal to 10.

$$\text{Median} = 10$$

11.7 MEASURES OF SKEWNESS

Frequency curves can be classified broadly as either symmetric or asymmetric (skewed). The frequency distribution of a variable is said to be symmetric when frequencies are symmetrically distributed about the mean, that is, when values equidistant from the mean have equal frequencies. The shape of frequency curves is very much affected by a few unusually high or low values. For example, the following distribution is symmetrical about its mean $\bar{x} = 4$.

$x =$	0	1	2	3	4	5	6	7	8
$f =$	1	8	28	56	70	56	28	8	1

The bell shaped frequency distribution is a special form of symmetric distribution called the normal distribution as shown in Fig. 11.4.
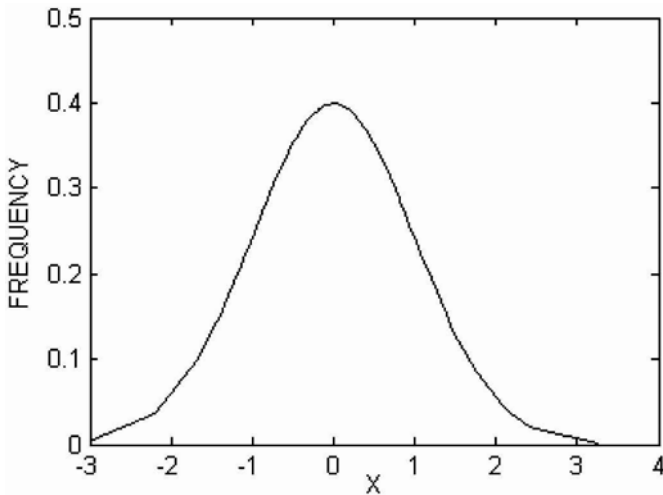
Fig. 11.4. Symmetric distribution.

In the case of an asymmetric distribution, the degree of departure from symmetry is called its skewness. If the shape of the distribution is such that the longer tail extends to the right, then the distribution is said to be skewed to the right or positively skewed (Fig. 11.5). A distribution skewed to the right contains a larger frequency of relatively low values and a few extremely high values. In such a distribution the modal value is generally smaller than the median value which in turn is smaller than the mean value. The distribution is skewed to the left when the longer tail extends to the left and is said to be negatively skewed (Fig. 11.6). A distribution skewed to the left contains larger frequencies of relatively high values and a few extremely low values.
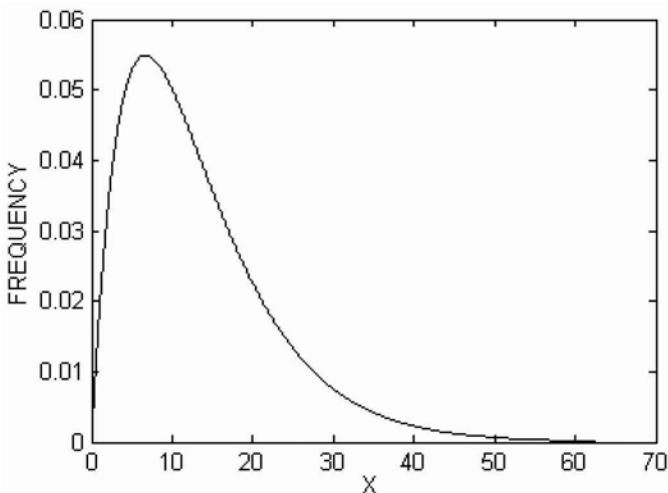

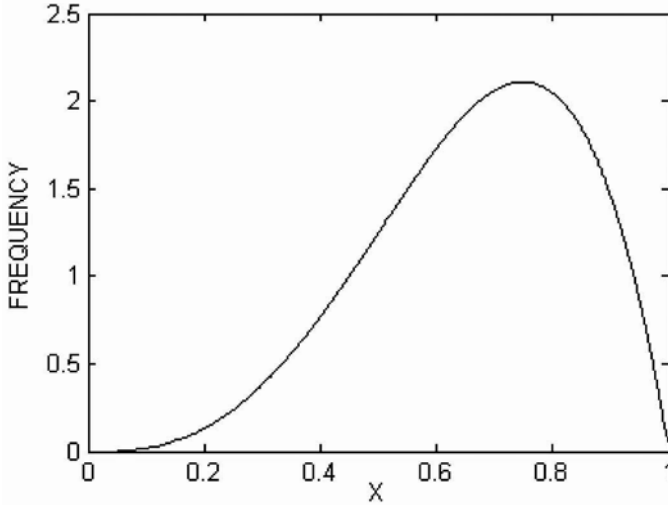**Fig. 11.5.** Asymmetric distribution skewed to the right.

Fig. 11.6. Asymmetric distribution skewed to the left.

The lack of symmetry of a distribution is indicated by the mean of the cubes of the deviation of the variable X from mean and is denoted as μ_3:

$$\mu_3 = \frac{\sum_{i=1}^{N}(x_i - \bar{x})^3}{N} \tag{11.16}$$

This quantity, when divided by the cube of the standard deviation, is a dimensionless number and is used as a measure of skewness denoted by γ_1

$$\gamma_1 = \frac{\mu_3}{\sigma^3} = \frac{1}{N} \frac{\sum_{i=1}^{N}(x_i - \bar{x})^3}{\sigma^3} \tag{11.17a}$$

For $\gamma_1 = 0$ the distribution is symmetrical; for $\gamma_1 > 0$ the distribution is skewed to the right; and for $\gamma_1 < 0$ the distribution is skewed to the left.

Another measure of skewness, proposed by Karl Pearson, is given as

$$\text{Skewness} = \frac{\text{mean} - \text{mode}}{\text{standard deviation}} \tag{11.17b}$$

When the mode can be accurately determined this coefficient is convenient to use.

11.8 MEASURE OF KURTOSIS (FLATTENING)

This is a measure of deviation from a normal distribution. A symmetrical distribution, while retaining its symmetry, may be distorted from the normal form by having a disproportionately large or small number of values in the intermediate range between the mean and the extreme values. This distortion

is known as kurtosis. It is indicated by the mean of the fourth power of the deviations of the variable X from the mean and is denoted as μ_4:

$$\mu_4 = \frac{\sum\limits_{i=1}^{N}(x_i - \bar{x})^4}{N} \tag{11.18}$$

This quantity, when divided by the fourth power of the standard deviation, is a dimensionless number and is used as a measure of kurtosis denoted by γ_2:

$$\gamma_2 = \frac{\mu_4}{\sigma^4} - 3 = \frac{1}{N}\frac{\sum\limits_{i=1}^{N}(x_i - \bar{x})^4}{\sigma^4} - 3 \tag{11.19}$$

Constant 3 is introduced in equation (11.19) so that γ_2 will be zero for a normal distribution. Based on the value of γ_2 three types of flattening shown in Fig. 11.7 are: For $\gamma_2 = 0$, the flattening is near to that of the normal curve; for $\gamma_2 < 0$, the distribution is platicurtic curve; and for $\gamma_2 > 0$, the distribution is a leptocurtic curve.
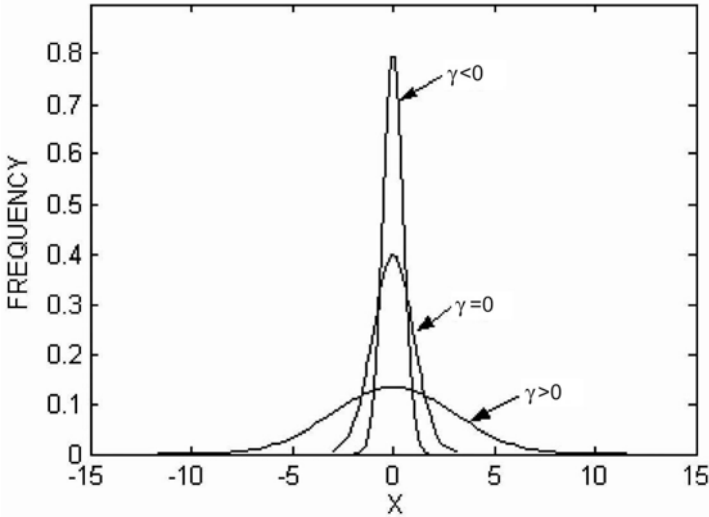

Fig. 11.7. Three types of flattening.

11.9 MOMENTS OF FREQUENCY DISTRIBUTION

The foregoing discussion shows that several statistical parameters are derived from the powers of the deviations of the individual values from the mean value. Similarly, the rth power of the deviation of the variable from the mean value is given as

$$\mu_r = \frac{1}{N}\sum\limits_{i=1}^{N}f_i(x_i - \bar{x})^r \tag{11.20}$$

This is usually called the rth moment of the distribution denoted by μ_r.

Obviously, it can be seen that mean is the first moment about the origin, variance is the second moment about the mean, skewness is the third moment about the mean divided by the cube of standard deviation. Moments of higher orders are not generally used.

11.10 STANDARD FREQUENCY DISTRIBUTIONS

Various theoretical and empirical frequency distributions have been applied to hydrometeorological and hydrologic series. The most useful and widely used amongst these include: (1) rectangular distribution, (2) binomial distribution, (3) Poisson distribution, (4) normal distribution, (5) gamma distribution, (6) Pearson distributions, (7) log-normal distribution, and (8) extreme value distributions.

11.10.1 Rectangular Distribution

Let a hydrometeorological variable X take on values x_1, x_2, x_3...x_i..., x_n with relative frequencies or probabilities of p_1, p_2, p_3..., p_i..., p_n (Table 11.2). If all the values x_1, x_2..., x_n occur with equal probabilities over the range from a to b then such a distribution is called a rectangular or a uniform height distribution (see Fig. 11.8). It is expressed as

$$p(x) = \frac{1}{(b-a)}, \qquad a \leq x \leq b \qquad (11.21)$$

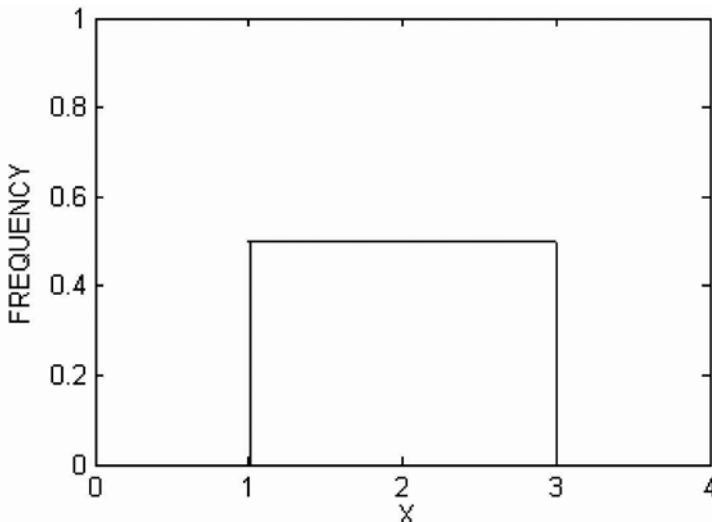The mean of the distribution is $(b + a)/2$ and the variance is $(b - a)^2/12$.

Fig. 11.8. Rectangular distribution.

11.10.2 Binomial Distribution

The binomial distribution is concerned with probabilities of occurrence or non-occurrence of an event (say, the occurrence or non-occurrence of rain, thunderstorm, etc.). It is a distribution of discrete values as shown in Fig. 11.9. In this distribution, the probability $P(x)$ or the relative frequency of x occurrences in a sample of n independent trials is given as

$$P(x) = \binom{n}{x} p^x q^{n-x} \tag{11.22}$$

where p is the probability of occurrence of an event x, and q is the probability of non-occurrence. Thus, $p + q = 1$. The mean, variance and skewness of the binomial distribution are expressed as:

$$\text{Mean} = np$$
$$\text{Variance} = npq$$
$$\text{Skewness} = (q - p)/\sqrt{npq}$$
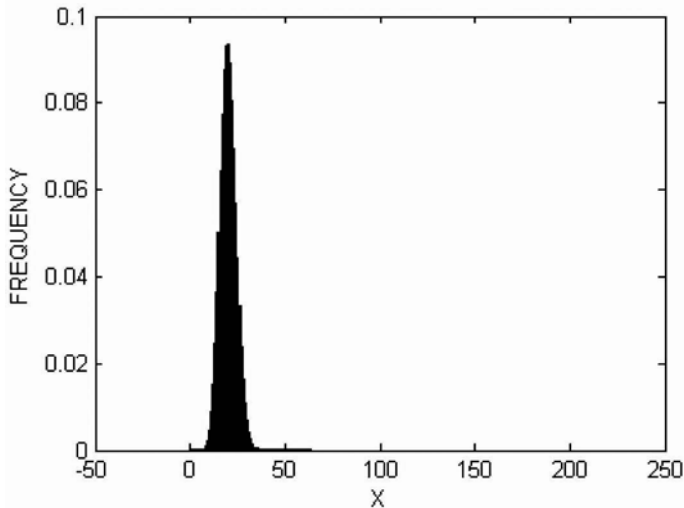
When $p = q$, the distribution is symmetrical.

Fig. 11.9. Binomial distribution.

Example 11.7: What is the probability that a 5-year design rainfall will occur three times in a 10-year period?

Solution: $T = 5$ years, $p = \dfrac{1}{5}$, $n = 10$, $x = 3$. The probability (P) of exactly x successes in n trials is:

$$P(x) = \binom{n}{x} p^x q^{n-x}$$

$$P(x=3) = \binom{10}{3}\left(\frac{1}{5}\right)^3\left(\frac{4}{5}\right)^7 = \frac{10\times9\times8}{3\times2\times1}\times(0.2)^3(0.8)^7 = 0.20$$

11.10.3 Poisson Distribution

This is also a distribution of discrete values, credited to Poisson. When the probability of occurrence in a trial is very small and the sample size is very large then the probability $P(x)$ of x occurrences in an infinite series of trials is given by

$$P(x) = \frac{m^x e^{-m}}{\lfloor x}$$
(11.23)

The mean of the Poisson distribution is m and the variance is m. This distribution is most useful for representing the frequency distribution of rare events as shown in Fig. 11.10.
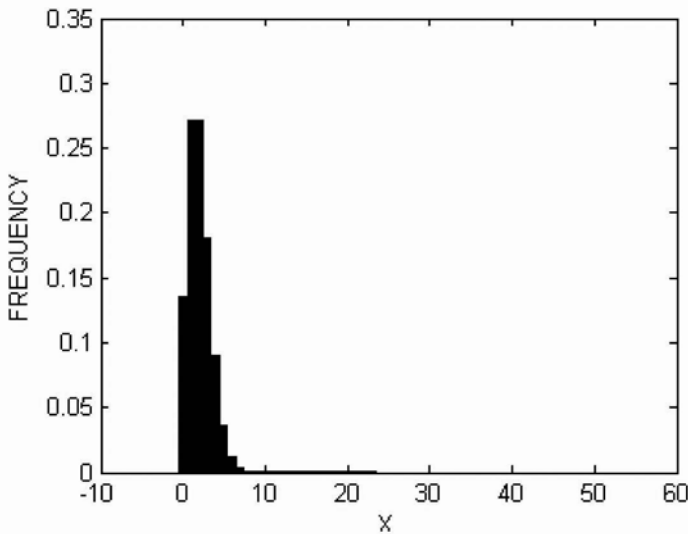

Fig. 11.10. Poisson distribution.

11.10.4 Normal Distribution

The binomial and Poisson distributions are distributions of discrete values. The normal distribution is a distribution of continuous variable. The probability density function of a normally distributed continuous variable X is given as

$$P(x) = \frac{1}{\sigma\sqrt{2\pi}} e^{\frac{-(x-\bar{x})^2}{2\sigma^2}}$$
(11.24)

The mean of the normal distribution is $\bar{x}$ and the variance is σ^2. If a continuous variable, X, with the range from $-\infty$ to ∞, is normally distributed with mean zero and SD, σ, then the probability density function is given by

$$P(x) = \frac{1}{\sigma\sqrt{2\pi}} e^{\frac{-x^2}{2\sigma^2}} \qquad (11.25)$$

The shape of the probability curve is symmetrical about the line $x = 0$, through the mean of the distribution.

The probability corresponding to any interval in the range of the variable is represented by the area under the curve given by equation (11.24) within that interval. In particular, the probability for the interval from the mean (zero) to the value x is given by the integral

$$P(x) = \frac{1}{\sigma\sqrt{2\pi}} \int_0^x e^{-\frac{x^2}{2\sigma^2}} dx \qquad (11.26)$$

This probability is therefore a function of $\frac{x}{\sigma}$. The values of the integral are given for different values of x/σ at intervals of 0.1 in any statistical textbook. The distribution is useful for estimating probabilities of excess or deficit rainfall. Figure 11.11 shows the standard normal distribution.
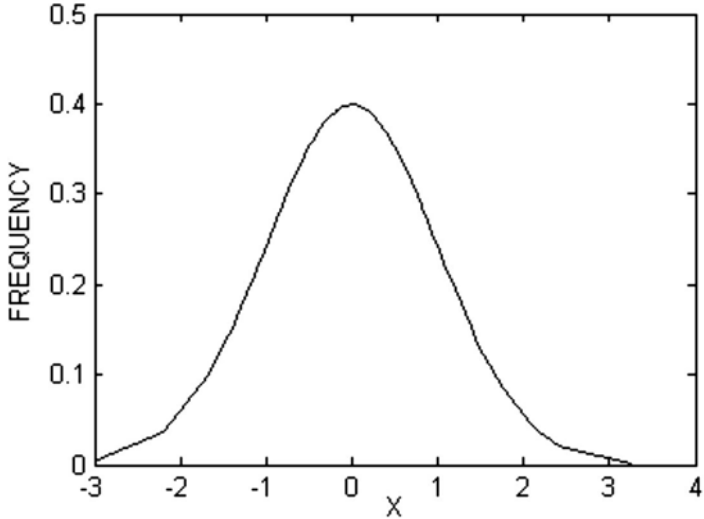

Fig. 11.11. Standard normal distribution.

11.10.5 Gamma (and Pearson Type III) Distribution

The integral

$$\Gamma(n) = \int_0^\infty e^{-x} x^{n-1} dx$$

converges if n is positive. It is a function of n called the gamma function. A continuous variable X which is distributed with the probability density

$$P(x) = \frac{1}{\beta\Gamma(\alpha)}\left(\frac{x}{\beta}\right)^{\alpha-1} e^{-x/\beta} \tag{11.27}$$

throughout the range 0 to ∞ is called a gamma distribution.

The mean of the gamma distribution is $\alpha\beta$ and variance $\alpha\beta^2$. The gamma distribution is widely used in hydrometeorological studies because it is easy to evaluate the gamma function. In greater use is a general case of gamma, called the Pearson Type III distribution where $Y=X-a$, and a is a parameter (or lower bound of X). This distribution has been widely adopted as the standard method for flood frequency analysis in a form known as the log-Pearson III distribution in which the transform $Y = \log(X - a)$ is used to reduce skewness. Although all three moments are required to fit the distribution, it is extremely flexible in that a zero will reduce the log-Pearson III distribution to a log-normal distribution and the Pearson Type III distribution to a normal distribution. Figure 11.12 shows the gamma distribution.
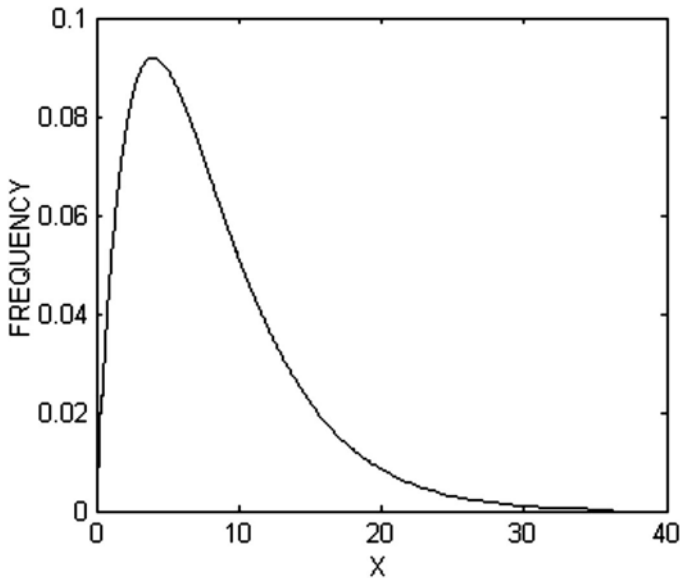

Fig. 11.12. Gamma distribution.

11.10.6 Extreme Value Distribution

The theory of extreme values considers the distribution of the largest (or smallest) values occurring in each group of repeated samples. According to the theory, the distribution of N largest (or smallest) values, each of which

is selected as one of m values, contained in each of N samples, asymptotically approaches a limiting form as m increases indefinitely. Gumbel (1958) was the first to employ the extreme value theory for analysis of flood frequencies. According to Gumbel (1958), the cumulative probability that any extreme value of a variable X will be equal to or less than the given value x approaches the double exponential function:

$$P(X \leq x) = \exp\left[-\exp\{-\alpha(x-u)\}\right] \tag{11.28}$$

The return period T of an extreme value equal to greater than x is given as

$$\frac{1}{T} = 1 - P(X \leq x) = 1 - \exp\left[-\exp\{-\alpha(x-u)\}\right]$$

or

$$x = u - \frac{1}{\alpha}\ln\left[\ln\frac{T}{T-1}\right] \tag{11.29}$$

Parameters α and u are given functions of the mean ($\bar{x}$) and SD (σ) of the extreme values as:

$$\frac{1}{\alpha} = \frac{\sqrt{6}}{\pi}\sigma$$

and

$$u = \bar{x} - \frac{c}{\alpha}$$

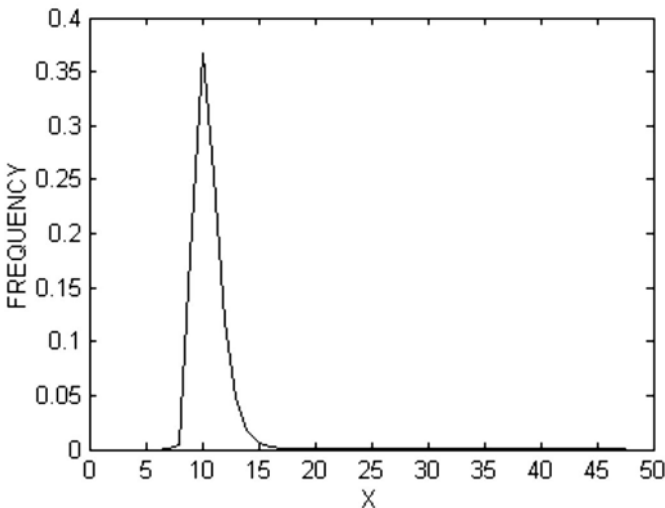where c is Euler's constant = 0.58. On substituting these values in equation (11.29) we have

Fig. 11.13. Extreme value distribution.

$$x = \bar{x} - \frac{c}{\alpha} - \frac{1}{\alpha} \ln \left(\ln \frac{T}{T-1} \right)$$

or

$$x = \bar{x} - \frac{\sqrt{6}}{\pi} \sigma \left[0.58 + \ln \left(\ln \frac{T}{T-1} \right) \right]$$

or

$$x = \bar{x} + K\sigma, \quad K = -\frac{\sqrt{6}}{\pi} \left(0.58 + \ln \left[\ln \frac{T}{T-1} \right] \right)$$

Figure 11.13 shows the extreme value distribution.

11.11 HOMOGENEITY OF DATA

Before population parameters are estimated on the basis of sample data, the homogeneity of data should be examined so that the assumption that the sample is from a single population can be justified. The most likely alternative to homogeneity in a series of data is some form of trend or oscillation and it can be examined by applying the Mann-Kendall rank test, the Run test or the double mass analysis. The Mann-Kendall rank test (Kendall and Stuart, 1961) is explained here.

Mann-Kendall Rank Test

The presence or absence of trends in a series can be determined by using the Mann-Kendall rank statistic τ. The statistic is computed from

$$\tau = \frac{4 \sum\limits_{i=1}^{N} n_i}{N(N-1)} - 1 \tag{11.30}$$

where n_i is the number of values larger than the ith value in the series subsequent to its position in the series of N values. Its expected value in a random series is zero and its standard deviation (σ) is given by

$$\sigma^2 = \frac{(4N+10)}{9N(N-1)} \tag{11.31}$$

The ratio of τ to the standard deviation σ gives an indication of trend or no trend in the data. For no trend in the data series, the value of τ/σ lies within the limits of ± 1.96 at the 5% level of significance.

To use this test we need to consider only the relative values of all terms in the series x_i under analysis. For computing τ for the series, compare the value of the first term of the series x_i with the values of all other terms in the series from the second to the Nth. Count the number of later terms whose values exceed x_1 and denote this number by n_1. Then compare the value of

the second term x_2 with the values of all later terms, count the number of later terms that exceed x_2 and determine this by n_2. Calculate this procedure for each term of the series to the x_{N-1} term and its corresponding number n_{N-1}. The Σn_i is given by the sum:

$$\sum_{i=1}^{N-1} n_i = n_1 + n_2 + n_3 + \ldots\ldots + n_{N-1} \tag{11.32}$$

Statistic τ can then be easily computed. The method of calculating τ is explained by the following numerical example.

Example 11.8: Rainfall values for the period 1901 to 1920 are given in the table below. Determine if there is a trend in the yearly values using the Mann-Kendall rank test.

Determination of the Mann-Kendall rank statistic

Year	Rainfall (x)	n_i	Year	Rainfall (x)	n_i
1901	2.5	15	1912	6.8	0
1902	3.1	11	1913	3.0	4
1903	1.4	17	1914	5.8	0
1904	6.9	0	1915	3.8	1
1905	2.9	11	1916	2.8	2
1906	4.2	6	1917	3.5	1
1907	1.9	12	1918	2.1	1
1908	5.5	4	1919	1.6	1
1909	3.9	5	1920	4.0	–
1910	6.0	2	–	–	94
1911	6.7	1			

Solution: We have $N = 20$, $\Sigma n_i = 94$, $\tau = \dfrac{4 \times 94}{20 \times 19} - 1 = -0.011$

$$\sigma = \sqrt{\frac{4 \times 20 + 10}{9 \times 20 \times 19}} = 0.162$$

$$\frac{\tau}{\sigma} = \frac{-0.011}{0.162} = -0.068$$

It is seen that the value of τ/σ is within the limits of ± 1.96 and hence there is no evidence of increasing or decreasing trend in the data series.

11.12 EMPIRICAL FREQUENCY ANALYSIS

11.12.1 Simple Rank Method or Probability Method

The probability that a random variable takes on a value in any particular interval can be determined from the mathematical form of its distribution. In

practice we have long periods of observed data of hydrometeorological variables. These data can be used to derive the probabilities for each of the values included in the data series with the use of a frequency method without bothering about the form of the distribution the variable follows. This can be achieved as follows.

Let us consider a chronological series of observations $x_1, x_2, x_3,..., x_N$ of a random variable X. If, in a series of N observations, we see that a value of magnitude x is exceeded m times out of N values then the probability of this value is given as

$$P = \frac{\text{number of observation exceeding the value } x}{\text{total number of observations}} \qquad (11.33)$$

Such simple probability for each of the values in the date series can be calculated from the ranked sample data. For this purpose, the values in the data series are first arranged in descending order of magnitude and ranks from 1 to N are assigned to each observation in the arranged series. Now the probability of any value x can be calculated just by knowing its rank in the series. It may lie between two values of ranks m and $m+1$. In that case, m values in the series are such that these are greater than x. Therefore m is the number of observations exceeding the value x in a series of N observations. The probability of occurrence $P(X \geq x)$ for a value of magnitude x, therefore, is

$$P(X \geq x) = \frac{m}{N} \qquad (11.34)$$

The return period T for an event of magnitude x, therefore, will be

$$T = \frac{1}{P(X \geq x)} = \frac{N}{m}$$

where T = return period (years), N = number of data values (years), and m = rank of the value in the series (the largest value having rank m = 1). This equation is the earliest formula designed for computing the probability plotting positions. Use of this formula is known as the California method, since it was first employed to plot flood data of the California streams.

11.12.2 Plotting Positions

Probability plotting is often used in hydrology and hydrometeorology to estimate probabilities of exceedance and recurrence intervals for certain random events, such as annual maximum rainfall, annual maximum discharge, etc. The probability estimates, obtained in this manner, are of great practical value for hydrologic design purposes. Many formulae have been developed for calculating exceedance probabilities and recurrence intervals for observed hydrological data. These formulae employ the system of ranking the data from the largest to the smallest and then the ranks are used to calculate the probability of exceedance for each of the ranked values.

Most of the plotting position formulae currently in use are of the form:

$$P(m) = \frac{m - a}{(N + 1 - 2a)} \tag{11.35}$$

where m = the rank value of x, m = 1, 2, …, N; N = the number of data values; $P(m)$ = the probability plotting position of event x of rank m; and a = a constant. Table 11.5 shows various formulae for computing plotting positions.

Table 11.5: Plotting position formulae

Name of formula	Year in which introduced	$T = \dfrac{1}{P(X \geq x)}$
California	1923	N/m
Hazen	1930	$2N/(2m - 1)$
Weibull	1939	$(N + 1)/m$
Chegodayev	1955	$(N + 0.4)/(m - 0.3)$
Blom	1958	$(N + 0.25)/(m - 0.375)$
Tukey	1962	$(3N + 1)/(3m - 1)$
Gringorten	1963	$(N + 0.12)/(m - 0.44)$
Cunnane	1989	$(N + 0.2)/(m - 0.4)$

It may be mentioned that all plotting formulae give practically the same results in the middle of the distribution but produce different plotting positions near the tails of the distribution. Yevjevich (1972) compared several plotting position formulae. The report recommended that the Gringorten formula should be used for the extreme value type-I (or Gumbel) distribution. The Chegodayev formula is commonly used in the former USSR states but the Weibull formula has been recommended as a standard since 1948. Plotting probability and the return period of a rank one event in a 50-year sample is given in Table 11.6.

Table 11.6: Plotting probability and return period of rank one event in a 50-year sample ($m = 1$ and $N = 50$)

Formula name	Formula	Plotting probability	Return period (T)
California	N/m	0.02	50
Hazen	$2N/(2m - 1)$	0.01	100
Weibull	$(N + 1)/m$	0.19	51
Chegodayev	$(N + 0.4)/(m - 0.3)$	0.014	72
Cunnane	$(N + 0.2)/(m - 0.4)$	0.012	84

Example 11.9: Annual maximum 1-day rainfall (cm) for the period 1901-1950 for New Delhi is given below. Estimate the values of the 2, 5, 10, 25 and 50-year rainfall by the California formula.

Year	0	1	2	3	4	5	6	7	8	9
190-		6.3	7.8	3.4	17.4	7.3	11.6	4.7	13.9	9.8
191-	15.0	16.9	17.0	7.4	14.6	9.4	7.1	8.8	5.4	3.9
192-	10.0	15.6	11.6	13.9	8.6	8.8	7.3	10.0	2.7	3.3
193-	13.8	11.3	15.7	16.3	11.9	11.8	23.2	11.0	3.9	6.2
194-	7.9	3.8	11.3	6.1	11.3	6.5	7.6	7.1	16.0	13.7
195-	11.4									

Solution: The data are ranked in the order of descending magnitude and each value is assigned a return period (T) equal to N/m and probability (P) equal to m/N where m is the rank number in the series and N is the total number of data.

x	Rank	$T = \dfrac{N}{m}$	$P(X \geq x) = \dfrac{m}{N}$	x	Rank	$T = \dfrac{N}{m}$	$P(X \geq x) = \dfrac{m}{N}$
23.2	1	50.0	0.02	9.8	26	1.92	0.52
17.4	2	25.0	0.04	9.4	27	1.85	0.54
17.0	3	16.67	0.06	8.8	28	1.78	0.56
16.9	4	12.5	0.08	8.8	29	1.72	0.58
16.3	5	10.0	0.10	8.6	30	1.67	0.60
16.0	6	8.33	0.12	7.9	31	1.61	0.62
15.7	7	7.14	0.14	7.8	32	1.56	0.64
15.6	8	6.25	0.16	7.6	33	1.52	0.66
15.0	9	5.55	0.18	7.4	34	1.47	0.68
14.6	10	5.0	0.20	7.3	35	1.43	0.70
13.9	11	4.55	0.22	7.3	36	1.39	0.72
13.9	12	4.16	0.24	7.1	37	1.35	0.74
13.8	13	3.85	0.26	7.1	38	1.32	0.76
13.7	14	3.57	0.28	6.5	39	1.28	0.78
11.9	15	3.33	0.30	6.3	40	1.25	0.80
11.4	16	3.13	0.32	6.2	41	1.22	0.82
11.3	17	2.94	0.34	6.1	42	1.19	0.84
11.8	18	2.78	0.36	5.4	43	1.16	0.86
11.6	19	2.63	0.38	4.7	44	1.14	0.88
11.6	20	2.50	0.40	3.9	45	1.11	0.90
11.3	21	2.38	0.42	3.9	46	1.09	0.92
11.3	22	2.27	0.44	3.8	47	1.06	0.94
11.0	23	2.17	0.46	3.4	48	1.04	0.96
10.0	24	2.08	0.48	3.3	49	1.02	0.98
10.0	25	2.0	0.50	2.7	50	1.0	1.0

The 2-year, 5-year, 10-year, 25-year and 50-year return period rainfall values are 10.0, 14.6, 16.3, 17.4 and 23.2 cm, respectively. *P* is the estimated

probability of occurrence of rainfall greater than that shown in the table. In this example, the probability that rainfall is more than 6.5 cm is 0.78, and that of less than 6.5 cm is $1 - p = 0.22$.

11.13 FREQUENCY ANALYSIS BY THE GUMBEL METHOD

11.13.1 Method of Moments

According to Gumbel (1958), the cumulative probability that any extreme value of a variable X will be equal to or less than x is given as:

$$P(X \le x) = \exp\left[-\exp\left\{-\alpha(x-u)\right\}\right] \tag{11.36}$$

Let $y = \alpha(x - u)$. Then, $x = u + \dfrac{1}{\alpha} y$. Parameters a and u are evaluated by the method of moments as:

$$\frac{1}{\alpha} = \frac{\sqrt{6}}{\pi}\sigma = 0.78\sigma \tag{11.37}$$

$$u = \bar{x} - \frac{c}{\alpha}$$

c = Euler's constant = 0.58. Therefore,

$$u = \bar{x} - 0.45\sigma$$

$$x = \bar{x} - 0.45\sigma + 0.78\sigma \cdot y$$

By definition,

$$T = \frac{1}{1 - P(X \le x)}$$

$$T = \frac{1}{1 - e^{-e^{-y}}}$$

$$y = -\log_e \log_e \frac{T}{T-1}$$

$\bar{x}$ and σ can be determined for a given series of data and then parameters α and u can be obtained. Thus, for any value of X, T can be calculated.

11.13.2 Method of Least Squares

The Gumbel method provides a straight line fit in the x and y plane. It has been pointed out by several workers that estimating the Gumbel distribution parameters by the method of moments may sometimes not be satisfactory. It has also been found that the method of moments does not give as good a fit as does the method of least squares. The use of the least square method was therefore recommended by Chow (1953). One can write:

$$x = A + By \tag{11.38}$$

where *A* and *B* are parameters which are given by the least square method as:

$$y = \log_e [\log_e \frac{T}{T-1}]$$

$$A = \frac{\sum x}{n} - \frac{B \sum y}{n}$$

$$B = \frac{\sum xy - n \bar{x} \bar{y}}{\sum y^2 - n \bar{y}^2}$$

The value of *T* can be obtained by the use of a plotting position formula. For the Gumbel model, the Weibull formula is most appropriate.

Example 11.10: Annual peak discharges (in 100 cumecs) for Damodar River at Rhondia for the period 1932–1952 (21 years) are given. Estimate the magnitude of the 25 and 100-year flood by the Gumbel method using the method of moments.

Year	1932	1933	1934	1935	1936	1937	1938	1939
Discharge $(10^2 \text{m}^3/\text{sec})$	29.6	64.0	48.0	181.2	70.8	58.8	120.1	79.9

Year	1940	1941	1942	1943	1944	1945	1946	1947
Discharge $(10^2 \text{m}^3/\text{sec})$	87.8	179.5	108.2	83.9	59.1	45.2	91.4	82.4

Year	1948	1949	1950	1951	1952			
Discharge $(10^2 \text{m}^3/\text{sec})$	65.0	77.0	95.7	111.2	51.2			

Solution: Method of Moments

S.No.	Discharge $(10^2 m^3/sec)$ (x)	S.No.	Discharge $(10^2 m^3/sec)$ (x)
1	29.6	12	83.9
2	64.0	13	59.1
3	48.0	14	45.2
4	181.2	15	91.4
5	70.8	16	82.4
6	58.8	17	65.0
7	120.1	18	77.0
8	79.9	19	95.7
9	87.8	20	111.2
10	179.5	21	51.2
11	108.2		

$$N = 21, \quad \sum x = 1789.0, \quad \sum x^2 = 182820.78, \quad \bar{x} = \frac{1}{N} \sum x = \frac{1}{21} \times 1789 = 85.19,$$

$$\overline{x^2} = \frac{1}{N} \sum x^2 = \frac{182820.78}{21} = 8705.75$$

$$\sigma^2 = \frac{N}{(N-1)} \left[\left(\overline{x^2} \right) - \left(\bar{x} \right)^2 \right] = \frac{21}{20} (8705.75 - 7257.34) = \frac{21}{20} \times 1448.41 = 1520.83$$

Therefore, $\sigma = 39.0$.

$$x_T = \bar{x} - 0.45\sigma + 0.78\sigma \cdot y_T$$
$$= 85.19 - 17.55 + 30.42 \, y_T$$
$$= 67.64 + 30.42 \, y_T$$

$$y_T = -\log_e \log_e \frac{T}{T-1}$$

$T = 25, \ y_T = 3.198; T = 100, \ y_T = 4.600$

$X_{25} = 67.64 + 30.42 \times 3.198 = 67.64 + 97.28$

$X_{25} = 164.92 \times 100 \approx 16492$ cumecs

$X_{100} = 67.64 + 30.42 \times 4.6 = 67.64 + 139.93 = 207.57 \times 100 \approx 20757$ cumecs

The peak discharge equals or exceeds 16492 and 20757 cumecs once every 25 and 100 years, respectively.

11.14 FREQUENCY FACTORS

Chow (1951) proposed the frequency method use as the general frequency equation for hydrologic frequency analysis. This can be expressed as

$$x_T = \bar{x} + k\sigma \tag{11.39}$$

where x_T = magnitude of an event of some given return period (T), $\bar{x}$ = mean of the record series, σ = standard deviation, and k = frequency factor. For two parameter distributions, the value of k varies only with the return period. It varies with the coefficient of skewness in skewed distributions and can be affected greatly by the sample size. For the normal, log-Pearson type III and extreme value type I distributions the tables showing theoretically derived values of the frequency factor k for selected values of the sample size (n) and the desired return periods have been tabulated by Chow (1964). Frequency factors for the extreme value type I or Gumbel distribution are shown in Table 11.7.

Table 11.7: Frequency factors for extreme value Type-I distribution

Sample Size	Return period (T)						
	10	*20*	*25*	*50*	*75*	*100*	*1000*
15	1.703	2.410	2.632	3.321	3.721	4.005	6.265
20	1.625	2.302	2.517	3.179	3.563	3.836	6.006
25	1.575	2.235	2.444	3.088	3.463	3.729	5.842
30	1.541	2.188	2.393	3.026	3.393	3.653	5.727
40	1.495	2.126	2.326	2.643	3.301	3.554	5.476
50	1.466	2.086	2.283	2.889	3.241	3.491	5.478
60	1.446	2.059	2.253	2.852	3.200	3.446	-
70	1.430	2.038	2.230	2.824	3.169	3.413	5.359
75	1.423	2.029	2.220	2.812	3.155	3.400	-
100	1.401	1.998	2.187	2.770	3.109	3.349	5.261

Example 11.11: The mean of the 1-day maximum rainfall at New Delhi in a 50-year record is 10.3 cm. The standard deviation is 4.6 cm. Estimate the magnitude of the 100-year rainfall.

Solution: $x_T = \bar{x} + k\sigma$, $\bar{x} = 10.3$, $\sigma = 4.6$. From Table 11.5, $k = 3.491$ for $n = 50$, $T = 100$. Therefore,

$$x_{100} = 10.3 + 3.491 \times 4.6 = 26.4 \text{ cm}$$

REFERENCES

Chow, V.T., 1951. A general formula for hydrologic frequency analysis. *Transactions, American Geophysical Union*, 32, pp. 231-237.

Chow, V.T., 1953. Frequency analysis of hydrologic data. Engineering Experiment Station Bulletin No. 414, 80 pp., University of Illinois, Urbana, Illinois.

Chow, V.T. (Editor), 1964. Handbook of Applied Hydrology. McGraw-Hill Publishing Company, New York.

Cunnane, C., 1989. Statistical distributions for flood frequency analysis. WMO Operational Hydrology Report No. 33, 72 pp., WMO, No. 718, Geneva, Switzerland.

Gumbel, E.J., 1958. Statistics of Extremes. 375 pp., Columbia University Press, Columbia, New York.

Kendall, M.G. and Stuart, A., 1961. The Advanced Theory of Statistics. Vol. 2, 676 pp., Griffin, London, U.K.

Langbein, W.B., 1949. Annual floods and the partial duration flood series. Transactions, American Geophysical Union, Vol. 30, No. 6, pp. 879-881.

Yevjevich, V., 1972. Probability and Statistics in Hydrology. 302 p., Water Resources Publication, Highlands Ranch, Colorado.

12 Foreshadowing Precipitation

Precipitation or rainfall is the major factor which influences hydrological and agricultural activities of any region, but rainfall is highly dependent on atmospheric weather systems. The weather systems thus play a determinant role in the production of rainfall. Forecast of rainfall is of considerable importance to hydrologists and agriculturists for making operational decisions. As mentioned in Chapter 1 under the scope of hydrometeorology, rainfall forecast is an important input in river flow warning as well as in efficient operation of multipurpose dams. It is well known that rainfall forecast is intimately linked with the safety of dams. In the case of a heavy rainfall warning the magnitude of inflow is determined and the reservoir is operated to accommodate the incoming flood waters. Because rainfall is a highly variable weather element, one of the important aspects of rainfall forecast is to identify those physical or natural factors which have the largest influence over rainfall. If these factors that control the rainfall of any region are identified then they can be used to provide a forecast of the behavior of rainfall well in advance. For example, there is a relation between the pressure in South America and subsequent rainfall in India. If the pressure is unusually high in Argentina and Chile during March and April there is likely to be a heavy monsoon rainfall in India in the following months of July and August. The forecasting of rainfall is therefore of considerable importance in agricultural and hydrological activities of the region. In this chapter, we deal with some of the techniques of rainfall forecasting. Before proceeding further, it will be beneficial to explain a few statistical concepts that are useful when we deal with forecasting methods on the basis of large historical volumes of data.

12.1 CORRELATION ANALYSIS

It frequently happens that the relationship between two variables, x and y, is very much marked, as has been pointed out above in the case of a relation between the pressure in South America and subsequent rainfall in India. The

straightforward way of establishing this relationship between two variables is to plot the pairs of their data on a graph paper—the x axis denoting one variable and the y axis the other variable. It will be seen that the distribution of points may closely lie along a straight line if there is a linear relationship between them. Such a line is called a regression line and the relationship can be used to make a forecast of y for any specified value of x or of x for any specified value of y.

If the line is used to forecast the value of y (dependent variable) from x (independent variable) it is called the regression line of y on x. If the line is used to forecast the value of x (dependent variable) from y (independent variable) then it is called the regression line of x on y.

In general, the regression line of y on x is not the same as the regression line of the x on y. First consider the line of regression of y on x as

$$y = a + bx \tag{12.1}$$

where b is the slope of the line. We determine constants a and b so that equation (12.1) yields for each value of x the best forecast estimate of the value of y. The term best estimate means to find a and b so as to minimize the sum of squares of deviations of actual values of y from their estimates given by equation (12.1).

Let (x_i, y_i) be the actual values of a point. For a given value of x_i, the forecast value of y_i will be $a + bx_i$. Thus we have to choose a and b so as to make $\sum_{i=1}^{n}(y_i - a - bx_i)^2$ a minimum, n is the number of observations. For a minimum value, the partial derivatives of the above expression with respect to a and b must be zero. The equations for determining these constants are

$$s = \sum_{i=1}^{n}(y_i - a - bx_i)^2 \tag{12.2}$$

$$\frac{ds}{da} = \sum_{i=1}^{n}(y_i - a - bx_i) = 0 \tag{12.3}$$

$$\frac{ds}{db} = \sum_{i=1}^{n}x_i(y_i - a - bx_i) = 0 \tag{12.4}$$

where s denotes the sum of deviations or forecast error. From equations (12.3) and (12.4) we have

$$\bar{y} = a - b\bar{x} \tag{12.5}$$

$$b = \frac{\sum_{i=1}^{n}x_i y_y - n\bar{x}\,\bar{y}}{\sum_{i=1}^{n}x_i^2 - n(\bar{x})^2} \tag{12.6}$$

$$b = \frac{\mu_{11}}{\sigma_x^2} \tag{12.7}$$

where the slope $\dfrac{\mu_{11}}{\sigma_x{}^2}$ is called the coefficient of regression of y on x, and $\bar{y}, \bar{x}$, σ_x and μ_{11} are, respectively, the mean of the y values, mean of the x values, standard deviation of the values of x and covariance of x and y for a data set of n values. These can be written as

$$\bar{y} = \frac{\sum\limits_{i=1}^{n} y_i}{n} \tag{12.8}$$

$$\bar{x} = \frac{\sum\limits_{i=1}^{n} x_i}{n} \tag{12.9}$$

$$\sigma_x^2 = \frac{\sum\limits_{i=1}^{n} x_i^2}{n} - (\bar{x})^2 \tag{12.10}$$

$$\mu_{11} = \frac{\sum\limits_{i=1}^{n} x_i y_i}{n} - \bar{x}\,\bar{y} \tag{12.11}$$

Similarly, for the regression line of x on y the slope of b' or the coefficient of regression of x on y can be expressed as

$$b' = \frac{\mu_{11}}{\sigma_y^2} \tag{12.12}$$

Coefficients b and b' measure the slopes of the regression lines. If there is no relationship between the two variables the regression lines will be horizontal or vertical. The product of the two coefficients of regression is symmetrical with respect to x and y. Its square root $\dfrac{\mu_{11}}{\sigma_x \sigma_y}$ is the coefficient of correlation, r:

$$r = \frac{\mu_{11}}{\sigma_x \sigma_y} \tag{12.13}$$

It is defined as the ratio of the covariance to the product of standard deviations of two variables x and y.

The equation for the line of regression of y on x has been found by minimizing the sum of the squares of the deviations of points from the line of regression of y on x. The mean of the sum of the square of deviations is called the standard error of estimate (S_y) of y from the regression equation. Its value is

$$S_y^2 = \sigma_y^2(1 - r^2) \tag{12.14a}$$

In the same way the mean squared deviations of points from the line of regression of x on y is S_x^2 where

$$S_x^2 = \sigma_x^2(1 - r^2) \tag{12.14b}$$

Since the sum of squares of deviations cannot be negative, it follows from equations (12.14b) that

$$r^2 \leq 1$$

or

$$-1 \leq r \leq +1$$

If $r = 1$ or $r = -1$, the sum of squares of deviations from either line of regression is zero and all the points lie on both lines of regression. These two lines then coincide and there is a linear relation between variables x and y giving perfect correlation. Thus, a correlation coefficient is a numerical quantity that expresses the degree of linear relationship or association between two variables and varies between -1 and $+1$.

In forecasting, we are often interested in foreshadowing the dependent variable from more than one independent variable. For example, we are interested in forecasting rainfall from, say, five known independent meteorological variables. We shall, therefore, deal with regression equations with more than one independent variable later in this chapter.

Example 12.1: The rainfall and temperature data at a station are given below. Find the forecasting relationship between rainfall and temperature and the coefficient of correlation.

Year	Rainfall (mm)	Temp (°C)
1951	36.1	27.8
1952	41.2	30.9
1953	41.1	31.3
1954	37.6	29.6
1955	34.1	26.0
1956	38.9	30.3
1957	33.8	27.2
1958	34.4	26.2
1959	33.5	25.7
1960	41.7	33.5

Solution: Let R be rainfall and T be temperature then the relation between R and T is given as:

$$R = a + bT$$
$$a = \bar{R} - b\bar{T}$$
$$b = \frac{\Sigma RT - n\bar{R}\bar{T}}{\Sigma T^2 - n(\bar{T})^2}$$

S.No.	Year	R	T	RT	R^2	T^2
1	1951	36.1	27.8	1003	1303	773
2	1952	41.2	30.9	1273	1697	955
3	1953	41.1	31.3	1286	1689	980
4	1954	37.6	29.6	1113	1414	876
5	1955	34.1	26.0	887	1163	676
6	1956	38.9	30.3	1179	1513	918
7	1957	33.8	27.2	919	1142	740
8	1958	34.4	26.2	901	1183	686
9	1959	33.5	25.7	861	1122	660
10	1960	41.7	33.5	1397	1739	1122
	Σ	372.4	288.5	10819	13965	8386

$$\overline{R} = 37.24$$

$$\overline{T} = 28.85$$

$$b = \frac{10819 - 10 \times 37.24 \times 28.85}{8386 - 10 \times 28.85 \times 28.85}$$

$$= 1.21$$

$$a = 37.24 - 1.21 \times 28.85$$

$$= 2.33$$

$$R = 2.33 + 1.21\ T$$

$$r = \frac{\Sigma RT - n\overline{R}\overline{T}}{\sqrt{\Sigma R^2 - n(\overline{R})^2} \times \sqrt{\Sigma T^2 - n(\overline{T})^2}}$$

$$r = \frac{10819 - 10 \times 37.24 \times 28.85}{\sqrt{13965 - 10 \times 37.24 \times 37.24} \times \sqrt{8386 - 10 \times 28.85 \times 28.85}} = 0.97$$

12.2 MEASURE OF VARIABILITY

The magnitude or a quantity of any hydrometeorological variable over a region, say rainfall, varies significantly from year to year because of the effects of several factors that control it. An average or a mean value is regarded as an estimate of the variable which gives us some information about the set of values. Often it is necessary to know how the values vary around their mean or average. For this purpose different parameters have been devised to measure the variation within a set of observations. The variation around the mean can best be explained by the term standard deviation which is a measure of the dispersion of the various values of the variable (x_i) about the mean value $\overline{x}$, $\overline{x} = \dfrac{\Sigma x_i}{N}$. The standard deviation (SD) is computed as:

$$SD = s_x = \sqrt{\frac{\sum (x_i - \bar{x})^2}{(N-1)}} \qquad (12.15)$$

The standard deviation has the same unit as the mean. The significance of the standard deviation and the mean value can be graphically demonstrated by plotting a scatter diagram showing the year to year percentage departures from the mean of the all-India summer monsoon rainfall for the period 1871-1990 as shown in Fig. 12.1. From this figure it can be seen that the departures of seasonal rainfall vary from –30% (1877) to +20% (1917) around a mean value. The mean summer monsoon seasonal rainfall (June-September) of India is about 85.2 cm with a standard deviation of 12.5 cm. The significance of the standard deviation and the mean value can be explained by plotting as shown in Fig. 12.1. The mean value is shown as a horizontal line through the data. The variation or confidence limits are shown as lines one standard deviation above $(\bar{x} + s_x)$ and below $(\bar{x} - s_x)$ the mean value. Statistical laws then say that in a normal case about 68% of the values of rainfall departures will be between two values of rainfall corresponding to $(\bar{x} + s_x)$ and $(\bar{x} - s_x)$. Sometimes, the confidence limit is set two times the standard deviation above and below the mean value, i.e., $[(\bar{x} + 2s_x), \ (\bar{x} - 2s_x)]$, respectively. Observations occurring outside the limits of the confidence band represent some special and unique performance of the monsoon system.
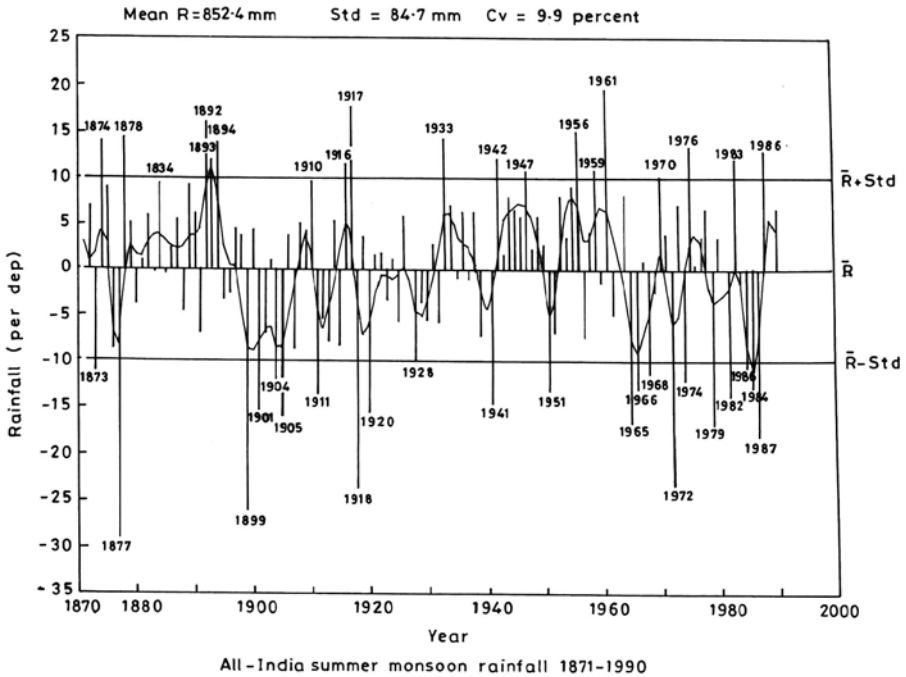
Fig. 12.1. Year-to-year percentage departure from mean of all-India monsoon seasonal (June–September) rainfall (1871-1990).

It may be pointed out that standard deviations of rainfall are generally comparable over two or many stations, but the wide differences in variability are due to the differences in the mean rainfall values. If we want to compare the variation of different sets of observations about their mean, it is then useful to express the variability in another form. For this purpose, the coefficient of variability is a useful parameter for assessing the regional characteristics of various regions. The coefficient of variability is found by expressing the standard deviation as a percentage of the mean value:

$$CV = \frac{s_x}{\bar{x}} \times 100$$

where CV is the coefficient of variation. Let us take, for example, a region with a coefficient of variation of 25 percent. That means

$$\frac{s_x}{\bar{x}} = \frac{25}{100} \text{ or } s_x = \frac{\bar{x}}{4}$$

and the annual rainfall in the region would occasionally deviate by as much as 25 percent from the mean annual rainfall. In other words, in about 68 years out of every 100 years, the rainfall in the region will be between $\bar{x} + \frac{\bar{x}}{4}$ and $\bar{x} - \frac{\bar{x}}{4}$, i.e., from an excess of 25% over the mean annual rainfall to a deficiency of 25% (or ±25% of the region's mean annual rainfall). The deviation will be over 25% in the rest of the 32 years—a deficiency of over 25% in about 16 years, and a surplus of over 25% in another 16 years. Similarly, where the coefficient of variability is 50%, the rainfall over the region would be less than half the normal in three years out of every 20 years. And that is a serious situation.

Example 12.2: The coefficient of variability of annual rainfall of a station based on 150 years of data is 50%. Find in how many years the station's rainfall was less than half of its normal rainfall. It is assumed that the annual rainfall follows a normal distribution.

Solution: The CV = 50%. Therefore $s_x = \frac{\bar{x}}{2}$. For normal distribution, in about 68 years out of every 100 years the rainfall for the station will be between the two values of rainfall corresponding to $\bar{x} + \frac{\bar{x}}{2}$ and $\bar{x} - \frac{\bar{x}}{2}$. Hence, the rainfall will be less than $\frac{\bar{x}}{2}$ in 16 years and will be more than $\frac{3\bar{x}}{2}$ in another 16 years. The annual rainfall of the station was less than half the normal in (16/100)×150 years i.e. 24 years.

12.3 GLOBAL SCALE FACTORS AFFECTING RAINFALL

Knowledge of the global scale natural factors influencing rainfall provide an insight to understand the physical processes behind rainfall, a fact first recognized by Sir Gilbert Walker in the beginning of the twentieth century. Modern research has enabled to understand the importance of global scale physical factors to global climate and the earth's environment. The methods of correlations as described in Section 12.1 have brought to light many interesting and suggestive relations.

12.3.1 Southern Oscillation

Sir Gilbert Walker (1908, 1918, 1924), from a correlation studies between the Indian monsoon rainfall and worldwide weather elements, discovered a curious sea-saw in the atmospheric surface pressure oscillation between the eastern equatorial Pacific Ocean and Indian Ocean. He found that when the pressure was high over the Pacific Ocean it tended to be low in the Indian Ocean, but once every 3 to 5 years, the pattern was reversed; that is, the pressure in the Indian Ocean became high, while there was low pressure in the eastern equatorial Ocean. This sea-saw oscillation of the atmospheric pressure was given the name Southern Oscillation (SO) by Sir Gilbert Walker. Later its importance was reiterated by Bjerknes in 1958, a meteorologist from Norway who found that the Southern Oscillation is the result of a cyclic warming and cooling of the surface of the central and eastern Pacific Ocean. This region of the Pacific Ocean is normally colder (sea surface temperature lower than 26°C) than its equatorial location would suggest, mainly because of the influence of northeasterly trade winds, a cold ocean current flowing up the coast of Chile, and to the upwelling of cold deep water off the coasts of Peru. The sudden appearance of warm waters off the coast of Peru was first reported by Dr. Luis Cananza, the President of the Geographical Society of Peru in 1891.

12.3.2 El Nino

As discussed above, the vast expanses of the central and eastern Pacific are the seat of lower than 26°C sea surface temperature (SST) and the lowest SST over tropical Pacific Ocean occurring in the waters off Peru and Ecuador coasts. At times, the SST fields over these regions are known to undergo an episodic warming over and above the seasonal cycle. Such an episodic warming of the equatorial Pacific SST is known as El Nino. During a warm episode the warming usually begins in April-May and reaches its mature phase around the end of December and decay during the following six months. The El Nino effect causes heavy rainfall over the coastal regions of northern Peru and Ecuador, but severe droughts in eastern Australia.

The El Nino is a Spanish word which means "the child" and was first used by Peruvian fisherman in the late 1800s to describe the warm water appearing off the coast of Peru around Christmas time. That is why it got the name El Nino, which denotes 'Christ Child' in local parlance. Today the term El Nino describes the warm phase of a naturally occurring sea surface temperature oscillation in the central and eastern Pacific Ocean.

At other times, the influence of cold water becomes more intense than usual; causing the surface of the central and eastern Pacific to cool and this is a La Nina event. This results in droughts in South America and heavy rainfall, even floods in eastern Australia. The reverse phenomenon, the cooling of the eastern Pacific waters, was at first called "Anti-El Nino" until it was realized that this literally meant the Anti-Christ. To avoid this connotation, it was renamed "La Nina" (or the girl).

El Nino is a major oceanic phenomenon which affects weather not only in the neighborhood of its occurrence, but even at far away locations through a complicated interactive process. Major El Nino events are closely associated with large scale changes in the atmospheric circulation over the Pacific Ocean. Around the time a major El Nino develops, the atmospheric pressure over the eastern Pacific decreases, whereas that over the Indian Ocean increases. When the El Nino event ends, that is, the abnormal warming of the ocean waters of the central Pacific ends, the atmospheric pressures in these regions swing back. This is what we have described as the Southern Oscillation. As the El Nino oscillation is associated with the Southern Oscillation, the combined phenomenon is called El Nino Southern Oscillation (ENSO). ENSO is the most notable and pronounced example of global climate variability on the interannual time-scale. Dramatic climatic effects were experienced worldwide in 1982-83 during the strongest El Nino of the twentieth century. During the 1982-83 El Nino, there were huge drought related fires in Borneo and Australia, drought related famines in India and east Africa, and flooding on the east coast of equatorial South America, in the Rocky Mountain region of the United States, and in Brazil south of the equator. At the same time prolonged droughts afflicted Australia, Indonesia, the Philippines, and South Africa.

12.3.3 Southern Oscillation Index

Southern Oscillation affects various meteorological and oceanographic conditions worldwide. Teleconnections are particularly pronounced during ENSO conditions. Many indices have been developed representing the strength of both SO and El Nino. We have seen that SO has a period varying from 3 to 5 years and consequently pressure departures (deviation from the mean value) and their trends are better indices than the absolute values of pressure. Several indices have been developed that indicate Southern Oscillation index (Troup, 1965; Wright, 1984; Ropelewski and Jones, 1987). The SO index (SOI) is most commonly calculated as the normalized difference between

the sea level pressure anomalies at Tahiti [17.5° S, 149.5° W] and Darwin [12.4° S, 130.9° E]. Figure 12.2 shows a plot of SOI. High negative values of the SOI indicate ENSO or warm events and high positive values of SOI La Nina or cold events. The SOI series has a maximum of value of +30 mm and a minimum of −35 mm.

Precipitation in the line Islands of the equatorial Pacific Ocean [latitude 0° to 10° N, longitude 160° W] has also been used as an index of ENSO conditions. Distinct precipitation surges occur in these normally dry islands under the ENSO conditions. Based on the strength and sign of the southern
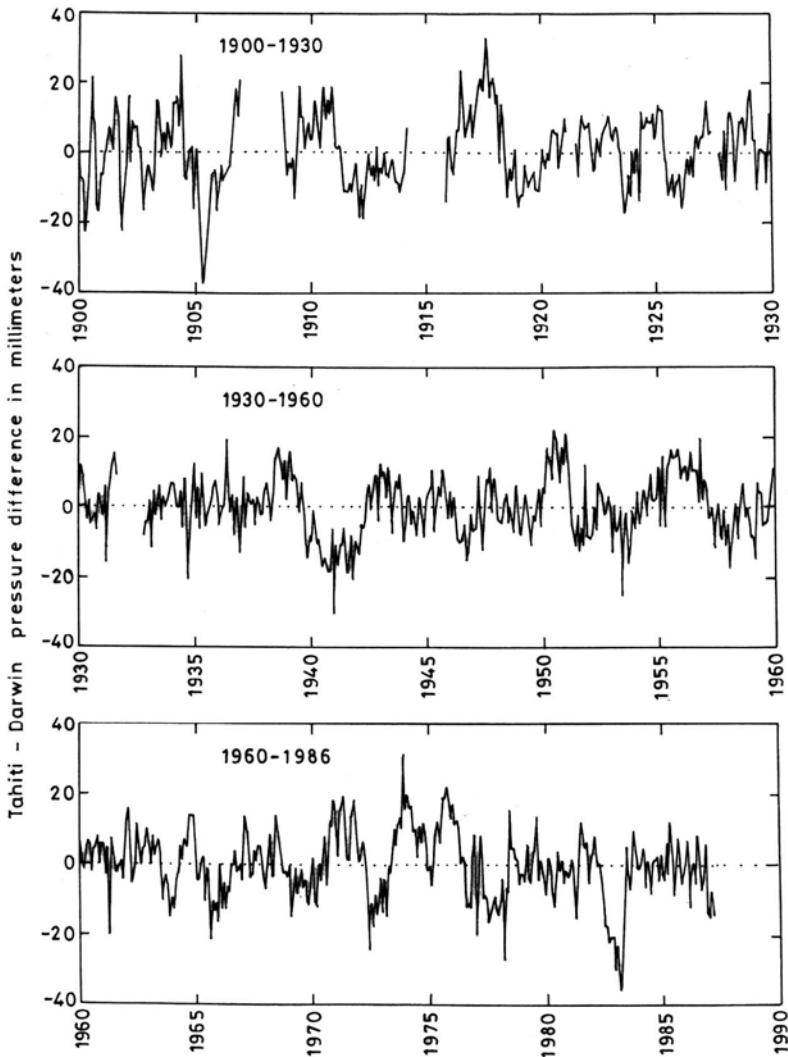
Fig. 12.2. Difference in monthly sea level pressure between Tahiti and Darwin. The sea level pressure difference is a measure of ENSO.

oscillation index, Table 12.1 gives a list of El Nino and La Nina years from 1900 to 2000.

Table 12.1 shows that there is no systematic time interval between two successive El Nino and La Nina years. On average the return period of the El Nino event varies from 2 to 7 years and of the La Nina event from 2 to 10 years. The intensity and duration of the events also vary and are hard to predict. El Nino often begins early in the year and peaks in the following December, but no two events behave in the same way. Typically an El Nino year lasts anywhere from 14 to 22 months but it can be much longer or shorter. El Nino is by no means a new phenomenon, and researchers are still working to determine whether global warming would intensify or otherwise affect El Nino.

Table 12.1: El Nino and La Nina years based on SOI

S.No	El Nino Years	Time Interval between El Nino Years	S.No	La Nina Years	Time Interval between La Nina Years
1	1899-1900	—	1	1903-1904	—
2	1902-1903	3	2	1906-1907	3
3	1905-1906	3	2	1908-1909	2
4	1911-1912	6	4	1916-1917	8
5	1914-1915	3	5	1920-1921	4
6	1918-1919	4	6	1924-1925	4
7	1923-1924	5	7	1928-1929	4
8	1925-1926	2	8	1931-1932	3
9	1930-1931	5	9	1938-1939	7
10	1932-1933	2	10	1942-1943	4
11	1939-1940	7	11	1949-1950	7
12	1940-1941	1	12	1954-1955	5
13	1941-1942	1	13	1964-1965	5
14	1946-1947	5	14	1970-1971	6
15	1951-1952	5	15	1973-1974	3
16	1953-1954	2	16	1975-1976	2
17	1957-1958	4	17	1984-1985	9
18	1963-1964	6	18	1988-1989	4
19	1965-1966	2	19	1995-1996	7
20	1969-1970	4	20	1998-1999	3
21	1972-1973	3	21	2000-2001	2
22	1976-1977	4			
23	1977-1978	1			
24	1982-1983	5			
25	1986-1987	4			
26	1991-1992	5			
27	1993-1994	2			
28	1994-1995	1			
29	1997-1998	3			

12.4 TYPES OF WEATHER FORECASTS

Rainfall forecasts for hydrological and agricultural purposes are done on three time scales, called ranges in a meteorological sense. These are:

- Short range over time scales of 1 to 3 days
- Medium range over time scales of 4 to 10 days
- Long range over time scales beyond 10 days

Each of the above forecasting range is of value for water management and planning purposes.

12.4.1 Short Range Forecast

Short range forecast is based on the synoptic situation prevailing at the time of forecast and is valid for 1 to 3 days. The term synoptic is from Greek and denotes the coherent view of an event as a whole. In this method meteorological elements are recorded at a fixed time at a number of weather stations all over the world. These data from the observation stations are then sent to their main forecasting centers. Observations are made at 03, 09, 15, 21 hrs GMT (Greenwich Mean Time). In India the time is IST (Indian Standard Time). Observations are made 5½ hours later than GMT. The meteorological elements, which are observed, are cloud cover, wind strength and direction, visibility, fog, thunderstorm, rain, snow, pressure, temperature, humidity, and change in pressure. There are more than 7000 weather stations on earth. These meteorological data are plotted on weather maps using international code of symbols and abbreviations. These are called synoptic or weather charts. The forecast of weather and rainfall for the next 2 to 3 days is made with the help of prevailing weather data of several stations based on changes in pressure, humidity, wind direction in upper and lower layers of atmosphere, current, and past weather conditions.

12.4.2 Medium Range Forecast

Forecasting of weather elements for periods of 4 to 10 days is beneficial for the management of multipurpose water resources dams. In many countries the medium range forecast aims at predicting the departures of anomalies of weather elements from long-term averages as described in Section 12.2 rather than forecasting the daily weather.

12.4.3 Long Range Forecast

Water resources management depends on the total quantity of rainfall received in a year or a season as well as its distribution within the year. The long range forecasting of rainfall therefore is made to foresee the general character of rainfall and other weather elements for a season in advance. These forecasts are usually expressed to state whether rainfall or any other meteorological

element in the period under consideration will be above or below normal and how much above or below. Attempts are being made to apply the existing knowledge of the worldwide relations of weather to the problems of long range forecasting using regression and auto-regression integrated moving average (ARIMA) methods.

12.5 DEVELOPMENT OF LONG RANGE FORECAST OF RAINFALL IN INDIA

In 1877 because of the failure of monsoon rainfall, a disastrous famine occurred in India. This caused the need for forecasting of monsoon rainfall of India. As shown in Fig. 12.1, the monsoon rainfall was deficient by about 30% of the normal value in 1877. The first attempt to forecast monsoon rainfall was initiated by H.F. Blanford, the chief Reporter of the India Meteorological Department (IMD) at the request of the then Government of India owing to the 1877 famine. With the knowledge of meteorology then available, Blanford found that the Himalayan snows greatly affect the climatic and weather conditions across the plains of northwest India. Recognizing this, he used the extent and depth of the Himalayan snow cover in the preceding winter for forecasting of the summer monsoon rainfall. The success of Blanford's tentative forecasts during 1882-85 encouraged him to start operational long range forecasting (LRF) of monsoon rainfall for the whole of India and Burma in 1886. Based on the antecedent Himalayan snow cover, the first empirical operational LRF for seasonal rainfall over India as a whole was issued on June 4, 1886. After this, John Elliot, who succeeded Blanford in 1895, found the linking of other weather factors over the whole of India and surrounding regions to monsoon rainfall. As a consequence, he used the following factors for the monsoon prediction:

(a) Himalayan snow cover (October-May),
(b) local peculiarities of premonsoon weather in India, and
(c) local peculiarities over the Indian Ocean and Australia.

Later, Sir Gilbert Walker (1908, 1918, 1924), then Director General of Observatories in India, made much progress in the seasonal forecasting of rainfall in India from a correlation analysis between monsoon rainfall and other worldwide weather elements, such as pressure, temperature, etc. He reasoned that since the monsoon circulation is a large scale global feature, any abnormalities in it should have prior indications by way of abnormalities in the weather elements elsewhere over the globe. Sir Walker, through his correlation between weather elements over different parts of the globe and the seasonal rainfall of India, discovered three different types of oscillations in the general circulation of the atmosphere. Of these, two in the Northern hemisphere—the North Atlantic Oscillation (NAO) and the North Pacific Oscillation (NPO)—and one in the Southern hemisphere i.e. the Southern Oscillation (SO). While the NAO and the NPO are mainly regional in nature,

the SO has since been recognized as the phenomenon with global-scale influence as pointed out in earlier section. The SO represents a tendency of high pressure over the Pacific Ocean to be associated with low pressure in the Indian Ocean and vice versa. The SO was later linked to the oceanic phenomenon, called El Nino, in the east equatorial Pacific Ocean characterized by warming of the sea surface along the Peru Coast. As SO is linked to the El Nino phenomenon, the combined phenomenon is called the El Nino-Southern Oscillation (ENSO) and this will be discussed afterwards.

The discovery of the SO drew the attention of Sir Walker to do further research on factors which have a close association with monsoon rainfall. As a consequence, he identified eight predictors for building an empirical forecasting model for monsoon rainfall in India. These eight predictors are briefly summarized as:

i. Pre-monsoon heavy snowfall over northern and western India: A heavy snowfall during the pre-monsoon generates a region of local high pressure over northwest India. Winds from this high pressure region are considered to be unfavorable for monsoon rains over Punjab and adjoining areas.

ii. Heavy rains at Zanzibar and Seychelles in April and May: The heavy rains at Zanzibar and Seychelles was an indication of the predominance of an equatorial flow pattern over the monsoon. This factor was also considered for monsoon rain.

iii. High pressure over South America: The relationship between the Indian Monsoon rainfall and the pressure over South America is apparently because of SO as pointed out earlier. According to the SO, this should favor the formation of low pressure over the Indian Ocean and consequently favorable for monsoon.

iv. High pressure around Mauritius and Australia in Spring: These conditions again reflect a predominance of equatorial flow. Consequently, these were found not favorable for monsoon.

v. During the previous year high pressure over India: This factor was found to be favorable for a good monsoon.

vi. Winds observed by ships in the Indian Ocean: These winds, especially in the month of May, provided a good indication of the propagation of monsoon.

vii. The onset of summer rains over Ethiopia in May: A large departure from the normal onset date of summer rains over Ethiopia was also reflected in the date of onset of the monsoon over India.

viii. Height of the Nile River: The height of the Nile River often provided a useful indication of the onset of summer rains over Ethiopia as well as the onset of monsoon over India.

It was later observed that high pressure over India pertaining to the previous year, which was considered favorable, was found to be of less value. Finally, in 1924, Sir Gilbert Walker, after considerable research, selected

six predictors and empirical regression-based forecasting models were developed for the prediction of seasonal rainfall in northwest India and the Indian Peninsula, separately. These predictors are listed in Table 12.2. The correlation technique, first proposed by Sir Gilbert Walker, for the prediction of monsoon rainfall is still being used with modifications and improvements.

The monsoons of South Asia are the most pronounced monsoon circulations over the globe and form an important component of the general circulation of the atmosphere. In recent years there has been a great deal of interest in the study of monsoons. This is because the tropics constitute the source of heat energy for driving the atmospheric circulation, and so an understanding of the atmospheric processes in the tropics is needed, even for the prediction of weather over extra tropics. Of considerable importance is the Southern Oscillation, which we discuss in what follows.

Table 12.2: Predictors for summer monsoon rains

Area	Predictors	Period
1. Indian Peninsula	1. South American Pressure	April – May
	2. South Rhodesia rain	October – April
	3. Dutch Harbor temperature	December – April
	4. Java Rain	October – February
	5. Zanzibar rain	May
	6. Cape Town pressure	September – November
2. Northwest India	1. South America pressure	April – May
	2. South Rhodesia rain	October – April
	3. Dutch Harbor temperature	March – April
	4. Equatorial pressure	January – May
	5. Snow accumulation	May
	6. Cape Town pressure	September – November

12.6 INDIAN SUMMER MONSOON AND SOUTHERN OSCILLATION INDEX

A significant correlation between the summer monsoon rainfall in India and the SOI was indicated by Sir Gilbert Walker. Until 1950, this factor showed a positive association with summer monsoon rainfall but there were wide variations in the magnitude of the correlation coefficient during different decades. It varied from about 0.02 to 0.78 for the Indian peninsula and from 0.13 to 0.63 for northwest India. Interestingly, Pant and Parthasarathy (1981) found the correlation coefficient of +0.59 between the monsoon rainfall of India as a whole and the SOI factor. Further, they showed that large departures of monsoon rainfall were well associated with large departures of the SOI values (Fig. 12.3) and elaborated that large rainfall departures were influenced by the interaction between the synoptic scale and global scale circulations and their associated anomalies. Moreover, in the last decade, the tendency

also appeared to have changed sign. Apparently, the knowledge about the Southern Oscillation and its relation with Indian monsoon is still inadequate.
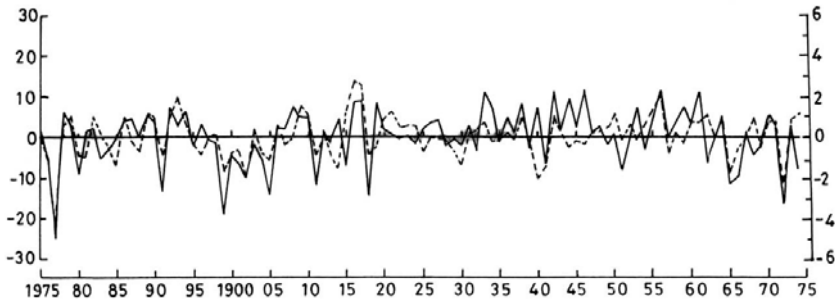

Fig. 12.3. Departure of rainfall amounts (June-August) from 100-year mean
(left scale, cm), ---- departures of Wright's southern oscillation index
(June-August) from 100-year mean (right scale).

In recent times, several improvements were effected in the long range forecasting techniques by incorporating new predictors whose association with the Indian monsoon was found to be better than the ones originally selected by Sir Gilbert Walker. Another innovation has been the inclusion of some circulation parameters based on the upper air observations. The LRF predictors, pertaining to the preceding winter and spring seasons, can be broadly classified into three groups representing the following features:

1. Pressures,
2. Upper winds and temperatures, and
3. Snow cover and atmospheric oscillation.

Before studying the long-range forecasting of Indian summer monsoon rainfall, it is worthwhile to briefly discuss the statistical techniques used.

12.7 STATISTICAL TECHNIQUES IN LONG RANGE FORECAST BASED ON IMPROVED PARAMETERS

Rainfall forecasts are required in the planning and management of rain water resources for agriculture and other human activities. Hence, in recent years the need for improved forecasting of monsoon rainfall in India has become increasingly important. Here we briefly describe rainfall forecasting using statistical techniques.

In many practical cases, a relationship is found to exist between observations of two or more variables. For example, a relationship is found to exist between the yield of a crop and the amount of rainfall. Sometimes the values of a variable are influenced by two or more variables. For example, the monsoon rainfall is affected by the Himalayan snow cover in May, the South American pressure and the Cape Town pressure. Such relationships

can be used to forecast one variable called the dependent variable from the knowledge of other related variables known as independent variables. Mathematical equations are then designed to express the relation between dependent and independent variables. Such an equation takes the form:

Crop yield $= a_0 + a_1$ (amount of rainfall)
Monsoon rainfall $= b_0 + b_1$ (Himalayan snow)
$+ b_2$ (South American pressure) $+ b_3$ (Cape Town pressure)

where a_0, a_1, b_0, b_1, b_2, and b_3 are coefficients determined from data. The statistical technique of quantifying such relationships among variables is known as correlation and regression analysis. When it is known that the values of a dependent variable is influenced by those of one independent variable, the problem is one simple correlation and regression analysis. If we are concerned with the combined influence of a group of variables upon another not included in that group, then our study becomes one of multiple regression and correlation analysis. However, the study of the effect of one variable upon another after eliminating the effects of other variables is the problem of partial correlation and regression analysis. The principles involved in multiple regression analysis is explained in what follows.

12.8 MULTIPLE REGRESSION ANALYSIS

A multiple regression equation is an equation for estimating a dependent variable, say Y, from independent variables X_1, X_2, X_3,..., X_K. Then the multiple regression equation is

$$Y = A + b_1 X_1 + b_2 X_2 + b_3 X_3 + ...b_K X_K \qquad (12.16)$$

where A is a constant, and b_0, b_1, b_2,..., b_K are referred to as partial regression coefficients. These coefficients can be determined by solving normal equations obtained by the method of least squares. If we take the deviations of the variables from their respective means, i.e., if $y = Y - \overline{Y}$, $x_1 = X_1 - \overline{X_1}$, $x_2 = X_2 - \overline{X_2}$, ...,$x_K = X_K - \overline{X_K}$ the regression equation (12.16) becomes

$$y = b_1 x_1 + b_2 x_2 + b_3 x_3 + ...b_K x_K \qquad (12.17)$$

Applying the method of least squares the following normal equations are obtained:

$$\sum x_1 y = b_1 \sum x_1^2 + b_2 \sum x_1 x_2 + ... + b_K \sum x_1 x_K$$

$$\sum x_2 y = b_1 \sum x_1 x_2 + b_2 \sum x_2^2 + ... + b_K \sum x_2 x_K$$

$$\sum x_3 y = b_1 \sum x_1 x_3 + b_2 \sum x_2 x_3 + ... + b_K \sum x_3 x_K \qquad (12.18)$$
...

$$\sum x_K y = b_1 \sum x_1 x_K + b_2 \sum x_2 x_K + \ldots + b_K \sum x_K^2$$

The above equations can be written in matrix form and can be solved using the matrix method:

$$\begin{bmatrix} \sum x_1^2 & \sum x_1 x_2 \ldots \sum x_1 x_K \\ \sum x_1 x_2 & \sum x_2^2 \ldots & \sum x_2 x_K \\ \sum x_1 x_3 & \sum x_2 x_3 \ldots \sum x_3 x_K \\ . \\ . \\ . \\ \sum x_1 x_K & \sum x_2 x_K \ldots \sum x_K^2 \end{bmatrix} \begin{bmatrix} b_1 \\ b_2 \\ b_3 \\ . \\ . \\ . \\ b_K \end{bmatrix} = \begin{bmatrix} \sum x_1 y \\ \sum x_2 y \\ \sum x_3 y \\ . \\ . \\ . \\ \sum x_K y \end{bmatrix} \qquad (12.19)$$

or

$$\begin{bmatrix} b_1 \\ b_2 \\ b_3 \\ . \\ . \\ . \\ b_K \end{bmatrix} = \begin{bmatrix} \sum x_1^2 & \sum x_1 x_2 \ldots \sum x_1 x_K \\ \sum x_1 x_2 & \sum x_2^2 \ldots & \sum x_2 x_K \\ \sum x_1 x_3 & \sum x_2 x_3 \ldots \sum x_3 x_K \\ . \\ . \\ . \\ \sum x_1 x_K & \sum x_2 x_K \ldots \sum x_K^2 \end{bmatrix}^{-1} \begin{bmatrix} \sum x_1 y \\ \sum x_2 y \\ \sum x_3 y \\ . \\ . \\ . \\ \sum x_K y \end{bmatrix} \qquad (12.20)$$

The values of b_1, b_2, b_3, ..., b_K can be obtained by finding the inverse of the matrix of sums of squares and sums of the products. Let the inverse of this matrix be defined as

$$\begin{bmatrix} \sum x_1^2 & \sum x_1 x_2 \ldots \sum x_1 x_K \\ \sum x_1 x_2 & \sum x_2^2 \ldots & \sum x_2 x_K \\ \sum x_1 x_3 & \sum x_2 x_3 \ldots \sum x_3 x_K \\ . \\ . \\ . \\ \sum x_1 x_K & \sum x_2 x_K \ldots \sum x_K^2 \end{bmatrix}^{-1} = \begin{bmatrix} C_{11} & C_{12} & C_{13} \ldots & C_{1K} \\ C_{21} & C_{22} & C_{23} & \ldots C_{2K} \\ C_{31} & C_{32} & C_{33} & \ldots C_{3K} \\ . \\ . \\ C_{K1} & C_{K2} & C_{K3} \ldots C_{KK} \end{bmatrix} \qquad (12.21)$$

where $C_{ij} = C_{ji}$. Consequently, the values of partial regression coefficients b_1, b_2, b_3, ..., b_K are

$$b_1 = C_{11} \sum x_1 y + C_{12} \sum x_2 y + \ldots + C_{1K} \sum x_k y$$

$$b_2 = C_{21} \sum x_1 y + C_{22} \sum x_2 y + \ldots + C_{2K} \sum x_k y$$

$$.$$
$$.$$
$$\qquad (12.22)$$

$$b_K = C_{K1} \sum x_1 y + C_{K2} \sum x_2 y + \ldots + C_{KK} \sum x_k y$$

If Y' represents the value of Y estimated from regression equation (12.23):

$$Y' = A + b_1 X_1 + b_2 X_2 + ... + b_K X_K \tag{12.23}$$

then the coefficient of multiple correlation is the simple correlation between Y and Y'. In terms of the deviations from the means, it will be the simple correlation between y and e where e is the value of y estimated from equation (12.24):

$$e = b_1 x_1 + b_2 x_2 + ... + b_K x_K \tag{12.24}$$

The multiple correlation coefficient defined as R is given by the following equation:

$$1 - R^2 = \frac{\Sigma d^2}{\Sigma d_o^2} \tag{12.25}$$

where d = deviation of observed Y from the estimated Y, and d_0 = deviation of observed Y from the mean.

or

$$1 - R^2 = \frac{\Sigma (Y - Y')^2}{\Sigma (Y - \bar{Y})^2} \tag{12.26}$$

Example 12.3: Determine the relation between y and x_1, x_2, x_3 from the following sum of squares and sums of products measured from their means based on 10 sets of observations:

$\Sigma x_1 y = 34$, $\Sigma x_1^2 = 32$, $\Sigma x_1 x_2 = 46$, $\Sigma x_2 y = 50$, $\Sigma x_2^2 = 68$, $\Sigma x_1 x_3 = 62$, $\Sigma x_3 y = 70$, $\Sigma x_3^2 = 128$, $\Sigma x_2 x_3 = 92$, $\Sigma y^2 = 40$

Solution: The multiple regression equation is:

$$y = b_1 x_1 + b_2 x_2 + b_3 x_3$$

Now the normal equations will be:

$$\Sigma x_1 y = b_1 \Sigma x_1^2 + b_2 \Sigma x_1 x_2 + b_3 \Sigma x_1 x_3$$

$$\Sigma x_2 y = b_1 \Sigma x_1 x_2 + b_2 \Sigma x_2^2 + b_3 \Sigma x_2 x_3$$

$$\Sigma x_3 y = b_1 \Sigma x_1 x_3 + b_2 \Sigma x_2 x_3 + b_3 \Sigma x_3^2$$

We have

$$34 = 32b_1 + 46b_2 + 62b_3$$

$$50 = 46b_1 + 68b_2 + 92b_3$$

$$70 = 62b_1 + 92b_2 + 128b_3$$

Solving the above equations by the matrix method we have:

$$\begin{bmatrix} 32 & 46 & 62 \\ 46 & 68 & 92 \\ 62 & 92 & 128 \end{bmatrix} \begin{bmatrix} b_1 \\ b_2 \\ b_3 \end{bmatrix} = \begin{bmatrix} 34 \\ 50 \\ 70 \end{bmatrix}$$

$$\begin{bmatrix} b_1 \\ b_2 \\ b_3 \end{bmatrix} = \begin{bmatrix} 32 & 46 & 62 \\ 46 & 68 & 92 \\ 62 & 92 & 128 \end{bmatrix}^{-1} \begin{bmatrix} 34 \\ 50 \\ 70 \end{bmatrix}$$

$$\begin{bmatrix} 32 & 46 & 62 \\ 46 & 68 & 92 \\ 62 & 92 & 128 \end{bmatrix}^{-1} = \begin{bmatrix} 1.1539 & -0.8846 & 0.0769 \\ -0.8846 & 1.2116 & -0.4423 \\ 0.0769 & -0.4423 & 0.2885 \end{bmatrix}$$

$$\begin{bmatrix} b_1 \\ b_2 \\ b_3 \end{bmatrix} = \begin{bmatrix} 1.1539 & -0.8846 & 0.0769 \\ -0.8846 & 1.2116 & -0.4423 \\ 0.0769 & -0.4423 & 0.2885 \end{bmatrix} \begin{bmatrix} 34 \\ 50 \\ 70 \end{bmatrix}$$

Partial regression coefficients b_1, b_2 and b_3 are:

$$\begin{aligned}
b_1 &= 1.1539 \times 34 - 0.8846 \times 50 + 0.0769 \times 70 \\
&= 39.2326 - 44.23 + 5.383 \\
&= 0.3856 \\
b_2 &= -0.8846 \times 34 + 1.2116 \times 50 - 0.4423 \times 70 \\
&= -30.0764 + 60.580 - 30.961 \\
&= -0.4574 \\
b_3 &= 0.0769 \times 34 - 0.4423 \times 50 + 0.2885 \times 70 \\
&= 2.6146 - 22.115 + 20.195 \\
&= 0.6946
\end{aligned}$$

The required equation is

$$y = 0.3856x_1 - 0.4574x_2 + 0.6946x_3$$

where y, x_1, x_2 and x_3 are departures from their mean values.

12.9 REQUIRED PARAMETERS IN LONG-RANGE FORECASTING OF INDIAN SUMMER MONSOON RAINFALL

As discussed above, the long range forecasting of Indian summer monsoon rainfall was started more than a century ago (Blanford, 1884). Since then many statistical techniques have been developed and used for the prediction of monsoon rainfall (Thapliyal 1990; Shukla and Paolino, 1983; Mooley et al., 1986; Bhalme et al., 1986; Shukla and Mooley, 1987; Gowarikar et al., 1991). Most of these studies are based on the statistical technique of multiple regression analysis as described in the preceding section.

Recently, researchers from the India Meteorological Department have developed a regression equation from a comprehensive set of 16 well established predictors to predict the monsoon rainfall. However, in developing the model each predictor is raised to a power which is given below:

$$y = A + b_1(x_1)^{P1} + b_2(x_2)^{P2} + ... + b_K(x_K)^{PK} \qquad (12.27)$$

The sixteen predictors are broadly classified into three groups, namely, (1) pressures, (2) upper winds and temperatures, and (3) snow cover and atmospheric oscillations. These 16 predictors are given in Table 12.3.

It should be noted that in spite of considerable research in long range forecasting in India, the technique is still not a perfect one.

Table 12.3: Predictor variables

Predictors	Detail
(a) Pressure parameters	
X1	Location of a 500 mb ridge over India along 75º E in April
X2	Darwin pressure in April
X3	Argentina pressure in April
X4	Indian Ocean equatorial pressure in January to May
X5	Northern hemisphere surface pressure anomalies from January to May
X6	50 mb east-west extent of trough-ridge pattern over northern hemisphere in January and February
(b) Upper winds and Temperature parameters	
X7	10 mb westerly wind over Balboa in January
X8	Central India minimum temperatures in May
X9	Northern India minimum temperatures in March
X10	Minimum temperatures over the east coast of India in March
X11	Northern hemispherical surface temperatures in January and February
(c) Snow cover and Atmospheric oscillations	
X12	Eurasian snow cover in previous December
X13	Himalayan snow cover from January to March
X14	The SO index (Tahiti-Darwin pressure) from March to May
X15	The El Nino category (measured by sea surface temperatures over the equatorial south-eastern Pacific of previous year)
X16	The El Nino category of current year (October of previous year to May of current year)

REFERENCES

Bhalme, H.N., Jadhav, S.K., Movley, D.A. and Ramana Murty, Bh. V., 1986. Forecasting of monsoon performance over India. *Journal of Climatology*, 6, pp. 347-354.

Blanford, H.F., 1884. On the connection of the Himalayan snowfall and seasons of droughts in India. *Proceedings Royal Society, London,* 37, pp. 3-22.

Gowarikar, V., Thapliyal, V., Kulshrestha, S.M., Mandal, G.S., Sen Roy, N. and Sikka, D.R., 1991. A power regression model for long range forecast of southwest monsoon rainfall over India. *Mausam*, 42, pp. 125-130.

Krishna Kumar, K., Soman, M.K. and Rupa Kumar, K., 1995. Season forecasting of Indian summer monsoon rainfall: A review. *Weather*, 50, pp. 449-467.

Mooley, D.A., Parathasarathy, B. and Pant, G.B., 1986. Relationships between Indian summer monsoon rainfall and location of the ridge at 500 mb level along 75° E. *Journal of Climatology and Applied Meteorology*, 15, p. 640.

Pant, G.B. and Parthasarthy, B., 1981. Some Aspects of an Association between the Southern Oscillation and Indian Summer Monsoon. *Arch. Met. Geoph. Biokl.*, Ser B, 29, pp. 245-252.

Ropelewski, C.F. and Jones, P.D., 1987. An extension of the Tahiti-Darwin Southern Oscillation Index. *Monthly Weather Review*, 115, pp. 2161-2165.

Sahai, A.K., Grimm, A.M., Satyan, V. and Pant, G.B., 2003. Long-term prediction of Indian summer monsoon rainfall from global SST evolution. *Climate Dynamics*, 20, pp. 855-863.

Shukla, J. and Mooley, D.A., 1987. Empirical prediction of the summer monsoon rainfall over India. *Monthly Weather Review*, 115, pp. 695-703.

Shukla, J. and Paolina, D.A., 1983. The southern oscillation and long range forecasting of summer monsoon rainfall over India. *Monthly Weather Review*, 111, pp. 1830-1837.

Thapliyal, V., 1990. Long range prediction of summer monsoon rainfall over India: Evolution and development of new models. *Mausam*, 44, pp. 339-346.

Troup, A.J., 1965. The Southern Oscillation. *Quart. J.R. Met. Soc*, 91, pp. 490-506.

Wright, P.B., 1984. Relationships between indices of the Southern Oscillation. *Monthly Weather Review*, 112, pp. 1913-1919.

Walker, G.T., 1908. Correlation in Seasonal Variation of Climate (Introduction). *Mem. India Meteorol. Dept.*, 20, pp. 117-124.

Walker, G.T., 1918. Correlation in Seasonal Variation of Weather. *Quart. J.R. Met. Soc.*, 44, pp. 223-224.

Walker, G.T., 1924. Correlation in Seasonal Variation of Weather – IX. A further study of World Weather. *Mem. India Meteorol. Dept.*, 24, pp. 275-332.

13 Evaporation

It has already been stated that precipitation in the form of rain and snow is the major source of water over the surface of the earth. Of this water, a sizable portion is lost as water vapor to the atmosphere by evaporation and transpiration. For example, of the 1170 mm of water that is received annually as precipitation in India about 597 mm (51%) of water is lost to the atmosphere through evaporation and transpiration and only the remainder is available to streams and soils and underground formations. In the United States, of the 750 mm of the average yearly precipitation received, about 70% is evaporated, thus reducing the total water obtained by about three fourth. These data illustrate the importance of evaporation for water resources development and water conservation. In countries where surface water storage is important over large areas, evaporation is even more significant.

Evaporation occurs from land and water bodies of the earth, whereas transpiration occurs from plant leaves through their stomata. Although these two processes are different but in hydrometeorology it is possible to treat them together, since the forcing mechanisms that cause evaporation and transpiration are controlled by similar meteorological factors, such as temperature, radiation, sunshine, humidity, wind, air pressure, soil moisture, and so on. The combined process is called evapotranspiration. The study of evaporation is fundamental for calculating water losses from reservoirs and lakes and evapotranspiration is fundamental to agriculture for modeling crop growth. In this chapter we will deal with evaporation, discuss its measurement and estimation techniques.

13.1 PHYSICS OF EVAPORATION

Evaporation occurs when there is free water surface, be it water in a pond or in the bare soil. Evaporation is defined as the process by which water in the liquid state is changed to the vapor or gaseous state. Obviously, evaporation can only occur when water is available. The evaporation process needs large

amounts of heat energy. For example, evaporation of one gram of water needs about 580 calories of heat energy. A source of heat may be direct solar energy, sensible heat from the air, heat from the ground or stored heat from the water itself

The physics of evaporation can best be explained by considering a body of water in a pond. The mass of water is made up of a large number of water molecules. These molecules are in a state of motion with their varying velocities dependent largely upon temperature. A slight increase in temperature causes an increase in the speed of molecules when some molecules in the water body acquire enough kinetic energy; they escape from the water surface into the overlying air and stay as vapor above the water surface. In a similar manner, the overlying air contains water molecules which are also in motion and some of them enter the water surface. In this way there is a continuous exchange of water molecules between the evaporating water surface and its overlying air. When the escaping molecules exceed the returning molecules the evaporation is said to occur. If returning molecules exceed the escaping molecules then there is condensation of water vapor.

Evaporation as a Net Rate of Vapor Flow

It was first recognized by John Dalton in 1802 that evaporation is a net rate of vapor transfer. Immediately near the water surface is a shallow layer of air whose temperature is the same as that of water. The motion of the escaping molecules produces pressure in a shallow layer. This pressure of the aqueous vapor is called the vapor pressure. This shallow layer may quickly become saturated with the water vapor corresponding to the water temperature. The vapor pressure of the air above the shallow layer or water surface depends upon its humidity and temperature. If the actual vapor pressure of this overlying air is less than that at the shallow layer or water surface, evaporation will occur. According to Dalton's law the rate of evaporation from the water surface is proportional to the difference between the vapor pressure (e_w) at the surface and the vapor pressure (e_a) in the overlying air. Mathematically,

$$E = C (e_w - e_a) \tag{13.1}$$

where E = evaporation in mm per day; e_w = the saturation vapor pressure corresponding to the temperature of shallow layer or water (in mm of mercury); e_a = the actual vapor pressure in the overlying air (in mm of mercury); and C = a coefficient depending upon the wind velocity and other factors affecting evaporation.

13.2 FACTORS AFFECTING EVAPORATION

Evaporation from a water surface is influenced by both meteorological and non-meteorological factors. Meteorological factors include solar radiation, temperature of water and overlying air, humidity, wind, and atmospheric

pressure. Non-meteorological factors include area of the water surface, depth of water, and the quality of the evaporating surface. These factors are briefly described in what follows.

Evaporation from the water surface is largely dependent on the available heat energy. Solar radiation is the dominant source of energy and sets broad limits of temperature. Values of solar radiation are high in the tropics (Chapter 4) and hence evaporation is considerably high.

Air and water temperature are related to solar radiation and hence evaporation increases if the temperature of the air and water surface is high. The surface temperature of water governs the vapor pressure gradient. If the temperature of the overlying air is high evaporation will proceed more rapidly, since the capacity of the air to absorb water vapor increases. Thus, in summer season or in hot countries evaporation is more than in winter season or cold countries.

Humidity affects evaporation. It is a measure of the extent to which air contains water vapor and consequently an indication of its capacity to absorb vapor due to evaporation from the water surface. If humidity of the air is more, evaporation will be less. Because water vapor during the process of evaporation moves from the point of higher vapor content to the point of lower vapor content, the rate of movement is governed by the difference of their vapor contents or the humidity gradient existing in the air. Thus, for rapid evaporation a steep humidity gradient away from the water surface is important.

The velocity of wind is also an important factor affecting evaporation. The process of evaporation removes water vapor from a water surface to a shallow air layer very near the water surface. When this shallow layer attains saturation then evaporation stops. If the turbulence is more or if the velocity of wind immediately above the water surface is sufficient, the saturated layer of air is easily removed by the wind and more opportunity for evaporation is created. Moderate wind velocity tends to maintain a steep humidity gradient and high evaporation rates.

Other meteorological factors remaining constant, a decrease in the atmospheric pressure as in high altitudes increases evaporation. Non-meteorological factors that influence evaporation are briefly discussed. The amount of evaporation is directly proportional to the area of the evaporating surface. If the exposed area is large, evaporation will be more and vice versa. The quality of water is also important. When a solute is dissolved in water, the vapor pressure of the solution is less than that of pure water and hence causes a reduction in evaporation. The rate of evaporation from lakes and rivers is more than that from saline sea water. The color and reflective (albedo) properties of evaporative surfaces influence evaporation. Evaporation from bare soils is often less than from open water surface because water is not always freely available.

13.3 MEASUREMENT OF EVAPORATION

The amount of evaporation, which is usually expressed in mm, from a water surface can be measured by exposing a vessel or pan of water. The water is filled in the pan up to a certain level and drop in water level is measured over a given time period (usually a day). It is found that evaporation from a large body of water, such as a lake and reservoir, is not the same as from a small pan. The evaporation obtained from a small pan is adjusted by a suitable pan coefficient, so as to obtain the evaporation from a large body of water. Different shapes of pans have been designed by different designers and different values of the pan coefficients have been given. Some of the important pans are described below.

  (i) **U.S. Weather Bureau Class A Pan-Evaporimeter:** This pan is 1210 mm (4 ft) in diameter, 255 mm (10 in.) deep and is mounted 150 mm (6 in.) above the ground on a wooden frame. The pan is filled with water and the depth of water is maintained between 180 mm and 200 mm. The drop in water level in one day is measured with a hook gauge in a stilling well. The pan is normally made of unpainted galvanized iron sheet. The evaporimeter is installed where other meteorological instruments are kept. The pan coefficient is about 0.6 to 0.8 with an average value of 0.7. The weather services throughout the world use this evaporimeter for measuring evaporation. The weather services report evaporation at different stations each day. Figure 13.1 shows the US Weather Bureau class A pan evaporimeter.
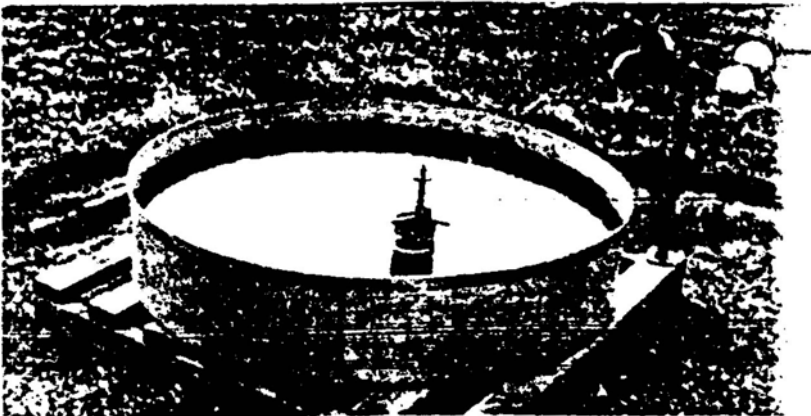
Fig. 13.1. U.S. Weather Bureau class A pan.

 (ii) **Colorado Sunken Pan:** This pan is 920 mm square and 460 mm deep and is made up of unpainted galvanized iron sheet. The pan is buried in the ground such that only 100-150 mm projects above the ground

surface. The water level in the pan is maintained almost at the ground level. Evaporation is measured by a point gauge. The main advantage of the sunken pan is that radiation and wind characteristics are similar to those of a lake. The pan coefficient is 0.75 to 0.86 with an average value of 0.78.

(iii) **U.S. Geological Survey Floating Pan:** This is a 900 mm square, 450 mm deep pan supported by drum floats in the middle of a raft (4250 mm × 48.50 mm) and is set floating in a lake. The water level in the pan is kept at the same level as the lake with the sides of the pan projecting 75 mm above. The pan coefficient is generally taken as 0.80. The pan more or less represents the characteristics of a lake.

The World Meteorological Organization (WMO) recommendations for the minimum number of evaporation stations needed for evaporation measurements in different geographical regions are given in Table 13.1.

Table 13.1: WMO criteria for evaporation stations

Region	Minimum density km^2/station
1. Arid regions	30,000
2. Humid temperate climate	50,000
3. Cold regions	100,000

13.4 EVAPORATION MEASUREMENT IN INDIA

In India, the U.S. Weather Bureau class A pan evaporimeters are used for the measurement of evaporation. Regular observations of evaporation are made at some 200 stations throughout the country by the India Meteorological Department (IMD). IMD (1980) has published monthly and annual mean evaporation values for 30 stations in India. The seasonal mean daily evaporation for some stations is given in Table 13.2 and the spatial variation of mean annual evaporation for the Indian region is shown in Fig. 13.2. There are also some records available which are maintained by agricultural and irrigation departments of the state governments. Figure 13.2 shows a variation in evaporation from 500 mm in northeast to 1500 mm in the dry part of western Rajasthan and Gujarat. The mean rate of evaporation in an arid and a semi arid region is often in excess of the local rainfall for that region. As a result, significant quantities of water are lost.

It is pointed out that for augmenting water storage and ensuring efficient management of water resources, it is most essential to obtain estimates of evaporation from large bodies of water, such as lakes and reservoirs. Pan measurements do not represent evaporation from large bodies of water, such as lakes or reservoirs. Many methods have been developed to estimate evaporation from lakes and reservoirs. These methods will be discussed in the following section.
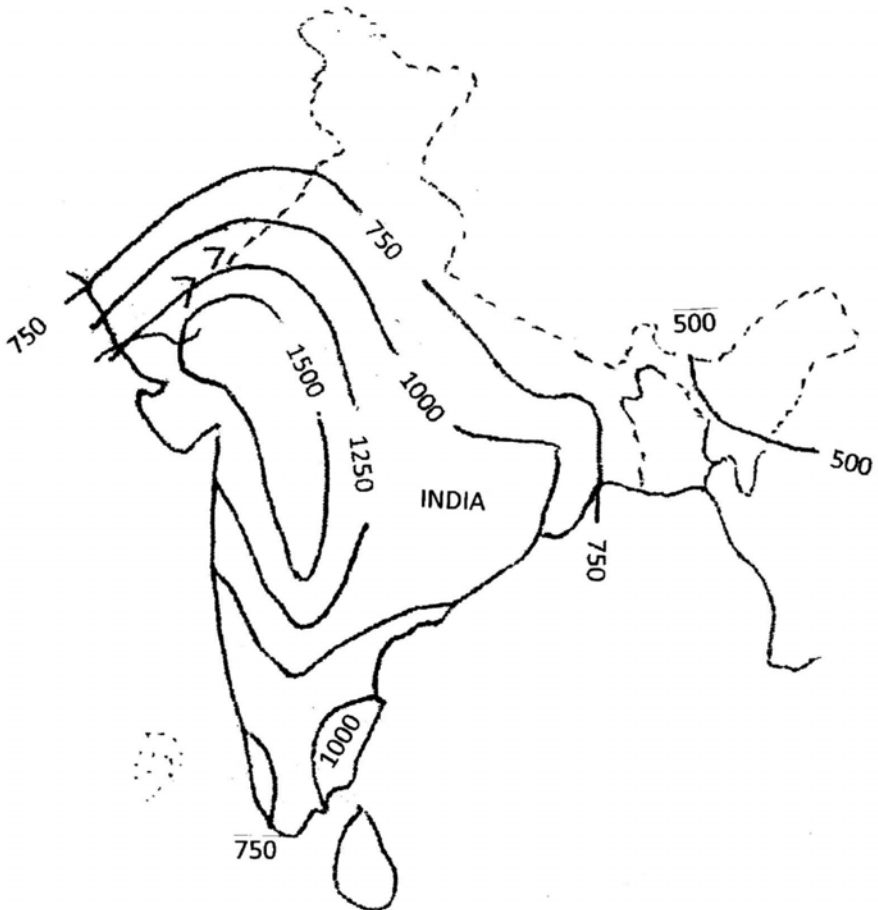
Fig. 13.2. Spatial variation of mean evaporation (mm) in India.

13.5 ESTIMATION OF EVAPORATION BY INDIRECT METHODS

To estimate the amount of evaporation the following methods are used when direct (evaporimeter) measurements cannot be obtained for lakes and reservoirs:

- Water budget methods
- Energy balance methods
- Vapor flow methods
- Empirical formulae
- Combination of energy and vapor flow methods
- Using pan coefficients.

Details of methods are found in several references, for example, Chang (1968), Oliver (1961), Wieisner (1970), and Penman (1963). Here, these methods are briefly discussed.

Table 13.2: Seasonwise mean daily evaporation in mm measured by the U.S.
Weather Bureau Class A pan evaporimeter in India

Station	*Winter (Dec-Feb.)*	*Hot weather (March-May)*	*SW-monsoon (June-Sept.)*	*Post monsoon (Oct.-Nov.)*	*Annual*
Agartala	3.2	6.5	4.5	3.2	4.4
Ahmedabad	5.8	11.2	6.7	6.3	7.5
Allahabad	2.6	7.2	5.5	3.5	4.7
Agra	3.5	10.5	8.0	4.3	6.6
Bangalore	4.8	7.2	4.1	3.7	4.9
Bikaner	3.2	9.5	9.5	5.4	6.9
Mumbai	3.7	5.6	3.5	3.9	4.2
Kolkata	3.0	5.7	4.1	3.6	4.1
Hyderabad	6.2	10.0	6.7	5.3	7.0
Jodhpur	2.1	5.6	4.4	2.8	3.7
Kota	4.6	12.4	8.8	5.6	7.8
Chennai	4.2	6.3	6.8	3.7	5.3
New Delhi	3.7	8.7	7.1	5.4	6.2
Patna	3.0	9.1	5.7	3.3	5.3
Roorkee	2.5	8.2	6.1	3.4	5.1
Trivandrum	4.1	4.4	3.8	3.7	4.0
Pune	5.2	10.3	4.7	4.9	6.3

13.5.1 Water Budget Method

The water budget method to determine evaporation from a lake or reservoir
is basically based on a balance between inflows, outflows, and a change in
the storage (Chow, 1964; Linsley et al., 1975). It involves writing the
hydrologic continuity equation for the lake and estimating evaporation from
the knowledge of other parameters. Thus, considering daily average values
for a lake, the water budget equation is written as:

$$P + R_1 + R_g = R_0 + R_s + E + T \pm \Delta S \tag{13.2}$$

or

$$E = P + R_1 + R_g - R_0 - R_s - T \pm \Delta S \tag{13.3}$$

where P = daily precipitation, R_1 = daily surface inflow into the lake,
R_g = daily groundwater inflow, R_0 = daily surface outflow from the lake,
R_s = daily seepage outflow, E = daily lake evaporation, T = daily transpiration,
and ΔS = change in lake storage in a day.

It is useful to deal with the net seepage outflow through the ground and
as such $R_g - R_s = 0$. Transpiration losses T can be considered to be insignificant.
Equation (13.3) becomes

$$E = P + R_1 - R_0 \pm \Delta S \tag{13.4}$$

(+ value for an increase in storage and – value for a decrease). All the terms in eq. (13.4) are in volume (m^3) or depth (mm) units for a given time period. If all other terms are known, E can be calculated. If the unit of time is kept large, say a week or more, better accuracy in the estimates of E is possible. The water budget method, although having the obvious advantage of being simple in theory but for various uncertainties and the possibilities of errors in measured variables, cannot be expected to give fairly accurate results. However, controlled studies for Lake Hefner in the U.S.A. have given fairly accurate results using this method.

Example 13.1: For a given year, 2500 km^2 lake received 40 cm of rainfall. The annual rate of flow measured was found to be 20 cumecs. Determine an estimate of evaporation from the lake during the year of record.

Solution: The basic hydrologic equation is: $E = P + R_1 – R_0 \pm \Delta S$. Considering $\Delta S = 0$ and $R_1 = 0$ we have $E = P – R_0$, 1 day = 86400 sec,

$$R_0 = \frac{20 \times 86400 \times 365 \times 100}{2500 \times 1000 \times 1000} \text{ cm} = 25.2 \text{ cm}$$

Therefore, $E = 40 – 25.2 = 14.8$ cm/year.

13.5.2 Energy Balance Method

The method is based upon the principle of conservation of heat energy and cooling produced by evaporation. Heat is dissipated during evaporation and the heat lost must be equal to the heat gained. If the total heat energy reaching the water surface and energy going out of the water surface and energy stored in the water body are known over a given time period, the amount of evaporation can be obtained.

We consider a body of water as shown in Fig. 13.3. The sources of heat responsible for the thermal balance at the water surface can be accounted for. This leads to the energy budget equation for the evaporating surface for a given period of time written as:

$$(1 – r) H_c = H_b + LE + H + H_a + G + H_s \tag{13.5}$$
$$(1 – r) H_c – H_b = LE + H + H_a + G + H_s \tag{13.6}$$
$$Q_n = LE + H + H_a + G + H_s \tag{13.7}$$

where Q_n = the net heat energy received by the water surface; H_c = solar radiation incident to water surface; r = albedo; rH_c = solar radiation reflected from the water surface of albedo r; $H_c (1 – r)$ = solar radiation into the water body; H_b = outgoing radiation from the water body; H = sensible heat transfer from air to water surface or in the opposite direction; LE = Heat energy used in evaporation and L, the latent heat of evaporation; G = heat flux into the ground; H_s = heat stored in the water body; and H_a = heat moved out or into the water body by water outflow or inflow.
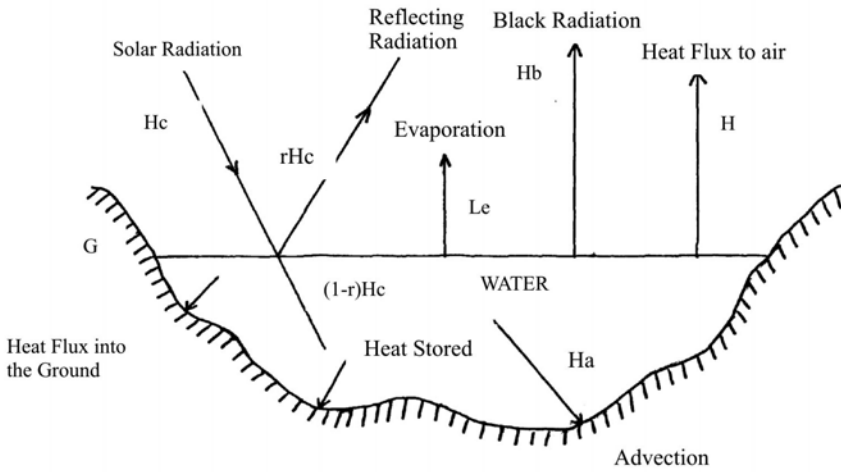
Fig. 13.3. Energy balance.

For many land surfaces the ground heat flux, *G,* is small and can be neglected. Also, if the time periods are small then terms H_s and H_a are very small and negligible. Therefore, equation (13.7) becomes

$$Q_n = LE + H \tag{13.8}$$

All the energy terms are in calories/cm^2 per day. All the terms except H can either be measured or evaluated indirectly. The sensible heat term H which cannot be evaluated is estimated using the Bowen ratio.

Bowen (1926) realized that the transport of vapor and the transport of heat are controlled by the same mechanism that is atmospheric turbulence, the one being governed by $(e_w - e_a)$ and other by $(T_w - T_a)$ and established Bowen's ratio β, given as

$$\beta = \frac{H}{EL} = 6.1 \times 10^{-4}\, p\, \frac{T_w - T_a}{e_w - e_a} \tag{13.9}$$

$$\beta = \gamma\, \frac{T_w - T_a}{e_w - e_a} \tag{13.10}$$

where p = the atmospheric pressure, T_w = the water surface temperature in °C , T_a = the air temperature in °C, e_w = the saturation vapor pressure corresponding to the water surface temperature T_w in mb, e_a = the vapor pressure of the air in mb and γ = the psychrometer constant with a value of 0.49 if temperature and vapor pressure are in °C and mm, respectively.

From equations (13.8) and (13.9), E can be evaluated as

$$Q_n = LE + \beta LE \tag{13.11}$$

$$E = \frac{Q_n}{L(1 + \beta)}$$

$$E = \frac{Q_n}{L} \frac{1}{1 + \gamma\left(\dfrac{T_w - T_a}{e_w - e_a}\right)} \tag{13.12}$$

The value of Q_n can be determined either directly from appropriate instruments or from an appropriate empirical formula. Bowen's ratio β can be determined from eq. (13.10) or from the principle of wet bulb hygrometry, measurements of temperature and humidity at two levels. The mean values of Bowen ratios (β) at various latitudes are given in Table 13.3.

Table 13.3: Mean value of β at different latitudes

Latitude (°N)	10	20	30	40	50	60	70
β	0.1	0.1	0.13	0.18	0.25	0.37	0.53

Example 13.2: The values of β and Q_n at the latitude 20° are 0.10 and 150 cal/cm^2/day. Determine the evaporation.

Solution: We have $E = \dfrac{Q_n}{L(1 + \beta)}$. Taking $L = 585$, and $E = \dfrac{150}{585(1 + 0.10)}$

$E = 0.23$ cm/day

The energy balance method for estimation of evaporation from a lake has been found to provide fairly accurate results when applied to periods of a week or more. However, the method involves a great deal of instrumental measurements, and it cannot therefore be readily used for want of such data which normally are not available for many stations throughout the world.

An acceptable relationship for computing the net radiation (Q_n) from meteorological data is given by the following equation:

$$Q_n = Q_A(1 - r)\left(a + b\frac{n}{N}\right) - \sigma T_a^4(0.56 - 0.09\sqrt{e_a}) \times \left(0.10 + 0.90\frac{n}{N}\right) \tag{13.13}$$

where Q_n = net incoming radiation in mm of evaporable water per day; Q_A = incident radiation outside the atmosphere on a horizontal surface expressed in mm of evaporable water per day, r = reflection coefficient or albedo, a = a constant depending upon the latitude of the station and is given by $a = 0.29 \cos \theta$, b = a constant with an average value of 0.52, θ = angle, n = actual hours of sunshine, N = theoretical duration of sunshine, σ = Stefan-Boltzmann constant = 2.01×10^{-9} mm of water per day per °K^4, e_a = actual vapor pressure of air in mm of mercury, and T_a = mean air temperature in degrees Kelvin (°K). Values of albedo (r) of some surfaces are given in Table 13.4 for use in the above formula.

Table 13.4: Values of albedo of some surfaces

Surface	Albedo
Water at 0-60° latitude (N)	<0.08
Water at 60-90° latitude (N)	<0.10
Snow	0.8
Earth's surface	0.15
Wood land	0.14
Tropical forest	0.13
Natural grassland	0.2

13.5.3 Vapor Flow Method

The vapor flow method of evaporation is based on the mass of water vapor transfer from the water surface to the atmosphere. As discussed in Section 13.1.1, Dalton (1802) showed that the rate of evaporation depends on the vapor pressure gradient between the evaporating surface and the air above, that is the difference between the saturated vapor pressure (e_w) at the water surface temperature and the vapor pressure (e_a) in the overlying air and a measure of vapor removal that should be a function of wind speed:

$$E = c\,f(u)\,(e_w - e_a) \tag{13.14}$$

where E is the rate of evaporation in mm per day and $f(u)$ is a function of wind. A more general form of equation (13.14) is given as

$$E = c(e_w - e_a)(a + bu) \tag{13.15}$$

where a, b and c are constants and u denotes an average wind speed at a suitable height. Terms e_w and e_a have their usual meaning and are already explained as above. The vapor flow method can be used for estimating evaporation if the velocity of wind and vapor distribution are known.

13.5.4 Empirical Formulae

Many empirical formulae to determine evaporation from lakes as a function of meteorological variables have been developed in various parts of the world. Chow (1964) gives a list of such formulae. Almost all formulae are based on Dalton's law and are of general form as shown in equation (13.15).

13.5.4.1 Meyer formula

Meyer (1915) derived a formula for estimating evaporation from shallow lakes in the U.S.A. His formula is:

$$E = k_M\,(e_w - e_a)\left(1 + \frac{U_9}{16}\right) \tag{13.16}$$

U_9 = the monthly mean wind velocity in km/hr at about 9 m above the ground, k_M = a coefficient accounting various factors with a value of 0.36 for large deep waters and 0.50 for small shallow waters, and E, e_w, and e_a are as defined in equation (13.1).

13.5.4.2 Rohwer's formula

Based on evaporation data from lakes and reservoirs in the U.S.A., Rohwer (1931) developed a formula for estimating evaporation as

$$E = 0.77 \ (1.465 - 0.000732 \ P) \ (0.44 + 0.0733 \ U_0) \ (e_w - e_a) \qquad (13.17)$$

where P = mean barometric pressure in mm of mercury, U_0 = mean wind velocity in km/hr at ground which can be taken at 0.6 m height, and E, e_w and e_a, are as defined in eq. (13.1).

13.5.4.3 Other empirical formulae

Other empirical formulae for estimation of evaporation are:
Penman (1948):

$$E = 0.40(1 + 0.27 \ U_0) \ (e_w - e_a) \qquad (13.18)$$
$$E = 0.35(1 + 0.0098 \ U_2) \ (e_w - e_a) \qquad (13.19)$$
$$E = 0.35(1 + U_2/100) \ (e_w - e_a) \qquad (13.20)$$

where U_0 and U_2 are wind velocity in miles/hr at surface and at 2 m, respectively, in equations (13.18) and (13.19). In equation (13.20), U_2 is wind velocity in miles/day at a height of 2 m.

Example 13.3: Estimate the average daily and monthly evaporation from a lake with the following data in the month of May: water temperature = 20°C; air temperature = 35°C; wind speed at 9 m = 20 km/hr; and relative humidity = 20%.

Solution: The saturation vapor pressure at 20°C and 35°C are found to be 17.5 mm and 42.2 mm, respectively. e_w = 17.5 mm of Hg; e_a = 42.2 × 0.20 = 8.4 mm of Hg. Using Meyer's formula we have

$$E \ (\text{mm/day}) = C\left(1 + \frac{U_9}{16}\right) (e_w - e_a)$$

C = 0.36 for the ordinary lake. Therefore,

E = 0.36(1+20/16)(17.5 − 8.4) = 0.36 × 2.25 × 9.1 = 7.4 mm/day

Total evaporation during the month of May = 7.4 × 31 = 229.4 mm

Example 13.4: Determine the average daily and the total volume of water evaporated during seven days from a lake of 200 ha surface area. The meteorological data are as follows: Water temperature = 20°C, RH = 40%, and wind speed at 1.0 m = 16 km/hr.

Solution: We can use Meyer's formula but the velocity at 9 m is to be estimated from the wind and elevation relation. We have

$$E = C\left(1 + \frac{U_9}{16}\right)(e_w - e_a)$$

The saturation vapor pressure at $20° = 17.5$ mm of Hg:

$$e_a = 17.5 \times 0.40 = 7.0 \text{ mm of Hg}$$

The wind speed is at 1.0 m, using the relation:

$$\frac{U_{h_1}}{U_{h_2}} = \left(\frac{h_1}{h_2}\right)^{\frac{1}{7}}$$

We can find the wind speed at 9 m:

$$U_9 = 16.0(9)^{1/7} = 16.0 \times 1.37 = 21.9 \text{ km/hr}$$

$$E = 0.36(17.5 - 7.0)\left(1 + \frac{21.9}{16}\right)$$

$$= 0.36 \times 10.5 \times 2.37 = 8.96 \text{ mm/day}$$

Volume of water evaporated in seven days $= 7 \times \left(\frac{8.96}{1000}\right) \times 200 \times 10^4$

$$= 125440 \text{ m}^3$$

13.5.5 Using Pan Coefficients

Direct measurements of evaporation by pan evaporimeters do not usually represent the evaporation rate from a lake or reservoir surface. As such these measurements cannot be applied to a lake or reservoir. This is mainly because a lake is large in size and deeper in depth and may be exposed to different wind speeds as compared to a pan. The small volume of water in the metallic pan is also greatly affected by temperature fluctuations due to solar radiations in contrast to the lake or reservoir. Hence evaporation from a lake is considerably less than that from measured pan evaporation. Therefore, pan evaporation data have to be adjusted to get the actual evaporation from lakes and reservoirs by applying a coefficient called a pan coefficient. The coefficient is expressed as the ratio of lake evaporation to pan evaporation and is given as

$$\text{Pan coefficient} = \frac{\text{Evaporation from the lake}}{\text{Evaporation from pan evaporimeter}}$$

The pan coefficient is determined by computing the lake evaporation theoretically and comparing it with the pan evaporation. Ratios of annual lake evaporation to pan evaporation are consistent from year to year and region to region, while monthly ratios often show considerable variation. On

an annual basis pan coefficients range from 0.67 to 0.82 with an average value of 0.7. Thus, on an annual basis, the lake evaporation is approximately 0.7 times the pan evaporation. Evaporation from the bare wet soil is about 0.6 times the pan evaporation. For the region of western Rajasthan in India, Khan and Bohra (1990) reported the pan coefficient of 0.67 on the annual basis. The values of pan coefficients for different pans are given in Table 13.5.

Table 13.5: Values of pan coefficients

Types of pan	*Average value*	*Range*
1. U.S. Weather Bureau Class A	0.7	0.60-0.80
2. Colorado Sunken	0.78	0.75-0.86
3. USGS Floating Pan	0.8	0.70-0.82

Example 13.5: In a given year the monthly pan evaporation from January to December near a reservoir site is listed below:

Month	J	F	M	A	M	J	J	A	S	O	N	D
Pan-evaporation (mm)	167	143	178	250	286	214	167	137	137	214	130	143

The water spread area of the reservoir in the beginning of January was 2.8 km^2 and at the end of December it was 2.5 km^2. Calculate the annual loss of water due to evaporation.

Solution: Cumulative evaporation (January-December) = 2166 mm

$$\text{Mean water spread area} = \frac{2.80 + 2.50}{2} = 2.65 \text{ km}^2$$

Apply the pan coefficient value of 0.70.

$$\text{Annual volume of water loss} = 0.7 \times 2.65 \times \frac{10^6 \times 2166}{10 \times 100} = 4.02 \times 10^6 \text{ m}^3$$

13.5.6 Combination of Energy and Vapor Flow Methods (Penman's Method)

In the development of this method both energy balance and vapor flow terms are incorporated. The method attempts to eliminate the problems of measurement of variables in both energy and vapor flow methods. The development of the method is discussed below.

The evaporation from the water surface, based on vapor flow method (or mass transfer), is given as

$$E = f(u) (e_w - e_a) \tag{13.21}$$

Here e_w is the saturation vapor pressure in the shallow layer near the water surface at its own temperature or at the water surface temperature. This temperature may not be the same as that of water and is also difficult to measure. In order to use equation (13.21), the saturation vapor pressure e_s of the air is used instead of e_w at the water temperature and related evaporation to the saturation deficit term $e_s - e_a$. Thus, we have

$$E_a = f(u) \ (e_s - e_a) \tag{13.22}$$

where E_a = evaporation for the hypothetical case of equal temperatures of air and water, e_s = saturation vapor pressure at air temperature, and e_a = actual vapor pressure at air temperature.

From equations (13.21) and (13.22) we have

$$\frac{E_a}{E} = \frac{e_s - e_a}{e_w - e_a} = 1 - \frac{e_w - e_s}{e_w - e_a} \times \frac{T_w - T_a}{T_w - T_a} \tag{13.23}$$

It can be seen from Fig. 13.4 (curve of saturation pressure with temperature) that $(e_w - e_s)/(T_w - T_a)$ or $(e_s - e_w)/(T_a - T_w)$ is the change of the saturated vapor pressure with temperature at T_a or the slope of the saturation vapor pressure curve.
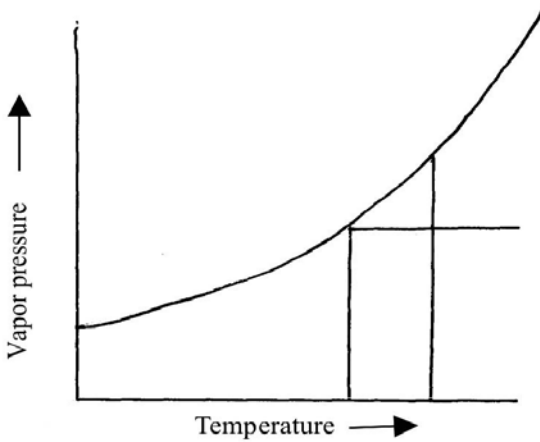
Fig. 13.4. Saturation vapor pressure with temperature.

Therefore, if $(e_w - e_s)/(T_w - T_a) = \Delta$ (slope of the vapor pressure curve), then substituting in equation (13.23) we have

$$\frac{E_a}{E} = 1 - \Delta \frac{T_w - T_a}{e_w - e_a} \tag{13.24}$$

From equation (13.12) we have

$$E = \frac{Q_n/L}{1 + \gamma \left(\dfrac{T_w - T_a}{e_w - e_a} \right)} \tag{13.25}$$

Substituting the value of $(T_w - T_a)/(e_w - e_a)$ in equation (13.25),

$$E(\Delta + \gamma) - \gamma E_a = \Delta Q_n/L$$

$$E = \frac{\Delta Q_n + \gamma E_a}{\Delta + \gamma} \tag{13.26}$$

where Q_n = net energy expressed in evaporation units, E_a = a function of wind speed at 2 m above ground, the saturated vapor pressure at mean air temperature and the actual vapor pressure at mean air temperature, γ = the psychrometric constant, and Δ = the slope of the saturation vapor pressure temperature curve (Fig. 13.4). The values of Δ obtained for some selected temperatures are as given below

Temp (degree centigrade)	Δ mm of Hg/°C
0	0.18
10	0.36
20	0.61
30	1.07

Using equation (13.26), evaporation can be calculated from readily available meteorological data. These estimates are most reliable when measured values of net radiation are used, but useful approximations are obtained when radiation is estimated from extraterrestrial solar radiation, sunshine temperature and humidity data.

13.5.7 Computation of Net Energy

The net energy Q_n used in equation (13.26) can be determined from equation (13.13) for the energy balance method. The equation is

$$Q_n = Q_A(1 - r)\left(a + b\,\frac{n}{N}\right) - \sigma T^4(0.51 - 0.09\sqrt{e_a})\left(0.10 + 0.90\,\frac{n}{N}\right) \tag{13.27}$$

The symbols have their meaning as explained in equation (13.13). Mean monthly values of possible hours of sunshine (N) as a function of latitude are given in Table 12.6 and the mean monthly values of solar radiation arriving at the outer limit of the atmosphere (Q_A) in gram calories per cm^2 per day as a function of latitude are given in Table 13.7.

The values of Q_A in Table 13.7 arriving at the earth's surface are based on the assumption that the atmosphere is perfectly transparent and there were no clouds. However, the amount of radiation depends on the latitude, season of the year, and degree of cloudiness. Thus, the values given in Table 13.7 must be adjusted to account for due to cloudiness. Generally this can be calculated by the following empirical relationship:

$$R_c = Q_A\left(a + b\,\frac{n}{N}\right) \tag{13.28}$$

Table 13.6: Mean monthly values of possible sunshine hours

Latitude North	J	F	M	A	M	J	J	A	S	O	N	D
0°	12.1	12.1	12.1	12.1	12.1	12.1	12.1	12.1	12.1	12.1	12.1	12.1
10°	11.6	11.8	12.1	12.4	12.6	12.7	12.6	12.4	12.9	11.9	11.7	11.5
20°	11.1	11.5	12	12.6	13.1	13.3	13.2	12.8	12.3	11.7	11.2	10.9
30°	10.4	11.1	12	12.9	13.7	14.1	13.9	13.2	12.4	11.5	10.6	10.2
40°	9.6	10.7	11.9	13.2	14.4	15	14.7	13.8	12.5	11.2	10	9.4
50°	8.6	10.1	11.8	13.8	15.4	16.4	16	14.5	12.7	10.8	9.1	8.1

Table 13.7: Mean monthly solar radiation at the outer limit of the atmosphere in gram calories per sq cm per day (Q_A)

North Latitude	J	F	M	A	M	J	J	A	S	O	N	D
0°	844	963	878	876	803	803	792	820	891	866	873	829
10°	631	795	821	914	912	947	912	887	856	740	666	599
20°	358	538	663	847	930	1001	941	843	719	528	397	318
30°	86	234	424	687	866	983	892	714	494	258	113	55
40°	0	3	143	518	875	1060	930	600	219	17	0	0
50°	0	0	55	518	903	1077	944	605	136	0	0	0

where R_c is the amount of radiation actually received at the earth's surface from the sun and sky, and n/N is a ratio of actual to possible sunshine hours. Some relationships are given as follows:

$$R_c = Q_A \left(0.18 + 0.55 \frac{n}{N} \right) \text{ for southern England} \qquad (13.29a)$$

$$R_c = Q_A \left(0.22 + 0.54 \frac{n}{N} \right) \text{ for Virginia, USA} \qquad (13.29b)$$

$$R_c = Q_A \left(0.25 + 0.54 \frac{n}{N} \right) \text{ for Canberra, Australia} \qquad (13.29c)$$

For the computation of evaporation by the combination of energy balance and vapor flow method, data on n, e_a, u, mean air temperature are needed. These can be obtained from actual observations or through available meteorological data for the region under consideration. Equations (13.26) and (13.27) together with values in Tables 13.6 and 13.7 enable computation of daily evaporation values.

Example 13.6: Calculate the evaporation from a lake situated at 40° latitude for a day of July during which the following mean values were obtained. Air temperature = 20°, relative humidity = 70%, average wind speed at 2 m level = 120 miles/day, and actual hours of sunshine = 7.6 hr (observed).

Solution:

$$E = \frac{\Delta Q_n + \gamma E_a}{\Delta + \gamma} \qquad (13.30)$$

Now Δ at 20°C = 0.61, and γ = 0.49 mm of mercury per °C (psychrometric constant). Q_n can be computed from the formula:

$$Q_n = Q_A(1-r)\left(a + b\frac{n}{N}\right) - \sigma T^4 (0.56 - 0.09\sqrt{e_a})\left(0.10 + 0.90\frac{n}{N}\right)$$

Assuming $a + b\frac{n}{N} = 0.18 + 0.55\frac{n}{N}$, and $Q_n = Q_c + Q_b$,

The saturation vapor pressure (e_s) at 20° C = 17.5 mm

The actual vapor pressure e_a = 17.5 × 70/100 = 12.3 mm

Solar radiation Q_A at 40° = 941 cal/cm²/day = 15.0 mm/day (59 cal = 1 mm of water evaporated)

Possible hours of sunshine (N) = 14.7 hours from Table 12.6.

$$Q_c = Q_A(1-\gamma)\left(0.18 + 0.55 \times \frac{n}{N}\right)$$
$$= 15.9 \times (1 - 0.05)(0.18 + 0.55 \times 7.6/14.7)$$
$$= 15.9 \times 0.95 \times 0.47$$
$$= 7.1 \text{ mm/day}$$

$$Q_b = \sigma T_a{}^4(0.56 - 0.09\sqrt{e_a})\left(0.1 + 0.9 \times \frac{n}{N}\right)$$
$$\sigma = 2.01 \times 10^{-9} \text{ mm of water/day/°K}^4$$
$$T = 273 + 20 = 293$$
$$\sigma T_a{}^4 = 2.01 \times 10^{-9} \times (293)^4 = 14.8 \text{ mm of water/day}$$
$$Q_b = 14.8(0.56 - 0.09\sqrt{12.3})(0.1 + .09 \times 7.6/14.7)$$
$$= 14.8 \times 0.24 \times 0.57 = 2.03 \text{ mm/day}$$
$$Q_n = Q_c - Q_b = 7.10 - 2.03 = 5.07 \text{ mm/day}$$

For computing E_a we can use Penman (1948) formula as given in equation (13.20):

$$E_a = 0.35\left(0.5 + \frac{U_2}{100}\right)(e_s - e_a)$$

U_2 is the wind speed in miles/day at 2 m height

$$E_a = 0.35(0.5 + 120/100)(17.5 - 12.3)$$
$$= 0.35 \times 1.7 \times 5.2 = 3.1 \text{ mm/day}$$

Now we have from equation (13.30):

$$E = \frac{0.61 \times 5.07 + 0.49 \times 3.1}{0.61 + 0.49} = \frac{3.09 + 1.52}{1.1} = 4.2 \text{ mm/day}$$

REFERENCES

Bowen, I.S., 1926. The ratio of heat losses by conduction and by evaporation from any water surface. *Phys. Rev.*, 27, pp. 779–789.

Chang, J.H., 1968. Climate and Agriculture., Aldine, Chicago.

Chow, V.T. (Ed)., 1964. Hand book of Applied Hydrology. McGraw Hill, New York, NYS.

Dalton, J., 1802. Experimental essays on the constitution of mixed gases on the force of steam or vapor from water and other liquids in different temperatures, both in a Torricelian vacuum and in air on evaporation and on the expansion of gases by heat. Manchester Lu. Phil. Soc. Mem. Proc. 5, 536–602.

India Meteorological Department, 1980. Evaporation data, 1969–1975, Parts I and II.

Khan, M.A. and Bohra, D.N., 1990. Water loss studies in the Sardar Samand Reservoir. *J. of Arid Environment*, 19, pp. 245–250.

Linsley, R.K., Kohler, M.A. and Paulhus, J.L.H., 1975. Hydrology for Engineers (2nd ed.), New York, McGraw-Hill, 340 pp.

Meyer, A.F., 1915. Computing runoff from rainfall and other physical data. *Trans. ASCE*, 79, pp. 1056–1115.

Oliver, H., 1961. Irrigation and climate. Edward Arnold, London.

Penman, H.L., 1948. Natural evaporation a review. *J of Hydrol.*, 13, 1, pp. 1–21.

Penman, H.L. et al., 1956. Discussion of evaporation. *Netherlands J. of Agr. Sci*, 4, pp. 87–97.

Penman, H.L., 1963. Vegetation and hydrology. Commonwealth Bureau of Soils Harpenden, Tech. communication, 53, 124.

Rohwer, C., 1931. Evaporation from free water surface. US Dept. Agr: Tech. Bull., 271.

Wieisner, C.J., 1970. Hydrometeorology. Chapman and Hall Ltd, London, UK.

14 <u>Droughts</u>

Worldwide the general connotation of the term drought in any area is significant shortage of water from the lack of rainfall. The rainfall in a given area is not the same every year and as discussed earlier it may range from half of the normal in one year to twice the normal the next year. This causes either too much of water from high rainfall resulting in floods or too less water from low rainfall resulting in droughts. The periodic cycle of floods and droughts is a bane to economy. In this chapter, we study abnormally low rainfall leading to droughts and in the subsequent chapter we will discuss abnormally high rainfall leading to floods.

Normally indigenous plants and human inhabitants of a region adapt their life cycles with the climatically expected or normal rainfall of that region. Therefore, the conditions which lead to droughts occur when plants and pastures fail due to abnormally low rainfall. The impact of a drought not only causes large scale damage to agriculture but also causes multitudes of people to lose jobs. It is known that there is no apparent coherence in the occurrence of droughts in time. This makes drought prediction rather difficult. However, if we understand the frequency of drought occurrences over an area as well as some of the global weather events that are linked to rainfall anomalies then it may be possible to anticipate drought risk over that area and take appropriate short-term actions to combat the drought and minimize its impact.

14.1 CAUSES OF DROUGHTS

The main cause of a drought is the deficiency of water. The availability of water over any region depends largely on rainfall which is considered to be highly variable in character. As a result there are often occasions when the actual rainfall amount over a particular region falls appreciably below the normal expected rainfall of that region. This causes a water shortage and eventually a drought which is manifested in terms of crop failure, and shortage

of water in lakes, rivers and storage reservoirs. As a result sufficient water is not available for various demands of agriculture, industry, hydro-power generation and other human activities. Droughts in various parts of the Southeast Asian countries are mainly due to the failure of rainfall from monsoons. As a matter of fact, a drought can occur in virtually all rainfall regions but it is more frequent in arid and semiarid zones. A definite characteristic of these areas is their aridity which, simply put, means the lack of available moisture. Any area can be said to be arid when its moisture inputs (rainfall) are exceeded by the moisture losses (evapotranspiration). Various climatic indices have been devised to measure the aridity of dry lands and these can be used to delimit dry land areas. However, it is important to note that although dry lands are normally deficient in moisture on an annual basis, the moisture inputs as rainfall are highly variable in both time and space. The extent and distribution of different climatic zones are given in Table 14.1. Of the world's total land area of 130.2 million km^2 about 48.5 million km^2 area is arid and semiarid (UNEP, 1997). The largest dry lands lie in Africa, Asia and Australia, as shown in Table 14.1. Arid areas commonly receive all of their average rainfall in just a few days.

Table 14.1: Climatic zones of the world (million km^2)

Continent	Cold	Humid	Dry sub humid	Semi arid	Arid	Total
Africa	0	10.1	2.7	5.2	11.7	29.7
Asia	10.8	12.3	3.5	6.9	9.1	42.6
Australia	0	2.2	0.5	3.1	3.0	8.8
Europe	0.3	6.2	1.8	1.1	0.1	9.5
North America	6.2	8.4	2.3	4.2	0.8	21.9
South America	0.4	11.9	2.1	2.6	0.7	17.7
Total	17.7	51.1	12.9	23.1	25.4	130.2

Recent studies on interactions between global circulation and deficiency of rainfall around the world show that during El Nino events the deficiency of rainfall can occur virtually anywhere in the world. The El Nino phenomenon which is believed to occur every two to seven years disrupts the global weather patterns. Researchers have found the strongest links between El Nino and abnormal rainfall deficiencies in Australia, India, Indonesia, the Philippines, Malaysia, Brazil, various African nations, the western Pacific Islands, Central America and various parts of the United States. Thus we find that the problem of droughts is very much complicated and it requires consistent research by meteorologists, hydrologists and agriculture scientists. As one of the effects of a drought is crop failure, the concept of evapotranspiration which is fundamental to the crop-water relationship is discussed first.

14.2 EVAPOTRANSPIRATION AND POTENTIAL EVAPOTRANSPIRATION

The concept of evaporation was introduced in Chapter 13. Evaporation occurs from soil and water surfaces, whereas transpiration occurs from plants through their stomata. Although these two processes are different and distinct, it is possible in most contexts to treat them together, since the forcing mechanisms are similar and the end result is the same. The combined loss of water by evaporation and transpiration is called evapotranspiration. The study of evapotranspiration is fundamental to agricultural purposes particularly in the dry farming areas, and in estimating the loss of water from the soil as well as from crops. Actually it refers to the total amount of water required to raise the crop for entire season. The study of evapotranspiration is fundamental to agricultural purposes, particularly in irrigation farming as to determine when to irrigate and how much to irrigate. Evapotranspiration has a controlling influence on the study of agriculture droughts which are discussed subsequently.

The actual evapotranspiration varies widely, depending on climatic factors such as temperature, radiation, cloud cover, sunshine hours, wind speed, and humidity; and the nature and property of vegetative cover and the amount of water available in the soil. In dry climate with sparse vegetation, evapotranspiration is limited by the amount of soil moisture and if more water is available there will be more vegetation productivity and evapotranspiration would correspondingly increase. The loss of water by evapotranspiration, therefore, depends not only on the climatic factors but also on the nature of crop grown and the stage of crop growth.

In spite of the continuous efforts of scientists, reliable estimates of regional evapotranspiration are extremely difficult to obtain, mainly because of its dependence on soil conditions and plant physiology; the advances in the knowledge of interactions underlying evapotranspiration and its all-round influence have been few and far in between. Because of this complexity, the concept of potential evapotranspiration (PET) has been introduced which no longer depends so critically on soil and plant factors but has been shown to primarily depend on climatic factors (Thornthwaite, 1948; Penman, 1948). PET is defined as the evapotranspiration that occurs when the ground is completely covered by actively growing vegetation under conditions of unlimited and unrestricted water supply. It represents the rate controlled entirely by atmospheric conditions and is the maximum possible in the prevailing meteorological conditions. The estimates of PET have applications in many fields, such as water balance studies, drought studies, seasonal irrigation requirement of crops and general hydrology.

PET can be estimated through direct measurement using lysimeters and evaporation pans. Secondly, a number of empirical formulae have been

developed for the determination of PET directly from meteorological data. The most well known and widely used methods of estimating PET are those of Thornthwaite (1948) and of Penman (1948). Thornthwaite's method is basically an empirical relationship between mean monthly PET and mean monthly temperature, wherein uniform values of wind and humidity have been assumed. Penman's method, which combines energy-budget and an aerodynamic approach (mass transfer), considers additional meteorological parameters of humidity, wind velocity and solar radiation which significantly affect PET as described in Chapter 13. Significant amounts of measured meteorological data requirement and relative complexity of Penman's method have, however, led to the widespread use of the simpler Thornthwaite method. The Thornthwaite method allows PET to be calculated from just two parameters: mean monthly temperature data and the average number of day light hours by month. The Thornthwaite's formula for the estimation of monthly PET is:

$$\text{PET} = 1.6\left(10\frac{t}{I}\right)^a \tag{14.1}$$

where PET = unadjusted PET (cm) per month (month of 30 days and 12 hours day time); t = mean temperature °C; I = annual or seasonal heat index = summation of 12 values of monthly heat indices defined as

$$I = \sum_{i=1}^{12}\left(\frac{t_i}{5}\right)^{1.514} \tag{14.2}$$

Here, t_i = temperature in °C of i-th month; and a = an empirical exponent

$$a = 0.675 \times 10^{-6}\ I^3 - 0.771 \times 10^{-4}\ I^2 + 0.1792 \times 10^{-1}\ I + 0.49239 \tag{14.3}$$

The unadjusted values of PET so obtained are then corrected for actual daylight hours and days in a month.

The Thornthwaite method has been used by several workers (for example, Krishna Kumar et al., 1987; Rao et al., 1971) for estimating annual PET values at several locations in India. There is a high variability in the distribution of PET in space and time due to different levels of moisture. The mean annual PET for India is shown in Fig. 14.1. The annual PET exceeds 200 cm over western Rajasthan and north Gujarat. In Assam, Kerala and along the west coast the annual PET is of the order of 120 to 140 cm. This map can be used to estimate the value of PET at any location for drought studies.
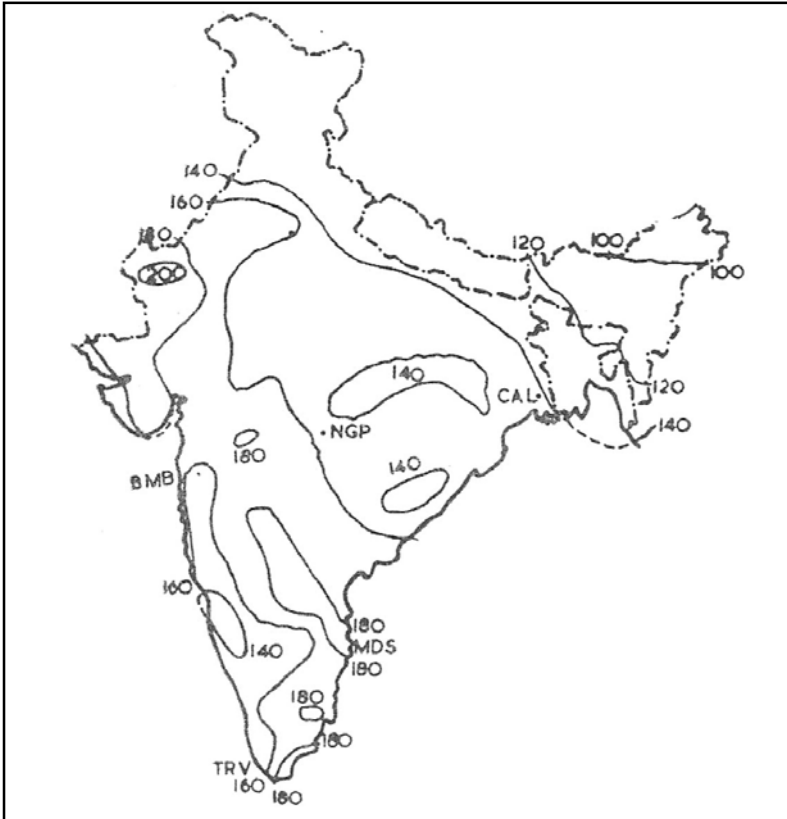
Fig. 14.1. Mean annual potential evapotranspiration (cm) over India.

14.3 TYPES OF DROUGHTS

Generally speaking drought means the scarcity of water from rainfall, but a simple definition like this does not bring forth the various aspects of the phenomenon of drought, because it means different things to different people. It should therefore be useful to look at some different definitions of droughts which depend on the type of drought. Various workers have defined a drought over a region differently considering their own needs.

14.3.1 Meteorological Drought

In defining a meteorological drought the most commonly used rainfall statistic is the mean (more usually called average or normal), which in the case of a normal or Gaussian distribution is the same as the median which is the value exceeded by half of the values. As such, a meteorological drought is primarily based on the deficiency of rainfall compared to normal rainfall of the region or in other words the "percentage of normal rainfall". It is defined

as a situation over a given area where the actual rainfall recorded significantly falls short of climatically expected rainfall of that area.

While assessing the severity of a drought period and the magnitude of its impact, several countries, such as Costa Rica, Israel, Jamaica, Botswana, Ethopia, Malaysia, Korea, Pakistan, the USA, Australia, and India, use in one form or another the criterion of a deficient rainfall by a certain "percentage of normal rainfall." Studying the drought situation in the USA, Bates (1935) found that drought occurred when annual rainfall was less than 75% of the normal value. Hoyt (1942) suggested that in humid and semi-arid climates droughts did not occur until the annual rainfall was as low as 85% of the mean. The British Rainfall Organization (1936) has defined an absolute drought as a period of at least 15 consecutive days to none of which is credited a rainfall of 2.5 mm or more. For India, the India Meteorological Department (IMD, 1971) has defined a drought as a situation occurring in a region when the annual rainfall is less than 75% of the normal. The drought is further classified as moderate when annual rainfall deficit is between 25 and 50% of the normal and severe drought when the deficiency is more than 50% of the normal.

If rainfall amounts are not normally distributed, a drought is best determined by defining the limits of a certain proportion of occurrences. For individual stations in Australia, Gibbs and Mehar (1957) used the criterion for drought years as those years with annual rainfall less than the first decile rainfall. The first decile is that rainfall amount which is not exceeded by the lowest 10 % of totals. The second decile is the amount of rainfall not exceeded by 20% of totals and so on. The following groupings of decile ranges were used in defining occurrences of droughts:

Very much above average	highest 10% of values	decile range 10
Much above average	next highest 10% of values	decile range 9
Above average	next highest 10% of values	decile range 8
Slightly above average	next highest 10% of values	decile range 7
Average	middle 20% of values	decile range 5 & 6
Slightly below average	next lower 10% of values	decile range 4
Below average	next lower 10% of values	decile range 3
Much below average	next lower 10% of values	decile range 2
Very much below average	lowest 10%	decile range 1

All these above mentioned definitions of a drought are based on rainfall as the only parameter. However, one cannot define a drought as a shortage of rainfall alone, since it does not take into account very important part played by soil moisture on which plants depend for their survival.

Example 14.1: The following table lists the July rainfalls (in mm) for Western Rajasthan for the years 1901 to 1990. Illustrate the method of determining deciles.

Year	Rainfall	Year	Rainfall	Year	Rainfall
1901	80	1931	56	1961	55
1902	32	1932	122	1962	119
1903	149	1933	44	1963	15
1904	41	1934	43	1964	154
1905	25	1935	131	1965	143
1906	54	1936	46	1966	61
1907	76	1937	164	1967	62
1908	220	1938	56	1968	75
1909	181	1939	14	1969	38
1910	57	1940	56	1970	52
1911	3	1941	79	1971	64
1912	102	1942	130	1972	27
1913	35	1943	168	1973	62
1914	104	1944	145	1974	103
1915	23	1945	162	1975	136
1916	87	1946	42	1976	122
1917	85	1947	20	1977	158
1918	1	1948	94	1978	209
1919	85	1949	113	1979	100
1920	87	1950	164	1980	107
1921	123	1951	38	1981	104
1922	80	1952	118	1982	85
1923	112	1953	79	1983	188
1924	81	1954	98	1984	56
1925	46	1955	11	1985	123
1926	91	1956	220	1986	98
1927	117	1957	67	1987	23
1928	82	1958	69	1988	119
1929	152	1959	134	1989	99
1930	90	1960	99	1990	208

Solution: The table as shown below illustrates the method of finding deciles. In this table the monthly rainfall values are rearranged in descending order. The first decile is determined as the value not exceeded by 10% of values, the second decile as that not exceeded by 20% of values and so on. The deciles are indicated in the table.

Rainfall	Year	Rainfall	Year	Rainfall	Year
1	1918	23	1915	35	1913
3	1911	23	1987	38	1951
11	1955	25	1905	38	1969
14	1939	25 1st Decile		41	1904
15	1963	27	1972	42	1946
20	1947	32	1902	43	1934

(Contd.)

(*Contd.*)

Rainfall	Year	Rainfall	Year	Rainfall	Year
44	1937	82	1928	119	1988
44 2nd decile		85	1982	122	1976
46	1925	85	1919	122	1932
46	1936	85	1917	123	1985
52	1970	85 5th decile		123	1921
54	1906	87	1916	130	1942
55	1961	87	1920	131	1935
56	1984	90	1930	131 8th decile	
56	1940	91	1926	134	1959
56	1938	94	1948	136	1975
56	1931	98	1986	143	1965
56 3rd decile		98	1954	145	1944
57	1910	99	1960	149	1903
61	1966	99	1967	151	1964
62	1957	99 6th decile		152	1929
62	1973	100	1979	158	1977
64	1971	102	1912	162	1945
67	1957	103	1974	162 9th decile	
69	1958	104	1981	164	1950
75	1968	104	1914	164	1937
76	1907	107	1980	168	1943
76 4th decile		112	1923	181	1909
79	1953	113	1949	188	1983
79	1941	117	1927	208	1990
80	1922	117 7th decile		209	1978
80	1901	118	1952	220	1956
81	1924	119	1962	220	1908

Lowest	1 mm
Decile 1	25 mm
Decile 2	44 mm
Decile 3	56 mm
Decile 4	76 mm
Decile 5	85 mm
Decile 6	99 mm
Decile 7	117 mm
Decile 8	131 mm
Decile 9	162 mm
Highest	220 mm

14.3.2 Agricultural Drought

An agricultural drought is defined as a situation over an area where the water deficiency has reached such an extent that the moisture available in the soil

may not be found sufficient for the normal growth of plants and trees. The basic concept is that agriculture depends not only on the availability of water from rainfall but also on local climate as represented by evapotranspiration (ET) as explained earlier. Several indicators, as the principal criteria for measuring an agricultural drought based on rainfall and potential evapotranspiration (PET), have been developed which are discussed in what follows.

14.3.2.1 Aridity index

The aridity index (AI), also called an index of moisture deficit, represents a lack of moisture under average climatic conditions. It is calculated on a daily, weekly, monthly, seasonal or annual basis as the ratio of rainfall to atmospheric demand usually expressed as potential evapotranspiration (Thornthwaite, 1948). It is expressed as

$$AI = \frac{\text{precipitation (P)}}{\text{potential evapotranspiration (PET)}} \qquad (14.4)$$

Rainfall provides the natural water availability for agriculture and PET is the water need for agriculture. If the calculated value of AI index is less than 1, then it indicates an annual moisture deficit in the soil. PET can be calculated using Thornthwaite's formula as described earlier. A more practical approach utilizes pan evaporation data as

$$PET = (0.70 \text{ to } 0.80) \times \text{pan evaporation} \qquad (14.5)$$

14.3.2.2 Soil moisture stress

Plants need specific amounts of water to have healthy and normal growth. This is the water need of crops. This amount should exceed PET which is defined as the amount of water that can evaporate and transpire from a well vegetated area under unlimited water. The actual amount of water for plant growth is however decreased when the moisture in the soil is depleted. This amount of water, actually used by plants, is defined as actual evapotranspiration (AET). The difference between PET and AET, PET - AET, indicates water deficit (WD) causing moisture stress or the shortage of moisture required to grow plants. The soil moisture stress is used to compute an agricultural drought index (ADI) as the ratio of water deficit to potential evapotranspiration which is expressed as

$$ADI = \frac{WD \times 100}{PET} \qquad (14.6)$$

WD is calculated on a weekly, monthly, seasonal or annual basis using the climatic water balance. The concept of water balance is explained in the following section.

14.3.2.3 Water balance

The water balance concept conveys the water in balance after making all allowances for gains and losses of water to any field for any period, say a day, a week, a month, a season, or a year. The water balance equation in its simplest form for a soil can be stated as:

$$P \quad = ET + RO + D + SM \qquad (14.7)$$

$$SM = P - (ET + RO + D) \qquad (14.8)$$

where P = precipitation, ET = evapotranspiration, RO = runoff, D = deep drainage and SM = soil moisture balance (all units are in terms of depth of water in mm).

Thus, day-to-day knowledge of soil moisture status can be gained by knowing climatic factors. The imbalance between the water demand of plants (more) and water supply (less) is nothing but water stress. This forms the basis for determining the moisture stress using water balance as a technique or device for agricultural droughts. Details of the procedure for computing water balance are given in Thornthwaite and Mather (1955) and are not discussed here.

14.3.3 Hydrological Drought

A hydrological drought deals with surface and subsurface water supplies (such as stream flow, reservoir/lake levels or ground water). Extended periods of deficient precipitation cause these water supplies to drop below normal. This drought is no different from others in regard to the fact it is caused by a lack of rainfall, but is different from others in one significant way. Hydrological droughts usually do not occur at the same time as others, instead they lag behind. This drought deals more with the effects the lack of rainfall has on the hydrological system as a whole. It takes a longer period of time for the lack of rainfall to show up in places, such as ground water, reservoir, and lake levels. When the flow in these places is affected significantly enough, this can have economic effects on the area on things, such as hydroelectric power plants, etc.

Although climate/weather is the main contributor to a hydrological drought, things such as changes in landscape, land use, and construction of dams, also have significant impacts on droughts. Such changes may not have a great effect on the immediate region, it is certain that it will impact the region downstream from the moisture. This is also true with a meteorological drought. An example of this type of thing occurring would be in the case of a drought in the Northern Great Plains. Since the Missouri River flows to the south, the lack of rainfall to the north will also impact the area downstream from the drought inflicted area. The changes in land/water use in the Great Plains will alter hydrological characteristics, such as flow and runoff rates, which in turn could cause a drought in the area downstream from the original

area to the north. This shows how land use changes/human alterations can alter the frequency of water shortages even when no meteorological drought is being observed.

Example 14.2: Annual rainfall data for a station for the period 1956-1990 is given below. Compute mean rainfall and identify the meteorological drought years.

Year	Rainfall (cm)	Year	Rainfall (cm)	Year	Rainfall (cm)
1956	40.3	1968	18.1	1980	52.3
1957	30.5	1969	40.2	1981	37.4
1958	50.4	1970	22.3	1982	39.3
1959	50.6	1971	38.2	1983	24.6
1960	35.0	1972	55.6	1984	36.5
1961	45.2	1973	50.4	1985	25.5
1962	17.5	1974	25.3	1986	25.3
1963	30.3	1975	50.4	1987	35.1
1964	30.5	1976	40.2	1988	45.6
1965	22.6	1977	62.5	1989	40.2
1966	22.5	1978	30.1	1990	35.0
1967	27.1	1979	30.1	–	–

Solution: 35-year mean = 36.1 cm. The meteorological drought is defined as the percentage of mean rainfall. The percentage of mean rainfall for each year is tabulated in columns 3 and 6 as shown below:

Year	Rainfall (cm)	% of mean	Year	Rainfall (cm)	% of mean
1956	40.3	112	1974	25.3	70
1957	30.5	84	1975	50.4	140
1958	50.4	140	1976	40.2	111
1959	50.6	140	1977	62.5	173
1960	35.0	97	1978	30.1	83
1961	45.2	125	1979	30.1	83
1962	17.5	48	1980	52.3	145
1963	30.3	84	1981	37.4	104
1964	30.5	84	1982	39.3	109
1965	22.6	63	1983	24.6	68
1966	22.5	62	1984	36.5	101
1967	27.1	75	1985	25.5	70
1968	18.1	50	1986	25.3	70
1969	40.2	111	1987	35.1	97
1970	22.3	62	1988	45.6	126
1971	38.2	106	1989	40.2	111
1972	55.6	154	1990	35.0	97
1973	50.4	140	–	–	–

Thus the drought years are: 1962, 1965, 1966, 1968, 1970, 1974, 1983, 1985, and 1986. In these years, rainfall was less than 75% of the mean.

14.4 DROUGHTS IN INDIA

India is one of the few countries of the world where rainfall is seasonal as described in Chapter 6. Also out of 142 million hectares of cultivated land in the country, 92 million hectares (about 65 percent) are under rain-fed agriculture. Consequently, agricultural production very much depends on monsoon rains. An incident of one drought year could reduce the crop yield by as much as 20 to 25 percent. It is, therefore, of crucial importance to study the magnitude and frequency of droughts in India in terms of rainfall deficiency with a view to locate the regions which are susceptible to frequent droughts on account of failure of rains.

14.4.1 Major Meteorological Droughts in India

On the basis of distribution of rainfall and other meteorological parameters, such as temperature, pressure, humidity and wind, the area of each state of India has been divided into homogenous meteorological subdivisions. There are in all 31 contiguous subdivisions (Fig. 14.2). Because of inherently variable character of the southwest monsoons there are often occasions when the actual rainfall in a year over these subdivisions falls appreciably below their respective normal rainfall. This causes acute shortages of water and consequently droughts. Dhar et al. (1979) and Parthasarthy et al. (1987) have evaluated the occurrence of droughts in each subdivision on the basis of rainfall deficiency. Two categories of droughts were defined by adopting the criteria of India Meteorological Department (1971) as described earlier. A rainfall deficiency of 26-50% from the normal over the area is considered as a moderate drought and a deficieny in excess of 50% as a severe drought. On the basis of this criterion, the drought over each meteorological subdivision was classified as moderate or severe during the monsoon period in each year of the period from 1871 to 1990.

The number of subdivisions affected by moderate to severe droughts and the percentage of area affected during the period from 1871 to 1990 are given in Table 14.2. It is seen from this table that there were 20 occasions when a large number of contiguous subdivisions of the country experienced deficient rainfall. During the 20 occasions of major droughts, it is seen that on an average 13 contiguous subdivisions came under drought conditions. The three worst droughts were in 1877, 1899, and 1918 when about 64 to 73 percent of the country faced wide spread drought conditions. Although there is no systematic time interval between two successive major drought years but on average over a long period of time one major drought year can be expected after an interval of about six years. Consequently this makes drought prediction rather difficult merely on the basis of rainfall deficiency.

During the 13-year period from 1878 to 1890, and during the 18-year period from 1921 to 1938 there were no drought years worth the name and the distribution of rainfall over the country as a whole was either normal or above normal.

Table 14.2: Major meteorological drought years of India

S.No	Drought year	Annual rainfall of India as a whole (cm)	Number of subdivisions affected by drought	% of area of India under drought	Time interval between drought years
1	1877	94.7	16	64	–
2	1891	101.7	9	34	14
3	1899	81.1	22	70	8
4	1901	97.2	12	38	2
5	1904	97.5	11	53	3
6	1905	92.0	15	47	1
7	1907	97.8	7	25	2
8	1911	96.7	11	40	4
9	1918	85.8	23	73	7
10	1920	92.2	14	51	2
11	1939	101.7	7	23	19
12	1941	95.7	12	42	2
13	1951	97.3	16	56	10
14	1965	87.2	14	54	14
15	1966	97.0	13	48	1
16	1972	84.9	12	41	6
17	1974	97.3	8	36	2
18	1979	96.2	8	36	5
19	1982	98.0	11	43	3
20	1987	96.5	16	57	5

14.4.2 Drought Magnitude

The magnitude of a drought cannot be directly measured. However, there are two indirect methods which give an idea of the magnitude of a drought: (i) deficiency in rainfall and (ii) extent of the area affected by a drought. The other indirect methods which also give an idea of the magnitude of a drought are: crop yield, stream flow, reservoir/lake level and ground water as pointed out in the case of hydrological droughts as well as relief offered to drought stricken people. Based on the monsoon rainfall deficiency and the area affected by a drought, the relative rankings for the 20 worst drought years of India are given in Table 14.3. It is seen from this table that the drought of 1918 was the worst drought of this country. During this drought 23 contiguous sub-divisions were affected and nearly 73 per cent of the total area of the country came under the grip of the drought. Dhar et al. (1978)

also found that the 1918 monsoon was the driest monsoon over the Indian area. However, it is seen from Table 14.3 that although the areal extent of the drought was the largest in the year 1918, but the deficiency of monsoon rainfall was the maximum in the years 1877 and 1899. The departure from the mean monsoon rainfall during these two drought years were of the order of -29 and -26 per cent respectively. The remaining 17 worst drought years were by and large not as severe as the years 1877, 1918 and 1899.
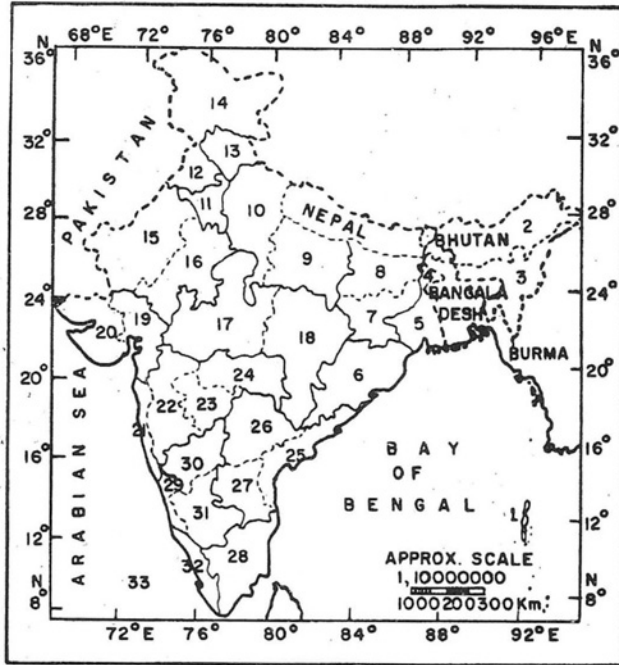
1 Bay Islands	12 Punjab	23 Marathwada
2 North Assam	13 Himachal Pradesh	24 Vidarbha
3 South Assam	14 Jammu & Kashmir	25 Coastal Andhra Pradesh
4 Sub-Himalayan West Bengal	15 West Rajasthan	26 Telangana
5 Gangetic West Bengal	16 East Rajasthan	27 Royalaseema
6 Orissa	17 West Madhya Pradesh	28 Tamil Nadu
7 Bihar Plateau	18 East Madhya Pradesh	29 Coastal Karnataka
8 Bihar Plains	19 Gujarat	30 North interior Karnataka
9 East Uttar Pradesh	20 Sourashtra and Kutch	31 South interior Karnataka
10 West Uttar Pradesh	21 Konkan	32 Kerala
11 Haryana	22 Madhya Maharashtra	33 Arabian Sea Islands

Fig. 14.2. Meteorological subdivisions of India.

Table 14.3: Rainfall deficiency in the monsoon period
during the major drought years

S.No.	Drought year	% of area of India affected	Rainfall deficiency (%)				
			Monsoon	June	July	August	September
1	1918	73	–24	11	–48	–10	–38
2	1899	70	–26	19	–32	–41	–40
3	1877	64	–29	–13	–40	–35	–14
4	1987	57	–18	–29	–25	–3	–19
5	1951	56	–13	–5	–7	–15	–29
6	1965	54	–17	–33	–3	–22	–16
7	1904	53	–12	10	–10	–19	–26
8	1920	51	–16	–12	6	–33	–29
9	1966	48	–13	2	–14	–19	–19
10	1905	47	–16	–44	–10	–16	0
11	1982	43	–14	–20	–21	10	–29
12	1941	42	–15	0	–21	–14	–21
13	1972	41	–24	–25	–33	–11	–25
14	1911	40	–14	17	–44	–13	1
15	1901	38	–15	–30	–19	7	–26
16	1974	36	–12	–35	0	–6	–14
17	1979	36	–17	–12	–18	–18	–19
18	1891	34	–7	–49	–6	–6	30
19	1907	25	–9	–5	–19	24	–42
20	1939	23	–7	–10	–8	–3	–11

14.4.3 Drought Frequency over Different Subdivisions

There is a large variability in monsoon rainfall in both space and time. Consequently, the Indian region experiences droughts or floods in some parts of the country or the other almost every year during the monsoon period (June to September). Frequencies of deficit rainfall during individual monsoon months and for the monsoon season as a whole for different subdivisions of the country during an 80-year period (1891-1970) were worked out by Dhar et al. (1979) and are given in Table 14.4. According to the Irrigation Commission, Government of India (1976), the areas where a drought (monsoon season as a whole) has occurred in 20 percent or more years are considered as 'drought areas' and the areas where a drought has occurred in more than 40 percent of the years as 'chronic drought areas.' With this criterion in mind, it is observed from Table 14.4 that there are eight subdivisions, namely, Haryana, Punjab, West Rajasthan, East Rajasthan, Gujarat, Saurashtra and Kutch, Telangana and Rayalaseema, which can be considered as drought areas. There is no subdivision which can be regarded as a chronic drought area. Apparently, those subdivisions of the country are liable to frequent droughts whose mean annual rainfall is less than 100 cm.

Table 14.4: Frequency (%) of deficient rainfall for different subdivisions

S. No.	Meteorological subdivision (See Fig. 14.2)	Annual rainfall (cm)	Frequency of deficient rainfall (%)				
			June	July	August	September	Monsoon
1.	North Assam	228	15	9	16	24	5
2.	South Assam	283	14	16	15	18	5
3.	Sub Himalayan West Bengal	280	23	29	29	30	10
4.	Gangetic West Bengal	142	31	23	20	34	9
5.	Orissa	149	30	28	20	29	5
6.	Bihar plateau	134	38	19	18	24	6
7.	Bihar plains	119	39	28	29	34	11
8.	East Uttar Pradesh	102	46	26	25	35	15
9.	West Uttar Pradesh	103	48	26	24	40	16
10.	Haryana	55	51	34	39	46	26
11.	Punjab	62	57	33	35	64	35
12.	Himachal Pradesh	175	46	30	31	48	18
13.	Jammu and Kashmir	100	46	30	31	51	20
14.	West Rajasthan	30	80	39	46	53	28
15.	East Rajasthan	67	53	33	35	45	21
16.	West Madhya Pradesh	103	45	25	31	43	15
17.	East Madhya Pradesh	135	38	23	21	30	10
18.	Gujarat	97	40	35	44	46	24
19.	Saurashtra and Kutch	52	50	46	46	55	33
20.	Konkan	294	26	23	39	34	13
21.	Madhya Maharashtra	100	31	24	31	31	18
22.	Marathwada	83	40	34	40	36	19
23.	Vidarbha	107	33	20	36	38	13
24.	Coastal Andhra Pradesh	100	34	26	34	28	14
25.	Telangana	91	43	29	33	40	23
26.	Rayalaseema	68	35	45	46	35	23
27.	Tamil Nadu	101	33	38	34	33	13
28.	Coastal Karnataka	333	19	24	31	35	10
29.	North Interior Karnataka	71	21	24	41	26	16
30.	South Interior Karnataka	115	30	28	38	33	19
31.	Kerala	295	23	28	36	40	11

14.5 EL NINO FACTOR RELATING TO DROUGHTS

El Nino was described in Chapter 12. Normally a high pressure belt hovers over the central southern and eastern equatorial Pacific Ocean and is counter balanced by a low pressure over Indonesia in the Indian Ocean. But once every 3 to 5 years, the pattern is reversed, that is, the pressure in the Indian Ocean becomes high while low in the eastern equatorial Pacific. The sea saw interaction between the two is called southern oscillation. When the differences in pressure become abnormally low, the trade winds in the western Pacific collapse, resulting in an extensive and abnormal warming of the Pacific. This phenomenon is known as El Nino; it normally starts in the month of December and is associated with northerly winds and heavy rainfall over the coastal regions of northern Peru and Ecuador. This is what is described in Chapter 12. Although this happens every December, to some extent, the term El Nino is used for severe warming which occurs every 3 to 5 years with far flung consequences.

Severe El Nino events occurred in 1877, 1884, 1891, 1899, 1911, 1918, 1925, 1941, 1957, 1972, 1982 and 1986 (Mooley and Parthasarthy, 1983). Every incarnation of El Nino is accompanied by a deficient rainfall virtually everywhere in the world. The extent of rainfall deficiency varies as does the magnitude of the pressure difference leading to El Nino. It was the lowest in 1972 and 1986 when the worst droughts occurred in different parts of the world.

14.5.1 El Nino and Droughts around the World

During an El Nino event, droughts can occur anywhere in the world, although strongest connections have been found between El Nino and severe droughts in Australia, India, Indonesia, the Philippines, Brazil, parts of east and south Africa, Central America and various parts of the United States. Droughts occur in each of these regions at different times during an event and in varying degrees of magnitudes.

Ropelewski and Halpert (1987) examined the association between El Nino events and regional precipitation patterns around the globe. A significant association was found in the regions of northeastern South America from Brazil up to Venezuela. During the 17 El Nino years, this region experienced 16 dry years. It is not uncommon to find rain forests burning during these dry periods. Their study found that areas also showed a strong tendency to be dry during El Nino years. Indonesia, Fiji, and Hawaii are usually prone to droughts during an El Nino year. Virtually all of Australia is subjected to abnormally low rainfall conditions during El Nino years but especially the eastern half faces extreme droughts. El Nino also plays a definite role in the southwest monsoon failure resulting in severe droughts in India. Mooley and Parthasarthy (1983) found that during the 22 El Nino years the monsoon rainfall over most parts of the country was below normal.

Thus, El Nino events considerably influence the amount of rain received in lower latitudes, especially in the equatorial Pacific and bordering tropical areas. The relationships in the mid-latitudes are not as pronounced nor are they as consistent in the way wet or dry weather patterns are influenced by El Nino.

14.5.2 El Nino and Indian Droughts

In India, the impacts of El Nino are most dramatic in the summer monsoon rainfall. The occurrence of El Nino produces deficient summer monsoon rainfall and consequent drought conditions over India. According to Mooley and Parthasarthy (1983), the worst years for the Indian summer monsoon are generally El Nino years. As shown in Chapter 12, El Nino occurred in 1899, 1902, 1905, 1911, 1914, 1918, 1923, 1925, 1930, 1932, 1939, 1940, 1941, 1946, 1951, 1953, 1957, 1963, 1965, 1969, 1972, 1976, 1977, 1982, 1986, 1991, 1993, 1994 and 1997. In this context, it is of interest to know whether the occurrence of El Nino exercises any influence on the annual amount of rainfall received in India. Corresponding to each of the El Nino years, the areal weighted average rainfall amount for the whole of India has been obtained from the IITM (1995) research report No. RR-065. The percentage departure of rainfall from normal rainfall was then worked out for each of the El Nino years. By the IMD (1971) definition, depending on the magnitude of percentage departure, the year was categorized as normal year, slight drought year, moderate drought year or severe drought year as indicated below:

Percentage departure from normal	Drought category
+10% to –10%	Normal year
–11% to –25%	Slight drought year
–25% to –50%	Moderate drought year
Less than –50%	Severe drought year

Table 14.5 gives details of the El Nino years along with all-India annual rainfall during the El Nino year and the rainfall departures from the normal. The average departure of all-India rainfall during 28 El Nino years works out to be 13%. There are 18 years (64% of the total number of El Nino years) having below normal rainfall. According to Table 14.5, seven El Nino years experienced deficit rainfall between 1 and 10 percent of normal rainfall, 13 between 11 and 20 percent and four between 20 and 30 percent and one El Nino year recorded a deficit of 31 percent of the normal rainfall.

Table 14.5: El Nino years and annual rainfall of whole of India
(Normal annual rainfall of India = 117 cm)

S.No	El Nino year	Intensity of El Nino	Annual Rainfall (cm)	% of departure from normal	Drought category
1	1899	S	81.1	−31	Moderate
2	1902	M	101.3	−13	Slight
3	1905	M	92.0	−21	Slight
4	1911	S	96.7	−17	Slight
5	1914	M	110.1	−6	Normal
6	1918	S	85.8	−27	Moderate
7	1923	–	103.2	−12	Slight
8	1925	S	106.4	−9	Normal
9	1930	M	108.2	−8	Normal
10	1932	–	105.9	−10	Normal
11	1939	M	101.7	−13	Slight
12	1940	–	113.2	−3	Normal
13	1941	S	95.7	−18	Slight
14	1946	–	123.2	+5	Normal
15	1951	–	97.3	−17	Slight
16	1953	M	113.0	−4	Normal
17	1957	S	100.7	−14	Slight
18	1963	–	109.5	−7	Normal
19	1965	M	87.3	−26	Moderate
20	1969	–	104.4	−11	Slight
21	1972	S	84.9	−28	Moderate
22	1976	M	104.6	−11	Slight
23	1977		119.5	+2	Normal
24	1982		98.0	−16	Slight
25	1986		99.4	−15	Slight
26	1991		100.5	−14	Slight
27	1993		116.8	0	Normal
28	1994		118.5	+1	Normal

14.6 ABSENCE OF TROPICAL DISTURBANCES AND INDIAN RAINFALL

There are three major meteorological factors that are considered to be related to the rainfall deficiency in India. These are: (1) late onset and early withdrawal of monsoons, (2) absence of tropical disturbances, and (3) prolonged breaks in monsoon rainfall. It is of considerable interest to know as to the extent of rainfall deficiency and consequent drought conditions that would result if the above meteorological factors happened to prevail.

Dhar et al. (1982, 1984) made an extensive study to find the extent of rainfall deficiency in India due to the absence of tropical disturbances during the summer monsoon months based on 80 years on rainfall data from 1891

to 1970. They found that in the 80-year period there were in all 22 June, 11 July, seven August, and three September months when the Indian area did not experience any tropical disturbances. These years are listed in Table 14.6.

Table 14.6: Years when the Indian region did not experience tropical disturbances in June to September months (1991-1970)

June	1891, 1899, 1901, 1909, 1910, 1912, 1913, 1919, 1921, 1922, 1923, 1924, 1926, 1930, 1931, 1938, 1942, 1946, 1957, 1958, 1960, 1966.
July	1901, 1907, 1908, 1911, 1915, 1916, 1924, 1931, 1953, 1955, 1967.
August	1901, 1905, 1930, 1932, 1961, 1962, 1966.
September	1913, 1929, 1952.

The tropical disturbances that occur during the summer monsoon months largely affect the Indian area north of latitude 15 degrees north. Hence, the influence of their non-occurrence was examined on the monsoon rainfall of the area north of 15 degrees north. In this area there are 21 meteorological subdivisions excluding hilly areas of the country. Using rainfall data of all available stations for the period 1891 to 1970, the areal average rainfall for the area north of 15 degrees north as a whole was computed for each of the four monsoon months for each year. By averaging the values of the 80 years, the mean areal rainfall for the months of June, July, August and September were estimated as 13.3 cm, 28.4 cm, 25.2 cm, and 17.0 cm, respectively.

While evaluating the amount of rainfall deficiency caused by the absence of tropical disturbances, the values of percentage departures of rainfall from the mean were then calculated for each of the 22 June months, 11 July months, seven August months and three September months which did not experience tropical disturbances. The percentage departures of rainfall in different years for the area above 15 degrees north are presented in Table 14.7.

Table 14.7 shows that in the absence of tropical disturbances, on average a deficiency of seven percent occurred in the month of June. The years 1899, 1909, 1910, 1913, 1919, 1921, 1922, 1930, 1938 and 1946 received normal to above normal rainfall in the month of June. The meteorological factors, such as early onset of monsoon, passage of lows, active monsoon conditions, position of trough axis, etc., accentuate the rainfall distribution. The years 1891, 1901, 1912, 1923, 1924, 1926, 1931, 1942, 1957, 1958, and 1965 received below normal rainfall. In these years, besides the absence of tropical disturbances, the onset of monsoon was late as well as monsoon conditions were weak. It was concluded that early or normal onset of monsoon coupled with active monsoon conditions may produce normal to above normal rainfall in spite of the absence of tropical disturbances.

Table 14.7: Percentage departures of rainfall in different years of monsoon months when no disturbances were experienced

June month		July month		August month		September month	
Year	*% departure*	*Year*	*% departure*	*Year*	*% departure*	*Year*	*% departure*
1891	−63	1901	−18	1901	+12	1913	−43
1899	+17	1907	−28	1905	−30	1929	−38
1901	−45	1908	+14	1930	−27	1952	−42
1909	+43	1911	−56	1932	−23	Average deficit	−41
1910	+43	1915	−26	1961	+12		
1912	−44	1916	−12	1962	−11		
1913	+57	1924	0	1966	−26		
1919	+21	1931	0	Average deficit	−13		
1921	+10	1953	+4				
1922	+19	1955	−18				
1923	−64	1957	−2				
1924	−49	Average deficit	−13				
1926	−69						
1930	+7						
1931	−46						
1938	+77						
1942	−2						
1946	+40						
1957	−19						
1958	−35						
1960	−3						
1965	−50						
Average deficit	−7						

In the month of July, on average a rainfall deficiency of 13 percent or as large as a deficiency of 56 percent or an excess rainfall of 14 percent from normal can occur. During the month of July, rainfall over India largely depends upon the position and strength of the monsoon trough, the activity of monsoon currents from the Arabian Sea and the Bay of Bengal and the passage of low pressure systems. If the monsoon trough shifts to the foot of Himalayas, a break in monsoon results which cause a decrease in the rainfall activity. It was observed that the absence of tropical disturbances coupled with setting in of prolonged monsoon-break conditions produced deficient rainfall in the July month of 1901, 1907, 1911, 1915, 1916, and 1955. The years 1908 and 1953 received above normal rainfall which was mainly because of the passage of low pressure systems from the Bay of Bengal.

In the August month, it was found that out of the seven years, five years experienced deficit rainfall ranging between 11 and 30 percent. As in the July month, the rainfall in August depends on the position and strength of the monsoon trough, the activity of monsoon currents from the Arabian Sea and the Bay of Bengal and the passage of low pressure systems from the Bay of Bengal. The deficient rainfall is caused if monsoon currents are weak and break-monsoon conditions prevail for a long time. In the absence of tropical disturbances, the years 1905, 1930, 1932, 1962 and 1966 experienced drought conditions. However, the years 1901 and 1961 received above normal rainfall which was due to the movement of low pressure systems from the Bay of Bengal.

In the September month, it was found that all the three years experienced severe drought conditions with an average rainfall deficiency of 41 percent. This comparison indicates that the maximum rainfall deficiency and the consequent drought can occur in the month of September due to the absence of tropical disturbances.

REFERENCES

Bates, C.G., 1935. Climatic characteristics of the plains. *In*: M Silcox, F. A. et al. (editors), Possibilities of shelterbelt planting in the plains region. Washington, D.C.

Dhar, O.N., Kulkarni, A.K. and Ghose, G.C., 1978. Rainfall distribution over Indian subdivisions during the wettest and the driest monsoons of the period 1901 to 1960. *Hydrological Sciences Bulletin*, *IAHS*, 23, 2.

Dhar, O.N., Rakhecha, P.R. and Kulkarni, A.K., 1979. Rainfall study of severe drought years of India. Proceedings, Hydrological Aspects of Droughts, New Delhi, Indian Institute of Technology, New Delhi.

Dhar, O.N., Mandal, B.N. and Rakhecha, P.R., 1982. Absence of tropical disturbances and rainfall distribution during the summer monsoon months over India. *Arch. Met. Geoph. Biokl.*, Ser. A, 31, pp. 117-126.

Dhar, O.N., Mandal, B.N. and Rakhecha, P.R., 1984. Rainfall distribution over India during the monsoon months in the absence of depressions and cyclonic storms. *Mausam*, 35, No. 1, pp. 309-314.

Government of India, 1976. Climate and Agriculture. Part IV of the Report of the National Commission on Agriculture, Ministry of Agriculture and Irrigation, New Delhi.

Gibbs, W.T. and Maher, J.V., 1967. Rainfall deciles as drought indicators. Bull. No. 48, Bureau of Meteorology, Melbourne, Australia.

Hoyt, W.G., 1942. Droughts. *In*: Meinzer O.E (ed.), Hydrology, Dover Publications, INC, New York, 579-591.

India Meteorological Department, 1971. Rainfall and droughts in India. Report of the Drought Research Unit, Meteorological Department, Poona.

Indian Institute of Tropical Meteorology (IITM), 1995. Monthly and seasonal rainfall series for all-India homogeneous regions and meteorological subdivisions; 1871-1994, IITM, Research Report No. RR-065, 113 pp.

Mooley, D.A. and Parthasarathy, B., 1983. Indian summer monsoon and El Nino. *PAGEOPH*, 121, No. 2, pp. 339-352.

Parthasarathy, B., Sontakke, N.A., Munot, A.A. and Kothawale, D.K., 1987. Droughts/Floods in the summer monsoon season over different meteorological subdivisions of India for the period 1871-1984. *Journal of Climatology*, 7, pp. 57-70.

Penman, H.L., 1948. Natural evaporation from open water, bare soil and grass. *Proc. Roy. Soc. Series A*, 193, pp. 120-145.

Ropelewski, C.F. and Halpert, M.F., 1987. Global and regional scale precipitation patterns associated with the El Nino Southern Oscillation. *Monthly Weather Rev.*, 119, pp. 1606-1626.

Thornthwaite, C.W., 1948. A approach towards a rational classification of climate. *Geog. Rev.*, 38, pp. 55-94.

Thornthwaite, C.W. and Mather, J.R., 1955. The water balance. Publications in Climatology, Laboratory of Climatology, Vol. 8, No. 1, 104 pp.

United Nations Environment Programme (UNEP), 1997. World Atlas of Desertification (2nd edition), Arnold, London, NW1 3BH, 182 pp.

15 Floods

Extreme hydrometeorological events that arise from unusually high and low precipitation are characterized by floods and droughts, respectively. In the previous chapter we have discussed unusually low rainfall leading to droughts. Apparently, floods and droughts are weather related phenomena and because of the differences in climate, topography and precipitation, their characteristics, such as magnitudes, duration of occurrence, time of occurrence, frequency of occurrence, number of occurrences, and time interval between occurrences, significantly vary from region to region. The damages caused by these weather events in terms of the loss of life, persons affected, environmental damage, social disruption, and economic losses are all too known. It has been estimated that in the United States, the average annual flood losses is more than four billion dollars and for India, it is of the order of seven billion Indian Rupees. It can, therefore, be said that floods are serious problems in virtually every country of the world. In order to control them and keep damages down to the lowest possible level, their prediction is fundamental. In this chapter we discuss floods and their hydrometeorology for understanding why we have floods?

Generally speaking, a flood means inundation caused by rivers overflowing their banks on account of heavy rainfall and/or melting of large amounts of snow. There are many small as well as large rivers all over the world. These rivers are subjected to flooding when heavy widespread rainfall occurs in their catchment areas. Because of the economic advantages of level grounds, easy accessibility to fresh water, and fertile alluvial soils, people throughout the world prefer to settle near rivers—flood plains which are low flat areas on either side of a river. Flood plains are normally dry but may be covered with water from the overflow of rivers at the time of floods due to heavy rains. It is obvious that the people living in the close proximity of rivers suffer from inundations caused by floods. About 400,000 km^2 of land in India is prone to flooding of which about 79,000 km^2 land is affected by floods almost every year. Although people have been responding to floods

from rivers since time immemorial and the national government of every country are making various efforts to control floods, much more is still to be done in order to mitigate floods.

15.1 DEFINITION OF FLOOD

Defining a flood is a difficult task, partly because floods are a complex phenomenon and partly because they are viewed differently by different people. In a hydrological sense, a flood is a relatively high flow which overtakes the natural channel provided for runoff (Chow, 1956). Ward (1978) defines that a flood is a body of water which rises to overflow land which is not normally submerged. In a hydrometeorological sense, a flood can be defined as a situation over a region where the rainfall amount is more than a certain amount of the normal for that region (WMO, 1975; IMD, 1971). Many countries use in some form or other the criterion of a given percentage of the normal as the definition of flood. The India Meteorological Department (IMD) (1971) has defined flood as a situation occurring in a subdivision in a year when the seasonal rainfall is more than 125 percent of the normal. If the rainfall is more than 125-150 percent of normal, it is called moderate flood and if rainfall is more than 150 percent of the normal, it is called a severe flood.

15.2 KINDS OF FLOODS

Different kinds of floods can be characterized in relation to meteorological processes. A brief discussion of these floods is given as follows.

15.2.1 Flash Floods

A flash flood is a flood that occurs suddenly without warning and lasts for a short time and is caused by thunderstorms. A thunderstorm, as defined by WMO, is one or more sudden electrical discharges, manifested by a flash of lightening and a sharp or rumbling sound (thunder). It usually develops in an unstable and moist atmosphere. A cumulus cloud is formed when warm moist air from the surface rises and is lifted to higher altitude and condenses. A matured thunderstorm often has a cellular structure with a diameter reaching 3 to 5 kilometers and its top exceeding 10 kilometers. Cells may occur singly or in clusters. Thunderstorms last on average of 15 to 30 minutes and are capable of producing hail and heavy rains. Heavy rains caused by thunderstorms can lead to flash flooding and landslides. Because of their small scale, there is no satisfactory method for predicting the occurrence of a thunderstorm. Thus disaster mitigation measures against thunderstorms and flash floods are rather difficult. Nevertheless much can be done by way of identifying areas and meteorological situations that favor the occurrence of a thunderstorm.

15.2.2 Heavy Rainfall Floods

Widespread heavy to very heavy rainfalls for periods of days occur from tropical and extra tropical storms. The rainfall area can be as large as 400,000 km^2 and point rainfall may range from 40 to 80 cm per day (Pisharoty and Asnani, 1957; Bao, 1987; Rakhecha and Pisharoty, 1996). Such heavy and widespread rains can produce severe and destructive floods. Floods in India occur mainly during the monsoon season from June to September. During this season, heavy to very heavy rainfalls for several days are caused by the penetration of tropical storms arising from the Bay of Bengal and the Arabian Sea.

15.2.3 Coastal Floods

Coastal floods are generally caused by storm surges generated from cyclonic storms. A storm surge is a large dome of water often 80 to 100 km wide and 4 to 8 m deep that sweeps across the coastline near where a cyclonic storm makes a landfall. The stronger the cyclonic storm and the shallower the offshore water, the higher the surge. Along the immediate coast the storm surge is the greatest threat to life and property. For example, a cyclonic storm of November 1979 which crossed the Andhra Coast on November 19 produced a peak storm surge of about 6 m high. The storm surge was responsible for killing as many as 15,000 people in and near the coastal area of Krishna district of Andhra Pradesh. Also, the hurricane Camille that struck the U.S.A. in 1969 caused a storm surge about 8 m high and inundated Pass Christian in Mississippi. There are similar examples of coastal flooding from cyclonic storms in other countries of the world. If the surge occurs near the mouth of a river falling into the sea, the river flow is backed up from the surge resulting in severe flooding over coastal areas and saltwater intrusion.

15.2.4 Dam Failure Floods

Dams are built across rivers to collect and store water to serve the needs of the people as well as reduce flood hazards. These dams are sometimes overtopped, due to the underestimation of design flood and spillway capacity. The failure of dams causes serious floods in the down stream areas. Floods due to dam failures have occurred in many countries of the world. For example, in 1979, the collapse of Machhu-2 dam in Gujarat caused deaths of about 2000 people in the Morui town. Heavy rainfall in the Hongu River catchment in China destroyed the Banqiao and Shimantan dams. Flash floods from the broken dams have caused deaths of thousands of people and widespread destruction to the downstream property. Some dam overtopping incidents in various parts of the world have resulted from the underestimation of design flood and/or operational problems with outlet works, as shown in Table 15.1.

<div align="center">**Table 15.1:** Dam overtopping incidents</div>

S. No.	Dam	Country	Year of Construction	Year of Overtopping
1	Brises	Australia	1924-1928	4 April 1929
2	Euclicles Da Cunha	Brazil	1958-1960	19 January 1977
3	Gibson	USA	1929	8 June 1964
4	Machhy-2	India	1967-1972	11 August 1979
5	Noppikoski	Sweden	1964-1967	7 September 1985
6	Sella Zerbino	Italy		13 August 1935
7	South Fork	USA	1838-1852	31 May 1889
8	Spitskop	South Africa	1970-1974	23 February 1988

15.3 CAUSES OF FLOODS

Floods occur due to a number of reasons most frequent of which is heavy rainfall associated with an unusual meteorological situation. When a large amount of rain falls in a few days, the ground becomes so wet that no more rain can seep through the soil. This rain water runs into the nearby river and the water level quickly becomes too high. Ultimately, the river cannot hold this extra water and the water overflows the river banks. In mountainous and colder regions of the world, the interplay of snow and ice with rain and temperature create critical flood conditions. Cyclones, hurricanes, or typhoons can form over seas and move towards coastlines. When they strike coasts, they cause huge destruction because of strong winds and flooding due to storm surge. A tropical cyclone in Bangladesh in November 1990 caused deaths of nearly 300,000 people, while Hurricane Mitch that struck Central America in October 1998 caused fatalities in excess of 11,000 and the total damage was estimated at over five billion U.S. dollars. In case of dam failure causing a flood, if enough dam spillways are not opened in times of heavy rainfall, the water builds up behind the dam in the reservoir. This water can then spill over the top of the dam. Apparently, flood is mostly a phenomenon of rivers and their surroundings. An area with no rivers may also suffer from floods if there is inadequate drainage.

15.4 EFFECTS OF FLOODS

Worldwide statistics in terms of significant damage, persons affected and the number of deaths caused by several kinds of weather related disasters during 1963-1992 is given in Table 15.2 (WMO, 1994). This table shows that throughout the world, floods rank as one of the most destructive among several weather related disasters.

Table 15.2: Major natural disasters around the world
during 1963-1992 (after WMO, 1994)

Natural Disaster	Significant Damage (in %)	Persons Affected (%)	Number of Deaths (in %)
Floods	32	32	26
Droughts	22	33	3
Earthquakes	10	4	13
Tropical Cyclones	30	20	25
Famine/Food Shortage	-	4	
Land Slides	-	-	7
Epidemics	-	-	17
Other Disasters	6	7	9

A total of 4.0 billion dollars of annual flood losses in the United States, an ever increasing percentage (Platt, 1979) result from catastrophic floods that have recurrence intervals of 100 years or more, or is caused by failure of a flood-protection project by exceeding the project design flood (Moss et al., 1978). The effects of a flood can be catastrophic, with the following consequences:

- Roads, railway lines, and bridges are broken,
- Houses are wrecked,
- Crops are damaged,
- People and animals are killed,
- Household items get damaged,
- The electricity and gas supplies are cut off,
- Diseases are spread,
- Beach erosion is caused,
- Coastal land loss is caused,
- Environmental pollution is caused,
- Social interruption is perpetrated, etc.

Table 15.3: Flood damage in India during 1953-1977

Parameter	Average Damage	Maximum Damage	Year of Maximum Damage
Area affected in km^2	78100	178900	1976
Population affected in million	24.6	61.5	1973
Crop area affected in km^2	33200	78000	1977
Value of crop affected in million rupees	1675	7055	1977
Homes damaged	806000	2428000	1971
Cattle lost	61224	292920	1977
Human lives lost	1132	9848	1977

In India, severe floods with serious consequences occurred during 25 years from 1953 to 1977 (Framji, 1983). Table 15.3 gives values of average yearly damage caused by floods and the year of the maximum damage.

15.5 SURFACE RUNOFF AND RUNOFF PROCESS

When rain falls, a part of it is first intercepted by vegetation. Some of it is stored in depressions on the ground surface and is known as depression storage which ultimately infiltrates or evaporates. Some of the rainfall is absorbed by the soil, the amount of which depends upon the soil moisture conditions existing at the time of rainfall. If the rain continues further, the water starts infiltrating to the water table and if the rate of rainfall exceeds the infiltration rate then excess water begins to flow overland and joins streams, rivers, lakes, oceans, etc. This flow of water is known as surface runoff. Part of rainfall which infiltrates moves laterally through upper crust of the soil without reaching the water table but joins streams as interflow or sub-surface flow and is considered as part of surface runoff. On the other hand the rainfall that reaches the groundwater table and later after a long time joins the river stream is known as groundwater runoff or base flow. The runoff thus actually consists of two portions, namely direct runoff and base flow. The direct runoff includes surface runoff, prompt subsurface runoff and rainfall on the channel surface. The base flow provides the dry weather flow in perennial rivers, while the surface runoff is important for the maximum flow or flood of the rivers. For the peak flood flow, the hydrologist is generally concerned with surface runoff and therefore the term runoff is exclusively used for surface runoff. The difference between the total rainfall and that which is intercepted is called effective rainfall. The difference between the effective rainfall and losses in the form of infiltration, evaporation, and depression storage is known as rainfall excess.

15.6 RUNOFF MEASUREMENTS

The magnitude of runoff in a river is measured by either its stage or its discharge. The stage of a river is the water level measured above a datum which can be the mean sea level or any arbitrary datum. The discharge of a flood in a river is the volume of water per unit time flowing past a cross section of the river. It is usually expressed as cubic meters per second (m^3/s). Measurement of runoff discharge in a river is important for design of flood control works. For example, the stage is important in defining the extent of the area inundated and the minimum elevation of any structure built on the flood plain as is the peak discharge for the design of spillways of dams. Considerable efforts are made in every country to measure, collect, and store stage and discharge data. The World Meteorologist Organization (WMO) recommendations for the minimum number of river gauging stations needed for discharge measurements in different geographical regions are given in Table 15.4.

Table 15.4: WMO criteria for river gauging stations

S. No.	Region	Minimum density (km^2/station)	Tolerable density (km^2/station)
1	Flat region of temperate, Mediterranean, and tropical zones	1000-2500	3000-10000
2	Mountainous regions of temperate, Mediterranean, and tropical zones	300-1000	1000-5000
3	Arid and polar zones	5000-20000	-

An adequate number of gauging stations must be sited in catchments of all major rivers so that their water potential can be assessed as accurately as possible. In India, stream flow observations are carried out by the states in their irrigation, hydroelectric, highway and public health departments. Apart from these, Indian Railways also carries out stream flow measurements at various railway bridges in the country. The Central Water Commission (CWC) has also been conducting stream flow observations at selected sites.

15.7 HYDROGRAPH

A hydrograph is the graphical representation of stream flow or discharge data with time at any section of a river. Time is always plotted on the X-axis and discharge on Y-axis as shown in Fig. 15.1. The hydrograph is the response of a given catchment for a rainfall input. It consists of flow in all the three phases of runoff, namely, surface runoff, interflow and base flow, and embodies in itself the integrated effects of a wide variety of catchment and rainfall characteristics. Thus two different rain events in a river catchment produce hydrographs differing from each other. Similarly, identical rain events in two different catchments produce hydrographs that are different. Figure 15.1 shows that a hydrograph has three main components: the rising limb, the crest segment and the falling or recession limb.

The rising limb reflects the characteristics of the catchment and storm rainfall. The initial high infiltration losses during the early period of a storm cause the discharge to rise rather slowly in the initial periods. As rainfall continues more and more flow from different parts of the catchment reach the measuring site. Similarly, infiltration losses also decrease with time. Thus, under a uniform storm over the catchment runoff increases rapidly with time. The crest segment is the most important part of a hydrograph as it contains peak flow. The peak flow occurs when runoff from various parts of the catchment simultaneously contributes the maximum amount of flow at the measuring site. Generally for large size catchments, peak flow occurs after the cessation of rainfall. Multiple peaked complex hydrographs in a
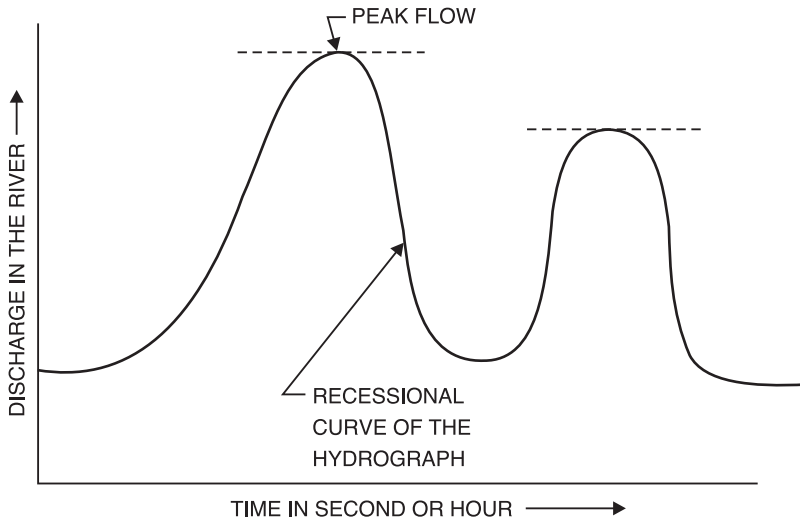
Fig. 15.1. A typical river hydrograph.

catchment can occur when two or more storms occur in close succession. The estimation of peak flow and its occurrence is very important in flood flow studies. A falling limb reflects the presence of subsurface runoff and the withdrawal of water from storage built up in the catchment. The falling limb begins at the point of inflection from the crest segment which marks the time at which inflow to the stream channels ceases. The shape of the falling limb is independent of the characteristics of the storm rainfall.

15.8 FLOOD CONTROL

The term 'flood control' is used to denote all efforts exercised to reduce damage to life and property caused by floods. From an extremely large flood occurring in a river the complete and strict control of the flood of negligible loss is neither physically possible nor economically feasible. However, there are ways by which to mitigate or minimize to some extent the impact of flood damage on people and property by adopting the following protective methods:

Structural methods of flood control:
- constructing storage and detention reservoirs,
- constructing levees and flood walls, in itself the integrated effects of a wide channel improvement, and
- constructing new channels or flood walls.

Non-structural methods:
- flood plain zoning, and
- flood forecasting.

15.8.1 Storage Reservoirs

Flood control storage reservoirs have been built on many streams and rivers to store flood waters. A storage reservoir holds a portion of the flood waters when the flood is rising and releases it later when the flood is receding.

15.8.2 Detention Reservoirs

A detention reservoir stores excess water during floods and releases it after the flood. It is similar to a storage reservoir but it is provided with large gated spillways and sluiceways to release the stored water in a controlled way. In the earlier stages of a flood, the gates are left open and the water is released, subjected to the safe carrying capacity of the channel downstream. In the later stages of the flood, when the discharge downstream exceeds the maximum capacity of the downstream channel, the gates are kept partially closed. There is basically no difference between the detention reservoir and a storage reservoir, except that the former has a larger spillway capacity and sluiceway capacity to permit rapid downstream flow just before or after a flood. The reservoir is quickly emptied and thus the full reservoir capacity is made available again for moderating a subsequent flood after a short interval. In this manner, the available capacity is more effectively utilized.

15.8.3 Levees

Levees, also called dikes, are earthen walls which are constructed parallel to the river flow at some suitable distance from the river. Such walls or embankments may be raised either on both sides of the river or only on one side for some suitable distance, where the river is passing through towns and cities or other places of importance. These embankments retain and confine the flood water in between them, thereby preventing them from spreading into adjoining lands and towns. The levees being earthen walls require much care and maintenance. Although levees provide protection from some floods, they can, being earthen, be eroded by large floods and cause enormous damage.

15.8.4 Flood Walls

Flood walls are used in a developed area where it is rather difficult to obtain enough land for the construction of levees. Because of flat slopes, levees require a very large base width. If the land is limited, it is more economical to construct flood walls. A flood wall is a reinforced concrete and cement (RCC) or masonry wall.

15.8.5 Channel Improvement

The improvement of river channels involves straightening, widening or deepening of channels to increase their discharge carrying capacity.

15.8.6 Floodways

Floodways are bypass and diversion channels into which part of the flood would be diverted during high floods. A floodway can be a natural or man-made channel and its location is controlled essentially by topography. Generally, wherever they are feasible, floodways offer an economical alternative to other structural flood control works.

15.8.7 Flood Plain Zoning

Flood plain zoning means restricting any human activity in the flood plains of a river. The areas affected by floods are divided into different zones in flood plain zoning. The area affected by flood increases as the flood discharge increases. The flood discharge depends upon the recurrence interval. Therefore, the flood plain zoning can be done according to the recurrence interval. For example, flood zones can be demarcated as zones of 1, 2, 5, 10, 15, or 100 year floods. Evidently, the area under a 100-year flood will be much more than under a 5-year flood. The basic objective of flood plain zoning is to restrict encroachment of the zone which frequently comes under the influence of flood. The areas which are prone to yearly flood may be put to agricultural uses. However, crops and vegetables grown in these zones should be of such types that they are harvested well before the start of the next rainy season.

15.8.8 Flood Forecasting

Flood forecasting for a river basically means estimating future stages or water levels in the river at selected places along the river during the flood season. The aim is to forecast river stage and its time of occurrence at a place along the river. For formulating flood forecasts, it is necessary to have relevant hydrological data, such as physical and geographical characteristics of the river catchment and flood plains, such as current levels of water and flow in the river; and hydrometeorological data, such as rainfall in the catchment and weather forecast. These data are then the basic input to flood forecasting techniques, which may include graphical techniques, rainfall-runoff models, unit hydrograph and computer models.

A flood forecasting system basically involves:

- hydrological and hydrometeorological observations,
- transmission of data to flood forecasting stations,
- data processing,
- formulating of flood forecasts at flood forecasting stations, and
- dissemination of flood forecasts to users.

Reliable forecasts of floods with sufficient lead time are of vital importance for people likely to be affected.

15.9 ESTIMATION OF PEAK FLOOD

The maximum or peak flood value generated by a river system is required for the design of flood control works, such as spillways for storage and detention reservoirs, waterway opening in bridges, height of flood walls and levees, highway and railway culverts, urban storm sewers, and many other flood control hydraulic structures. To estimate the magnitude of a flood peak the following methods are used when direct (current meter) measurements cannot be obtained:

- Rational method
- Empirical methods
- Unit hydrograph methods
- Flood frequency methods

The use of a particular method depends upon the desired objective, the available data and the importance of the flood control project.

15.9.1 Rational Method

This method of estimating the peak flood discharge is based on physical and hydraulic properties of catchments and their effects on storm rainfall. The peak flood discharge value is given as:

$$Q = 0.278 \ CIA \qquad (15.1)$$

where Q = peak flood discharge in m^3/s, C = runoff coefficient, A = catchment area in km^2, I = rainfall intensity in mm/hr with the selected recurrence interval T (years) and duration equal to the catchment's time of concentration (t_c) in minutes.

The time of concentration is defined as the time which would be required for surface runoff from the remotest part of the catchment to reach the outlet or the point of interest on the water course. The time will vary, depending on the slope and characteristics of land surfaces. There are a number of empirical equations for the estimation of the time of concentration. For small drainage basins, the time of concentration was given by Kirpich (1940) as:

$$t_c = 0.01947 L^{0.77} S^{-0.385} \qquad (15.2)$$

where t_c is the time of concentration in minutes, L is the maximum length of travel of water in meters and S is the slope of the catchment.

Coefficient C represents the integrated effect of catchment losses and therefore depends upon the nature of the surface, surface slope, and rainfall intensity. Some typical values of the coefficient C are given in Table 15.5. The rainfall intensity corresponding to the time of concentration t_c and the desired recurrence interval T for the catchment can be found from rainfall-frequency-duration relationship.

Table 15.5: Values of coefficient *C*

Type of Area	Value of C
Flat residential area	0.4
Moderately steep residential area	0.6
Built up areas—impervious	0.8
Rolling lands and clay loam soils	0.5
Hilly areas, forests, clay, and loamy soils	0.5
Flat cultivated lands and sandy soils	0.2

Example 15.1: Determine the peak discharge for use in the design of a bridge with the following data:

Catchment area   = 20 hectares
Time of concentration   = 20 minutes
Intensity of rainfall during 20 minutes = 120 mm/hour
Runoff coefficient   = 0.6

Solution:

$Q = 0.278\ CIA$
$A = 0.2\ \text{km}^2$
$I = 120\ \text{mm/hr}$
$C = 0.6$
$Q = 0.278 \times 0.6 \times 120 \times 0.2 = 4\ \text{m}^3/\text{s}$

Example 15.2: Determine the peak discharge for use in the design of a culvert. The catchment has the following characteristics:

Mains stream length = 10.50 m
Catchment area   = 1.85 km²
Slope   = 0.006
Runoff coefficient   = 0.30

The maximum depth of rainfall with a 25-year return period is as follows:

Duration (min)	5	10	20	30	40	60
Raindepth (min)	17	26	40	50	57	62

Solution: The time of concentration is calculated using equation:

$t_c = 0.01947L^{0.77} \times S^{-0.385}$
$\quad = 0.01947(1050)^{0.77} \times (.006)^{-0.385}$
$\quad = 0.01947 \times 211.99 \times 7.168$
$\quad = 29.6\ \text{minutes}$

Maximum depth of rainfall for a duration of 29.6 minutes

$= 40 + (50 - 40)/10 \times 9.6$
$= 49.6\ \text{mm}$

Average intensity = (49.6/29.6) × 60 = 100.5 mm/hr

$Q = 0.278 \times 30 \times 100.5 \times 1.85 = 15.5$ m^3/s

15.9.2 Empirical Formulae

Several empirical formulae to determine peak flood discharge as a function of the catchment area have been developed in various parts of the world. Chow (1964) lists such formulae. Almost all formulae use catchment area as a parameter affecting the flood beak and neglect flood frequency as parameter. These empirical formulae are applicable only in the region from which they were developed and when applied to other areas they give approximate values. Some of the more commonly used formulae are discussed below:

15.9.2.1 Dicken formula

Dicken made the first attempt in India to derive a general formula for estimating the peak flood (Q) as a function of catchment area (A) on the basis of studies conducted for determining waterway capacities for bridges. His formula is

$$Q = CA^{3/4} \tag{15.3}$$

where Q = peak flood in m^3/s, C = Dicken's constant with a value between 6 and 30, and A = catchment area in km^3. The formula is widely used in north and central India. The values of C for catchments located in the north Indian plains, north Indian hilly regions, central India and the coastal Andhra and Orissa are 6, 11-14, 14-28, and 22-28, respectively.

15.9.2.2 Ryves formula

Ryves modified Dicken's formula for application to river catchments in southern India. His formula is:

$$Q = CA^{2/3} \tag{15.4}$$

where Q = peak flood in m^3/s, C = Ryves coefficient, and A = Catchment area in km^2. The values of C for catchments located within 80 km from the east coast, 80-60 km from the east coast and near hills are 6.8, 8.5, and 10.2, respectively.

15.9.2.3 Inglish and Desouza formula

Based on the flood data of catchments in Western Ghats in Maharashtra, Inglish and Desouza (1930) developed a formula for estimating flood peak as:

$$Q = 124A/(A + 10.4)^{1/2} \tag{15.5}$$

where Q = peak flood in m^3/s, and A = catchment area in km^2.

15.9.2.4 Other empirical formulae

There are other empirical formulae which relate peak flood discharge to catchment area and flood frequency. Fuller (1914) gave the formula for catchments in the USA as:

$$Q = CA^{0.8}(1 + 0.8 \log T) \qquad (15.6)$$

where Q = peak flood in m^3/s with a frequency of T years, A = catchment area in km^2, and C = a constant with values between 0.18 and 1.88.

15.9.2.5 Bairel and Mellwraith formula

Based on the highest recorded floods throughout the world, Bairel and Mellwraith (1951) developed a formula for estimating peak flood as:

$$Q = 0.3025A/ (278 + A)^{0.78} \qquad (15.7)$$

Example 15.3: Estimate the maximum flood for the following catchments by using an appropriate empirical formulae:

(i) A_1= 40 km^2 in Western Ghats of Maharashtra
(ii) A_2 = 40 km^2 in Gangetic plains
(iii) A_3 = 40 km^2 in the Cauvery delta of Tamil Nadu
(iv) What is the peak flood value for A = 40 km^2 using world's maximum flood formula?

Solution: 1. For the catchment in Western Ghats in Maharashtra, the Inglish formula is used.

$$Q = 124A/(A + 10.4)^{1/2}$$
$$= 124 \times 40/(40 + 10.4)^{1/2}$$
$$= 4960/7.10 = 699 \text{ m}^3/\text{s}$$

2. For the catchment in the Gangetic plains Dicken's formula with C = 6.0 is used.
$$Q = 6(40)^{0.75}$$
$$= 6 \times 15.9 = 95.4 \text{ m}^3/\text{s}$$

3. For the catchment in the Cauvery delta of Tamil Nadu, the Ryves formula is used with C = 6.8.
$$Q = 6.8(40)^{2/3}$$
$$= 6.8 \times 11.7 = 79.5 \text{ m}^3/\text{s}$$

4. The maximum peak flood value based on world's maximum flood formula.
$$Q = 3025 \times 40/ (278 + 40)^{0.78}$$
$$= 121000/ 89.5 = 1352 \text{ m}^3/\text{s}$$

15.9.3 Unit Hydrograph Method

In 1932 Sherman developed the concept of the unit hydrograph (*UH*) for determining the surface or direct runoff hydrograph (*DRH*) from the effective rainfall hyetograph (*ERH*). The unit hydrograph, or simply unit graph, of a watershed is defined as the *DRH* resulting from one unit (1 inch or 1 centimeter) of effective rainfall (*ER*) occurring uniformly over the watershed at a uniform rate during a unit period of time. This unit period is not necessarily equal to unity; it can be any finite-period duration up to the time of concentration. This unit period of *ER* is the period for which the *UH* is determined for a watershed. As soon as this period changes, so does the *UH* for the watershed. This means that there can be as many *UHs* for a watershed as periods of *ER*. Often used are 1-hour *UH*, 6-hour *UH*, 12-hour *UH*, or 1-day *UH*. Here the duration of one hour, six hours, 12 hours, or one day is not the duration for which the *UH* occurs, but it is the duration of the *ER* for which the *UH* is derived. Since *ER* is assumed constant during its duration *D* for which the *UH* is derived, the effective rainfall intensity (*ERI*) is 1/*D*.

The unit hydrograph is based on certain postulates which can be stated as follows: (1) For a given drainage basin, the duration of surface runoff is constant for all uniform-intensity storms of the same duration, regardless of differences in the total volume of surface runoff. (2) For a given drainage basin, if two uniform-intensity storms of the same length produce different total volumes of surface runoff, then the rates of surface runoff at corresponding times, after the beginning of two storms, are in the same proportion to each other as their total volumes of surface runoff. (3) The time distribution of surface runoff from a given storm period is independent of concurrent runoff from antecedent storm periods. Postulates 1 and 2 together make up the principle of proportionality. In other words, if the duration of *ER* is fixed but its volume changes, then the duration of *ERH* does not change but its ordinates do in proportion to the volume of *ER*. The third postulate is the principle of superposition, which allows the decomposition of a complex *ERH* into rectangular blocks or pulses and then superimposing on one another hydrographs of these rectangular pulses, each of steady intensity, to obtain the total *DRH*.

As stated in the definition of the unit hydrograph, it is assumed that *ER* is uniformly distributed within its duration. This means that the rainfall intensity is uniform throughout the watershed during the time rain falls. The other assumption is that it is uniformly distributed throughout the watershed. This means that uniform runoff occurs from all parts of the watershed. Since *ER* is defined as that portion of rainfall that produces surface runoff, all abstractions must be subtracted from rainfall and in order for *ER* to be uniform, abstractions must be uniform throughout the watershed.

The above postulates, together with the definition and the assumptions, constitute what is now referred to as the unit hydrograph theory. The theory fundamentally assumes that the watershed is linear and time invariant. That

is, *DRH* is derived from *ERH* by a linear operation. Once the assumption of linearity and time invariance is recognized, the theory can be applied to any linear and time-invariant system (Singh, 1988, 1989) and is, no way, restricted to computing the surface runoff hydrograph only. It is this reason that it has been employed to derive the unit sediment hydrograph, the unit pollutant graph, the unit groundwater hydrograph, the unit interflow hydrograph, among others. Thus, in a generic sense, the behavior of a linear time-invariant system that receives input and produces output can be described by the theory. By conservation of mass, the volume of input must be equal to the volume of output.

The dimensions of the *UH* can be expressed in two ways. First, if *UH* is derived from *DRH* due to *ER* of specified duration whose depth is not unity, then the dimensions of the *UH* ordinates will be equal to the dimensions of runoff divided by the dimension of the depth of *ER*. Runoff can, however, be expressed either in terms of discharge having volumetric rate units or specific discharge having volumetric rate per unit area or intensity units. Therefore, the dimensions of the *UH* ordinates are either the dimensions of discharge per unit depth or the dimensions of discharge per unit area per unit depth. Let L denote the dimension of length and T the dimension of time. Then, the two forms of the dimensions of the *UH* ordinates are: (1) L^2/T and (2) $1/T$.

Limitations of the Unit Hydrograph Theory

The unit hydrograph theory is only an approximation and its postulates are not strictly valid. Nevertheless, it is a useful practical tool and is amenable to linear mathematics whose methods are simple and best understood.

The *ER* of a specified duration seldom occurs uniformly over the watershed of a reasonable size. The spatial variation generally becomes more pronounced as the watershed size increases. Rain storms that produce intense rainfall usually do not extend over large areas. The nonuniform distribution of rainfall can cause variation in the hydrograph shape. However, errors in the *UH* due to nonuniformity in areal distribution can be minimized by decomposing the watershed into subwatersheds, each being small enough to ensure approximately uniform areal distribution, deriving the *UH* for each subwatershed, and then appropriately combining these *UHs* to develop the *UH* for the entire watershed.

The *ER* seldom occurs uniformly, even for as short a duration as five minutes. However, the effect of temporal variation of rainfall intensity on the *UH* shape depends principally on the watershed size. For example, rainfall bursts lasting only a few minutes may produce well-defined peaks in the runoff hydrograph from small watersheds, but may cause little change in the runoff hydrograph shape from large watersheds. The effect of temporal variation can be minimized by employing the instantaneous unit hydrograph (*IUH*).

All watersheds in nature are nonlinear; some are more linear and some are less. They are linear only by assumption. If hydrographs from storms of the same duration are compared, their ordinates are not found to be in proportion to their corresponding runoff amounts. The peaks of *UHs* for small rainfall events are usually lower than those for larger ones.

Mathematical Equations of Unit Hydrograph

In order to avoid ambiguity in the interpretation of the *UH*, it must be emphasized that it corresponds to a particular duration of the *ER* and has volume of one unit (i.e., 1 inch or 1 cm). Because *ER* is assumed to occur uniformly, its duration is sufficient to define its uniform intensity. This duration is referred to as the unit storm duration and may change from one application to another. Thus, for a given watershed there can be a large number of *UHs*, each corresponding to a specific duration of *ER*.

Let *ERH* of a *D*-hour duration be denoted as

$$I(t) = I, \ 0 \leq t < D; \quad I(t) = 0, \ t \geq D \tag{15.8}$$

with *I* as a constant *ER* intensity (L/T), the *D*-hour *UH* as $h(D, t)$ and the resulting *DRH* as $Q(t)$. Then, applying the principle of proportionality one obtains

$$Q(t) = h(D, t) \, I(t) \, D = h(D, t) \, I \, D \tag{15.9}$$

The quantity $I \, D$ denotes the volume of *ER*. This equation states that the *DRH* is proportional to the *ER* volume. When, $I \, D = 1$, the *DRH* and *UH* are numerically the same.

Let an *ERH* be a complex hyetograph composed of an *n* number of pulses, each of duration *D* hours. Let the intensity of pulse *j* be I_j, $j = 1, 2, 3, \ldots, n$, and the *DRH* of pulse *j* be $Q_j(t)$. If the *D*-hour *UH* is $h(D, t)$, then the *DRH* due to the complex hyetograph can be expressed as

$$Q(t) = \sum_{j=1}^{n} Q_j(t - (j-1)D) \tag{15.10}$$

Now, note that Q_1 starts at $t = 0$, Q_2 starts at $t - D$, and Q_j starts at $t - (j - 1)D$. The individual *DRHs* can be expressed as

$Q_1(t) = h(D, t) \, I_1 \, D$
$Q_2(t - D) = h(D, t - D) \, I_2 \, D, \quad h(D, t - D) = 0, \ t \leq D$
$Q_3(t - 2D) = h \, (D, t - 2D) \, I_2 \, D, \quad h(D, t - 2D) = 0, \ t \leq 2D$ (15.11)
.

.
$Q_n(t - (n - 1) \, D) = h \, (D, t - (n - 1) \, D) \, I_n \, D,$
$h \, (D, t - (n - 1) \, D) = 0, \ t \leq (n - 1) \, D$

Thus, the *DRH* can be expressed as

$$Q(t) = \sum_{j=1}^{n} h(D, t - (j-1)D) \, I_j \, D \tag{15.12}$$

Since the *DRH* at any time *t* is the result of the *ERH* pulses occurring up to that time but not subsequent to it, equation (15.12) must be modified as

$$Q(t) = \sum_{j=1}^{t} h(D, t - (j-1)D) \, DI_j \, D \qquad (15.13)$$

For purposes of simplicity, time *t* can be taken as a discrete variable taking on values at *D* time intervals.

The difficulty arising from the dependence of the *UH* on the duration of *D* of the *ER* is circumvented by letting *D* tend to be instantaneous. The *UH* so obtained is called the instantaneous unit hydrograph (*IUH*). Thus, the *IUH*, $h(0, t) = h(t)$ is a hypothetical *UH* due to the *ER* whose duration tends to zero as a limit, but whose volume remains unity (say, 1 cm). Clearly, the *IUH* is independent of the duration of *ER*. Mathematically,

$$h(t) = h(0, t) = \lim_{D \to 0} h(D, t) \qquad (15.14)$$

and

$$\delta(t) = \lim_{D \to 0} I(t, D) \, D \qquad (15.15)$$

where $\delta(t)$ is the Dirac Delta function occurring at $t = 0$. Physically, this function can be thought of as a spike of infinitesimally small thickness and infinitely large height such that the area under the spike is 1. Therefore, equation (15.13) can be expressed as

$$Q(t) = \int_{o}^{t} h(t - \tau) \, I(\tau) \, d\tau, \quad h(\tau) = 0, \quad \tau \leq 0 \qquad (15.16)$$

Because mathematical operations are linear, equation (15.16) can also be written as

$$Q(t) = \int_{o}^{t} h(\tau) \, I(t - \tau) \, d\tau \qquad (15.17)$$

with

$$h(t) \geq 0 \qquad \text{for any } t \geq 0$$

$$\lim_{t \to \infty} h(t) = 0$$

and

$$\int_{0}^{\infty} h(s) \, ds = 1$$

Experimental evidence shows that

$$\int (t - \bar{t}) \, h(t) \, dt > 0 \qquad (15.18)$$

where $\bar{t}$ is the centroid of the *IUH* located at the t-axis:

$$\bar{t} = \int_0^\infty t\, h(t)\, dt \qquad (15.19)$$

where equation (15.19) states that the *IUH* must be skewed to the right, that is, its peak must be to the left of the centroid with a long tail extending to the right.

If the duration of the *ER* is indefinitely long and its intensity is one unit per unit of time (say, 1 cm/hr), then the hydrograph so obtained is termed the summation hydrograph or S-hydrograph. This hydrograph assumes a deformed S-shape and its ordinates ultimately approach the rate of *ER* in the limit or at the time of equilibrium. If the *ERH* is broken down into pulses each of duration *D* hours, then the *SH* will be obtained by superimposing the *DRHs* due to individual pulses. For this *ERH*, *SH*, *U(t)*, are obtained from equation (15.13) as

$$U(t) = \sum_{j=1}^{t} h(D, t - (j-1)D)\, D \qquad (15.20)$$

$$= \sum_{j=1}^{t} Q(D, t - (j-1)D)$$

Clearly, if *D* tends to 0, $h(D, t - (j-1)D)$ tends to $h(t)$, the lower limit for summation will approach the origin, and

$$U(t) = \int_0^t h(s)\, ds \qquad (15.21)$$

Now, the relations between *IUH*, *UH*, and *SH* can be derived. From the definitions of the *UH* and *IUH*, one can write

$$h(D, t) = \frac{1}{D} \int_{t-D}^{t} h(s)\, ds \qquad (15.22)$$

Similarly, the relation between *UH* an *SH* can be expressed as

$$h(D, t) = \frac{1}{D} [U(t) - U(t - D)] \qquad (15.23)$$

As *D* tends to 0,

$$h(t) = \frac{dU(t)}{dt} \qquad (15.24)$$

It may be instructions to summarize that three hydrographs—*IUH*, *UH*, and *SH*—are ascribed to three distinct characteristics of the effective rainfall—volume, duration, and intensity—as shown below:

<div align="center">Effective Rainfall Characteristics</div>

Hydrograph	Volume	Duration	Intensity
IUH	Unity	Zero	Indefinite
UH	Unity	Finite	1/Duration
SH	Indefinite	Indefinite	Unity

It may also be noted that the time to the peak of $h(D, t)$ can be determined by differentiating equation (15.23) with respect to t, and equating the derivative to zero:

$$h(t) - h(t - D) = 0 \qquad (15.25)$$

Equation (15.25) states that the peak of $h(D, t)$ occurs at a time when the ordinate of the *IUH* is equal to the ordinate at D time units earlier. The *SH* attains its maximum value at a time equal to D hours less than the time base of the initial $h(D, t)$.

Unit Hydrograph Models

The unit hydrograph theory has been extensively applied to develop rainfall-runoff models. There is a large range of *UH*-based models, including empirical, conceptual, and physically based (Singh, 1988). However, for economy of space, only a simple conceptual model will be presented to illustrate the power of the *UH* theory. To develop a conceptual model, a watershed is represented by a network of linear elements, such as reservoirs and channels. This network can be defined using the laws of geomorphology or arbitrarily to best mimic the flow pattern in the watershed. Rainfall is reduced to the effective rainfall by subtracting infiltration. Then, an instantaneous *ER* is routed through the network of reservoirs and/or channels to obtain the *IUH* of the watershed. By convoluting this *IUH* with *ERH*, *DRH* is obtained.

A linear reservoir can be defined by a linear relation between storage S and surface runoff Q as

$$S = KQ \qquad (15.26)$$

where K is the residence time. The water balance of the reservoir can be expressed as

$$\frac{dS}{dt} = I(t) - Q(t) \qquad (15.27)$$

where I is *ER*, and t is time. Substitution of equation (15.27) in equation (15.26) yields

$$\frac{dQ}{dt} + \frac{1}{K} Q = \frac{I}{K} \qquad (15.28)$$

For an instantaneous $I(t)$, represented by $\delta(t)$, $Q(t)$ will reduce to $h(t)$. Therefore, equation (15.28) can be expressed as

$$\frac{dh}{dt} + \frac{1}{K} h = \frac{\delta(t)}{K} \tag{15.29}$$

For $h(0) = 0$, solution of equation (15.29) is

$$h(t) = \frac{1}{K} \exp\left(-t/K\right) \tag{15.30}$$

If n linear reservoirs are arranged in series, then the *IUH* of this cascade is:

$$h(t) = \frac{1}{K \; \Gamma(n)} \left(\frac{t}{k}\right) \exp\left(-\frac{t}{K}\right) \tag{15.31}$$

Equation (15.31) is a gamma function and is known as the Nash model (1957).

A linear channel is defined by a linear rating curve or a linear relation between flow cross-section $A(t)$ and discharge Q:

$$A = C(x) \; Q \tag{15.32}$$

where $C(x)$ is a constant at a channel section and varies with distance and has the connotation of the inverse of the velocity, and x is the distance along the channel. The continuity equation for a channel in one dimensional form can be written as

$$\frac{\partial Q}{\partial x} + \frac{\partial A}{\partial t} = 0 \tag{15.33}$$

Substitution of equation (15.32) in equation (15.33) produces

$$\frac{\partial Q}{\partial x} + C(x) \frac{\partial Q}{\partial t} = 0 \tag{12.34}$$

The inflow to the channel is at the upstream and can be denoted as $Q(x_0, t)$. A linear channel simply translates the flow by the time equal to the travel time, T. Thus, the solution of equation (15.34) is

$$Q(x_1, t) = Q(x_0, t - T), \quad T = C(x_1 - x_0) \tag{15.35}$$

where x_1 denotes the downstream end of the channel reach. If the inflow is given by the delta function $\delta(t)$ occurring at the upstream end of the channel, the *IUH* of the channel is

$$h(t) = \delta(t - T) \tag{15.36}$$

The linear reservoirs and linear channels can be arranged in a way that best represents the watershed. Dooge (1959) employed a network of linear channels and reservoirs to represent the watershed. Since all operations are linear, the

IUH of the network can be derived with little difficulty. For any $I(t)$, the *DRH* can be determined by convolving the *IUH* with $I(t)$ as

$$Q(t) = \int_0^t h(t - \tau)\, I(\tau)\, d\tau \qquad (15.37)$$

For practical purposes, equation (15.37) can also be expressed in discrete form.

Channel Flow Routing

The channel flow routing is performed using either systems-based approach or a hydraulic approach. The unit hydrograph theory is applicable to both approaches if they are linear. The systems-based approach based on the Muskingum method is perhaps the most popular. This method is comprised of equation (15.27) and a linear storage-discharge relation expressed as

$$S = k\, [wI + (1 - w)Q] \qquad (15.38)$$

where S is the storage of water within the channel reach, I is the inflow rate, Q is the outflow, and w and k are routing parameters. For a delta function inflow, $\delta(t)$, the *IUH* of the Muskingum method is obtained by substituting equation (15.38) in equation (15.27) and solving the combined equation:

$$h(t) = -\frac{w}{1 - w}\, \delta(t) + \frac{1}{k\,(1 - w)^2}\, \exp[-\frac{t}{k\,(1 - w)}] \qquad (15.39)$$

where $I(O)$ is $I(t)$ at $t = 0$. By convoluting equation (15.39) with $I(t)$, the outflow discharge $Q(t)$ can be obtained.

On the other hand, in a hydraulic approach the St. Venant equations are employed. The unit hydrograph theory has been applied to several linearized forms of these equations. One simple approximation is the kinematic diffusion approximation (Dooge, 1973; Singh, 1996) expressed as

$$\left(gh_0 - \frac{u_0^2}{4} \right) \frac{\partial^2 Q}{\partial x^2} = 3gS_0\, \frac{\partial Q}{\partial x} + \frac{2gS_0}{u_0}\, \frac{\partial Q}{\partial t} \qquad (15.40)$$

where h_0 is the flow depth at the reference discharge, u_0 is the velocity at the reference discharge, Q is the perturbation discharge around the reference discharge, g is the acceleration due to gravity, S_0 is the bed slope, x is the distance along the channel, and t is time. The reference discharge may correspond to the steady uniform flow. For an instantaneous flow at the upstream end of the channel reach, $\delta(t)$, the *IUH* of the channel reach described by equation (15.40) is:

$$h(t) = \frac{x}{\sqrt{4\pi D t^2}}\, \exp\left[-\frac{(x - at)^2}{4Dt} \right] \qquad (15.41)$$

where $a = 1.5\ u_0$, and

$$D = \frac{Q_0}{2S_0}\left(1 - \frac{F^2}{4}\right), \quad F = \frac{u_0}{\sqrt{g\ h_0}} \qquad (15.42)$$

where F is Froude number corresponding to the reference discharge, and D is hydraulic diffusivity. By convoluting equation (15.35) with the upstream discharge, the outflow (or routed) discharge can be obtained.

Derivation of Unit Hydrograph

Unit hydrograph is a very useful tool in flood estimation. Its main advantage is that instead of giving only the value of the peak flood magnitude, it can generate the entire flood hydrograph corresponding to any rainstorm. The unit hydrograph from an isolated storm can be prepared as follows:

(1) A number of isolated storm hydrographs caused by intense rainfalls over the catchment area are selected. It is desirable to select the hydrograph having the largest volume of runoff, preferably 2.5 cm to 5.0 cm.
(2) Estimate the duration of rainfall effective in producing direct runoff.
(3) Separate the hydrographs into direct runoff and base flow.
(4) Measure the total volume under each of the direct runoff hydrograph (DRH).
(5) The volume under the respective hydrographs is divided by the catchment area to obtain the depth of excess rainfall values.
(6) The ordinates of the various DRHs are divided by the respective excess rainfall values so as to obtain the ordinates of the unit hydrographs.

A number of unit hydrographs of a given duration are derived in this manner and then plotted on a common pair of axes. Because of rainfall variations in space and time, the various unit hydrographs thus determined may not be identical. It is a common practice to adopt a mean of such curves as the unit hydrograph of a given duration for the catchment. For deriving the mean curve the average of peak flows and time to peaks are first calculated. Then a mean curve of best fit is drawn.

Example 15.4: A uniform effective rainfall of a certain storm occurred for four hours over a catchment having an area of 1600 km². The ordinates of resulting flow are given below. Derive and plot the 4-hr unit hydrograph assuming a constant base flow of 100 m³/sec.

Time (day)	Flow (m³/sec)	Time (day)	Flow (m³/sec)
1	100	8	280
2	1000	9	218
3	839	10	180
4	630	11	155

5	520	12	130
6	420	13	110
7	350	14	100

Solution: The ordinates of the unit hydrograph are calculated in tabular form as follows:

Time day	Ordinates of hydrograph (m³/sec)	Base flow (m³/sec)	Ordinates of DRH (m³/sec)	Ordinates of 4-hr U.H (m³/sec)
1	100	100	0	0
2	1000	100	900	90
3	830	100	730	73
4	630	100	530	53
5	520	100	420	42
6	420	100	320	32
7	350	100	250	25
8	280	100	180	18
9	218	100	118	12
10	180	100	80	8
11	155	100	55	6
12	130	100	30	3
13	110	100	10	1
14	100	100	0	0
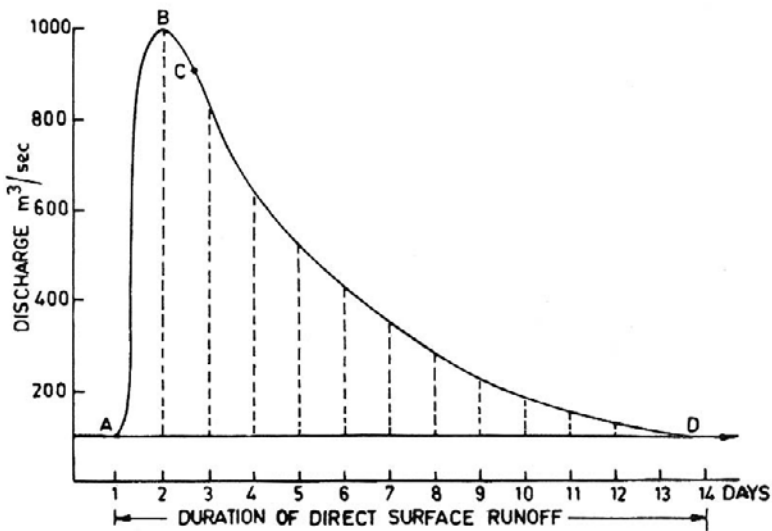
Fig. 15.2. Flood hydrograph for a storm of 4-h duration.

1. The hydrograph is first plotted as shown in Fig. 15.2.
2. The base flow (horizontal line AD is base flow) is separated to get ordinates of the DRH.
3. The area under DRH is calculated which is the volume of surface runoff.

$$= \frac{1}{2}\big[\Sigma \text{ ordinates}\big] \times \text{interval}$$

$$= \frac{1}{2} [0 + 900 + 730 + 530 + 420 + 320 + 250 + 180 + 118 + 80 + 55$$

$$+ \ 30 + 10 + 0] \times 60 \times 60 \times 24$$

$$= \frac{3623 \times 3600 \times 24}{2}$$

$$= 1.565 \times 10^8 \text{ m}^3$$

4. Rainfall excess = Volume of the DRH/catchment area

$$= \frac{1.565 \times 10^8}{1600 \times 1000 \times 1000} \times 100$$

$$= 10 \text{ cm}$$

5. The ordinates of the DRH are divided by 10 to obtain the ordinates of unit hydrograph and are plotted as shown in Fig. 15.3.
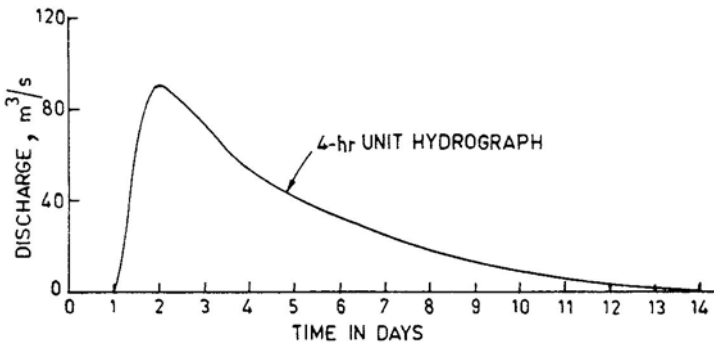
Fig. 15.3. Unit hydrograph for the catchment.

15.9.4 Flood Frequency Method

The empirical formulae presented in the previous section are some of the methods of estimating flood peaks. However, their applicability in modern hydrology for flood control works and large water projects is limited.

In flood control works, one would like to have estimates of flood peaks with various probabilities of exceedance. Such estimates are obtained by

frequency analysis of flood data at a river gauging site. One of the commonly used data series for this purpose is the annual flood series. The highest observed flood value at a site during a year is called the annual maximum flood value. If the annual peak flood value occurring in each year is selected for a number of years then these values constitute an annual flood series. The probability of occurrence of a flood in this series can be determined by frequency analysis.

The annual flood data series is arranged in descending order of magnitude and the probability (P) of each value being equaled or exceeded is calculated by the plotting position formula:

$$P = \frac{m}{N+1} \tag{15.43}$$

where m = order of the flood value, and N = total number of flood values.

The recurrence interval, T, is calculated as

$$T = \frac{1}{P} = \frac{N+1}{m} \tag{15.44}$$

The above equation is an empirical formula and there are several other such empirical formulae available for calculating P. Having calculated P or T for all the values in the series, the flood values are plotted against their recurrence intervals (T) on semi log or log-log paper. By a suitable plot, the flood value for any recurrence interval can be estimated.

This simple empirical procedure often yields satisfactory results for small extrapolation but errors increase with increasing extrapolation. Various frequency distribution functions are available. Gumbel's extreme value distribution, log-normal distribution, and log-Pearson type III distribution are commonly used analytical methods and are described in Chapter 11.

Example 15.5: For a river site, the recorded annual maximum flood values are given below. Estimate the flood with a return period of 25 and 50 years and what would be the probability of a flood of magnitude equal to or exceeding 100 m^3/s.

Year	Flood (m^3/s)	Year	Flood (m^3/s)	Year	Flood (m^3/s)
1950	130	1957	125	1964	85
1951	120	1958	112	1965	75
1952	76	1959	89	1966	60
1953	143	1960	89	1967	84
1954	160	1961	78	1968	108
1955	96	1962	90	1969	106
1956	80	1963	102	1970	83
				1971	95

Solution: $N = 22$

Calculation of the return periods for the flood data

m	Flood (m³/s)	P= m/(N+1)	T= 1/P	m	Flood (m³/s)	P=m/(N+1)	T=1/P
1	160	0.043	23.3	12	90	0.522	1.9
2	143	0.087	14.5	13	89	-	-
3	130	0.13	7.7	14	89	0.609	1.7
4	125	0.174	5.8	15	85	0.652	1.5
5	120	0.217	4.6	16	84	0.696	1.4
6	112	0.261	3.8	17	83	0.739	1.3
7	108	0.364	3.3	18	86	0.783	1.3
8	106	0.348	2.9	19	78	0.826	1.2
9	102	0.391	2.6	20	76	0.87	1.2
10	96	0.435	2.3	21	75	0.913	1.1
11	95	0.478	2.1	22	60	0.957	1.1
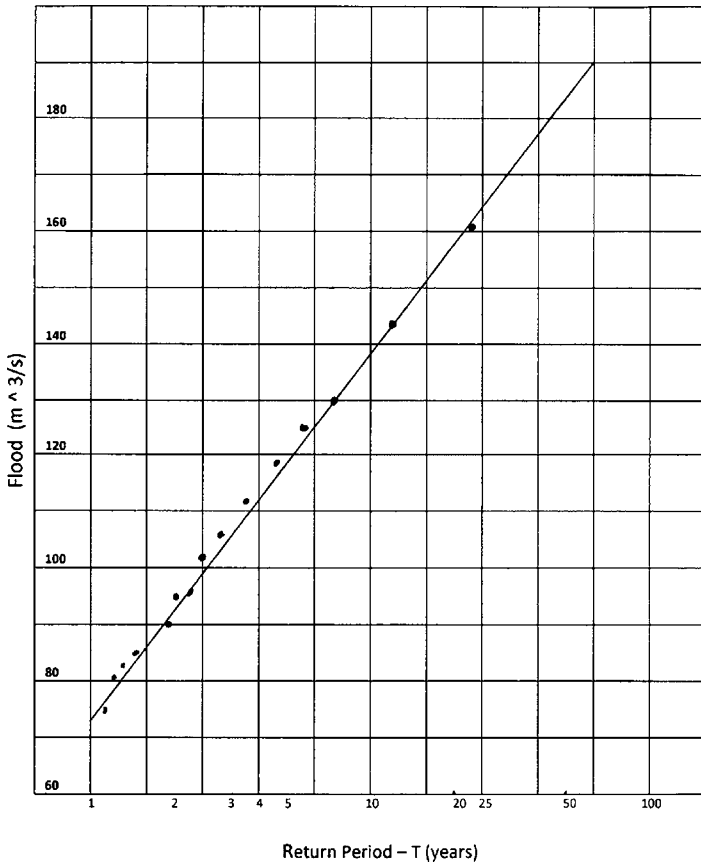
Fig. 15.4. Return period of different flood values.

A graph is plotted between the flood and the return period on a semi-log paper (Fig. 15.4). From this curve, the flood values for the return periods 25 and 50 years are 163 and 184 m^3/s, respectively. For a flood of 100 m^3/s, the return period is 2.5 years and the probability is 0.40.

15.10 FLOODS IN INDIAN RIVERS

15.10.1 River Systems of India

India has about 120 major and medium rivers and a number of minor rivers that flow in different parts of the country. From the standpoint of flood geomorphology, these rivers of India can be grouped broadly into two major systems. The first system includes all the large rivers and their tributaries of the Himalayan region and the second consists of the rivers of the central and peninsular India as has been mentioned in Chapter 1. Table 15.6 summarizes some of the important hydrologic and physiographic characteristics of the major rivers of India.

Table 15.6: Hydrological characteristics of the Indian rivers (Rao, 1975)

River	Catchment area (km^2)	Main river length (km)	Peak flood (m^3/s)	Mean slope (%)	Sediment load (10^6t/year)
Indus	468068	2880	32880	0.18	100
Ganga	1050000	2525	72915	0.28	329
Brahmaputra	580000	2900	72700	0.18	597
Mahanadi	141589	851	44827	0.05	15.7
Narmada	98796	1312	69000	0.08	70
Tapi	65145	724	41700	0.1	25
Godavari	312812	1465	78800	0.04	170
Krishna	258948	1401	33600	0.09	4
Pennar	55213	597	13394	0.25	-
Cauvery	81155	800	12913	0.17	1.5

There is a distinct difference between the two systems in terms of peak discharge, sediment load and channel morphology. The Himalayan rivers have a high dynamic environment with much variability in flood discharge and sediment load. By comparison, central and peninsular rivers are more stable because of low channel gradients.

15.10.2 Flood Characteristics of Indian Rivers

The magnitude of a flood is measured by either its stage or discharge. Systematic measurements of stage and discharge of Indian rivers at different sites are available since about 1950, as most of the gauging sites were established after India attained independence in 1947.

Table 15.7: Flooding characteristics of some Indian rivers

	Name of the river	Site	Mean flood (m^3/s)	Highest flood (m^3/s)	% of mean (%)	Lowest flood (m^3/s)	% of mean (%)	SD (m^3/s)	Coefficient of skewness
1	Ganga	Raiwala	6055	19133	316	236	4	2747	1.3
2	Yamuna	Tajewala	4400	15942	362	1218	28	2803	2.1
3	Ganga	Farakka	55776	72900	130	39413	71	7979	0.03
4	Sutlej	Bhakra	3941	9203	233	1727	43	1664	1.1
5	Ravi	Madhopur	4351	26052	598	1600	37	3458	2.9
6	Kosi	Sunakhambikhola	8178	17445	213	4578	56	2834	1.9
7	Sone	Dehri	17873	34235	192	5125	29	7503	0.2
8	Damodar	Rhondia	6328	14761	233	1727	27	3103	0.6
9	Baitarni	Akhyapada	3687	9203	250	1274	35	1985	1.3
10	Mahanadi	Naraj	29269	44827	153	11157	38	2731	-0.4
11	Narmada	Garudeshwar	25399	69400	273	11892	47	12781	1.3
12	Tapi	Kathore	9698	25500	263	3270	34	5883	1.4
13	Godavari	Dowleshwarm	29207	78800	270	11490	39	12378	1.9
14	Krishna	Vijayawada	14775	39000	264	7187	49	4516	2.1
15	Pennar	Nellore	3623	13394	370	170	5	3281	1.7
16	Kaveri	K.R. Sagar	2641	6205	235	-	-	1142	1.5

High magnitude flood events with serious consequences occur in different rivers of the country. On average about 6 to 8 high magnitude floods occur every year. However, such floods generally occur in August and September, when heavy and widespread rains associated with tropical disturbances fall over the previously saturated wet soils. Table 15.7 summarizes flood characteristics for some sites on major rivers in India, where highest and lowest flood discharges are compared with mean flood discharges in each river catchment. Table 15.7 reveals that most rivers show a high mean discharge, a large variability and a pronounced positive skewness. The positive skewness values suggest the occurrence of a few very large floods in the short term records. The highest flood discharges are between 6205 and 79950 m^3/s and the lowest flood discharges between 170 and 39413 m^3/s. The extreme highest and lowest floods vary from about 4 to 600 percent of the respective mean flood value. Also the magnitude of the highest flood discharges deviate from the mean discharges by as much as 2 to 3 times the standard deviation.

15.11 HIGHEST FLOODS IN INDIA

Information on the highest floods, such as their date of occurrence, stage height, and flood discharge, are available for a number of sites on major rivers in India. The highest flood discharges at different sites are listed in Table 15.8. The locations of these floods are shown in Fig. 15.5. Table 15.8 shows that 12 major rivers in India have records at about 32 sites with peak discharges ranging from about 1170 m^3/s for a 133 km^2 area to about 72,900 m^3/s for a 935,000 km^2 area. The highest flood of 72,900 km^2 was recorded on the mighty Ganga River in 1954. The 1968 flood on the Tapi River at Ukai was the highest since 1849, the 1970 flood on the Narmada River was the highest for the last 107 years and the 1982 flood on the Mahanadi River was the highest since 1834. It is remarkable to find that the highest floods of 9340 m^3/s for a 735 km^2 area and 16,307 m^3/s for a 1930 km^2 area occurred in the arid region of the state of Gujarat. Figure 15.5 shows that most of the extreme floods have occurred in the northern and the central river basins, the areas most frequently impacted by monsoon depressions occurring in the Bay of Bengal. Apparently, the areas of northern and central parts of India are the regions of great risk to human life and property.

When the highest 32 flood values are plotted against their drainage areas and an envelope curve is drawn, as shown in Fig. 15.6, it is seen that the remarkable floods at many sites fall far below the envelope line indicating that a much greater flood than has been experienced could occur on most rivers. The envelope curve can be considered as an indicator of the reasonable limits for estimating maximum floods.
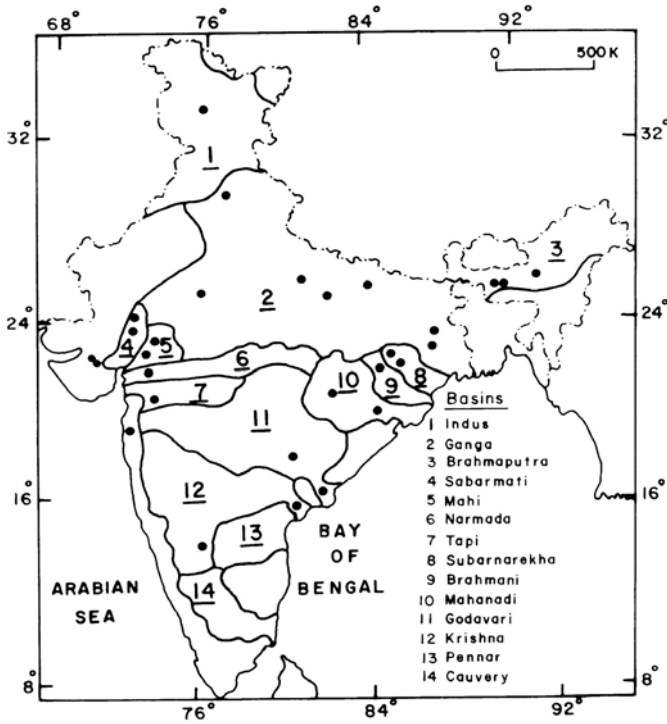
Fig. 15.5. Major river basins in India and locations of the highest floods
(after Rakhecha, 2002).
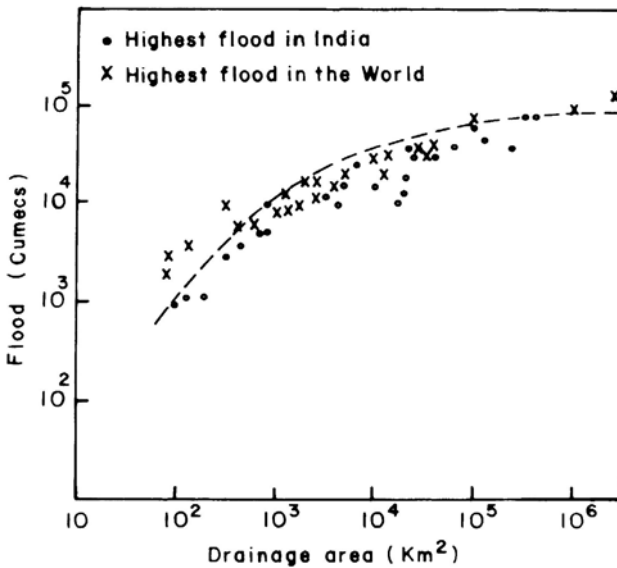
Fig. 15.6. Envelope curve of the highest floods in India compared with the
highest floods in the world (after Rakhecha, 2002).

Table 15.8: Highest floods in the major river basins in India

S. No.	River Basin	Stream	Site	Area (km^2)	Flood (m^3/s)	Year
1	Brahamaputra	Gish	-	133	1170	July. 1968
2	Mahi	Kharm	Patadungri	212	1177	-
3	Subarnarekha	Ramiala	Ramiala	328	3108	Sept. 1982
4	Kutch	Moj	Moj	440	3981	-
5	Kutch	Brahmani	Brahmani	699	5450	-
6	Kutch	Machhu	Machhu-1	735	9340	Aug. 1979
7	Kutch	Damanganga	Damanganga	1813	12900	-
8	Kutch	Machhu	Machhu-2	1930	16307	Aug. 1979
9	Godavari	Kadam	Kadam	2590	13450	Aug. 1958
10	Sabarmati	Banas	Dantiwada	2862	11950	Aug. 1973
11	Mahi	Mahi	Chandangarh	4320	8160	Aug. 1977
12	Sabarmati	Sabarmati	Dharoi	5540	14150	Aug. 1973
13	Indus	Ravi	Madhopur	6087	26052	Sept. 1988
14	Ganga	Yamuna	Tajewala	11059	15947	Sept. 1947
15	Ganga	Tons	Meja Rol	17400	10800	July. 1971
16	Brahmani	Brahmani	Bolani	18070	13570	Aug. 1974
17	Mahanadi	Mahanadi	Kantamel	19600	15400	Sept. 1977
18	Ganga	Damodar	Rhondia	19900	18100	Aug. 1935
19	Ganga	Ganga	Rishikesh	21800	16000	Aug. 1924
20	Ganga	Chambal	Jhalawar	22584	37000	Aug. 1969
21	Mahi	Mahi	Kadana	25491	33000	-
22	Godavari	Indravati	Barthagudern	40000	24860	Aug. 1976
23	Ganga	Betwa	Sahijna	43870	43800	July. 1971
24	Ganga	Kosi	Barakshetra	59052	23085	Aug. 1924
25	Tapi	Tapi	Ukai	62225	42475	Aug. 1968
26	Ganga	Sone	Kolewar	67878	36800	July. 1971
27	Narmada	Narmada	Garudeshwar	88000	69400	Sept. 1970
28	Mahanadi	Mahanadi	Naraj	127000	44827	Aug. 1982
29	Krishna	Krishna	Vijayawada	257000	39000	July. 1903
30	Godavari	Godavari	Dowlaish-waram	309000	78800	Sept. 1959
31	Brahamaputra	Brahama-putra	Pandu	404000	72700	Aug. 1962
32	Ganga	Ganga	Farakka	935000	72900	Aug. 1954

15.12 COMPARISON OF THE HIGHEST FLOODS IN INDIA WITH WORLD'S HIGHEST FLOODS

It is of interest to compare the highest floods recorded in India with those recorded in other parts of the world. Rodier and Roche (1984) have given the data for the 40 highest floods from different countries of the world. These data are given in Table 15.9. The available world flood data indicate

that the highest floods with peak discharges ranging from 250 m³/s for a 32 km² area to 370,000 m³/s for a 46,40,000 km² area have been observed in different rivers of the world. For comparison, the world's highest floods are plotted along with the highest Indian floods in Fig. 15.6. The figure shows that the flood discharges for the Indian rivers are remarkably comparable with the highest flood discharges recorded in the world for drainage areas larger than about 1000 km². However, for areas less than 1000 km², India's highest floods are considerably lower in magnitude. The records given in Tables 15.7 and 15.8 indicate that two floods recorded in India were record breaking floods in the world as they far exceeded any other flood for the same drainage size. The first flood was on the Machhu River on 11 August 1979, which destroyed the Machhu-2 dam. This flood peak of 16,307 m³/s from 1930 km² was caused as a result of exceptionally heavy rainfall in the Machhu River basin. During the period 10-12 August 1979, the Machhu River basin received nearly four times the mean basin rainfall for August (Rakhecha and Mandal, 1983). The second flood was on the Narmada River on 6 September 1970. This flood peak of 69,400 m³/s from 88,000 km² was caused by a depression during which several stations recorded rainfalls exceeding 20 cm in 24 hours. The Narmada River is a west flowing river. For west flowing rivers, such as the Narmada River, the magnitude of the floods frequently gets amplified because the depressions move parallel to and in concert with the river flow.

Table 15.9: Highest floods in the world

No.	River	Country	Area (km²)	Flood (m³/s)
1	San Rafael	USA	3.2	250
2	L. San Gorgonio	USA	4.5	311
3	Halawa	USA	12	762
4	SF Wailua	USA	58	2470
5	Buey	Cuba	73	2060
6	Papenoo	France	78	2200
7	San Bartolo	Mexico	81	3000
8	Quinne	France	143	4000
9	Quaieme	France	330	10400
10	Yate	France	435	5700
11	Little Nemaha	USA	549	6370
12	Haast	New Zealand	1020	7690
13	Midfork	USA	1360	8780
14	Cithuatlam	Mexico	1370	13500
15	Pioneer	Australia	1490	9840
16	Hualien	Taiwan (China)	1500	11900
17	Nyoda	Japan	1560	13510
18	Kiso	Japan	1680	11150
19	West Nueces	USA	1800	15600

20	Machhu	India	1930	16307
21	Tamshui	Taiwan (China)	2110	16700
22	Shingu	Japan	2350	19025
23	Pedernales	USA	2450	12500
24	Daeryoung Gang	North Korea	3020	13500
25	Yoshino	Japan	3750	14470
26	Cagayan	Philippines	4244	17550
27	Tone	Japan	5110	16900
28	Nueces	USA	5504	17400
29	Eel	USA	8060	21300
30	Pecos	USA	9100	26800
31	Betsiboka	Madagascar	11800	22000
32	Toedong Gang	North Korea	12175	29000
33	Han	South Korea	23880	37000
34	Jhelam	Pakistan	29000	31100
35	Hanjiang	China	41400	40000
36	Mangoky	Madagascar	50000	38000
37	Narmada	India	88000	69400
38	Changjiang	China	1010000	110000
39	Lena	USSR	2430000	189000
40	Amazonas	Brazil	4640000	370000

REFERENCES

Bao, C.L., 1987. Synoptic Meteorology in China. Springer Verlag, Berlin, 269 pp.

Chow, V.T., 1956. Hydrologic Studies of Floods in the United State. Int. Ass. Scientific Hydrol. Publ. 42, pp. 134-170.

Chow, V.T. (editor), 1964. Hand Book of Applied Hydrology,. McGraw-Hill Book Co., New York.

Dooge, J.C.I., 1959. A general theory of the unit hydrograph. *Journal of Geophysical Research*, 64, 2, pp. 241-256.

Dooge, J.C.I., 1960. The routing of groundwater recharge through typical elements of linear storage. *IASH Bulletin*, 52, pp. 286-300.

Dooge, J.C.I., 1973. Linear theory of hydrologic systems. Technical Bulletin No. 1468, 327 pp., U.S. Department of Agriculture, Agricultural Service, Beltsville, Maryland.

Famji, K.K., 1983. Manual of Flood Control Methods and Practices. ICID, New Delhi.

Fuller, W.E., 1914. Flood Flows. *Trans. Am. Soc. Civ. Eng.*, 17, pp. 564-617.

India Meteorological Department, 1971. Rainfall and Droughts in India. Report of the Drought Research Unit. IMD publ. Poona.

Inglish, G.C. and Desoyza, A.J., 1930. A Critical Study of Runoff and Floods of Catchments of the Bombay Presidency. PWD, Tech. paper No. 30.

Kirpich, Z.P., 1940. Time of Concentration of Small Agricultural Watersheds. *Civil Engr.*, 30, No. 6, p. 361.

Moss, J.H., Baker, V.R., Doehring, D.O., Patton, P.C., and Wolman, M.G., 1978. Floods and People—A Geological Perspective. Report of the Committee on Geology and Public Policy, Geol. Soc. Am., 7 pp.

Nash, J.E., 1957. The form of the instantaneous unit hydrograph. IASH Publication, 45, 3, pp. 114-121.

Pisharoty, P.R. and Asnani, G.C. 1957. Rainfall Around Monsoon Depressions over India. *J. Met. Geophys*, 8. pp. 1-6.

Platt, R.H., 1979. Options to Improve Federal Non Structural Response to Floods. U.S. Water Resources Council, Washington, D.C., 102 pp.

Rakhecha, P.R., 2002. Highest Floods in India. Proc. Int. Symposium on Extraordinary Floods. IAHS Publ., 271, pp. 107-172.

Rakhecha, P.R. and Mandal, B.N., 1983. Estimation of Peak Flood at Machhu-2 Dam on the Day of Disaster of 11 August 1979. *Vayu Mandal*, 13, pp 71-73.

Rakhecha, P.R. and Pisharoty, P.R., 1996. Heavy Rainfall During Monsoon Season Point and Spatial Distribution. *Current Sci*., 71, pp. 177-186.

Rao, K.L., 1975. India's Water Wealth. Orient Longman, New Delhi, 255 pp.

Rodier, J.A. and Roche, M., 1984. World Catalogue of Maximum Observed Floods. IAHS Publ. No. 143.

Sherman, L.K., 1932. Stream flow from rainfall by the unit graph method. *Engineering News Record*, 108, pp. 501-505.

Singh, V.P., 1988. Hydrologic Systems: Vol. 1. Rainfall-Runoff Modeling. Prentice Hall, Englewood Cliffs, New Jersey.

Singh, V.P., 1989. Hydrologic Systems: Vol. 2. Watershed Modeling. Prentice Hall, Englewood Cliffs, New Jersey.

Singh, V.P., 1996. Kinematic Wave Modeling in Water Resources: Surface Water Hydrology. John Wiley & Sons, New York.

Ward, R., 1978. Floods, A Geographical Perspective. The MacMillan Press. London.

WMO (World Meteorological Organization), 1975. Drought and Agriculture. WMO Tech. Note No. 138. WMO No. 392.

World Weather Extremes

World Rainfall Extremes

Highest Annual Average	1168 cm	Mt Waialeale, HAWAII	32 years
Highest Annual Total	2299 cm	Cherrapunji, INDIA	Aug 1860 – July 1861
Highest Monthly Total	930 cm	Cherrapunji, INDIA	July 1861
Highest Daily Rainfall	188 cm	Cilaos, LA REUNION	15–16 Mar 1952
Lowest Annual Average	0.05 cm	Arica, CHILE	59 years
Most Rainy Days per Year	325 days	Bahia Felix, CHILE	

Wind Extremes

Maximum Wind Gust (World)	371 km/h	Mt Washington, USA	12 April 1934
Maximum Wind Gust (Australia)	267 km/h	Varanus Island, WA and Learmonth, WA	10 April 1996 and 22 March 1999

Pressure Extremes

Highest Pressure (World)	1083.8 hPa	Agata, RUSSIA	31 December 1986

Temperature Extremes

Highest (World)	57.8°C	El Azizia, LIBYA	13 September 1922
Lowest (World)	-89.6°C	Vostok, ANTARCTICA	21 July 1983
Highest (Australia)	50.7°C	Oodnadatta, SA	2 Janaury 1960
Highest (Africa)	57.8°C	El Azizia, LIBYA	13 September 1922
Highest (Antarctica)	15.0°C	Vanda, ANTARCTICA	Date not known
Highest (Asia)	54.0°C	Tirat Tsvi, ISRAEL	21 July 1942
Highest (Europe)	50.0°C	Seville, SPAIN	4 August 1881
Highest (North America)	56.7°C	Death Valley, CALIFORNIA	10 July 1913
Highest (South America)	48.9°C	Rivadavia, ARGENTINA	11 December 1905

Lowest (Australia)	-23.0°C	Charlotte Pass, NSW	29 June 1994
Lowest (Africa)	-23.9°C	Ifrane, MOROCCO	11 February 1935
Lowest (Antarctica)	-89.6°C	Vostok, ANTARCTICA	21 July 1983
Lowest (Asia)	-67.7°C	Oimekon, SIBERIA	6 February 1933
Lowest (Europe)	-55.0°C	Ust- Shchugor, RUSSIA	Date not known
Lowest (North America)	-62.8°C	Snag (Yukon), CANADA	3 February 1947
Lowest (South America)	-32.8°C	Sarmiento, ARGENTINA	1 June 1907

Index